COLD-FORMED STEEL DESIGN

THIRD EDITION

Wei-Wen Yu, Ph.D., P.E.
Curators' Professor Emeritus of Civil Engineering
Director, Center for Cold-Formed Steel Structures
University of Missouri-Rolla

JOHN WILEY & SONS, INC.

New York • Chichester • Weinheim • Brisbane • Singapore • Toronto

This publication is designed to provide accurate and authoritative information in regard to the subject matter covered. It is sold with the understanding that the publisher is not engaged in rendering professional services. If professional advice or other expert assistance is required, the services of a competent professional person should be sought.

PREFACE

This third edition of the book has been prepared to provide readers with a better understanding of the analysis and design of the thin-walled, cold-formed steel structures that have been so widely used in building construction and other areas in recent years. It is a revised version of my book, *Cold-Formed Steel Design,* published by John Wiley & Sons, Inc. in 1991. All the revisions are based on the 1996 edition of the AISI Specification with the Supplement No. 1 which combines the Allowable Stress Design (ASD) and the Load and Resistance Factor Design (LRFD) methods.

The material was originally developed for graduate courses and short courses in the analysis and design of cold-formed steel structures and is based on experience in design, research, and development of American Iron and Steel Institute (AISI) design criteria.

Throughout the book, descriptions of the structural behavior of cold-formed steel members and connections are given from both the theoretical and the experimental points of view. The reasons and justification for the various design provisions of the AISI Specification are discussed at length. Consequently the text will not only be instructive for students but can serve as a major source of reference for structural engineers and researchers.

Of the published book's 14 chapters, Chapters 2 through 9 have been completely revised according to the combined ASD/LRFD Specification. Other chapters have been updated on the basis of available information. Chapter 14 is a new chapter on residential construction.

Chapter 1 includes a general discussion of the application of cold-formed steel structures and a review of previous research. It also discusses the development of design specifications, and the major differences between the design of cold-formed and hot-rolled steel structural members. Because of the many research projects in the field that have been conducted worldwide during the past 25 years, numerous papers have been presented at various conferences and published in a number of engineering journals. At the same time, new design criteria have been developed in various countries. These new developments are reviewed in this chapter.

Since material properties play an important role in the performance of structural members, the types of steels and their most important mechanical properties are described in Chapter 2. In addition to the revision of Table 2.1, new information on the use of low-ductility steel has been included in Article 2.4. Article 2.10 includes additional information on test methods

In Chapter 3, the strength of thin elements and design criteria are discussed to acquaint the reader with the fundamentals of local buckling and postbuckling strength of thin plates and with the basic concepts used in design. This chapter has been completely revised to include detailed information on design basis with a revised Table 3.1 for safety factors and resistance factors.

Chapter 4 deals with the design of flexural members. Because the AISI design provisions were revised extensively during 1996–1999, this chapter has been completely rewritten to cover the design of beams using both ASD and LRFD methods. It also includes new information on perforated elements, distortional buckling, and beams having one flange fastened to a standing seam roof system.

The design procedures for compression members are discussed in Chapter 5. This chapter has been brought up to date by using the newly revised equations for computing the nominal buckling stress with the revised factor of safety. Design information on compression members having one flange through-fastened to deck or sheathing has also been added.

In 1996, the AISI Specification included new design provisions on combined tensile load and bending, as discussed in Chapter 6. Revisions have also been made on the design of beam-columns using ASD and LRFD methods.

Chapter 7 covers the design of cylindrical tubes. This revised chapter reflects the minor changes made in the 1996 edition of the AISI Specification and Supplement No. 1.

Like the member design, the design of connections has been updated in Chapter 8 for using the ASD and LRFD methods with additional provisions for shear lag and staggered holes. New design information on screw connections and press joints have been added.

Because various types of structural systems, such as shear diaphragms and shell roof structures, have become increasingly popular in building construction, Chapter 9 contains design information on these types of structural systems. It also contains the current design procedure for wall studs on the basis of the 1996 Specification.

The sectional properties of standard corrugated sheets are discussed in Chapter 10 because they have long been used in buildings for roofing, siding, and other applications.

Steel decks are widely used in building construction. Consequently the updated information in Chapter 11 on their use in steel-deck-reinforced composite slabs and composite beams is timely.

Chapter 12 contains an introduction to the design of cold-formed stainless steel structural members supplementing the information on cold-formed carbon steel structural members in other chapters. This chapter is based on the ASCE Standard for the design of cold-formed stainless steel structural members.

The increasing use of computers for design work warrants the brief introduction that is given in Chapter 13 for the computer-aided design of cold-formed steel structures.

During recent years, cold-formed steel members have been used increasingly for residential construction. The new Chapter 14 includes recently developed design information on residential steel framing.

It is obvious that a book of this nature would not have been possible without the cooperation and assistance of many individuals, organizations, and institutions. It is based primarily on the results of continuing research programs on cold-formed steel structures that have been sponsored by the American Iron and Steel Institute (AISI), the American Society of Civil Engineers (ASCE), the Metal Building Manufacturers Association (MBMA), the Metal Construction Association (MCA), the National Science Foundation (NSF), the Rack Manufacturers Institute (RMI), the Steel Deck Institute (SDI), the Steel Stud Manufacturers Association (SSMA), and others at various universities. The publications related to cold-formed steel structures issued by AISI and other establishments have been very helpful for the preparation of this book.

I am especially indebted to the late Professor George Winter of Cornell University, who made contributions of pronounced significance to the building profession in his outstanding research on cold-formed steel structures and in the development of AISI design criteria. A considerable amount of material used in this book is based on Dr. Winter's publications.

My sincere thanks go to Mr. David Jeanes, Senior Vice President of the American Iron and Steel Institute, for permission to quote freely from the AISI Specification and the Commentary thereon. An expression of appreciation is also due to the many organizations and individuals that granted permission for the reproduction of quotations, graphs, tables, and photographs. Credits for the use of such materials are given in the text.

I also wish to express my sincere thanks to Mr. Roger L. Brockenbrough, Dr. Helen Chen, Dr. Samuel J. Errera, Dr. James M. Fisher, Mr. Richard B. Heagler, Professor Gregory J. Hancock, Professor Roger A. LaBoube, Mr. Jay W. Larson, Professor Teoman B. Pekoz, and Dr. Benjamin W. Schafer for their individual reviews of various parts of the manuscript. Their suggestions and encouragement have been of great value to the improvement of this book.

I am very grateful to Mrs. Laura Richardson for her careful typing and kind assistance. The financial assistance provided by the University of Missouri-Rolla through the Curators' Professorship and the Center for Cold-Formed Steel Structures is appreciated.

This book could not have been completed without the help and encouragement of my wife, Yueh-Hsin. I am most grateful for her patience, understanding, and assistance.

Wei-Wen Yu

Rolla, Missouri
March 2000

CONTENTS

1 Introduction

1.1 GENERAL REMARKS

In steel construction, there are two main families of structural members. One is the familiar group of hot-rolled shapes and members built up of plates. The other, less familiar but of growing importance, is composed of sections cold-formed from steel sheet, strip, plates, or flat bars in roll-forming machines or by press brake or bending brake operations.[1.1,1.2,1.3*] These are cold-formed steel structural members. The thickness of steel sheets or strip generally used in cold-formed steel structural members ranges from 0.0149 in. (0.4 mm) to about $\frac{1}{4}$ in. (6.4 mm). Steel plates and bars as thick as 1 in. (25 mm) can be cold-formed successfully into structural shapes.[1.1,1.4,1.314]

Although cold-formed steel sections are used in car bodies, railway coaches, various types of equipment, storage racks, grain bins, highway products, transmission towers, transmission poles, drainage facilities, and bridge construction, the discussions included herein are primarily limited to applications in building construction. For structures other than buildings, allowances for dynamic effects, fatigue, and corrosion may be necessary.[1.314]

The use of cold-formed steel members in building construction began in about the 1850s in both the United States and Great Britain. However, such steel members were not widely used in buildings until around 1940. The early development of steel buildings has been reviewed by Winter.[1.5–1.7]

Since 1946 the use and the development of thin-walled cold-formed steel construction in the United States have been accelerated by the issuance of various editions of the "Specification for the Design of Cold-Formed Steel Structural Members"[1.314] of the American Iron and Steel Institute (AISI). The earlier editions of the specification were based largely on the research sponsored by AISI at Cornell University under the direction of George Winter since 1939. It has been revised subsequently to reflect the technical developments and the results of continuing research.[1.267]

In general, cold-formed steel structural members provide the following advantages in building construction:

1. As compared with thicker hot-rolled shapes, cold-formed light members can be manufactured for relatively light loads and/or short spans.

---

*The references are listed at the back of the book.

1
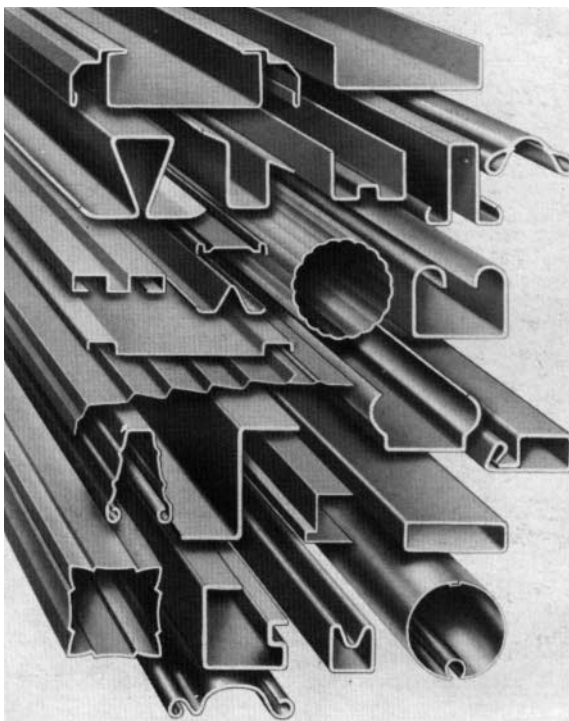
Figure 1.1   Various shapes of cold-formed sections.[1.1]

2. Unusual sectional configurations can be produced economically by cold-forming operations (Fig. 1.1), and consequently favorable strength-to-weight ratios can be obtained.
3. Nestable sections can be produced, allowing for compact packaging and shipping.
4. Load-carrying panels and decks can provide useful surfaces for floor, roof, and wall construction, and in other cases they can also provide enclosed cells for electrical and other conduits.
5. Load-carrying panels and decks not only withstand loads normal to their surfaces, but they can also act as shear diaphragms to resist force in their own planes if they are adequately interconnected to each other and to supporting members.

Compared with other materials such as timber and concrete, the following qualities can be realized for cold-formed steel structural members.[1.8,1.9]

1. Lightness
2. High strength and stiffness

3. Ease of prefabrication and mass production
4. Fast and easy erection and installation
5. Substantial elimination of delays due to weather
6. More accurate detailing
7. Nonshrinking and noncreeping at ambient temperatures
8. Formwork unneeded
9. Termite-proof and rotproof
10. Uniform quality
11. Economy in transportation and handling
12. Noncombustibility
13. Recyclable material

The combination of the above-mentioned advantages can result in cost saving in construction.

1.2   TYPES OF COLD-FORMED STEEL SECTIONS AND THEIR APPLICATIONS

Cold-formed steel structural members can be classified into two major types:

1. Individual structural framing members
2. Panels and decks

The design and the usage of each type of structural members have been reviewed and discussed in a number of publications.[1.5–1.75,1.267–1.285]

1.2.1   Individual Structural Framing Members

Figure 1.2 shows some of the cold-formed sections generally used in structural framing. The usual shapes are channels (C-sections), Z-sections, angles, hat sections, I-sections, T-sections, and tubular members. Previous studies have indicated that the sigma section (Fig. 1.2*d*) possesses several advantages such as high load-carrying capacity, smaller blank size, less weight, and larger torsional rigidity as compared with standard channels.[1.76]

In general, the depth of cold-formed individual framing members ranges from 2 to 12 in. (51 to 305 mm), and the thickness of material ranges from 0.048 to about $\frac{1}{4}$ in. (1.2 to about 6.4 mm). In some cases, the depth of individual members may be up to 18 in. (457 mm), and the thickness of the member may be $\frac{1}{2}$ in. (13 mm) or thicker in transportation and building construction. Cold-formed steel plate sections in thicknesses of up to about $\frac{3}{4}$ or 1 in. (19 or 25 mm) have been used in steel plate structures, transmission poles, and highway-sign support structures.
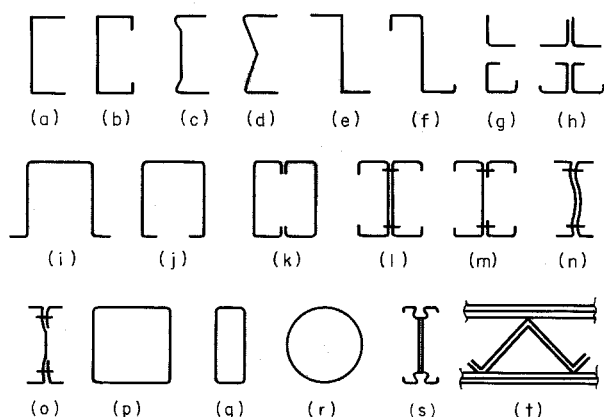
Figure 1.2   Cold-formed sections used in structural framing.[1.6]

In view of the fact that the major function of this type of individual framing member is to carry load, structural strength and stiffness are the main considerations in design. Such sections can be used as primary framing members in buildings up to six stories in height.[1.278] Figure 1.3 shows a two-story building. In tall multistory buildings the main framing is typically of heavy hot-rolled shapes and the secondary elements may be of cold-formed steel members such as steel joists, decks, or panels (Figs. 1.4 and 1.5). In this case the heavy hot-rolled steel shapes and the cold-formed steel sections supplement each other.[1.264]

As shown in Figs. 1.2 and 1.6 through 1.10, cold-formed sections are also used as chord and web members of open web steel joists, space frames, arches, and storage racks.

1.2.2   Panels and Decks

Another category of cold-formed sections is shown in Fig. 1.11. These sections are generally used for roof decks, floor decks, wall panels, siding material, and bridge forms. Some deeper panels and decks are cold-formed with web stiffeners.

The depth of panels generally ranges from $1\frac{1}{2}$ to $7\frac{1}{2}$ in. (38 to 191 mm), and the thickness of materials ranges from 0.018 to 0.075 in. (0.5 to 1.9 mm). This is not to suggest that in some cases the use of 0.012 in. (0.3 mm) steel ribbed sections as load-carrying elements in roof and wall construction would be inappropriate.

Steel panels and decks not only provide structural strength to carry loads, but they also provide a surface on which flooring, roofing, or concrete fill can be applied, as shown in Fig. 1.12. They can also provide space for electrical
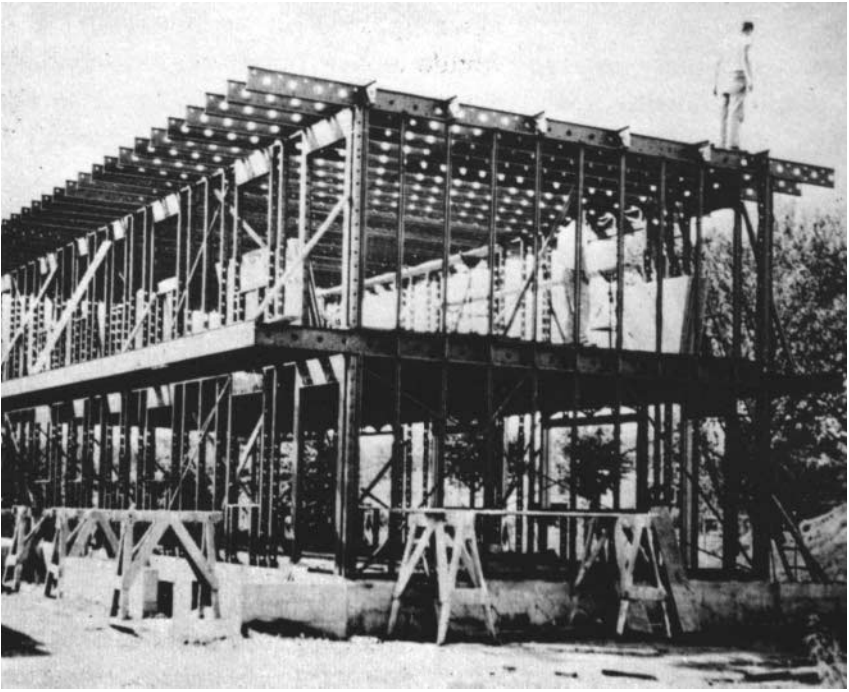
Figure 1.3   Building composed entirely of cold-formed steel sections. (*Penn Metal Company.*)[1.7]

conduits, or they can be perforated and combined with sound absorption material to form an acoustically conditioned ceiling. The cells of cellular panels are also used as ducts for heating and air conditioning.

In the past, steel roof decks were successfully used in folded-plate and hyperbolic paraboloid roof construction,[1.13,1.22,1.26,1.30,1.34,1.35,1.72,1.77–1.84] as shown in Figs. 1.13 and 1.14. The world's largest light-gage steel primary structure using steel decking for hyperbolic paraboloids, designed by Lev Zetlin Associates, is shown in Fig. 1.15.[1.82] In many cases, roof decks are curved to fit the shape of an arched roof without difficulty. Some roof decks are shipped to the field in straight sections and curved to the radius of an arched roof at the job site (Fig. 1.16). In other buildings, roof decks have been designed as the top chord of prefabricated open web steel joists or roof trusses (Fig. 1.17).[1.85,1.86] In Europe, TRP 200 decking (206 mm deep by 750 mm pitch) has been used widely. In the United States, the standing seam metal roof has an established track record in new construction and replacement for built-up and single ply systems in many low-rise buildings.

Figure 1.11 also shows corrugated sheets which are often used as roof or wall panels and in drainage structures. The use of corrugated sheets as exterior
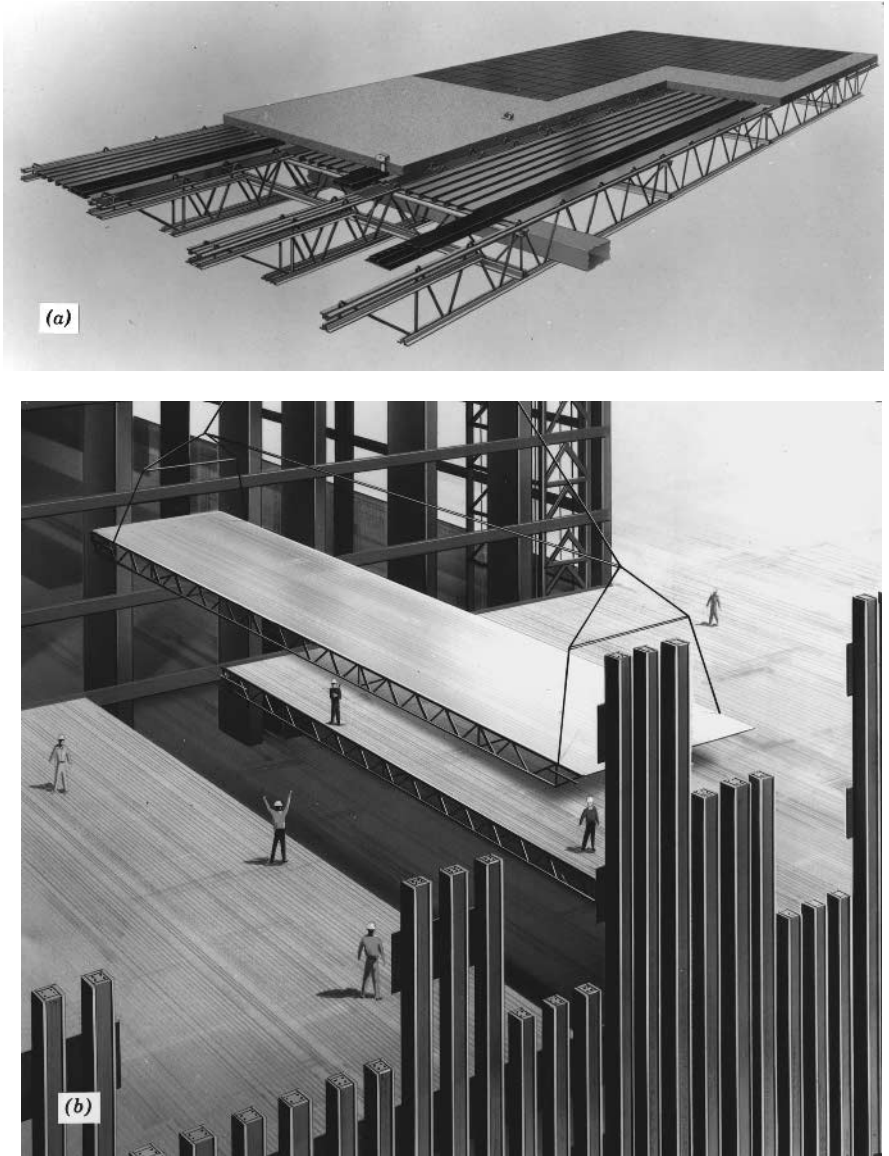
Figure 1.4   (*a*) Composite truss-panel system used in World Trade Center Building, New York City; prefabricated by Laclede Steel Company. (*b*) Placement of prefabricated composite floor panel section in World Trade Center Building. (*Port of New York Authority*.)
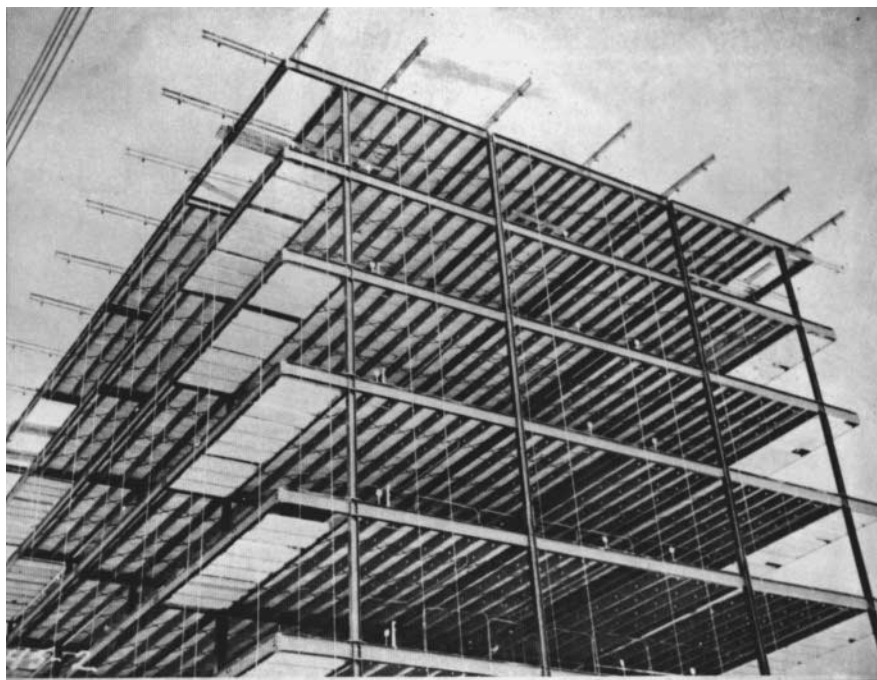
Figure 1.5   Cold-formed steel joists used together with hot-rolled shapes (*Stran-Steel Corporation*.)

curtain wall panels is illustrated in Fig. 1.18*a*. It has been demonstrated that corrugated sheets can be used effectively in the arched roofs of underground shelters and drainage structures.[1.87–1.89]

The pitch of corrugations usually ranges from $1\frac{1}{4}$ to 3 in. (32 to 76 mm), and the corrugation depth varies from $\frac{1}{4}$ to 1 in. (6.4 to 25 mm). The thickness of corrugated steel sheets usually ranges from 0.0135 to 0.164 in. (0.3 to 4.2 mm). However, corrugations with a pitch of up to 6 in. (152 mm) and a depth of up to 2 in. (51 mm) are also available. See Chap. 10 for the design of corrugated steel sheets based on the AISI publications.[1.87,1.88] Unusually deep corrugated panels have been used in frameless stressed-skin construction, as shown in Fig. 1.18*b*. The self-framing corrugated steel panel building proved to be an effective blast-resistant structure in the Nevada tests conducted in 1955.[1.90]

Figure 1.19 shows the application of standing seam roof systems. The design of beams having one flange fastened to a standing seam roof system is discussed in Chap. 4.

In the past four decades, cold-formed steel deck has been successfully used not only as formwork, but also as reinforcement of composite concrete floor and roof slabs.[1.55,1.91–1.103] The floor systems of this type of composite steel deck-reinforced concrete slab are discussed in Chap. 11.

(a)

(b)
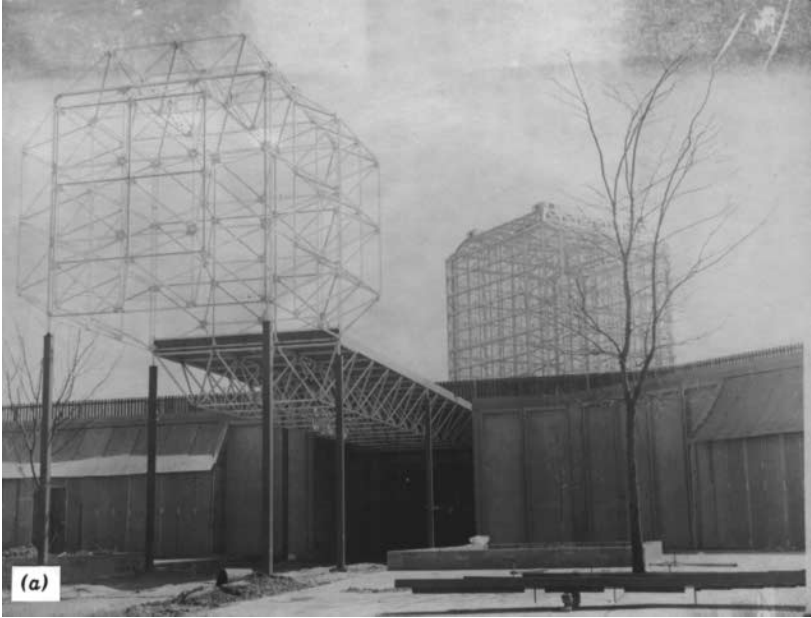
Figure 1.6 Cold-formed steel sections used in space frames (*Unistrut Corporation.*)
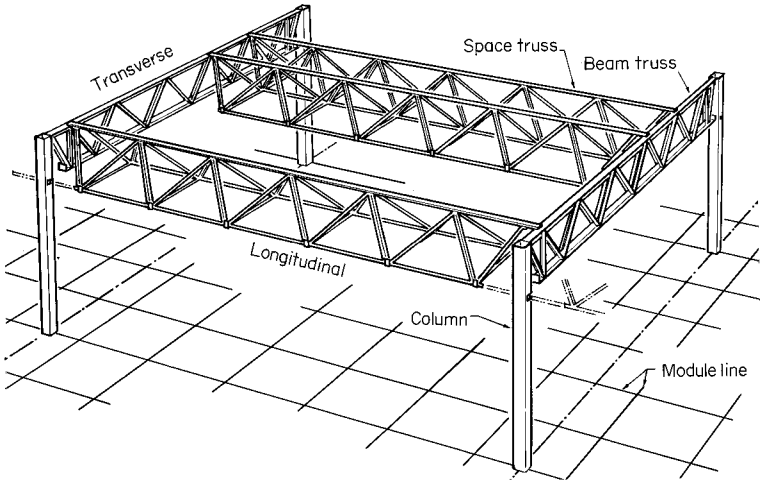
Figure 1.7 Cold-formed steel members used in space grid system. (*Butler Manufacturing Company.*)

1.3 STANDARDIZED METAL BUILDINGS AND INDUSTRIALIZED HOUSING

Standardized single-story metal buildings have been widely used in industrial, commercial, and agricultural applications. Metal building systems have also been used for community facilities such as recreation buildings, schools, and churches[1.104,1.105] because standardized metal building provides the following major advantages:

Figure 1.8 Cold-formed steel members used in a 100 × 220 × 30-ft (30.5 × 67.1 × 9.2-m) triodetic arch. (*Butler Manufacturing Company.*)
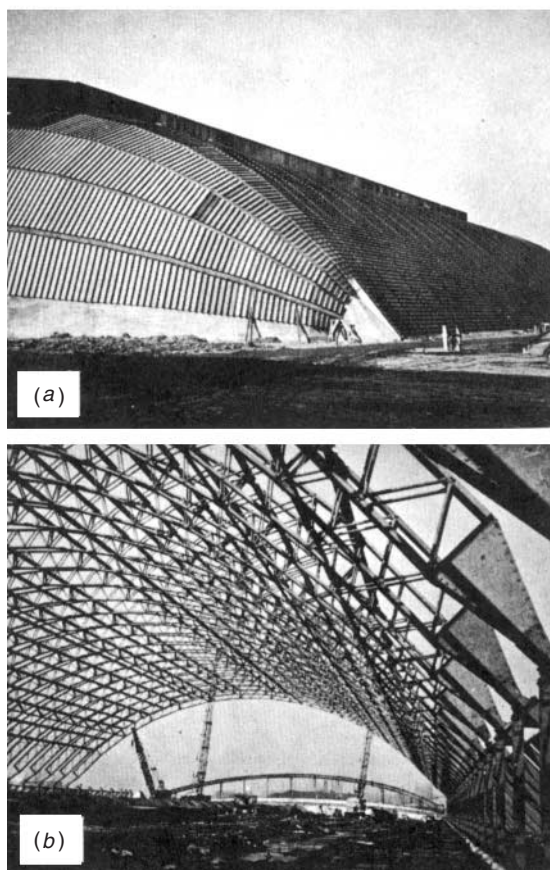
Figure 1.9 Hangar-type arch structures using cold-formed steel sections. (*Armco Steel Corporation.*)[1.6]

1. Attractive appearance
2. Fast construction
3. Low maintenance
4. Easy extension
5. Lower long-term cost

In general, small buildings can be made entirely of cold-formed sections (Fig. 1.20), and relatively large buildings are often made of welded steel plate rigid frames with cold-formed sections used for girts, purlins, roofs, and walls (Fig. 1.21).

The design of pre-engineered standardized metal buildings is often based on the Low Rise Building Systems Manual issued by the Metal Building

Figure 1.10   Rack Structures. (*Unarco Materials Storage.*)
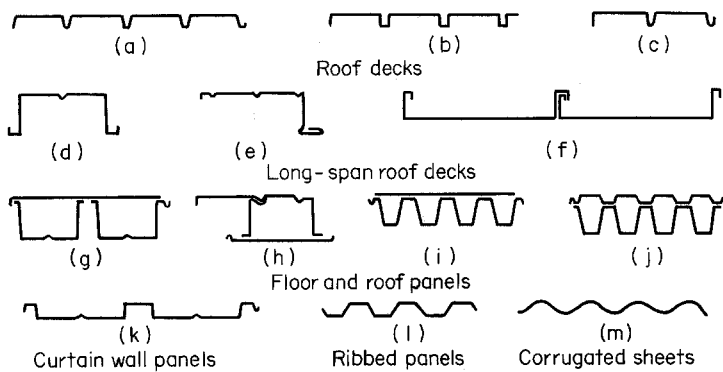
Figure 1.11   Decks, panels and corrugated sheets.
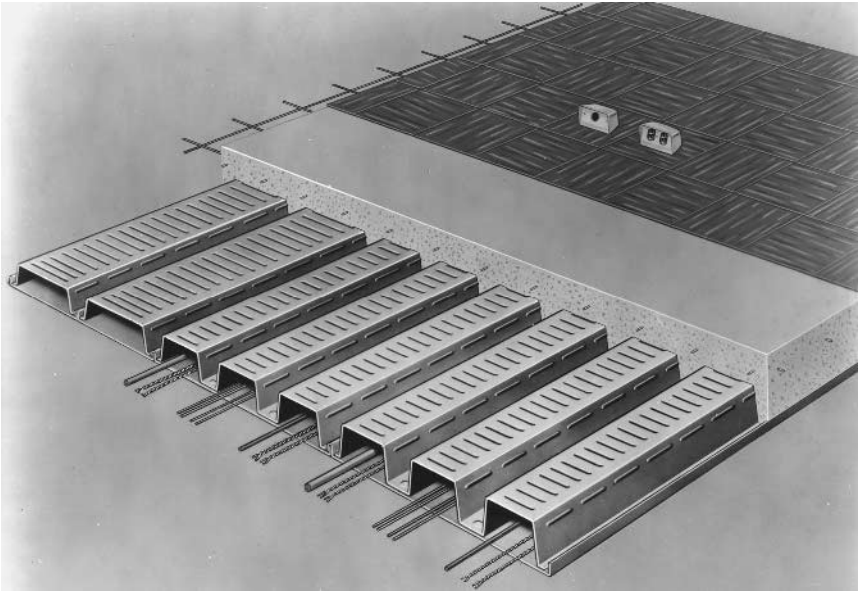
Figure 1.12 Cellular floor panels. (*H. H. Robertson Company.*)

Manufacturers Association.[1.106] This document contains design practices, commentary, design examples, common industry practices, guide specifications, bibliography, glossary, and appendix. The design of single-story rigid
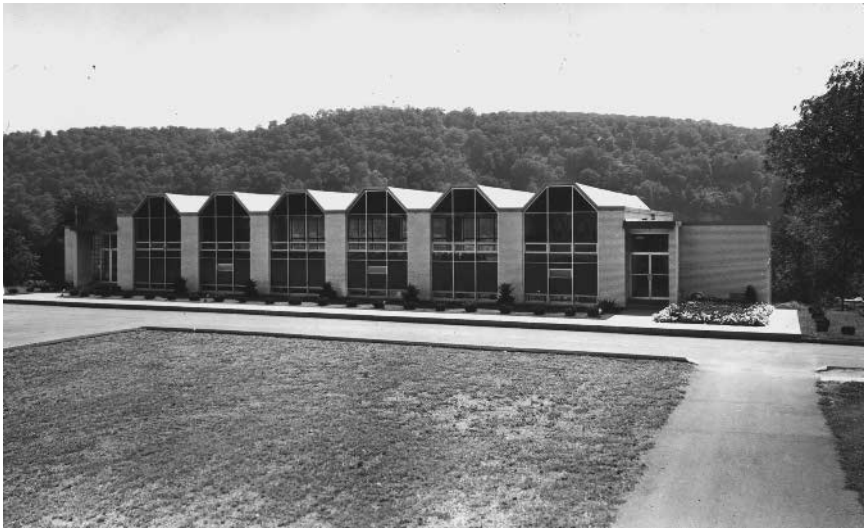
Figure 1.13 Cold-formed steel panels used in folded-plate roof. (*H. H. Robertson Company.*)
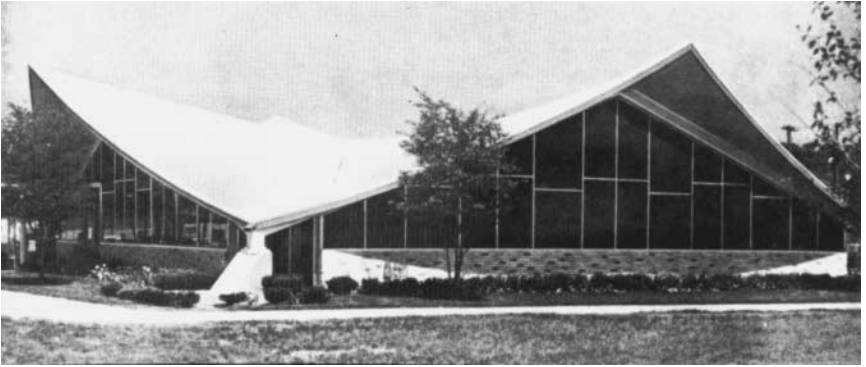
Figure 1.14 Hyperbolic paraboloid roof of welded laminated steel deck. (*Reprinted from Architectural Record, March 1962, copyrighted by McGraw-Hill Book Co., Inc.*)[1.79]

frames is treated extensively by Lee et al.[1.107] In Canada the design, fabrication, and erection of steel building systems are based on a standard of Canadian Sheet Steel Building Institute.[1.108]

Industrialized housing can be subdivided conveniently into (1) panelized systems and (2) modular systems.[1.109,1.278] In panelized systems, flat wall, floor, and roof sections are prefabricated in a production system, transported

Figure 1.15 Superbay hangar for American Airlines Boeing 747s in Los Angeles. (*Lev Zetlin Associates, Inc.*)[1.82]
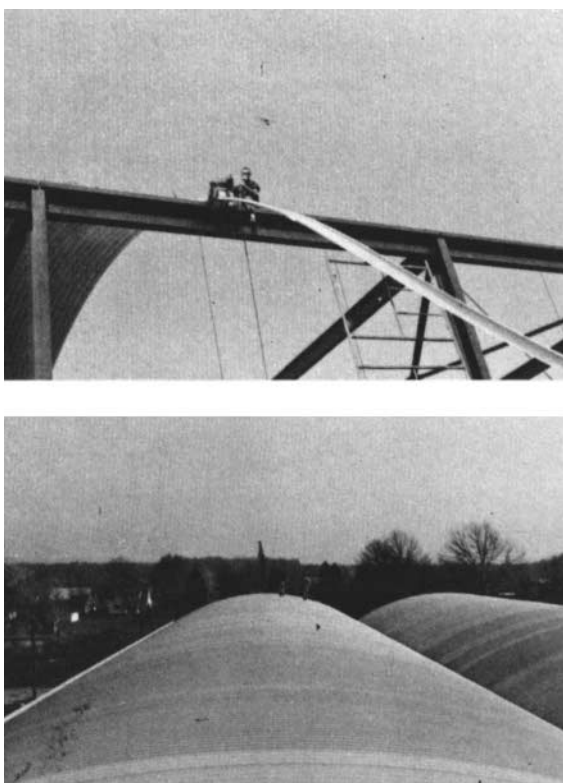
Figure 1.16 Arched roof curved at job site. (*Donn Products Company.*)

to the site, and assembled in place. In modular systems, three-dimensional housing-unit segments are factory-built, transported to the site, lifted into place, and fastened together.

In the 1960s, under the School Construction Systems Development Project of California, four modular systems of school construction were developed by Inland Steel Products Company (modular system as shown in Fig. 1.17), Macomber Incorporated (V-Lok modular component system as shown in Fig. 1.22), and Rheem/Dudley Buildings (flexible space system).[1.110] These systems have been proven to be efficient structures at reduced cost. They are successful not only for schools but also for industrial and commercial buildings throughout the United States.

In 1970 Republic Steel Corporation was selected by the Department of Housing and Urban Development under the Operation Breakthrough Program to develop a modular system for housing.[1.111] Panels consisting of steel facings with an insulated core were used in this system.

Building innovation also includes the construction of unitized boxes. These boxes are planned to be prefabricated of room size, fully furnished, and stacked in some manner to be a hotel, hospital, apartment, or office build-

Figure 1.17   Steel deck is designed as top chord of prefabricated open web steel joists. (*Inland-Ryerson Construction Products Company.*)

ing.[1.25,1.112] For multistory buildings these boxes can be supported by a main framing made of heavy steel shapes.

In the past, cold-formed steel structural components have been used increasingly in low-rise buildings and residential steel framing. Considerable research and development activities have been conducted continuously by numerous organizations and steel companies.[1.21,1.25,1.27,1.28,1.113–116,1.280–1.301] In addition to the study of the load-carrying capacity of various structural components, recent research work has concentrated on (1) joining methods, (2) thermal and acoustical performance of wall panels and floor and roof systems, (3) vibrational response of steel decks and floor joists, (4) foundation wall panels, (5) trusses, and (6) energy considerations.

In Europe and other countries many design concepts and building systems have been developed. For details, see Refs. 1.25, 1.40–1.43, 1.117, 118, 1.268, 1.270, 1.271, 1.273, 1.275, 1.290, 1.293, and 1.297.

1.4   METHODS OF FORMING

Three methods are generally used in the manufacture of cold-formed sections such as illustrated in Fig. 1.1:

1. Cold roll forming
2. Press brake operation
3. Bending brake operation
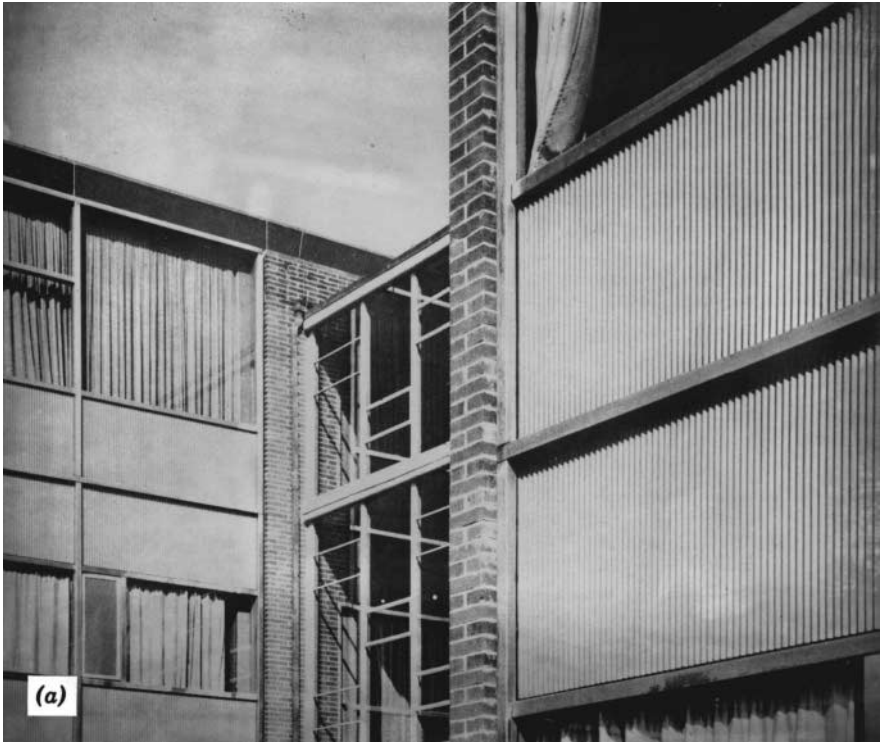
Figure 1.18 (*a*) Exterior curtain wall panels employing corrugated steel sheets.[1.87] (*b*) Frameless stressed-skin construction (*Behlen Manufacturing Company*.)

Figure 1.19 Application of standing seam roof systems. (*Butler Manufacturing Company.*)

1.4.1 Cold Roll Forming[1.1,1.119]

The method of cold roll forming has been widely used for the production of building components such as individual structural members, as shown in Fig. 1.2, and some roof, floor, and wall panels and corrugated sheets, as shown in Fig. 1.11. It is also employed in the fabrication of partitions, frames of windows and doors, gutters, downspouts, pipes, agricultural equipment, trucks, trailers, containers, railway passenger and freight cars, household appliances,
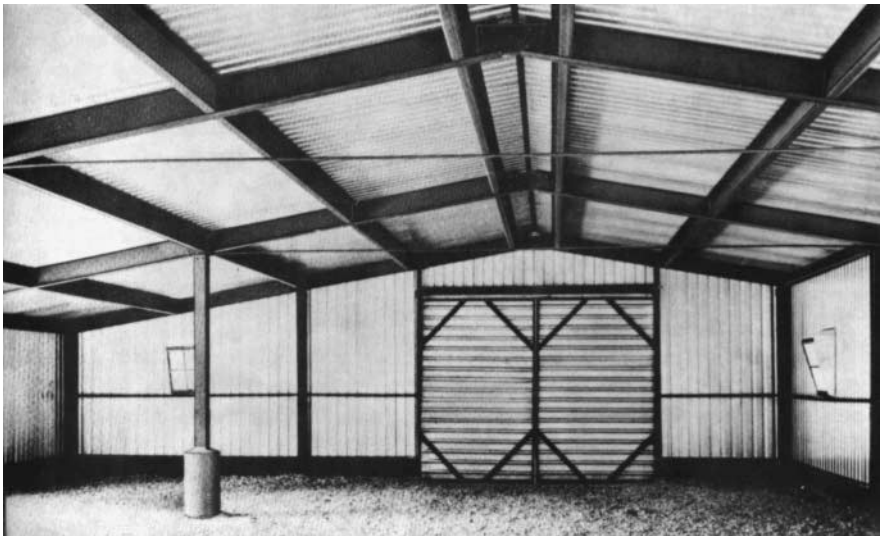
Figure 1.20 Small building made entirely of cold-formed sections. (*Stran-Steel Corporation.*)[1.6]

Figure 1.21   Standardized building made of fabricated rigid frame with cold-formed sections for girts, purlins, roofs, and walls. (*Armco Steel Corporation.*)

and other products. Sections made from strips up to 36 in. (915 mm) wide and from coils more than 3000 ft (915 m) long can be produced most economically by cold roll forming.

The machine used in cold roll forming consists of pairs of rolls (Fig. 1.23) which progressively form strips into the final required shape. A simple section may be produced by as few as six pairs of rolls. However, a complex section may require as many as 15 sets of rolls. Roll setup time may be several days.

The speed of the rolling process ranges from 20 to 300 ft/min (6 to 92 m/min). The usual speed is in the range of 75 to 150 ft/min (23 to 46 m/min). At the finish end, the completed section is usually cut to required lengths by an automatic cutoff tool without stopping the machine. Maximum cut lengths are usually between 20 and 40 ft (6 and 12 m).

As far as the limitations for thickness of material are concerned, carbon steel plate as thick as $\frac{3}{4}$ in. (19 mm) can be roll-formed successfully, and stainless steels have been roll-formed in thicknesses of 0.006 to 0.30 in. (0.2 to 7.6 mm). The size ranges of structural shapes that can be roll-formed on standard mill-type cold roll forming machines are shown in Fig. 1.24.

The tolerances in roll forming are usually affected by the section size, the product type, and the material thickness. The following limits are given by
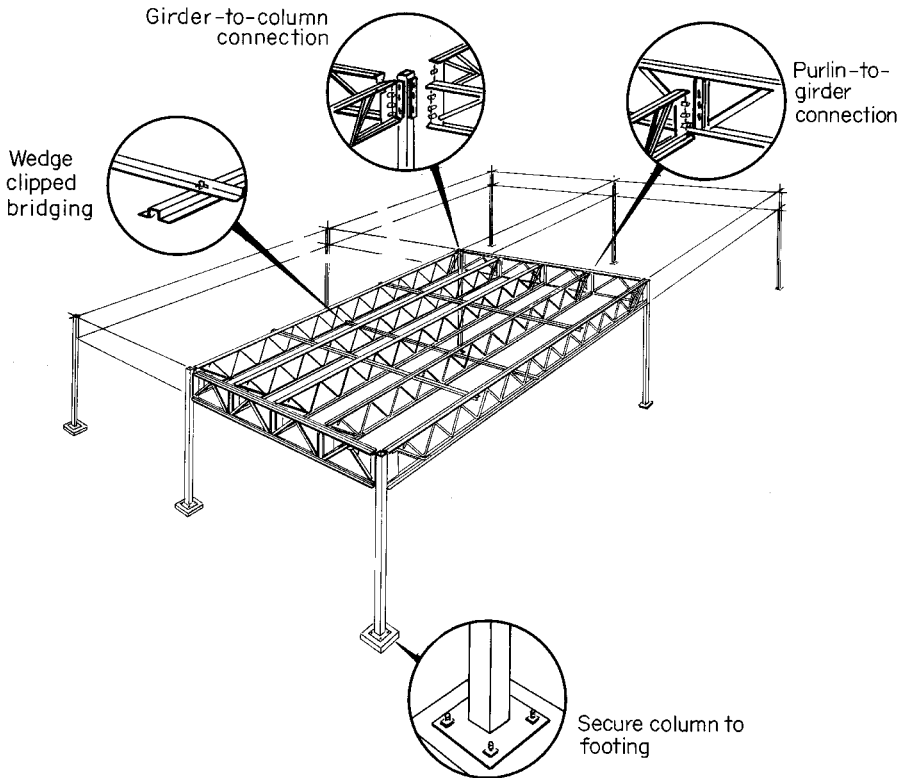
Figure 1.22   V-Lok modular component system. (*Macomber Incorporated.*)

Kirkland[1.1] as representative of commercial practice, but they are not necessarily universal:

Piece length, using automatic cutoff	$\pm\frac{1}{64}$ to $\frac{1}{8}$ in. (0.4 to 3.2 mm)
Straightness and twist	$\frac{1}{64}$ to $\frac{1}{4}$ in. (0.4 to 6.4 mm) in 10 ft (3 m)
Cross-section dimensions	
Fractional	$\pm\frac{1}{64}$ to $\frac{1}{16}$ in. (0.4 to 1.6 mm)
Decimal	± 0.005 to 0.015 in. (0.1 to 0.4 mm)
Angles	$\pm 1°$ to $2°$

Table 1.1 gives the fabrication tolerances as specified by the Metal Building Manufacturers Association (MBMA) for cold-formed steel channels and Z-sections to be used in metal building systems.[1.106] All symbols used in the table are defined in Fig. 1.25. The same tolerances are specified in the Stan-
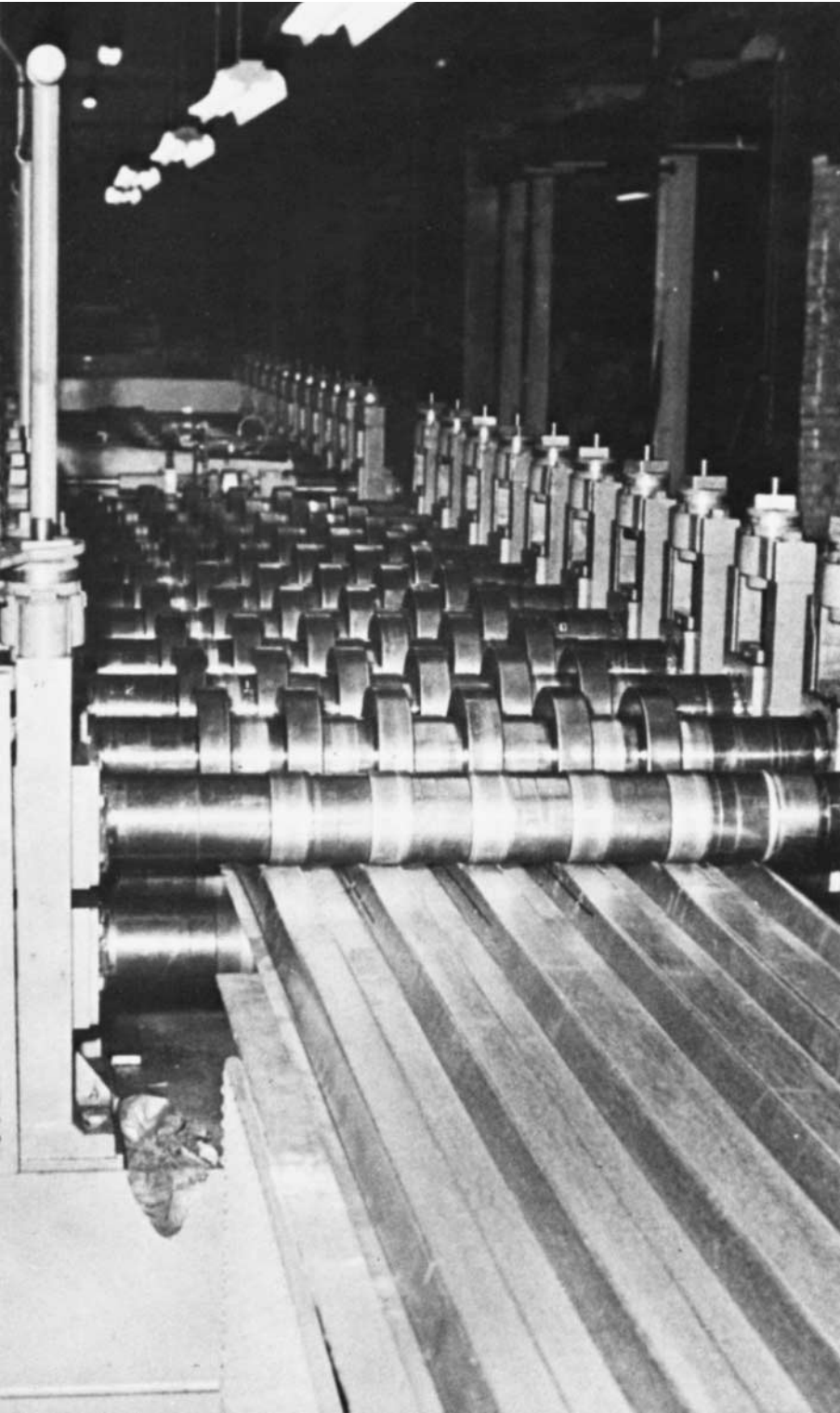
Figure 1.23   Cold roll forming machine.
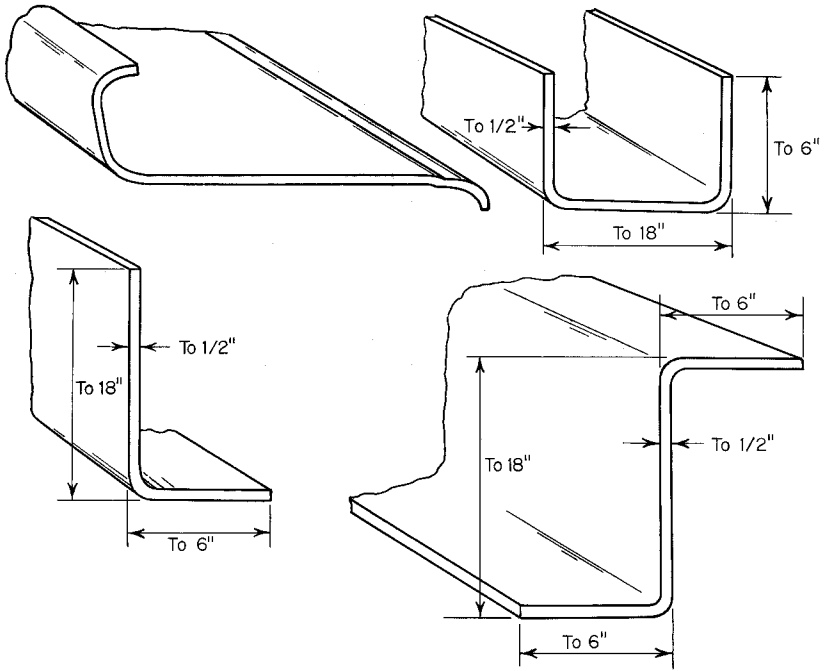
Figure 1.24   Size ranges of typical roll-formed structural shapes.[1.1]

dard of the Canadian Sheet Steel Building Institute.[1.108] For additional information on roll forming see Ref. 1.119.

1.4.2   Press Brake

The press brake operation may be used under the following conditions:

1. The section is of simple configuration.
2. The required quantity is less than about 300 linear ft/min (91.5 m/min).
3. The section to be produced is relatively wide [usually more than 18 in. (457 mm)] such as roof sheets and decking units.

The equipment used in the press brake operation consists essentially of a moving top beam and a stationary bottom bed on which the dies applicable to the particular required product are mounted, as shown in Fig. 1.26.

Simple sections such as angles, channels, and Z-sections are formed by press brake operation from sheet, strip, plate, or bar in not more than two operations. More complicated sections may take several operations.

It should be noted that the cost of products is often dependent upon the type of the manufacturing process used in production. Reference 1.120 indi-

TABLE 1.1   MBMA Table on Fabrication Tolerances

Dimension	Tolerances, in.	
	+	−
Geometry		
D	$\frac{3}{16}$	$\frac{3}{16}$
B	$\frac{3}{16}$	$\frac{3}{16}$
d	$\frac{3}{8}$	$\frac{1}{8}$
θ_1	$3°$	$3°$
θ_2	$5°$	$5°$
Hole location		
E_1	$\frac{1}{8}$	$\frac{1}{8}$
E_2	$\frac{1}{8}$	$\frac{1}{8}$
E_3	$\frac{1}{8}$	$\frac{1}{8}$
S_1	$\frac{1}{16}$	$\frac{1}{16}$
S_2	$\frac{1}{16}$	$\frac{1}{16}$
F	$\frac{1}{8}$	$\frac{1}{8}$
P	$\frac{1}{8}$	$\frac{1}{8}$
L	$\frac{1}{8}$	$\frac{1}{8}$
Chamber C	$\frac{1}{4}\left(\dfrac{\text{L ft}}{10}\right)$, in.	
Minimum thickness t	$0.95 \times$ design t	

Note: 1 in. = 25.4 mm.

cates that in addition to the strength and dimensional requirements, a designer should also consider other influencing factors, such as formability, cost and availability of material, capacity and cost of manufacturing equipment, flexibility in tooling, material handling, transportation, assembly, and erection.

1.5   RESEARCH AND DESIGN SPECIFICATIONS

1.5.1   The United States

During the 1930s the acceptance and the development of cold-formed steel construction in the United States faced difficulties due to the lack of an appropriate design specification. Various building codes made no provision for cold-formed steel construction at that time.

It became evident that the development of a new design specification for cold-formed steel construction was highly desirable not only because the performance of thin cold-formed structural members under load differs in several
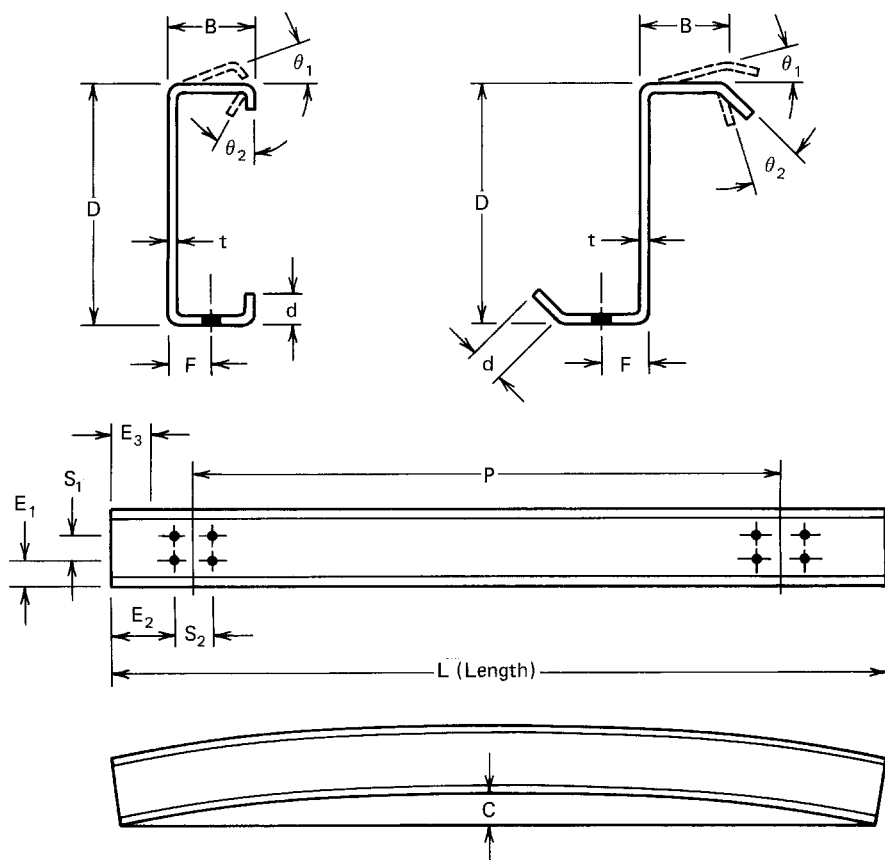
Figure 1.25   Symbols used in MBMA table.[1.106]

significant respects from that of heavy hot-rolled steel sections, but also the forms, shapes, connections, and fabrication practices which have been developed in cold-formed steel construction differ in many ways from those of heavy steel structures. As a result, design specifications for heavy hot-rolled steel construction cannot possibly cover the design features of cold-formed steel construction completely.

Realizing the need of a special design specification and the absence of factual background and research information, the AISI Committee on Building Research and Technology (then named Committee on Building Codes) sponsored a research project at Cornell University in 1939 for the purpose of studying the performance of light-gage cold-formed steel structural members and of obtaining factual information for the formulation of a design specification. Research projects have been carried out continuously at Cornell University and other universities since 1939.
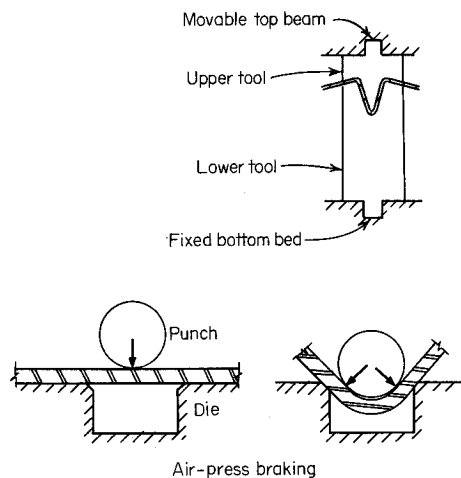
Figure 1.26   Press braking.[1.2.2.16]

The investigations on structural behavior of cold-formed steel structures conducted at Cornell University by Professor George Winter and his collaborators resulted in the development of methods of design concerning the effective width for stiffened compression elements, the reduced working stresses for unstiffened compression elements, web crippling of thin-walled cold-formed sections, lateral buckling of beams, structural behavior of wall studs, buckling of trusses and frames, unsymmetrical bending of beams, welded and bolted connections, flexural buckling of thin-walled steel columns, torsional–flexural buckling of concentrically and eccentrically loaded columns in the elastic and inelastic ranges, effects of cold forming on material properties, performance of stainless steel structural members, shear strength of light-gage steel diaphragms, performance of beams and columns continuously braced with diaphragms, hyperbolic paraboloid and folded plate roof structures, influence of ductility, bracing requirements for channels and Z-sections loaded in the plane of the web, mechanical fasteners for cold-formed steel, interaction of local and overall buckling, ultimate strength of diaphragm-braced channels and Z-sections, inelastic reserve capacity of beams, strength of perforated compression elements, edge and intermediate stiffeners, rack structures, probability analysis, and C- and Z-purlins under wind uplift.[1.5–1.7,1.31,1.121,1.122,1.133–1.136]

Recent Cornell research under the direction of Professor Teoman Pekoz included effect of residual stress on column strength, maximum strength of columns, distortional buckling of beams, perforated wall studs, storage racks, load eccentricity effects on lipped-channel columns, bending strength of standing seam roof panels, behavior of longitudinally stiffened compression elements, probabilistic examination of element strength, direct strength prediction of members using numerical elastic buckling solutions, laterally

braced beams with edge stiffened flanges, and steel members with multiple longitudinal intermediate stiffeners.[1.220,1.273,1.302–1.308]

In addition to the Cornell work, numerous research projects on cold-formed steel members, connections, and structural systems have been conducted at many individual companies and many other universities in the United States.[1.121–1.143,1.267,1.302–1.305,1.309,1.311] Forty-three universities were listed in the first edition of this book published in 1985. Research findings obtained from these projects have been presented at various national and international conferences and are published in the conference proceedings and the journals of different engineering societies.[1.43,1.117,1.118,1.124–1.132,1.144–1.147,1.272–1.276,1.302–1.308] In 1990, the Center for Cold-Formed Steel Structures was established at the University of Missouri-Rolla to provide an integrated approach for handling research, teaching, technical services, and professional activity.[1.312]

Since 1975 the ASCE Committee on Cold-Formed Members has conducted surveys of current research on cold-formed structures and literature surveys.[1.133–1.136,1.139–1.141] Thirty-eight research projects were reported in Ref. 1.136. In Ref. 1.141, about 1300 publications were classified into 18 categories. These reports provide a useful reference for researchers and engineers in the field of cold-formed steel structures. In 1996, the Center for Cold-Formed Steel Structures conducted a survey of recent research. Reference 1.309 lists 48 projects carried out in seven countries.

As far as the design criteria are concerned, the first edition of the "Specification for the Design of Light Gage Steel Structural Members" prepared by the AISI Technical Subcommittee under the chairmanship of Milton Male was issued by the American Iron and Steel Institute in 1946. This allowable stress design (ASD) specification was based on the findings of the research conducted at Cornell University up to that time and the accumulated practical experience obtained in this field. It was revised by the AISI committee under the chairmanships of W. D. Moorehead, Tappan Collins, D. S. Wolford, J. B. Scalzi, K. H. Klippstein, and S. J. Errera in 1956, 1960, 1962, 1968, 1980, and 1986 to reflect the technical developments and results of continuing research.

In 1991, the first edition of the load and resistance factor design (LRFD) specification[1.313] was issued by AISI under the chairmanship of R. L. Brockenbrough and the vice chairmanship of J. M. Fisher. This specification was based on the research work discussed in Ref. 1.248. In 1996, the AISI ASD Specification[1.4] and the LRFD Specification[1.313] were combined into a single specification[1.314] under the chairmanship of R. L. Brockenbrough and the vice chairmanship of J. W. Larson. The revisions of various editions of the AISI Specification are discussed in Ref. 1.267. In Ref. 1.315, Brockenbrough summarized the major changes made in the 1996 AISI Specification. See also Ref. 1.316 for an outline of the revised and new provisions. In 1999, a Supplement to the 1996 edition of the AISI Specification was issued by the Institute.[1.333] (The AISI specification is entitled "Specification for the Design of Cold-Formed Steel Structural Members." It is distinguished from the

American Institute of Steel Construction specification for the design of hot-rolled shapes.[1.148])

The AISI Specification has gained both national and international recognition since its publication. It is accepted as the design standard for cold-formed steel structural members in the National Building Code, sponsored by the Building Officials Conference of America, the Standard Building Code, sponsored by the Southern Building Code Congress International, and the Uniform Building Code of the International Conference of Building Officials. This design standard is now used wholly or partly by most of the cities and other jurisdictions in the United States having building codes. The design of cold-formed steel structural members based on the AISI Specification is briefly included in several textbooks and engineering handbooks.[1.13,1.149–1.158,1.318–1.320]

In addition to the issuance of the design specification, AISI published the first edition of the *Light Gauge Steel Design Manual* in 1949, prepared by the Manual Subcommittee under the chairmanship of Tappan Collins. It was subsequently revised in 1956, 1961, 1962, 1968–1972, 1977, 1983, 1986, and 1996.[1.159]

The 1996 AISI Design Manual includes the following eight parts: I—Dimensions and Properties, II—Beam Design, III—Column Design, IV—Connections, V—Specification, VI—Commentary, VII—Supplementary Information, and VIII—Test Procedures. Illustrative examples are given in Parts I, II, III, IV, and VIII for calculating sectional properties and designing members and connections. Part I also includes information on the availability and properties of steels which are referenced in the Specification. It contains tables of sectional properties of channels, Z-sections, angles, and hat-sections with useful equations for computing sectional properties. The development of this new AISI Design Manual is discussed by Kaehler and Seaburg in Ref. 1.317.

It should be noted that the provisions of the AISI Specification and the data contained in the Design Manual are applicable to carbon and low-alloy steels only. They do not apply to stainless steels or to nonferrous metals whose stress–strain curves and some other characteristics of structural behavior are substantially different from those of carbon and low-alloy steels. For the design of stainless steel structural members, see Ref. 12.9 and Chap. 12.

It should also be noted that at the present time there are no standard sizes for cold-formed steel members. The sections listed in the tables of Part I of the 1996 edition of the Design Manual are not necessarily stock sections with optimum dimensions. They are included primarily as a guide for design.

In some other countries, the cold-formed steel shapes may be standardized. The standardization of shapes would be convenient for the designer, but it may be limited for particular applications and new developments.

Commentaries on several earlier editions of the AISI design specification were prepared by Professor Winter of Cornell University and published by

AISI in 1958, 1961, 1962, and 1970.[1.161] In the 1983 and 1986 editions of the Design Manual, the format used for the simplified commentary was changed in that the same section numbers are used in the Commentary as in the Specification. For the 1996 edition of the Specification, the AISI Commentary, prepared by Wei-Wen Yu, contains a brief presentation of the characteristics and the performance of cold-formed steel members, connections, and systems.[1.310] In addition, it provides a record of the reasoning behind, and the justification for, various provisions of the Specification. A cross reference is provided between various provisions and more than 100 publications.

In 1998, the American Iron and Steel Institute established a new Committee on Framing Standards to develop consensus standards for cold-formed steel framing to be used in residential construction. For details, see Chap. 14.

In addition to the AISI publications, many trade associations and professional organizations have special design requirements for using cold-formed steel members as floor decks, roof decks, and wall panels,[1.103,1.162,1.330–1.332] open web steel joists,[1.163] transmission poles,[1.45,1.48,1.164,1.321–1.323] storage racks,[1.165,1.166] shear diaphragms,[1.167–1.169] composite slabs,[1.103,1.170,1.324,1.325] metal buildings,[1.106] light framing systems,[1.171] guardrails, structural supports for highway signs, luminaries, and traffic signals,[1.88] and automotive structural components.[1.172,1.173]

In Refs. 1.62, 1.73, and 1.174, Johnson has reviewed the previous research work together with the development of design techniques for cold-formed steel structural members. In 1993, AISI published a Guide for Preliminary Design of Cold-Formed Steel C- and Z-Members (Ref. 1.266).

1.5.2   Other Countries

In other countries, research and development in cold-formed steel members, connections, and structural systems has been actively conducted at many institutions and individual companies during the past three decades. Design specifications and recommendations are now available in Australia and New Zealand,[1.69,1.175,1.326] Austria,[1.176] Canada,[1.177–1.180,1.327] the Czech Republic,[1.181] Finland,[1.182] France,[1.183,1.184] India,[1.185] Japan,[1.186] the Netherlands,[1.187] the People's Republic of China,[1.188] the Republic of South Africa,[1.189] Sweden,[1.191–1.193] Romania,[1.190] the United Kingdom,[1.49,1.72,1.194,1.195] Germany,[1.196–1.198] Russia,[1.199] and elsewhere. Some of the recommendations are based on limit states design. The AISI Design Manual has previously been translated into several other languages.[1.200–1.204]

In the past, the European Convention for Constructional Steelwork (ECCS), through its Committee TC7 (formerly 17), prepared several documents for the design and testing of cold-formed sheet steel used in buildings.[1.205–1.214] Recently, the European Committee for Standardization published Part 1.3 of the Eurocode 3 for cold-formed, thin-gage members and sheeting.[1.328] This work was initiated by the Commission of the European Communities and was

carried out in collaboration with a working group of the ECCS. The design of cold-formed steel sections is also covered in Refs. 1.66, 1.69, 1.215, 1.216, 1.217, and 1.268.

With regard to research work, many other institutions have conducted numerous extensive investigations in the past. References 1.40–1.43, 1.71, 1.117, 1.118, 1.124–1.147, 1.158, 1.218, 1.237, 1.268–1.276, and 1.302–1.309 contain a number of papers on various subjects related to thin-walled structures from different countries. Comparisons between various design rules are presented in Refs. 1.239 and 1.240.

1.6   GENERAL DESIGN CONSIDERATIONS OF COLD-FORMED STEEL CONSTRUCTION

The use of thin material and cold-forming processes results in several design problems for cold-formed steel construction different from those of heavy hot-rolled steel construction. The following is a brief discussion of some problems usually encountered in design.

1.6.1   Local Buckling and Postbuckling Strength of Thin Compression Elements

Since the individual components of cold-formed steel members are usually so thin with respect to their widths, these thin elements may buckle at stress levels less than the yield point if they are subjected to compression, shear, bending, or bearing. Local buckling of such elements is therefore one of the major design considerations.

It is well known that such elements will not necessarily fail when their buckling stress is reached and that they often will continue to carry increasing loads in excess of that at which local buckling first appears.

Figure 1.27 shows the buckling behavior and postbuckling strength of the compression flange of a hat-section beam with a compression flange having a width-to-thickness ratio of 184 tested by Winter. For this beam the theoretical buckling load is 500 lb (2.2 kN), while failure occurred at 3460 lb (15.4 kN).[1.7]

Figure 1.28 shows the buckling behavior of an I-beam having an unstiffened flange with a width-to-thickness ratio of 46.[1.7] The beam failed at a load about 3.5 times that at which the top flange stress was equal to the theoretical critical buckling value. These pictures illustrate why the postbuckling strength of compression elements is utilized in design.

Prior to 1986, different procedures were used in the AISI Specification for the design of beams and columns with different types of compression elements. The current design methods for beams, columns, and beam-columns are discussed in Chap. 4, 5, and 6, respectively.
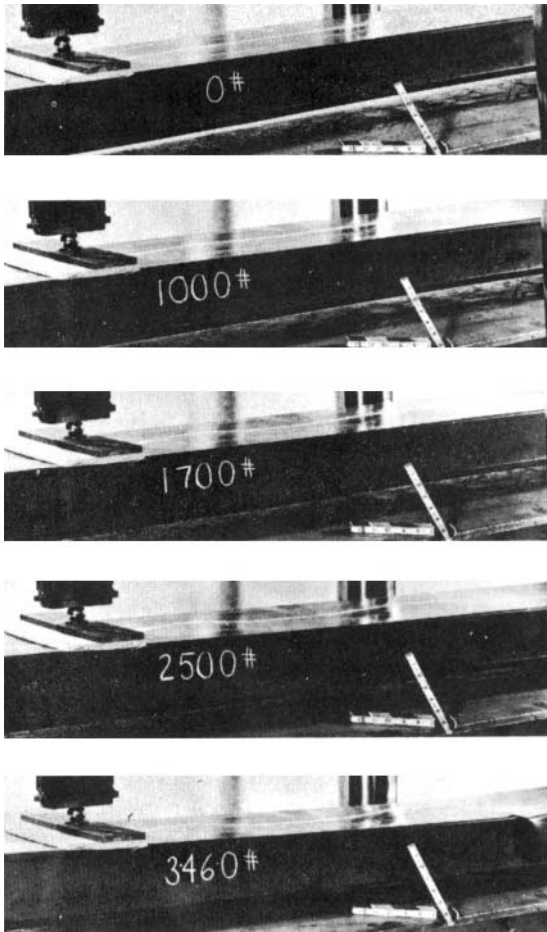
Figure 1.27   Consecutive load stages on hat-shaped beam.[1.7]

1.6.2   Torsional Rigidity

Because the torsional rigidity of open sections is proportional to t^3, cold-formed steel sections consisting of thin elements are relatively weak against torsion. Figure 1.29 shows the twist of a channel-shaped unbraced beam when it is loaded in the plane of its web. In this case, the shear center is outside the web and the applied load initiates rotation.

Because cold-formed steel sections are relatively thin and in some sections the centroid and shear center do not coincide, torsional–flexural buckling may be a critical factor for compression members. In addition, distortional buckling may govern the design for certain members used as beams or columns.
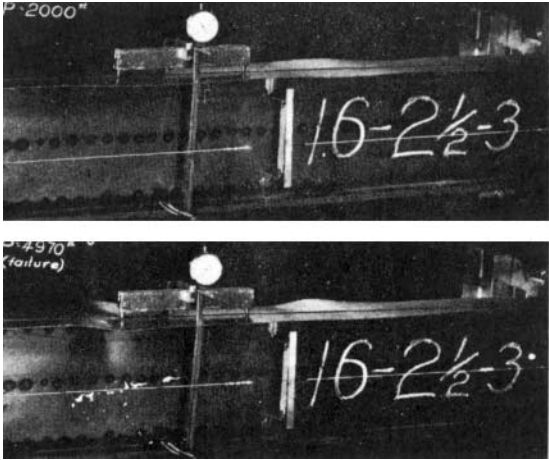
Figure 1.28   Consecutive load stages on I-beam.[1.7]

1.6.3   Stiffeners in Compression Elements

The load-carrying capacity and the buckling behavior of compression components of beams and columns can be improved considerably by the use of
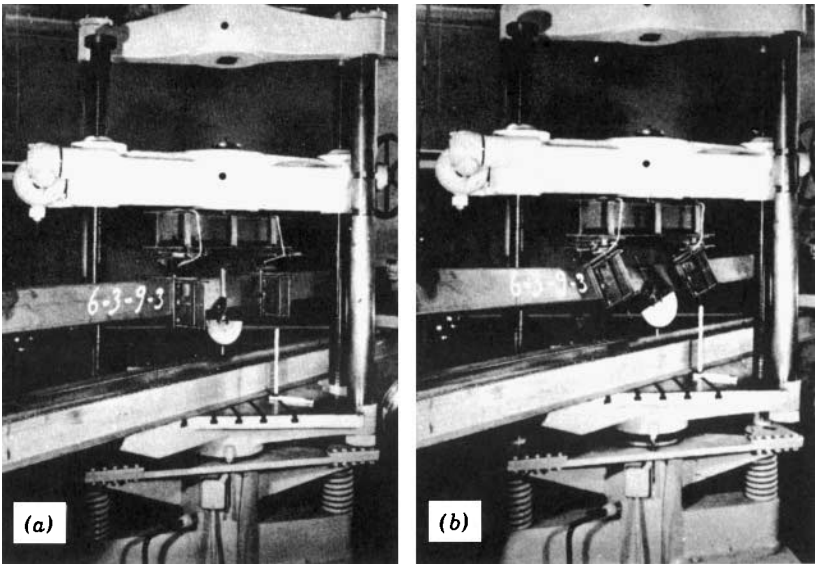
Figure 1.29   Twist of unbraced channel loaded in plane of its web.[1.6] (*a*) Before loading. (*b*) Near maximum load.

edge stiffeners or intermediate stiffeners. Provisions for the design of such stiffeners have been developed from previous research. However, this type of stiffener generally is not practical in hot-rolled shapes and built-up members.

1.6.4   Variable Properties of Sections Having Stiffened or Unstiffened Compression Elements

For a section having a stiffened, partially stiffened, or unstiffened compression element, the entire width of the element is fully effective when the width-to-thickness ratio of the element is small or when it is subjected to low compressive stress. However, as stress increases in the element having a relatively large width-to-thickness ratio, the portions adjacent to the supported edges are more structurally effective after the plate buckles. As a result, the stress distribution is nonuniform in the compression element. In the design of such members the sectional properties are based on a reduced effective area.

The effective width of a compression element not only varies with the unit stress applied but also depends on its width-to-thickness ratio. For a given beam having a compression flange with a relatively large width-to-thickness ratio, the effective section modulus S decreases with an increase in the yield point of steel used because the effective width of the compression flange becomes smaller when it is subjected to a higher unit stress. The strength of such a beam is therefore not directly proportional to the yield point of the steel. The same is true for the compression members.

1.6.5   Connections

In bolted connections the thickness of connected parts is usually much thinner in cold-formed steel construction than in heavy construction. The steel sheet or strip may have a small spread between yield point and tensile strength. These are major influences that make the behavior of the cold-formed steel bolted connection differ from that of heavy construction, particularly for bearing and tension stress. Modified design provisions have been developed in the AISI Specification for cold-formed steel bolted connections.

In welded connections, resistance welding is probably the most important means in cold-formed steel fabrication. Arc welds (groove welds, arc spot welds, arc seam welds, fillet welds, and flare groove welds) are often used for connecting cold-formed steel members to each other as well as for connecting cold-formed sections to hot-rolled shapes. Arc spot welds without prepunched holes and arc seam welds are often used for connecting panels or decks to supporting beams or to each other.

In addition to bolted and welded connections, screws are often used for cold-formed steel construction. Design provisions for determining the shear and tensile strengths of screw connections are included in the current AISI Specification.

1.6.6 End Bearing Strength of Webs

Web crippling is often a critical problem for cold-formed steel structural members for two reasons. First, the use of stamped or rolled-in end bearing stiffeners (or stiffeners under concentrated loads) is frequently not practical in cold-formed steel construction. Second, the depth-to-thickness ratio of the webs of cold-formed steel members is usually large and generally exceeds that of hot-rolled shapes. Figure 1.30 illustrates the pattern of web crippling of an I-section.

Special design criteria for web crippling of cold-formed steel sections included in the AISI Specification have been developed on the basis of extensive research.

1.6.7 Thickness Limitations

The ranges of thickness generally used in various types of cold-formed steel structural members are described in Art. 1.2 of this chapter. However, they should not be considered as thickness limitations.

In the design of cold-formed steel structural members the important factors are the width-to-thickness ratio of compression elements and the unit stress used; the thickness of the steel itself is not a critical factor. Members formed of relatively thin steel sheet will function satisfactorily if designed in accordance with the AISI Specification.

The durability of lightweight steel construction has been studied by Cissel and Quinsey.[1.241,1.242] It was found that the durability of cold-formed steel
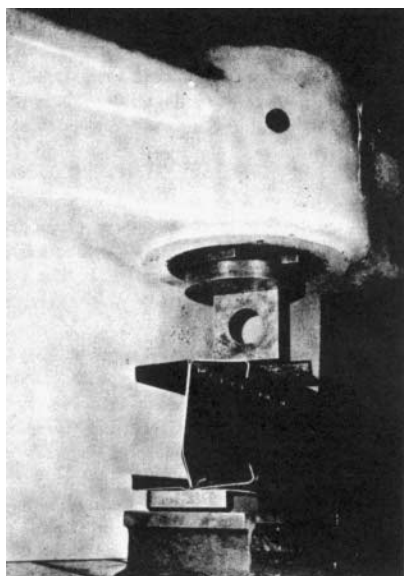
Figure 1.30   Test for end bearing strength of thin webs.[1.6]

sections is primarily dependent upon the protective treatment applied to the sheet and not necessarily upon the thickness of the sheet itself.[1.243] For galvanized cold-formed steel there is high corrosion resistance. Available data indicate that the corrosion rate of galvanized sheets in the atmosphere is practically linear; that is, for the same base metal thickness a sheet having double the weight of coating of another sheet can be expected to last twice as long before rusting of the base metal sets in.[1.244–1.246] It is therefore unnecessary to limit the minimum thickness for cold-formed steel sections merely for the purpose of protecting the steel from corrosion. The accepted methods of protection are discussed in Sec. 5 of Part III of the 1977 AISI design manual.[1.159] Recent tests of coil-coated steel panels are reported in Ref. 1.329.

1.6.8   Plastic Design

A complete plastic design method is not included in the AISI Specification because most cold-formed steel shapes have width-to-thickness ratios considerably in excess of the limits required by plastic design. Such members with large width-to-thickness ratios are usually incapable of developing plastic hinges without local buckling. However, since 1980 the AISI Specification has included design provisions to utilize the inelastic reserve capacity of flexural members. For details, see Art. 4.2.2.2.

1.6.9   Linear Method for Computing Properties of Formed Sections

If the thickness of the formed section is uniform the computation of properties of such sections can be simplified by using a linear or "midline" method. In this method the material of the section is considered to be concentrated along the centerline or midline of the steel sheet and the area elements are replaced by straight or curved "line elements." The thickness dimension t is introduced after the linear computations have been completed. Thus the total area $A = L \times t$, and the moment of inertia of the section $I = I' \times t$, where L is the total length of all line elements and I' is the moment of inertia of the centerline of the steel sheet. The properties of typical line elements are shown in Fig. 1.31. Example 1.1 illustrates the application of the linear method.

Example 1.1   Determine the full section modulus S_x of the channel section shown in Fig. 1.32a. Use the linear method.

Solution.   The midline of the cross section is shown in Fig. 1.32b.

1. *Flat Width of Flanges* (element 1)

$$L_f = 1.5 - 0.292 = 1.208 \text{ in.}$$

$$I_1 = \left(\frac{\cos^2\theta}{12}\right) l^3 = \frac{ln^2}{12}$$

$$I_2 = \left(\frac{\sin^2\theta}{12}\right) l^3 = \frac{lm^2}{12}$$

$$I_1 = \frac{l^3}{12}, \quad I_2 = 0 \qquad I_1 = 0, \quad I_2 = \frac{l^3}{12} \qquad I_{12} = \left(\frac{\sin\theta\cos\theta}{12}\right) l^3 = \frac{lmn}{12}$$

$$I_3 = la^2 + \frac{l^3}{12} = l\left(a^2 + \frac{l^2}{12}\right) \qquad I_3 = la^2 \qquad I_3 = la^2 + \frac{ln^2}{12} = l\left(a^2 + \frac{n^2}{12}\right)$$

θ (expressed in radians) $= 0.01745\,\theta$ (expressed in degrees and decimals thereof)

$$l = (\theta_2 - \theta_1) R$$

$$c_1 = \frac{\sin\theta_2 - \sin\theta_1}{\theta_2 - \theta_1} R, \qquad c_2 = \frac{\cos\theta_1 - \cos\theta_2}{\theta_2 - \theta_1} R$$

$$I_1 = \left[\frac{\theta_2 - \theta_1 + \sin\theta_2\cos\theta_2 - \sin\theta_1\cos\theta_1}{2} - \frac{(\sin\theta_2 - \sin\theta_1)^2}{\theta_2 - \theta_1}\right] R^3$$

$$I_2 = \left[\frac{\theta_2 - \theta_1 - \sin\theta_2\cos\theta_2 + \sin\theta_1\cos\theta_1}{2} - \frac{(\cos\theta_1 - \cos\theta_2)^2}{\theta_2 - \theta_1}\right] R^3$$

$$I_{12} = \left[\frac{\sin^2\theta_2 - \sin^2\theta_1}{2} + \frac{(\sin\theta_2 - \sin\theta_1)(\cos\theta_2 - \cos\theta_1)}{\theta_2 - \theta_1}\right] R^3$$

$$I_3 = \left(\frac{\theta_2 - \theta_1 + \sin\theta_2\cos\theta_2 - \sin\theta_1\cos\theta_1}{2}\right) R^3, \quad I_4 = \left(\frac{\theta_2 - \theta_1 - \sin\theta_2\cos\theta_2 + \sin\theta_1\cos\theta_1}{2}\right) R^3, \quad I_{34} = \left(\frac{\sin^2\theta_2 - \sin^2\theta_1}{2}\right) R^3$$

Case I: $\theta_1 = 0, \theta_2 = 90°$ **Case II:** $\theta_1 = 0, \theta_2 = \theta$

$$l = \theta R$$

$$c_1 = \frac{R\sin\theta}{\theta}$$

$$c_2 = \frac{R(1-\cos\theta)}{\theta}$$

$l = 1.57 R, c = 0.637 R$
$I_1 = I_2 = 0.149 R^3$
$I_{12} = -0.137 R^3$
$I_3 = I_4 = 0.785 R^3$
$I_{34} = 0.5 R^3$

$$I_1 = \left(\frac{\theta + \sin\theta\cos\theta}{2} - \frac{\sin^2\theta}{\theta}\right) R^3, I_2 = \left[\frac{\theta - \sin\theta\cos\theta}{2} - \frac{(1-\cos\theta)^2}{\theta}\right] R^3$$

$$I_{12} = \left[\frac{\sin^2\theta}{2} + \frac{\sin\theta(\cos\theta - 1)}{\theta}\right] R^3$$

$$I_3 = \left(\frac{\theta + \sin\theta\cos\theta}{2}\right) R^3, \quad I_4 = \left(\frac{\theta - \sin\theta\cos\theta}{2}\right) R^3$$

$$I_{34} = \left(\frac{\sin^2\theta}{2}\right) R^3$$

Figure 1.31   Properties of line elements.[1.159]
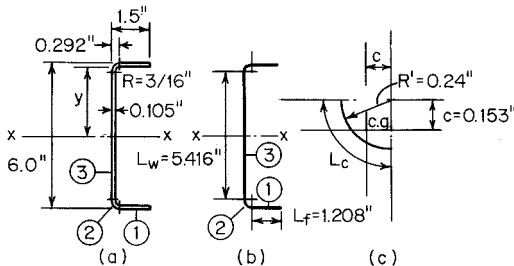
Figure 1.32   Example 1.1.

2. *Distance from x–x Axis to Centerline of Flange*

$$3.0 - \frac{0.105}{2} = 2.948 \text{ in.}$$

3. *Computation of Properties of 90° Corner* (element 2) (Fig. 1.32c)

$$R' = 0.1875 + \frac{0.105}{2} = 0.240 \text{ in.}$$

$$L_c = 1.57 (0.240) = 0.377 \text{ in.} \qquad \text{(Fig. 1.31)}$$

$$c = 0.637 (0.240) = 0.153 \text{ in.} \qquad \text{(Fig. 1.31)}$$

4. *Flat Width of Web* (element 3)

$$L_w = 6.0 - 2(0.292) = 5.416 \text{ in.}$$

5. *Distance from x–x Axis to c.g. of Corner*

$$y = \frac{5.416}{2} + 0.153 = 2.861 \text{ in.}$$

6. *Linear* I'_x, *Moment of Inertia of Midlines of Steel Sheets*

$$\text{Flanges: } 2(1.208)(2.948)^2 = 21.00$$

$$\text{Corners: } 2(0.377)(2.861)^2 = 6.17$$

$$\text{Web: } \tfrac{1}{12}(5.416)^3 = \underline{13.24}$$

$$\text{Total} \quad 40.41 \text{ in.}^3$$

7. *Actual* I_x

$$I_x = I'_x t = 40.41(0.105) = 4.24 \text{ in.}^4$$

8. *Section Modulus*

$$S_x = \frac{I_x}{d/2} = \frac{4.24}{3.0} = 1.41 \text{ in.}^3$$

The accuracy of the linear method for computing the properties of a given section depends on the thickness of the steel sheet to be used and the configuration of the section. For the thicknesses of steel sheets generally used in cold-formed steel construction the error in the moment of inertia determined by the linear method is usually negligible, particularly for relatively deep

sections made of thin material. For example, as indicated in Table 1.2, the expected errors in the computed moment of inertia of the two arbitrarily chosen channel sections as shown in Fig. 1.33 are less than 1% if the material is $\frac{1}{4}$ in. or thinner.

For cylindrical tubes, the error in the computed moment of inertia about the axis passing through the center of the tube determined by the linear method varies with the ratio of mean diameter to wall thickness D/t; the smaller the ratio, the larger error. The expected errors in the moment of inertia are approximately 2.7% and 0.2% for D/t ratios of 6 and 20, respectively, if the wall thickness is $\frac{1}{4}$ in. Errors smaller than the above values are expected for materials thinner than $\frac{1}{4}$ in.

1.6.10   Tests for Special Cases

In Art. 1.1 it was indicated that in cold-formed steel construction, unusual sectional configurations can be economically produced by cold-forming operations. However, from the point of view of structural design, the analysis and design of such unusual members may be very complex and difficult. In many cases it may be found that their safe load-carrying capacity or deflection cannot be calculated on the basis of the design criteria presently included in the AISI Specification.[1.314] For this case the AISI Specification permits their structural performance to be determined by load tests conducted by an independent testing laboratory or by a manufacturer's laboratory. It is not the intent of the AISI provision, however, to substitute load tests for design calculations.

A detailed discussion on the method of testing is beyond the scope of this book. However, when tests are found necessary to determine structural performance of cold-formed sections and assemblies, Chapter F of the AISI Specification and Part VIII of the AISI Design Manual should be used for the evaluation of test results and the determination of allowable load-carrying capacities. In some cases the test results may be evaluated by an experienced laboratory or consultant.

TABLE 1.2   Expected Error in I_x

Channel Section	Thickness of Material (in.)	Expected Error in I_x (%)
A	0.50	3.3
	0.25	0.7
	0.10	0.1
B	0.50	0.6
	0.25	0.15
	0.10	0.02

Note: 1 in. = 25.4 mm.
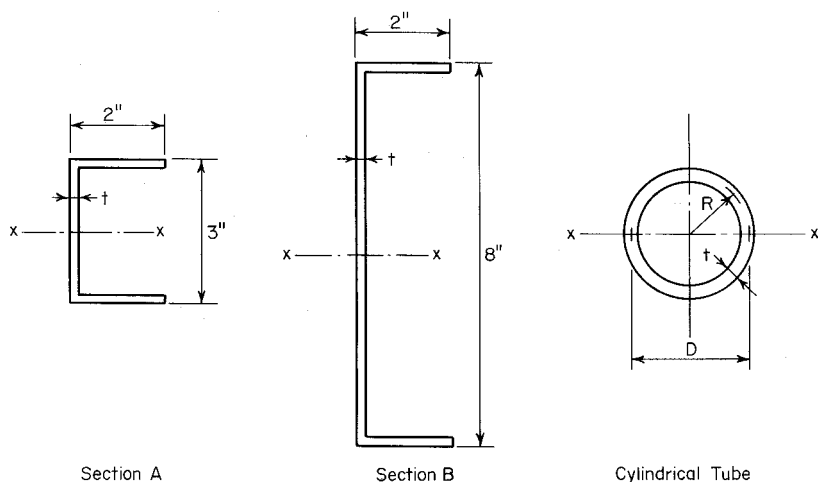
Figure 1.33   Sections used for studying the accuracy of the linear method.

1.6.11   Cold Work of Forming

It is well known that the mechanical properties of steel are affected by cold work of forming. The AISI Specification permits utilizing the increase in yield point from a cold-forming operation subjected to certain limitations. Articles 2.7 and 2.8 discuss the influence of cold work on the mechanical properties of steel and the utilization of the cold work of forming, respectively.

1.7   ECONOMIC DESIGN AND OPTIMUM PROPERTIES

The basic problem of economic design is to achieve the least expensive construction that satisfies the design requirements. One of the conditions required for the low cost of the erected structure is that the weight of the material be kept to a minimum, which is associated with the maximum structural efficiency.

It has been shown by numerous investigators that for a given loading system, the maximum efficiency can be obtained when all the possible modes of failure occur at the same time.

In practice, such ideal conditions may not be obtained easily because of unavoidable limitations, such as preselected shapes and specific dimensional limitations. However, it can be shown that in some cases there may be a possible mode of failure that will result in a maximum efficiency within the practical limitations.

The efficiency of the use of high-strength steel depends on the type of mode of failure. Under certain conditions, such as long columns having large slenderness ratios, the failure is usually limited by overall elastic buckling.

For this case the use of high-strength steel may not result in an economic design because the performance of structural members under the above-mentioned conditions will be the same for different grades of steel. For this reason the use of high-strength steel for these cases may not be justified as far as the overall cost is concerned.

In any event the general aim should always be to utilize the full potential strength of the steel that can be used in fabrication by designing the detail outline of the section for maximum structural efficiency. Flexibility of the cold-forming process to produce an endless variety of shapes is ideal for this purpose.[1.225,1.247]

2 Materials Used in Cold-Formed Steel Construction

2.1 GENERAL REMARKS

Because material properties play an important role in the performance of structural members, it is important to be familiar with the mechanical properties of the steel sheets, strip, plates, or flat bars generally used in cold-formed steel construction before designing this type of steel structural member. In addition, since mechanical properties are greatly affected by temperature, special attention must be given by the designer for extreme conditions below $-30°F$ $(-34°C)$ and above $200°F$ $(93°C)$.

Sixteen steels are specified in the 1996 edition of the AISI Specification[1.314] and the Supplement (Ref. 1.333):

ASTM A36, Carbon Structural Steel

ASTM A242, High-Strength Low-Alloy Structural Steel

ASTM A283, Low and Intermediate Tensile Strength Carbon and Steel Plates

ASTM A500, Cold-Formed Welded and Seamless Carbon Steel Structural Tubing in Round and Shapes

ASTM A529, High-Strength Carbon–Manganese Steel of Structural Quality

ASTM A570, Steel, Sheet and Strip, Carbon, Hot-Rolled, Structural Quality

ASTM A572, High-Strength Low-Alloy Columbium–Vanadium Structural Steel

ASTM A588, High-Strength Low-Alloy Structural Steel with 50 ksi (345 MPa) Minimum Yield Point to 4 in. (100 mm) Thick

ASTM A606, Steel, Sheet and Strip, High-Strength, Low-Alloy, Hot-Rolled and Cold-Rolled, with Improved Atmospheric Corrosion Resistance

ASTM A607, Steel, Sheet and Strip, High-Strength, Low-Alloy, Columbium or Vanadium, or both, Hot-Rolled and Cold-Rolled

ASTM A611 (Grades A, B, C, and D), Structural Steel (SS), Sheet, Carbon, Cold-Rolled

ASTM A653 (SS Grades 33, 37, 40, and 50 Classes 1 and 3; HSLAS Types A and B, Grades 50, 60, 70 and 80), Steel Sheet, Zinc-Coated (Galvanized) or Zinc-Iron Alloy-Coated (Galvannealed) by the Hot-Dip Process

ASTM A715 (Grades 50, 60, 70 and 80), Steel Sheet and Strip, High-Strength, Low-Alloy, Hot-Rolled, and Steel Sheet, Cold-Rolled, High-Strength, Low-Alloy with Improved Formability

ASTM A792 (Grades 33, 37, 40, and 50A), Steel Sheet, 55% Aluminum–Zinc Alloy-Coated by the Hot-Dip Process

ASTM A847, Cold-Formed Welded and Seamless High-Strength, Low-Alloy Structural Tubing with Improved Atmospheric Corrosion Resistance

ASTM A875 (SS Grades 33, 37, 40, and 50 Classes 1 and 3, HSLAS Types A and B, Grades 50, 60, 70, and 80) Steel Sheet, Zinc–5% Aluminum Alloy-Coated by the Hot-Dip Process

See Table 2.1 for the mechanical properties of these 16 steels.

In addition to the above-listed steels, other steel sheet, strip, or plates can also be used for structural purposes provided such material conforms to the chemical and mechanical requirements of one of the listed specifications or other published specification that establishes its properties and suitability[1.314] for the type of application. Information on proprietary steels can be found from their producers.

From a structural standpoint, the most important properties of steel are

1. Yield point or yield strength
2. Tensile strength
3. Stress–strain characteristics
4. Modulus of elasticity, tangent modulus, and shear modulus
5. Ductility
6. Weldability
7. Fatigue strength
8. Toughness

In addition, formability and durability are also important properties for thin-walled cold-formed steel structural members.

2.2 YIELD POINT, TENSILE STRENGTH, AND STRESS–STRAIN CURVE

The strength of cold-formed steel structural members depends on the yield point or yield strength, except in connections and in those cases where elastic local buckling or overall buckling is critical. As indicated in Table 2.1, the

yield points of steels listed in the AISI Specification range from 24 to 80 ksi (165 to 552 MPa).

There are two general types of stress–strain curves, as shown in Fig. 2.1. One is of the sharp-yielding type (Fig. 2.1a) and the other is of the gradual-yielding type (Fig. 2.1b). Steels produced by hot rolling are usually sharp yielding. For this type of steel, the yield point is defined by the level at which the stress–strain curve becomes horizontal. Steels that are cold-reduced or otherwise cold-worked show gradual yielding. For gradual-yielding steel, the stress–strain curve is rounded out at the "knee" and the yield strength is determined by either the offset method or the strain-underload method.[2.2,2.3]

In the offset method, the yield strength is the stress corresponding to the intersection of the stress–strain curve and a line parallel to the initial straight-line portion offset by a specified strain. The offset is usually specified as 0.2%, as shown in Fig. 2.2a. This method is often used for research work and for mill tests of stainless and alloy steels. In the strain-underload method, the yield strength is the stress corresponding to a specified elongation or extension under load. The specified total elongation is usually 0.5%, as shown in Fig. 2.2b. This method is often used for mill tests of sheet or strip carbon and low-alloy steels. In many cases, the yield points determined by these two methods are similar.

The ultimate tensile strength of steel sheets or strip used for cold-formed steel sections has little direct relationship to the design of such members. The load-carrying capacities of cold-formed steel flexural and compression members are usually limited by yield point or buckling stresses that are less than the yield point of steel, particularly for those compression elements having relatively large flat-width ratios and for compression members having relatively large slenderness ratios. The exceptions are bolted and welded connections, the strength of which depends not only on the yield point but also on the ultimate tensile strength of the material. For this reason, in the design of bolted and welded connections where stress concentration may occur and the consideration of ultimate strength in the design is essential, the AISI Specification includes special design provisions to ensure that adequate safety is provided for the ultimate strength of the connection. As indicated in Table 2.1, the minimum ultimate tensile strengths of the steels listed in the AISI Specification range from 42 to 100 ksi (290 to 690 MPa). The ratios of tensile strength to yield point F_u/F_y range from 1.13 to 1.88. Previous studies indicated that the effects of cold work on formed steel members depend largely upon the spread between the tensile and the yield strength of the virgin material.

2.3   MODULUS OF ELASTICITY, TANGENT MODULUS, AND SHEAR MODULUS

Modulus of Elasticity, E

The strength of members that fail by buckling depends not only on the yield point but also on the modulus of elasticity E and the tangent modulus E_t. The

TABLE 2.1 Mechanical Properties of Steels Referred to in Section A3.1 of the AISI Specification[1.314,1.333]

Steel Designation	ASTM Designation	Thickness (in.)	Minimum Yield Point or Yield Strength F_y (ksi)	Minimum Tensile Strength F_u (ksi)	F_u/F_y	Minimum Elongation (%) in 2-in. Gage Length
Carbon structural steel	A36		36	58–80	1.61	23
High-strength	A242	$\frac{3}{4}$ and under	50	70	1.40	21
low-alloy		$\frac{3}{4}$ to $1\frac{1}{2}$	46	67	1.46	21
structural steel						
Low and intermediate	A283					
tensile strength	A		24	45–60	1.88	30
carbon steel plates	B		27	50–65	1.85	28
	C		30	55–75	1.83	25
	D		33	60–80	1.82	23
Cold-formed welded	A500					
and seamless	Round tubing					
carbon steel	A		33	45	1.36	25
structural tubing	B		42	58	1.38	23
in rounds and shapes	C		46	62	1.35	21
	D		36	58	1.61	23
	Shaped tubing					
	A		39	45	1.15	25
	B		46	58	1.26	23
	C		50	62	1.24	21
	D		36	58	1.61	23
High-strength	A529 Gr. 42	$\frac{1}{2}$ in.	42	60–85	1.43	22
carbon–manganese	50	max.	50	70–100	1.40	21
steel						

Type of steel	Designation	Thickness (in.)	Min. yield (ksi)	Tensile (ksi)	Ratio	Elong. (%)
Hot-rolled carbon steel sheets and strips of structural quality	A570 Gr. 30	0.0255	30	49	1.63	21
	33	to	33	52	1.58	18
	36	0.2299	36	53	1.47	17
	40		40	55	1.38	15
	45		45	60	1.33	13
	50		50	65	1.30	11
High-strength low-alloy columbium–vanadium steels of structural quality	A572 Gr. 42		42	60	1.43	24
	50		50	65	1.30	21
	60		60	75	1.25	18
	65		65	80	1.23	17
High-strength low-alloy structural steel with 50 ksi minimum yield point	A588	4 in. and under	50	70	1.40	21
Hot-rolled and cold-rolled high-strength low-alloy steel sheet and strip with improved corrosion resistance	A606					
	Hot-rolled as rolled cut length		50	70	1.40	22
	Hot-rolled as rolled coils		45	65	1.44	22
	Hot-rolled annealed or normalized		45	65	1.44	22
	Cold-rolled		45	65	1.44	22

TABLE 2.1 (*Continued*)

Steel Designation	ASTM Designation	Thickness (in.)	Minimum Yield Point or Yield Strength F_y (ksi)	Minimum Tensile Strength F_u (ksi)	F_u/F_y	Minimum Elongation (%) in 2-in. Gage Length
Hot-rolled and cold-rolled high-strength low-alloy columbiun and/or vanadiuim steel sheet and strip	A607 Class I Gr. 45		45	60	1.33	Hot-rolled 23
						Cold-rolled 22
	50		50	65	1.30	Hot-rolled 20
						Cold-rolled 20
	55		55	70	1.27	Hot-rolled 18
						Cold-rolled 18
	60		60	75	1.25	Hot-rolled 16
						Cold-rolled 16
	65		65	80	1.23	Hot-rolled 14
						Cold-rolled 15
	70		70	85	1.21	Hot-rolled 12
						Cold-rolled 14
	Class 2 Gr. 45		45	55	1.22	Hot-rolled 23
						Cold-rolled 22
	50		50	60	1.20	Hot-rolled 20
						Cold-rolled 20
	55		55	65	1.18	Hot-rolled 18
						Cold-rolled 18
	60		60	70	1.17	Hot-rolled 16
						Cold-rolled 16
	65		65	75	1.15	Hot-rolled 14
						Cold-rolled 15
	70		70	80	1.14	Hot-rolled 12
						Cold-rolled 14

Cold-rolled carbon structural steel sheet	A611				
	A	25	42	1.68	26
	B	30	45	1.50	24
	C	33	48	1.45	22
	D	40	52	1.30	20
Zinc-coated or zinc–iron alloy-coated steel sheet	A653 SS				
	33	33	45	1.36	20
	37	37	52	1.41	18
	40	40	55	1.38	16
	50 Class 1	50	65	1.30	12
	50 Class 3	50	70	1.40	12
	HSLAS Type A				
	50	50	60	1.20	20
	60	60	70	1.17	16
	70	70	80	1.14	12
	80	80	90	1.13	10
	HSLAS Type B				
	50	50	60	1.20	22
	60	60	70	1.17	18
	70	70	80	1.14	14
	80	80	90	1.13	12
Hot-rolled and cold-rolled high-strength low-alloy steel sheets and strip with improved formability	A715				
	Gr. 50	50	60	1.20	22
	60	60	70	1.17	18
	70	70	80	1.14	16
	80	80	90	1.13	14

TABLE 2.1 (*Continued*)

Steel Designation	ASTM Designation	Thickness (in.)	Minimum Yield Point or Yield Strength F_y (ksi)	Minimum Tensile Strength F_u (ksi)	F_u/F_y	Minimum Elongation (%) in 2-in. Gage Length
55% aluminum–zinc	A792					
alloy-coated steel	Gr. 33		33	45	1.36	20
sheet by the hot-dip	37		37	52	1.41	18
process	40		40	55	1.38	16
	50A		50	65	1.30	12
Cold-formed welded	A847		50	70	1.40	19
and seamless high-						
strength, low-alloy						
structural tubing						
with improved at-						
mospheric corrosion						
resistance						
Zinc–5% aluminum	A875 SS					
alloy–coated steel	Gr. 33		33	45	1.36	20
sheet by the hot-dip	37		37	52	1.41	18
process	40		40	55	1.38	16
	50 (Class 1)		50	65	1.30	12
	50 (Class 3)		50	70	1.40	12
	HSLAS Type A					
	Gr. 50		50	60	1.20	20
	60		60	70	1.17	16
	70		70	80	1.14	12
	80		80	90	1.13	10

HSLAS Type B				
Gr. 50	50	60	1.20	22
60	60	70	1.17	18
70	70	80	1.14	14
80	80	90	1.13	12

Notes:

1. The tabulated values are based on ASTM standards.[2.1] 1 in. = 25.4 mm; 1 ksi = 6.9 MPa.

2. Section A3.3.2 allows the use of A653 SS80, A611 Grade E, A792 Grade 80, and A875 SS80 steels under special conditions. Properties of these SS80, Grade E, and Grade 80 steels are F_y = 80 ksi, F_u = 82 ksi, F_u/F_y = 1.03. Elongations are not specified.
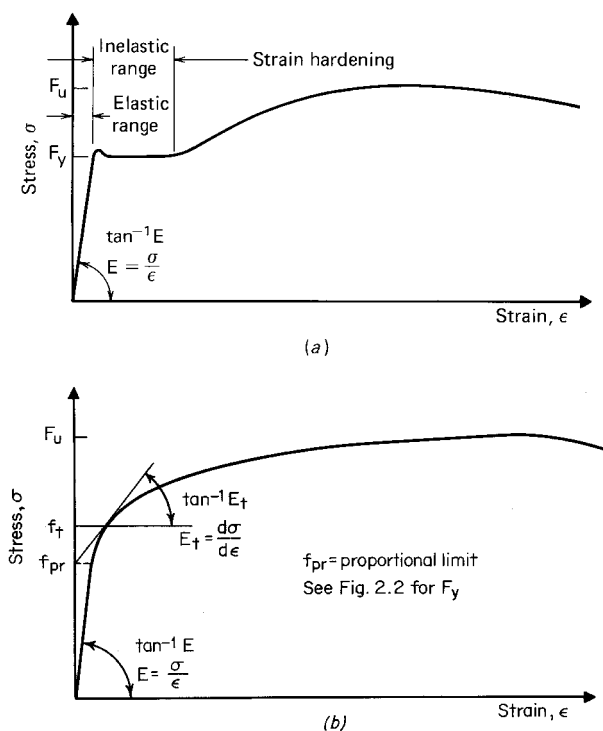
Figure 2.1   Stress–strain curves of carbon steel sheet or strip (*a*) Sharp-yielding. (*b*) Gradual-yielding.

modulus of elasticity is defined by the slope of the initial straight portion of the stress–strain curve. The measured values of E on the basis of the standard methods[2.4,2.5] usually range from 29,000 to 30,000 ksi (200 to 207 GPa). A value of 29,500 ksi (203 GPa) is recommended by AISI in its specification for design purposes.[1.314] This value is slightly higher than 29,000 ksi (200 GPa) currently used in the AISC specification.[1.148]

Tangent Modulus, E_t

The tangent modulus is defined by the slope of the stress–strain curve at any point, as shown in Fig. 2.1*b*. For sharp yielding, $E_t = E$ up to the yield point, but with gradual yielding, $E_t = E$ only up to the proportional limit. Once the stress exceeds the proportional limit, the tangent modulus E_t becomes progressively smaller than the initial modulus of elasticity. For this reason, for moderate slenderness the sharp-yielding steels have larger buckling strengths than gradual-yielding steels. Various buckling provisions of the AISI speci-
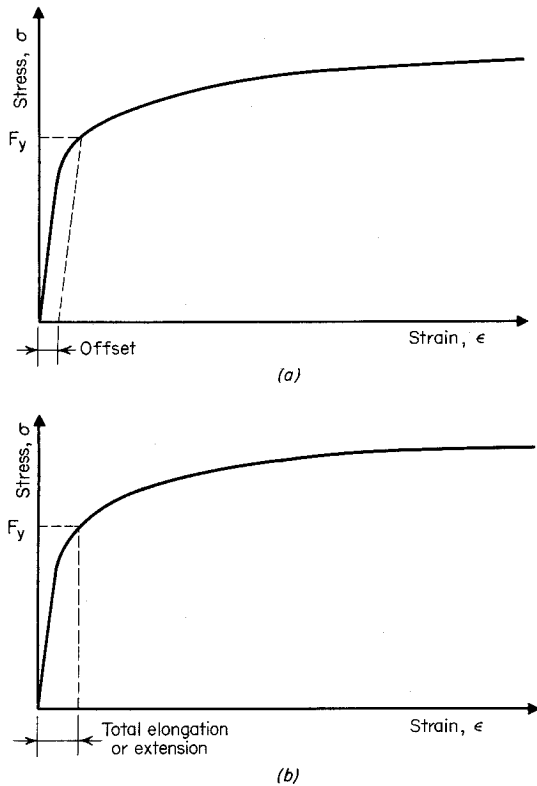
Figure 2.2   Determination of yield point for gradual-yielding steel. (*a*) Offset method (*b*) Strain-underload method.

fication have been written for gradual-yielding steels whose proportional limit is usually not lower than about 70% of the specified minimum yield point.

Shear Modulus, *G*

By definition, shear modulus, *G*, is the ratio between the shear stress and the shear strain. It is the slope of the straight line portion of the shear stress–strain curve. Based on the theory of elasticity, the shear modulus can be computed by the following equation:[2.52]

$$G = \frac{E}{2(1 + \mu)} \tag{2.1}$$

where E is the tensile modulus of elasticity and μ is the Poisson's ratio. By using $E = 29,500$ ksi (203 GPa) and $\mu = 0.3$ for steel in the elastic range,

the value of shear modulus, G, is taken as 11,300 ksi (78 GPa) in the AISI Specification. This G value is used for computing the torsional buckling stress for the design of beams, columns, and wall studs.

2.4 DUCTILITY

Ductility is defined as "an extent to which a material can sustain plastic deformation without rupture." It is not only required in the forming process but is also needed for plastic redistribution of stress in members and connections, where stress concentration would occur.

Ductility can be measured by (1) tension test, (2) bend test, or (3) notch test. The permanent elongation of a tensile test specimen is widely used as the indication of ductility. As shown in Table 2.1, for the customary range in thickness of steel sheet, strip, or plate used for cold-formed steel structural members, the minimum elongation in 2-in. (50.8-mm) gage length varies from 10 to 30%.

The ductility criteria and performance of low-ductility steels for cold-formed members and connections have been studied by Dhalla, Winter, and Errera at Cornell University.[2.6–2.9] It was found that the ductility measurement in a standard tension test includes (1) local ductility and (2) uniform ductility. Local ductility is designated as the localized elongation at the eventual fracture zone. Uniform ductility is the ability of a tension coupon to undergo sizeable plastic deformations along its entire length prior to necking. This study also revealed that for the different ductility steels investigated, the elongation in 2-in. (50.8-mm) gage length did not correlate satisfactorily with either the local or the uniform ductility of the material. In order to be able to redistribute the stresses in the plastic range to avoid premature brittle fracture and to achieve full net-section strength in a tension member with stress concentrations, it is suggested that (1) the minimum local elongation in a $\frac{1}{2}$-in. (12.7-mm) gage length of a standard tension coupon including the neck be at least 20%; (2) the minimum uniform elongation in a 3-in. (76.2-mm) gage length minus the elongation in a 1-in. (25.4-mm) gage length containing neck and fracture be at least 3%; and (3) the tensile-strength-to-yield-point ratio F_u/F_y be at least 1.05.[2.9] In this method, the local and uniform elongations are established in accordance with Part VIII of the AISI Design Manual or the following procedure:

1. Tensile coupons are prepared according to ASTM designation A370,[2.2] except that the length of the central reduced section [$\frac{1}{2}$ in. (12.7 mm) uniform width] of the coupon is at least $3\frac{1}{2}$ in. (89 mm). Gage lines are scribed at $\frac{1}{2}$ in. (12.7 mm) intervals along the entire length of the coupon.

2. Upon completion of the coupon test, the following two permanent plastic deformations are measured:

   a. Linear elongation in a 3-in. (76.2-mm) gage length e_3, in inches, including the fractured portion, preferably having occurred near the middle third of the gage length; and

   b. Linear elongation in a 1-in. (25.4-mm) gage length e_1, in inches, including the fractured portion.

3. The local elongation ϵ_l and the uniform elongation ϵ_u are computed as follows:

$$\epsilon_l = 50(5e_1 - e_3) \quad \% \tag{2.2}$$

$$\epsilon_u = 50(e_3 - e_1) \quad \% \tag{2.3}$$

For a rough differentiation of low ductility from higher ductility steels, Ref. 2.9 suggests that (1) the minimum elongation in a 2-in. (50.8-mm) gage length be at least 7% and (2) the minimum tensile-strength-to-yield-point ratio be at least 1.05.

These research findings and suggestions have received careful review and consideration during the revision of the AISI Specification in 1980. Section A3.3.1 of the 1986 edition of the AISI Specification requires that the tensile-strength-to-yield-point ratio F_u/F_y be not less than 1.08 and the elongation in a 2-in. (50.8-mm) gage length be not less than 10% for steels not listed in the specification and used for structural members and connections. These requirements are slightly higher than the corresponding values suggested in Ref. 2.9 because the AISI Specification refers to the conventional tensile tests.[2.2] These minimum requirements would ensure adequate ductility. When an 8-in. (203-mm) gage length is used, the minimum elongation is 7%. This specified elongation was derived from the conversion formula given in Sec. S30 of Ref. 2.2. The above discussed ductility requirements are retained in the 1996 edition of the AISI Specification.

During the past 20 years, a low-strain-hardening ductile (LSHD) steel that has reasonable elongation but very low F_u/F_y ratio has been developed for building purlins and girts. The results of coupon tests reported in Ref. 2.10 show that even though the F_u/F_y ratio of this type of steel is less than the specified minimum ratio of 1.08 and the elongation in a 2-in. (50.8-mm) gage length may be less than 10%, the local elongation in a $\frac{1}{2}$-in. (12.7-mm) gage length across the fracture exceeds 20% and the uniform elongation outside the fracture exceeds 3%. On the basis of limited number of tests, the same publication indicates that the AISI design provisions for flexural members with regard to effective width, lateral buckling, and nominal bending strength based on initiation of yielding are applicable to beams fabricated from LSHD steel. Consequently, the AISI Specification permits the use of such material

in the 1989 Addendum and the 1996 edition for the design of purlins and girts which support roof deck or wall panels provided that the steel can satisfy the requirements of modified Sec. A3.3.1.[1.4,1.314] When purlins and girts are subject to combined axial load and bending, the applied axial load P should not exceed 15% of the allowable axial load, P_n/Ω_c, for the ASD method because the use of such a LSHD steel for columns and beam-columns would require additional study. For the LRFD method, $P_u/\phi P_n \leq 0.15$. In the above expressions, P_n is the nominal column strength, Ω_c is the safety factor for column design, P_u is the column load based on the factored loads, and ϕ is the resistance factor.

The required ductility for cold-formed steel structural members depends mainly on the type of application and the suitability of the material. The same amount of elongation that is considered necessary for individual framing members may not be needed for such applications as roof panels and siding, which are formed with large radii and are not used in service with highly stressed connections or other stress raisers. For this reason, the performance of Structural Steel (SS) Grade 80 of A653, Grade E of A611, Grade 80 of A792, and SS Grade 80 of A875 steels used for roofing, siding, and similar applications has been found satisfactory, even though for these grades of steels the F_u/F_y ratios are less than the AISI requirements (1.03 vs. 1.08) and elongations are unspecified. The use of such steels, which do not meet the AISI ductility requirements of Sec. A3.3.1, is permitted by Sec. A3.3.2 of the Specification for multiple-web configurations provided that (1) the yield strength, F_y, used for beam design is taken as 75% of the specified minimum yield point or 60 ksi (414 MPa), whichever is less, and (2) the tensile strength, F_u, used for connection design is taken as 75% of the specified minimum tensile strength or 62 ksi (427 MPa), whichever is less.

During recent years, studies have been made to determine the ductility of Structural Steel (SS) Grade 80 of A653 steel and the performance of flexural members and connections using such a low-ductility steel.[2.53–2.61] Based on the research findings reported by Wu, Yu, LaBoube and Pan in Refs. 2.53, 2.54, and 3.124, the following exception clause was added in Sec. A3.3.2 of the Supplement to the 1996 edition of the Specification for determining the flexural strength of multiple-web decks using SS Grade 80 of A653 steel and similar low-ductility steels:[1.333]

Exception: For multiple-web configurations, a reduced yield point, $R_b F_y$, shall be permitted for determining the nominal flexural strength in Section C3.1.1 (a), for which the reduction factor, R_b, shall be determined as follows:

(a) Stiffened and Partially Stiffened Compression Flanges

For $w/t \leq 0.067\ E/F_y$

$$R_b = 1.0 \tag{2.4}$$

For $0.067\ E/F_y < w/t < 0.974\ E/F_y$

$$R_b = 1 - 0.26 \left[\frac{wF_y}{tE} - 0.067 \right]^{0.4} \tag{2.5}$$

For $0.974\ E/F_y \leq w/t \leq 500$

$$R_b = 0.75 \tag{2.6}$$

(b) Unstiffened Compression Flanges
   For $w/t \leq 0.0173\ E/F_y$

$$R_b = 1.0 \tag{2.7}$$

For $0.0173\ E/F_y < w/t \leq 60$

$$R_b = 1.079 - 0.6\sqrt{\frac{wF_y}{tE}} \tag{2.8}$$

where E = modulus of elasticity
   F_y = yield point as specified in Section A7.1 $\leq$ 80 ksi (552 MPa)
   t = thickness of section
   w = flat width of compression flange

The above Exception Clause does not apply to the use of steel deck for composite slabs, for which the steel deck acts as the tensile reinforcement of the slab.

Alternatively, the suitability of such steels for any configuration shall be demonstrated by load tests according to the provisions of Sec. F1 of the AISI Specification. Design strengths based on these tests should not exceed the strengths calculated according to Chaps. B through E of the Specification, using the specified minimum yield point, F_y, and the specified minimum tensile strength, F_u.

2.5 WELDABILITY

Weldability refers to the capacity of a steel to be welded into a satisfactory, crack-free, sound joint under fabrication conditions without difficulty. It is basically determined by the chemical composition of the steel and varies with types of steel and the welding processes used.
   The ''Structural Welding Code—Sheet Steel'' (ANSI/AWS D1.3) provides welding processes for shielded metal arc welding (SMAW), gas metal arc welding (GMAW), flux cored arc welding (FCAW), and submerged arc welding (SAW).

2.6   FATIGUE STRENGTH AND TOUGHNESS

Fatigue strength is important for cold-formed steel structural members sub-jected to vibratory, cyclical, or repeated loads. The basic fatigue property is the fatigue limit obtained from the *S–N* diagram (*S* being the maximum stress and *N* being the number of cycles to failure) which is established by tests. In general, the fatigue-to-tensile-strength ratios for steels range from 0.35 to 0.60. This is for plain specimens; the fatigue strength of actual members is often governed by details or connections. For cold-formed steel members, the influence of repeated loading on steel sections and connections has been stud-ied at the University of New Mexico, the United States Steel Research Lab-oratory,[2.11–2.13] and the University of Manitoba.[2.62]

With regard to the use of cold-formed steel members in building construc-tion, no specific provisions for fatigue strength are at present included in the AISI Specification. The AISI Committee on Specifications is currently (1999) developing the fatigue design provisions on the basis of Klippstein's research work as summarized by LaBoube and Yu in Ref. 2.72.

Toughness is the extent to which a steel absorbs energy without fracture. It is usually expressed as energy absorbed by a notched specimen in an impact test. Additionally, the toughness of a smooth specimen under static loads can be measured by the area under the stress–strain diagram. In general, there is not a direct relation between the two types of toughness.

2.7   INFLUENCE OF COLD WORK ON MECHANICAL PROPERTIES OF STEEL

The mechanical properties of cold-formed sections are sometimes substan-tially different from those of the steel sheet, strip, plate, or bar before forming. This is because the cold-forming operation increases the yield point and ten-sile strength and at the same time decreases the ductility. The percentage increase in tensile strength is much smaller than the increase in yield strength, with a consequent marked reduction in the spread between yield point and tensile strength. Since the material in the corners of a section is cold-worked to a considerably higher degree than the material in the flat elements, the mechanical properties are different in various parts of the cross section. Figure 2.3 illustrates the variations of mechanical properties from those of the parent material at the specific locations in a channel section and a joist chord after forming tested by Karren and Winter.[2.14] For this reason, buckling or yielding always begins in the flat portion due to the lower yield point of the material. Any additional load applied to the section will spread to the corners.

Results of investigations conducted by Winter, Karren, Chajes, Britvec, and Uribe[2.14–2.17] on the influence of cold work indicate that the changes of me-chanical properties due to cold work are caused mainly by strain hardening and strain aging, as illustrated in Fig. 2.4,[2.15] in which curve *A* represents the
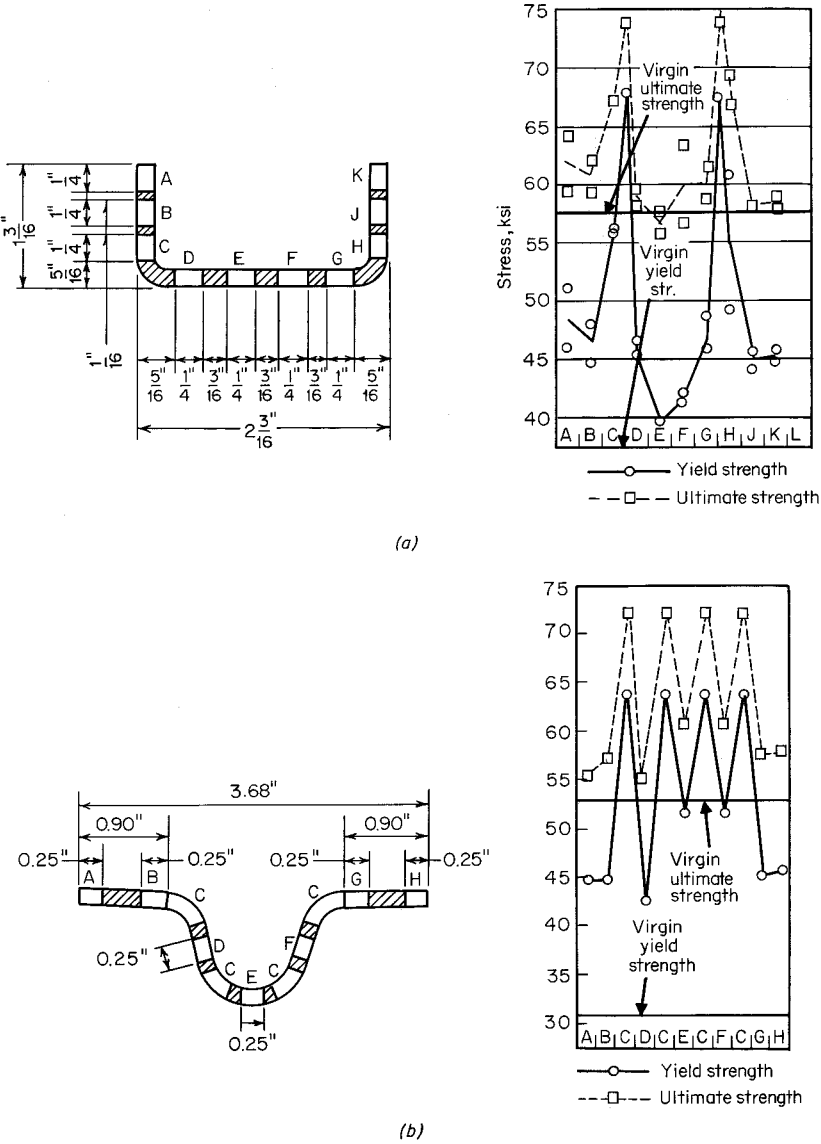
Figure 2.3 Effect of cold work on mechanical properties in cold-formed steel sections.[2.14] (*a*) Channel section. (*b*) Joist chord.

stress–strain curve of the virgin material. Curve *B* is due to unloading in the strain-hardening range, curve *C* represents immediate reloading, and curve *D* is the stress–strain curve of reloading after strain aging. It is interesting to note that the yield points of both curves *C* and *D* are higher than the yield point of the virgin material and that the ductilities decrease after strain hard-
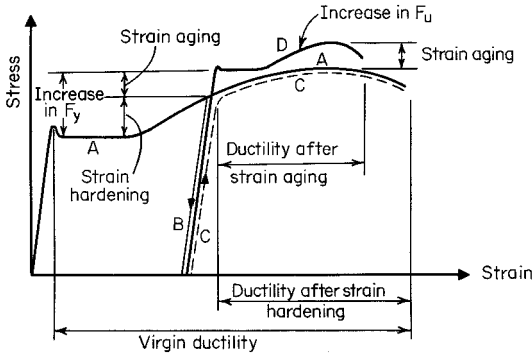
Figure 2.4   Effects of strain hardening and strain aging on stress–strain characteristics.[2.15]

ening and strain aging. In addition to strain hardening and strain aging, the changes in mechanical properties produced by cold work are also caused by the direct and inverse Bauschinger effect. The Bauschinger effect refers to the fact that the longitudinal compression yield strength of the stretched steels is smaller than the longitudinal tension yield strength, as shown in Fig. 2.5a.[2.17] The inverse Bauschinger effect produces the reverse situation in transverse direction, as shown in Fig. 2.5b.[2.17]

The effects of cold work on the mechanical properties of corners usually depend on (1) the type of steel, (2) the type of stress (compression or tension), (3) the direction of stress with respect to the direction of cold work (transverse or longitudinal), (4) the F_u/F_y ratio, (5) the inside-radius-to-thickness ratio (R/t), and (6) the amount of cold work. In general, the increase of the yield point is more pronounced for hot-rolled steel sheets than for cold-reduced sheets.

Among the above items, the F_u/F_y and R/t ratios are the most important factors to affect the change in mechanical properties of formed sections. Virgin material with a large F_u/F_y ratio possesses a large potential for strain hardening. Consequently as the F_u/F_y ratio increases, the effect of cold work
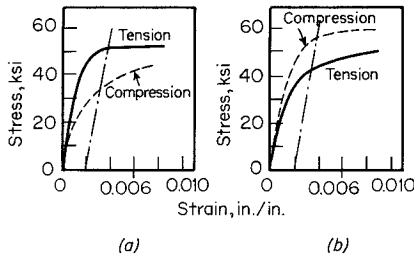

Figure 2.5   (a) Bauschinger effect. (b) Inverse Bauschinger effect.[2.17]

on the increase in the yield point of steel increases. Small inside-radius-to-thickness ratios R/t correspond to a large degree of cold work in a corner, and therefore, for a given material, the smaller the R/t ratio, the larger the increase in yield point (Fig. 2.6).

Investigating the influence of cold work, Karren derived the following equations for the ratio of corner yield strength to virgin yield strength:[2.16]

$$\frac{F_{yc}}{F_y} = \frac{B_c}{(R/t)^m} \qquad (2.9)$$

where

$$B_c = 3.69 \frac{F_u}{F_y} - 0.819 \left(\frac{F_u}{F_y}\right)^2 - 1.79 \qquad (2.10)$$

$$m = 0.192 \frac{F_u}{F_y} - 0.068 \qquad (2.11)$$

and F_{yc} = corner yield strength, ksi
  F_y = virgin yield strength, ksi
  F_u = virgin ultimate tensile strength, ksi
  R = inside bend radius, in.
  t = sheet thickness, in.

Figure 2.6 shows the relationship of F_{yc}/F_y and R/t for various ratios of F_u/F_y.
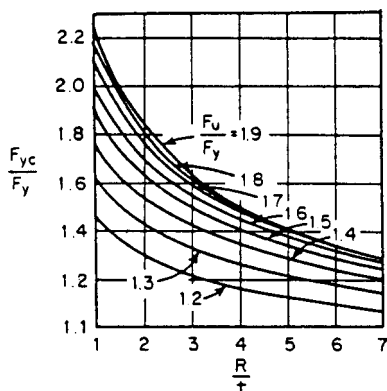

Figure 2.6 Relationship between F_{yc}/F_y and R/t ratios based on various values of F_u/F_y.[2.16]

With regard to the full-section properties, the tensile yield strength of the full section may be approximated by using a weighted average as follows:

$$F_{ya} = CF_{yc} + (1 - C)F_{yf} \qquad (2.12)$$

where F_{ya} = full-section tensile yield strength, ksi
  F_{yc} = average tensile yield strength of corners, = $B_c F_y/(R/t)^m$, ksi
  F_{yf} = average tensile yield strength of flats, ksi
  C = ratio of corner area to total cross-sectional area

Good agreement between the computed and the tested stress–strain characteristics for a channel section and a joist chord section is shown in Figs. 2.7 and 2.8.

In the last three decades, additional studies have been made by numerous investigators. These investigations dealt with the cold-formed sections having large R/t ratios and with thick materials. They also considered residual stress distribution, simplification of design methods, and other related subjects. For details, see Refs. 2.18 to 2.29 and 2.73. References 2.63 to 2.65 present recent research findings related to stainless steels.

2.8   UTILIZATION OF COLD WORK OF FORMING

The AISI Specification permits utilization of the increase in material properties that results from a cold-forming operation. The provisions of Section A7.2 of the AISI Specification are applicable only to compact sections.
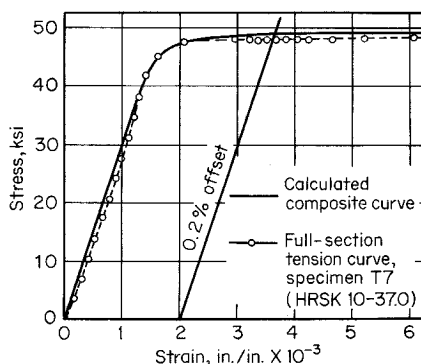

Figure 2.7   Tensile stress–strain relationship of roll-formed channel section.[2.14]
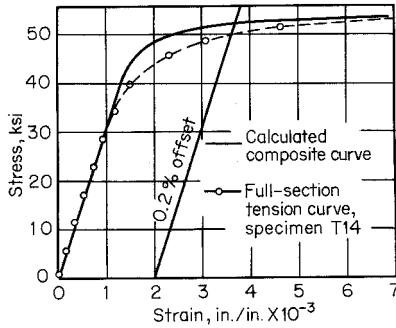
Figure 2.8 Tensile stress–strain relationship of roll-formed joist chord.[2.14]

Whenever the cold work of forming is utilized in design, the mechanical properties of axially loaded *compact** compression members and flexural members having a compact compression flange should be determined on the basis of either (1) full-section tensile tests or (2) stub column tests, or (3) should be computed by Eq. (2.12).

In the application of Eq. (2.12), F_{yf} is the weighted-average tensile yield point of the flat portions determined in accordance with Art. 2.10 or the virgin yield point, F_{yc} is the tensile yield point of corners, which may be either computed by Eq. (2.9) or obtained from Fig. 2.6 on the basis of the material used and the R/t ratio of the corner. The formula does not apply where F_u/F_y is less than 1.2, R/t exceeds 7, and/or the maximum included angle exceeds 120°. The increase in yield point of corners having R/t ratios exceeding 7 was discussed in Refs. 2.18, 2.24, and 2.73.

When the increased strength of axially loaded tension members due to cold work is used in design, the yield point should either be determined by full-section tensile tests or computed by Eq. (2.12).

The AISI Specification limits the provisions for the utilization of the cold work of forming to those sections of the specification concerning tension members (Sec. C2), bending strength of flexural members (Sec. C3.1 excluding Section C3.1.1(b)), concentrically loaded compression members (Sec. C4), combined axial load and bending (Sec. C5), cylindrical tubular members (Sec. C6), and wall studs (Sec. D4). For other provisions of the specification the design of the structural member should be based on the mechanical properties of the plain material prior to the forming operation.

---

*A compact compression member refers to a section for which the reduction factor ρ determined in accordance with Art. 3.5 equals unity. The definition of ''compact section'' in reference to the AISI Specification is not identical with the AISC Specifications[1.148] for ''compact section'' which refer to plastic design and is more stringent than the AISI requirements.[1.314]

The following examples illustrate the use of the AISI provisions on the utilization of cold work for determining the average yield point of steel.

Example 2.1   Determine the average tensile yield point of steel F_{ya} for the flange of a given channel section to be used as a beam (Fig. 2.9). Consider the increase in strength resulting from the cold work of forming. Use the AISI Specification and A653 SS40 steel ($F_y = 40$ ksi and $F_u = 55$ ksi).

Solution

1. *Check AISI Requirements.*
   A. In order to use Eq. (2.12) for computing the average tensile yield point for the beam flange, the channel must have a compact compression flange, that is $\rho = 1.0$.

      Assume that on the basis of Arts. 3.5.1, 3.5.2, and 3.5.3, the reduction factor ρ is found to be unity, then Eq. (2.12) can be used to determine F_{ya}.
   B. When Eq. (2.9) is used to determine the tensile yield point of corners F_{yc}, the following three requirements must be satisfied:

$$F_u/F_y \geq 1.2, \qquad R/t \leq 7, \qquad \theta \leq 120°$$

Since the actual values are $F_u/F_y = 55/40 = 1.375$, $R/t = 0.1875/0.135 = 1.389$, and $\theta = 90°$, which all satisfy the AISI requirements, Eq. (2.9) can be used to determine F_{yc}.
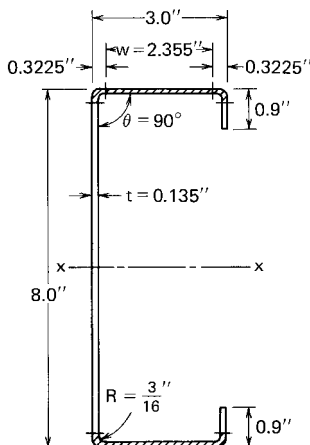

Figure 2.9   Example 2.1.

2. *Calculation of F_{yc}.* According to Eq. (2.9),

$$F_{yc} = \left[\frac{B_c}{(R/t)^m}\right]F_y$$

where

$$B_c = 3.69(F_u/F_y) - 0.819(F_u/F_y)^2 - 1.79 = 1.735$$

$$m = 0.192(F_u/F_y) - 0.068 = 0.196$$

Therefore,

$$F_{yc} = \left[\frac{1.735}{(1.389)^{0.196}}\right](40) = 1.627(40) = 65.08 \text{ ksi}$$

3. *Calculation of F_{ya}.* By using $F_{yc} = 65.08$ ksi, $F_{yf} = $ virgin yield point $= 40$ ksi, and

$$C = \frac{\text{total cross-sectional area of two corners (Table 4.1)}}{\text{full cross-sectional area of flange}}$$

$$= \frac{2 \times 0.054}{(2 \times 0.054) + (2.355 \times 0.135)} = 0.254$$

the average tensile yield point of the beam flange can be computed from Eq. (2.12) as follows:

$$F_{ya} = CF_{yc} + (1 - C)F_{yf} = 46.37 \text{ ksi}$$

The above value of F_{ya} can be used for tension and compression flanges. It represents a 16% increase in yield point as compared with the virgin yield point of steel.

Example 2.2   Determine the average yield point of steel F_{ya} for the axially loaded compression member, as shown in Fig. 2.10. Consider the increase in strength resulting from the cold work of forming. Use A570 Grade 33 steel ($F_y = 33$ ksi and $F_u = 52$ ksi).

Solution

1. *Check AISI Requirements.*
   A. Determination of reduction factor. Assume that on the basis of Arts. 3.5.1, 3.5.2, and 3.5.3, the reduction factor ρ is found to be unity, then Eq. (2.12) can be used to determine F_{ya}.
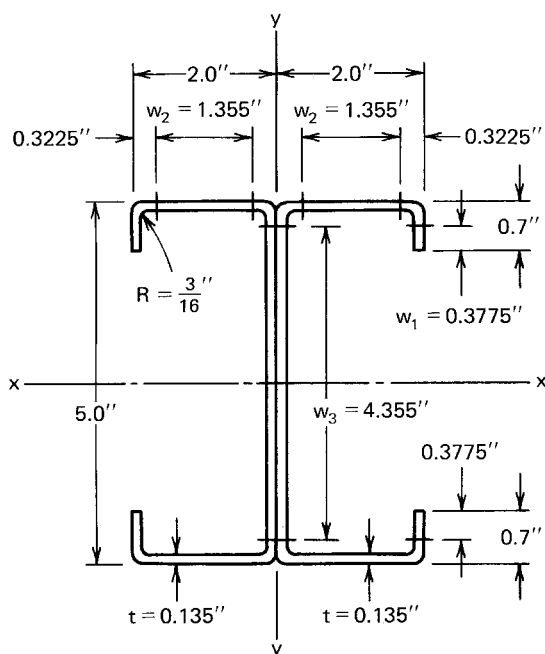
Figure 2.10   Example 2.2.

B. Review of F_u/F_y, R/t, and θ

$$F_u/F_y = 52/33 = 1.576 > 1.2 \qquad \text{(OK)}$$
$$R/t = 0.1875/0.135 = 1.389 < 7 \qquad \text{(OK)}$$
$$\theta = 90° < 120° \qquad \text{(OK)}$$

Therefore, Eq. (2.9) can be used to compute F_{yc}.

2. *Calculation of F_{yc}.* From Eq. (2.9),

$$B_c = 3.69(F_u/F_y) - 0.819(F_u/F_y)^2 - 1.79 = 1.991$$
$$m = 0.192(F_u/F_y) - 0.068 = 0.235$$

and

$$F_{yc} = \left[\frac{B_c}{(R/t)^m}\right]F_y = \left[\frac{1.991}{(1.389)^{0.235}}\right](33) = 1.843(33) = 60.82 \text{ ksi}$$

3. *Calculation of F_{ya}.* By using

$$F_{yc} = 60.82 \text{ ksi}$$

$$F_{yf} = 33 \text{ ksi}$$

$$C = \frac{\text{total corner area}}{\text{total area of full section}}$$

$$= \frac{8(0.054)}{2.54} = 0.17$$

and

$$F_{ya} = CF_{yc} + (1 - C)F_{yf} = 37.73 \text{ ksi}$$

The above computed F_{ya} represents a 14% increase in yield point when the strength increase from the cold work of forming is considered only for the corners.

In the Canadian specification[1.177] Eq. (2.13) is used to compute the average tensile yield point F_y' of the full section of tension or compression members. This simpler equation is also applicable for the full flange of flexural members.

$$F_y' = F_y + \frac{5D}{W^*} (F_u - F_y) \tag{2.13}$$

where D = number of 90° corners. If other angles are used, D is the sum of the bend angles divided by 90°.

W^* = ratio of the length of centerline of the full flange of flexural members, or of the entire section of tension or compression members, to the thickness t.

Equation (2.13) is based on a study conducted by Lind and Schroff.[2.19,2.25] By using a linear strain-hardening model and Karren's experimental data,[2.16] Lind and Schroff concluded that the increase in yield point depends only on the R/t ratio and the hardening margin ($F_u - F_y$). In order to take the cold-work strengthening into account, it is merely necessary to replace the virgin yield points by the virgin ultimate strength over a length of $5t$ in each 90° corner. Reference 2.30 indicates that the R/t ratio has little or no effect on the average tensile yield point of the full section because when R/t is small, the volume undergoing strain hardening is also small, while the increase in yield point is large. Conversely when R/t is large, the volume is

proportionately large, but the increase in yield point is small. The correlations between the test data and the AISI and Canadian Specifications are reported by Schuster and Sloof in Ref. 2.73.

Example 2.3   For the channel section used in Example 2.1, determine the average yield point of steel F'_y for the beam flange by using Eq. (2.13).

Solution. Based on the type of steel and the dimensions used in Example 2.1, the following values can be obtained:

$$F_y = 40 \text{ ksi}$$

$$F_u = 55 \text{ ksi}$$

$$D = 2$$

$$W^* = \frac{(\text{arc length of two } 90° \text{ corners}) + (\text{flat width of flange})}{t}$$

$$= \frac{2(1.57)(R + t/2) + 2.355}{0.135}$$

$$= \frac{2(1.57)(0.1875 + 0.0675) + 2.355}{0.135} = 23.38$$

By using Eq. (2.13), the average yield point of steel for the beam flange is

$$F'_y = 40 + \frac{5(2)}{23.38}(55 - 40) = 46.42 \text{ ksi}$$

This value provides a good agreement with the value of $F_{ya} = 46.37$ ksi computed in Example 2.1 on the basis of the AISI Specification.

Example 2.4   For the I-section used in Example 2.2, determine the average yield point of steel F'_y for the compression member. Use Eq. (2.13).

Solution. By using the data given in Example 2.2, the following values can be obtained:

$$F_y = 33 \text{ ksi}$$

$$F_u = 52 \text{ ksi}$$

$$D = 2(4) = 8$$

$$W^* = \frac{2 \times \text{length of the midline of each channel section}}{t}$$

$$= \frac{2[2(0.3775 + 1.355) + 4.355 + 4(1.57)(0.1875 + 0.0675)]}{0.135}$$

$$= 139.6$$

From Eq. (2.13), the average yield point of steel for the compression member is

$$F'_y = 33 + \frac{5(8)}{139.6}(52 - 33) = 38.44 \text{ ksi}$$

The above value is about 2% greater than the value of $F_{ya} = 37.73$ ksi computed in Example 2.2 on the basis of the AISI Specification.

2.9   EFFECT OF TEMPERATURE ON MECHANICAL PROPERTIES OF STEEL

The mechanical properties of steel discussed in Art. 2.2 are based on the data obtained from tests conducted at room temperature. These mechanical properties will be different if the tests are performed at elevated temperatures.

The effect of elevated temperatures on the mechanical properties of steels and the structural strength of steel numbers has been the subject of extensive investigations for many years.[2.31–2.37] In Ref. 2.34, Uddin and Culver presented the state of the art accompanied by an extensive list of references. In addition, Klippstein has reported detailed studies of the strength of cold-formed steel studs exposed to fire.[2.35,2.36] The effect of elevated temperatures on the yield point, tensile strength, and modulus of elasticity of steel plates and sheet steels is shown graphically in Fig. 2.11. For additional information on steel plates, see Ref. 2.32. It should be noted that when temperatures are below zero, the yield point, tensile strength, and modulus of elasticity of steel are generally increased. However, the ductility and toughness are reduced. Therefore, great care must be exercised in designing cold-formed steel structures for extreme low-temperature environments particularly when subjected to dynamic loads. Reference 1.229 discusses structural sandwich panels at low temperature.

The load-carrying capacities of structural members are affected by the elevated temperature not only because the mechanical properties of steel vary with temperature, but also because the thermal stresses may be induced due to the restraint of expansion and secondary stresses may be developed due to the additional deformation caused by thermal gradients.
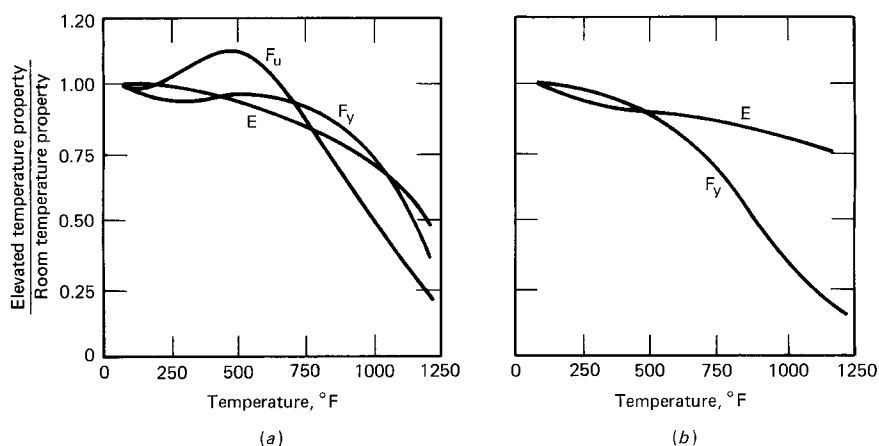
Figure 2.11   Effect of temperature on mechanical properties of low-carbon steel. (*a*) Steel plates (A36). (*b*) Steel sheets.[2.35, 2.36]

2.10   TESTING OF FULL SECTIONS AND FLAT ELEMENTS

When testing of full sections and flat elements is required to determine the yield strength, the procedures and methods used for testing and the evaluation of test results should be based on Chapter F of the AISI Specification.[1.314]

Figure 2.12 illustrates the typical full-section tension specimen and the compression tests conducted at Cornell University for the investigation of the influence of cold work.[2.14]

Because welding influences the material properties due to cold work,[2.41] the effect of any welding on mechanical properties of a member should be determined on the basis of full section specimens containing within the gage length such welding as the manufacturer intends to use. Any necessary allowance for such effect should be made in the structural use of the member.[1.314]

In addition to the tests for determining material properties, Chap. F of the AISI Specification[1.314] also includes the test requirements for special cases. These provisions can be used to obtain design values when the composition or configuration of elements, assemblies, connections, or details of cold-formed steel structural members is such that calculation of their strength cannot be made in accordance with Chaps. A through E of the AISI Specification. Six test methods for use with the 1996 edition of the AISI Specification are included in Part VIII of the Design Manual. These test methods are dealing with (a) rotational–lateral stiffness for beam-to-panel assemblies, (b) stub-column test for determining the effective area of cold-formed steel columns, (c) determination of uniform and local ductility, (d) mechanically fastened cold-formed steel connections, (e) cantilever test for cold-formed steel diaphragms, and (f) base test for purlins supporting a standing seam roof system. In 1999, new Standard Procedures for Panel and Anchor Structural Tests were
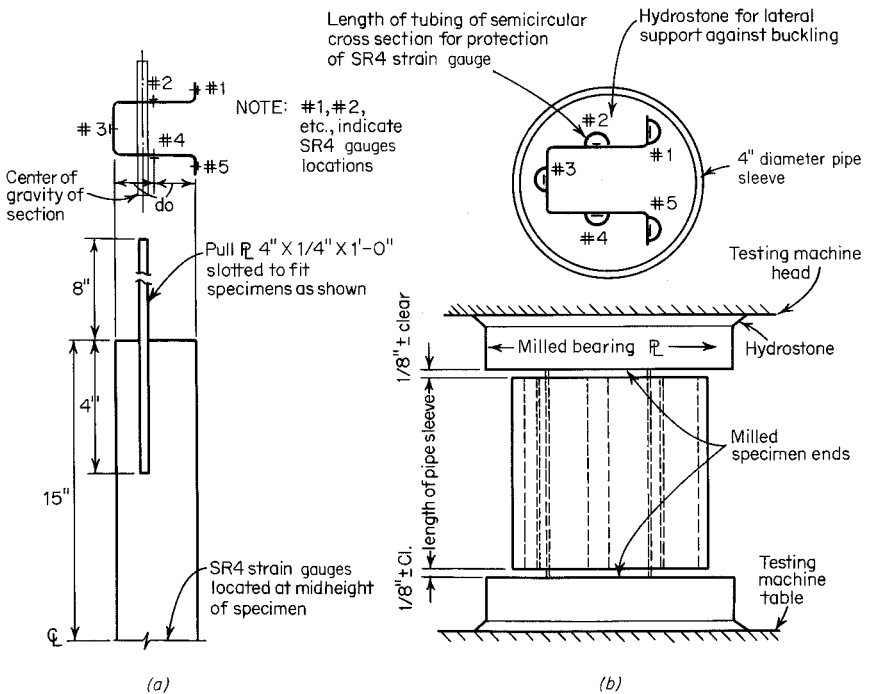
Figure 2.12 (*a*) Typical full-section tension specimen. (*b*) Full-section compression test.[2.14]

added in the Supplement to the 1996 edition of the Specification. Detailed discussion of test methods is beyond the scope of this book.

2.11 RESIDUAL STRESSES DUE TO COLD FORMING

Residual stresses are stresses that exist in the member as a result of manufacturing and fabricating processes. In the past, the distribution of residual stresses and the effect of such stresses on the load-carrying capacity of steel members have been studied extensively for hot-rolled wide-flange shapes and welded members.[2.42–2.44] For these structural shapes, the residual stresses are caused by uneven cooling after hot rolling or welding. These stresses are often assumed to be uniform across the thickness of the member.

Based on a selected residual stress pattern in W-shapes, Galambos derived a general formula for the stress–strain relationship of hot-rolled wide-flange cross sections.[2.45] He concluded that residual stresses cause yielding earlier than is expected if they are neglected, and they cause a reduction in the stiffness of the member. As shown in Fig. 2.13, even though the effect of the residual stress may not be very great as far as the ultimate stress is concerned,
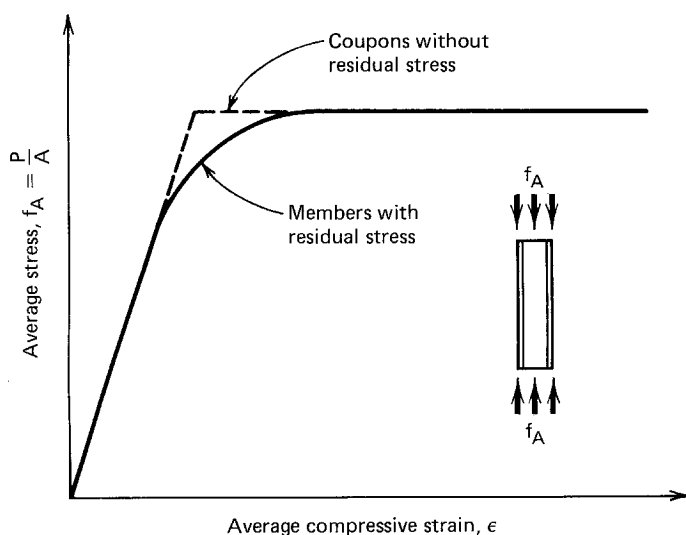
Figure 2.13   Effect of residual stress on stress–strain relationship of hot-rolled W-shapes.

the residual stress will nevertheless lower the proportional limit, and the inelastic behavior of these members cannot be predicted correctly without consideration of the residual stress.

In the past, the residual stress distribution in cold-formed steel members has been studied analytically and experimentally by a number of investigators.[2.26,2.27,2.46–2.49] Figure 2.14, adapted from Ref. 2.26, shows Ingvarsson's measured residual stresses in the outer and inner surfaces of a channel section. The average measured residual stresses for the same channel section are shown in Fig. 2.15. It is expected that the effect of such stresses on the stress–strain relationship of cold-formed members is similar to that for hot-rolled shapes, even though for the former, the residual stress results from cold rolling or cold bending.

In the design of cold-formed steel members, the AISI buckling provisions have been written for a proportional limit that is considerably lower than the yield point of virgin steel. The assumed proportional limit seems justified for the effect of residual stresses and the influence of cold work discussed in Art. 2.7.

2.12   EFFECT OF STRAIN RATE ON MECHANICAL PROPERTIES

The mechanical properties of sheet steels are affected by strain rate. References 2.50, 2.51, and 2.66–2.71 present a review of literature and discuss the
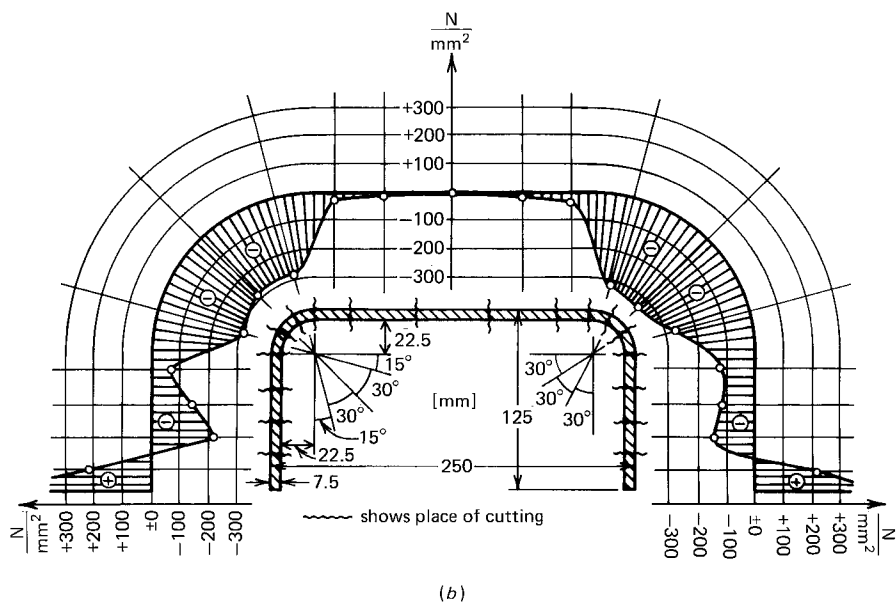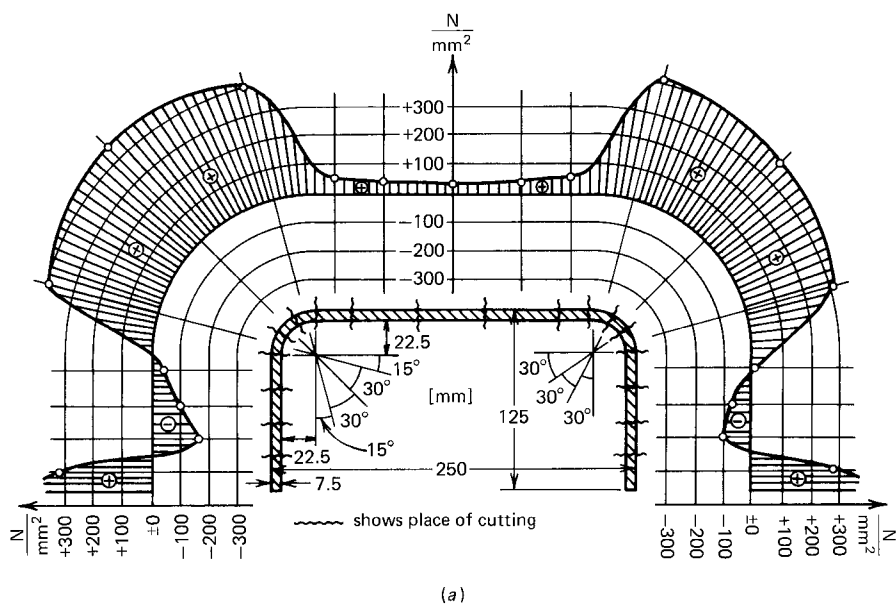
Note: 1mm = 0.039 in.; 1 N/mm² = 0.145 ksi

Figure 2.14   Measured longitudinal residual stress distribution in (*a*) outer and (*b*) inner surfaces of cold-formed steel channel.[2.26]

Note: 1mm = 0.039 in.; 1 N/mm^2 = 0.145 ksi

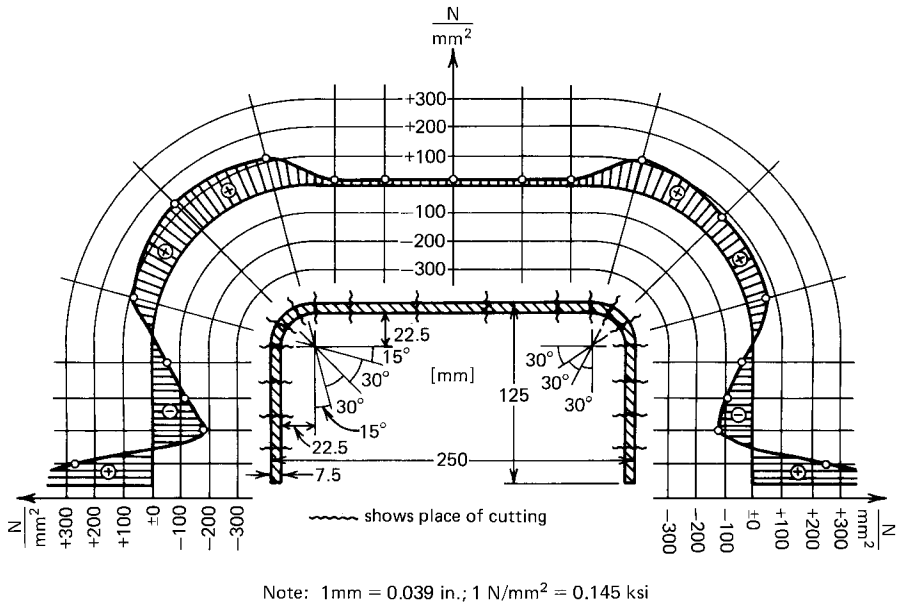**Figure 2.15**   Average measured longitudinal residual stresses in cold-formed steel channel.[2.26]

results of a recent study of the effect of strain rate on material properties of a selected group of sheet steels and the structural strength of cold-formed steel members conducted by Kassar, Pan, and Yu. This information is useful for the design of automotive structural components and other members subjected to dynamic loads.

3 Strength of Thin Elements and Design Criteria

3.1 GENERAL REMARKS

In cold-formed steel design, individual elements of cold-formed steel structural members are usually thin and the width-to-thickness ratios are large. These thin elements may buckle locally at a stress level lower than the yield point of steel when they are subject to compression in flexural bending, axial compression, shear, or bearing. Figure 3.1 illustrates local buckling patterns of certain beams and columns, where the line junctions between elements remain straight and angles between elements do not change.

Since local buckling of individual elements of cold-formed steel sections has often been one of the major design criteria, the design load should be so determined that adequate safety is provided against failure by local instability with due consideration given to the postbuckling strength.

It is well known that a two-dimensional compressed plate under different edge conditions will not fail like one-dimensional members such as columns when the theoretical critical local buckling stress is reached. The plate will continue to carry additional load by means of the redistribution of stress in the compression elements after local buckling occurs. This is a well-known phenomenon called postbuckling strength of plates. The postbuckling strength may be several times larger than the strength determined by critical local buckling stress, as discussed in Chap. 1.

In view of the fact that postbuckling strength of a flat plate is available for structural members to carry additional load, it would be proper to design such elements of cold-formed steel sections on the basis of the postbuckling strength of the plate rather than based on the critical local buckling stress. This is true in particular for elements having relatively large width-to-thickness ratios. The use of postbuckling strength has long been incorporated in the design of ship structures, aircraft structures, and cold-formed steel structures.

Before discussing any specific design problems, it is essential to become familiar with the terms generally used in the design of cold-formed steel structural members and to review the structural behavior of thin elements.

3.2 DEFINITIONS OF GENERAL TERMS

The following definitions of general terms are used in cold-formed steel design:[1.314]
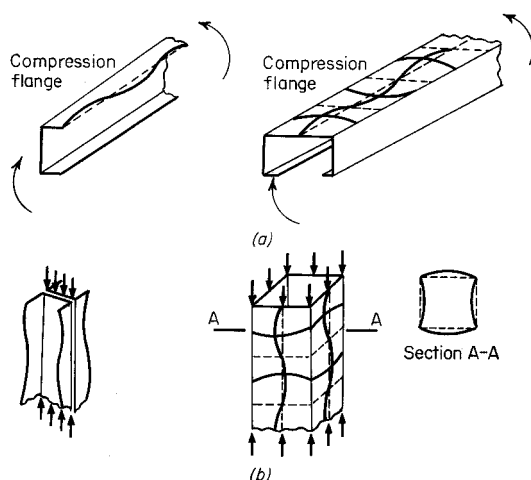
Figure 3.1   Local buckling of compression elements. (*a*) Beams. (*b*) Columns.

1. *Unstiffened Compression Element* (*u.c.e.*). An unstiffened compression element is a flat compression element that is stiffened at only one edge parallel to the direction of stress. As shown in Fig. 3.2, the vertical leg of an angle section and the compression flange of a channel section and an inverted-hat section are unstiffened compression elements. In addition, the portion of the cover plate in the built-up section beyond the center of connection is also considered as an unstiffened compression element if the spacings of the connections are close enough.

2. *Stiffened or Partially Stiffened Compression Element* (*s.c.e.*). A stiffened or partially stiffened compression element is a flat compression element of which both edges parallel to the direction of stress are stiffened either by a web, flange, stiffening lip, intermediate stiffener, or the like (Fig. 3.3). For the built-up section illustrated in Fig. 3.3, the portion of the compression flange between two centerlines of connections can be considered as a stiffened
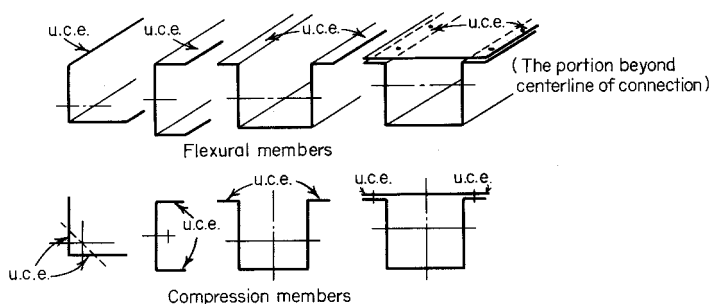

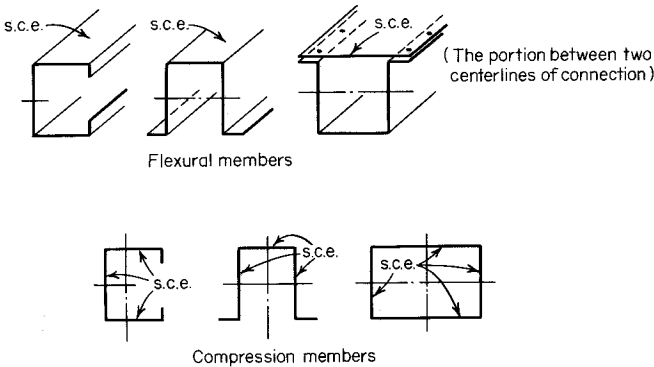**Figure 3.2**   Sections with unstiffened compression elements.

Figure 3.3 Sections with stiffened or partially stiffened compression elements.

compression element if the spacing of the connections meets the requirement of Art. 8.10 on the spacing of connections in compression elements.

3. *Multiple-Stiffened Element.* A multiple-stiffened element is an element that is stiffened between webs, or between a web and a stiffened edge, by means of intermediate stiffeners which are parallel to the direction of stress (Fig. 3.4). The portion between adjacent stiffeners or between a web and an intermediate stiffener or between an edge and an intermediate stiffener is called a "subelement." See Art. 3.5.3.3 for other limitations.

4. *Flat Width w.* The flat width w used in the design of cold-formed steel structural members is the width of the straight portion of the element and does not include the bent portion of the section. For unstiffened flanges, the flat width w is the width of the flat projection of the flange measured from the end of the bend adjacent to the web to the free edge of the flange, as shown in Fig. 3.5a. As shown in Fig. 3.5b, for a built-up section the flat width of the unstiffened compression element is the portion between the center of the connection and the free edge. The flat width w of a stiffened element is the width between the adjacent stiffening means exclusive of bends, as shown in Fig. 3.6a. For the composite section shown in Fig. 3.6b, the flat width of the stiffened compression flange is the distance between the centers of connections.

5. *Flat-Width-to-Thickness Ratio.* The flat-width-to-thickness ratio is the ratio of the flat width of an element measured along its plane to its thickness.
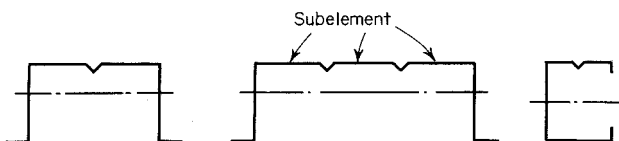

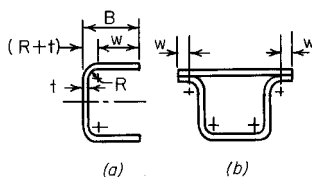**Figure 3.4** Sections with multiple-stiffened compression elements.

Figure 3.5   Flat width of unstiffened compression elements.

Section B1 of the AISI Specification includes the following maximum w/t ratios for flange elements and maximum h/t ratios for web elements:[1.333]

a. MAXIMUM   FLAT-WIDTH-TO-THICKNESS   RATIOS   FOR   FLANGES*
Maximum allowable overall flat-width-to-thickness ratios, w/t, disregarding intermediate stiffeners and taking as t the actual thickness of the element, shall be as follows:

1. Stiffened compression element having one longitudinal edge connected to a web or flange element, the other stiffened by:
   Simple lip   60
   Any other kind of stiffener
   i) when $I_s < I_a$ 60
   ii) when $I_s \geq I_a$ 90
2. Stiffened compression element with *both* longitudinal edges connected to other stiffened elements   500
3. Unstiffened compression element   60

It should be realized that in cold-formed steel design, unstiffened compression elements with w/t ratios exceeding approximately 30 and stiffened compression elements with w/t ratios exceeding approximately 250 may develop noticeable deformation under design loads without detriment to load-carrying capacity.[1.314]
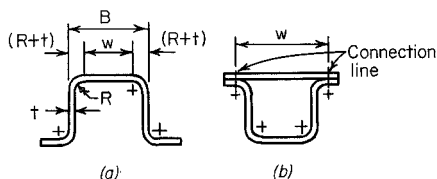

Figure 3.6   Flat width of stiffened compression elements.

*When flange curling or movement of the beam flange toward the neutral axis is important, the flange width is limited by Eq. (4.110) in Art. 4.2.6.2.

b. MAXIMUM DEPTH-TO-THICKNESS RATIOS FOR WEBS   The h/t ratio of the webs of flexural members as defined in Art. 3.5.1.2 shall not exceed the following limitations:
   1. For unreinforced webs: $(h/t)_{max} = 200$
   2. For webs which are provided with transverse stiffeners satisfying the requirements of Art. 4.3.2
   When using bearing stiffeners only, $(h/t)_{max} = 260$
   When using bearing stiffeners and intermediate stiffeners, $(h/t)_{max} = 300$

Where a web consists of two or more sheets, the h/t ratio shall be computed for the individual sheets.

6. *Effective Design Width b.* The effective design width b is a reduced design width for computing sectional properties of flexural and compression members when the flat-width-to-thickness ratio of an element exceeds a certain limit. Figure 3.7 shows effective design widths of flexural and comparison members.

7. *Thickness t.* The thickness t used in the calculation of sectional properties and the design of cold-formed sections should be the thickness of base steel. Any thickness of coating material should be deducted from the overall thickness of steel. See Appendix A for the thickness of base metal. In the AISI Specification it is specified that the uncoated minimum thickness of the cold-formed product as delivered to the job site shall not at any location be less than 95% of the thickness used in the design. An exception is at bends, such as corners, where the thickness may be less due to cold-forming effects. However, the thinning is usually on the order of 1 to 3% and can be ignored in calculating sectional properties.

8. *Torsional–Flexural Buckling.* Torsional–flexural buckling is a mode of buckling in which compression members can bend and twist simultaneously without change in cross-sectional shape. This type of buckling mode is critical, in particular when the shear center of the section does not coincide with the centroid. See Chap. 5 for the design of compression members which may be subject to torsional–flexural buckling.

9. *Point-Symmetric Section.* A point-symmetric section is a section symmetrical about a point (centroid). A Z-section having equal flanges is a point-symmetric section.

10. *Yield Point F_y.* In ASTM Specifications and other publications, the terms ''yield point'' and ''yield strength'' are often used for steels having different stress–strain characteristics. The term ''yield point'' used in the AISI Specification applies to either yield point or yield strength. Table 2.1 of Chap. 2 lists various yield points.

11. *Stress.* In the 1996 edition of the AISI Specification, the term ''stress'' means force per unit area.
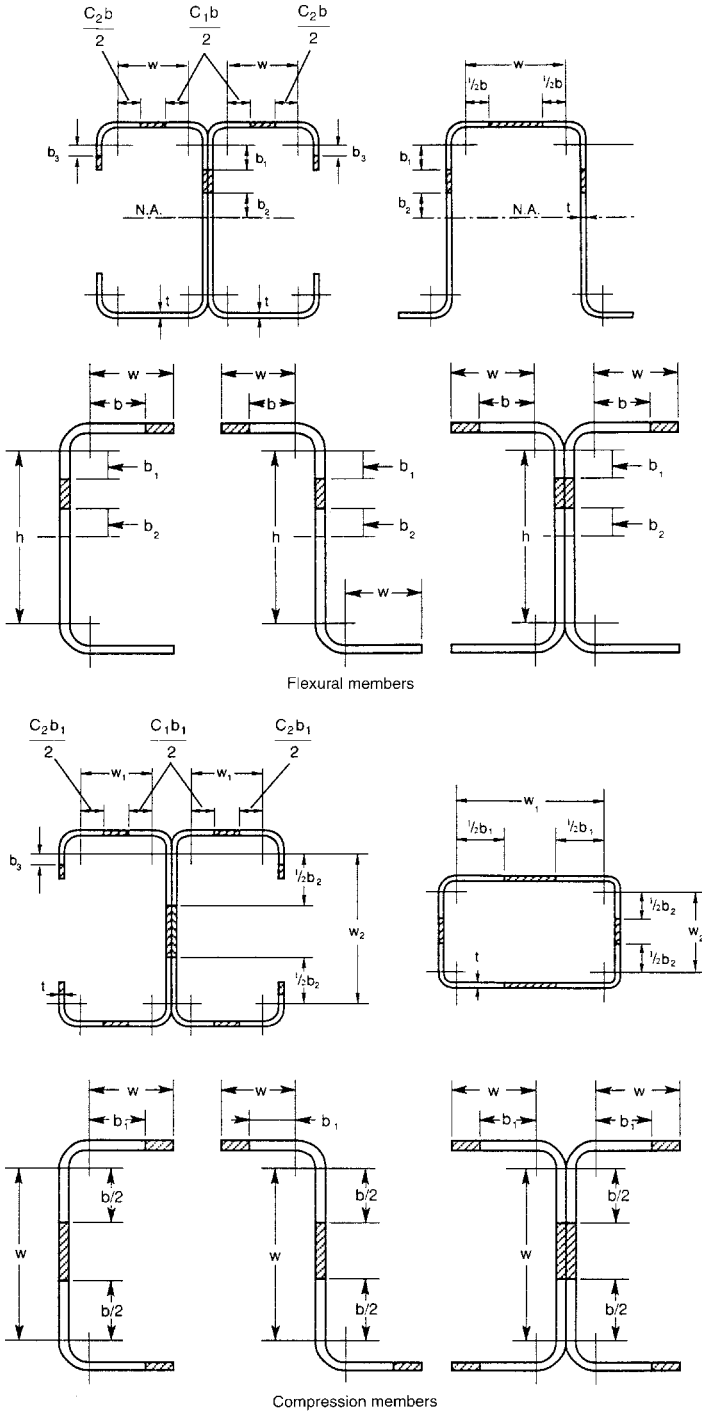
Figure 3.7   Effective design width of flexural and compression members.

TABLE 3.1   Safety Factors, Ω, and Resistance Factors, ϕ, Used in the 1996 Edition of the AISI Specification[1.314, 1.333]

Type of Strength	ASD Safety Factor, Ω	LRFD Resistance Factor, ϕ
(a) Stiffeners		
Transverse stiffeners	2.00	0.85
Shear stiffeners[a]	1.67	0.90
(b) Tension members		
For yielding	1.67	0.90
For fracture away from the connection	2.00	0.75
For fracture at the connection (see connections)		
(c) Flexural members		
Bending strength		
For sections with stiffened or partially stiffened compression flanges	1.67	0.95
For sections with unstiffened compression flanges	1.67	0.90
Laterally unbraced beams	1.67	0.90
Beams having one flange through-fastened to deck or sheathing (C- or Z-sections)	1.67	0.90
Beams having one flange fastened to a standing seam roof system	1.67	0.90
Web design		
Shear strength[a]	1.67	0.90
Web crippling		
For single unreinforced webs	1.85	0.75
For I-sections	2.00	0.80
For two nested Z-sections	1.80	0.85
(d) Concentrically loaded compression members	1.80	0.85
(e) Combined axial load and bending		
For tension	1.67	0.95
For compression	1.80	0.85
For bending	1.67	0.90–0.95
(f) Cylindrical tubular members		
Bending strength	1.67	0.95
Axial compression	1.80	0.85
(g) Wall studs and wall assemblies		
Wall studs in compression	1.80	0.85
Wall studs in bending	1.67	0.90–0.95
(h) Diaphragm construction	2.00–3.00	0.50–0.65
(i) Welded connections		
Groove welds		
Tension or compression	2.50	0.90
Shear (welds)	2.50	0.80
Shear (base metal)	2.50	0.90

TABLE 3.1   (*Continued*)

Type of Strength	ASD Safety Factor, Ω	LRFD Resistance Factor, ϕ
Arc spot welds		
Welds	2.50	0.60
Connected part	2.50	0.50–0.60
Minimum edge distance	2.00–2.22	0.60–0.70
Tension	2.50	0.60
Arc seam welds		
Welds	2.50	0.60
Connected part	2.50	0.60
Fillet welds		
Longitudinal loading (connected part)	2.50	0.55–0.60
Transverse loading (connected part)	2.50	0.60
Welds	2.50	0.60
Flare groove welds		
Transverse loading (connected part)	2.50	0.55
Longitudinal loading (connected part)	2.50	0.55
Welds	2.50	0.60
Resistance Welds	2.50	0.65
Shear lag effect	2.50	0.60
(j) Bolted connections		
Minimum spacing and edge distance	2.00–2.22	0.60–0.70
Tension strength on net section		
With washers		
Double shear connection	2.00	0.65
Single shear connection	2.22	0.55
Without washers	2.22	0.65
Bearing strength	2.22	0.55–0.70
Shear strength of bolts	2.40	0.65
Tensile strength of bolts	2.00–2.25	0.75
Shear lag effect	2.22	0.65
Flat sheet with staggered holes	2.22	0.65
(k) Screw connections	3.00	0.50
(l) Rupture		
Shear rupture	2.00	0.75
Block shear rupture		
For bolted connections	2.22	0.65
For welded connections	2.50	0.60

[a] When $h/t \leq 0.96 \sqrt{Ek_v/F_y}$, $\Omega = 1.50$, $\phi = 1.0$

12. *Confirmatory Test.* A confirmatory test is a test made on members, connections, and assemblies that are designed according to the AISI Specification or its specific references. It is used to compare actual versus calculated performance.

13. *Performance Test.* A performance test is a test on structural members, connections, and assemblies whose performance cannot be determined by the AISI Specification or its specific references. The design values may be determined by the results of performance tests and the requirements stipulated in Sec. F1 of the AISI Specification.

14. *Virgin Steel.* Virgin steel refers to steel as received from the producer or warehouse before being cold-worked as a result of fabricating operations.

15. *Virgin Steel Properties.* Virgin steel properties are mechanical properties (yield point, tensile strength, and elongation) of the virgin steel. These properties are established according to standard tests.

16. *Specified Minimum Yield Point.* The specified minimum yield point is the lower limit of yield point that must be equalled or exceeded in a specification test to qualify a lot of steel for use in a cold-formed steel structural member designed at that yield point.

17. *Cold-Formed Steel Structural Members.* Cold-formed steel structural members are shapes that are manufactured by press-braking blanks sheared from sheets, cut length of coils or plates, or by roll forming cold- or hot-rolled coils or sheets; both forming operations being performed at ambient room temperature, that is, without manifest addition of heat such as would be required for hot forming.

18. *ASD* (*Allowable Stress Design*). The allowable stress design approach is a method of proportioning structural components (members, connectors, connecting elements, and assemblages) such that the allowable stress, allowable force, or allowable moment is not exceeded by the required strength when the structure is subjected to all appropriate combinations of nominal loads. See Art. 3.3.1.

19. *LRFD* (*Load and Resistance Factor Design*). The load and resistance factor design approach is a method of proportioning structural components (members, connectors, connecting elements, and assemblages) such that no applicable limit state is exceeded when the structure is subjected to all appropriate load combinations. See Art. 3.3.2.

20. *Nominal Loads.* The nominal loads are magnitudes of the loads specified by the applicable code not including load factors.

21. *Required Strength.* The required strength is the load effect (force, moment, as appropriate) acting on the structural component determined by structural analysis from the factored loads for LRFD or nominal loads for ASD (using most appropriate critical load combinations).

22. *Nominal Strength, R_n.* The nominal strength is the capacity of a structure or component to resist the effects of loads, as determined by specified

material properties and dimensions using equations derived from accepted principles of structural mechanics or by field tests or laboratory tests of scaled models, allowing for modeling effects, and differences between laboratory and field conditions.

23. *Design Strength.* For the ASD method, the allowable design strength (force, moment, as appropriate) provided by the structural component is determined by R_n/Ω, where R_n is the nominal strength and Ω is the safety factor. For the LRFD method, the design strength is determined by the factored resistance, ϕR_n, where ϕ is the resistance factor.

24. *Resistance Factor ϕ.* The resistance factor is a factor that accounts for unavoidable deviations of the actual strength from the nominal value. It is usually less than unity.

25. *Safety Factor, Ω.* The safety factor is defined as a ratio of the stress (or strength) at incipient failure to the computed stress (or strength) at design load.

In the design of cold-formed steel structural members, different safety factors are used in some of the design provisions of the AISI Specification in accordance with the type of structural behavior. Table 3.1 gives a summary of the safety factors and resistance factors used in the AISI Specification.

3.3 DESIGN BASIS

Prior to 1996, the American Iron and Steel Institute issued two separate specifications for the design of cold-formed steel structural members, connections, and structural assemblies. One was for the *allowable stress design* (ASD) method,[1.4] and the other was for the *load and resistance factor design* (LRFD) method.[1.313] These two design specifications were combined into a single standard in 1996.[1.314] Both methods are now equally acceptable for the design of cold-formed steel structures, even though they may or may not produce identical designs. However, the two methods should not be mixed in designing the various cold-formed steel components of a structure.

3.3.1 Allowable Stress Design (ASD)

Since the issuance of the first AISI Specification in 1946, the design of cold-formed steel structural members and connections in the United States and some other countries has been based on the allowable stress design method. In this method, the *required strengths* (axial forces, bending moments, shear forces, etc.) for structural members and connections are computed from structural analysis by using the nominal loads or specified working loads for all applicable load combinations as discussed in Art. 3.3.1.2. The allowable *design strength* permitted by the specification is determined by the nominal strength and the specified safety factor.

3.3.1.1   Design Format for the ASD Method   For the ASD method, the *required strength, R,* should not exceed the allowable *design strength, R_a,* as follows:

$$R \leq R_a \tag{3.1}$$

Based on Sec. A5.1.1 of the AISI specification, the allowable design strength is determined by Eq. (3.2):

$$R_a = \frac{R_n}{\Omega} \tag{3.2}$$

where R_n = nominal strength
Ω = safety factor corresponding to R_n (See Table 3.1)

In Eq. (3.2), the nominal strength is the strength or capacity of the element or member for a given limit state or failure mode. It is computed by the design equations provided in Chaps. B through E of the AISI Specification using sectional properties (cross-sectional area, moment of inertia, section modulus, radius of gyration, etc.) and material properties.

The safety factors provided in Chaps. C through E of the AISI Specification are summarized in Table 3.1. These factors are used to compensate for uncertainties inherent in the design, fabrication, and erection of structural components and connections as well as uncertainties in the estimation of applied loads. It should be noted that for the ASD method, the same safety factor is used for dead and live loads. For wind, earthquake, and combined forces, see Art. 3.3.1.2.

3.3.1.2   Load Combinations for the ASD Method   When the ASD method is used, the following load combinations should be considered according to Sec. A5.1.2 of the AISI Specification:

$$D \tag{3.3a}$$

$$D + L + (L_r \text{ or } S \text{ or } R_r) \tag{3.3b}$$

$$D + (W \text{ or } E) \tag{3.3c}$$

$$D + L + (L_r \text{ or } S \text{ or } R_r) + (W \text{ or } E) \tag{3.3d}$$

where D = dead load
E = earthquake load
L = live load due to intended use and occupancy
L_r = roof live load
R_r = rain load, except for ponding
S = snow load
W = wind load

The above load combinations are based on the ASCE *Standard on Minimum Design Loads for Buildings and Other Structures.*[3.149] For the impact loads on a structures, reference may be made to AISC publications[1.148, 3.150] for building design and the MBMA publication for the design of metal buildings.[1.106]

When wind or earthquake load acts in combination with dead and/or live loads, it has been a general practice to permit the allowable design strength to be increased by a factor of one-third because the action of wind or earthquake on a structure is highly localized and of very short duration. Instead of the above-mentioned design practice, in Sec. A5.1.3 of the AISI Specification this is accomplished by permitting a 25% reduction in the combined load effects without the increase of the allowable design strength. This load reduction should only be used for strength calculations. Section A5.1.3 of the Specification also specifies that when the seismic load model is limit state based, the resulting earthquake load is to be multiplied by 0.67.

In addition to the above-specified loads, due consideration should also be given to the loads due to (1) fluids with well-defined pressures and maximum heights, (2) weight and lateral pressure of soil and water in soil, (3) ponding, and (4) self-straining forces and effects arising from contraction or expansion resulting from temperature, shrinkage, moisture changes, creep in component materials, movement due to different settlement, and combinations thereof.

3.3.2   Load and Resistance Factor Design (LRFD)

During recent years, the load and resistance factor design (LRFD) or limit states design (LSD) method has been used in the United States (on a limited basis) and other countries for the design of steel structures.[1.177, 1.209, 3.150, 3.151] The advantages of the LRFD method are (1) the uncertainties and the variabilities of different types of loads and resistances are accounted for by use of multiple factors, and (2) by using probability theory, all designs can ideally achieve a consistent reliability. Thus, the LRFD approach provides the basis for a more rational and refined design method than is possible with the allowable stress design method.

In order to develop the load and resistance factor design criteria for cold-formed, carbon, and low-alloy steel structural members, a research project was conducted at the University of Missouri-Rolla under the direction of Wei-Wen Yu with consultation of T. V. Galambos and M. K. Ravindra. This project, which was initiated in 1976, was sponsored by the American Iron and Steel Institute and supervised by the AISI Subcommittee on Load and Resistance Factor Design.[1.248] Based on the studies made by Rang, Supornsilaphachai, Snyder, Pan, and Hsiao, the AISI Load and Resistance Factor Design Specification for Cold-Formed Steel Structural Members with Commentary was published in August 1991 on the basis of the 1986 edition of the AISI ASD Specification with the 1989 Addendum.[1.313, 3.152] The background infor-

mation and research findings for developing the AISI LRFD criteria have been documented in 14 progress reports of the University of Missouri-Rolla and are summarized in Refs. 1.248, and 3.153–3.159. As discussed in Art. 3.3, the 1996 edition of the AISI Specification includes both the ASD and LRFD methods.

3.3.2.1 Design Format for the LRFD Method

As discussed in Art. 3.3.1.1, the allowable stress design method employs only one factor of safety for dead and live loads under a given limit state. A limit state is the condition at which the structural usefulness of a load-carrying element or member is impaired to such an extent that it becomes unsafe for the occupants of the structure, or the element no longer performs its intended function. For cold-formed steel members, typical limit states are yielding, buckling, post-buckling strength, shear lag, web crippling, excessive deflection, and others. These limits have been established through experience in practice or in the laboratory, and they have been thoroughly investigated through analytical and experimental research.

Unlike allowable stress design, the LRFD approach uses multiple load factors and resistance factors to provide a refinement in the design that can account for the different degrees of the uncertainties and variabilities of analysis, design, loading, material properties, and fabrication. The design format for satisfying the structural safety requirement is expressed in Eq. (3.4):

$$\phi\, R_n \geq \Sigma\gamma_i Q_i \qquad (3.4)$$

where R_n = nominal resistance
$\quad\ Q_i$ = load effect
$\quad\ \phi$ = resistance factor corresponding to R_n
$\quad\ \gamma_i$ = load factor corresponding to Q_i
$\quad \phi R_n$ = design strength
$\ \Sigma\gamma_i Q_i$ = required resistance or required strength for factored loads

The nominal resistance R_n is the total strength of the element or member for a given limit state, computed from sectional and material properties according to the applicable design criteria. The resistance factor ϕ accounts for the uncertainties and variabilities inherent in R_n, and it is usually less than unity, as listed in Table 3.1. The load effects Q_i are the forces (axial force, bending moment, shear force, etc.) on the cross section determined from the structural analysis and γ_i are the corresponding load factors that account for the uncertainties and variabilities of the applied loads. The load factors are usually greater than unity, as given in Art. 3.3.2.2.

For the design of cold-formed members using carbon and low-alloy steels, the values of ϕ, R_n, γ_i, and load combinations are given in the 1996 edition of AISI Specification.[1.314]

3.3.2.2   Load Factors and Load Combinations for the LRFD Method   In the AISI Specification, the following load factors and load combinations are included for the design of cold-formed steel structural members and connections:

$$1.4D + L \tag{3.5a}$$

$$1.2D + 1.6L + 0.5 \, (L_r \text{ or } S \text{ or } R_r) \tag{3.5b}$$

$$1.2D + 1.6 \, (L_r \text{ or } S \text{ or } R_r) + (0.5L \text{ or } 0.8W) \tag{3.5c}$$

$$1.2D + 1.3W + 0.5L + 0.5 \, (L_r \text{ or } S \text{ or } R_r) \tag{3.5d}$$

$$1.2D + 1.5E + 0.5L + 0.2 \, S \tag{3.5e}$$

$$0.9D - (1.3W \text{ or } 1.5E) \tag{3.5f}$$

All symbols were defined previously.
Exceptions:

1. The load factor for E in Eqs. (3.5e) and (3.5f) shall equal 1.0 when the seismic load model specified by the applicable code or specification is limit state based.
2. The load factor for L in Eqs. (3.5c), (3.5d), and (3.5e) shall be equal to 1.0 for garages, areas occupied as places of public assembly, and all areas where the live load is greater than 100 psf.
3. For wind load on individual purlins, girts, wall panels, and roof decks, multiply the load factor for W by 0.9.
4. The load factor for L_r in Eq. (3.5c) shall equal 1.4 in lieu of 1.6 when the roof live load is due to the presence of workmen and materials during repair operations.

The above load factors and load combinations listed in Eqs. (3.5a) through (3.5f) are based on the ASCE/ANSI recommendations[3.149] with the following minor modifications:[1.310, 3.152]

1. In Eq. (3.5a), the load combination is (1.4D + L) instead of ASCE/ANSI value of 1.4D. This is due to the fact that the dead load of cold-formed steel structures is usually smaller than that of heavy construction.
2. In Exception (4), the load factor used for the nominal roof live load, L_r, is 1.4 instead of the ASCE/ANSI value of 1.6. The use of a relatively small load factor is because the roof live load is due to the presence of workmen and materials during repair operations and therefore can be considered as a type of construction load.

3. For roof and wall construction, the load factor for the nominal wind load W to be used for the design of individual purlins, girts, wall panels, and roof decks should be multiplied by a reduction factor of 0.9 as permitted by Exception (3). This is because these elements are secondary members subjected to a short duration of wind load and can be designed for a smaller reliability than primary members such as beams and columns. With this reduction factor, designs comparable to the current practice are obtained.

In addition to the above modifications, the following load combination is included in the AISI Commentary for roof and floor composite construction:[1.310]

$$1.2D_s + 1.6C_w + 1.4C \tag{3.6}$$

where D_s = weight of steel deck
C_w = nominal weight of wet concrete during construction
C = nominal construction load, including equipment, workmen, and formwork, but excluding the weight of wet concrete

The above suggestion provides safe construction practices for cold-formed steel decks and panels that otherwise may be damaged during construction. In Eq. (3.6), the load factor used for the weight of wet concrete is 1.6 because delivering methods are such that an individual sheet can be subjected to this load. The use of a load factor of 1.4 for the construction load reflects a general practice of 33% strength increase for concentrated loads in the allowable design approach.

3.3.2.3   Design Strength, ϕR_n

The design strength is the usable capacity of a structural component or connection to be used for design purposes. As shown in Eq. (3.4), design strength is obtained by multiplying the nominal resistance R_n by a reduction factor ϕ to account for the uncertainties and variabilities of the nominal strength.

Nominal Resistance R_n. The nominal resistance or nominal strength R_n is the capacity of a structural component or connection to resist load effects (axial force, bending moment, shear force, etc.). It is determined by computations using specified material properties and dimensions in the design criteria derived from accepted principles of structural mechanics and/or by tests, taking account of the effects of manufacturing and fabrication processes. For the design of cold-formed members using carbon and low-alloy steels, Chaps. C through E of the AISI Specification[1.314] provide the equations needed for determining the nominal strengths of tension members, flexural members, compression members, cylindrical tubular members, wall studs, connections,

and joints. It should be noted that for the purpose of consistency, the same nominal strength equations are used in the AISI Specification for the ASD and LRFD methods.

Resistance Factor ϕ. The resistance factor ϕ is a reduction factor to account for unavoidable deviations of the actual strength from the nominal value prescribed in the design specification. These deviations may result from the uncertainties and variabilities in (1) the material properties (i.e., yield stress, tensile strength, modulus of elasticity, etc.), (2) the geometry of the cross section (i.e, depth, width, thickness, etc. to be used for computing area, moment of inertia, section modulus, radius of gyration, etc.), and (3) the design methods (i.e., assumptions, approximations of theoretical formulas, etc.).

In the development of the AISI LRFD criteria,[3.159] the resistance factors were derived from a combination of (1) probabilistic modeling,[3.160, 3.161] (2) calibration of the new criteria to the ASD approach,[3.162] and (3) evaluations of the new LRFD criteria by judgment and past experience. The development was aided by a comparative study of the ASD and LRFD methods.[3.157, 3.163] The procedures used for developing the resistance factors for cold-formed steel design consisted of the following five steps:

1. Analyze the available information and test data to obtain the statistical value (mean values and coefficients of variation) of resistance and load effects.
2. Assume the mean values and coefficients of variation of the variable for which no statistical information is available.
3. Compute the reliability index implied in the applicable ASD Specification.
4. Select the target reliability index.
5. Develop the resistance factors according to the selected target reliability index for different types of members with the limit state being considered.

Details of Steps 1, 2, and 3 are presented in several progress reports of the University of Missouri-Rolla and are summarized in Ref. 3.162. Based on the probability distribution shown in Fig. 3.8 and the first order probabilistic theory, the reliability index β can be computed by Eq. (3.7):[1.248, 3.152]

$$\beta = \frac{\ell n(R_m / Q_m)}{\sqrt{V_R^2 + V_Q^2}} \tag{3.7}$$

where R_m = mean value of resistance
$R_m = R_n(P_m\, M_m\, F_m)$
Q_m = mean value of load effect
V_R = coefficient of variation of resistance = σ_R / R_m
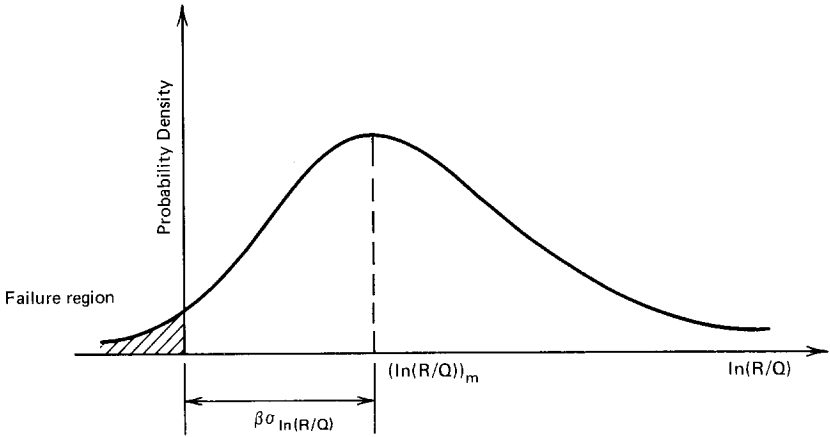$V_R = \sqrt{V_P^2 + V_M^2 + V_F^2}$

Figure 3.8 Definition of reliability index.

V_Q = coefficient of variation of load effect = σ_Q/Q_m
σ_R = standard deviation of resistance
σ_Q = standard deviation of load effect
P_m = mean ratio of the experimentally determined ultimate load to the predicted ultimate load of test specimens
M_m = mean ratio of the tested material properties to specified minimum values
F_m = mean ratio of the actual sectional properties to nominal values
V_P = coefficient of variation of ratio P
V_M = coefficient of variation of ratio M
V_F = coefficient of variation of ratio F

The reliability index β is a measure of the safety of the design. As shown in Fig. 3.8, a limit state is reached when $\ell n(R/Q) = 0$. The shaded area represents the probability of exceeding the limit states. The smaller the shaded area, the more reliable the structure. Because the distance between the mean value of $[\ell n(R/Q)]_m$ and the failure region is defined as $\beta[\sigma_{\ell n(R/Q)}]$, when two designs are compared, the one with the larger β is more reliable.

As far as the target reliability index β_0 is concerned, research findings indicated that for cold-formed steel members, the target reliability index may be taken as 2.5 for gravity loads. In order to ensure that failure of a structure is not initiated in connections, a higher value of 3.5 was selected for connections using cold-formed carbon steels. Even though these two target values are somewhat lower than those recommended by the ASCE/ANSI code (i.e., 3.0 and 4.5 for members and connections, respectively),[3.149] they are essentially the same targets used for the AISC LRFD Specification.[3.150]

On the basis of the load combination of $(1.2D + 1.6L)$ with an assumed D/L ratio of $1/5$ and the available statistical data, it can be shown that the resistance factor ϕ can be determined as follows:[1.310]

$$\phi = \frac{1.521 \, M_m F_m P_m}{\exp(\beta_o \sqrt{V_R^2 + V_Q^2})} \tag{3.8}$$

where β_o is the target reliability index. For practical reasons, it is desirable to have relatively few different resistance factors. Table 3.1 lists the resistance factors for the design of various types of members using carbon and low-alloy steels.

If the ϕ factor is known, the corresponding safety factor, Ω, for allowable stress design can be computed for the load combination $(1.2D + 1.6L)$ as follows:[1.310]

$$\Omega = \frac{1.2D/L + 1.6}{\phi(D/L + 1)} \tag{3.9}$$

where D/L is the dead-to-live load ratio for the given condition.

3.4 SERVICEABILITY

Article 3.3 deals only with the strength limit state. A structure should also be designed for the serviceability limit state as required by Sec. A8 of the AISI Specification.[1.314]

Serviceability limit states are conditions under which a structure can no longer perform its intended functions. Strength considerations are usually not affected by serviceability limit states. However, serviceability criteria are essential to ensure functional performance and economy of design.

The conditions which may require serviceability limits are listed in the AISI Commentary as follows:[1.310]

1. Excessive deflections or rotations which may affect the appearance or functional use of the structure and deflections which may cause damage to nonstructural elements.
2. Excessive vibrations which may cause occupant discomfort of equipment malfunctions.
3. Deterioration over time, which may include corrosion or appearance considerations.

When checking serviceability, the designer should consider appropriate service loads, the response of the structure, and the reaction of building occupants.

Service loads that may require consideration include static loads, snow or rain loads, temperature fluctuations, and dynamic loads from human activities, wind-induced effects, or the operation of equipment. The service loads are actual loads that act on the structure at an arbitrary point in time. Appropriate

service loads for checking serviceability limit states may only be a fraction of the nominal loads.

The response of the structure to service loads can normally be analyzed assuming linear elastic behavior. Serviceability limits depend on the function of the structure and on the perceptions of the observer. Unlike the strength limit states, general serviceability limits cannot be specified that are applicable to all structures. The AISI Specification does not contain explicit requirements; however, guidance is generally provided by the applicable building code. In the absence of specific criteria, guidelines may be found in Refs. 3.164–3.167.

3.5 STRUCTURAL BEHAVIOR OF COMPRESSION ELEMENTS AND DESIGN CRITERIA

3.5.1 Stiffened Compression Elements

3.5.1.1 *Stiffened Elements under Uniform Compression*

Yielding. The strength of a stiffened compression element such as the compression flange of a hat section is governed by yielding if its w/t ratio is relatively small. It may be governed by local buckling as shown in Fig. 3.9 at a stress level less than the yield point if its w/t ratio is relatively large.

Elastic Local Buckling Stress of Plates. Considering a simply supported square plate subjected to a uniform compression stress in one direction, it will buckle in a single curvature in both directions, as shown in Fig. 3.10. However, for individual elements of a section, the length of the element is usually much larger than the width, as illustrated in Fig. 3.9.

The critical buckling stress of a plate as shown in Fig. 3.11 can be determined by solving Bryan's differential equation based on small deflection theory (i.e., the significant deflection at buckling is of the order of the thickness of the plate or less) as follows:
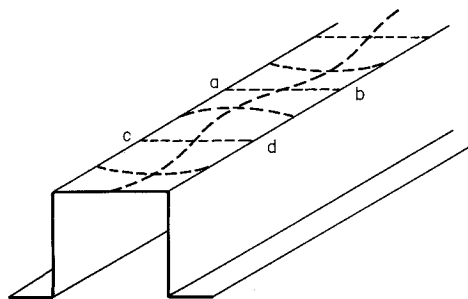

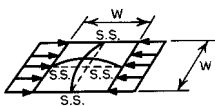**Figure 3.9**   Local buckling of stiffened compression flange of hat-shaped beam.[1.161]

Figure 3.10   Square plate subjected to compression stress.

$$\frac{\partial^4 \omega}{\partial x^4} + 2 \frac{\partial^4 \omega}{\partial x^2 \, \partial y^2} + \frac{\partial^4 \omega}{\partial y^4} + \frac{f_x t}{D} \frac{\partial^2 \omega}{\partial x^2} = 0 \qquad (3.10)$$

where

$$D = \frac{Et^3}{12(1 - \mu^2)}$$

and

E = modulus of elasticity of steel = 29.5×10^3 ksi (203 GPa)
t = thickness of plate
μ = Poisson's ratio = 0.3 for steel in the elastic range
ω = deflection of plate perpendicular to surface
f_x = compression stress in x direction

If m and n are the numbers of half sine waves in the x and y directions, respectively, the deflected shape of the rectangular plate as shown in Fig. 3.11 may be represented by a double series:

$$\omega = \sum_{m=1}^{\infty} \sum_{n=1}^{\infty} A_{mn} \sin \frac{m\pi x}{a} \sin \frac{n\pi y}{w} \qquad (3.11)$$

The above equation is satisfied with boundary conditions because for $x = 0$, a and $y = 0$, w (a and w being the length and width of the plate, respectively) the computed deflection equals zero. Since $\partial^2 \omega / \partial x^2 = 0$ and $\partial^2 \omega / \partial y^2 = 0$ at four edges, Eq. (3.11) also satisfies the condition that the edge moments equal zero because
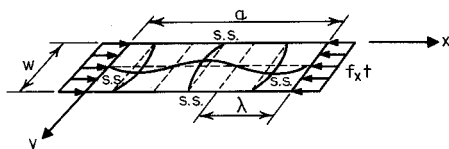

Figure 3.11   Rectangular plate subjected to compression stress.

$$M_x = -D \left(\frac{\partial^2 \omega}{\partial x^2} + \mu \frac{\partial^2 \omega}{\partial y^2} \right)$$

$$M_y = -D \left(\frac{\partial^2 \omega}{\partial y^2} + \mu \frac{\partial^2 \omega}{\partial x^2} \right)$$

Solving Eq. (3.10) by using Eq. (3.11), one can then obtain the following equation:

$$\sum_{m=1}^{\infty} \sum_{n=1}^{\infty} A_{mn} \left[\pi^4 \left(\frac{m^2}{a^2} + \frac{n^2}{w^2} \right)^2 - \frac{f_x t}{D} \frac{m^2 \pi^2}{a^2} \right] \sin \frac{m \pi x}{a} \sin \frac{n \pi y}{w} = 0 \quad (3.12)$$

It is obvious that the solution can be obtained if either $A_{mn} = 0$ or the quantity in square brackets equals zero. The former condition means that no buckling will occur, which is not applicable to this particular case.

By solving

$$\pi^4 \left(\frac{m^2}{a^2} + \frac{n^2}{w^2} \right)^2 - \frac{f_x t}{D} \frac{m^2 \pi^2}{a^2} = 0$$

one can obtain an equation for critical local buckling stress as follows:

$$f_{cr} = f_x = \frac{D \pi^2}{t w^2} \left[m \left(\frac{w}{a} \right) + \frac{n^2}{m} \left(\frac{a}{w} \right) \right]^2 \quad (3.13)$$

In Eq. (3.13) the minimum value in square brackets is $n = 1$, that is, only one half sine wave occurs in the y direction. Therefore

$$f_{cr} = \frac{k D \pi^2}{t w^2} \quad (3.14)$$

where

$$k = \left[m \left(\frac{w}{a} \right) + \frac{1}{m} \left(\frac{a}{w} \right) \right]^2 \quad (3.15)$$

Substituting the value of D in Eq. (3.14), Eq. (3.16) represents a general equation for critical local buckling stress for a rectangular plate subjected to compression stress in one direction:

$$f_{cr} = \frac{k \pi^2 E}{12(1 - \mu^2)(w/t)^2} \quad (3.16)$$

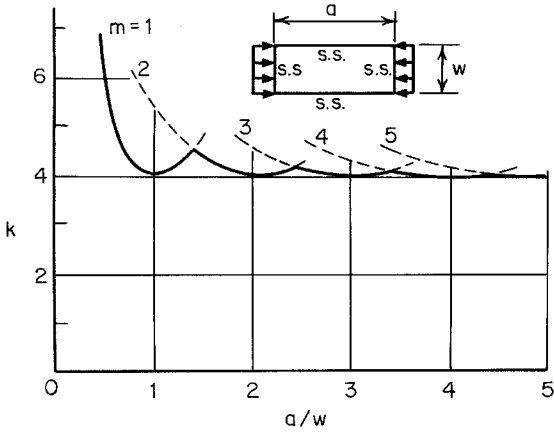The value of k used in Eq. (3.16) is shown in Fig. 3.12 for different a/w ratios.

Figure 3.12   Buckling coefficient for flat rectangular plates.[3.1]

It should be noted that when the a/w ratio is an integer, the value of k equals 4. This value of k is also applicable for relatively large a/w ratios.

From Fig. 3.12 and Eq. (3.15) it can be seen that the transition from m to $m + 1$ half sine waves occurs at the condition when the two corresponding curves have equal ordinates, that is,

$$m\left(\frac{w}{a}\right) + \frac{1}{m}\left(\frac{a}{w}\right) = (m + 1)\left(\frac{w}{a}\right) + \frac{1}{m + 1}\left(\frac{a}{w}\right)$$

or

$$\frac{a}{w} = \sqrt{m(m + 1)}$$

For a long plate,

$$\frac{a}{w} \simeq m$$

or

$$\lambda = \frac{a}{m} \simeq w \tag{3.17}$$

where λ is the length of the half sine wave.

Equation (3.17) indicates that the number of half sine waves increases with the increase of a/w ratios. For a long plate, the length of the half sine waves

equals approximately the width of the plate, and therefore square waves are formed, as shown in Fig. 3.11.

In structural engineering, the long plate having a relatively large a/w ratio is of particular interest because such a long plate often represents the case of individual elements of the sections generally used in structures. As shown in Fig. 3.12, whenever the aspect ratio a/w exceeds about 4, a value of $k = 4$ can be used for determining the critical buckling stress for a plate simply supported along four edges and subjected to compression stress in one direction, that is,

$$f_{cr} = \frac{\pi^2 E}{3(1 - \mu^2)(w/t)^2} \tag{3.18}$$

Equation (3.18) is also applicable to a square plate.

The values of k for a long rectangular plate subjected to different types of stress (compression, shear, or bending) and under different boundary conditions (simply supported, fixed, or free edge) are tabulated in Table 3.2.

Buckling of Plates in the Inelastic Range. When the compression stress in a plate in only one direction exceeds the proportional limit of the steel, the plate becomes an anisotropic plate which has different properties in different directions of the plate.

In 1924 Bleich proposed the following differential equation for inelastic buckling:[3.3]

$$\left(\tau \frac{\partial^4 \omega}{\partial x^4} + 2\sqrt{\tau} \frac{\partial^4 \omega}{\partial x^2 \, \partial y^2} + \frac{\partial^4 \omega}{\partial y^4} \right) + \frac{f_x t}{D} \frac{\partial^2 \omega}{\partial x^2} = 0 \tag{3.19}$$

where $\tau = E_t/E$, and E_t is the tangent modulus of steel.

Applying the modified boundary conditions, one can then obtain the following critical buckling stress for plastic buckling of the plate:

$$f_{cr} = \frac{k\pi^2 E\sqrt{\tau}}{12(1 - \mu^2)(w/t)^2} = \frac{k\pi^2 \sqrt{EE_t}}{12(1 - \mu^2)(w/t)^2} \tag{3.20}$$
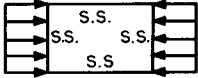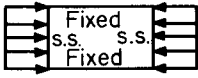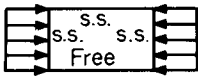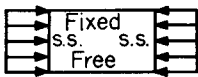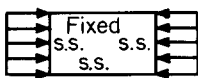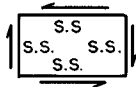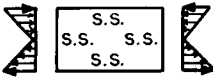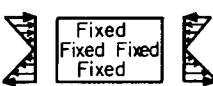
The wavelength for a long plate is

$$\lambda = \sqrt[4]{\tau}w \tag{3.21}$$

In Eqs. (3.19) and (3.20), $\sqrt{\tau} = \sqrt{E_t/E}$ is the plasticity reduction factor for a simply supported plate subjected to a uniform compression stress in one direction [case (a) of Table 3.2]. This factor varies with the type of loading and the edge support conditions. For example, a value of E_s/E has been found to be an appropriate plasticity reduction factor for case (c) of Table 3.2. The

TABLE 3.2 Values of k for Determining Critical Buckling Stress[3.2]

$$f_{cr} = k \frac{\pi^2 E}{12(1 - \mu^2)(w/t)^2}$$

Case	Boundary condition	Type of stress	Value of k for long plate
(a)	s.s. / s.s. s.s. / s.s	Compression	4.0
(b)	Fixed / s.s. s.s. / Fixed	Compression	6.97
(c)	s.s. / s.s. s.s. / Free	Compression	0.425
(d)	Fixed / s.s. s.s. / Free	Compression	1.277
(e)	Fixed / s.s. s.s. / s.s.	Compression	5.42
(f)	s.s / s.s. s.s. / s.s.	Shear	5.34
(g)	Fixed / Fixed Fixed / Fixed	Shear	8.98
(h)	s.s. / s.s. s.s. / s.s.	Bending	23.9
(i)	Fixed / Fixed Fixed / Fixed	Bending	41.8

value E_s is the secant modulus. It has been used in the "Specification for the Design of Cold-Formed Stainless Steel Structural Members."[1.160,3.4,3.5,3.11] Additional information on local buckling coefficients and plasticity reduction factors can be found in Refs. 3.1, 3.6–3.11.

Postbuckling Strength and Effective Design Width. Unlike one-dimensional structural members such as columns, stiffened compression elements will not collapse when the buckling stress is reached. An additional load can be carried by the element after buckling by means of a redistribution of stress. This phenomenon is known as postbuckling strength and is most pronounced for elements with large w/t ratios.

The mechanism of the postbuckling action can easily be visualized from a square plate model as shown in Fig. 3.13. It represents the portion *abcd* of the compression flange of the hat section illustrated in Fig. 3.9. As soon as the plate starts to buckle, the horizontal bars in the grid of the model will act as tie rods to counteract the increasing deflection of the longitudinal struts.

In the plate, the stress distribution is uniform prior to its buckling, as shown in Fig. 3.14a. After buckling, a portion of the prebuckling load of the center strip transfers to the edge portion of the plate. As a result, a nonuniform stress distribution is developed, as shown in Fig. 3.14b. The redistribution of stress continues until the stress at the edge reaches the yield point of the steel and then the plate begins to fail (Fig. 3.14c).

The postbuckling behavior of a plate can be analyzed by using large deflection theory. The following differential equation for large deflection buckling of a plate was introduced by von Karman in 1910:

$$\frac{\partial^4 \omega}{\partial x^4} + 2\frac{\partial^4 \omega}{\partial x^2\,\partial y^2} + \frac{\partial^4 \omega}{\partial y^4} = \frac{t}{D}\left(\frac{\partial^2 F}{\partial y^2}\frac{\partial^2 \omega}{\partial x^2} - 2\frac{\partial^2 F}{\partial x\,\partial y}\frac{\partial^2 \omega}{\partial x\,\partial y} + \frac{\partial^2 F}{\partial x^2}\frac{\partial^2 \omega}{\partial y^2}\right)$$

$$(3.22)$$

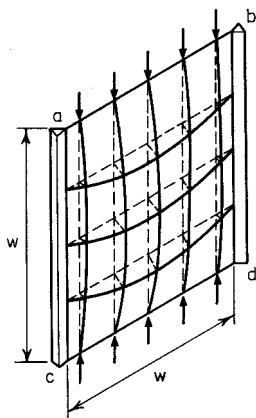where F is a stress function defining the median fiber stress of the plate, and

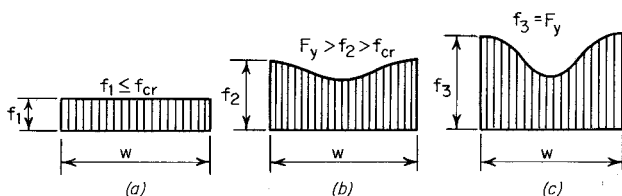**Figure 3.13** Square plate model for postbuckling action.[1.161]

Figure 3.14   Consecutive stages of stress distribution in stiffened compression elements.

$$f_x = \frac{\partial^2 F}{\partial y^2}$$

$$f_y = \frac{\partial^2 F}{\partial x^2}$$

$$\tau_{xy} = -\frac{\partial^2 F}{\partial x \, \partial y}$$

It has been found that the solution of the differential equation for large deflection theory has little application in practical design because of its complexity. For this reason, a concept of "effective width" was introduced by von Karman et al. in 1932.[3.12] In this approach, instead of considering the nonuniform distribution of stress over the entire width of the plate w, it is assumed that the total load is carried by a fictitious effective width b, subject to a uniformly distributed stress equal to the edge stress f_{max}, as shown in Fig. 3.15. The width b is selected so that the area under the curve of the actual nonuniform stress distribution is equal to the sum of the two parts of the equivalent rectangular shaded area with a total width b and an intensity of stress equal to the edge stress f_{max}, that is,

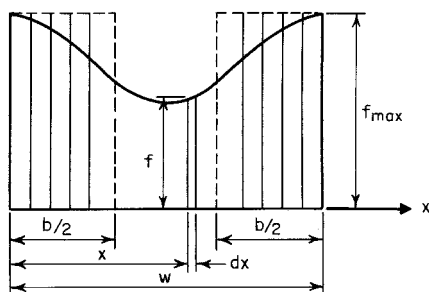$$\int_0^w f \, dx = b f_{max} \tag{3.23}$$

Figure 3.15   Effective width of stiffened compression element.

It may also be considered that the effective width b represents a particular width of the plate which just buckles when the compressive stress reaches the yield point of steel. Therefore for a long plate, the theoretical value of b may be determined as follows:

$$f_{cr} = F_y = \frac{\pi^2 E}{3(1 - \mu^2)(b/t)^2} \tag{3.24}$$

or

$$b = Ct \sqrt{\frac{E}{F_y}} = 1.9t \sqrt{\frac{E}{F_y}} \tag{3.25}$$

where

$$C = \frac{\pi}{\sqrt{3(1 - \mu^2)}} = 1.9 \tag{3.26}$$
$$\mu = 0.3$$

Equation (3.25) is the von Karman formula for the design of stiffened elements derived in 1932.

Whenever $w > b$,

$$f_{cr} = \frac{\pi^2 E}{3(1 - \mu^2)(w/t)^2} \tag{3.18}$$

or

$$w = Ct \sqrt{\frac{E}{f_{cr}}} \tag{3.27}$$

From Eqs. (3.25) and (3.27), the following relationship of b and w can be obtained:

$$\frac{b}{w} = \sqrt{\frac{f_{cr}}{F_y}} \tag{3.28}$$

Based on his extensive investigation on light-gage cold-formed steel sections, Winter indicated that Eq. (3.25) is equally applicable to the element in which the stress is below the yield point.[3.13] Therefore Eq. (3.25) can then be rewritten as

$$b = Ct \sqrt{\frac{E}{f_{max}}} \qquad (3.29)$$

where f_{max} is the maximum edge stress of the plate. It may be less than the yield point of steel.

In addition, results of tests previously conducted by Sechler and Winter indicate that the term C used in Eq. (3.29) depends primarily on the nondimensional parameter

$$\sqrt{\frac{E}{f_{max}}} \left(\frac{t}{w}\right) \qquad (3.30)$$

It has been found that a straight-line relationship exists between $\sqrt{E/f_{max}}$ (t/w) and the term C, as shown in Fig. 3.16. The following equation for the term C has been developed by Winter on the basis of his experimental investigation:[3.13, 3.14]

$$C = 1.9 \left[1 - 0.475 \left(\frac{t}{w}\right) \sqrt{\frac{E}{f_{max}}} \right] \qquad (3.31)$$

It should be noted that the straight line in Fig. 3.16 starts at a value of 1.9 for $\sqrt{E/f_{max}}(t/w) = 0$, which represents the case of an extremely large w/t ratio with relatively high stress. For this particular case, the experimental determinations are in substantial agreement with von Karman's original formula [Eq. (3.25)].

Consequently, in 1946 Winter presented the following modified formula for computing the effective width b for plates simply supported along both longitudinal edges:
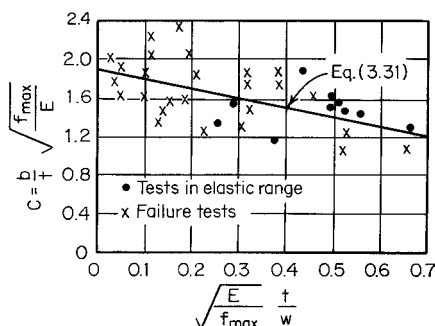

Figure 3.16   Experimental determination of effective width.[3.13]

$$b = 1.9t \sqrt{\frac{E}{f_{\max}}} \left[1 - 0.475 \left(\frac{t}{w}\right) \sqrt{\frac{E}{f_{\max}}} \right] \tag{3.32}$$

It should be noted from Eq. (3.32) that the effective width depends not only on the edge stress $f_{\max}$ but also on the w/t ratio.

Equation (3.32) may be written in terms of the ratio of $f_{cr}/f_{\max}$ as

$$\frac{b}{w} = \sqrt{\frac{f_{cr}}{f_{\max}}} \left(1 - 0.25 \sqrt{\frac{f_{cr}}{f_{\max}}} \right) \tag{3.33}$$

From the above equation it can be shown that a compressed plate is fully effective, $b = w$, when the ratio of w/t is less than

$$\left(\frac{w}{t}\right)_{\lim} = 0.95 \sqrt{\frac{E}{f_{\max}}} \tag{3.34}$$

and that the first wave occurs at a stress equal to $f_{cr}/4$.

In summary, it may be considered that Eqs. (3.32) and (3.33) are generalizations of Eqs. (3.25) and (3.28) in two respects: (1) by introducing $f_{\max}$ for F_y, the equations can be applied to service loads as well as to failure loads, and (2) by introducing empirical correction factors, the cumulative effects of various imperfections, including initial deviations from planeness, are accounted for.

During the period from 1946 to 1968, the AISI design provision for the determination of the effective design width was based on Eq. (3.32). A long-time accumulated experience has indicated that a more realistic equation, as shown in Eq. (3.35), may be used in the determination of the effective width b:[1.161]

$$b = 1.9t \sqrt{\frac{E}{f_{\max}}} \left[1 - 0.415 \left(\frac{t}{w}\right) \sqrt{\frac{E}{f_{\max}}} \right] \tag{3.35}$$

Figure 3.17 illustrates the correlation between Eq. (3.35) and the results of tests conducted by Sechler and Winter. It should be noted that Sechler's tests were carried out on disjointed single sheets, not on structural shapes. Hence the imperfect edge conditions account for many low values in his tests.

In view of the fact that Eq. (3.35) correlates well with the stiffened compression elements with little or no rotational restraints along both longitudinal edges (i.e., $k = 4$), this equation can be generalized as shown below for determining the effective width of stiffened elements having different rotational edge restraints:
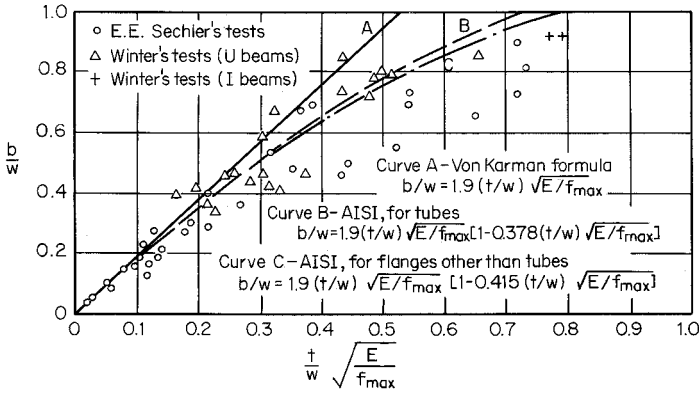
Figure 3.17   Correlation between test data on stiffened compression elements and design criteria.[3.15]

$$b = 0.95t \sqrt{\frac{kE}{f_{max}}} \left[1 - 0.208 \left(\frac{t}{w} \right) \sqrt{\frac{kE}{f_{max}}} \right] \qquad (3.36)$$

where k is the local buckling coefficient. The above equation is being used in the Canadian standard.[1.177]

In Ref. 3.16, Johnson pointed out that Eq. (3.36) can be modified for the effects of inelastic buckling by replacing E by ηE, where η is a plasticity reduction factor.

It should be noted that Eq. (3.35) may be rewritten in terms of the f_{cr}/f_{max} ratio as follows:

$$\frac{b}{w} = \sqrt{\frac{f_{cr}}{f_{max}}} \left(1 - 0.22 \sqrt{\frac{f_{cr}}{f_{max}}} \right) \qquad (3.37)$$

Therefore, the effective width, b, can be determined as

$$b = \rho w \qquad (3.38)$$

where ρ = reduction factor

$$= (1 - 0.22/\sqrt{f_{max}/f_{cr}})/\sqrt{f_{max}/f_{cr}}$$

$$= (1 - 0.22/\lambda)/\lambda \le 1 \qquad (3.39)$$

In Eq. (3.39), λ is a slenderness factor determined below.

$$\lambda = \sqrt{f_{max}/f_{cr}} = \sqrt{f_{max}[12(1 - \mu^2)(w/t)^2]/(k\pi^2 E)}$$
$$= (1.052/\sqrt{k})(w/t)\sqrt{f_{max}/E} \tag{3.40}$$

in which k, w/t, f_{max}, and E were previously defined. The value of μ was taken as 0.3.

Figure 3.18 shows the relationship between ρ and λ. It can be seen that when $\lambda \leq 0.673$, $\rho = 1.0$.

Based on Eqs. (3.38) through (3.40), the 1986 edition of the AISI Specification adopted the following nondimensional format in Sec. B2.1 for determining the effective design width, b, for uniformly compressed stiffened elements.[3.17,3.18] The same design equations are used in the 1996 edition of the AISI Specification.

a. *Strength* (*Load Capacity*) *Determination*

$$\text{1. When } \lambda \leq 0.673, \qquad b = w \tag{3.41}$$

$$\text{2. When } \lambda > 0.673, \qquad b = \rho w \tag{3.42}$$

where b = effective design width of uniformly compressed element for strength determination

w = flat width of compression element

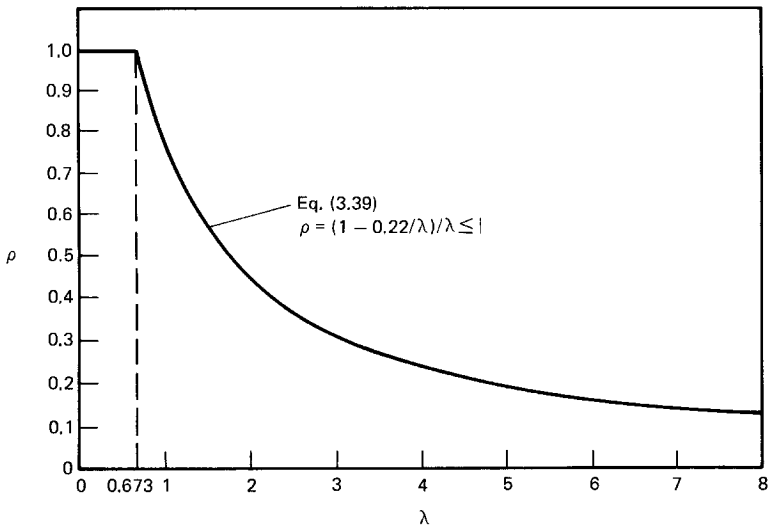ρ = reduction factor determined from Eq. (3.39):

Figure 3.18 Reduction factor, ρ, vs. slenderness factor, λ.

$$\rho = \left(1 - \frac{0.22}{\lambda}\right) \Big/ \lambda \leq 1 \tag{3.43}$$

where λ = plate slenderness factor determined from Eq. (3.44):

$$\lambda = \frac{1.052}{\sqrt{k}} \left(\frac{w}{t}\right) \sqrt{\frac{f}{E}} \tag{3.44}$$

where k = plate buckling coefficient
 = 4.0 for stiffened elements supported by a web on each longitudinal edge as shown in Fig. 3.19
t = thickness of compression element
E = modulus of elasticity
f = maximum compressive edge stress in the element without considering the safety factor

Figure 3.20 is a graphic presentation of Eqs. (3.43) and (3.44) plotted for $k = 4.0$ and $E = 29,500$ ksi (203 GPa). It can be used for determination of the effective design width of stiffened elements with a given w/t ratio and compressive stress. Note that the limiting w/t ratio, $(w/t)_{\text{lim}}$, is $219.76/\sqrt{f}$. When $w/t \leq (w/t)_{\text{lim}}$, no reduction of the flat width is required for stiffened elements supported by a web on each longitudinal edge.
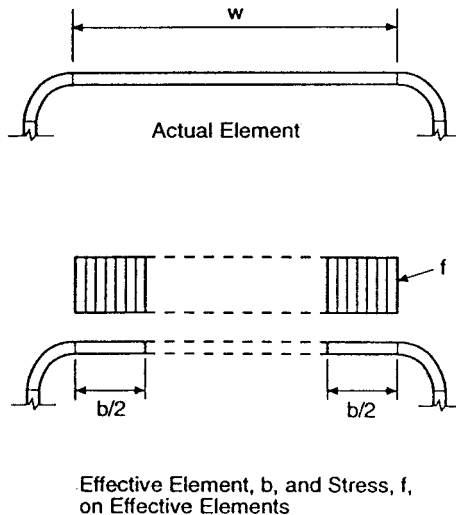

Effective Element, b, and Stress, f,
on Effective Elements

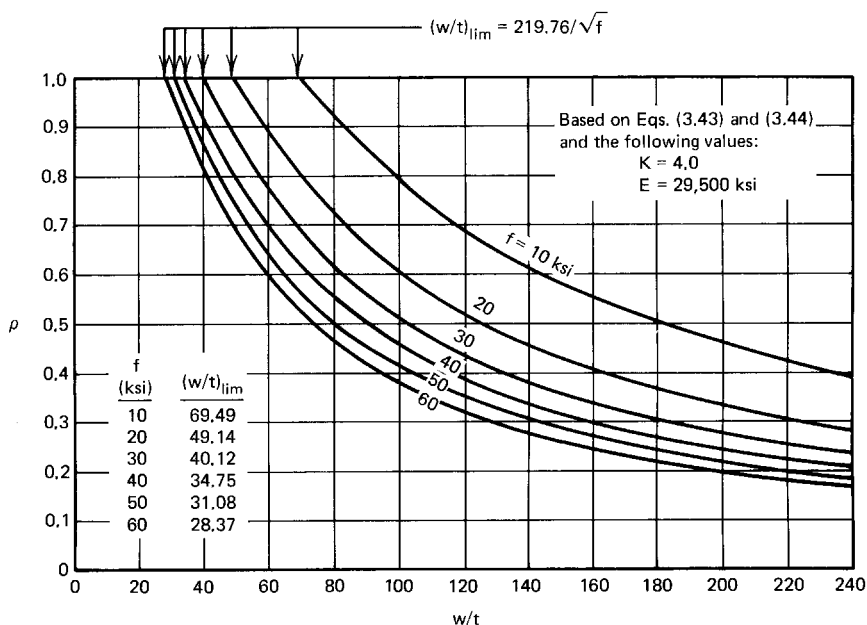**Figure 3.19**   Stiffened elements.[1.314]

Figure 3.20   Reduction factory ρ for stiffened compression elements.

b. *Deflection Determination*

$$\text{1. When } \lambda \leq 0.673, \qquad b_d = w \qquad\qquad (3.45)$$

$$\text{2. When } \lambda > 0.673, \qquad b_d = \rho w \qquad\qquad (3.46)$$

where b_d = effective design width of compression element for deflection determination

w = flat width of compression element

ρ = reduction factor determined from Eq. (3.43)

λ = plate slenderness factor determined from Eq. (3.47):

$$\lambda = (1.052/\sqrt{k})(w/t)(\sqrt{f_d/E}) \qquad (3.47)$$

f_d = compressive stress computed on the basis of the effective section for deflection determination

k, t, and E are the same as that defined above for strength determination.

The above method (Eqs. 3.45 through 3.47) can be used to obtain a conservative effective width, b_d, for deflection calculation. It is included in Sec. B2.1(b) of the AISI Specification as Procedure I. Figure 3.20 can also be used

for the determination of the effective width for deflection calculation using this Procedure.

For stiffened compression elements supported by a web on each longitudinal edge, a study conducted by Weng and Pekoz indicated that Eqs. (3.48) through (3.51) can yield a more accurate estimate of the effective width, b_d, for deflection analysis. The following equations are included in the AISI Specification as Procedure II:

When $\lambda \leq 0.673$,

$$\rho = 1 \qquad\qquad (3.48)$$

When $0.673 < \lambda < \lambda_c$,

$$\rho = (1.358 - 0.461/\lambda)/\lambda \qquad\qquad (3.49)$$

When $\lambda \geq \lambda_c$,

$$\rho = (0.41 + 0.59\sqrt{F_y/f_d} - 0.22/\lambda)/\lambda \qquad\qquad (3.50)$$

where $\lambda_c = 0.256 + 0.328 \, (w/t)\sqrt{F_y/E}$ (3.51)

and λ is defined by Eq. (3.47).

Example 3.1   For the given thin plate supported along both longitudinal edges as shown in Fig. 3.21, determine the following items:

1. The critical buckling stress.
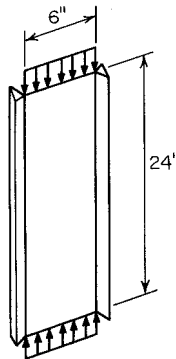2. The critical buckling load.

Figure 3.21   Example 3.1.

3. The ulitmate load.
   Given:

   $$t = 0.06 \text{ in.}$$
   $$E = 29.5 \times 10^3 \text{ ksi}$$
   $$F_y = 50 \text{ ksi}$$
   $$\mu = 0.3$$

Solution

1. *Critical Buckling Stress* [Eq. (3.16)]. Since the aspect ratio is 4, use $k = 4.0$ as follows:

   $$
   \begin{aligned}
   f_{cr} &= \frac{k\pi^2 E}{12(1 - \mu^2)(w/t)^2} \\
   &= \frac{4(3.1416)^2 \times (29.5 \times 10^3)}{12(1 - 0.3^2)(6/0.06)^2} \\
   &= 10.665 \text{ ksi}
   \end{aligned}
   $$

2. *Critical Buckling Load.* $P_{cr} = Af_{cr} = 6(0.06) \times (10.665) = 3.839$ kips
3. *Ultimate Load.* The ultimate load can be computed from the effective width b determined by Eq. (3.41) or Eq. (3.42). From Eq. (3.44),

   $$
   \begin{aligned}
   \lambda &= \frac{1.052}{\sqrt{k}} \left(\frac{w}{t}\right) \sqrt{\frac{f}{E}} \\
   &= \frac{1.052}{\sqrt{4}} \left(\frac{6.0}{0.06}\right) \sqrt{\frac{50}{29,500}} \\
   &= 2.166
   \end{aligned}
   $$

   Since $\lambda > 0.673$, $b = \rho w$, where

   $$
   \begin{aligned}
   \rho &= \left(1 - \frac{0.22}{\lambda}\right) \bigg/ \lambda \\
   &= \left(1 - \frac{0.22}{2.166}\right) \bigg/ 2.166 \\
   &= 0.415
   \end{aligned}
   $$

Therefore, the effective design width and the ultimate load are computed as follows:

$$b = \rho w = 0.415(6.0) = 2.49 \text{ in.}$$

$$P_{\text{ult}} = A_{\text{eff}}F_y = 2.49(0.06)(50) = 7.47 \text{ kips}$$

It is seen that here the ultimate load of 7.47 kips is almost twice the critical buckling load of 3.839 kips.

Example 3.2 Compute the effective design width of the compression flange of the beam shown in Fig. 3.22.

a. For strength determination—assume that the compressive stress in the flange without considering the safety factor is 25 ksi.
b. For deflection determination—assume that the compressive stress in the flange under the service or allowable load is 15 ksi.

Solution

1. *Strength Determination.* As the first step, compute λ by using Eq. (3.44) with the following values:

$$k = 4.0$$

$$w = 15.00 - 2(R + t)$$

$$= 15.00 - 2(0.1875 + 0.105) = 14.415 \text{ in.}$$

$$\frac{w}{t} = \frac{14.415}{0.105} = 137.286$$

$$f = 25 \text{ ksi}$$

$$E = 29,500 \text{ ksi}$$

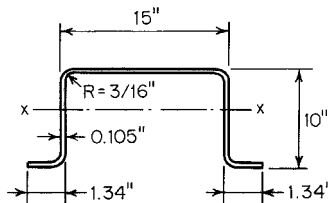$$\lambda = \frac{1.052}{\sqrt{4}}(137.286)\sqrt{\frac{25}{29,500}} = 2.102$$

Figure 3.22 Example 3.2.

Since $\lambda > 0.673$, compute the reduction factor ρ according to Eq. (3.43):

$$\rho = \left(1 - \frac{0.22}{2.102}\right)\bigg/ 2.102 = 0.426$$

Therefore, the affective design width for strength determination is

$$b = \rho w = (0.426)(14.415) = 6.14 \text{ in.}$$

2. *Deflection Determination.* By using Eq. (3.47) and $f_d = 15$ ksi,

$$\lambda = \frac{1.052}{\sqrt{4}}(137.286)\sqrt{\frac{15}{29{,}500}} = 1.628$$

Since $\lambda > 0.673$,

$$\rho = \left(1 - \frac{0.22}{1.628}\right)\bigg/ 1.628 = 0.531$$

Therefore, the effective design width for deflection determination is

$$b = \rho w = (0.531)(14.415) = 7.654 \text{ in.}$$

Example 3.3   Calculate the effective width of the compression flange of the box section (Fig. 3.23) to be used as a beam bending about the *x*-axis. Use $F_y = 33$ ksi. Assume that the beam webs are fully effective and that the bending moment is based on initiation of yielding.

Solution.   Because the compression flange of the given section is a uniformly compressed stiffened element, which is supported by a web on each longitudinal edge, the effective width of the flange for strength determination can be computed by using Eqs. (3.41) through (3.44) with $k = 4.0$.

Assume that the bending strength of the section is based on *Initiation of Yielding* (Procedure I of Sec. C3.1.1 of the AISI specification), $\bar{y} \geq 2.50$ in. Therefore, the slenderness factor λ for $f = F_y$ can be computed from Eq. (3.44). i.e.,

$$\lambda = (1.052/\sqrt{k})(w/t)\sqrt{f/E}$$
$$= (1.052/\sqrt{4.0})(6.1924/0.06)\sqrt{33/29{,}500} = 1.816$$

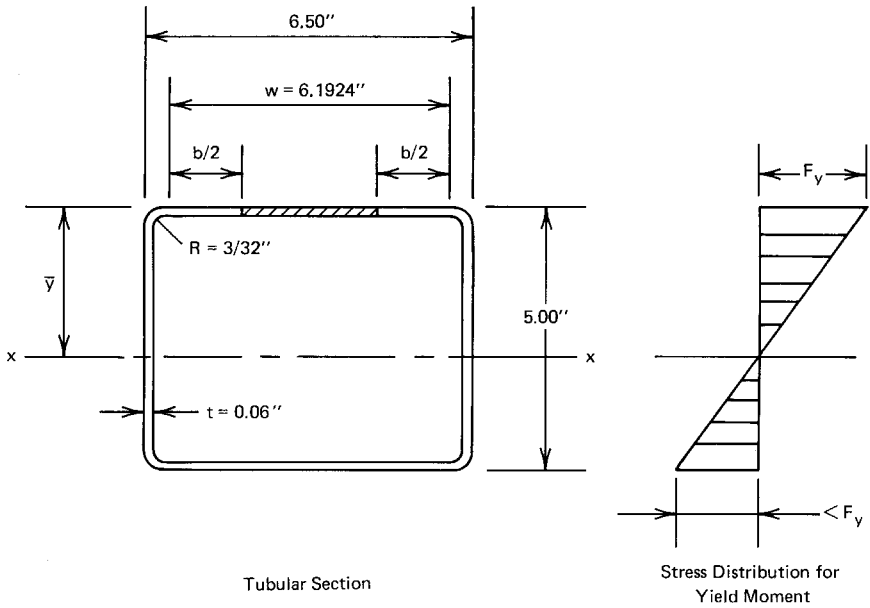Since $\lambda > 0.673$, use Eqs. (3.42) and (3.43) to compute the effective width, b, as follows:

Figure 3.23   Example 3.3.

$$b = \rho w = [(1 - 0.22/\lambda)/\lambda]w$$
$$= [(1 - 0.22/1.816)/1.816](6.1924) = 3.00 \text{ in.}$$

The above discussion on the structural design of stiffened compression elements is based on the AISI Specification.[1.314] In other countries the design equations and methods for determining the effective design width may be different as compared with the AISI formulas. For example, in the Japanese Standard[1.186] the effective design width is independent of the flat-width ratio w/t. This approach is similar to Eq. (3.52), which was derived by Lind et al.[3.20, 3.21] on the basis of their statistical analysis of the available experimental results:

$$b = 1.64t \sqrt{\frac{E}{f_{\max}}} \tag{3.52}$$

Equation (3.52) was used in the Canadian Standard during the period from 1974 through 1984. However, the design equation used in the current Canadian Standard[1.177] would provide the same effective design width as permitted by the AISI formula for stiffened compression elements.

In the British Standard the effective design width is determined by the w/t ratio and the design equations given in Ref. 1.194. For the design of steel decks and panels, European recommendations[1.209] have adopted Winter's formula as given in Eqs. (3.38) to (3.40). In Refs. 1.183, 1.184, and 3.22 the French recommendations give an effective design width similar to that permitted by the AISI Specification.

The effective design widths of the stiffened compression element as determined by several design specifications are compared in Fig. 3.24. Reference 1.147 includes comparisons of different specifications being used in Australia, China, East Europe, Japan, North America, and West Europe. Additional information on effective design width can be found in Refs. 3.23 to 3.37.

Influence of Initial Imperfection on Effective Design Width. The load-carrying capacity of stiffened compression elements is affected by the initial imperfection of the plate. The larger the initial imperfection, the smaller the capacity.

The influence of initial imperfection on the effective design width has previously been studied by Hu et al.[3.38] and by Abdel-Sayed.[3.39] Figure 3.25 shows the theoretical ratio of effective width to actual width b/w affected by various values of initial imperfections. Imperfect plates have also been studied
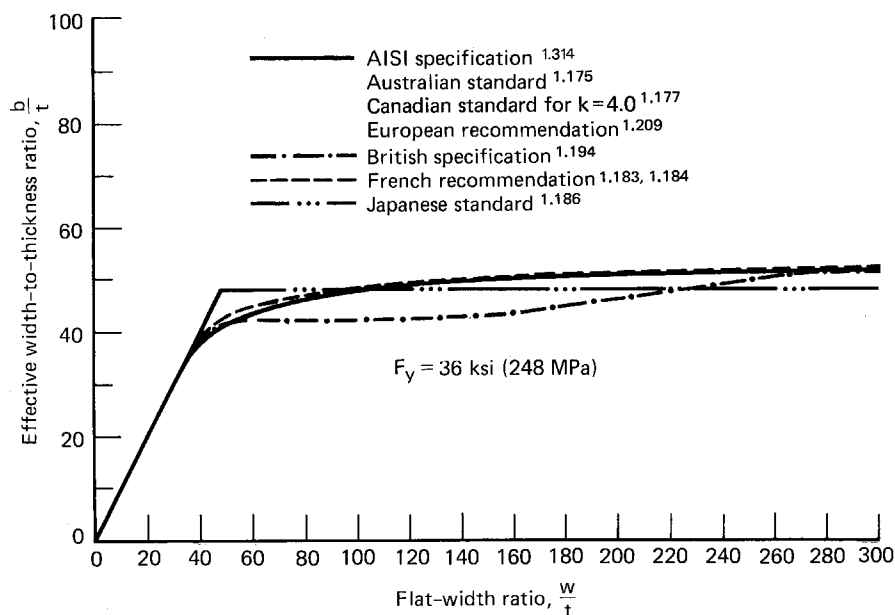

Figure 3.24 Comparison of effective design widths for load determination by using various design specifications.
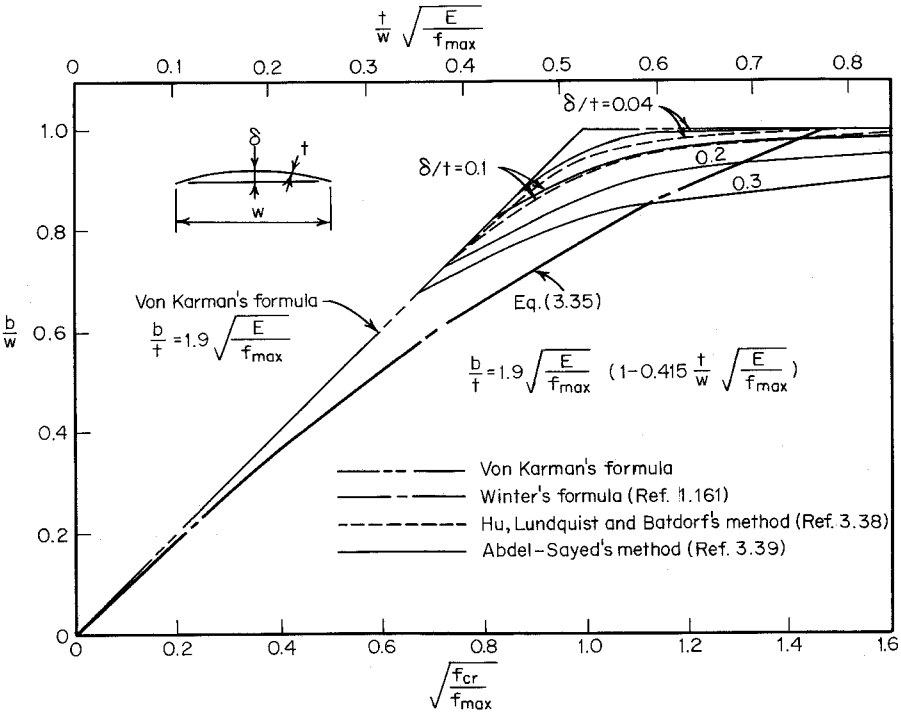
Figure 3.25   Effect of initial imperfection on effective design width.

extensively by Dawson and Walker,[3.40] Sherbourne and Korol,[3.41] Hancock,[3.42] and Maquoi and Rondal.[3.43]

Influence of Impact Loading on Effective Design Width. Previous discussion on effective width was concerned with the compression elements subjected to static loading. This type of loading condition is primarily applicable to the design of cold-formed steel members used in building construction.

As indicated in Art. 1.1, cold-formed steel members are also used in car bodies, railway coaches, various types of equipment, storage racks, highway products, and bridge construction, all of which are subjected to dynamic loads. Since members subjected to dynamic loads behave differently than those subjected to static loads, the question arises as to whether direct application of the AISI design criteria based on static loading is appropriate. In order to develop the necessary information on this topic, research work has been conducted by Culver and his collaborators at Carnegie-Mellon University to study analytically and experimentally the behavior of thin compression elements, beams, and columns subjected to dynamic or time-dependent loading.[3.44–3.49] It was found that the effective design width formula [Eq. (3.35)] satisfies both the static and the dynamic results to the same degree of

accuracy.[3.44, 3.46] Figure 3.26 shows the correlation between the test data and Eq. (3.35). In this figure β' is the ratio of the time duration of the stress pulse to the fundamental period of the compression flange treated as a simply supported plate. This subject has been studied at the University of Missouri-Rolla under a project on automotive structural components.[3.50, 2.67–2.71]

3.5.1.2 Beam Webs and Stiffened Elements with Stress Gradient

When a flexural member is subjected to bending moment, the compression portion of the web may buckle due to the compressive stress caused by bending. Figure 3.27 shows a typical pattern of bending failure of beam webs.

Prior to 1986, the design of beam webs in the United States was based on the full web depth and the allowable bending stress specified in the 1980 and earlier editions of the AISI Specification. In order to unify the design methods for webs and compression flanges, the "effective web depth approach" was adopted in the 1986 edition of the AISI Specification.[1.4]

Web Buckling Due to Bending Stress. The buckling of disjointed flat rectangular plates under bending with or without longitudinal loads has been investigated by Timoshenko, Schuette, McCulloch, Johnson, and Noel.[3.1, 3.2] The
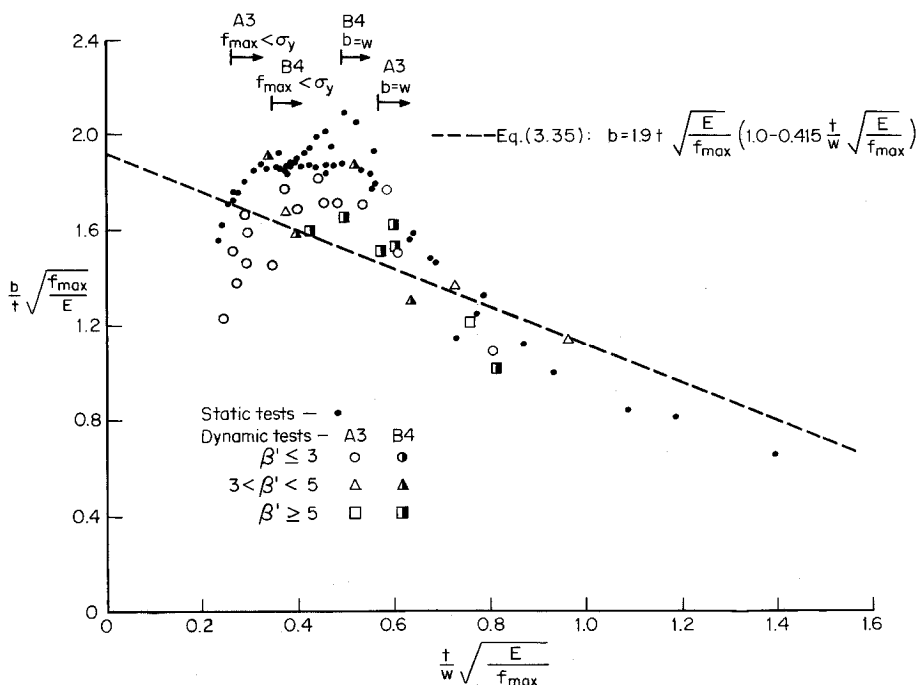

Figure 3.26 Correlation between effective design width formula and test data.[3.46]
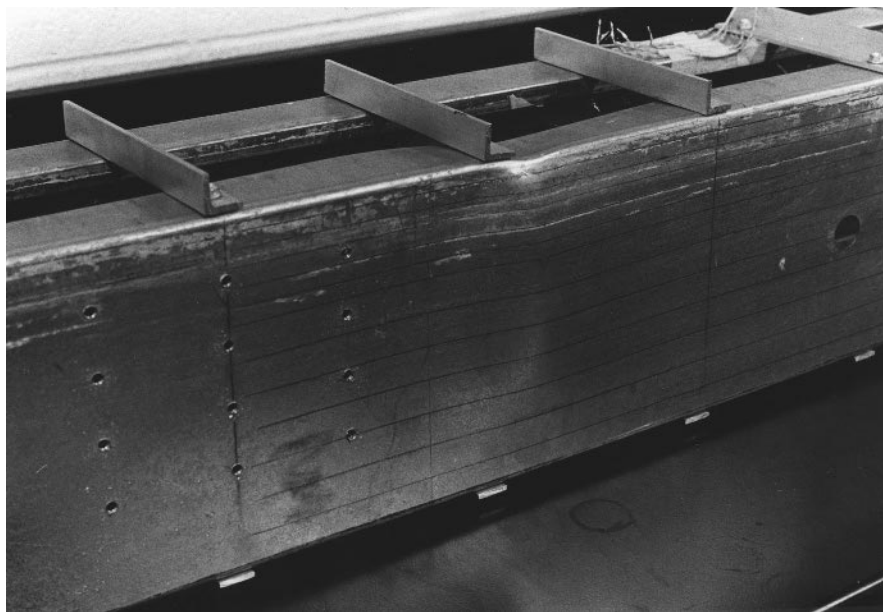
Figure 3.27   Typical bending failure pattern for channel sections.[3.60]

theoretical critical buckling stress for a flat rectangular plate under pure bending can be determined by

$$f_{cr} = \frac{k\pi^2 E}{12(1 - \mu^2)(h/t)^2} \qquad (3.53)$$

where h is the depth of the web and k is the buckling coefficient. For long plates the value of k was found to be 23.9 for simple supports and 41.8 for fixed supports as listed in Table 3.2. The relationships between the buckling coefficient and the aspect ratio a/h are shown in Fig. 3.28. When a simply supported plate is subjected to a compressive bending stress higher than the tensile bending stress, the buckling coefficient k is reduced according to the bending stress ratio f_c/f_t as shown in Fig. 3.29.[3.7]

In practice the bending strength of a beam web is not only affected by the web slenderness ratio h/t, the aspect ratio a/h, and the bending stress ratio f_c/f_t, but it also depends on the mechanical properties of material (E, F_y, and μ) and the interaction between flange and web components. In addition, the buckling coefficient k for the web is influenced by the actual edge restraint provided by the beam flange. Because the derivation of an exact analytical solution for the stability and the postbuckling strength of plate assemblies is extremely cumbersome, the AISI design criteria have been based on the results of tests.
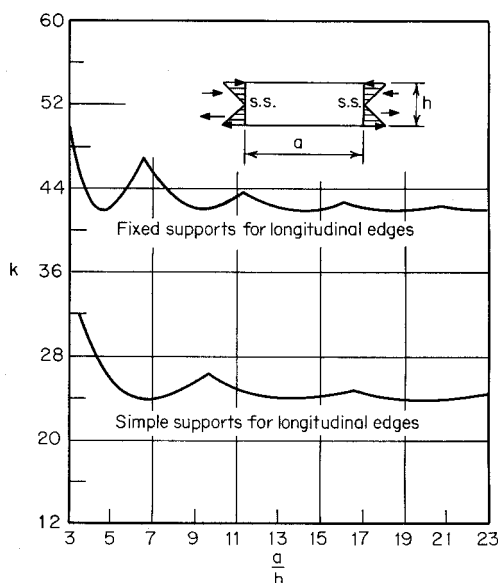
Figure 3.28 Bending buckling coefficients of plates vs. aspect ratio a/h.[3.1]

Postbuckling Strength and Effective Depth of Webs. In the past, several design formulas for computing the effective web depth have been developed by Berg-felt, Thomasson, Kallsner, Hoglund, DeWolf, Gladding, LaBoube, and Yu[3.51–3.61] to account for the actual buckling strength and the postbuckling behavior of beam webs. The effective web depth approach has been used in several specifications.[3.62, 3.63] In 1986, Cohen and Pekoz[3.64] evaluated the test results reported by LaBoube and Yu,[3.59–3.61] Cohen and Pekoz,[3.64] Kallsner,[3.54] Johnson,[3.65] He,[3.66] and van Neste,[3.67] and developed the needed design for-mulas for webs connected to stiffened, unstiffened, and partially stiffened compression flanges. Some statistical data on the correlation are given in Ref. 3.17.

Consequently, the following design equations were included in Sec. B2.3 of the 1986 edition of the AISI Specification for computing the effective width of webs and stiffened elements with stress gradient as shown in Fig. 3.30. The same equations are used in the 1996 edition of the AISI Specification.

a. *Strength (Load Capacity) Determination.* The effective width b_1 is de-termined from Eq. (3.54):

$$b_1 = b_e/(3 - \psi) \tag{3.54}$$

The effective width b_2 is determined from either Eq. (3.55) or Eq. (3.56) depending on the value of ψ:
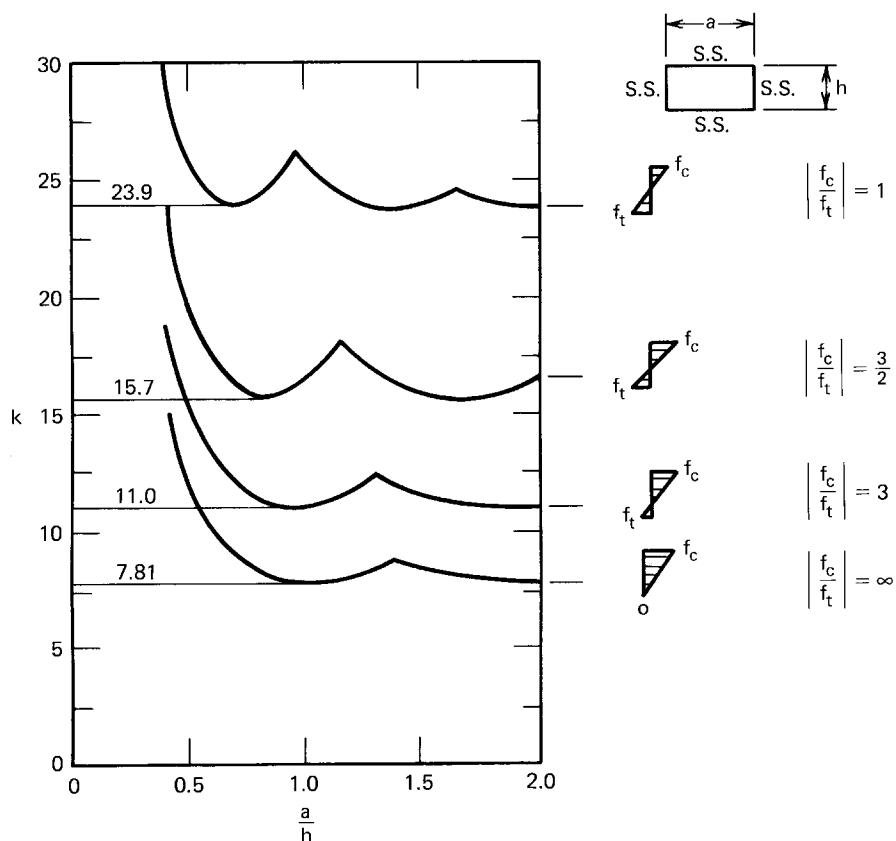
Figure 3.29 Buckling coefficient k for simply supported plates subjected to nonuniform longitudinal bending stress.[3.7] (*Reproduced with permission from Chatto & Windus, London.*)

$$\text{For } \psi \le -0.236, \qquad b_2 = b_e/2 \qquad (3.55)$$

$$\text{For } \psi > -0.236, \qquad b_2 = b_e - b_1 \qquad (3.56)$$

where b_e = effective width b computed from Eqs. (3.41) through (3.44) with the compressive stress f_1 substituted for f and with the buckling coefficient k computed as follows:

$$k = 4 + 2(1 - \psi)^3 + 2(1 - \psi) \qquad (3.57)$$

$$\psi = f_2/f_1 \qquad (3.58)$$
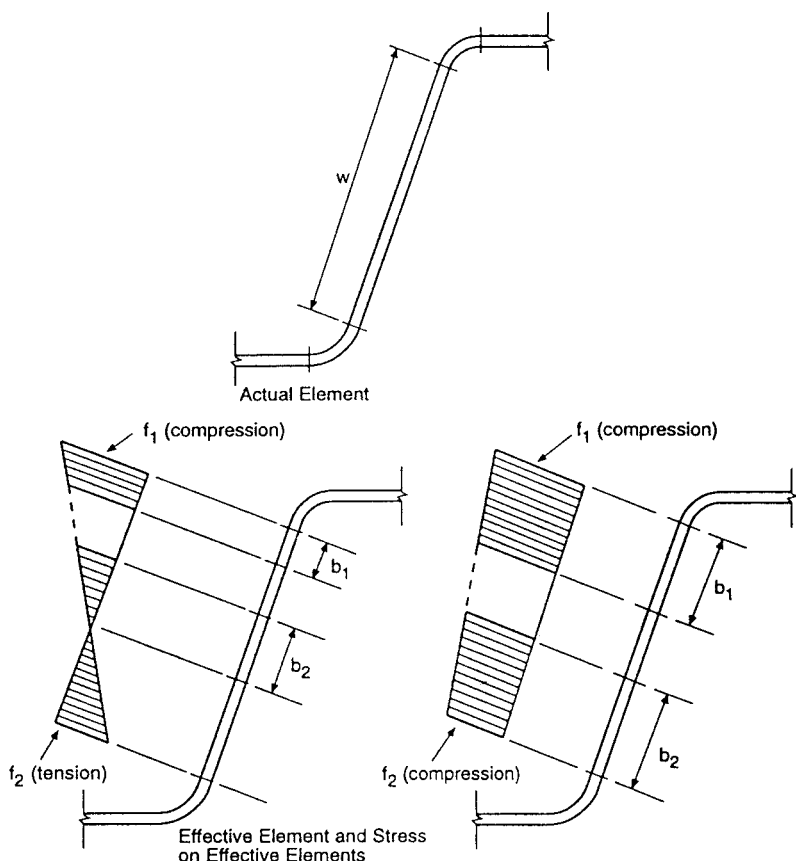
Figure 3.30 Stiffened elements with stress gradient and webs.[1.314]

f_1, f_2 = stresses shown in Fig. 3.30 calculated on the basis of the ef-
fective section. As shown in Fig. 3.30, f_1 is compression $(+)$
and f_2 can be either tension $(-)$ or compression $(+)$. In case
f_1 and f_2 are both compression, $f_1 \geq f_2$.

From Fig. 3.30, it can be seen that the summation of b_1 and b_2 should
not exceed the compression portion of the web calculated on the basis
of the effective section. When the value of $(b_1 + b_2)$ exceeds the com-
pression portion of the web, the web is fully effective.

b. *Deflection Determination.* The effective widths in computing deflections
at a given load shall be determined in accordance with Eqs. (3.54)
through (3.58) except that f_{d1} and f_{d2} are substituted for f_1 and f_2,
where f_{d1}, f_{d2} = computed stresses f_1 and f_2 as shown in Fig. 3.30.
Calculations are based on the effective section at the load for which
deflections are determined.

In 1998, the design equations in Sec. B2.3 were further studied by Schafer and Pekoz for improvements over a wider range of ψ values.[3.168] These research findings will be useful for future revision of the Specification.

Example 3.4   For the box section used in Example 3.3, it can be shown that the distance from the top compression fiber to the neutral axis is 2.908 in. if the beam webs are fully effective. Check these two beam webs and determine whether they are fully effective according to Eqs. (3.54) through (3.58) for load determination. Use $F_y = 33$ ksi.

Solution. From Fig. 3.31, stresses f_1 and f_2 are computed as follows:

$$f_1 = 33(2.754/2.908) = 31.25 \text{ ksi (compression)}$$

$$f_2 = 33(1.938/2.908) = 22.00 \text{ ksi (tension)}$$

According to Eqs. (3.57) and (3.58),

$$\psi = f_2/f_1 = -22.00/31.25 = -0.704$$

$$k = 4 + 2(1 - \psi)^3 + 2(1 - \psi)$$

$$= 4 + 2(1 + 0.704)^3 + 2(1 + 0.704) = 17.304$$

$$h = 4.693 \text{ in.}$$

$$h/t = 4.693/0.06 = 78.21 < 200 \text{ O.K.}$$

(see Art. 3.2 for the maximum h/t ratio)

The effective depth b_e of the web can be computed in accordance with Eqs. (3.41) through (3.44) for uniformly compressed stiffened elements with f_1 substituted for f, h/t substituted for w/t, and the k value computed above. From Eq. (3.44),
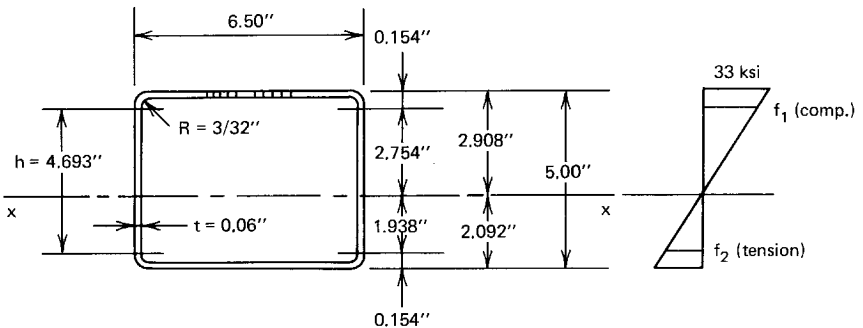

Figure 3.31   Example 3.4.

$$\lambda = (1.052/\sqrt{k})(h/t)\sqrt{f_1/E}$$

$$= (1.052/\sqrt{17.304})(78.21)\sqrt{31.25/29500} = 0.644$$

Since $\lambda < 0.673$, $b_e = h = 4.693$ in. Therefore

$$b_1 = b_e/(3 - \psi) = 4.693/(3 + 0.704) = 1.267 \text{ in.}$$

Because $\psi < -0.236$, from Eq. (3.55),

$$b_2 = b_e/2 = 2.347 \text{ in.}$$

$$b_1 + b_2 = 1.267 + 2.347 = 3.614 \text{ in.}$$

Since $b_1 + b_2 > 2.754$ in., the compression portion of the web is fully effective.

3.5.2 Unstiffened Compression Elements

3.5.2.1 *Unstiffened Elements under Uniform Compression*

Yielding. An unstiffened compression element, such as the flange of the I-shaped column shown in Fig. 3.32*a*, may fail in yielding if the column is short and its w/t ratio is less than a certain value. It may buckle as shown in Fig. 3.32*b* at a predictable unit stress, which may be less than the yield point, when its w/t ratio exceeds that limit.

Local Buckling. The elastic critical local buckling stress for a uniformly compressed plate can also be determined by Eq. (3.16), which gives

$$f_{cr} = \frac{k\pi^2 E}{12(1 - \mu^2)(w/t)^2} \tag{3.16}$$

where E = modulus of elasticity
 μ = Poisson's ratio
 w/t = flat-width-to-thickness ratio
 k = a constant depending upon conditions of edge support and the aspect ratio a/w

For a long rectangular plate simply supported along three sides, with one unloaded free edge as shown in Fig. 3.33, $k = 0.425$. However, when the restraining effect of the web is considered, k may be taken as 0.5 for the design of an unstiffened compression flange.

If the steel exhibits sharp yielding and an unstiffened compression element is ideally plane, the element will buckle at the critical stress determined by
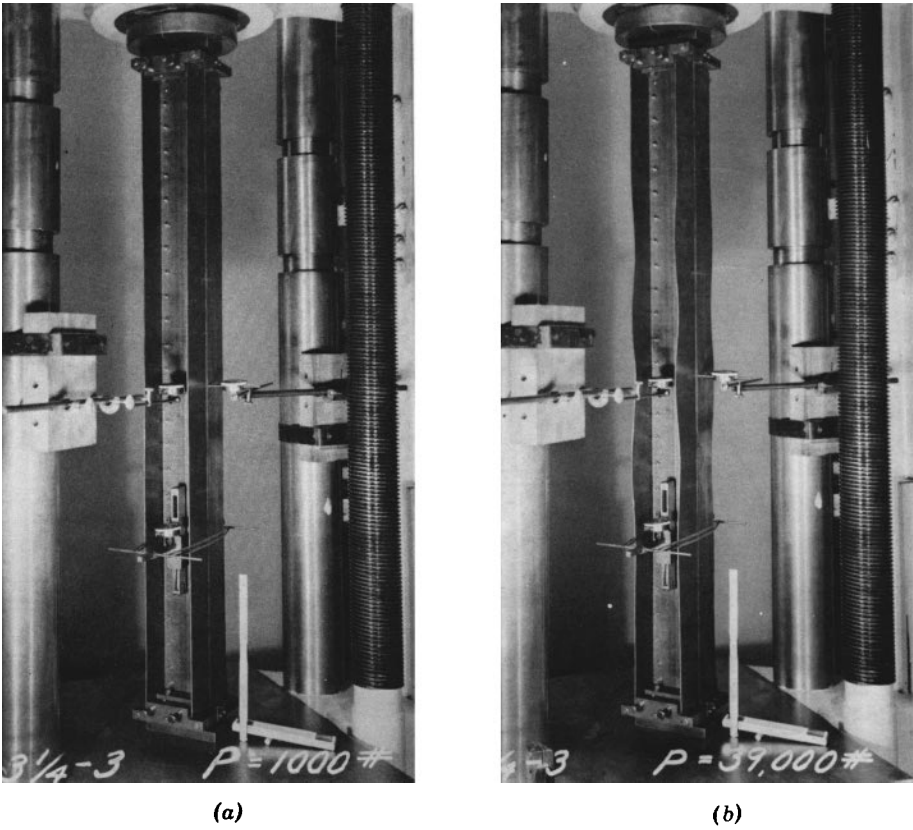
Figure 3.32   Local buckling of unstiffened compression elements.[1.6]
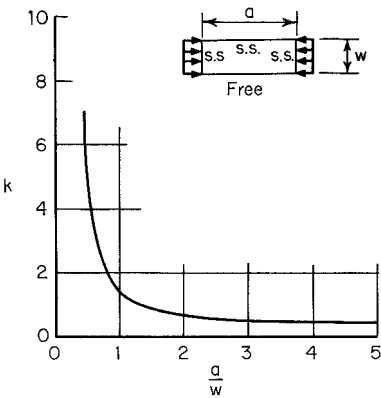

Figure 3.33   Buckling coefficient for rectangular plates simply supported along three sides with one unloaded edge free.[3.7]

Eq. (3.16) with the upper limit of F_y (Fig. 3.34). However, such ideal conditions may not exist, and an element with a moderate w/t ratio may buckle below the theoretical elastic buckling stress.

On the basis of experimental evidence a straight line B is drawn in Fig. 3.34, representing those stresses at which sudden and pronounced buckling occurred in the tests. The 1980 edition of the AISI Specification considered that the upper limit of such buckling is at $w/t = 63.3/\sqrt{F_y}$, and that the endpoint of the line is at $w/t = 144/\sqrt{F_y}$.[3.68]* In this region the element will buckle inelastically. If $w/t \leq 63.3/\sqrt{F_y}$, the element will fail by yielding represented by horizontal line A.

Additional experimental and analytical investigations on the local buckling of unstiffened compression elements in the elastic range have been conducted by Kalyanaraman, Pekoz, and Winter.[3.8,3.69–3.71] These studies considered the effects of initial imperfection and rotational edge restraint on the local buckling of compression elements. By using the procedure outlined in Ref. 3.8, a more realistic value of the local buckling coefficient can be calculated for compression elements of cold-formed steel members.

Figure 3.35 shows the correlation between the test data and the predicted maximum stresses.

Postbuckling Strength. When the w/t ratio of an unstiffened element exceeds about 25, the element distorts more gradually at a stress about equal to the theoretical local buckling stress (curve D in Fig. 3.34) and returns to its
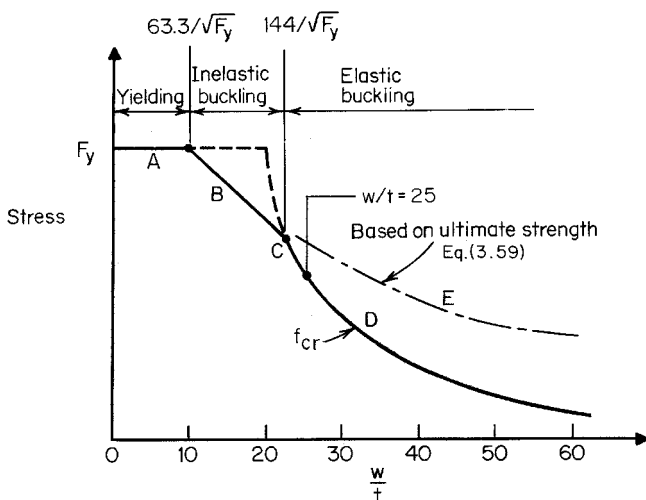
Figure 3.34 Maximum stress for unstiffened compression elements.[1.161]

*When the yield point of steel is less than 33 ksi (228 MPa), the endpoint of line B is $w/t = 25$.
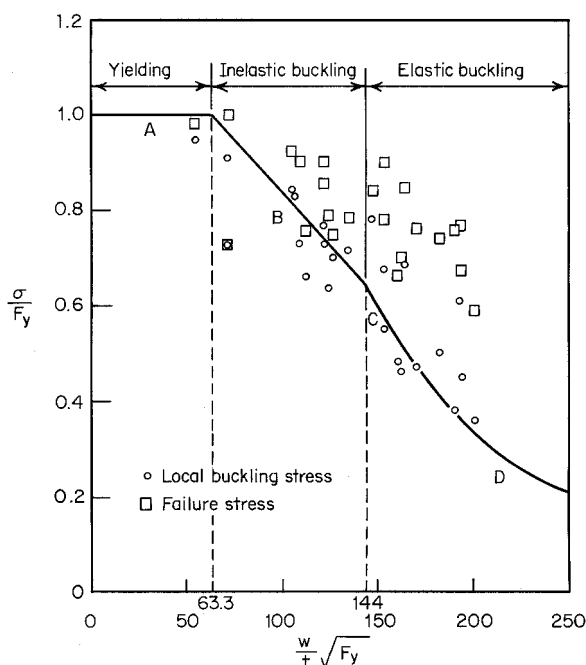
Figure 3.35 Correlation between test data on unstiffened compression elements and predicted maximum stress.[1.161,3.13]

original shape upon unloading because the buckling stress is considerably below the yield point. Sizable waving can occur without permanent set being caused by the additional stress due to distortion. Such compression elements show a considerable postbuckling strength.

Based upon the tests made on cold-formed steel sections having unstiffened compression flanges, the following equation has been derived by Winter for the effective width of unstiffened compression elements, for which the post-buckling strength has been considered:[3.13]

$$b = 0.8t \sqrt{\frac{E}{f_{max}}} \left[1 - 0.202 \left(\frac{t}{w} \right) \sqrt{\frac{E}{f_{max}}} \right] \tag{3.59}$$

where f_{max} is the stress in the unstiffened compression element at the supported edge (Fig. 3.36). Curve E in Fig. 3.34 is based on Eq. (3.59) and represents the ultimate strength of the element, which is considerably larger than the elastic buckling stress.

Based on a selected local buckling coefficient of $k = 0.5$, Eq. (3.59) can be generalized as follows:
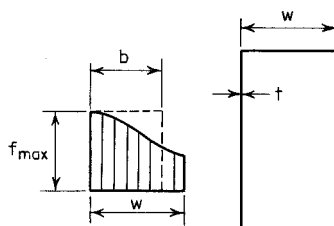
Figure 3.36 Effective width of unstiffened compression element.

$$b = 1.13t \sqrt{\frac{kE}{f_{max}}} \left[1 - 0.286 \left(\frac{t}{w} \right) \sqrt{\frac{kE}{f_{max}}} \right] \tag{3.60}$$

where k is the local buckling coefficient for unstiffened compression elements. Figure 3.37 shows a comparison between Eq. (3.36) for stiffened elements and Eq. (3.60) for unstiffened elements.

Equation (3.59) can also be written in terms of f_{cr}/f_{max} as

$$\frac{b}{w} = 1.19 \sqrt{\frac{f_{cr}}{f_{max}}} \left(1 - 0.3 \sqrt{\frac{f_{cr}}{f_{max}}} \right) \tag{3.61}$$
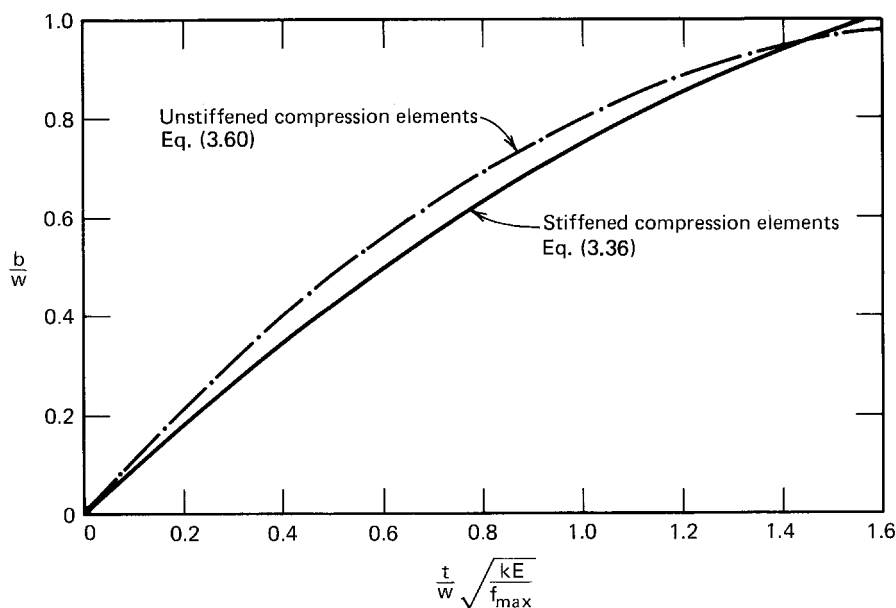
Figure 3.37 Comparison of generalized equations for stiffened and unstiffened compression elements.

where f_{cr} is the elastic local buckling stress determined by Eq. (3.16) with a value of $k = 0.5$. The above equation is practically identical to the empirical formula derived by Kalyanaraman et al. on the basis of some additional results of tests.[3.70]

Based on Eq. (3.61), the reduction factor ρ for the effective width design of unstiffened elements can be determined as follows:

$$\rho = 1.19(1 - 0.3/\lambda)/\lambda \qquad (3.62)$$

where λ is defined in Eq. (3.44).

Prior to 1986, it had been a general practice to design cold-formed steel members with unstiffened flanges by using the allowable stress design approach. The effective width equation was not used in the AISI Specification due to lack of extensive experimental verification and the concern for excessive out-of-plane distortions at service loads.

In the 1970s, the applicability of the effective width concept to unstiffened elements under uniform compression was studied in detail by Kalyanaraman, Pekoz, and Winter.[3.69–3.71] The evaluation of the test data using $k = 0.43$ is presented and summarized by Pekoz in Ref. 3.17, which shows that Eq. (3.43) gives a conservative lower bound to the test results of unstiffened compression elements. In addition to the strength determination, the same study also investigated the out-of-plane deformations in unstiffened elements. The results of theoretical calculations and test results on sections having unstiffened elements with $w/t = 60$ are presented in Ref. 3.17. It was found that the maximum amplitude of the out-of-plane deformations at failure can be twice the thickness as the w/t ratio approaches 60. However, the deformations are significantly less at service loads.

Based on the above reasons and justifications, the following provisions were included for the first time in Sec. B3.1 of the 1986 AISI Specification for the design of uniformly compressed unstiffened elements. The same approach is retained in the 1996 Specification.

a. *Strength* (*Load Capacity*) *Determination.* The effective widths, b, of unstiffened compression elements with uniform compression are determined in accordance with Eqs. (3.41) through (3.44) with the exception that k is taken as 0.43 and w as defined in Art. 3.2. See Fig. 3.5.

b. *Deflection Determination.* The effective widths used in computing deflections are determined in accordance with Eqs. (3.45) through (3.47) except that f_d is substituted for f and $k = 0.43$.

Example 3.5   Determine the critical buckling stress and critical buckling load for the thin sheet simply supported at three edges and one edge free, as shown in Fig. 3.38.
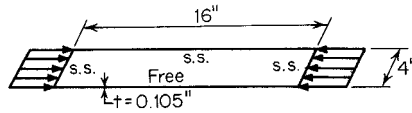
Figure 3.38   Example 3.5.

Solution

1. The critical buckling stress of the unstiffened compression element based on Eq. (3.16) is

$$f_{cr} = \frac{k\pi^2 E}{12(1 - \mu^2)(w/t)^2}$$

$$= \frac{0.425\pi^2(29.5 \times 10^3)}{12(1 - 0.3^2)(4/0.105)^2} = 7.808 \text{ ksi}$$

   In the above calculation, the value of $k = 0.425$ is slightly conservative (see Fig. 3.33).

2. The critical buckling load is

$$P_{cr} = Af_{cr} = 4(0.105)(7.808) = 3.279 \text{ kips}$$

Example 3.6   Calculate the effective width of the compression flange of the channel section (Fig. 3.39) to be used as a beam. Use $F_y = 33$ ksi. Assume that the beam web is fully effective and that lateral bracing is adequately provided.
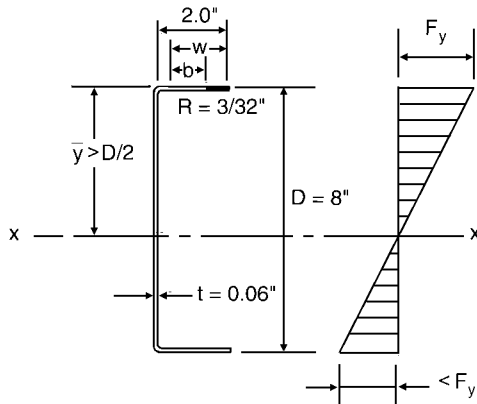
Figure 3.39   Example 3.6.

Solution. Because the compression flange of the given channel is a uniformly compressed unstiffened element, which is supported at only one edge parallel to the direction of the stress, the effective width of the flange for load determination can be computed by using Eqs. (3.41) through (3.44) with $k = 0.43$.

According to Eq. (3.44), the slenderness factor λ for $f = F_y$ is

$$\lambda = (1.052/\sqrt{k})(w/t)\sqrt{f/E}$$
$$= (1.052/\sqrt{0.43})(1.8463/0.06)\sqrt{33/29,500} = 1.651$$

Since $\lambda > 0.673$, use Eqs. (3.42) and (3.43) to calculate the effective width, b, as follows:

$$b = \rho w = [(1 - 0.22/\lambda)/\lambda]w$$
$$= [(1 - 0.22/1.651)/1.651](1.8463) = 0.97 \text{ in.}$$

3.5.2.2 Unstiffened Compression Elements with Stress Gradient

In concentrically loaded compression members and in flexural members where the unstiffened compression element is parallel to the neutral axis, the stress distribution is uniform before buckling. However, in some cases, such as the lips of the beam section shown in Fig. 3.40, which are turned in or out and are perpendicular to the neutral axis, the compression stress is not uniform but varies in proportion to the distance from the neutral axis.

An exact determination of the buckling condition of such elements is complex. When the stress distribution in the lip varies from zero to the maximum, the buckling coefficient k may be obtained from Fig. 3.41.[3.7] The local buckling of unstiffened elements under nonuniform compression is also discussed by Kalyanaraman in Ref. 3.169.

In Sec. B3.2 of the AISI Specification, the effective widths of unstiffened compression elements and edge stiffeners with stress gradient are treated as uniformly compressed elements with the stress f to be the maximum compressive stress in the element. This design approach was found to be adequate by Rogers and Schuster on the basis of the comparisons made with the available test data.[3.170]
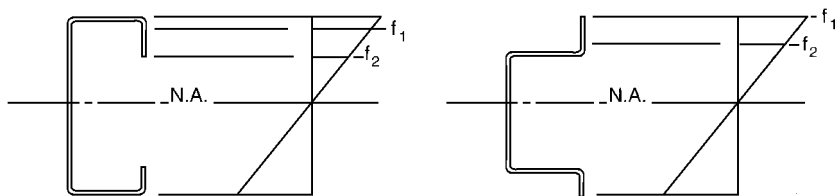
Figure 3.40   Unstiffened lip subjected to stress gradient.
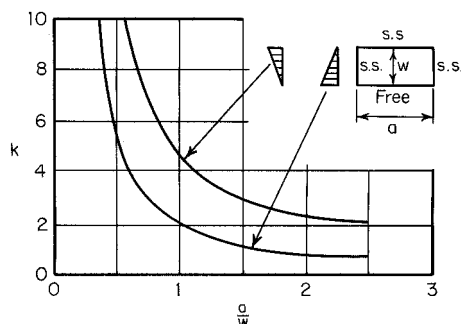
Figure 3.41 Buckling coefficient for unstiffened compression elements subjected to nonuniform stress.[3.7]

3.5.3 Uniformly Compressed Elements with Stiffeners

3.5.3.1 Uniformly Compressed Elements with One Intermediate Stiffener
In the design of cold-formed steel beams, when the width-to-thickness ratio of the stiffened compression flange is relatively large, the structural efficiency of the section can be improved by adding an intermediate stiffener, even though the area of the intermediate stiffener may be reduced. For example, if the stiffened compression flange of the hat section shown in Fig. 3.42 has a b_o/t ratio of 200 with $f = 33$ ksi (228 MPa), the efficiency of the compression flange as indicated by the factor ρ in Fig. 3.20 is only 27%. If one intermediate stiffener is added at the middle, the w/t ratio of each subelement may be assumed to be 95, and the factor ρ for subelements with the same stress is found to be 52%, which represents a significant improvement. Similar comparisons can be made for other values of w/t ratios.

The buckling behavior of rectangular plates with central stiffeners is discussed in Ref. 3.7. The load-carrying capacity of an element with a longitudinal intermediate stiffener has been studied by Höglund,[3.72] König,[3.73] König and Thomasson,[3.74] and Desmond, Pekoz, and Winter.[3.75–3.77]

Recently, this subject was studied by Bernard, Bridge, and Hancock.[3.171,3.172] Both local buckling and distortional buckling in the compression flange of profiled steel decks were discussed by the authors.
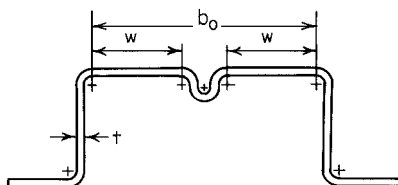
Figure 3.42 Section with multiple-stiffened compression elements.

As far as the design provisions are concerned, the 1980 edition of the AISI Specification included the requirements for the minimum moment of inertia of the intermediate stiffener for multiple-stiffened compression elements. When the size of the actual intermediate stiffener did not satisfy the required minimum moment of inertia, the load-carrying capacity of the member had to be determined either on the basis of a flat element disregarding the intermediate stiffener or through tests. For some cases, this approach could be unduly conservative.[3.17]

The AISI design provisions were revised in 1986 on the basis of the research findings reported in Refs. 3.75 through 3.77. According to Sec. B4.1 of the 1996 edition of the AISI Specification, the effective design width of subelements using only one intermediate stiffener at the middle is determined as follows:

a. *Strength (Load Capacity) Determination*

Case I: $b_o/t \leq S$ $\qquad$ (3.63)

$$I_a = 0 \text{ (no intermediate stiffener needed)} \qquad (3.64)$$

$$b = w \qquad (3.65)$$

$$A_s = A_s' \qquad (3.66)$$

Case II: $S < b_o/t < 3S$ $\qquad$ (3.67)

$$I_a = \{[50(b_o/t)/S] - 50\}t^4 \qquad (3.68)$$

b is calculated according to Eqs. (3.41) to (3.44), where

$$k = 3(I_s/I_a)^{1/2} + 1 \leq 4 \qquad (3.69)$$

$$A_s = A_s'(I_s/I_a) \leq A_s' \qquad (3.70)$$

Case III: $b_o/t \geq 3S$ $\qquad$ (3.71)

$$I_a = \{[128(b_o/t)/S] - 285\}t^4 \qquad (3.72)$$

b is calculated according to Eqs. (3.41) to (3.44), where

$$k = 3(I_s/I_a)^{1/3} + 1 \leq 4 \qquad (3.73)$$

$$A_s = A_s'(I_s/I_a) \leq A_s' \qquad (3.74)$$

In the above equations

A_s = reduced area of the stiffener to be used in computing the overall effective sectional properties; the centroid of the stiffener is to be considered located at the centroid of the full area of the stiffener, and the moment of inertia of the stiffener about its own centroidal axis is that of the full section of the stiffener

A'_s = effective area of the stiffener

b = effective width of subelement

b_o = overall flat width as shown in Fig. 4.43

I_a = adequate moment of inertia of stiffener, so that each subelement will behave as a stiffened element

I_s = moment of inertia of the full stiffener about its own centroidal axis parallel to the element to be stiffened

k = buckling coefficient

S = 1.28 $\sqrt{E/f}$ (3.75)
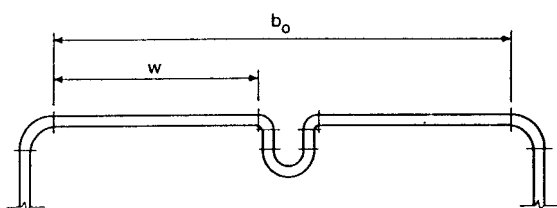
Actual Elements
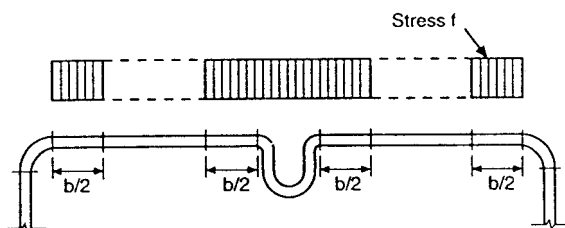
Effective Elements and Stress
on Effective Elements

Stiffener Section

Figure 3.43   Elements with one intermediate stiffener.[1.314]

t = thickness of compression element

w = flat width of subelement as shown in Fig. 3.43

b. *Deflection Determination.* The effective widths to be used for computing deflection are the same as those determined for strength except that f_d is substituted for f, where f_d is the computed compressive stress in the element being considered.

3.5.3.2 Uniformly Compressed Elements with an Edge Stiffener

An edge stiffener is used to provide a continuous support along a longitudinal edge of the compression flange to improve the buckling stress. Even though in most cases the edge stiffener takes the form of a simple lip (Fig. 3.44), other types of stiffeners, as shown in Fig. 3.45, can also be used for cold-formed steel members.[3.78, 3.173]

In order to provide necessary support for the compression element, the edge stiffener must possess sufficient rigidity. Otherwise it may buckle perpendicular to the plane of the element to be stiffened.

Both theoretical and experimental investigations on the local stability of flanges stiffened by lips and bulbs have been conducted in the past.[3.75–3.82] The design requirements included in the 1996 edition of the AISI Specification for uniformly compressed elements with an edge stiffener are based on the analytical and experimental investigations on adequately stiffened, partially stiffened elements, and unstiffened elements conducted by Desmond, Pekoz, and Winter[3.75, 3.76] with additional studies carried out by Pekoz and Cohen.[3.17] These AISI design provisions were developed on the basis of the critical buckling criterion and the ultimate strength criterion. According to Sec. B4.2 of the current (1996) AISI Specification, the effective width of the uniformly compressed elements with an edge stiffener can be calculated as follows:

a: *Strength* (*Load Capacity*) *Determination*

Case I: $w/t \leq S/3$ (3.76)
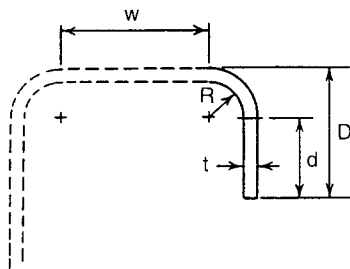
Figure 3.44 Edge stiffener.
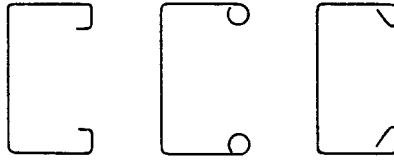
Figure 3.45 Edge stiffeners other than simple lip.[3.78]

$$I_a = 0 \quad \text{(no edge stiffener needed)} \tag{3.77}$$

$$b = w \tag{3.78}$$

$$d_s = d'_s \quad \text{for simple lip stiffener} \tag{3.79}$$

$$A_s = A'_s \quad \text{for other stiffener shapes} \tag{3.80}$$

Case II: $S/3 < w/t < S$ $\tag{3.81}$

$$I_a = 399\{[(w/t)/S] - \sqrt{k_u/4}\}^3 t^4 \tag{3.82}$$

$$n = 1/2$$

$$C_2 = I_s/I_a \leq 1 \tag{3.83}$$

$$C_1 = 2 - C_2 \tag{3.84}$$

b is calculated according to Eqs. (3.41) to (3.44), where

$$k = C_2^n(k_a - k_u) + k_u \tag{3.85}$$

$$k_u = 0.43$$

For simple lip stiffener with $140° \geq \theta \geq 40°$ and $D/w \leq 0.8$ where θ is as shown in Fig. 3.46,

$$k_a = 5.25 - 5\,(D/w) \leq 4.0 \tag{3.86}$$

$$d_s = C_2 d'_s \tag{3.87}$$

For stiffener shape other than simple lip,

$$k_a = 4.0$$

$$A_s = C_2 A'_s \tag{3.88}$$

Case III: $w/t \geq S$ $\tag{3.89}$
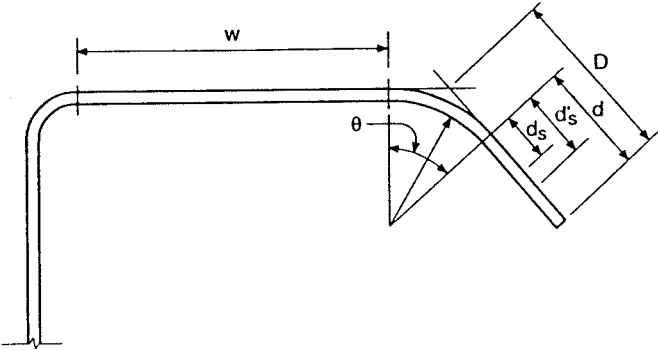
D, d = Actual stiffener dimensions

d'_s , d_s = Effective stiffener dimensions used
for calculating section properties
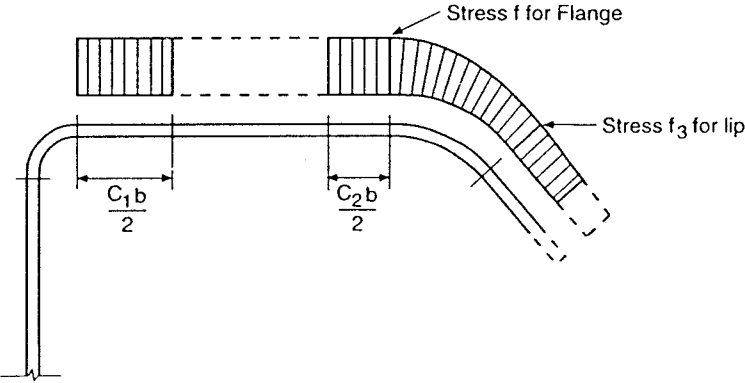
Effective Element and Stress on Effective Element and Stiffener

Figure 3.46   Compression element with an edge stiffener.[1.314]

$$I_a = \{[115(w/t)/S] + 5\}t^4 \qquad (3.90)$$

C_1, C_2, b, k, d_s, and A_s are calculated per Case II with $n = 1/3$.

In the above equations

A_s = reduced area of the edge stiffener to be used in computing the overall effective sectional properties

A_s' = effective area of the stiffener; the round corner between the stiffener and the element to be stiffened is not considered as a part of the stiffener

b = effective width of the uniformly compressed element

C_1 = coefficient defined in Fig. 3.46.

C_2 = coefficient defined in Fig. 3.46.

D = overall depth defined in Figs. 3.44 and 3.46

d = flat width of the edge stiffener defined in Figs. 3.44 and 3.46*

d_s = reduced effective width of the edge stiffener calculated according to the above formulas, is to be used in computing the overall effective sectional properties (see Fig. 3.46)

d_s' = effective width of the edge stiffener calculated according to Eqs. (3.41) to (3.44) with $k = 0.43$ (see Fig. 3.46)

I_a = adequate moment of inertia of the edge stiffener, so that the compression element will behave as a stiffened element

I_s = moment of inertia of the full edge stiffener about its own centroidal axis parallel to the element to be stiffened; the round corner between the stiffener and the element to be stiffened is not considered as a part of the stiffener

k = buckling coefficient

n = constant

S = $1.28\sqrt{E/f}$

  = w/t ratio of the fully effective stiffened element

t = thickness of compression element

w = flat width of compression element as shown in Figs. 3.44 and 3.46

For the simple stiffener shown in Fig. 3.46,

$$I_s = (d^3 t \sin^2 \theta)/12 \tag{3.91}$$

$$A_s' = d_s' t \tag{3.92}$$

The distribution of longitudinal stresses in compression elements with an edge stiffener are shown in Fig. 3.47 for all three cases.[3.17]

The above-described AISI design criteria are intended to account for the inability of the edge stiffener to prevent distortional buckling by

---

*Since proprietary tests conducted in 1989 revealed that lip lengths with a d/t ratio of greater than 14 gave unconservative results, the AISI Commentary includes an upper limit of $d/t = 14$ pending further research.
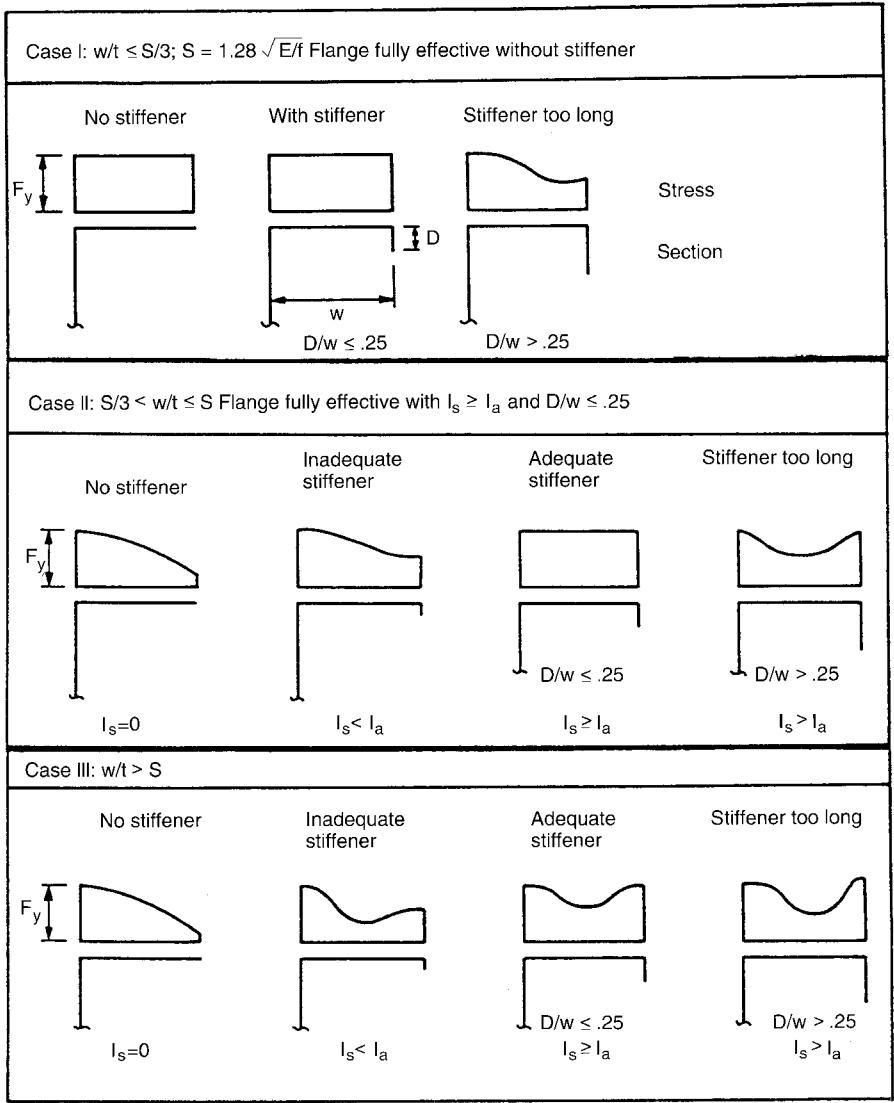
Figure 3.47   Edge stiffener design criteria.[3.17]

reducing the local buckling coefficient, k, for calculating the effective design width of the compression element. Because the empirical equations were derived on the basis of the tests of back-to-back sections with strong restraint against web buckling, recent research demonstrates that these AISI design equations may provide unconservative strength predictions for laterally braced beams and columns with edge stiffened flanges when the distortional buckling mode of the compression flange

is critical.[3.168] Additional discussions of distortional buckling are given in Art. 4.2.3.6 for beams and in Art. 5.7 for columns.

b. *Deflection Determination.* The effective widths to be used for computing deflection are the same as that determined for strength except that f_d is substituted for f, where f_d is the computed compressive stress in the element being considered.

Example 3.7 Compute the effective width of the compression flange of the channel section with an edge stiffener as shown in Fig. 3.48. Assume that the channel is used as a beam and that lateral bracing is adequately provided. Use $F_y = 33$ ksi. Also compute the reduced effective width of the edge stiffener.

Solution

A. *Effective Width of the Compression Flange.* Because the compression flange is an uniformly compressed element with an edge stiffener, its effective width should be determined according to Eqs. (3.76) through (3.90).

  As the first step, the flat width w, w/t ratio, and $S = 1.28\sqrt{E/f}$ are computed as follows:

$$w = 3.5 - 2(R + t) = 3.163 \text{ in.}$$

$$w/t = 3.163/0.075 = 42.17$$

$$S = 1.28\sqrt{E/f} = 1.28\sqrt{29{,}500/33} = 38.27$$

Since $w/t > S$, use Case III and Eq. (3.90) to compute the required moment of inertia of the edge stiffener I_a. By using Eq. (3.90),
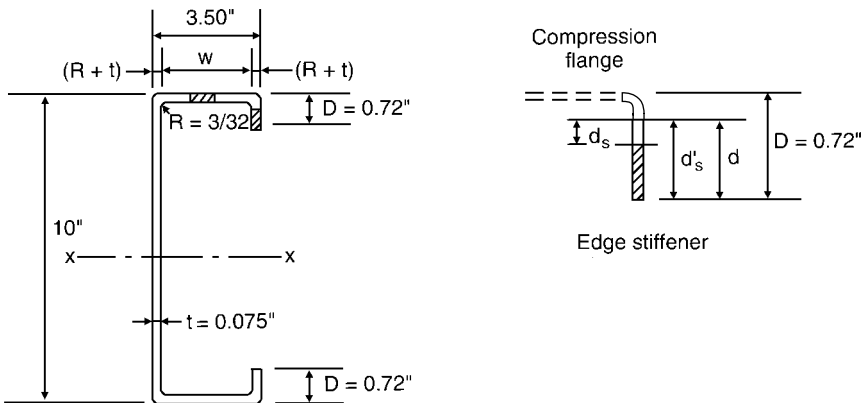
Figure 3.48 Example 3.7.

$$I_a = \{[115(w/t)/S] + 5\}t^4 = \{[115(42.17)/38.27] + 5\}(0.075)^4$$

$$= 131.7(0.075)^4 = 4.167 \times 10^{-3} \text{ in.}^4$$

For the simple lip edge stiffener used for the given channel section,

$$D = 0.720 \text{ in. (see Fig. 3.48)}$$

$$d = D - (R + t) = 0.551 \text{ in.}$$

$$d/t = 0.551/0.075 = 7.35 < 14 \text{ (maximum limit of the } d/t\text{)}$$

$$I_s = d^3t/12 = 1.047 \times 10^{-3} \text{ in.}^4$$

$$D/w = 0.72/3.163 = 0.228$$

By using Eq. (3.85), the buckling coefficient k can be computed as follows:

$$k = C_2^n(k_a - k_u) + k_u$$

where $C_2 = I_s/I_a = 0.251 < 1$
$\quad\quad\quad n = 1/3$
$\quad\quad\quad k_u = 0.43$

For a simple lip stiffener with $\theta = 90°$ and $D/w < 0.8$,

$$k_a = 5.25 - 5(D/w) = 4.11 > 4.0, \text{ use } k_a = 4.0$$

$$k = (0.251)^{1/3}(4 - 0.43) + 0.43 = 2.68$$

Use $k = 2.68$ to calculate the effective width of the compression flange as follows:

$$\lambda = (1.052/\sqrt{k})(w/t)\sqrt{f/E}$$

$$= (1.052/\sqrt{2.68})(42.17)\sqrt{33/29,500} = 0.906 > 0.673$$

The effective width of the compression flange is

$$b = \rho w = [(1 - 0.22/\lambda)/\lambda]w = [(1 - 0.22/0.906)/0.906](3.163)$$

$$= 2.643 \text{ in.}$$

B. *Reduced Effective Width of the Edge Stiffener.* The reduced effective width of the edge stiffener with stress gradient can be computed according to Sec. B3.2 of the AISI Specification. Using $k = 0.43$, $d/t = 7.35$, and a conservative $f = F_y$, the slenderness factor λ is

$$\lambda = (1.052/\sqrt{0.43})(7.35)\sqrt{33/29{,}500} = 0.394 < 0.673$$

Therefore, the effective width of the edge stiffener is

$$d'_s = d = 0.551 \text{ in.}$$

The reduced effective width of the edge stiffener is

$$d_s = C_2 d'_s = 0.251\,(0.551) = 0.138 \text{ in.}$$

3.5.3.3 Multiple-Stiffened Elements with More Than One Intermediate Stiffener and Edge Stiffened Elements with Intermediate Stiffeners

As discussed in Art. 3.5.3.1, the AISI design provisions for uniformly compressed elements with one intermediate stiffener were revised in 1986 on the basis of the 1981 Cornell research.[3.75–3.77] Because this Cornell project did not cover the multiple-stiffened elements with more than one intermediate stiffener and the edge stiffened elements with intermediate stiffeners, the 1986 and 1996 editions of the AISI Specification have the same design provisions as the 1980 edition of the AISI Specification for these cases.

In the current 1996 AISI Specification, the following minimum moment of inertia is required for an intermediate stiffener in Sec. B5 of the Specification:

$$I_{min} = [3.66\sqrt{(w/t)^2 - 0.136E/F_y}]t^4 \geq 18.4\,t^4 \tag{3.93}$$

where w/t = width-to-thickness ratio of the larger stiffened subelement. If the actual moment of inertia of the full intermediate stiffener, I_s, does not satisfy the minimum requirement of Eq. (3.93), the intermediate stiffener is disregarded for the determination of the effective width of stiffened elements. The problem involved in the determination of the load-carrying capacities of members having such inadequately stiffened compression elements is complex because the buckling wave tends to spread across the intermediate stiffener (overall or distortional buckling) rather than being limited to individual waves occurring on both sides of the stiffener (local buckling). Once such a spreading wave occurs, the stiffened compression element is hardly better than an element without intermediate stiffeners. For this reason, the sectional properties of members having inadequately stiffened compression flanges are determined on the basis of flat elements disregarding the intermediate stiffeners. The same is true for edge stiffened elements with intermediate stiffeners.

Effective Stiffeners. If a number of stiffeners were to be placed between webs at such distances that the resulting subelements have w/t ratios of a considerable magnitude, there would be a rapid cumulative loss of effectiveness

with increasing distance from the web. This is due to the fact that the slightly waved subelements and the intermediate stiffeners are not as effective as complete webs.

Section B5.a of the AISI Specification specifies that when the spacing of intermediate stiffeners between two webs is such that for the subelement between stiffeners $b < w$, only two intermediate stiffeners (those nearest each web) shall be considered effective.

Similarly, Sec. B5.b of the AISI Specification specifies that when the spacing of intermediate stiffeners between a web and an edge stiffener is such that for the subelement between stiffeners $b < w$, only one intermediate stiffener, that nearest the web, shall be considered effective.

If intermediate stiffeners are spaced so closely that for the elements between stiffeners $b = w$, all the stiffeners may be considered effective according to Sec. B5.c of the AISI Specification. In computing the flat width-to-thickness ratio of the entire multiple-stiffened element, such element shall be considered as replaced by an "equivalent element" without intermediate stiffeners whose width, b_o, is the full width between webs or from web to edge stiffener, and whose equivalent thickness, t_s, is determined as follows:

$$t_s = \sqrt[3]{12 I_{sf}/b_o} \qquad (3.94)$$

where I_{sf} = moment of inertia of the full area of the multiple-stiffened element, including the intermediate stiffeners, about its own centroidal axis. The moment of inertia of the entire section shall be calculated assuming the "equivalent element" to be located at the centroidal axis of the multiple-stiffened element, including the intermediate stiffener. The actual extreme fiber distance shall be used in computing the section modulus.

In the Canadian Standard, the equivalent thickness t_s is determined in accordance with Eq. (3.95):[1.177]

$$t_s = t \left[\frac{1}{2} \left(\frac{b_o}{p} \right) + \left(\frac{3 I_s}{p t^3} \right)^{1/2} \right]^{1/3} \qquad (3.95)$$

where p is the perimeter length of the multiple-stiffened element. Other symbols were defined previously.

The above equation is based on Lind's study of longitudinally stiffened sheets. Reference 3.83 indicates that an isotropic plate with an equivalent thickness t_s [Eq. (3.95)] would have the same buckling load as the orthotropic plate having longitudinal stiffeners.

Effective Design Width. Results of tests of cold-formed steel sections having intermediate stiffeners showed that the effective design width of a subelement of the multiple-stiffened compression elements is less than that of a single-

stiffened element with the same w/t ratio.[1.161] This is true particularly when the w/t ratio of the subelement exceeds about 60.

This phenomenon is due to the fact that, in beam sections, the normal stresses in the flanges result from shear stresses between web and flange. The web generates the normal stresses by means of the shear stress which transfers to the flange. The more remote portions of the flange obtain their normal stress through shear from those close to the web. For this reason there is a difference between webs and intermediate stiffeners. The latter is not a shear-resisting element and does not generate normal stresses through shear. Any normal stress in the intermediate stiffener must be transferred to it from the web or webs through the flange portions. As long as the subelement between web and stiffener is flat or is only very slightly buckled, this stress transfer proceeds in an unaffected manner. In this case the stress in the stiffener equals that at the web, and the subelement is as effective as a regular single-stiffened element with the same w/t ratio. However, for subelements having larger w/t ratios, the slight waves of the subelement interfere with complete shear transfer and create a "shear lag" problem which results in a stress distribution as shown in Fig. 3.49.

For multiple-stiffened compression elements or wide stiffened elements with edge stiffeners, the effective widths of subelements are determined by the following equations:

1. If $w/t \leq 60$,

$$b_e = b \tag{3.96}$$

2. If $w/t > 60$,

$$b_e = b - 0.10t \left(\frac{w}{t} - 60 \right) \tag{3.97}$$
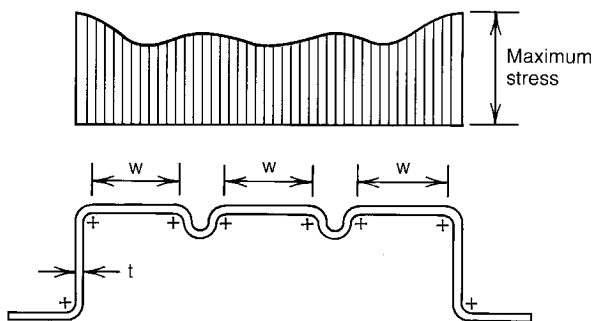
Figure 3.49 Stress distribution in compression flange with intermediate stiffeners.[1.161]

where w/t = flat-width-to-thickness ratio of subelement or element
b_c = effective design width of subelement or element
b = effective design width determined for single-stiffened compression element in accordance with Eqs. (3.41) to (3.44)

The above simple reduction formula has been verified by the results of tests.[1.161] The same approach is also used in the Canadian Standard.[1.177]

Effective Stiffener Area. Since the stress in the stiffener is less than the stress along the longitudinal web, as shown in Fig. 3.49, the efficiency of the stiffener is reduced for elements having large w/t ratios. For this reason, when we compute the effective sectional properties for a member having intermediate stiffeners and when the w/t ratio of the subelement exceeds 60, the effective stiffener area can be computed as follows:[1.4, 1.161, 1.314]

1. If $60 < w/t < 90$,

$$A_{ef} = \alpha A_{st} \tag{3.98}$$

where

$$\alpha = \left(3 - \frac{2b_e}{w}\right) - \frac{1}{30}\left(1 - \frac{b_e}{w}\right)\left(\frac{w}{t}\right) \tag{3.99}$$

2. If $w/t \geq 90$,

$$A_{ef} = \frac{b_e}{w} A_{st} \tag{3.100}$$

In the above equations, A_{ef} and A_{st} refer only to the area of the stiffener section, exclusive of any portion of adjacent elements. In the calculation of sectional properties, the centroid of the full section of the stiffener and the moment of inertia of the stiffener about its own centroidal axis shall be that of the full section of the stiffener.

The structural behavior and strength of cold-formed steel members with multiple longitudinal intermediate stiffeners have recently been investigated by Papazian, Schuster, and Sommerstein,[3.174] Schafer and Pekoz,[3.175, 3.176] and Acharya and Schuster.[3.177, 3.178] These studies considered the distortional buckling of the entire stiffened elements as a unit (Fig. 3.50a), and local buckling of the subelements between stiffeners (Fig. 3.50b). The AISI Specification and the Canadian Standard were compared with the analytical and experimental results. Improved design methods were proposed by the authors.

(*a*)

(*b*)
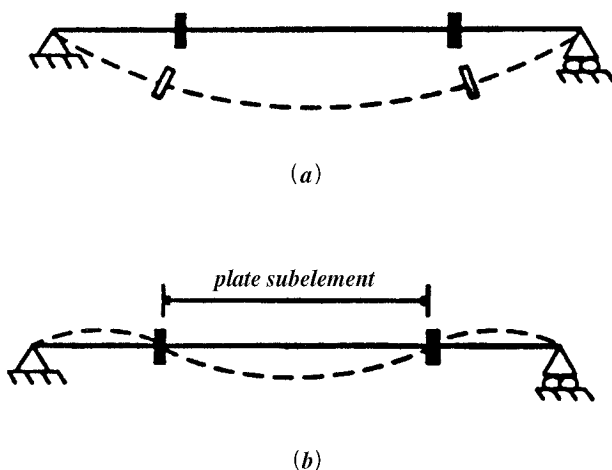
Figure 3.50   Buckling modes of multiple-stiffened elements with longitudinal inter-mediate stiffeners.[3.176] (*a*) Distortional buckling mode. (*b*) Local buckling mode.

3.6   STRUCTURAL BEHAVIOR OF PERFORATED ELEMENTS

In cold-formed steel structural members, holes are sometimes provided in webs and/or flanges of beams and columns for duct work, piping, and other construction purposes, as shown in Fig. 1.3. For steel storage racks (Fig. 1.10), various types of holes are often used for the purpose of easy assembly. The presence of such holes may result in a reduction of the strength of individual component elements and of the overall strength of the member depending on the size, shape and arrangement of holes, the geometric configuration of the cross section, and the mechanical properties of the material used.

The exact analysis and the design of steel sections having perforated elements are complex, in particular when the shapes and the arrangement of the holes are unusual. Even though limited information is available for relatively thick steel sections[1.148, 1.165, 3.84–3.86] on the basis of previous investigations,[3.87–3.90] these design criteria may not be applicable completely to perforated cold-formed steel sections due to the fact that local buckling is usually a major concern for thin-walled structural members.

For perforated cold-formed steel structural members the load-carrying capacity of the member is usually governed by the buckling behavior and the postbuckling strength of the component elements. The critical buckling loads for perforated plates and members have been studied by numerous investigators.[3.91–3.111] The effect of circular holes on the buckling coefficients in compression is shown in Fig. 3.51. Figure 3.52 shows the effect of a central square hole on the buckling coefficient for a simply supported square plate, in which the top curve was computed by the finite-element method developed
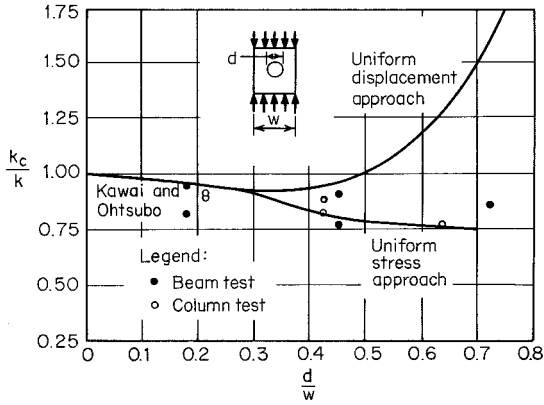
Figure 3.51   Effect of circular hole on buckling coefficient in compression.[3.99]

by Yang.[3.112] The test data obtained from the testing of beams and columns are also shown in these two figures.[3.99]

In Figs. 3.51 and 3.52, k is the buckling coefficient for square plates without holes, k_c is the buckling coefficient for perforated square plates having a circular hole, k_s is the buckling coefficient for perforated square plates having a square hole, d is the diameter of circular holes, h is the width of square holes, and w is the width of the plate.

The postbuckling strength of perforated compression elements has also been studied by Davis and Yu in Ref. 3.99. It was found that Winter's effective-width equation for a solid plate [Eq. (3.35)] can be modified for the determination of the effective width of perforated stiffened elements. Even though the bucking load for the perforated stiffened element is affected more
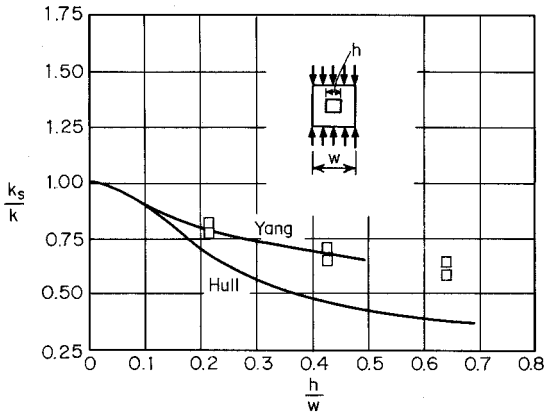
Figure 3.52   Effect of square hole on buckling coefficient in compression.[3.99]

by square holes than by circular holes, the postbuckling strength of the elements with square and circular holes was found to be nearly the same if the diameter of a circular hole was the same as the width of a square hole.

The effect of perforations on the design of industrial steel storage racks has been accounted for by using net section properties determined by stub column tests.[1.165]

Considering the effect of holes on shear buckling of a square plate, the reduction of the bucking coefficients has been studied by Kroll,[3.113] Rockey, Anderson, and Cheung,[3.114, 3.115] and Narayanan and Avanessian.[3.101] Figure 3.53 shows the buckling coefficients in shear affected by holes.

3.6.1   Stiffened Elements with Circular Holes

Based on the Cornell study presented in Ref. 3.100, Sec. B2.2 of the AISI Specification includes the following brief provisions for determining the effective width of uniformly compressed stiffened elements with circular holes.

a. *Strength* (*Load Capacity*) *Determination.* The effective width, b, of stiffened elements with uniform compression having circular holes shall be determined as follows:

for $0.50 \geq \dfrac{d_h}{w} \geq 0$, and $\dfrac{w}{t} \leq 70$ and

center-to-center spacing of holes $\geq 0.50w$, and $\geq 3d_h$,
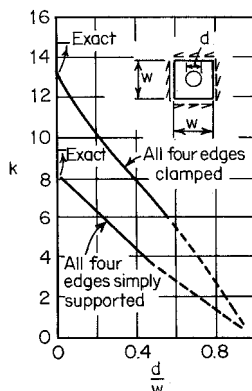
Figure 3.53   Effect of circular hole on buckling coefficient in shear.[3.114]

$$b = w - d_{\text{h}} \qquad \text{when } \lambda \leq 0.673 \tag{3.101}$$

$$b = \frac{w\left[1 - \dfrac{(0.22)}{\lambda} - \dfrac{(0.8d_{\text{h}})}{w}\right]}{\lambda} \leq (w - d_{\text{h}}) \tag{3.102}$$

$$\text{when } \lambda > 0.673$$

where w = flat width
$\quad\quad d_{\text{h}}$ = diameter of holes
$\quad \lambda$ is as defined in Eq. (3.44)

b. *Deflection Determination.* The effective width, b_{d}, used in deflection calculations shall be equal to b determined in accordance with Eqs. (3.41) to (3.44) except that f_{d} is substituted for f, where f_{d} is the computed compressive stress in the element being considered.

3.6.2   C-Section Webs with Holes under Stress Gradient

During recent years, numerous studies have been conducted to investigate the structural behavior and strength of perforated elements and members subjected to tension, compression, bending, shear, and web-crippling. [3.179–3.193, 3.197–3.200] Based on the research work conducted by Shan et al. at the University of Missouri-Rolla,[3.184, 3.197] the following requirements are included in a new Section B2.4 of the Specification for determining the effective depth of C-section webs with holes under stress gradient:[1.333]

a. *Strength (Load Capacity) Determination.* When $d_{\text{o}}/h < 0.38$, the effective widths, b_1 and b_2, shall be determined by Section B2.3 (a) of the Specification by assuming no hole exists in the web. When $d_{\text{o}}/h > 0.38$, the effective width shall be determined by Section B3.1(a) of the Specification, assuming the compression portion of the web consists of an unstiffened element adjacent to the hole with $f = f_1$, as shown in Fig. 3.30.

b. *Deflection Determination.* The effective widths shall be determined by Section B2.3 (b) of the Specification by assuming no hole exists in the web.

where d_{o} = depth of web hole
$\quad\quad b$ = length of web hole
$\quad b_1, b_2$ = effective widths defined by Fig. 3.30
$\quad\quad h$ = depth of flat portion of the web measured along the plane of the web

Because the above requirements are based on the experimental study, these provisions are applicable only within the following limits:

1. $d_o/h < 0.7$
2. $h/t \leq 200$
3. holes centered at mid-depth of the web
4. clear distance between holes ≥ 18 in. (457 mm)
5. for non-circular holes, corner radii $\geq 2\ t$
6. for non-circular holes, $d_o \leq 2.5$ in. (64 mm) and $b \leq 4.5$ in. (114 mm)
7. circular hole diameter ≤ 6 in. (152 mm)
8. $d_o > 9/16$ in. (14 mm)

Although these provisions are based on the tests of C-sections having the web hole centered at mid-depth of the section, the provisions may be conservatively applied to sections for which the full unreduced compression region of the web is less than the tension region. Otherwise, the web strength must be determined by tests.[1.333]

The design provisions apply to any hole pattern that fits within equivalent virtual holes, as shown in Figs. 3.54 and 3.55. Figure 3.54 shows the dimensions b and d_o for a multiple hole pattern that fits within a non-circular virtual hole; while Fig. 3.55 illustrates the dimension d_o for a rectangular hole that exceeds the limits of 2.5 in. (64 mm) $\times$ 4.5 in. (114 mm), but still fits within an allowable circular virtual hole. For each case, the provisions apply to the geometry of the virtual hole, not the actual hole or holes.[1.333]

For the effect of web holes on the shear strength and web crippling strength of C-sections, see Art. 4.3 on the design of beam webs.

3.7   PLATE BUCKLING OF STRUCTURAL SHAPES

In Art. 3.5 a discussion was made on the local buckling of stiffened and unstiffened compression elements, for which the edges were assumed to be
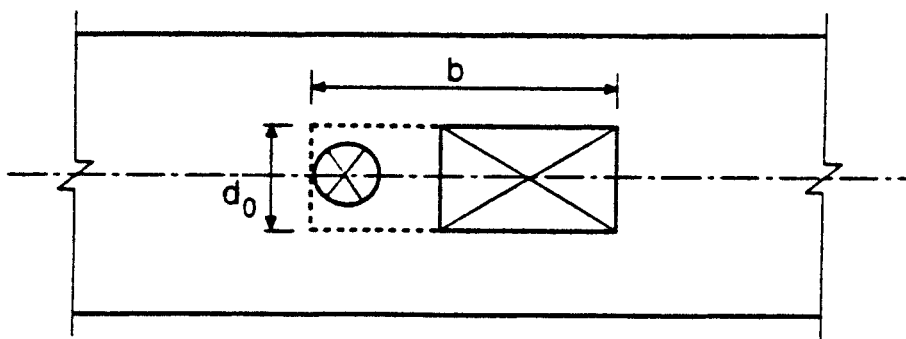
Figure 3.54   Virtual hole method for multiple openings.[1.333]
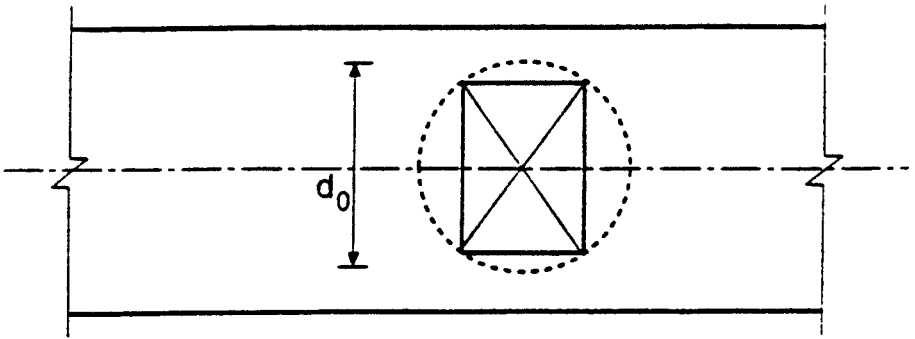
Figure 3.55 Virtual hole method for opening exceeding limit.[1.333]

simply supported. If the actual restraining effects of adjoining cross-sectional elements are taken into account, the plate buckling coefficient k for box sections, channels, and Z-sections used as columns can be found from Fig. 3.56. These curves are based on the charts developed by Kroll, Fisher, and Heimerl.[3.116] Additional information can be found from Refs. 1.94, 1.158 3.8, 3.80, 3.117–3.123, 3.194, 3.195 and in Chap. 5 on compression members.

The advantages of using numerical solution for the design of cold-formed steel members are discussed by Schafer and Pekoz in Refs. 3.194 and 3.195. The element interaction can be handled properly by the numerical solution.
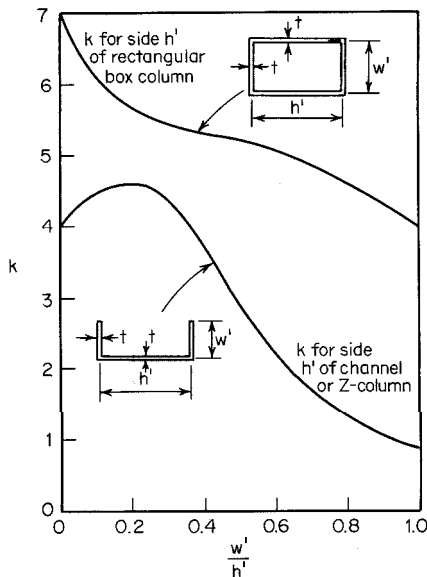
Figure 3.56 Plate buckling coefficient k for side h' of columns.

3.8 ADDITIONAL INFORMATION

The strength of thin compression elements and the current design criteria were discussed in this chapter on the basis of the publications referred to in the text. Additional information on the strength of compression elements and members can also be found in Refs. 3.124 through 3.148.

The structural behavior of webs of beams subjected to shear, or bearing is discussed in Chap. 4 on the design of flexural members. The buckling behavior of cylindrical tubular members is discussed in Chap. 7 on cylindrical tubular members.

4 Flexural Members

4.1 GENERAL REMARKS

Beams are used to support transverse loads and/or applied moment. Cold-formed steel sections, such as I-sections, channels, Z-shapes, angles, T-sections, hat sections, and tubular members (Fig. 1.2) and decks and panels (Fig. 1.11) can be used as flexural members.

In the design of cold-formed steel flexural members, consideration should first be given to the moment-resisting capacity and the stiffness of the member. It may be found that in many cases, the moment of inertia of the section is not a constant value but varies along the span length due to the noncompactness of the thin-walled section and the variation of the moment diagram. The design method is discussed in this chapter. Second, the webs of beams should be checked for shear, combined bending and shear, web crippling, and combined bending and web crippling.

In addition to the design features discussed above, the moment-resisting capacity of the member may be limited by lateral buckling of the beam, particularly when the section is fabricated from thin material and laterally supported at relatively large intervals. For this reason, flexural members must be braced adequately in accordance with the bracing requirements prescribed in the AISI Specification; otherwise a low design moment has to be used. For some sections, distortional buckling may be critical.

Unlike hot-rolled heavy steel sections, in the design of thin-walled cold-formed steel beams, special problems such as shear lag and flange curling are also considered to be important matters due to the use of thin material. Furthermore, the design of flexural members can be even more involved if the increase of steel mechanical properties due to cold work is to be utilized.

Based on the above general discussion, the following design features are considered in this chapter with some design examples for the purpose of illustration:

1. Bending strength and deflection
2. Design of webs for shear, combined bending and shear, web crippling, and combined bending and web crippling
3. Bracing requirements
4. Shear lag
5. Flange curling

146

In general, long-span, shallow beams are governed by deflection and medium-length beams are controlled by bending strength. For short-span beams, shear strength may be critical.

For design tables and charts, reference should be made to Part II of the AISI Design Manual.

4.2   BENDING STRENGTH AND DEFLECTION

4.2.1   Introduction

In the design of flexural members, sufficient bending strength must be provided, and at the same time the deflection of the member under service loads should not exceed specific limitations.

A. ASD Method

According to the design format discussed in Art 3.3.1.1 for the ASD method, Eq. (4.1) gives the following structural safety requirement for the flexural or bending strength:

$$M \leq M_a \tag{4.1}$$

where M = required flexural strength or bending moment for ASD computed from nominal loads or working loads

      M_a = allowable design flexural strength or bending moment determined by Eq. (4.2):

$$M_a = \frac{M_n}{\Omega_b} \tag{4.2}$$

In Eq. (4.2), Ω_b = factor of safety for flexural or bending strength

      = 1.67 on the basis of Sec. 3.1.1 of the AISI Specification

      M_n = smallest nominal flexural strength or moment determined from the following four design considerations:

1. Section strength or bending moment of the cross section calculated in accordance with Art. 4.2.2
2. Lateral–torsional buckling strength calculated in accordance with Art. 4.2.3
3. Section strength of beams having one flange through-fastened to deck or sheathing determined in accordance with Art. 4.2.4
4. Section strength of beams having one flange fastened to a standing seam roof system determined in accordance with Art. 4.2.5

In addition to the above-listed four cases, consideration should also be given to shear lag problems for unusually short span beams (see Art. 4.2.6). The current AISI design provisions do not consider torsional effects, such as those resulting from loads that do not pass through the shear center of the cross section.[1.333] For torsional analysis, see Appendix B.

B. LRFD Method

Based on the design format discussed in Art. 3.3.2.1 for the LRFD method, the structural safety requirement for the flexural or bending strength is expressed in Eq. (4.3):

$$M_u \leq \phi_b M_n \qquad (4.3)$$

where M_u = required flexural strength or bending moment for LRFD computed from factored loads (see Arts. 3.3.2.1 and 3.3.2.2)

ϕ_b = resistance factor for reducing the flexural strength or bending moment

= 0.95 for the nominal section strength of flexural members with stiffened or partially stiffened compression flanges (Art. 4.2.2)

= 0.90 for the nominal section strength of flexural members with unstiffened compression flanges (Art. 4.2.2), the nominal lateral-torsional buckling strength (Art. 4.2.3), the section strength of beams having one flange through-fastened to deck or sheathing (Art. 4.2.4), and the section strength of beams having one flange fastened to a standing seam roof system (Art. 4.2.5).

$\phi_b M_n$ = design flexural strength or bending moment

M_n was defined in Item A for the ASD method.

4.2.2   Section Strength or Bending Moment of the Cross Section

Section C3.1.1 of the 1996 edition of the AISI Specification includes two design procedures for calculating the section strength of flexural members. Procedure I is based on ''Initiation of Yielding'' and Procedure II is based on ''Inelastic Reserve Capacity.'' Both design procedures are discussed in this Article.

4.2.2.1 Initiation of Yielding   In Procedure I of the AISI Specification, the nominal moment, M_n, of the cross section is the effective yield moment, M_y, determined on the basis of the effective areas of flanges and the beam web. The effective width of the compression flange and the effective depth of the web can be computed from the design equations presented in Chapter 3.

Similar to the design of hot-rolled steel shapes, the yield moment M_y of a cold-formed steel beam is defined as the moment at which an outer fiber (tension, compression, or both) first attains the yield point of steel. This is

the maximum bending capacity to be used in elastic design. Figure 4.1shows several types of stress distribution for yield moment based on different locations of the neutral axis. For balanced sections (Fig. 4.1a) the outer fibers in the compression and tension flanges reach the yield point at the same time. However, if the neutral axis is eccentrically located, as shown in Figs. 4.1b and c, the initial yielding takes place in the tension flange for case b and in the compression flange for case c.

Based on the above discussion, the nominal section strength for initiation of yielding is calculated by using Eq. (4.4):

$$M_n = M_y = S_e F_y \qquad (4.4)$$
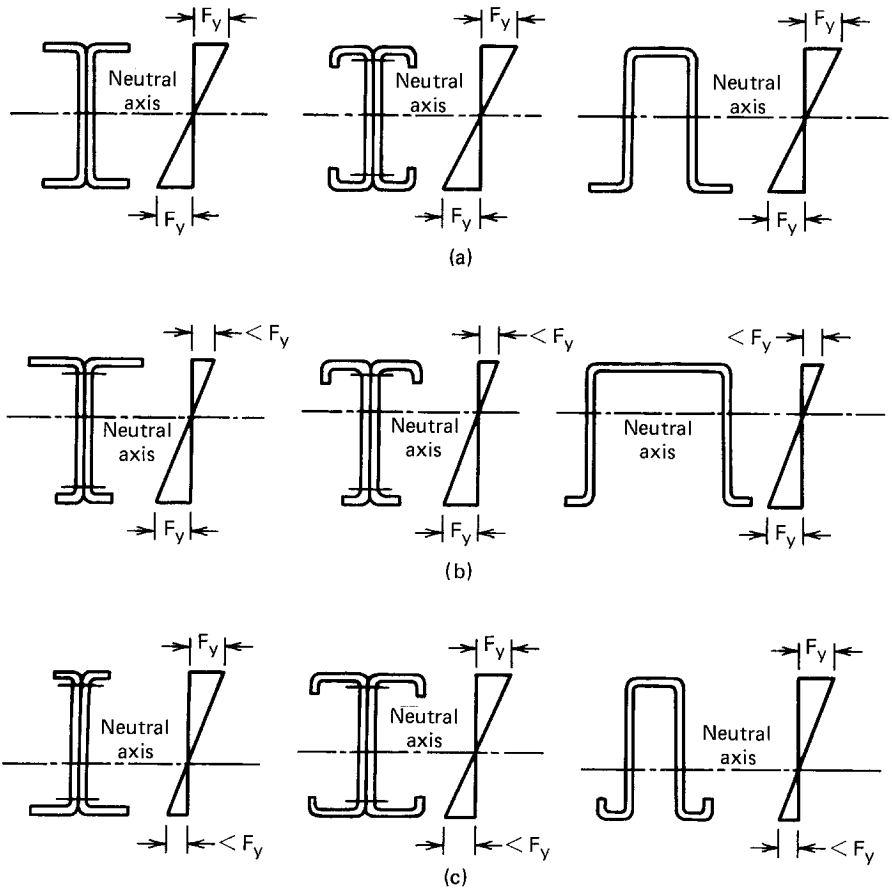
Figure 4.1   Stress distribution for yield moment. (a) Balanced sections. (b) Neutral axis close to compression flange (initial yielding in tension flange). (c) Neutral axis close to tension flange (initial yielding in compression flange).

where F_y = design yield stress

S_e = elastic section modulus of the effective section calculated with the extreme compression or tension fiber at F_y.

In cold-formed steel design, S_e is usually computed by using one of the following two cases:

1. If the neutral axis is closer to the tension than to the compression flange as shown in Fig. 4.1c, the maximum stress occurs in the compression flange, and therefore the plate slenderness ratio λ and the effective width of the compression flange are determined by the w/t ratio and $f = F_y$ in Eq. (3.44). Of course, this procedure is also applicable to those beams for which the neutral axis is located at the mid-depth of the section as shown in Fig. 4.1a.

2. If the neutral axis is closer to the compression than to the tension flange as shown in Fig. 4.1b, the maximum stress of F_y occurs in the tension flange. The stress in the compression flange depends on the location of the neutral axis, which is determined by the effective area of the section. The latter cannot be determined unless the compressive stress is known. The closed-form solution of this type of design is possible but would be a very tedious and complex procedure. It is therefore customary to determine the sectional properties of the section by successive approximation.

The calculation of the nominal moment on the basis of initiation of yielding and the determination of the design moment are illustrated in Examples 4.1 through 4.4.

Example 4.1   Use the ASD and LRFD methods to check the adequacy of the I-section with an unstiffened compression flange as shown in Fig. 4.2. The nominal moment for section strength is computed on the basis of initiation of yielding by using $F_y = 50$ ksi. Assume that lateral bracing is adequately provided. The dead load moment $M_D = 30$ in.-kips and the live load moment $M_L = 150$ in.-kips.
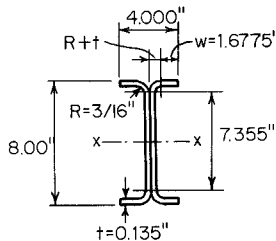
Figure 4.2   Example 4.1.

Solution

A. ASD Method

1. *Calculation of Sectional Properties.* The sectional properties of the corner element can be obtained from Table 4.1. For $R = \frac{3}{16}$ in. and $t = 0.135$ in.,

$$I_x = I_y = 0.0003889 \text{ in.}^4$$

$$A = 0.05407 \text{ in.}^2$$

$$x = y = 0.1564 \text{ in.}$$

For the unstiffened flange,

$$w = \frac{4.000}{2} - (R + t) = 1.6775 \text{ in.}$$

$$w/t = 1.6775/0.135 = 12.426 < 60 \qquad \text{O.K. according to Art. 3.2.}$$

Since the compression flange is an unstiffened element and the neutral axis is either at mid-depth or closer to the tension flange, use Eqs. (3.41) through (3.44) with $k = 0.43$ and $f = F_y = 50$ ksi. Therefore

TABLE 4.1   One 90° Corner, Dimensions and Properties

Dimensions		Properties			
Thickness t (in.)	Inside Radius R (in.)	Moment of Inertia $I_x = I_y$ (in.^{4})	Centroid Coordinates $x = y$ (in.)	Area A (in.^{2})	Blank Width (in.)
0.135	0.1875	0.0003889	0.1564	0.05407	0.3652
0.105	0.1875	0.0002408	0.1373	0.03958	0.3495
0.075	0.0938	0.0000301	0.0829	0.01546	0.1865
0.060	0.0938	0.0000193	0.0734	0.01166	0.1787
0.048	0.0938	0.0000128	0.0658	0.00888	0.1724
0.036	0.0625	0.00000313	0.0464	0.00452	0.1170

Notes: (1) Stock width of blank taken at $t/3$ distance from inner surface.
　　　　(2) 1 in. = 25.4 mm.

$$\lambda = \frac{1.052}{\sqrt{k}}\left(\frac{w}{t}\right)\sqrt{\frac{f}{E}} \tag{3.44}$$

$$= \frac{1.052}{\sqrt{0.43}}(12.426)\sqrt{\frac{50}{29,500}}$$

$$= 0.821 > 0.673$$

$$\rho = \left(1 - \frac{0.22}{\lambda}\right)\Big/\lambda \tag{3.43}$$

$$= \left(1 - \frac{0.22}{0.821}\right)\Big/0.821$$

$$= 0.892$$

$$b = \rho w = 0.892(1.6775)$$

$$= 1.4963 \text{ in.}$$

By using the effective width of the compression flange and assuming the web is fully effective, the location of the neutral axis, the moment of inertia I_x and the elastic section modulus of the effective section S_e can be computed as follows.

Element	Area A (in.²)	Distance from Top Fiber y (in.)	Ay (in.³)	Ay^2 (in.⁴)
Top flange	2(1.4963)(0.135) = 0.4040	0.0675	0.0273	0.0018
Top corners	2(0.05407) = 0.1081	0.1564	0.0169	0.0026
Webs	2(7.355)(0.135) = 1.9859	4.0000	7.9436	31.7744
Bottom corners	2(0.05407) = 0.1081	7.8436	0.8479	6.6506
Bottom flange	2(1.6775)(0.135) = 0.4529	7.9325	3.5926	28.4983
Total	3.0590		12.4283	66.9277

$$y_{cg} = \frac{\Sigma(Ay)}{\Sigma A} = \frac{12.4283}{3.0590} = 4.063 \text{ in.}$$

Since $y_{cg} > d/2 = 4.00$ in., initial yield occurs in the compression flange. Prior to computing the moment of inertia, check the web for full effectiveness by using Fig. 4.3 as follows:

$$f_1 = 50(3.7405/4.063) = 46.03 \text{ ksi (compression)}$$

$$f_2 = -50(3.6145/4.063) = -44.48 \text{ ksi (tension)}$$

$$\psi = f_2/f_1 = -0.966 \tag{3.58}$$
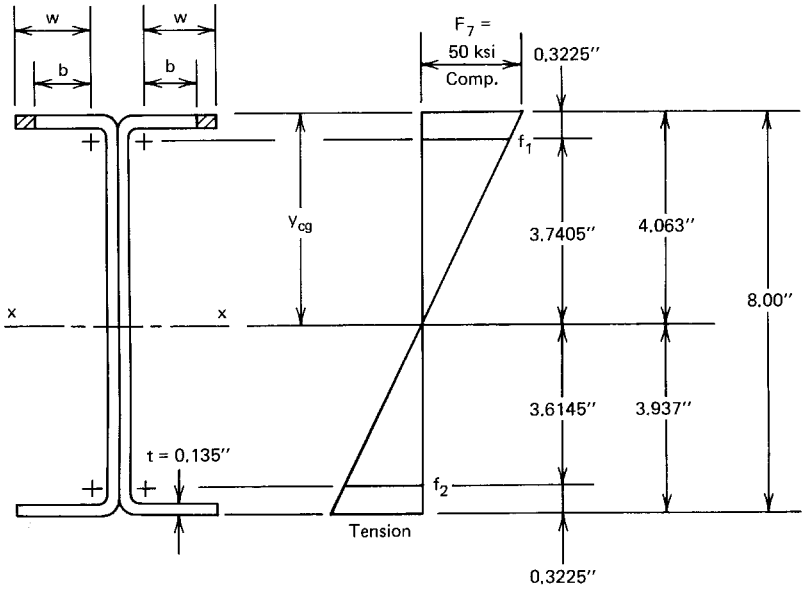
Figure 4.3 Stress distribution in webs.

$$k = 4 + 2(1 - \psi)^3 + 2(1 - \psi) \tag{3.57}$$
$$= 4 + 2[1 - (-0.966)]^3 + 2[1 - (-0.966)]$$
$$= 23.13$$
$$h = 7.355 \text{ in.}$$
$$h/t = 7.355/0.135 = 54.48 < 200$$

O.K. according to Art. 3.2.

$$\lambda = \frac{1.052}{\sqrt{23.13}} (54.48) \sqrt{\frac{46.03}{29,500}} = 0.471 < 0.673 \tag{3.44}$$

$$\rho = 1.0 \tag{3.43}$$
$$b_e = h = 7.355 \text{ in.}$$
$$b_1 = b_e/(3 - \psi) \tag{3.54}$$
$$= 7.355/[3 - (-0.966)] = 1.855 \text{ in.}$$

Since $\psi < -0.236$,

$$b_2 = b_e/2 = 3.6775 \text{ in.} \tag{3.55}$$
$$b_1 + b_2 = 1.855 + 3.6775 = 5.5325 \text{ in.}$$

Since $(b_1 + b_2)$ is greater than the compression portion of the web of 3.7405 in., the web is fully effective as assumed. The total I_x is

$$\sum (Ay^2) = 66.9277$$

$$2I_{\text{web}} = 2(\tfrac{1}{12})(0.135)(7.355)^3 = 8.9522$$

$$-\left(\sum A\right)(y_{\text{cg}})^2 = (3.0590)(4.063)^2 = \underline{-50.4979}$$

$$I_x = 25.3820 \text{ in.}^4$$

The elastic section modulus relative to the top fiber is

$$S_e = \frac{I_x}{y_{\text{cg}}} = \frac{25.3820}{4.063} = 6.247 \text{ in.}^3$$

2. *Nominal and Allowable Design Moments*. The nominal moment for section strength is

$$M_n = S_e F_y = (6.247)(50) = 312.35 \text{ in.- kips}$$

The allowable design moment is

$$M_a = M_n/\Omega_b = 312.35/1.67 = 187.0 \text{ in.-kips}$$

3. *Required Moment*. Based on the load combination discussed in Art. 3.3.1.2, the required moment for the given dead load moment and live load moment is computed as follows:

$$M = M_D + M_L \tag{3.3b}$$

$$= 30 + 150 = 180 \text{ in.-kips}$$

Since $M < M_a$, the I-section is adequate for the ASD method.

B. LRFD Method

1. *Nominal and Design Moments*. The nominal moment for the LRFD method is the same as that used for the ASD method, i.e.,

$$M_n = 312.35 \text{ in.-kips}$$

The design moment for the I-section having an unstiffened compression flange ($\phi_b = 0.90$) is

$$\phi_b M_n = 0.90(312.35) = 281.12 \text{ in.-kips}$$

2. *Required Moment.* According to the load factors and the load combinations discussed in Art. 3.3.2.2, the required moment for the given dead load moment and live load moment can be computed as follows:

$$M_{u1} = 1.4D + L$$

$$= 1.4 \ (30) + 150 = 192.00 \text{ in.-kips}$$

$$M_{u2} = 1.2D + 1.6L$$

$$= 1.2(30) + 1.6 \ (150) = 276.00 \text{ in.-kips} \Leftarrow \text{controls}$$

Since $M_u < \phi_b M_n$, the I-section is also adequate for the LRFD method.

Example 4.2   For the channel section with an edge stiffener as shown in Fig. 4.4, determine the allowable design moment (M_a) about the *x*-axis for the ASD method and the design moment $(\phi_b M_n)$ for the LRFD method. Assume that the yield point of steel is 50 ksi and that lateral bracing is adequately provided. Use the linear method. The nominal moment is determined by initiation of yielding.
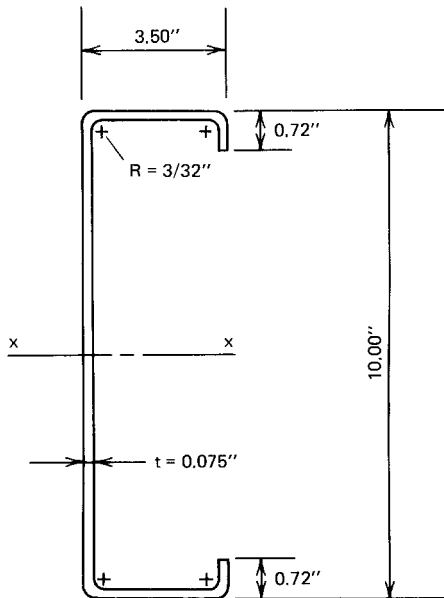
Figure 4.4   Example 4.2 (same as Fig 3.48).

Solution

A. ASD Method

1. *Calculation of Sectional Properties.* In order to simplify the calculation, line elements, as shown in Fig. 4.5, are used for the linear method.
   i. *Corner element* (Figs. 1.31 and 4.5)

$$R' = R + \frac{t}{2} = 0.131 \text{ in.}$$

   Arc length

$$L = 1.57R' = 0.206 \text{ in.}$$
$$c = 0.637R' = 0.0836 \text{ in.}$$

   ii. *Effective width of the compression flange.* For the given channel section with equal flanges, the neutral axis is located either at the mid-depth or closer to the tension flange. Therefore, use $f = F_y =$
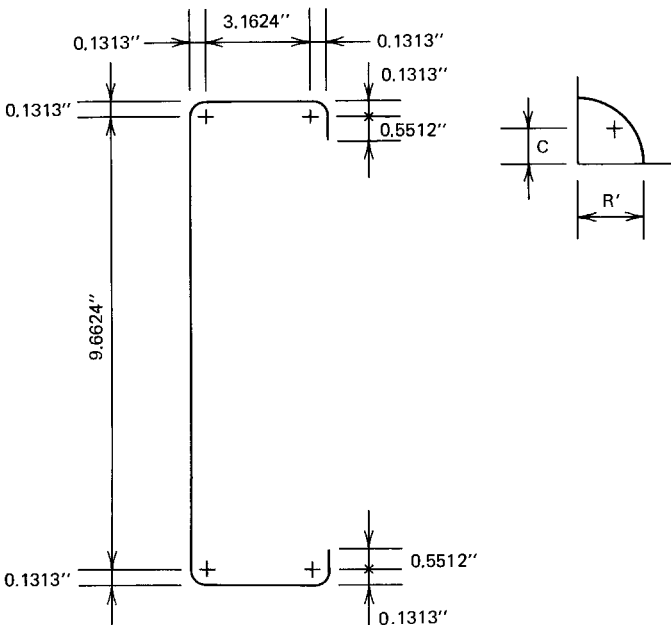
Figure 4.5   Line elements.

50 ksi to compute the effective width of the compression flange. For the compression flange,

$$w = 3.50 - 2(R + t) = 3.1624 \text{ in.}$$
$$w/t = 3.1624/0.075 = 42.17$$

According to Eq. (3.75)

$$S = 1.28\sqrt{E/f} = 1.28\sqrt{29,500/50} = 31.09$$

Since $w/t > S$, use Case III of Art. 3.5.3.2 and Eq. (3.90) to compute the required moment of inertia of the edge stiffener I_a as follows:

$$I_a = \{[115(w/t)/S] + 5\}t^4$$
$$= \{[115(42.17)/31.09] + 5\}(0.075)^4 = 5.093 \times 10^{-3} \text{ in.}^4$$

For the simple lip edge stiffener used for the given channel section,

$$D = 0.720 \text{ in.}$$
$$d = D - (R + t) = 0.5512 \text{ in.}$$
$$d/t = 0.5512/0.075 = 7.35 < 14 \text{ (maximum } d/t)$$

By using Eq. (3.91), the moment of inertia of the full edge stiffener is

$$I_s = d^3t/12 = 1.047 \times 10^{-3} \text{ in.}^4$$
$$C_2 = I_s/I_a = 0.206 < 1.0$$
$$D/w = 0.72/3.1624 = 0.228$$

Since $D/w < 0.8$ and $\theta = 90^0$, according to Eq. (3.86),

$$k_a = 5.25 - 5(D/w) = 4.11 > 4.0$$

Use $k_a = 4.0$
According to Eq. (3.85),

$$k = C_2^n(k_a - k_u) + k_u$$

$$= (C_2)^{1/3}(4.0 - 0.43) + 0.43$$

$$= (0.206)^{1/3}(3.57) + 0.43$$

$$= 2.54 < 4.0$$

Use $k = 2.54$ to calculate the plate slenderness factor for the compression flange as follows:

$$\lambda = (1.052/\sqrt{k})(w/t)\sqrt{f/E}$$

$$= (1.052/\sqrt{2.54})(42.17)\sqrt{50/29,500} = 1.146 > 0.673$$

The effective width of the compression flange is

$$b = \rho w = [(1 - 0.22/\lambda)/\lambda]w$$

$$= [(1 - 0.22/1.146)/1.146](3.1624) = 2.230 \text{ in.}$$

iii. *Effective width of the edge stiffener.* The reduced effective width of the edge stiffener with stress gradient can be computed in accordance with Art. 3.5.3.2 or Section B3.2 of the AISI Specification. Using $k = 0.43$, $d/t = 7.35$ and a conservative $f = F_y$, the slenderness factor is

$$\lambda = (1.052/\sqrt{0.43})(7.35)\sqrt{50/29,500} = 0.485 < 0.673$$

Therefore, the effective width of the edge stiffener is

$$d_s' = d = 0.5512 \text{ in.}$$

Based on Eq. (3.87), the reduced effective width of the edge stiffener is

$$d_s = C_2 d_s' = 0.206(0.5512) = 0.113 \text{ in.}$$

The above calculation indicates that the compression stiffener is not fully effective.

iv. *Location of neutral axis and computation of I_x and S_x*

a. *Location of neutral axis based on full web element.* Assuming that the web element (Element 7 in Fig. 4.6) is fully effective, the neutral axis can be located by using the following table. See Fig. 4.6 for dimensions of elements.
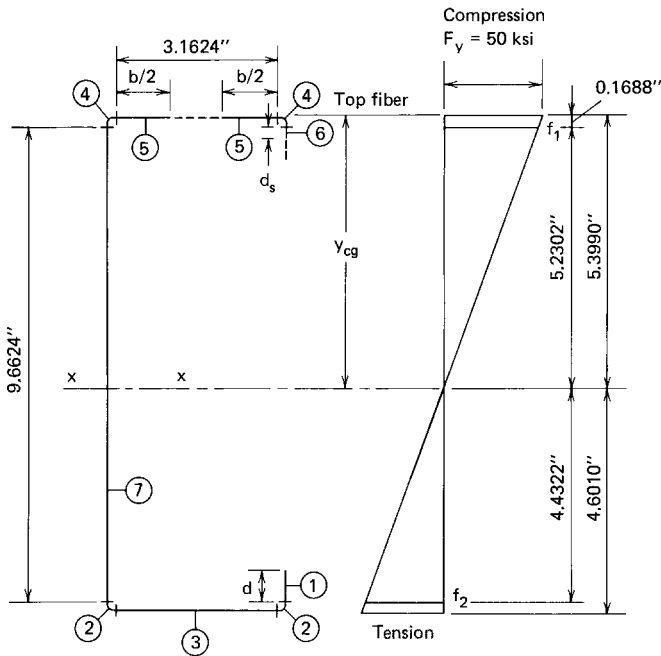
Figure 4.6   Effective lengths and stress distribution using fully effective web.

Element	Effective Length L (in.)	Distance from Top Fiber y (in.)	Ly (in.²)
1	0.5512	9.5556	5.2670
2	2(0.206) = 0.4120	9.9148	4.0849
3	3.1624	9.9625	31.5054
4	2(0.206) = 0.4120	0.0852	0.0351
5	2.2300	0.0375	0.0836
6	0.1130	0.2254	0.0255
7	9.6624	5.0000	48.3120
Total	16.5430		89.3135

$$y_{cg} = \frac{\Sigma(Ly)}{\Sigma L} = \frac{89.3135}{16.5430} = 5.399 \text{ in.}$$

Use Art. 3.5.1.2 or Section B2.3 of the AISI Specification to check the effectiveness of the web element. From Fig. 4.6,

$$f_1 = 50(5.2302/5.399) = 48.44 \text{ ksi} \qquad \text{(compression)}$$

$$f_2 = -50(4.4322/5.399) = -41.05 \text{ ksi} \qquad \text{(tension)}$$

$$\psi = f_2/f_1 = -0.847$$

$$k = 4 + 2(1 - \psi)^3 + 2(1 - \psi) = 20.30$$

$$h/t = 9.6624/0.075 = 128.83 < 200 \qquad \text{O.K.}$$

$$\lambda = \frac{1.052}{\sqrt{20.30}} (128.83) \sqrt{\frac{48.44}{29,500}} = 1.219 > 0.673$$

$$\rho = [1 - 0.22/\lambda]/\lambda = 0.672$$

$$b_e = \rho h = 0.672 \times 9.6624 = 6.4931 \text{ in.}$$

$$b_1 = b_e/(3 - \psi) = 1.6878 \text{ in.}$$

Since $\psi < -0.236$,

$$b_2 = b_e/2 = 3.2465 \text{ in.}$$

$$b_1 + b_2 = 4.9343 \text{ in.}$$

Since the value of $(b_1 + b_2)$ is less than 5.2302 in. shown in Fig. 4.6, the web element is not fully effective as assumed. The neutral axis should be relocated by using the partially effective web. The procedure is interative as illustrated below.

b. *Location of neutral axis based on ineffective web elements.* As the first iteration, the ineffective portion of the web can be assumed as follows:

$$5.2302 - (b_1 + b_2) = 5.2302 - 4.9343 = 0.2959 \text{ in.}$$

Therefore, the effective lengths of all elements are shown in Fig. 4.7 using partially effective web.

Element	Effective Length L (in.)	Distance from Top Fiber y (in.)	Ly (in.^{2})
1	0.5512	9.5556	5.2670
2	0.4120	9.9148	4.0849
3	3.1624	9.9625	31.5054
4	0.4120	0.0852	0.0351
5	2.2300	0.0375	0.0836
6	0.1130	0.2254	0.0255
7	7.6787	5.9919	46.0100
8	1.6878	1.0127	1.7092
	16.2471		88.7207

$$y_{cg} = \frac{88.7207}{16.2471} = 5.461 \text{ in.}$$

Figure 4.7   Effective lengths and stress distribution using partially effective web (first iteration).

From Fig. 4.7,

$$f_1 = 48.45 \text{ ksi} \qquad \text{(compression)}$$

$$f_2 = -40.01 \text{ ksi} \qquad \text{(tension)}$$

$$\psi = -0.826$$

$$k = 19.83$$

$$h/t = 128.83$$

$$\lambda = \frac{1.052}{\sqrt{19.83}} (128.83) \sqrt{\frac{48.45}{29,500}} = 1.233 > 0.673$$

$$\rho = [1 - 0.22/1.233]/1.233 = 0.666$$

$$b_e = \rho h = 6.4352 \text{ in.}$$

$$b_1 = b_e/(3 - \psi) = 1.6820 \text{ in.}$$

$$b_2 = b_e/2 = 3.2176 \text{ in.}$$

$$b_1 + b_2 = 4.8996 \text{ in.}$$

Because the above computed value of $(b_1 + b_2)$ is less than the previous value of 4.9343 in. by 0.7%, additional iterations are required.

For the second iteration, the ineffective portion of the web is

$$5.2922 - (b_1 + b_2) = 5.2922 - 4.8966 = 0.3926 \text{ in.}$$

By using the same procedure shown above, the neutral axis can be relocated as follows:

Element	Effective Length L (in.)	Distance from Top Fiber y (in.)	Ly (in.²)	Ly^2 (in.³)
1	0.5512	9.5556	5.2670	50.3298
2	0.4120	9.9148	4.0849	40.5009
3	3.1624	9.9625	31.5054	313.8727
4	0.4120	0.0852	0.0351	0.0030
5	2.2300	0.0375	0.0836	0.0031
6	0.1130	0.2254	0.0255	0.0057
7	7.5878	6.0373	45.8098	276.5675
8	1.6820	1.0098	1.6985	1.7151
	16.1504		88.5098	682.9977

$$y_{cg} = \frac{88.5098}{16.1504} = 5.481 \text{ in.}$$

From Fig. 4.8,

$$f_1 = 48.46 \text{ ksi} \qquad \text{(compression)}$$

$$f_2 = -39.68 \text{ ksi} \qquad \text{(tension)}$$

$$\psi = -0.819$$

$$k = 19.68$$

$$h/t = 128.83$$

$$\lambda = \frac{1.052}{\sqrt{19.68}} (128.83) \sqrt{\frac{48.46}{29,500}} = 1.238 > 0.673$$

$$\rho = [1 - 0.22/1.238]/1.238 = 0.664$$

$$b_e = \rho h = 6.4158 \text{ in.}$$

$$b_1 = b_e/(3 - \psi) = 1.6800 \text{ in.}$$
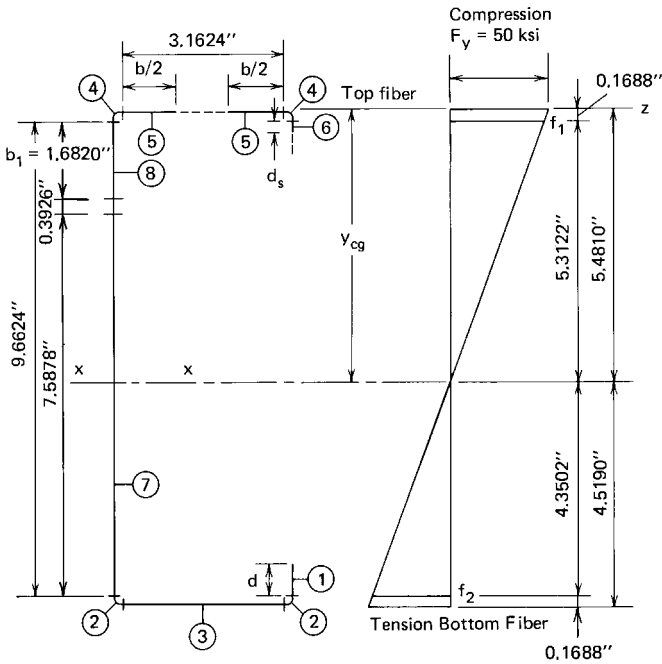
Figure 4.8 Effective lengths and stress distribution using partially effective web (second interaction).

$$b_2 = b_e/2 = 3.2079 \text{ in.}$$

$$b_1 + b_2 = 4.8879 \text{ in.}$$

Because the above computed value of $(b_1 + b_2)$ is approximately equal to the value of $(b_1 + b_2)$ computed from the first iteration, it is acceptable. Better accuracy can be obtained by using additional iterations.

c. *Moment of inertia and section modulus.* The moment of inertia based on line elements is

$$I'_1 = \frac{1}{12}(0.5512)^3 = 0.0140$$

$$I'_6 = \frac{1}{12}(0.113)^3 = 0.0001$$

$$I'_7 = \frac{1}{12}(7.5878)^3 = 36.4054$$

$$I'_8 = \frac{1}{12}(1.6820)^3 = 0.3965$$

$$\sum (Ly^2) = \underline{682.9977}$$

$$I_z' = 719.8137 \text{ in.}^3$$

$$-\left(\sum L\right)(y_{cg})^2 = -(16.1504)(5.481)^2 = \underline{-485.1800}$$

$$I_x' = 234.6337 \text{ in.}^3$$

$$I_x = I_x't = (234.6337)(0.075) = 17.598 \text{ in.}^4$$

$$S_x = \frac{17.598}{5.481} = 3.211 \text{ in.}^3$$

2. *Nominal and Allowable Design Moments.* The nominal moment for section strength is

$$M_n = S_e F_y = S_x F_y = 3.211(50) = 160.55 \text{ in.-kips}$$

The allowable design moment is

$$M_a = M_n/\Omega_b = 160.55/1.67 = 96.14 \text{ in.-kips}$$

B. LRFD Method

The nominal moment for the LRFD method is the same as that computed for the ASD method. From Item *A* above, the nominal moment about the x-axis of the channel section is

$$M_n = 160.55 \text{ in.-kips}$$

Based on Art. 4.2.1 or Sec. C3.1.1 of the AISI Specification, the design moment for the channel section having a partially stiffened compression flange ($\phi_b = 0.95$) is

$$\phi_b M_n = 0.95(160.55) = 152.52 \text{ in.-kips}$$

Example 4.3 For the hat section with a stiffened compression flange as shown in Fig. 4.9, determine the allowable design moment (M_a) about the x-axis for the ASD method and the design moment ($\phi_b M_n$) for the LRFD method. Assume that the yield point of steel is 50 ksi. Use the linear method. The nominal moment is determined by initiation of yielding.
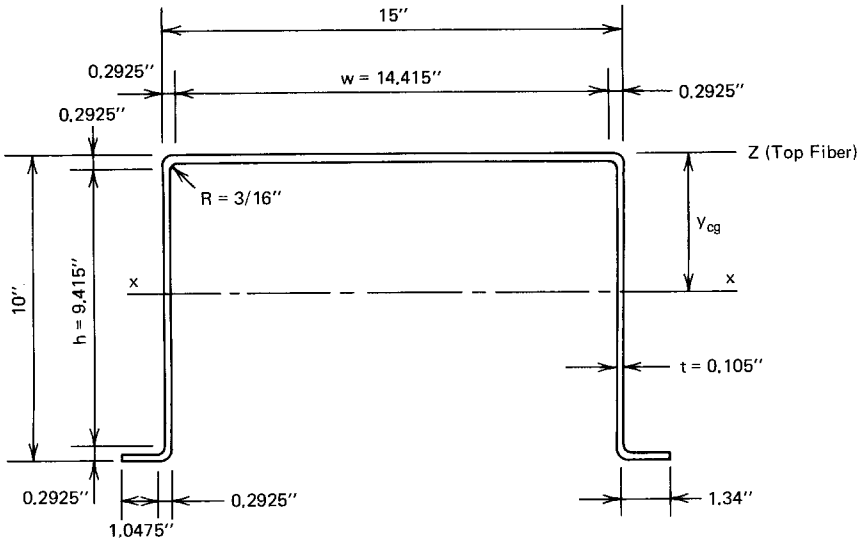
Figure 4.9   Example 4.3.

Solution

A. ASD Method

1. *Calculation of Sectional Properties.* In order to use the linear method, midline dimensions are shown in Fig. 4.10.

   A. *Corner element* (Figs. 1.31 and 4.10)

$$R' = R + t/2 = 0.240 \text{ in.}$$

   Arc length

$$L = 1.57R' = 0.3768 \text{ in.}$$

$$c = 0.637R' = 0.1529 \text{ in.}$$

   B. *Location of neutral axis*

   a. *First approximation.* For the compression flange,

$$w = 15 - 2(R + t) = 14.415 \text{ in.}$$

$$\frac{w}{t} = 137.29$$
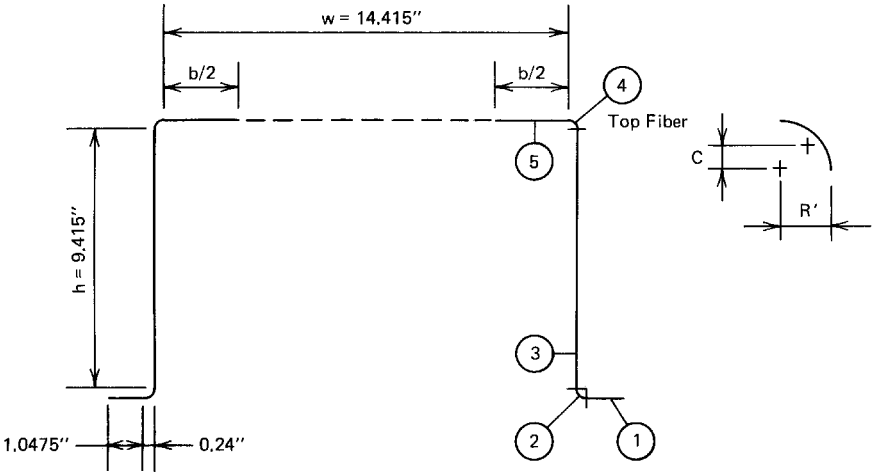
Figure 4.10 Line elements.

Using Eqs. (3.41) through (3.44) and assuming $f = F_y = 50$ ksi.

$$\lambda = \frac{1.052}{\sqrt{4}} (137.29) \sqrt{\frac{50}{29,500}} = 2.973 > 0.673$$

$$\rho = \left(1 - \frac{0.22}{2.973}\right) \Big/ 2.973 = 0.311$$

$$b = \rho w = 0.311(14.415) = 4.483 \text{ in.}$$

By using the effective width of the compression flange and assuming that the web is fully effective, the neutral axis can be located as follows:

Element	Effective Length L (in.)	Distance from Top Fiber y (in.)	Ly (in.^{2})
1	$2 \times 1.0475 = $ 2.0950	9.9475	20.8400
2	$2 \times 0.3768 = $ 0.7536	9.8604	7.4308
3	$2 \times 9.4150 = $ 18.8300	5.0000	94.1500
4	$2 \times 0.3768 = $ 0.7536	0.1396	0.1052
5	4.4830	0.0525	0.2354
Total	26.9152		122.7614

$$y_{cg} = \frac{\Sigma (Ly)}{\Sigma L} = \frac{122.7614}{26.9152} = 4.561 \text{ in.}$$

Because the distance y_{cg} is less than the half-depth of 5.0 in., the neutral axis is closer to the compression flange and, therefore, the maximum stress occurs in the tension flange. The maximum compressive stress can be computed as follows:

$$f = 50 \left(\frac{4.561}{10 - 4.561} \right) = 41.93 \text{ ksi}$$

Since the above computed stress is less than the assumed value, another trial is required.

b. *Second approximation.* After several trials, assuming that

$$f = 40.70 \text{ ksi}$$
$$\lambda = 2.682 > 0.673$$
$$b = 4.934 \text{ in.}$$

Element	Effective Length L (in.)	Distance from Top Fiber y (in.)	Ly (in.^{2})	Ly^2 (in.^{3})
1	2.0950	9.9475	20.8400	207.3059
2	0.7536	9.8604	7.4308	73.2707
3	18.8300	5.0000	94.1500	470.7500
4	0.7536	0.1396	0.1052	0.0147
5	4.9340	0.0525	0.2590	0.0136
Total	27.3662		122.7850	751.3549

$$y_{cg} = \frac{122.7850}{27.3662} = 4.487 \text{ in.}$$

$$f = 50 \left(\frac{4.487}{10 - 4.487} \right) = 40.69 \text{ ksi}$$

Since the above computed stress is close to the assumed value, it is OK.

C. *Check the effectiveness of the web.* Use Art. 3.5.1.2 or Section B2.3 of the AISI Specification to check the effectiveness of the web element. From Fig. 4.11,

Figure 4.11   Effective lengths and stress distribution using fully effective web.

$$f_1 = 50(4.1945/5.513) = 38.04 \text{ ksi} \qquad \text{(compression)}$$

$$f_2 = -50(5.2205/5.513) = -47.35 \text{ ksi} \qquad \text{(tension)}$$

$$\psi = f_2/f_1 = -1.245$$

$$k = 4 + 2(1 - \psi)^3 + 2(1 - \psi)$$

$$= 4 + 2(2.245)^3 + 2(2.245) = 31.12$$

$$h/t = 9.415/0.105 = 89.67 < 200 \qquad \text{O.K.}$$

$$\lambda = \frac{1.052}{\sqrt{31.12}} (89.67) \sqrt{\frac{38.04}{29,500}} = 0.607 < 0.673$$

$$b_e = h = 9.415 \text{ in.}$$

$$b_1 = b_e/(3 - \psi) = 2.218 \text{ in.}$$

Since $\psi < -0.236$,

$$b_2 = b_e/2 = 4.7075 \text{ in.}$$

$$b_1 + b_2 = 6.9255 \text{ in.}$$

Because the computed value of $(b_1 + b_2)$ is greater than the compression portion of the web (4.1945 in.), the web element is fully effective.

D. *Moment of inertia and section modulus.* The moment of inertia based on line elements is

$$2I_3' = 2\left(\frac{1}{12}\right)(9.415)^3 = 139.0944$$

$$\sum(Ly^2) = \underline{751.3549}$$

$$I_z' = 890.4493 \text{ in.}^3$$

$$-(\Sigma L)(y_{cg})^2 = -27.3662(4.487)^2 = \underline{-550.9683} \text{ in.}^3$$

$$I_x' = 339.4810 \text{ in.}^3$$

The actual moment of inertia is

$$I_x = I_x't = (339.4810)(0.105) = 35.646 \text{ in.}^4$$

The section modulus relative to the extreme tension fiber is

$$S_x = 35.646/5.513 = 6.466 \text{ in.}^3$$

2. *Nominal and Allowable Design Moments.* The nominal moment for section strength is

$$M_n = S_e F_y = S_x F_y = (6.466)(50) = 323.30 \text{ in.-kips}$$

The allowable design moment is

$$M_a = M_n/\Omega_b = 323.30/1.67 = 193.59 \text{ in.-kips}$$

B. LRFD Method

The nominal moment for the LRFD method is the same as that computed for the ASD method. From Item *A* above, the nominal moment about the *x*-axis of the hat section is

$$M_n = 323.30 \text{ in.-kips}$$

Based on Art. 4.2.1 or Sec. C3.1.1 of the AISI Specification, the design moment for the hat section having a stiffened compression flange ($\phi_b = 0.95$) is

$$\phi_b M_n = 0.95 (323.30) = 307.14 \text{ in.-kips}$$

Example 4.4   For the section with an intermediate stiffener as shown in Fig. 4.12, determine the allowable design moment (M_a) about the x-axis for the ASD method and the design moment ($\phi_b M_n$) for the LRFD method. Use the linear method with F_y = 33 ksi. The nominal moment is determined by initiation of yielding.

Solution

A. ASD Method

1. *Calculation of Sectional Properties.* Using the linear method as shown in Fig. 4.13.
   A. *Corner element* (Figs. 1.31 and 4.13).

$$R' = R + \frac{t}{2} = 0.1313 \text{ in.}$$

   Arc length

$$L = 1.57R' = 1.57(0.1313) = 0.2063 \text{ in.}$$
$$c = 0.637R' = 0.637(0.1313) = 0.0836 \text{ in.}$$

   B. *Location of neutral axis*
      a. *First approximation.* For the top compression flange,

$$b_o = 12 - 2(R + t) = 11.6624 \text{ in.}$$
$$b_o/t = 11.6624/0.075 = 155.50 \text{ in.}$$

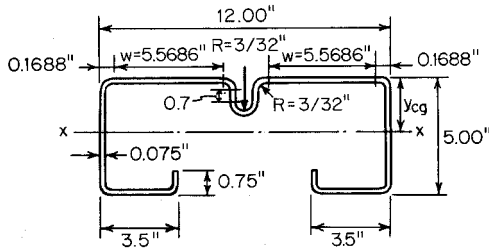   Assuming that $f = F_y$ and using Eq. (3.75),
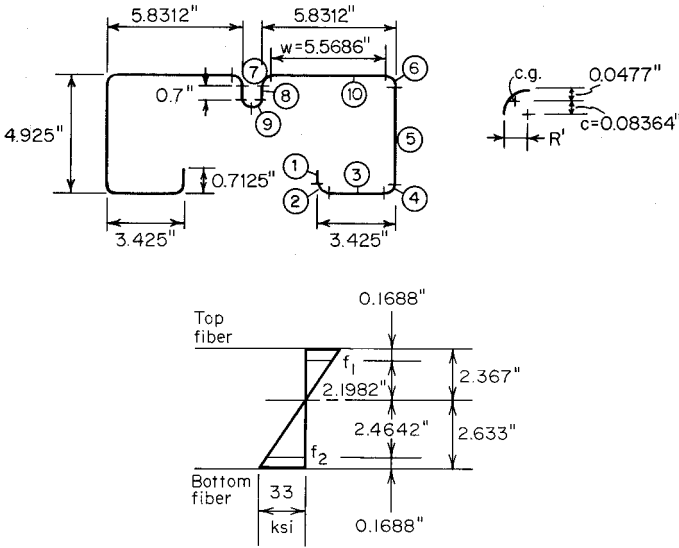

Figure 4.12   Example 4.4.

Figure 4.13   Example 4.4; line elements.

$$S = 1.28\sqrt{E/f} = 1.28\sqrt{29{,}500/33} = 38.27$$

Since $b_o/t > (3S = 114.81)$, use Eq. (3.72) of Art. 3.5.3.1 to compute the required moment of inertia of the intermediate stiffener as follows:

$$I_a = \{[128(b_o/t)/S] - 285\}t^4$$

$$= \{[128(155.50)/38.27] - 285\}(0.075)^4 = 7.439$$

$$\times 10^{-3} \text{ in.}^4$$

The actual moment of inertia of the full intermediate stiffener (Elements 7, 8, and 9 in Fig. 4.13) about its own centroidal axis parallel to the top compression flange is computed below.

$$I'_s = 2\left(\frac{1}{12}\right)(0.7)^3 + 4(0.2063)(0.35 + 0.0836)^2$$

$$= 0.2123 \text{ in.}^3$$

$$I_s = I'_s t = 0.2123(0.075) = 15.923 \times 10^{-3} \text{ in.}^4$$

According to Eq. (3.73),

$$k = 3(I_s/I_a)^{1/3} + 1 = 3(15.923/7.439)^{1/3} + 1$$

$$= 4.866 > 4$$

use $k = 4$. The effective width of the multiple-stiffened element (Element 10 in Fig. 4.13) on the basis of $f = F_y = 33$ ksi is computed as follows:

$$w = 5.5686 \text{ in.}$$

$$w/t = 5.5686/0.075 = 74.248$$

$$\lambda = \frac{1.052}{\sqrt{4}} (74.248) \sqrt{\frac{33}{29,500}} = 1.306 > 0.673$$

$$b = \rho w = \left\{ \left[1 - \frac{0.22}{1.306} \right] \bigg/ 1.306 \right\} (5.5686)$$

$$= 3.5456 \text{ in.}$$

For the stiffened element (Element 8) of the intermediate stiffener,

$$k = 4.0$$

By using a conservative value of $f = F_y$, and

$$w/t = 0.7/0.075 = 9.33$$

$$\lambda = \frac{1.052}{\sqrt{4}} (9.33) \sqrt{\frac{33}{29,500}} = 0.164 < 0.673$$

$$b = w = 0.70 \text{ in.}$$

$$A'_s = [2(0.7) + 4(0.2063)](0.075)$$

$$= 0.1669 \text{ in.}^2$$

$$A_s = A'_s(I_s/I_a) = 0.1669(15.923/7.439)$$

$$= 0.3572 \text{ in.}^2 > A'_s$$

use $A_s = A'_s = 0.1669$ in.^{2} The neutral axis can then be located by using the following table with an assumption that the web is fully effective.

Element	Effective Length L (in.)		Distance from Top Fiber y (in.)	Ly (in.^{2})
1	$2 \times 0.5812 =$	1.1624	4.5406	5.2780
2	$2 \times 0.2063 =$	0.4126	4.9148	2.0278
3	$2 \times 3.1624 =$	6.3248	4.9625	31.3868
4	$2 \times 0.2063 =$	0.4126	4.9148	2.0278
5	$2 \times 4.6624 =$	9.3248	2.5000	23.3120
6	$2 \times 0.2063 =$	0.4126	0.0852	0.0352
7	$2 \times 0.2063 =$	0.4126	0.0852	0.0352
8	$2 \times 0.7000 =$	1.4000	0.5188	0.7263
9	$2 \times 0.2063 =$	0.4126	0.9524	0.3930
10	$2 \times 3.5456 =$	7.0912	0.0375	0.2659
Total		27.3662		65.4880

$$y_{cg} = \frac{\Sigma\,(Ly)}{\Sigma\,L} = \frac{65.4880}{27.3662} = 2.393 \text{ in.} < 2.50 \text{ in.}$$

$$f = \left(\frac{2.393}{5 - 2.393}\right)(33) = 30.29 \text{ ksi}$$

Since the computed value is considerably less than 33 ksi, additional trials are required. After several trials, it was found that the stress should be about 29.68 ksi.

b. *Additional approximation.* Assuming

$$f = 29.68 \text{ ksi}$$

$$\lambda = 1.239 > 0.673$$

$$b = 3.6964 \text{ in.}$$

Element	Effective Length L (in.)	Distance from Top Fiber y (in.)	Ly (in.^{2})	Ly^2 (in.^{3})
1	1.1624	4.5406	5.2780	23.9653
2	0.4126	4.9148	2.0278	9.9664
3	6.3248	4.9625	31.3868	155.7570
4	0.4126	4.9148	2.0278	9.9664
5	9.3248	2.5000	23.3120	58.2800
6	0.4126	0.0852	0.0352	0.0030
7	0.4126	0.0852	0.0352	0.0030
8	1.4000	0.5188	0.7263	0.3768

Element	Effective Length L (in.)	Distance from Top Fiber y (in.)	Ly (in.^{2})	Ly^2 (in.^{3})
9	0.4126	0.9524	0.3930	0.3743
10	$2 \times 3.6964 =$ 7.3928	0.0375	0.2772	0.0104
Total	27.6678		65.4993	258.7026

$$y_{cg} = \frac{65.4993}{27.6678} = 2.367 \text{ in.}$$

$$f = \left(\frac{2.367}{5 - 2.367}\right)(33) = 29.67 \text{ ksi}$$

Since the computed stress is close to the assumed value of 29.68 ksi, it is O.K.

To check if the web is fully effective, refer to Fig. 4.13:

$$f_1 = 33 \left(\frac{2.1982}{2.633}\right) = 27.55 \text{ ksi} \qquad \text{(compression)}$$

$$f_2 = -33 \left(\frac{2.4642}{2.633}\right) = -30.88 \text{ ksi} \qquad \text{(tension)}$$

$$\psi = f_2/f_1 = -1.121$$

$$k = 4 + 2(1 - \psi)^3 + 2(1 - \psi) = 27.33$$

$$h/t = 4.6624/0.075 = 62.17 < 200 \qquad \text{O.K.}$$

$$\lambda = \frac{1.052}{\sqrt{27.33}} (62.17) \sqrt{\frac{27.55}{29,500}} = 0.382 < 0.673$$

$$b_e = h = 4.6624 \text{ in.}$$

$$b_1 = b_e/(3 - \psi) = 4.6624/4.121 = 1.131 \text{ in.}$$

Since $\psi < -0.236$,

$$b_2 = b_e/2 = 2.3312 \text{ in.}$$

$$b_1 + b_2 = 3.4622 > 2.1982 \text{ in.}$$

The web is fully effective as assumed.

C. *Total I_x and S_x.*

$$2I_5' = 2 \times \tfrac{1}{12} \times (4.6624)^3 = \quad 16.8918$$

$$2I_1' = 2 \times \tfrac{1}{12} \times (0.5812)^3 = \quad 0.0327$$

$$2I_8' = 2 \times \tfrac{1}{12} \times (0.7)^3 = \quad 0.0572$$

$$2(I_2' + I_4' + I_6' + I_7' + I_9') = \quad 0.0034$$

$$\sum (Ly^2) = \underline{258.7026}$$

$$275.6877$$

$$-\left(\sum L\right)(y_{cg})^2 = -27.6678(2.367)^2 = \underline{-158.0141}$$

$$I_x' = 120.6736 \text{ in.}^3$$

$$I_x = I_x't = 120.6736(0.075) = 9.0505 \text{ in.}^4$$

$$S_x = \frac{9.0505}{5 - 2.367} = 3.4373 \text{ in.}^3$$

2. *Nominal and Allowable Design Moments.* The nominal moment for section strength is

$$M_n = S_e F_y = S_x F_y = (3.4373)(33) = 113.431 \text{ in.-kips}$$

The allowable design moment is

$$M_a = M_n/\Omega_b = 113.431/1.67 = 67.92 \text{ in.-kips}$$

B. LRFD Method

The nominal moment for the LRFD method is the same as that computed for the ASD method. From above calculations, the nominal moment about the *x*-axis of the section is

$$M_n = 113.431 \text{ in.-kips}$$

Based on Art. 4.2.1 or Sec. C3.1.1 of the AISI Specification, the design moment for the given section having a uniformly compressed flange with one intermediate stiffener ($\phi_b = 0.95$) is

$$\phi_b M_n = 0.95(113.431) = 107.76 \text{ in.-kips}$$

4.2.2.2 *Effects of Cold Work on Bending Strength*   The bending strength of cold-formed steel sections discussed above was based on the mechanical properties of the virgin material. The effects of cold work were completely neglected.

When the effects of cold work are utilized in the determination of bending strength, the computation can be performed by one of the following two design approaches.

1. Consider the increase in yield point at corners due to cold work and neglect the effects of cold work in all flat portions of the section. As discussed in Chap. 2, the increase in yield point can be found either by the use of Eq. (2.9) or by tests.
2. Consider the effects of cold work for corners and all flat elements. Equation (2.12) can be used to compute the average yield point of the entire section.

In any design approach, the following procedures may be used:[2.17]

1. Subdivide the section into a number of elements. Assume a position of the neutral axis and the strain in the top fiber. Compute the strains in various elements based on the assumed neutral axis and the top fiber strain.
2. Determine the stresses from the stress–strain relationship of the material in various elements for the computed strains.
3. Locate the neutral axis by iteration until

$$\sum \sigma \Delta A = 0$$

is satisfied. Then the bending moment can be approximated by

$$M = \sum \sigma y \Delta A$$

where σ = stress
ΔA = area for element
y = distance between center of gravity of each element and neutral axis

Results of a study by Winter and Uribe indicate that for the steels commonly used in thin-walled cold-formed steel construction, considering the effects of cold work only in the corners of the formed sections, the moment capacities can be increased by 4 to 22% compared with those obtained when neglecting cold work.[2.17]

If the effects of cold work are considered in both the flats and the corners, the increase in bending strength ranges from 17 to 41% above the virgin value.

It can be seen that a substantial advantage can be obtained by using the increase in strength of the material. Figure 4.14, reproduced from Ref. 2.17, shows a comparison of the ultimate moments computed for three different conditions. It should be noted that the effects of cold work as shown in Fig. 4.14 may not be directly applied to other configurations because the relative influence of corners or flats on the increase in bending strength depends mainly on the configuration of the section, and the spread between the tensile strength and yield point of the virgin material. Attention should be given to the limitations of Sec. A7.2 of the AISI Specification when the effects of cold work are used in design.

4.2.2.3   *Inelastic Reserve Capacity of Beams*   Prior to 1980, the inelastic reserve capacity of beams was not included in the AISI Specification because most cold-formed steel shapes have width-to-thickness ratios considerably in excess of the limits required by plastic design. Because of the use of large width-to-thickness ratios for beam flange and web, such members are usually incapable of developing plastic hinges without local buckling.
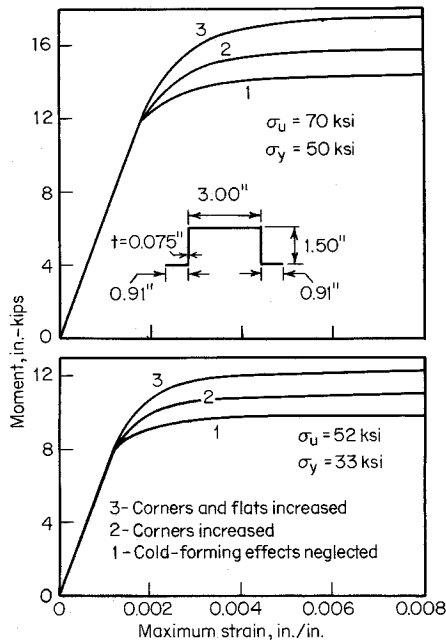

Figure 4.14   Comparison of ultimate moments computed for three different conditions.[2.17]

In the 1970s research work on the inelastic strength of cold-formed steel beams was carried out by Reck, Pekoz, Winter, and Yener at Cornell University.[4.1–4.4] These studies showed that the inelastic reserve strength of cold-formed steel beams due to partial plastification of the cross section and the moment redistribution of statically indeterminate beams can be significant for certain practical shapes. With proper care, this reserve strength can be utilized to achieve more economical design of such members. In Europe, a study has been made by von Unger on the load-carrying capacity of transversely loaded continuous beams with thin-walled section, in particular of roof and floor decks with trapezoidal profiles.[4.5] In addition, the buckling strength and load-carrying capacity of continuous beams and steel decks have also been studied by some other investigators.[4.6–4.9]

In order to utilize the available inelastic reserve strength of certain cold-formed steel beams, new design provisions based on the partial plastification of the cross section were added in the 1980 edition of the AISI Specification. The same provisions are retained in the 1986 and the 1996 editions of the specification. According to Procedure II of Sec. C3.1.1 of the specification, the nominal section strengths, M_n, of those beams satisfying certain specific limitations can be determined on the basis of the inelastic reserve capacity with a limit of $1.25M_y$ or $1.25S_e F_y$. In the above expression, M_y is the effective yield moment determined according to Art. 4.2.2.1. The ratio of M_n/M_y represents the inelastic reserve strength of a beam cross section.

The nominal moment M_n is the maximum bending capacity of the beam by considering the inelastic reserve strength through partial plastification of the cross section. The inelastic stress distribution in the cross section depends on the maximum strain in the compression flange, ϵ_{cu}. Based on the Cornell research work on hat sections having stiffened compression flanges,[4.1] the AISI design provision included in Sec. C3.1.1 of the specification limits the maximum compression strain to be $C_y \epsilon_y$, that is,

$$\epsilon_{cu} = C_y \epsilon_y \tag{4.5}$$

where ϵ_y = yield strain, = F_y/E, in./in.
   E = modulus of elasticity of steel, = 29.5×10^3 ksi (203 GPa)
   F_y = yield point of steel, ksi
   C_y = a factor determined as follows:

1. Stiffened compression elements without intermediate stiffeners
   a. When $w/t \leq \lambda_1$

$$C_y = 3.0 \tag{4.6}$$

   b. When $\lambda_1 < w/t < \lambda_2$

$$C_y = 3 - 2\left(\frac{w/t - \lambda_1}{\lambda_2 - \lambda_1}\right) \tag{4.7}$$

c. When $w/t \geq \lambda_2$

$$C_y = 1.0 \tag{4.8}$$

where

$$\lambda_1 = \frac{1.11}{\sqrt{F_y/E}}$$

$$\lambda_2 = \frac{1.28}{\sqrt{F_y/E}}$$

The relationship between C_y and the w/t ratio of the compression flange is shown in Fig. 4.15.

2. Unstiffened compression elements

$$C_y = 1.0 \tag{4.9}$$

3. Multiple-stiffened compression elements and compression elements with edge stiffeners

$$C_y = 1.0 \tag{4.10}$$

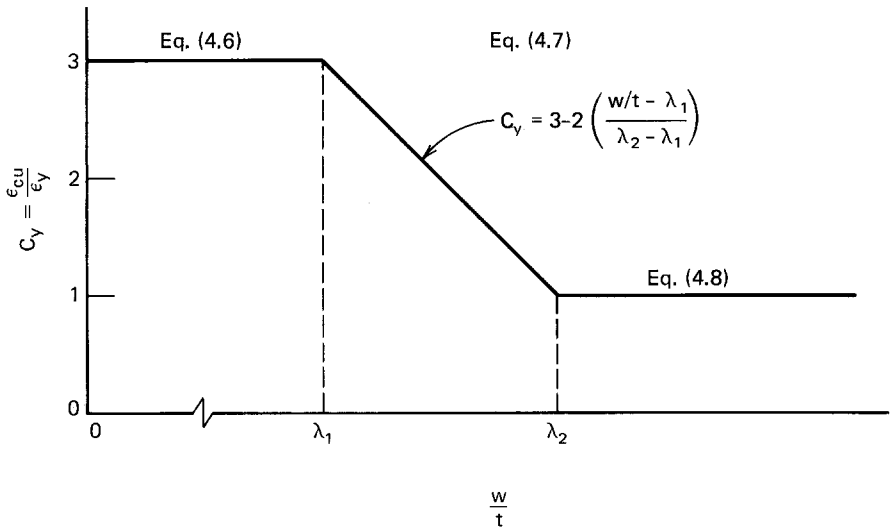No limit is placed on the maximum tensile strain in the AISI Specification.

Eq. (4.6)   Eq. (4.7)

$$C_y = 3 - 2\left(\frac{w/t - \lambda_1}{\lambda_2 - \lambda_1}\right)$$

Eq. (4.8)

$C_y = \dfrac{\epsilon_{cu}}{\epsilon_y}$

$\dfrac{w}{t}$

Figure 4.15   Factor C_y for stiffened compression elements without intermediate stiffeners.

On the basis of the maximum compression strain ϵ_{cu} allowed in Eq. (4.5), the neutral axis can be located by using Eq. (4.11), and the nominal moment M_n can be determined by using Eq. (4.12) as follows:

$$\int \sigma \, dA = 0 \qquad (4.11)$$

$$\int \sigma y \, dA = M_n \qquad (4.12)$$

where σ is the stress in the cross section.

For hat sections Reck, Pekoz, and Winter gave the following equations for the nominal moments of sections with yielded tension flange and sections with tension flange not yielded.

a. Sections with Yielded Tension Flange at Nominal Moment.[4.1] For the stress distributions shown in Fig. 4.16, Eqs. (4.13) to (4.18) are used for computing the values of y_c, y_t, y_p, y_{cp}, y_{tp}, and M_n. For the purpose of simplicity, midline dimensions are used in the calculation.
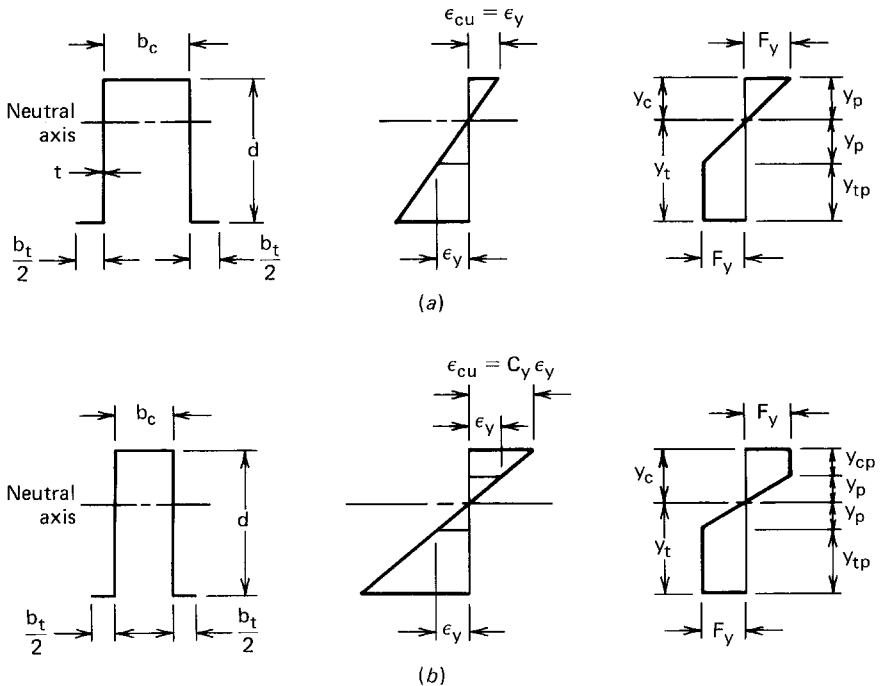

Figure 4.16 Stress distribution in sections with yielded tension flange at nominal moment.[4.1]

$$y_c = \frac{b_t - b_c + 2d}{4} \tag{4.13}$$

$$y_t = d - y_c \tag{4.14}$$

$$y_p = \frac{y_c}{\epsilon_{cu}/\epsilon_y} \tag{4.15}$$

$$y_{cp} = y_c - y_p \tag{4.16}$$

$$y_{tp} = y_t - y_p \tag{4.17}$$

$$M_n = F_y t \left[b_c y_c + 2y_{cp} \left(y_p + \frac{y_{cp}}{2} \right) + \frac{4}{3} (y_p)^2 \right.$$
$$\left. + 2y_{tp} \left(y_p + \frac{y_{tp}}{2} \right) + b_y y_t \right] \tag{4.18}$$

b. Sections with Tension Flange Not Yielded at Nominal Moment.[4.1] For the stress distribution shown in Fig. 4.17, y_c is computed from the following quadratic equation:

$$y_c^2 \left(2 - \frac{1}{C_y} - C_y \right) + y_c(b_c + 2C_y d + C_y b_t) - (C_y d^2 + C_y b_t d) = 0 \tag{4.19}$$

Subsequently, the values of y_t, y_p, and y_{cp} can be computed from Eqs. (4.14), (4.15), and (4.16), respectively.

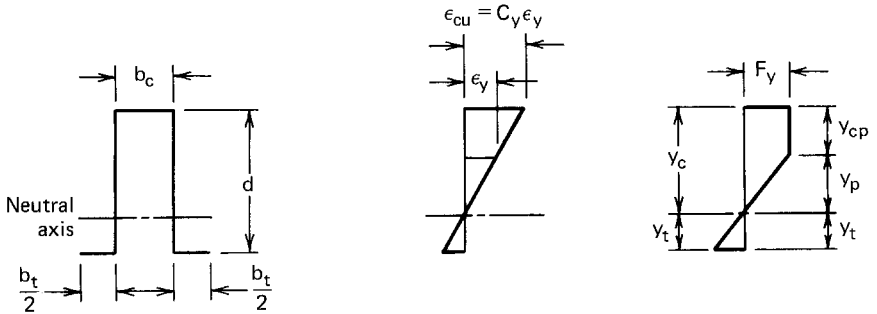If $y_p > y_t$, then case 4.2.2.3b applies and the nominal moment M_n is computed as follows:

Figure 4.17   Stress distribution in sections with tension flange not yielded at nominal moment.[4.1]

$$M_n = F_y t \left[b_c y_c + 2 y_{cp} \left(y_p + \frac{y_{cp}}{2} \right) + \frac{2}{3} (y_p)^2 \right.$$
$$\left. + \frac{2}{3} (y_t)^2 \left(\frac{\sigma_t}{F_y} \right) + b_y y_t \left(\frac{\sigma_t}{F_y} \right) \right] \quad (4.20)$$

In Eq. (4.20), $\sigma_t = F_y C_y y_t / y_c$.

It should be noted that according to Sec. C3.1.1 of the AISI Specification, Eqs. (4.18) and (4.20) can be used only when the following conditions are met:

1. The member is not subject to twisting, lateral, torsional, or torsional–flexural buckling.
2. The effect of cold forming is not included in determining the yield point F_y.
3. The ratio of the depth of the compression portion of the web to its thickness does not exceed λ_1.
4. The shear force does not exceed $0.35 F_y$ times the web area, ht.
5. The angle between any web and the vertical does not exceed 30°.

It should also be noted that when applicable, effective design widths should be used in the calculation.

Example 4.5 For the hat section (3 × 3 × 0.105 in.) shown in Fig. 4.18, determine the allowable design moment (M_a) about the x-axis for the ASD method and the design moment ($\phi_b M_n$) for the LRFD method. Consider the inelastic reserve capacity according to Sec. C3.1.1 of the 1996 edition of the AISI Specification. Use $F_y = 33$ ksi and assume that lateral support is adequately provided.
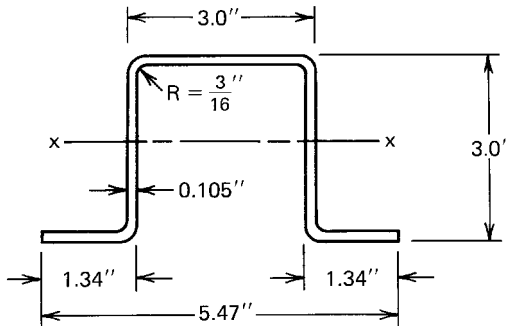

Figure 4.18 Example 4.5.

Solution

A. ASD Method

1. *Dimensions of Section.* By using the midline dimensions and square corners, the widths of compression and tension flanges and the depth of webs are computed as follows.

Width of compression flange,

$$b_c = 3 - 0.105 = 2.895 \text{ in.}$$

Width of tension flange,

$$b_t = 2(1.34 - 0.105/2) = 2.576 \text{ in.}$$

Depth of webs,

$$d = 3 - 0.105 = 2.895 \text{ in.}$$

All dimensions are shown in Fig. 4.19a. Check the effective width of the compression flange

$$w = 3 - 2(3/16 + 0.105) = 2.415 \text{ in.}$$
$$w/t = 2.415/0.105 = 23$$
$$k = 4.0$$
$$f = F_y = 33 \text{ ksi}$$
$$\lambda = (1.052/\sqrt{4})(23)(\sqrt{33/29,500}) = 0.405 < 0.673$$
$$b = w = 2.415 \text{ in.}$$

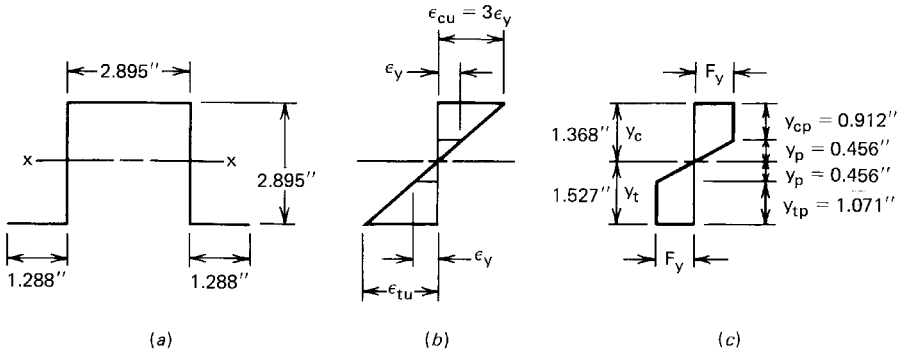Therefore, the compression flange is fully effective.

Figure 4.19 Stress distribution. (*a*) Midline dimensions. (*b*) Strain. (*c*) Stress.

2. *Strain Diagram.* The w/t ratio of the stiffened compression flange is

$$\frac{w}{t} = 23$$

$$\lambda_1 = 1.11/\sqrt{F_y/E}$$

$$= 1.11/\sqrt{33/29,500} = 33.2$$

Since $w/t < (\lambda_1 = 33.2)$, according to Eq. (4.6), $C_y = 3.0$. Therefore $\epsilon_{cu} = 3\epsilon_y$, as shown in Fig. 4.19b.

3. *Stress Diagram.* The values of y_c, y_t, y_p, y_{cp}, and y_{tp} are computed by using Eqs. (4.13) to (4.17) as follows:

$$y_c = \frac{b_t - b_c + 2d}{4} = \frac{2.576 - 2.895 + 2 \times 2.895}{4} = 1.368 \text{ in.}$$

$$y_t = d - y_c = 2.895 - 1.368 = 1.527 \text{ in.}$$

$$y_p = \frac{y_c}{\epsilon_{cu}/\epsilon_y} = \frac{1.368}{3} = 0.456 \text{ in.}$$

$$y_{cp} = y_c - y_p = 1.368 - 0.456 = 0.912 \text{ in.}$$

$$y_{tp} = y_t - y_p = 1.527 - 0.456 = 1.071 \text{ in.}$$

All dimensions are shown in Fig. 4.19c.

4. *Nominal Moment M_n.* In order to utilize the inelastic reserve capacity, the AISI requirements must be checked.

$$\frac{y_c}{t} = \frac{1.368}{0.105} = 13.03 < (\lambda_1 = 33.2) \qquad \text{(O.K.)}$$

Therefore, the nominal moment is

$$M_n = F_y t[b_c y_c + 2y_{cp}(y_p + y_{cp}/2) + \tfrac{4}{3}(y_p)^2$$

$$+ 2y_{tp}(y_p + y_{tp}/2) + b_t y_t]$$

$$= 33(0.105)[(2.895 \times 1.368) + 2(0.912)(0.456 + 0.912/2)$$

$$+ \tfrac{4}{3}(0.456)^2 + 2(1.071)(0.456 + 1.071/2) + (2 \times 1.288)(1.527)]$$

$$= 41.43 \text{ in.-kips}$$

5. *Yield Moment M_y.* Based on the method illustrated in Example 4.3, S_e for the given hat section is 0.992 in.[3] Therefore

$$M_y = S_eF_y = 0.992(33) = 32.74 \text{ in.-kips}$$

$$1.25M_y = 1.25(32.74) = 40.93 \text{ in.-kips}$$

6. *Allowable Design Moment M_a.* Because M_n exceeds $1.25M_y$, use

$$M_n = 1.25M_y = 40.93 \text{ in.-kips}$$

$$M_a = M_n/\Omega_b = 40.93/1.67 = 24.51 \text{ in.-kips}$$

B. LRFD Method

The nominal moment for the LRFD method is the same as that computed for the ASD method. From Item *A* above, the nominal moment about the *x*-axis of the hat section is

$$M_n = 40.93 \text{ in.-kips}$$

Based on Art. 4.2.1 or Sec. C3.1.1 of the AISI Specification, the design moment for the hat section having a stiffened compression flange ($\phi_b = 0.95$) is

$$\phi_bM_n = 0.95(40.93) = 38.88 \text{ in.-kips}$$

Example 4.6   For the I-section with unequal flanges as shown in Fig. 4.20, determine the allowable design moment (M_a) about the *x*-axis for the ASD method and the design moment (ϕ_bM_n) for the LRFD method. Consider the inelastic reserve capacity and use $F_y = 50$ ksi. Assume that lateral support is adequately provided to prevent lateral buckling.

Solution

A. ASD Method

1. *Dimensions of Section.* By using the midline dimensions and square corners, the widths of compression and tension flanges and the depth of webs are computed as follows: The flat width of the unstiffened compression flange according to Art. 3.2 is,

$$w = 2.5 - (R + t) = 2.5 - (3/16 + 0.135) = 2.1775 \text{ in.}$$

$$w/t = 2.1775/0.135 = 16.13$$

For $f = F_y = 50$ ksi in the top fiber and $k = 0.43$ for the unstiffened flange,
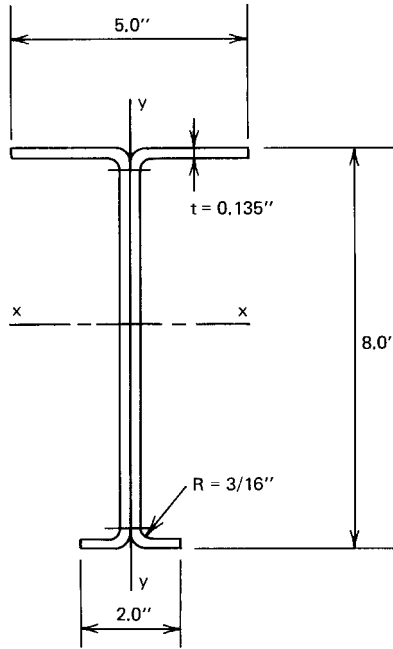
Figure 4.20   Example 4.6.

$$\lambda = \frac{1.052}{\sqrt{0.43}} \ (16.13) \ \sqrt{\frac{50}{29,500}} = 1.065 > 0.673$$

$$b = \rho w = [(1 - 0.22/\lambda)/\lambda]w = 1.622 \text{ in.}$$

$$b_c/2 = b + (R + t/2) = 1.622 + (3/16 + 0.135/2) = 1.877 \text{ in.}$$

$$b_c = 3.754 \text{ in.}$$

Width of the tension flange,

$$b_t/2 = 1 - t/2 = 1 - 0.135/2 = 0.9325 \text{ in.}$$

$$b_t = 1.865 \text{ in.}$$

Depth of webs

$$d = 8.0 - t = 8.0 - 0.135 = 7.865 \text{ in.}$$

All midline dimensions are shown in Fig. 4.21a.

2. *Strain Diagram.* For unstiffened compression flange, $C_y = 1.0$. Therefore
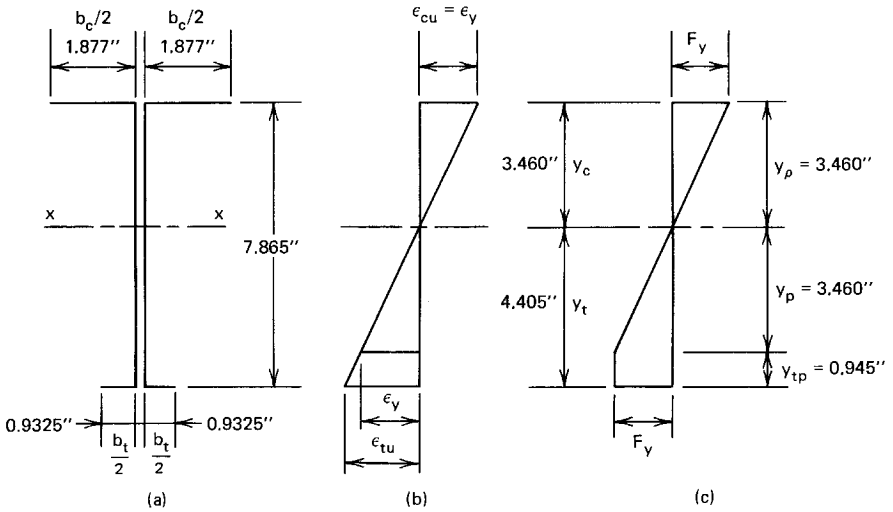
Figure 4.21   Stress distribution. (*a*) Midline dimensions. (*b*) Strain. (*c*) Stress.

$$\epsilon_{cu} = \epsilon_y$$

as shown in Fig. 4.21*b*.

3. *Stress Diagram.* The values of y_c, y_t, y_p, and y_{tp} are computed by using Eqs. (4.13) to (4.17) as follows:

$$y_c = \frac{b_t - b_c + 2d}{4} = \frac{1.865 - 3.754 + 2(7.865)}{4} = 3.46 \text{ in.}$$

$$y_t = d - y_c = 7.865 - 3.46 = 4.405 \text{ in.}$$

$$y_p = \frac{y_c}{\epsilon_{cu}/\epsilon_y} = y_c = 3.46 \text{ in.}$$

$$y_{cp} = 0$$

$$y_{tp} = y_t - y_p = 4.405 - 3.46 = 0.945 \text{ in.}$$

All dimensions are shown in Fig. 4.21*c*.

4. *Nominal Moment.* In order to satisfy the AISI requirements for using the inelastic reserve capacity, check the y_c/t ratio against the limit of λ_1.

$$\frac{y_c}{t} = \frac{3.46}{0.135} = 25.63$$

$$\lambda_1 = 1.11 \sqrt{F_y/E} = 1.11 \sqrt{50/29,500} = 26.96$$

Since $y_c/t < \lambda_1$, O.K. Therefore, the nominal moment is

$$M_n = F_y t[b_c y_c + \tfrac{4}{3}(y_p)^2 + 2y_{tp}(y_p + y_{tp}/2) + b_t y_t]$$

$$= 50(0.135)[(3.754 \times 3.46) + \tfrac{4}{3}(3.46)^2$$

$$+ \ 2(0.945)(3.46 + 0.945/2)$$

$$+ \ 1.865(4.405)]$$

$$= 301.05 \text{ in.-kips}$$

5. *Yield Moment.* Based on the method illustrated in Example 4.1, the effective yield moment, M_y, is

$$M_y = 248.0 \text{ in.-kips}$$

$$1.25 \ M_y = 310.0 \text{ in.-kips}$$

6. *Nominal Moment and Allowable Design Moment.* Because M_n is less than $1.25 \ M_y$, use M_n for the nominal moment, i.e.,

$$M_n = 301.05 \text{ in.-kips}$$

The allowable design moment is

$$M_a = M_n/\Omega_b = 301.05/1.67 = 180.27 \text{ in.-kips}$$

B. LRFD Method

The nominal moment for the LRFD method is the same as that computed for the ASD method. From Item *A* above, the nominal moment about the *x*-axis of the I-section with unequal flanges is

$$M_n = 301.05 \text{ in.-kips}$$

Based on Art. 4.2.1 or Sec. C3.1.1 of the AISI Specification, the design moment for the I-section having an unstiffened compression flange ($\phi_b = 0.90$) is

$$\phi_b M_n = 0.90(301.05) = 270.95 \text{ in.-kips}$$

4.2.2.4   Economic Design for Bending Strength   The above discussion and design examples are based on the fact that the allowable design moment is determined for a given section for which the dimensions are known. In the design of a new section, the dimensions are usually unknown factors. The selection of the most favorable dimensions can be achieved by using the

optimum design technique. This is a very complex nonlinear problem which can only be solved by computer analysis.[1.247] However, if the depth and the thickness of the section are known, previous study has shown that the maximum moment-to-weight ratio usually occur in the neighborhood of the flange width determined by Eq. (4.21) or (4.22) as applicable.

1. For unstiffened compression flanges,

$$w = 0.43t \sqrt{\frac{E}{f}} \qquad (4.21)$$

2. For stiffened compression flanges supported by a web on each longitudinal edge,

$$w = 1.28t \sqrt{\frac{E}{f}} \qquad (4.22)$$

where w = flat width for compression flange
t = thickness of steel
E = modulus of elasticity
f = maximum compressive edge stress in the element without considering the safety factor

The economic design of continuous beams and long-span purlins is discussed in Refs. 4.11 and 4.12.

4.2.2.5 Deflection of Flexural Members

For a given loading condition, the deflection of flexural members depends on the magnitude, location, and type of the applied load, the span length, and the bending stiffness EI, in which the modulus of elasticity in the elastic range is 29.5×10^3 ksi (203 GPa) and I is the moment of inertia of the beam section.

Similar to the bending strength calculation, the determination of the moment of inertia I for calculating the deflection of steel beams is based on the effective areas of the compression flange and beam web, for which the effective widths are computed for the compressive stress developed from the bending moment. If the compression flange and the beam web are fully effective, the moment of inertia is obviously based on the full section. In this case, the moment of inertia is a constant value along the entire beam length. Otherwise, if the moment of inertia is on the basis of the effective areas of the compression flange and/or beam web, the moment of inertia may vary along the beam span because the bending moment usually varies along the beam length, as shown in Fig. 4.22.

In the design of thin-walled cold-formed steel sections, the method to be used for deflection calculation is based on the accuracy desired in the analysis.
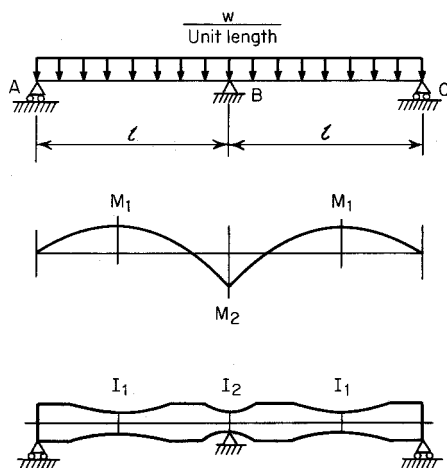
Figure 4.22 Bending moment and variable moments of inertia for two-span contin-
uous beam under uniform load.[4.14].

If a more exact deflection is required, a computer program or a numerical
method may be used in which the beam should be divided into a relatively
large number of elements according to variable moments of inertia. The de-
flection calculation for such a beam is too complicated for hand calculation.
On the other hand, if an approximate analysis is used, the deflection of a
simply supported beam may be computed on the basis of a constant moment
of inertia determined for the maximum bending moment. The error so intro-
duced is usually small and on the conservative side.[3.13] For continuous spans,
the deflection of the beam may be computed either by a rational analysis[4.13]
or by a method using a conventional formula in which the average value of
the positive and negative moments of inertia I_1 and I_2 will be used as the
moment of inertia I.[4.14] This simplified method and other approaches have
been used in Refs. 4.6 and 4.7 for a nonlinear analysis of continuous beams.

Example 4.7 Determine the moment of inertia of the I-Section (Fig. 4.2) to
be used for deflection calculation when the I-section is loaded to the allowable
design moment as determined in Example 4.1 for the ASD method.

Solution From Example 4.1, the allowable design moment for the given
I-section is 187.0 in.-kips. The estimated compressive stress in the top fiber
under the allowable design moment is

$$f = \frac{My_{cg}}{I_x} = \frac{187.0(4.063)}{25.382} = 29.93 \text{ ksi}$$

The same stress of $f = 29.93$ ksi will be assumed in the calculation of the
effective design width for deflection calculation.

By using Eqs. (3.45) through (3.47) and the same procedure employed in Example 4.1, the effective width b_d of the unstiffened flange can be computed as follows:

$$w = 1.6775 \text{ in.}$$
$$w/t = 12.426$$
$$k = 0.43$$
$$f = 29.93 \text{ ksi}$$
$$\lambda = \frac{1.052}{\sqrt{0.43}} (12.426) \sqrt{\frac{29.93}{29,500}} = 0.635 < 0.673$$
$$\rho = 1.0$$
$$b_d = w = 1.6775 \text{ in.}$$

Using the full width of the compression flange and assuming the web is fully effective, the neutral axis is located at the mid-depth (i.e., $y_{cg} = 4.0$ in.). Prior to computing the moment of inertia, check the web for effectiveness as follows:

$$f_1 = 29.93 \left(\frac{4 - 0.3225}{4}\right)$$
$$= 27.52 \text{ ksi) (compression)}$$
$$f_2 = -29.93 \left(\frac{4 - 0.3225}{4}\right)$$
$$= -27.52 \text{ ksi} \quad \text{(tension)}$$
$$\psi = f_2/f_1 = -1.0$$
$$k = 4 + 2(1 - \psi)^3 + 2(1 - \psi) = 24.0$$
$$h/t = 54.48$$
$$\lambda = \frac{1.052}{\sqrt{24}} (54.48) \sqrt{\frac{27.52}{29,500}}$$
$$= 0.357 < 0.673$$
$$\rho = 1.0$$
$$b_e = h = 7.355 \text{ in.}$$
$$b_1 = b_e/(3 - \psi) = 7.355/(3 + 1) = 1.839 \text{ in.}$$

Since $\psi < -0.236$,

$$b_2 = b_e/2 = 3.6775 \text{ in.}$$

$$b_1 + b_2 = 1.839 + 3.6775 = 5.5165 \text{ in.}$$

Since $(b_1 + b_2)$ is greater than the compression portion of the web of 3.6775 in., the web is fully effective as assumed. Because both the compression flange and the web are fully effective, the moment of inertia I_x of the full section can be computed as follows:

Element	Area A (in.²)	Distance from Mid-Depth y (in.)	Ay^2 (in.⁴)
Flanges	4(1.6775)(0.135) = 0.9059	3.9325	14.0093
Corners	4(0.05407) = 0.2163	3.8436	3.1955
Webs	2(7.355)(0.135) = 1.9859	0	0
Total	3.1081		17.2048

$$2I_{web} = 2 \times \frac{1}{12} (0.135)(7.355)^3 = \underline{8.9522}$$

$$I_x = 26.1570 \text{ in.}^4$$

$$f = \frac{M_x y_{cg}}{I_x} = \frac{187.0(4.0)}{26.1570} = 28.60 \text{ ksi}$$

In view of the fact that the computed stress of 28.60 ksi is less than the assumed value of 29.93 ksi, the moment of inertia I_x computed on the basis of the full section can be used for deflection calculation without additional iteration.

Example 4.8   Compute the moment of inertia of the hat section (Fig. 4.9) to be used for deflection calculation when the hat section is loaded to the allowable design moment as determined in Example 4.3 for the ASD method.

Solution

1. *First Approximation.* From Example 4.3, the allowable design moment is 193.59 in.-kips. The estimated compressive stress in the top flange under the allowable moment is

$$f = \frac{M_x y_{cg}}{I_x} = \frac{193.59(4.487)}{35.646} = 24.37 \text{ ksi}$$

The same stress of $f = 24.37$ ksi will be assumed in the calculation of the effective design width for deflection determination.

Using Eqs. (3.45) through (3.47) and the same procedure employed in Example 4.3, the effective width b_d of the stiffened compression flange is computed as follows:

$$w = 14.415 \text{ in.}$$
$$w/t = 137.29$$
$$k = 4.0$$
$$f = 24.37 \text{ ksi}$$

$$\lambda = \frac{1.052}{\sqrt{4}} (137.29) \sqrt{\frac{24.37}{29,500}} = 2.076 > 0.673$$

$$\rho = \left(1 - \frac{0.22}{2.076}\right) \Big/ 2.076 = 0.431$$

$$b_d = \rho w = 0.431(14.415) = 6.213 \text{ in.}$$

By using the effective width of the compression flange and assuming the web is fully effective, the moment of inertia can be computed from the line elements shown in Fig. 4.10 as follows:

Element	Effective Length L (in.)	Distance from Top Fiber y (in.)	Ly (in.²)	Ly^2 (in.³)
1	2(1.0475) = 2.0950	9.9476	20.8400	207.3059
2	2(0.3768) = 0.7536	9.8604	7.4308	73.2707
3	2(9.415) = 18.8300	5.0000	94.1500	470.7500
4	2(0.3768) = 0.7536	0.1396	0.1052	0.0147
5	6.2130	0.0525	0.3262	0.0171
Total	28.6452		122.8522	751.3584

$$y_{cg} = \frac{122.8522}{28.6452} = 4.289 \text{ in.}$$

The total I_x is

$$2I_3' = 2\left(\frac{1}{12}\right)(9.415)^3 = \quad 139.0944$$

$$\sum (Ly^2) = \underline{\quad 751.3584}$$

$$890.4528$$

$$-\left(\sum L\right)(y_{cg}^2) = -28.6452(4.289)^2 = \underline{-526.9434}$$

$$I_x' = \quad 363.5094 \text{ in.}^3$$

$$I_x = I_x't = 363.5094(0.105) = \quad 38.168 \text{ in.}^4$$

The compressive stress in the top fiber is

$$f = \frac{M_x y_{cg}}{I_x} = \frac{193.59(4.289)}{38.168}$$

$$= 21.75 \text{ ksi} < \text{ the assumed value (no good)}$$

2. *Second Approximation.* Assuming $f = 21.00$ ksi and using the same values of w/t and k,

$$\lambda = \frac{1.052}{\sqrt{4}} (137.29) \sqrt{\frac{21.00}{29,500}} = 1.927 > 0.673$$

$$\rho = 0.460$$

$$b_d = \rho w = 6.631 \text{ in.}$$

Element	Effective Length L (in.)	Distance from Top Fiber y (in.)	Ly (in.²)	Ly^2 (in.³)
1 to 4	22.4322		122.5260	751.3413
5	6.6310	0.0525	0.3481	0.0183
Total	29.0632		122.8741	751.3596

$$y_{cg} = 4.228 \text{ in.}$$

The total I_x is

$$2I'_3 = \quad 139.0944$$

$$\sum (Ly^2) = \quad \underline{751.3596}$$

$$890.4540$$

$$-\left(\sum L\right)(y^2_{cg}) = -29.0632(4.228)^2 = \underline{-519.5333}$$

$$I'_x = \quad 370.9207 \text{ in.}^3$$

$$I_x = I'_x t = \quad 38.947 \text{ in.}^4$$

$$f = \frac{M_x y_{cg}}{I_x} = \frac{193.59(4.228)}{38.947} = \quad 21.01 \text{ ksi}$$

Since the computed value of f is close to the assumed value of 21.00 ksi, the moment of inertia for deflection calculation under the allowable design moment is 38.947 in.[4] It is of interest to note that the difference between the I values computed from the first and second approximations is only about 2%.

4.2.3 Lateral–Torsional Buckling Strength

Cold-formed steel flexural members, when loaded in the plane of the web, may twist and deflect laterally as well as vertically if braces are not adequately provided. In the design of flexural members, the moment capacity is not only governed by the section strength of the cross section as discussed in Art. 4.2.2 but is also limited by the lateral buckling strength of the member. This article contains the design methods for determining the lateral buckling strength of singly, doubly, and point-symmetric sections according to the actual number and location of braces. The design of braces is discussed in Art. 4.4.

4.2.3.1 Doubly and Singly Symmetric Sections.   When a simply supported, locally stable I-beam is subject to a pure moment M as shown in Fig. 4.23, the following differential equations for the lateral–torsional buckling of such a beam are given by Galambos in Ref. 2.45:

$$EI_y u^{iv} + M\phi'' = 0 \tag{4.23}$$

$$EC_w \phi^{1v} - GJ\phi'' + Mu'' = 0 \tag{4.24}$$

where M = pure bending moment
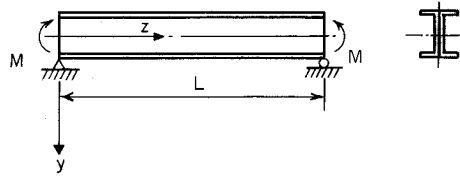$\quad\quad E$ = modulus of elasticity

Figure 4.23   Simply supported beam subjected to end momens.

G = shear modulus = $E/2(1 + \mu)$
I_y = moment of inertia about y axis
C_w = warping constant of torsion of the cross section (see Appendix B)
J = St. Venant torsion constant of cross section approximately determined by $\frac{1}{3} \Sigma b_i t_i^3$
u = deflection of shear center in x direction
ϕ = angle of twist

The primes indicate differentiation with respect to z.

Considering the simply supported condition, the end sections cannot deflect or twist; they are free to warp, and no end moment exists about the y axis. The boundary conditions are

$$u(0) = u(L) = \phi(0) = \phi(L) = 0 \tag{4.25}$$

$$u''(0) = u''(L) = \phi''(0) = \phi''(L) = 0 \tag{4.26}$$

The solution of Eqs. (4.23) and (4.24) gives the following equation for the critical lateral buckling moment:

$$M_{cr} = \frac{n\pi}{L} \sqrt{EI_y GJ\left(1 + \frac{n^2\pi^2 EC_w}{GJL^2}\right)} \tag{4.27}$$

where L is the span length and $n = 1, 2, 3, \ldots$.

The deflected shape of the beam is

$$\phi = C \sin\left(\frac{n\pi z}{L}\right) \tag{4.28}$$

and the lateral deflection u can be determined by

$$u = \frac{CML^2 \sin(n\pi z/L)}{n^2\pi^2 EI_y} \tag{4.29}$$

The deflection history of the I-beam is shown in Fig. 4.24. When $M < M_{cr}$
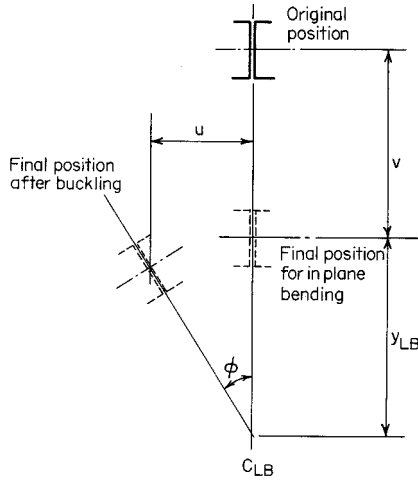
Figure 4.24   Positions of I-beam after lateral buckling.

and $M = M_{cr}$ but lateral buckling has not yet occurred, the beam deflects in the y direction. The vertical deflection v can be obtained from Eq. (4.30) for in-plane bending,

$$EI_x v'' = - M \qquad (4.30)$$

Solving Eq. (4.30) and using the boundary conditions $v(0) = v(L) = 0$, the deflection equation is[2.45]

$$v = \frac{ML^2}{2EI_x} \left[\left(\frac{z}{L} \right) - \left(\frac{z}{L} \right)^2 \right] \qquad (4.31)$$

When the beam buckles laterally, the section rotates about the center of rotation C_{LB}. This point is located at a distance of y_{LB} below the shear center of the section as determined by Eq. (4.32),

$$y_{LB} \simeq \frac{u}{\phi} = \frac{ML^2}{n^2 \pi^2 EI_y} \qquad (4.32)$$

From Eq. (4.27), for $n = 1$, the lowest critical moment for lateral buckling of an I-beam is equal to

$$M_{cr} = \frac{\pi}{L} \sqrt{EI_y GJ \left(1 + \frac{\pi^2 EC_w}{GJL^2} \right)} \qquad (4.33)$$
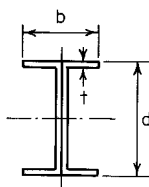
Since for I-beams (Fig. 4.25)

Figure 4.25   Dimensions of I-beam.

$$C_w \simeq \frac{b^3 t d^2}{24} \tag{4.34}$$

$$I_y \simeq \frac{b^3 t}{6} \tag{4.35}$$

Equation (4.33) can then be rewritten as follows:

$$M_{cr} = \frac{\pi}{L} \sqrt{EI_y GJ + \frac{E^2 I_y^2 d^2}{4}\left(\frac{\pi}{L}\right)^2} \tag{4.36}$$

Consequently the critical stress for lateral buckling of an I-beam subjected to pure bending is given by

$$\sigma_{cr} = \frac{M_{cr}}{S_x} = \frac{M_{cr}d}{2I_x}$$
$$= \frac{\pi^2 E}{2(L/d)^2} \sqrt{\left(\frac{I_y}{2I_x}\right)^2 + \left(\frac{JI_y}{2(1+\mu)I_x^2}\right)\left(\frac{L}{\pi d}\right)^2} \tag{4.37}$$

where S_x is the section modulus and I_x is the moment of inertia of the full section about the x axis. The unpublished data of 74 tests on lateral buckling of cold-formed steel I-sections of various shapes, spans, and loading conditions have demonstrated that Eq. (4.37) applies to cold-formed steel sections with reasonable accuracy.[1.161]

In Eq. (4.37) the first term under the square root represents the strength due to lateral bending rigidity of the beam, and the second term represents the St. Venant torsional rigidity. For thin-walled cold-formed steel sections, the first term usually exceeds the second term considerably.

For I-beams with unequal flanges, the following equation has been derived by Winter for the elastic lateral buckling stress.[1.161,3.84,4.15]

$$\sigma_{cr} = \frac{\pi^2 E d}{2L^2 S_{xc}}\left(I_{yc} - I_{yt} + I_y \sqrt{1 + \frac{4GJL^2}{\pi^2 I_y E d^2}}\right) \tag{4.38}$$

where S_{xc} is the section modulus relative to the compression fiber, and I_{yc} and

I_{yt} are the moments of inertia of the compression and tension portions of the full section, respectively, about the centroidal axis parallel to the web. Other symbols were defined previously. For equal-flange sections, $I_{yc} = I_{yt} = I_y/2$, Eqs. (4.37) and (4.38) are identical.

As previously discussed, in Eq. (4.38) the second term under the square root represents the St. Venant torsional rigidity, which can be neglected without much loss in economy. Therefore Eq. (4.38) can be simplified as shown in Eq. (4.39) by considering $I_y = I_{yc} + I_{yt}$ and neglecting the term of $4GJL^2/\pi^2 I_y E d^2$:

$$\sigma_{cr} = \frac{\pi^2 E d I_{yc}}{L^2 S_{xc}} \tag{4.39}$$

Equation (4.39) was derived on the basis of a uniform bending moment. It is rather conservative for the case of unequal end moments. For this reason it may be modified by multiplying the right-hand side by a bending coefficient C_b,[1.161,3.84]

$$\sigma_{cr} = \frac{C_b \pi^2 E}{L^2 S_{xc}/d I_{yc}} \tag{4.40}$$

where C_b is the bending coefficient, which can conservatively be taken as unity. During the period from 1968 to 1996, the bending coefficient was calculated from $C_b = 1.75 + 1.05(M_1/M_2) + 0.3(M_1/M_2)^2$, but must not exceed 2.3. Here M_1 is the smaller and M_2 the larger bending moment at the ends of the unbraced length, taken about the strong axis of the member. The ratio of end moments M_1/M_2 is positive when M_1 and M_2 have the same sign (reverse curvature bending) and negative when they are of opposite signs (single curvature bending).

The above equation for C_b was replaced by the following equation in the 1996 edition of the AISI Specification:

$$C_b = \frac{12.5 M_{max}}{2.5 M_{max} + 3 M_A + 4 M_B + 3 M_C}$$

where M_{max} = absolute value of maximum moment in the unbraced segment
M_A = absolute value of moment at quarter point of unbraced segment
M_B = absolute value of moment at centerline of unbraced segment
M_C = absolute value of moment at three-quarter point of unbraced segment

This newly adopted equation for bending coefficient was derived from Ref. 4.156. It can be used for various shapes of moment diagrams within the

unbraced segment and gives more accurate results for fixed-end beams and moment diagrams which are not straight lines.

Consequently, the simplified, elastic critical moment for lateral buckling of doubly-symmetric I-beams can be calculated from the elastic critical buckling stress given in Eq. (34.40) and the section modulus relative to the compression fiber as follows:

$$(M_{cr})_e = \sigma_{cr}S_{xc} = \frac{C_b \pi^2 E d I_{yc}}{L^2} \tag{4.41}$$

The above design formula is used in Sec. C3.1.2 of the 1996 edition of the AISI Specification as Eq. (C3.1.2-15).

It should be noted that Eq. (4.40) applies to elastic buckling of cold-formed steel beams when the computed theoretical buckling stress is less than or equal to the proportional limit σ_{pr}. However, when the computed stress exceeds the proportional limit, the beam behavior will be governed by inelastic buckling. For extremely short beams, the maximum moment capacity may reach the full plastic moment M_p for compact sections. A previous study[4.16] has indicated that for wide-flange beams having an average shape factor of 10/9,

$$M_p = (10/9)M_y = (10/9)F_y S_x \tag{4.42}$$

where M_p = full plastic moment
M_y = yield moment, = $S_x F_y$

This means that the stress in extreme fibers may reach a hypothetical value of $(10/9)F_y$ when $L^2 S_{xc}/dI_{yc} \simeq 0$ if we use the elastic section modulus to compute moment.

As in the previous design approach for compression members (Ref. 1.4), the effective proportional limit (or the upper limit of the elastic buckling) may be assumed to be equal to one-half the maximum stress,

$$\sigma_{pr} = \frac{1}{2}(10/9)F_y = 0.56F_y \tag{4.43}$$

As shown in Fig. 4.26, the corresponding $L^2 S_{xc}/dI_{yc}$ ratio for $\sigma_{cr} = \sigma_{pr}$ is $1.8\pi^2 E C_b/F_y$.

When the theoretical critical stress exceeds σ_{pr}, the critical stress for inelastic buckling may be represented by the following parabolic equation:
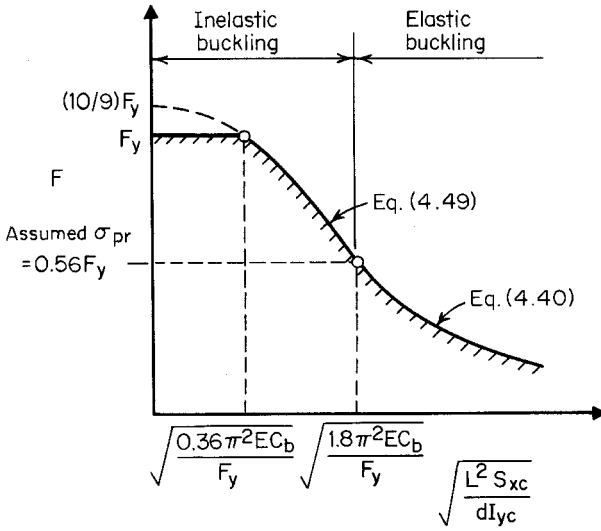
Figure 4.26 Maximum lateral buckling stress for I-beams.

$$(\sigma_{cr})_I = F_y \left[A - \frac{1}{B} \left(\frac{F_y}{\sigma_{cr}} \right) \right] \tag{4.44}$$

where A and B are constants that can be determined by the following conditions:

1. When $L = 0$,

$$(\sigma_{cr})_I = (10/9)F_y \tag{4.45}$$

2. When $\dfrac{L^2 S_{xc}}{d I_{yc}} = \dfrac{1.8\pi^2 E C_b}{F_y}$,

$$(\sigma_{cr})_I = 0.56 F_y \tag{4.46}$$

By solving Eq. (4.44), A and B are found as follows:

$$A = 10/9 \tag{4.47}$$

$$B = 3.24 \tag{4.48}$$

Therefore Eq. (4.44) can be rewritten as

$$(\sigma_{cr})_I = F_y \left\{ \frac{10}{9} - \frac{1}{3.24} \left[\frac{F_y(L^2 S_{xc}/dI_{yc})}{C_b \pi^2 E} \right] \right\}$$

$$= \frac{10}{9} F_y \left\{ 1 - \frac{10}{36} \left[\frac{F_y(L^2 S_{xc}/dI_{yc})}{C_b \pi^2 E} \right] \right\}$$

(4.49)

This is the theoretical equation for lateral buckling in the inelastic range.

Even though the maximum stress computed by Eq. (4.49) as shown in Fig. 4.26 is larger than F_y, a conservative approach has been used by AISI to limit the maximum stress to F_y.

By using the inelastic critical buckling stress given in Eq. (4.49) and the section modulus relative to the compression fiber, the inelastic critical moment for lateral buckling of I-beams can be computed as follows:

$$(M_{cr})_I = (\sigma_{cr})_I S_{xc} \leq M_y$$

$$= \frac{10}{9} M_y \left[1 - \frac{10}{36} \frac{M_y}{(M_{cr})_e} \right] \leq M_y$$

(4.50)

where M_y is the yield moment and $(M_{cr})_e$ is the elastic critical moment defined in Eq. (4.41). Equation (4.50) is being used in Sec. C3.1.2 of the 1996 edition of the AISI Specification. It is used only for $(M_{cr})_e > 0.56 M_y$ as shown in Fig. 4.27. Hill has demonstrated that the equations derived for I-sections can also be used for channels with satisfactory accuracy.[4.17]

For cold-formed steel design, Eqs. (4.40) and (4.49) were used in the 1968 and 1980 editions of the AISI Specification to develop the design equations for lateral buckling of I-beams and channels. In the 1986 and 1996 editions of the AISI Specification, in addition to the use of Eqs. (4.41) and (4.50) for determining the critical moment, new design formulas for lateral buckling
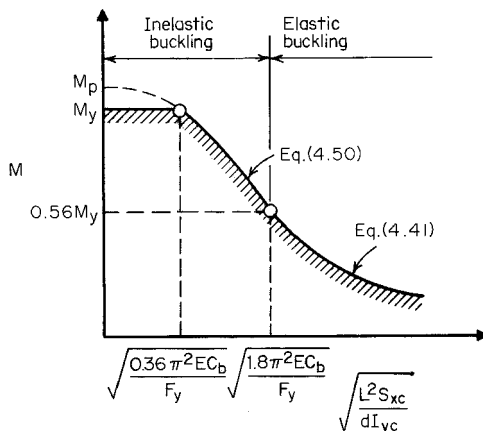

Figure 4.27   Maximum lateral buckling moment for I-beams.

strength were added as alternative methods. These additional equations were developed from the previous study conducted by Pekoz and Winter on torsional–flexural buckling of thin walled sections under eccentric load. The AISI Specification also considers the effect of local buckling on lateral buckling strength of beams.

Specifically, Section C3.1.2 of the 1996 edition of the AISI Specification provides Eq. (4.51) for computing the elastic critical moment on the basis of the torsional–flexural buckling theory. It is used for singly and doubly symmetric sections bending about the symmetry axis perpendicular to the web.

$$(M_{cr})_e = C_b r_0 A \sqrt{\sigma_{ey} \sigma_t} \tag{4.51}$$

where A = full cross-sectional area

$$\sigma_{ey} = \frac{\pi^2 E}{(K_y L_y / r_y)^2} \tag{4.52}$$

$$\sigma_t = \frac{1}{A r_0^2} \left[GJ + \frac{\pi^2 E C_w}{(K_t L_t)^2} \right] \tag{4.53}$$

K_y, K_t = effective length factors for bending about the y-axis and for twisting

L_y, L_t = unbraced length for bending about the y-axis and for twisting

$r_0 = \sqrt{r_x^2 + r_y^2 + x_0^2}$

r_x, r_y = radii of gyration of the cross section about the centroidal principal axes

x_0 = distance from the shear center to the centroid along the principal x-axis, taken as negative

Other terms were defined previously. For singly symmetric sections, the x-axis is the axis of symmetry oriented such that the shear center has a negative x-coordinate. The basis for Eq. (4.51) is discussed by Pekoz in Ref. 3.17. A comparison of Eqs. (4.41) and (4.51) shows that these two equations give similar results for channels having $I_x > I_y$.[3.17] However, for channel sections having $I_x < I_y$ with large $K_y L_y / r_y$ ratios, the simplified Eq. (4.41) provides very conservative results as compared with Eq. (4.51).

For singly symmetric sections bending about the centroidal axis perpendicular to the symmetry axis, the elastic critical moment based on the torsional–flexural buckling theory can be computed by using Eq. (4.54):

$$(M_{cr})_e = C_s A \sigma_{ex} [j + C_s \sqrt{j^2 + r_0^2 (\sigma_t / \sigma_{ex})}] / C_{TF} \tag{4.54}$$

where C_s = +1 for moment causing compression on the shear center side of the centroid

C_s = −1 for moment causing tension on the shear center side of the centroid

$$\sigma_{ex} = \frac{\pi^2 E}{(K_x L_x / r_x)^2} \tag{4.55}$$

C_{TF} = $0.6 - 0.4(M_1/M_2)$, where M_1 is the smaller and M_2 the larger bending moment at the ends of the unbraced length, and where M_1/M_2, the ratio of end moments, is positive when M_1 and M_2 have the same sign (reverse curvature bending) and negative when they are of opposite sign (single curvature bending). When the bending moment at any point within an unbraced length is larger than that at both ends of this length, and for members subject to combined axial load and bending moment, C_{TF} shall be taken as unity.

K_x = effective length factor for bending about the x-axis

L_x = unbraced length for bending about the x-axis

$$j = \frac{1}{2I_y}\left[\int_A x^3 \, dA + \int_A xy^2 \, dA\right] - x_0 \tag{4.56}$$

$$= \beta_y/2. \text{ See Appendix C for computation of } \beta_y. \tag{4.57}$$

Other terms were defined previously.

The derivation of Eq. (4.54) is presented in Chap. 6 for beam-columns. See Eqs. (6.46) and (6.50).

It should be noted that Eqs. (4.51) and (4.54) can be used only when the computed value of $(M_{\mathrm{cr}})_e$ does not exceed $0.56M_y$, which is considered to be the upper limit for the elastic buckling range. When the computed $(M_{\mathrm{cr}})_e$ exceeds $0.56M_y$, the inelastic critical moment can be computed from Eq. (4.50). The elastic and inelastic critical moments are shown in Fig. 4.28.

The above discussion dealt only with the lateral buckling strength of locally stable beams. For locally unstable beams, the interaction of the local buckling
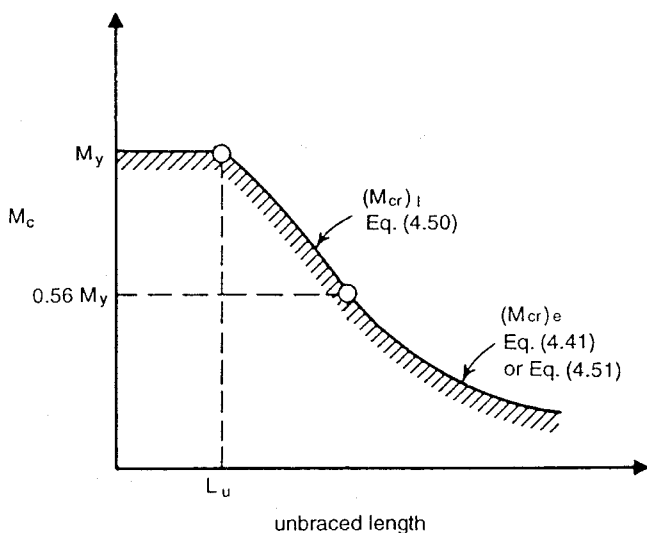

Figure 4.28 Elastic and inelastic critical lateral buckling moments for members bending about centroidal axis perpendicular to the web.

of compression elements and the overall lateral buckling of beams may result in a reduction of the lateral buckling strength of the member. The effect of local buckling on critical moment is considered in Sec. C3.1.2 of the 1986 and 1996 editions of the AISI Specification, in which the nominal lateral buckling strength is determined as follows:

$$M_n = M_c \left(\frac{S_c}{S_f} \right)$$ (4.58)

where M_c = elastic or inelastic critical moment whichever is applicable
S_c = elastic section modulus of the effective section calculated at a stress M_c/S_f in the extreme compression fiber
S_f = elastic section modulus of the full unreduced section for the extreme compression fiber

In Eq. (4.58), the ratio of S_c/S_f is used to account for the effect of local buckling on lateral buckling strength of beams.

The equations developed above for the uniform bending moment can also be used for other loading conditions with reasonable accuracy.[1.161,4.18] If more accurate results are desired, the theoretical critical value for a concentrated load at the center of a simply supported beam can be computed as[3.3]

$$P_{cr} = K \frac{\sqrt{EI_y GJ}}{L^2}$$ (4.59)

where K is a coefficient to be taken from Table 4.2 based on the parameter

TABLE 4.2   Coefficients K in Eq. (4.59)[3.3]

$\dfrac{GJ}{EC_w} L^2$	Loads Acts at		
	Centroid	Top Flange	Bottom Flange
0.4	86.4	51.3	145.6
4	31.9	20.2	50.0
8	25.6	17.0	38.2
16	21.8	15.4	30.4
24	20.3	15.0	27.2
32	19.6	14.8	26.3
48	19.0	14.8	23.5
64	18.3	14.9	22.4
80	18.1	14.9	21.7
96	17.9	15.1	21.1
160	17.5	15.3	20.0
240	17.4	15.6	19.3
320	17.2	15.7	18.9
400	17.2	15.8	18.7

GJL^2/EC_w. For symmetrical I-sections, $C_w \simeq I_y d^2/4$, where d is the depth of the section.

For a uniformly distributed load, the critical load is

$$w_{cr} = K \frac{\sqrt{EI_y GJ}}{L^3} \tag{4.60}$$

where K is to be taken from Table 4.3.

4.2.3.2 Point-Symmetric Sections. Point-symmetric sections such as Z-sections with equal flanges will buckle laterally at lower strengths than doubly and singly symmetric sections. A conservative design approach has been and is being used in the AISI Specification, in which the elastic critical moment is taken to be one-half of those permitted for I-beams or channels. Therefore instead of using Eq. (4.51), the following equation is used for determining the elastic critical moment for point-symmetric Z-sections bending about the centroidal axis perpendicular to the web:

$$(M_{cr})_e = \frac{C_b r_0 A \sqrt{\sigma_{ey} \sigma_t}}{2} \tag{4.61}$$

In lieu of Eq. (4.61), the following simplified equation can be used to calculate the elastic critical moment for Z-sections:

TABLE 4.3   Coefficients K in Eq. (4.60)[3.3]

$\dfrac{GJ}{EC_w} L^2$	Loads Acts at		
	Centroid	Top Flange	Bottom Flange
0.4	143.0	92.9	222.0
4	53.0	36.3	77.3
8	42.6	30.4	59.4
16	36.3	27.4	48.0
24	33.8	26.6	43.4
32	32.6	26.1	40.4
48	31.5	25.8	37.6
64	30.5	25.7	36.2
80	30.1	25.7	35.1
128	29.0	26.0	33.3
200	29.0	26.4	32.1
280	28.8	26.5	31.4
360	28.7	26.6	31.0
400	28.6	26.6	30.7

$$(M_{cr})_e = \frac{C_b \pi^2 E d I_{yc}}{2L^2} \tag{4.62}$$

All symbols used in Eqs. (4.61) and (4.62) are defined in Art. 4.2.3.1.

4.2.3.3   AISI Design Criteria for Lateral Buckling Strength of Singly, Doubly, and Point-Symmetric Sections

The following excerpts are adopted from Sec. C3.1.2 of the Supplement to the 1996 edition of the AISI Specification, which provide the needed design equations for computing the critical lateral–torsional buckling stress.[1.333] The application of the AISI design criteria is illustrated in Examples 4.9 through 4.11.

C3.1.2.1   Lateral–Torsional Buckling Strength for Open Cross Section Members

For laterally unbraced segments of singly, doubly, and point-symmetric sections* subject to lateral–torsional buckling, the nominal flexural strength, M_n, shall be calculated as follows:

$$M_n = S_c F_c \tag{4.63}$$

$$\Omega_b = 1.67 \text{ (ASD)}$$

$$\phi_b = 0.90 \text{ (LRFD)}$$

where S_c = elastic section modulus relative to the extreme compression fiber of effective section calculated at a stress F_c

F_c = elastic or inelastic critical lateral–torsional buckling stress calculated as follows:

For $F_e \geq 2.78 F_y$

$$F_c = F_y \tag{4.64a}$$

For $2.78 F_y > F_e > 0.56 F_y$

$$F_c = \frac{10}{9} F_y \left(1 - \frac{10 F_y}{36 F_e} \right) \tag{4.64b}$$

For $F_e \leq 0.56 F_y$

---

*The provisions of this Section apply to I-, Z-, C- and other singly symmetric section flexural members (not including multiple-web deck, U- and closed box-type members, and curved or arch members). The provisions of this Section do not apply to laterally unbraced compression flanges of otherwise laterally stable sections. Refer to Section C3.1.3 for C- and Z-purlins in which the tension flange is attached to sheathing.

$$F_c = F_e \qquad (4.64c)$$

where

F_e = elastic critical lateral–torsional buckling stress calculated according to (a) or (b) below:

  (a) For singly, doubly, and point-symmetric sections:

$$F_e = \frac{C_b r_0 A}{S_f} \sqrt{\sigma_{ey}\sigma_t} \text{ for bending about the symmetry axis} \qquad (4.65)$$

S_f = elastic section modulus of the full unreduced section relative to the extreme compression fiber

For singly symmetric sections, x-axis is the axis of symmetry oriented such that the shear center has a negative x-coordinate.

For point-symmetric sections, use $0.5F_e$. x-axis of Z-sections is the centroidal axis perpendicular to the web.

Alternatively, F_e can be calculated using the equation given in (b) for doubly symmetric I-sections or point-symmetric sections.

For singly symmetric sections bending about the centroidal axis perpendicular to the axis of symmetry:

$$F_e = \frac{C_s A \sigma_{ex}}{C_{TF} S_f} [j + C_s \sqrt{j^2 + r_0^2(\sigma_t / \sigma_{ex})}] \qquad (4.66)$$

C_s = +1 for moment causing compression on the shear center side of the centroid

C_s = −1 for moment causing tension on the shear center side of the centroid

$$\sigma_{ex} = \frac{\pi^2 E}{(K_x L_x / r_x)^2} \qquad (4.67)$$

$$\sigma_{ey} = \frac{\pi^2 E}{(K_y L_y / r_y)^2} \qquad (4.68)$$

$$\sigma_t = \frac{1}{A r_0^2}\left[GJ + \frac{\pi^2 E C_w}{(K_t L_t)^2} \right] \qquad (4.69)$$

A = full unreduced cross-sectional area

$$C_b = \frac{12..5 M_{max}}{2.5 M_{max} + 3 M_A + 4 M_B + 3 M_C} \qquad (4.70)$$

where M_{max} = absolute value of maximum moment in the unbraced segment

      M_A = absolute value of moment at quarter point of unbraced segment

      M_B = absolute value of moment at centerline of unbraced segment

      M_C = absolute value of moment at three-quarter point of unbraced segment

C_b is permitted to be conservatively taken as unity for all cases. For cantilevers or overhangs where the free end is unbraced, C_b shall be taken as unity. For members subject to combined compressive axial load and bending

moment (Section C5.2), C_b shall be taken as unity.

$$E = \text{modulus of elasticity} \tag{4.71}$$

$$C_{TF} = 0.6 - 0.4 \, (M_1/M_2)$$

where M_1 is the smaller and M_2 the larger bending moment at the ends of the unbraced length in the plane of bending, and where M_1/M_2, the ratio of end moments, is positive when M_1 and M_2 have the same sign (reverse curvature bending) and negative when they are of opposite sign (single curvature bending). When the bending moment at any point within an unbraced length is larger than that at both ends of this length, and for members subject to combined compressive axial load and bending moment (Section C5.2), C_{TF} shall be taken as unity.

r_o = polar radius of gyration of the full cross section about the shear center
$\quad = \sqrt{r_x^2 + r_y^2 + x_0^2}$

r_x, r_y = radii of gyration of the full cross section about the centroidal principal axes

G = shear modulus

K_x, K_y, K_t = effective length factors for bending about the x- and y-axes, and for twisting

L_x, L_y, L_t = unbraced length of compression member for bending about the x- and y-axes, and for twisting

x_O = distance from the shear center to the centroid along the principal x-axis, taken as negative

J = St. Venant torsion constant of the cross section

C_W = torsional warping constant of the cross section

$$j = \frac{1}{2I_y} \left[\int_A x^3 dA + \int_A xy^2 dA \right] - x_0 \tag{4.72}$$

(b) For I- or Z-sections bent about the centroidal axis perpendicular to the web (x-axis): In lieu of (a), the following equations may be used to evaluate F_e:

$$F_e = \frac{C_b \pi^2 E d I_{yc}}{S_f L^2} \quad \text{for doubly symmetric I-sections} \tag{4.73a}$$

$$= \frac{C_b \pi^2 E d I_{yc}}{2 S_f L^2} \quad \text{for point-symmetric Z-sections} \tag{4.73b}$$

d = depth of section

L = unbraced length of the member

I_{yc} = moment of inertia of the compression portion of a section about the centroidal axis of the entire section parallel to the web, using the full unreduced section.

Other terms are defined in (a).

According to Sec. C3.1.2 of the 1996 AISI Specification, it can be seen that for members bent about the centroidal axis perpendicular to the web, calculation of

lateral–torsional buckling strength is unnecessary when the unbraced length does not exceed a length, L_u, which is determined for $M_e = 2.78M_y$ (or $F_e = 2.78F_y$) (see Fig. 4.28). The following equations are given in Part II of the AISI Design Manual[1.159] for computing L_u:

(a) For singly, doubly, and point-symmetric sections:

$$L_u = \left\{ \frac{GJ}{2C_1} + \left[\frac{C_2}{C_1} + \left(\frac{GJ}{2C_1} \right)^2 \right]^{0.5} \right\}^{0.5} \tag{4.74}$$

    (1) For singly and doubly symmetric sections:

$$C_1 = \frac{7.72}{AE} \left[\frac{K_y F_y S_f}{C_b \pi r_y} \right]^2$$

$$C_2 = \frac{\pi^2 E C_w}{(K_t)^2}$$

    (2) For point-symmetric sections:

$$C_1 = \frac{30.9}{AE} \left[\frac{K_y F_y S_f}{C_b \pi r_y} \right]^2$$

$$C_2 = \frac{\pi^2 E C_w}{(K_t)^2}$$

(b) For I- or Z-sections bent about the centroidal axis perpendicular to the web (x-axis): In lieu of (a), the following equations may be used:
    (1) For doubly symmetric I-sections:

$$L_u = \left[\frac{0.36C_b \pi^2 E d I_{yc}}{F_y S_f} \right]^{0.5} \tag{4.75a}$$

    (2) For point-symmetric Z-sections:

$$L_u = \left[\frac{0.18C_b \pi^2 E d I_{yc}}{F_y S_f} \right]^{0.5} \tag{4.75b}$$

In addition, Part II of the Design Manual provides beam design charts for determining the nominal flexural strengths of C-sections and Z-sections with lips. These charts were prepared for $F_y = 33$ and 55 ksi (228 and 379 MPa) with $C_b = 1.0$. The torsional unbraced length $(K_t L_t)$ is assumed to be equal to the unbraced length about the y-axis $(K_y L_y)$.

Example 4.9 For the I-beam used in Example 4.1, what is the maximum spacing of lateral supports in order to use the nominal moment of 312.35 in.-kips determined for section strength? Assume that the I-section is to be used

as a simple beam with a span length of 10 ft to support a uniform load (see Fig. 4.29).

Solution. In order to use the nominal moment for section strength, the maximum spacing of lateral supports can be determined from the following equation:

M_n (for section strength) $= M_n$ (for lateral–torsional buckling strength)

From Eqs. (4.4) and (4.63),

$$S_e F_y = S_c F_c$$

As shown in Fig. 4.28, when $L \leq L_u$, $M_c = M_y$ (or $F_c = F_y$) and $S_e = S_c$. Assume that the elastic critical moment of the I-section is determined according to Sec. C3.1.2.1 (b) of the AISI Specification. For $F_c = F_y$,

$$F_e \geq 2.78 \ F_y$$

By substituting Eq. (4.73a) for F_e into the above expression, then

$$\frac{\pi^2 E C_b d I_{yc}}{S_f L^2} \geq 2.78 \ F_y$$

Therefore,

$$L \leq \sqrt{\pi^2 E C_b d I_{yc}/(2.78 S_f F_y)}$$

where $E = 29.5 \times 10^3$ ksi
$C_b = 1.0$ (assumed value)
$d = 8.0$ in.
$F_y = 50$ ksi
$I_{yc} = 0.724$ in.[4] (see the following calculation)
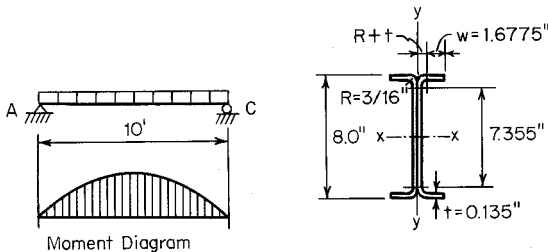
Figure 4.29   Example 4.9

Element	Area A (in.^{2})	Distance from y Axis, x (in.)	Ax^2 (in.^{4})
Flanges	4(1.6775)(0.135) = 0.9059	1.1613	1.2217
Corners	4(0.05407) = 0.2163	0.1564	0.0053
Webs	2(7.355)(0.135) = 1.9859	0.0675	0.0090
Total	3.1081		1.2360

$$I_{\text{flanges}} = 4 \times \tfrac{1}{12} \times 0.135(1.6775)^3 = 0.2124$$

$$I_y = 1.4484 \text{ in.}^4$$

$$I_{yc} = \tfrac{1}{2}I_y = 0.724 \text{ in.}^4$$

$S_f = 6.54$ in.^{3} (see the following calculation)

Element	Area A (in.^{2})	Distance from Mid-Depth y (in.)	Ay^2 (in.^{4})
Flanges	4(1.6775)(0.135) = 0.9059	3.9325	14.0093
Corners	4(0.05407) = 0.2163	3.8436	3.1955
Webs	2(7.355)(0.135) = 1.9859	0	0
Total	3.1081		17.2048

$$2I_{\text{web}} = 2 \times \tfrac{1}{12}(0.135)(7.355)^3 = 8.9522$$

$$I_x = 26.1570 \text{ in.}^4$$

$$S_f = \frac{I_x}{8/2} = 6.54 \text{ in.}^3$$

The maximum unbraced length between lateral supports is

$$L = \sqrt{\frac{\pi^2(29{,}500)(1)(8)(0.724)}{2.78(6.54)(50)}} = 43.1 \text{ in.}$$

Alternatively, the above unbraced length can be calculated directly from Eq. (4.75a). Actually, the beam may be braced at one-third span length with an

unbraced length of 40 in. as shown in Fig. 4.30. For segment CD, $C_b = 1.01$, which is practically the same as the assumed value of 1.0.

Example 4.10 Determine the allowable uniform load if the I-beam used in Example 4.9 is braced laterally at both ends and midspan. See Fig. 4.31. Use the value of C_b determined by the formula included in the AISI Specification and $F_y = 50$ ksi. Use the ASD method and the LRFD method with an assumed dead load-to-live load ratio $D/L = 1/5$.

Solution

A. ASD Method

1. *Nominal Moment for Section Strength.* From Example 4.1, the *nominal moment for section strength* according to Eq. (4.4) is

$$(M_n)_1 = S_e F_y = 312.35 \text{ in.-kips}$$

2. *Nominal Moment for Lateral–Torsional Buckling Strength.* From Example 4.9, $S_f = 6.54$ in.^{3} and $I_{yc} = 0.724$ in.^{4} Considering the lateral supports at both ends and midspan and the moment diagram shown in Fig 4.31, the bending coefficient C_b for segment AB can be calculated by using Eq. (4.70) as follows:

$$C_b = \frac{12.5 M_{\text{max}}}{2.5 M_{\text{max}} + 3 M_1 + 4 M_2 + 3 M_3}$$

where $M_{\text{max}} = wL^2/8$ at midspan
$M_1 = 7wL^2/128$ at $1/4$ point of unbraced segment
$M_2 = 12wL^2/128$ at midpoint of unbraced segment
$M_3 = 15wL^2/128$ at $3/4$ point of unbraced segment
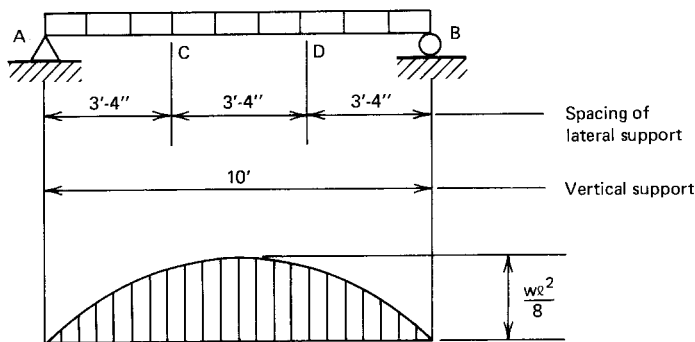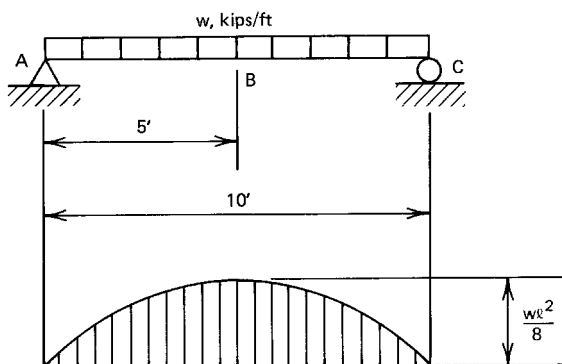

Figure 4.30 Lateral supports.

Figure 4.31 Example 4.10.

$$C_b = \frac{12.5(wL^2/8)}{2.5(wL^2/8) + 3(7wL^2/128) + 4(12wL^2/128) + 3(15wL^2/128)}$$
$$= 1.30$$

This C_b value is less than $C_b = 1.75$, which was used in the 1986 AISI Specification.

Using Eq. (4.73a),
$$F_e = \frac{\pi^2 E C_b d I_{yc}}{S_f L^2}$$

$$= \frac{\pi^2(29{,}500)(1.30)(8)(0.724)}{(6.54)\left(5 \times 12\right)^2} = 93.11 \text{ ksi}$$

$$0.56 \, F_y = 28.00 \text{ ksi}$$

$$2.78 \, F_y = 139.00 \text{ ksi}$$

Since $2.78 \, F_y > F_e > 0.56 \, F_y$, from Eq. (4.64b)

$$F_c = \frac{10}{9} F_y \left(1 - \frac{10F_y}{36F_e}\right)$$

$$= \frac{10}{9} (50) \left[1 - \frac{10(50.0)}{36(93.11)}\right]$$

$$= 47.27 \text{ ksi}$$

Based on Eq. (4.63), the nominal moment for lateral–torsional buckling strength is

$$(M_n)_2 = S_c F_c$$

in which S_c is the elastic section modulus of the effective section calculated at a compressive stress of $f = 47.27$ ksi. By using the same procedure illustrated in Example 4.1, $S_c = 6.294$ in.[3] Therefore, the *nominal moment for lateral–torsional buckling strength* is

$$(M_n)_2 = (6.294)(47.27) = 297.5 \text{ in.-kips}$$

3. *Allowable Uniform Load.* Because $(M_n)_2 < (M_n)_1$, lateral–torsional buckling strength governs the design. Use $M_n = 297.5$ in.-kips to determine the allowable moment as follows:

$$M_a = M_n / \Omega_b$$
$$= 297.5 / 1.67 = 178.14 \text{ in.-kips}$$

The maximum moment at midspan is $wL^2/8$ ft-kips:

$$\frac{wL^2}{8}(12) = 178.14 \text{ in.-kips}$$

Then the allowable uniform load is

$$w = 1.188 \text{ kips/ft}$$

It should be noted that the allowable load computed above is based on the bending moment. It should also be checked for shear, web crippling, deflection, and other requirements as applicable.

B. LRFD Method

Use the same method employed above for the ASD method, the governing nominal moment for lateral–torsional buckling strength is

$$M_n = 297.5 \text{ in.-kips}$$

Since the I-section has an unstiffened flange, the resistance factor as listed in Table 3.1 and discussed in Art. 4.2.1 is 0.90.

Therefore, the design moment is

$$\phi_b M_n = 0.90(297.5) = 267.75 \text{ in.-kips}$$

Based on the load combination of Eq. (3.5a), the required moment is

$$M_u = 1.4M_D + M_L = 1.4M_D + 5M_D = 6.4M_D$$

where M_D = bending moment due to dead load
$\quad\quad M_L$ = bending moment due to live load

Similarly, based on the load combination of Eq. (3.5*b*), the required moment is

$$M_u = 1.2M_D + 1.6M_L = 1.2M_D + 1.6(5M_D) = 9.2M_D$$

A comparison of the above computations indicates that for a given member, the load combination of Eq. (3.5*b*) allows a smaller moment M_D than the load combination of Eq. (3.5*a*). Therefore, the bending moment M_D can be computed from $M_u = \phi_b M_n$ as follows:

$$9.2M_D = 267.75 \text{ in.-kips}$$

Therefore,

$$M_D = \frac{267.75}{9.2} = 29.10 \text{ in.-kips}$$

$$M_L = 5M_D = 145.50 \text{ in.-kips}$$

The allowable moment is

$$M_a = M_D + M_L = 29.10 + 145.50 = 174.60 \text{ in.-kips}$$

The allowable uniform load can be calculated as follows:

$$\frac{wL^2}{8}(12) = 174.60 \text{ in.-kips}$$

$$w = 1.164 \text{ kips/ft}$$

It can be seen that the allowable uniform load computed on the basis of the LRFD method is similar to that computed from the ASD method. The difference is only about 2%.

Example 4.11   For the singly symmetric channel section ($8 \times 2 \times 0.06$ in.) shown in Fig. 4.32, determine the nominal moment for lateral–torsional buckling strength according to Sec. C3.1.2 of the Supplement to the 1996 edition of the AISI Specification. Assume that the channel is used as a simply supported beam to support a concentrated load at midspan and lateral supports are located at one-fourth of the span length. Use $F_y = 33$ ksi, $K_y L_y = K_t L_t = 2.5$ ft.
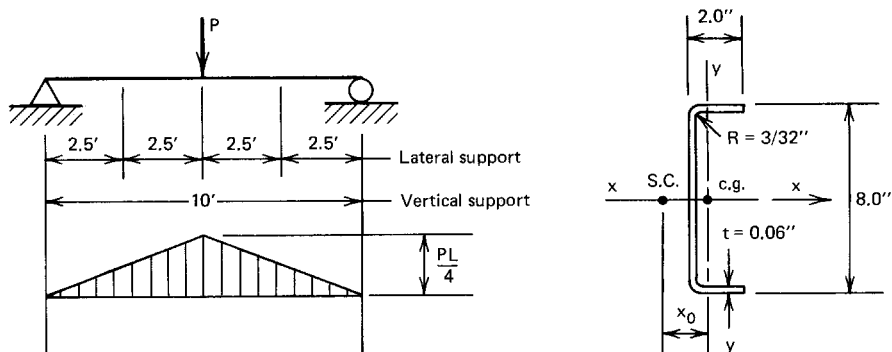
Figure 4.32 Example 4.11.

Solution

1. *Sectional Properties.* By using the design formulas given in Part I of the AISI Design Manual, the following full section properties can be calculated:

$$A = 0.706 \text{ in.}^2 \qquad x_0 = -0.929 \text{ in.}$$

$$S_f = 1.532 \text{ in.}^3 \qquad r_o = 3.14 \text{ in.}$$

$$r_x = 2.945 \text{ in.} \qquad J = 0.000848 \text{ in.}^4$$

$$r_y = 0.569 \text{ in.} \qquad C_w = 2.66 \text{ in.}^6$$

2. *Elastic Critical Lateral–Torsional Buckling Stress, F_e.* Because the given channel section is subject to a moment bending about the symmetry axis (x-axis), the elastic critical lateral–torsional buckling stress can be determined according to Eq. (4.65) as follows:

$$F_e = \frac{C_b r_0 A}{S_f} \sqrt{\sigma_{ey} \sigma_t}$$

For two central segments, the value of C_b can be computed from Eq. (4.70) as follows:

$$C_b = \frac{12.5 M_{\max}}{2.5 M_{\max} + 3M_1 + 4M_2 + 3M_3}$$

where $M_{\max} = PL/4$ at midspan
$\qquad M_1 = 5PL/32$ at $\frac{1}{4}$ point of unbraced segment
$\qquad M_2 = 6PL/32$ at midpoint of unbraced segment

$$M_3 = 7PL/32 \text{ at } \tfrac{3}{4} \text{ point of unbraced segment}$$

$$C_b = \frac{12.5(PL/4)}{2.5(PL/4) + 3(5PL/32) + 4(6PL/32) + 3(7PL/32)}$$

$$= 1.25$$

$$\sigma_{ey} = \frac{\pi^2 E}{(K_y L_y/r_y)^2} = \frac{\pi^2(29,500)}{(2.5 \times 12/0.569)^2} = 104.74 \text{ ksi}$$

$$\sigma_t = \frac{1}{A r_0^2} \left[GJ + \frac{\pi^2 E C_w}{(K_t L_t)^2} \right]$$

$$= \frac{1}{(0.706)(3.14)^2} \left[(11,300)(0.000848) \right.$$

$$\left. + \frac{\pi^2(29,500)(2.66)}{(2.5 \times 12)^2} \right]$$

$$= 125.0 \text{ ksi}$$

Therefore, the elastic critical lateral–torsional buckling stress is

$$F_e = \frac{(1.25)(3.14)(0.706)}{(1.532)} \sqrt{(104.74)(125.0)} = 206.96 \text{ ksi}$$

3. *Critical Lateral–Torsional Buckling Stress, F_c.*

$$0.56F_y = 18.48 \text{ ksi}$$

$$2.78F_y = 91.74 \text{ ksi}$$

Since $F_e > 2.78\ F_y$, then according to Eq. (4.64a)

$$F_c = F_y$$

4. *Nominal Moment M_n.* The compressive stress in the extreme fiber is

$$f = F_c = F_y = 33 \text{ ksi}$$

By using the same procedure illustrated in Example 4.1 with the above compressive stress, the elastic section modulus of the effective section is

$$S_c = 1.211 \text{ in.}^3$$

Based on Eq. (4.63), the nominal moment for lateral–torsional buckling strength is

$$M_n = S_c F_c = (1.211)(33) = 39.96 \text{ in.-kips}$$

5. It should be noted that the above calculation is based on Sec. C3.1.2.1(a) of the AISI Specification.[1.333] If Sec. C3.1.2.1(b) is used to compute F_e, then according to Eq. (4.73a),

$$F_e = \frac{\pi^2 E C_b d I_{yc}}{S_f L^2}$$

$$= \frac{\pi^2 (29{,}500)(1.25)(8.0)(0.1145)}{(1.532)(2.5 \times 12)^2} = 241.78 \text{ ksi}$$

Since $F_e > 2.78 \, F_y = 91.74$ ksi, then based on Eq. (4.64a),

$$F_c = F_y$$

The compressive stress is also

$$f = F_c = F_y = 33 \text{ ksi}$$

The elastic section modulus of the effective section is

$$S_c = 1.211 \text{ in.}^3$$

The nominal moment is

$$M_n = 39.96 \text{ in.-kips}$$

It can be seen that for the given channel section with quarter point lateral supports, Sec. C3.1.2.1 (a) and Sec. C3.1.2.1 (b) give the same nominal moment for lateral–torsional buckling strength.

4.2.3.4 Box Sections
Closed sections such as box shapes have relatively larger torsional stiffness as compared with open sections such as I-beams, channels, and Z-sections discussed in Arts. 4.2.3.1 and 4.2.3.2. As far as lateral buckling is concerned, these closed, double-web sections are more stable than single-web open sections, and therefore any use of box sections will result in an economical design if lateral stability of the beam is essential.

In Ref. 4.18, Winter indicated that for box beams the bending strength is unaffected by lateral buckling even when the length-to-width ratio is as high as 100 for a steel having a yield point of 33 ksi (228 MPa).

Previous editions of the AISI Specification contained in Sec. D3.3 a conservative design provision for lateral buckling of box beams, in which laterally

unbraced box sections can be designed without any strength reduction for lateral buckling consideration if the ratio of the unsupported length to the distance between the webs of the section does not exceed $0.086E/F_y$. In 1999, this design requirement was replaced by Sec. C3.1.2.2 in the Supplement to the 1996 Edition of the AISI Specification.[1.333]

For a box section subjected to a uniform bending moment as shown in Fig. 4.23, the elastic critical moment for lateral buckling is[3.84]

$$(M_{cr})_e = \frac{\pi}{L} \sqrt{EI_y GJ}$$

All terms are defined in Art. 4.2.3.1, except that the torsional constant J may be determined by the following equation for a box section having a uniform thickness:[4.157]

$$J = \frac{2b^2 d^2 t}{(b + d)}$$

where b = midline or centerline dimension of the flange
      d = midline or centerline dimension of the web
      t = wall thickness

When a box section is subject to a nonuniform bending moment, the above equation for the elastic critical moment can be modified by a bending coefficient C_b as follows:

$$(M_{cr})_e = \frac{C_b \pi}{L} \sqrt{EI_y GJ} \tag{4.76}$$

Consequently, the elastic critical lateral–torsional buckling stress F_e can be determined by Eq. (4.77) as given in Sec. C3.1.2.2 of the Supplement to the 1996 edition of the AISI Specification as follows:[1.333]

$$F_e = \frac{C_b \pi}{LS_f} \sqrt{EI_y GJ} \tag{4.77}$$

in which S_f is the elastic section modulus of the full unreduced section relative to the extreme compression flange.

Based on Eq. (4.77), the following equation for L_u can be derived from $F_e = 2.78\, F_y$:

$$L_u = \frac{0.36C_b\pi}{F_yS_f} \sqrt{EI_yGJ} \qquad (4.78)$$

The calculation of lateral–torsional buckling strength is unnecessary when the laterally unbraced length does not exceed L_u. Otherwise, the critical lateral–torsional buckling stress F_c should be determined from Sec. C3.1.2.1 using the value of F_e calculated from Eq. (4.77).

4.2.3.5 *Laterally Unbraced Compression Flanges* The problems discussed in Arts. 4.2.3.1 and 4.2.3.2 dealt with the type of lateral buckling of I-beams, channels, and Z-shaped sections for which the entire cross section rotates and deflects in the lateral direction as a unit. But this is not the case for U-shaped beams and the combined sheet-stiffener sections as shown in Fig. 4.33. For the latter, when it is loaded in such a manner that the brims and the flanges of stiffeners are in compression, the tension flange of the beams remains straight and does not displace laterally; only the compression flange tends to buckle separately in the lateral direction, accompanied by out-of-plane bending of the web, as shown in Fig. 4.34, unless adequate bracing is provided.

The precise analysis of the lateral buckling of U-shaped beams is rather complex. The compression flange and the compression portion of the web act not only like a column on an elastic foundation, but the problem is also complicated by the weakening influence of the torsional action of the flange. For this reason, the design procedure for determining the allowable design stress for laterally unbraced compression flanges is based on the considerable simplification of an analysis presented by Douty in Ref. 4.19. See Sec. 2 of Part VII of the AISI design manual for cold-formed steel.[1.159]

Notes:
1. Arrows indicate probable direction of collapse due to shear.
2. b is portion of tension flange supporting web.
3. h is distance from tension flange to centroid of equivalent column.
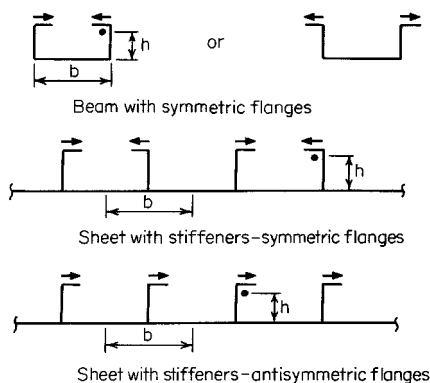
Beam with symmetric flanges

Sheet with stiffeners–symmetric flanges

Sheet with stiffeners–antisymmetric flanges

Figure 4.33 Three possible types of supporting elastic frame for equivalent column.[4.19]
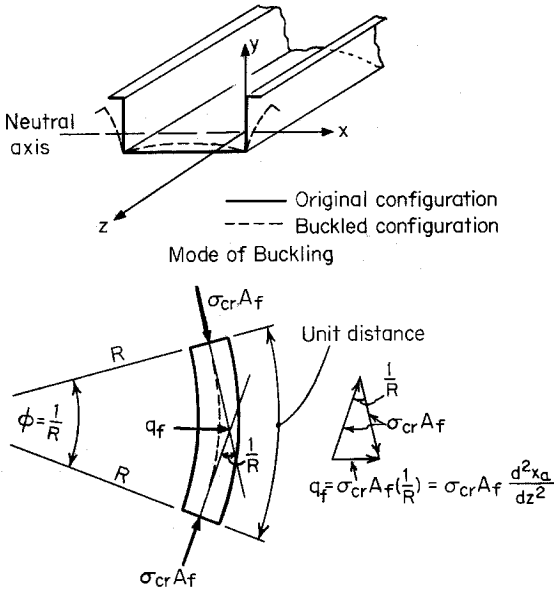
Figure 4.34   Force normal to buckled flange.[4.19]

When the compression flange of a U-shaped beam is subject to the critical bending forces $\sigma_{cr}A_f$ (σ_{cr} being the critical stress and A_f the area of the flange), the component of these forces normal to the buckling flange is

$$q_f = \sigma_{cr}A_f \frac{d^2 x_a}{dz^2} \tag{4.79}$$

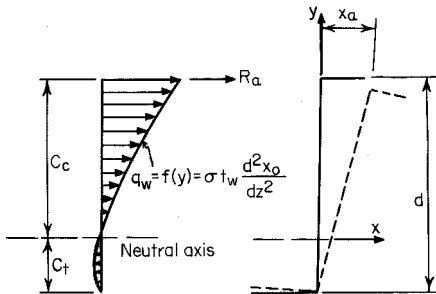(see Fig. 4.34). In the same manner, the component on a unit strip of the buckled web as shown in Fig. 4.35 is

Figure 4.35   Force normal to buckled web.[4.19]

$$q_{w} = \sigma t_{w} \frac{d^2 x}{dz^2} \qquad (4.80)$$

As a result, the total lateral force R_a transmitted to the compression flange by the buckled web is

$$\sigma_{cr} \frac{A_{web}}{12C_c/(3C_c - C_t)} \frac{d^2 x_a}{dz^2} \qquad (4.81)$$

where A_{web} is the area of the web, and C_c and C_t are the distance from the neutral axis to the extreme compression fiber and the extreme tension fiber, respectively (Fig. 4.35).

Consequently, the equation of equilibrium of the compression flange is

$$EI_f \frac{d^4 x_a}{dz^4} + \sigma_{cr} \left[A_f + \frac{A_{web}}{12C_c/(3C_c - C_t)} \right] \frac{d^2 x_a}{dz^2} = 0 \qquad (4.82)$$

and the corresponding nontrivial eigenvalue leads to

$$\sigma_{cr} = \frac{\pi^2 E}{(L/r)^2} \qquad (4.83)$$

where

$$r = \sqrt{\frac{I_f}{A_f + A_{web}/[12C_c/(3C_c - C_t)]}} \qquad (4.84)$$

which is the radius of gyration of the effective column consisting of the compression flange and a part of the compression portion of the web having a depth of $[(3C_c - C_t)/12C_c]d$, where d is the depth of the beam.

The above analysis is for the type of column supported on an elastic foundation where the elastic support is provided by the remaining portion of the web and the tension flange acting together as an elastic frame. The effect of torsional weakening in the combined flexural–torsional stability of the effective column can be determined by the theorem of minimum potential energy:[4.19]

$$U = V_1 + V_2 + U_w$$

$$= \frac{1}{2} \int_0^L [EI_y(u'')^2 + EC_w(\phi'')^2 + GJ(\phi')^2]dz$$

$$= + \frac{1}{2} \int_0^L (C_1 u^2 - 2C_2 u\phi + C_3 \phi^2)dz$$

$$- \frac{P}{2} \int_0^L \left[(u')^2 + 2y_0 u'\phi' + \left(\frac{I_p}{A}\right)(\phi')^2 \right]dz \qquad (4.85)$$

where U = change in the entire potential energy of system consisting of effective column and its supporting elastic frame

V_1 = strain energy accumulated in bent and twisted column

V_2 = strain energy of deflected supporting frame

U_w = change in potential energy of external forces acting on system

I_y = moment of inertia of column about its vertical y-axis

u = horizontal displacement of shear center

ϕ = rotation of column

J = torsional constant of column

y_0 = vertical distance between shear center and centroid of column

I_p = polar moment of inertia of column about its shear center

C_w = warping constant

$C_1 = \delta_\phi / (\delta_u \delta_\phi - \delta_{u\phi}^2)$

$C_2 = \delta_{u\phi} / (\delta_u \delta_\phi - \delta_{u\phi}^2)$

$C_3 = \delta_u / (\delta_u \delta_\phi - \delta_{u\phi}^2)$

δ_u = horizontal displacement of shear center due to a unit load

$\delta_{u\phi}$ = horizontal displacement of shear center due to a unit moment

δ_ϕ = rotation of column due to a unit moment

By solving Eq. (4.85) and applying considerable simplifications, the following expressions can be obtained for the stability of the effective column on an elastic foundation taking the torsional weakening of the flange into consideration:[4.19]

1. When $\beta L^2 / P_e \leq 30$,

$$P_{cr} = T \left(1 + \frac{\beta L^2}{\pi^2 P_e} \right) P_e \qquad (4.86)$$

2. When $\beta L^2 / P_e > 30$,

$$P_{cr} = T \left(0.6 + \frac{2}{\pi} \sqrt{\frac{\beta L^2}{P_e}} \right) P_e \qquad (4.87)$$

where P_{cr} = critical load of equivalent column

$\quad P_e$ = Euler critical load, = $\pi^2 EI/L^2$

$\quad \beta$ = spring constant, = $1/D$

$\quad D$ = lateral deflection of column centroid due to a unit force applied to web at level of column centroid

$\quad L$ = unbraced length of equivalent column

$\quad T$ = torsional reduction factor determined as follows:

1. If $L \geq L'$,

$$T = T_0 = \frac{h}{h + 3.4y_0} \tag{4.88}$$

2. If $L < L'$,

$$T = T_0 \left(\frac{L}{L'}\right) = \left(\frac{h}{h + 3.4y_0}\right)\left(\frac{L}{L'}\right) \tag{4.89}$$

where $L' = \pi\sqrt[4]{2I(h/t)^3} = 3.7\sqrt[4]{I(h/t)^3}$

$\quad y_0$ = distance from centroid of equivalent column to its shear center

$\quad h$ = distance from tension flange to centroid of equivalent column

For beams with a large distance between bracing, the following expression for P_{cr} may be used:

$$P_{cr} = T_0\sqrt{4\beta EI} \tag{4.90}$$

From the value of P_{cr} given above, the equivalent slenderness ratio $(L/r)_{eq}$ can then be determined as follows:

$$\left(\frac{L}{r}\right)_{eq} = k\sqrt{\frac{\pi^2 E}{P_{cr}/A_c}} = \frac{490}{\sqrt{P_{cr}/A_c}} \tag{4.91}$$

where k is an experimental correction factor for the postbuckling strength and equals $1/1.1$, and A_c is the cross-sectional area of the equivalent column.

The allowable compression stress F_a for the ASD method can be computed from the column formula (Chap. 5) on the basis of this equivalent slenderness ratio. To obtain the allowable compression bending stress in the extreme compression fiber F_b', the axial stress F_a may be extrapolated linearly from the centroid level and adjusted for the different factors of safety used for beam yielding and column buckling, that is,

$$F_b' = \frac{\Omega_c}{\Omega_b} \left(\frac{C_c}{y_c}\right) F_a \tag{4.92}$$

where Ω_c = safety factor used for column buckling
$\quad\Omega_b$ = safety factor used for beam yielding
$\quad y_c$ = distance from neutral axis of beam to centroid of equivalent column

The design method developed in Ref. 4.19 has been compared with the results of more than one hundred tests (Fig. 4.36). It has been found that discrepancies are within about 30% on the conservative side and about 20% on the nonconservative side.

Based on the analysis and simplifications, the following ten-step design procedure has been included in the AISI design manual since 1962.[1.159]

1. Determine the location of the neutral axis and define as the "equivalent column" the portion of the beam from the extreme compression fiber to a level that is a distance of $[(3C_c - C_t)/12C_c]d$ from the extreme compression fiber. In this expression, C_c and C_t are the distances from the neutral axis to the extreme compression and tension fibers, respectively, and d is the depth of the section.

2. Determine the distance y_0 measured parallel to the web from the centroid of the equivalent column to its shear center. (If the cross section of the equivalent column is of angle or T-shape, its shear center is at the intersection of web and flange; if of channel shape, the location of the shear center is obtained from Art. 4.4. If the flanges of the channel are of unequal width, for an approximation take w as the mean of the two flange widths, or compute the location of the shear center by rigorous methods.)

3. To determine the spring constant β, isolate a portion of the member 1 in. (25.4 mm) long, apply a force of 0.001 kip (4.45 N) perpendicular to the
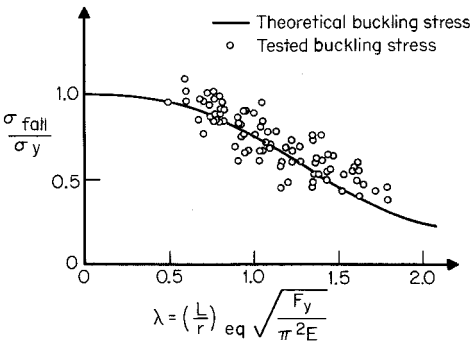

Figure 4.36 Comparison between analysis and tests.[4.19]

web at the level of the column centroid, and compute the corresponding lateral deflection D of the centroid. Then the spring constant is

$$\beta = \frac{0.001}{D} \tag{4.93}$$

4. Calculate

$$T_0 = \frac{h}{h + 3.4y_0} \tag{4.94}$$

where h is the distance from the tension flange to the centroid of the equivalent column in inches.

5. a. If the flange is laterally braced at two or more points, calculate

$$P_e = \frac{290{,}000I}{L^2} \tag{4.95}$$

$$C = \frac{\beta L^2}{P_e} \tag{4.96}$$

$$L' = 3.7 \sqrt[4]{I \left(\frac{h}{t}\right)^3} \tag{4.97}$$

where I = moment of inertia of equivalent column about its gravity axis parallel to web, in.[4]
L = unbraced length of equivalent column, in.

If $C \leq 30$, compute

$$P_{cr} = TP_e \left(1 + \frac{\beta L^2}{\pi^2 P_e}\right) \tag{4.98}$$

If $C > 30$, compute

$$P_{cr} = TP_e \left(0.60 + 0.635 \sqrt{\frac{\beta L^2}{P_e}}\right) \tag{4.99}$$

In both cases, if $L \geq L'$,

$$T = T_0$$

and $L < L'$,

$$T = \frac{T_0 L}{L'} \tag{4.100}$$

b. If the flange is braced at less than two points, compute

$$P_{cr} = T_0 \sqrt{4\beta EI} \tag{4.101}$$

6. Determine the slenderness ratio of the equivalent column,

$$\left(\frac{KL}{r}\right)_{eq} = \frac{490}{\sqrt{P_{cr}/A_c}} \tag{4.102}$$

where A_c is the cross-sectional area of the equivalent column.

7. From Eqs. (5.54), (5.55), and (5.56) compute the stress F_n corresponding to $(KL/r)_{eq}$.

8. The design compression bending stress based on previous factors of safety is

$$F_{b2} = 1.15 F_n \left(\frac{C_c}{y_c}\right) \leq F_y \tag{4.103}$$

where C_c = distance from neutral axis of beam to extreme compression fiber
y_c = distance from neutral axis of beam to centroid of equivalent column

The critical moment is $M_c = F_{b2} S_f$.
Use Eq. (4.58) or Eq. (4.63) to compute M_n.

Example 4.12   Determine the design compression bending stress in the compression flanges (top flanges of the U-shaped section shown in Fig. 4.37. Assume that the compression flanges are laterally braced at the third points with unbraced lengths of 48 in. The yield point of steel is 33 ksi.

Solution

1. *Location of Neutral Axis and Determination of Equivalent Column* (Fig. 4.37)
   a. *Location of neutral axis*
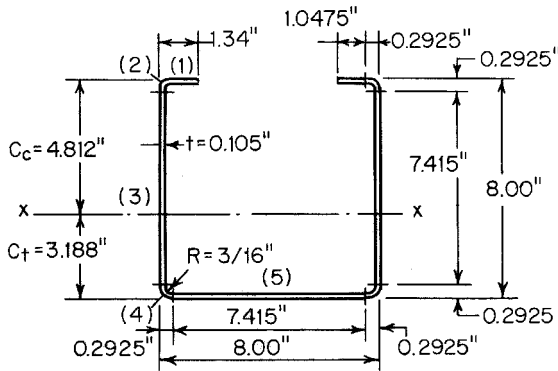
Figure 4.37 Example 4.12.

Element	Area A (in.^{2})		Distance from Top Fiber y (in.)	Ay (in.^{3})
1	2(1.0475)(0.105)	= 0.2200	0.0525	0.0116
2	2(0.0396)(Table 4.1)	= 0.0792	0.1373	0.0109
3	2(7.415)(0.105)	= 1.5572	4.0000	6.2288
4	2(0.0396)	= 0.7920	7.8627	0.6227
5	7.415(0.105)	= 0.7786	7.9475	6.1879
Total		2.7142		13.0619

$$C_c = \frac{13.0619}{2.7142} = 4.812 \text{ in.}$$

$$C_t = 8.0 - 4.812 = 3.188 \text{ in.}$$

b. *Equivalent column.* Based on step 1 of the procedure, the equivalent column used in design is an angle section as shown in Fig. 4.38. The depth of the equivalent column can be determined as follows:

$$\left(\frac{3C_c - C_t}{12C_c}\right) d = \left[\frac{3(4.812) - 3.188}{12(4.812)}\right] \times 8.00 = 1.558 \text{ in}$$

2. *Determination of y_0* (*Distance from Centroid of Equivalent Column to Its Shear Center*) (Fig. 4.38). The centroid of the equivalent column can be located as follows:
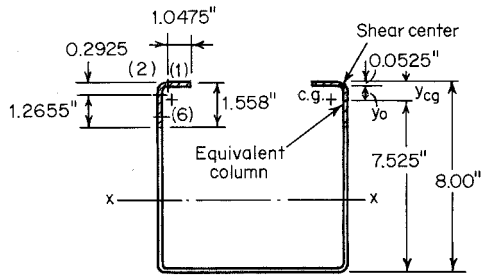
Figure 4.38   Equivalent column.

Element	Area A (in.^{2})	Distance from Top Fiber y (in.)	Ay (in.^{3})
1	1.0475(0.105) $= 0.1100$	0.0525	0.0058
2	0.0396(Table 4.1) $= 0.0396$	0.1373	0.0055
6	1.2655(0.105) $= \underline{0.1329}$	0.9253	$\underline{0.1230}$
Total	0.2825		0.1343

$$y_{cg} = \frac{0.1343}{0.2825} = 0.475 \text{ in.}$$

From Appendix B it can be seen that the shear center of an angle section is located at the intersection of two legs. Therefore, the distance y_0 between the centroid and the shear center of the equivalent column is

$$y_0 = y_{cg} - \frac{t}{2} = 0.475 - 0.0525 = 0.4225 \text{ in.}$$

3. *Calculation of Spring Constant β.* The spring constant β can be computed from Eq. (4.93) as

$$\beta = \frac{0.001}{D}$$

for a portion of the member 1 in. in length. Here D is the lateral deflection of the column centroid due to a force of 0.001 kip applied to the web at the level of the column centroid (Fig. 4.39). Using the moment-area method (Fig. 4.40), the deflection D can be computed:

$$D = \frac{(7.4725)^3}{3EI \times 10^3} + \frac{(7.4725)^2(7.895)}{2EI \times 10^3}$$
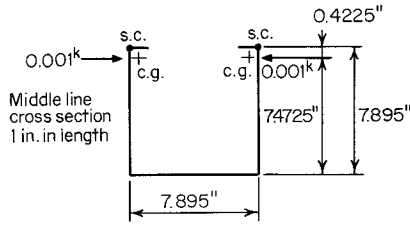
Figure 4.39 Force applied to web for computing spring constant.

where $E = 29.5 \times 10^3$ ksi and

$$I = \frac{1}{12}(0.105)^3 = 96.5 \times 10^{-6} \text{ in.}^4$$

Therefore

$$D = \frac{359.50}{(29.5 \times 10^3)(96.5 \times 10^{-6})10^3} = 0.1263 \text{ in.}$$

$$\beta = \frac{1}{D \times 10^3} = \frac{1}{126.3} = 7.918 \times 10^{-3}$$

4. *Computation of T_0* [Eq. (4.94)]

$$T_0 = \frac{h}{h + 3.4y_0} = \frac{7.525}{7.525 + 3.4(0.4225)} = 0.840$$

5. *Determination of P_{cr}.* In order to determine P_{cr}, we should first compute the moment of inertia of the equivalent column about its y-axis parallel to the web (Fig. 4.41) as follows:
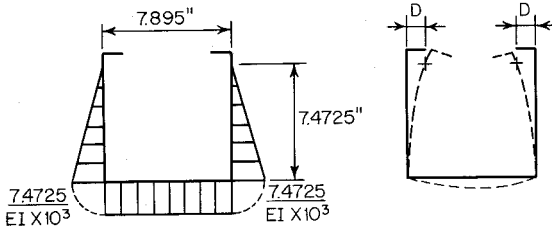
Figure 4.40 Lateral deflection of equivalent column.
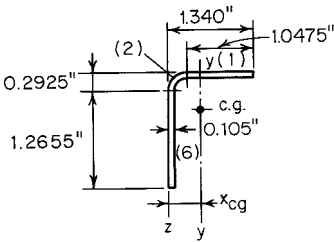
Figure 4.41   Dimensions of equivalent column.

Element	Area A (in.^{2})	Distance from z axis, x (in.)	Ax (in.^{3})	Ax^2 (in.^{4})
1	0.1100	0.8163	0.0898	0.0733
2	0.0396	0.1373	0.0055	0.0008
6	0.1329	0.0525	0.0070	0.0004
Total	0.2825		0.1023	0.0745

$$x_{cg} = \frac{0.1023}{0.2825} = 0.362 \text{ in.}$$

I values of the individual elements about their own centroidal axes parallel to the web are

$$I'_1 = \frac{1}{12}(0.105)(1.0475)^3 = \quad 0.0101$$

$$I'_2 = \quad 0.0002$$

$$I'_6 = \quad \underline{0.0000}$$

$$I'_1 + I'_2 + I'_6 = \quad 0.0103$$

$$\sum (Ax^2) = \quad \underline{0.0745}$$

$$I_z = \quad 0.0848 \text{ in.}^4$$

$$-\left(\sum A\right)(x_{cg}^2) = -0.2825(0.362)^2 = \underline{-0.0370}$$

$$I_y = \quad 0.0478 \text{ in.}^4$$

and

$$A = 0.2825 \text{ in.}^2$$

Since the compression flange is braced at the third points, the values of P_e, C, and L' can be computed from Eqs. (4.95) to (4.97):

$$P_e = 290,000 \frac{I}{L^2} = \frac{290,000(0.0478)}{48^2} = 6.016 \text{ kips}$$

$$C = \frac{\beta L^2}{P_e} = \frac{7.918 \times 10^{-3}(48)^2}{6.016} = 3.032$$

$$L' = 3.7 \sqrt[4]{I\left(\frac{h}{t}\right)^3} = 3.7 \sqrt[4]{0.0478\left(\frac{7.525}{0.105}\right)^3} = 42.61 \text{ in.}$$

Since C is less than 30 and L is greater than L', from Ezq. (4.98),

$$P_{cr} = T_0 P_e \left(1 + \frac{\beta L^2}{\pi^2 P_e}\right)$$

$$= 0.840(6.016)\left[1 + \frac{7.918 \times 10^{-3}(48)^2}{\pi^2(6.016)}\right]$$

$$= 0.840(6.016)(1 + 0.307) = 6.605 \text{ kips}$$

6. *Determination of $(KL/r)_{eq}$ for Equivalent Column* [Eq. (4.102)]

$$\left(\frac{KL}{r}\right)_{eq} = \frac{490}{\sqrt{P_{cr}/A_c}}$$

$$= \frac{490}{\sqrt{6.60/0.2825}} = 101.3$$

7. *Determination of Compression Stress F_n. From Eq. (5.56),*

$$F_e = \frac{\pi^2 E}{(KL/r)_{eq}^2} = \frac{\pi^2(29,500)}{(101.3)^2} = 28.37 \text{ ksi}$$

$$\lambda_c = \sqrt{\frac{F_y}{F_e}} = \sqrt{\frac{33}{28.37}}$$

$$= 1.08 < 1.5$$

$$F_n = \left(0.658^{\lambda_c^2}\right)F_y = \left(0.658^{1.08^2}\right)(33)$$

$$= 20.25 \text{ ksi}$$

8. *Design Compression Bending Stress* [Eq. (4.103)]

$$F_{b2} = 1.15F_n \left(\frac{C_c}{y_c}\right)$$

$$= 1.15(20.25)\frac{4.812}{4.337} = 25.84 \text{ ksi} < (F_y = 33 \text{ ksi}) \qquad (\text{O.K.})$$

Once the design compression bending stress is computed, the critical or nominal moment can be calculated as $M_c = F_{b2}S_c$.

In 1964, Haussler presented rigorous methods for determining the strength of elastically stabilized beams.[4.20] In his methods, Haussler also treated the unbraced compression flange as a column on an elastic foundation and maintained more rigor in his development. A comparison of Haussler's method with Douty's simplified method indicates that the latter may provide a smaller critical stress.

In the early 1990s, the flexural behavior of standing seam roof panels with laterally unsupported compression flanges was restudied by Serrette and Pe-koz.[4.158–4.162]Based on the available test data and the analytical results from elastic finite strip buckling analysis, the authors introduced two design methods in Ref. 4.161 to estimate the maximum moment capacity of sections subjected to an interaction between local and distortional buckling. It was assumed that distortional buckling may be taken as local overall buckling behavior. Both methods used the design philosophy currently used in the AISI Specification for local–lateral buckling interaction. Method A used a derived analytical expression for distortional buckling and Method B used a modified version of Douty's formulation discussed in this Article. It was concluded that Method A gives somewhat better results than method B and is consistent with the present formulation for flexural, torsional, and torsional–flexural buckling.

4.2.3.6 Distortional Buckling   The flexural strength of cold-formed steel beams bending about the major-axis may be limited by local buckling, lateral buckling, or distortional buckling. As shown in Fig. 4.42, the local buckling mode of a channel section for major-axis bending consists of buckling of the compression portion of the web, the compression flange, and edge stiffener without movement of the line junction between the flange and edge stiffener. For this type of limit state, the section strength of the member is determined according to Art. 4.2.2. For the flange distortional buckling mode, the flange and edge stiffener rotate about the flange–web junction with some rotational resistant provided by the web. This mode of failure occurs at considerably longer wavelengths than local buckling but generally shorter wavelength than lateral buckling. Distortional buckling can occur simultaneously with local buckling. Section B4.2 of the AISI Specification accounts for the inability of
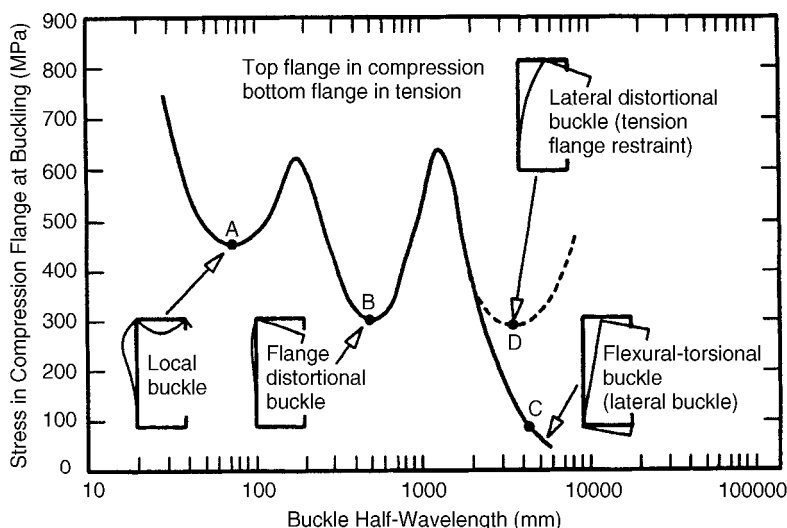
Figure 4.42 Channel section purlin buckling stress versus half-wavelength for major-axis bending.[1.69]

the stiffener to prevent flange distortional buckling by reducing the local buckling coefficient, k, to be less than 4.0 for the partially stiffened compression flange. The reduced buckling coefficient is then used to compute the effective width of the flange element. However, Kwon and Hancock have found that the AISI approach is unconservative for distortional buckling of channel sections composed of high-strength steel of a yield stress of 80 ksi (550 MPa).[1.69,1.158]

Since 1962, the distortional buckling problem of cold-formed steel flexural members has been studied by Douty,[4.19] Haussler, [4.20] Desmond, Pekoz and Winter,[3.76,3.77] Hancock,[1.69,4.163,4.164] Hancock, Rogers, and Schuster,[4.165] Serrette and Pekoz,[4.158–4.162] Buhagiar, Chapman, and Dowling[4.166] Davies and Jiang[4.167,4.1.68] Schafer and Pekoz, [3.168,3.175,3.176,3.195] Bambach, Merrick, and Hancock,[3.173] Bernard, Bridge, and Hancock, [3.171,3.172] Ellifritt, Glover, and Hren,[4.169] and others. Design provisions for distortional buckling are included in the Australian/New Zealand Standard[1.175] and discussed by Hancock in Ref. 1.69.

4.2.4 Beams Having One Flange Through-Fastened to Deck or Sheathing

When roof purlins or wall girts are subject to the suction force due to wind load, the compression flange of the member is laterally unbraced, but the tension flange is supported by the deck or sheathing. The bending capacity of this type of flexural member is less than the fully braced member, but is

greater than the laterally unbraced condition because of the rotational restraint provided by the panel-to-purlin (or girt) connection. The rotational stiffness has been found to be a function of the member thickness, sheet thickness, fastener type and fastener location.

In the past, the bending capacity of flexural members having the tension flange through-fastened to deck or sheathing has been investigated by a large number of investigators in various countries.[4.30–4.40] Based on the results of these studies, reduction factors for the effective yield moment have been developed for simple and continuous span conditions. These factors are given in Sec. C3.1.3 of the 1996 edition of the AISI Specification. It should be noted that the R factors for simple span C- and Z-sections up to 8.50 in. (216 mm) in depth have been increased from the 1986 Specification based on Fisher's study (Ref. 4.170). In view of the fact that these reduction factors were based on the available experimental data, their use for design is limited only to the conditions listed in the specification. For the convenience of readers, the following excerpts are adopted from the AISI Specification:

C3.1.3   Beams Having One Flange Through-Fastened to Deck or Sheathing

This section does not apply to a continuous beam for the region between inflection points adjacent to a support, or to a cantilever beam.

The nominal flexural strength, M_n, of a C- or Z-section loaded in a plane parallel to the web, with the tension flange attached to deck or sheathing and with the compression flange laterally unbraced shall be calculated as follows:

$$M_n = RS_eF_y$$

$$\Omega_b = 1.67 \text{ (ASD)} \tag{4.104}$$

$$\phi_b = 0.90 \text{ (LRFD)}$$

where R is obtained from Table C3.1.3-1 for simple span C- or Z-sections, and

$$R = 0.60 \text{ for continuous span C-sections}$$

$$= 0.70 \text{ for continuous span Z-sections}$$

S_e and F_y are defined in Section C3.1.1. The reduction factor, R, shall be limited to roof and wall systems meeting the following conditions:

(1) Member depth less than 11.5 in. (292 mm).
(2) Member flanges shall have edge stiffeners.
(3) $60 \leq$ depth/thickness ≤ 170
(4) $2.8 \leq$ depth/flange width ≤ 4.5.
(5) $16 \leq$ flat width/thickness of flange ≤ 43.

(6) For continuous span systems, the lap length at each interior support in each direction (distance from center of support to end of lap) shall not be less than 1.5 d.

(7) Member span length shall be no greater than 33 ft (10 m).

(8) For continuous span systems, the longest member span length shall not be more than 20% greater than the shortest span length.

(9) Both flanges shall be prevented from moving laterally at the supports.

(10) Roof or wall panels shall be steel sheets with 50 ksi (345 MPa) minimum yield strength and a minimum of 0.018 in. (0.46 mm) base metal thickness, having a minimum rib depth of 1-1/4 in. (32 mm), spaced a maximum of 12 in. (305 mm) on centers and attached in a manner to effectively inhibit relative movement between the panel and purlin flange.

(11) Insulation shall be glass fiber blanket 0 to 6 in. (152 mm) thick compressed between the member and panel in a manner consistent with the fastener being used.

(12) Fastener type: minimum No. 12 self-drilling or self-tapping sheet metal screws or 3/16-in. (4.76-mm) rivets, having washers 1/2 in. (12.7 mm) diameter.

(13) Fasteners shall not be standoff type screws.

(14) Fasteners shall be spaced not greater than 12 in. (305 mm) on centers and placed near the center of the beam flange, and adjacent to the panel high rib.

(15) The design yield strength of the member shall not exceed 60 ksi (414 MPa).

If variables fall outside any of the above-stated limits, the user must perform full-scale tests in accordance with Section F1 of the *Specification,* or apply a rational analysis procedure. In any case, the user is permitted to perform tests, in accordance with Section Fl, as an alternate to the procedure described in this section.

For simple span members, R shall be reduced for the effects of compressed insulation between the sheeting and the member. The reduction shall be calculated by multiplying R from Table C3.1.3-1 by the following correction factor, r.

$$r = 1.00 - 0.01t_i \text{ when } t_i \text{ is in inches} \tag{4.105}$$

$$r = 1.00 - .0004t_i \text{ when } t_i \text{ is in millimeters} \tag{4.106}$$

t_i = thickness of uncompressed glass fiber blanket insulation

TABLE C3.1.3-1   Simple Span C- or Z-Section R Values

Depth Range, in. (mm)	Profile	R
$d \leq 6.5$ (165)	C or Z	0.70
6.5 (165) $< d \leq 8.5$ (216)	C or Z	0.65
8.5 (216) $< d \leq 11.5$ (292)	Z	0.50
8.5 (216) $< d \leq 11.5$ (292)	C	0.40

4.2.5 Beams Having One Flange Fastened to a Standing Seam Roof System

Standing seam roofs were first introduced in the 1930s.[4.171] Because standing seam roof panels are attached to supporting purlins with a clip that is concealed in the seam, this type of roof system has proved to be a cost-effective roof membrane due to its superior weathertightness, its ability to provide consistent thermal performance, and low maintenance requirements with its ability to adjust to thermal expansion and contraction.[4.172]

For C- or Z-purlins supporting a standing seam roof system, the bending capacity is greater than the bending strength of an unbraced member and maybe equal to the bending strength of a fully braced member. The bending capacity is governed by the nature of the loading, gravity or uplift, and the nature of the particular standing seam roof system. Due to the availability of numerous types of standing seam roof systems, an analytical method for computing positive and negative bending capacities has not been developed. Consequently, Section C3.1.4 was added in the 1996 edition of the AISI Specification for beams having one flange fastened to a standing seam roof system. In this Section, it is specified that the nominal flexural strength, M_n, of a C- or Z-section, loaded in a plane parallel to the web with the top flange supporting a standing seam roof system shall be determined using discrete point bracing and the provisions of Section C3.1.2.1 or shall be calculated as follows:

$$M_n = RS_eF_y \tag{4.107}$$

$$\Omega_b = 1.67 \text{ (ASD)}$$

$$\phi_b = 0.90 \text{ (LRFD)}$$

where

R = reduction factor determined by the "Base Test Method for Purlins Supporting a Standing Seam Roof System" provided in Appendix A of the Supplement to the 1996 edition of the Specification
S_e and F_y are defined in Section C3.1.1 of the AISI Specification.

For additional design information, see Ref. 4.172, which includes detailed discussion and design examples using standing seam roof systems. The major advantage of the base test is that a simple span test may be used to predict performance of continuous span systems for reducing experimental costs. The concepts for the base test was developed by T. M. Murray and his associates at Virginia Polytechnic Institute & State University.

When standing seam roof panel systems are tested according to the ASTM E1592 Standard,[4.193] the new Specification Section C3.1.5[1.333] prescribes that

the evaluation of test results should follow the Standard Procedures for Panel and Anchor Structural Tests of Part VIII of the AISI *Cold-Formed Steel Design Manual*.[1.159] The strength under uplift loading should also be evaluated by this procedure. When three or more assemblies are tested, safety factors and resistance factors should be determined in accordance with the procedure of Specification Section F1.1(b) with the target reliability index and statistical data provided in the Specification. The justifications for these variables are discussed in the AISI Commentary.[1.333] When the number of physical test assemblies is less than 3, a safety factor of 2.0 and a resistance factor of 0.5 should be used.

4.2.6 Unusually Wide Beam Flanges and Unusually Short Span Beams

When beam flanges are unusually wide, special consideration should be given to the possible effects of shear lag and flange curling, even if the beam flanges, such as tension flanges, do not buckle. Shear lag depends on the type of loading and the span-to-width ratio and is independent of the thickness. Flange curling is independent of span length but depends on the thickness and width of the flange, the depth of the section, and the bending stresses in both flanges.

4.2.6.1 Shear Lag   For conventional structural members with ordinary dimensions, the effect of shear deformation on flange stress distribution is negligible. However, if the flange of a beam is unusually wide relative to its span length, the effect of shear deformation on bending stress is pronounced. As a result, the bending stresses in both compression and tension flanges are nonuniform and decrease with increasing distance from the web, as shown in Fig. 4.43 for a box-type beam and an I-section. This phenomenon is known as shear lag.

Analytical and experimental investigations of the problem on shear lag have previously been conducted by Hildebrand and Reissner,[4.41] Winter,[4.42]

Box-type beam   I-section beam
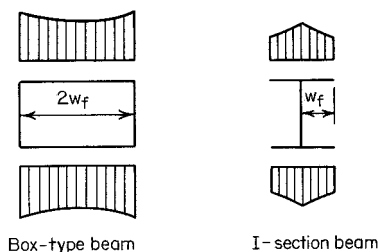
Figure 4.43 Stress distribution in both compression and tension flanges of beams due to shear lag.

Miller,[4.43] and Tate.[4.44,4.45] Recently this subject has been investigated by Malcolm and Redwood,[4.46] Parr and Maggard,[4.47] Van Dalen and Narasimham,[4.48] Lamas and Dowling,[4.49] and in Refs. 4.50 through 4.55.

In their paper, Hildebrand and Reissner concluded that the amount of shear lag depends not only on the method of loading and support and the ratio of span to flange width but also on the ratio of G/E and the ratio $m = (3I_w + I_s)/(I_w + I_s)$, where I_w and I_s are the moments of inertia of webs and of cover plates, respectively, about the neutral axis of the beam.

Based on the theory of plane stress, Winter analyzed the shear lag problem and developed tabular and graphic data,[4.42] from which the effective width of any given beam section can be obtained directly for use in design. The ratios of the maximum and minimum bending stresses in beam flanges were computed and verified by the results of 11 I-beam tests. It was indicated that shear lag is important for beams with wide flanges subjected to concentrated loads on fairly short spans; the smaller the span-to-width ratio, the larger the effect. For beams supporting uniform loads, shear lag is usually negligible except that the L/w_f ratio is less than about 10, as shown in Fig. 4.44. Winter also concluded that for a given span-to-width ratio, the effect of shear lag is practically the same for box beams, I-beams, T-beams, and U-shaped beams.

Table 4.4 is a summary of the ratios of effective design width to actual width based on the results obtained by several investigators.[4.45]

In Table 4.4 w_f is the width of the flange projection beyond the web for I-beams and half the distance between webs for multiple-web sections (Fig. 4.43); L is the span length. It should be noted that the values obtained by Hildebrand and Reissner were for $G/E = 0.375$ and $m = 2$.

As far as the design criteria are concerned, the "effective width" concept used in the design of compression elements (Art. 3.5) can also be applied to the design of beams whenever the shear lag problem is critical.

Based on the results of Winter's investigation,[4.42] design provisions for shear lag have been developed as included in Sec. B1.1(c) of the AISI Spec-
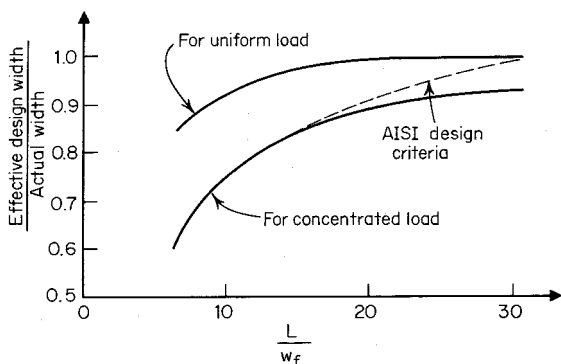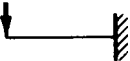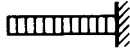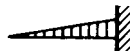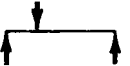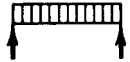

Figure 4.44   Analytical curve for determining effective width of flange of short-span beams.[4.42]

TABLE 4.4   Ratio of Effective Design Width to Actual Width for Wide Flanges

Loading Condition	Investigator	L/w_f						
		6	8	10	12	16	20	30
(cantilever, point load)	Hildebrand Reissner	0.830	0.870	0.895	0.913	0.934	0.946	
(cantilever, uniform load)	Hildebrand and Reissner	0.724	0.780	0.815	0.842	0.876	0.899	
(cantilever, triangular load)	Hildebrand and Reissner	0.650	0.710	0.751	0.784	0.826	0.858	
(simple beam, central point load)	Hildebrand and Reissner	0.686	0.757	0.801	0.830	0.870	0.895	0.936
	Winter	0.550	0.670	0.732	0.779	0.850	0.894	0.945
	Miller			0.750				
(simple beam, off-center point load)	Hildebrand and Reisser	0.610	0.686	0.740	0.778	0.826	0.855	0.910
(simple beam, uniform load)	Hiildebrand and Reisser	0.830	0.897	0.936	0.957	0.977	0.985	0.991
	Winter	0.850	0.896	0.928	0.950	0.974	0.984	0.995
	Miller			0.875				

ification.[1.314] It is specified that when the effective span L of the beam is less than $30w_f$ and when it carries one concentrated load or several loads spaced farther apart than $2w_f$, the ratio of effective design width to actual width of the tension and compression flanges shall be limited to the value given in Table 4.5 in accordance with the L/w_f ratio.

In the application of Table 4.5 the effective span length of the beam is the full span for simple-span beams, the distance between inflection points for continuous beams, or twice the length of cantilever beams. The symbol w_f indicates the width of the flange projection beyond the web for I-beams and similar sections or half the distance between webs for multiple-web sections, including box or U-type sections (Fig. 4.43). When I-beams and similar sections are stiffened by lips at outer edges, w_f shall be taken as the sum of the flange projection beyond the web plus the depth of the lip.

The above tabulated ratios are also plotted in Fig. 4.44 for comparison with the analytical values. The AISI design values are slightly larger than the analytical results when L/w_f ratios exceed about 16.

Although the above discussed provision relative to shear lag is applicable to tension and compression flanges, local buckling in compression as discussed in Art. 3.5 may be a critical factor and should also be investigated. The shear lag problem is of particular importance in the analysis and design of aircraft and naval structures. In cold-formed steel building construction, however, it is infrequent that beams are so wide that they would require considerable reduction of flange widths.

Example 4.13 Compute the nominal moment for the beam section shown in Fig. 4.45 if it is used to support a concentrated load on a simple span of 2 ft. Assume that the minimum yield point of steel is 40 ksi.

TABLE 4.5   Maximum Allowable Ratio of Effective Design Width to Actual Width for Short, Wide Flanges

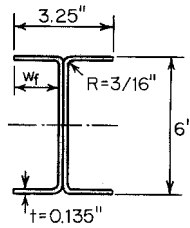| L/w_f	Effective Design Width/Actual Width
30	1.00
25	0.96
20	0.91
18	0.89
16	0.86
14	0.82
12	0.78
10	0.73
8	0.67
6	0.55

Figure 4.45 Example 4.13.

Solution. From Fig. 4.45,

$$w_f = \tfrac{1}{2}(3.25) - 0.135 = 1.490 \text{ in.}$$

$$30w_f = 44.70 \text{ in.}$$

$$L = 2 \text{ ft} = 24 \text{ in.}$$

Since $L < 30w_f$ and the beam is subject to a concentrated load, shear lag is an important factor.

Using Table 4.5 for $L/w_f = 16.1$, the ratio of effective design width to actual width is 0.86. The effective design widths for both compression and tension flanges are

$$b' = 0.86 \times 1.49 = 1.28 \text{ in.}$$

See Fig. 4.45a.
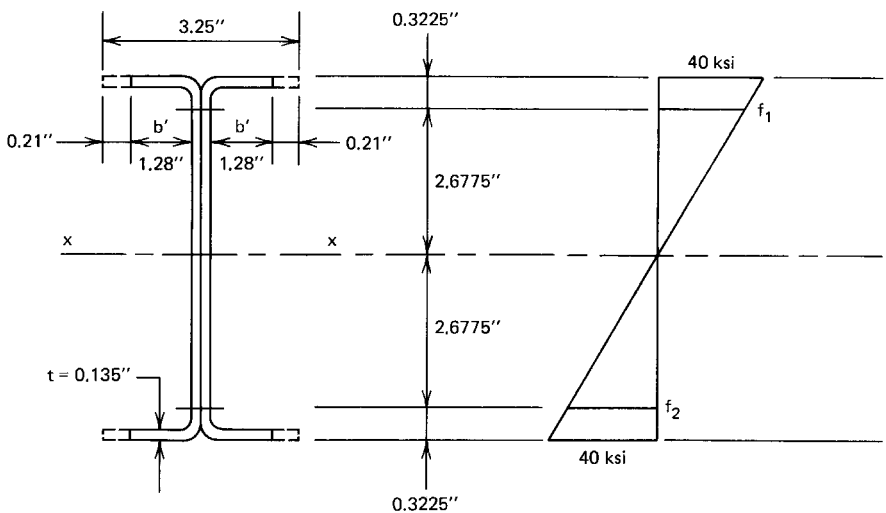
Figure 4.45a.

To check if web is fully effective according to Art. 3.5.1.2.

$$f_1 = 40(26.775/3) = 35.7 \text{ ksi} \qquad \text{(compression)}$$

$$f_2 = 35.7 \text{ ksi} \qquad \text{(tension)}$$

$$\phi = f_2/f_1 = -1.0$$

$$k = 4 + 2[1 - (-1)]^3 + 2[1 - (-1)] = 24$$

$$\lambda = 1.052(5.355/0.135)\sqrt{35.7/29,500}/\sqrt{24}.$$

$$= 0.296$$

Since $\lambda < 0.673$, $\rho = 1.0$

$$b_e = 5.355 \text{ in.}$$

$$b^1 = b_e/(3 - \psi) = 5.355/[3 - (-1)] = 1.339 \text{ in.}$$

For $\psi = -1$, which is less than -0.236,

$$b_2 = b_e/2 = 5.355/2 = 2.678 \text{ in.}$$

$$b_1 + b_2 = 1.339 + 2.678 = 4.017 \text{ in.}$$

Since $(b_1 + b_2)$ is larger than the compression portion of the web of 2.6775 in., the web is fully effective.

Based on the method discussed previously, the effective section modulus is

$$S_e = 3.4 \text{ in.}^3$$

The nominal moment is

$$M_n = S_e F_y = 3.4 \times 40 = 136 \text{ in.-kips}$$

The nominal moment determined above for shear lag should be checked for local buckling. Since $w = \frac{1}{2}(3.25) - (0.1875 + 0.135) = 1.3025$ in.

$$\frac{w}{t} = \frac{1.3025}{0.135} = 9.62$$

$$\lambda = [1.052/\sqrt{0.43}](9.62)\sqrt{40/29,500} = 0.568 < 0.673$$

$$b = w = 1.3025 \text{ in.}$$

The nominal moment is

$$M_n = S_x(\text{full section})(40)$$

In view of the fact that the nominal moment determined above for local buckling consideration is larger than that determined for shear lag, the nominal moment of 136 in.-kips will govern the design.

Example 4.14   For the tubular section shown in Fig. 4.46, determine the nominal moment if the member is to be used as a simply supported beam to carry a concentrated load at midspan. Assume that the span length is 5 ft and $F_y = 50$ ksi.

Solution

1. *Nominal Moment based on Effective Width of Compression Flange.* For the compression flange,

$$\frac{w}{t} = \frac{8 - 2(3/32 + 0.06)}{0.06} = \frac{7.693}{0.06} = 128.2$$

Based on Eqs. (3.41) through (3.44),

$$\lambda = [1.052/\sqrt{k}](w/t)\sqrt{f/E}$$
$$= [\sqrt{1.052}/\sqrt{4}](128.2)\sqrt{50/29,500} = 2.776 > 0.673$$
$$\rho = (1 - 0.22/\lambda)/\lambda = (1 - 0.22/2.776)/2.776 = 0.332$$
$$b = \rho w = 0.332(7.693) = 2.554 \text{ in.}$$

See Fig. 4.47.

Assume that the web is fully effective, the distance y_{cg} can be determined as follows:
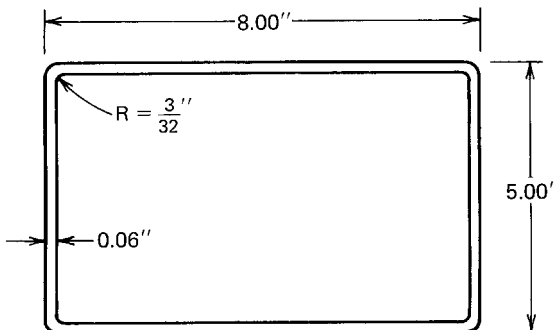
Figure 4.46   Example 4.14.
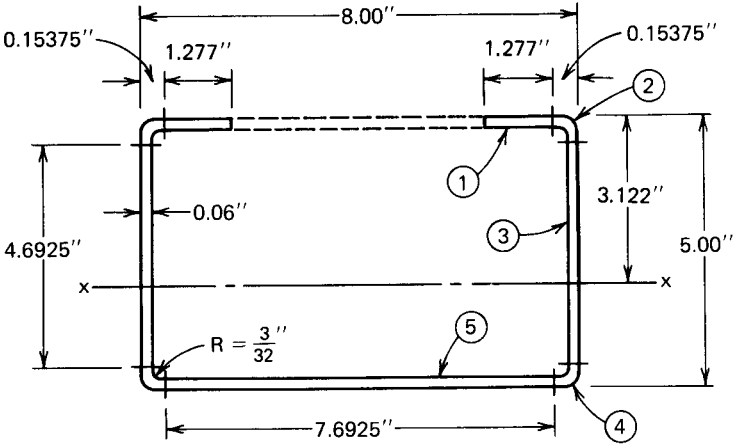
Figure 4.47   Effective width of compression flange for postbuckling strength.

Element	Area A (in.^{2})	Distance from Top Fiber y (in.)	Ay (in.^{3})	Ay^2 (in.^{4})
1	$2.554 \times 0.06 = 0.1532$	0.030	0.0046	0.00014
2	$2 \times 0.01166 = 0.0233$	0.073	0.0017	0.0013
3	$2 \times 4.6925 \times 0.06 = 0.5631$	2.500	1.4078	3.5194
4	$2 \times 0.01166 = 0.0233$	4.927	0.1148	0.5656
5	$7.6925 \times 0.06 = \underline{0.4616}$	4.970	$\underline{2.2942}$	$\underline{11.4019}$
Total	1.2245		3.8231	15.48717
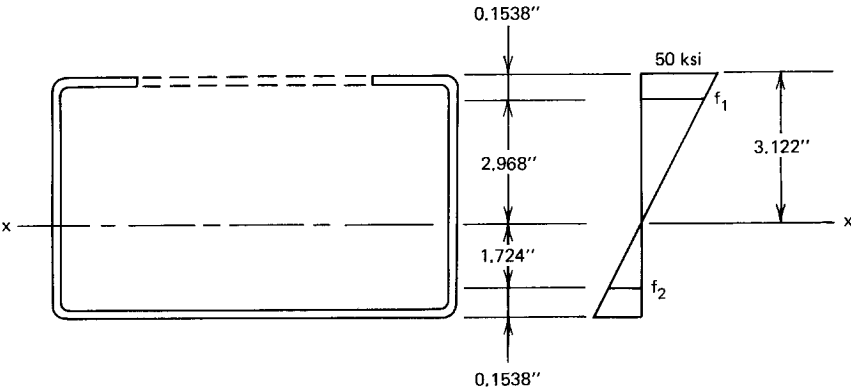
Figure 4.47a.

$$y_{cg} = \frac{\Sigma(Ay)}{\Sigma A} = 3.122 \text{ in.}$$

1. To check if the web is fully effective (see Fig. 4.47a).

   $f_1 = 50(2.968/3.122) = 47.53 \text{ ksi}$ \qquad (compression)

   $f_2 = 50(1.724/3.122) = 27.61 \text{ ksi}$ \qquad (tension)

   $\psi = f_2/f_1 = -27.61/47.53 = -0.581$

   $k = 4 + 2[1 - (-0.581)]^3 + 2[1 - (-0.581)] = 15.066$

   $\lambda = [1.052/\sqrt{15.066}](4.692/0.06)[\sqrt{47.53/29,500}]$

   $\quad = 0.851 > 0.673$

   $\rho = (1 - 0.22/\lambda)/\lambda = (1 - 0.22/0.851)/0.851 = 0.871$

   $b_e = 0.871(4.692) = 4.087 \text{ in.}$

   $b_1 = b_e/(3 - \psi) = 4.087/(3 + 0.581) = 1.141 \text{ in.}$

Since $\psi < -0.236$, $b_2 = b_e/2 = 4.087/2 = 2.0435$ in. $b_1 + b_2 = 1.141 + 2.0435 = 3.1845 > 2.968$ in. (compression portion of the web). The web is fully effective.

The total I_x is

$$\sum (Ay^2) = \quad 15.4872$$

$$I_{webs} = 2 \times \tfrac{1}{2}(0.06)(4.6925)^3 = \quad 1.0333$$

$$-\left(\sum A\right)(y_{cg}^2) = -1.2245(3.122)^2 = \underline{-11.9351}$$

$$I_x = \quad 4.5850 \text{ in.}^4$$

The section modulus is

$$S_x = \frac{I_x}{y_{cg}} = \frac{4.5850}{3.122} = 1.469 \text{ in.}^3$$

The nominal moment about the x-axis is

$$M_n = 1.469(50) = 73.45 \text{ in.-kips}$$

2. *Nominal Moment based on Shear Lag Consideration.* According to Figs. 4.43 and 4.46,

$$w_f = \frac{8 - 2(0.06)}{2} = 3.94 \text{ in.}$$

$$\frac{L}{w_f} = \frac{5 \times 12}{3.94} = 15.23 < 30$$

Because the L/w_f ratio is less than 30, and the member carries a concentrated load, additional consideration for shear lag is needed. Using Table 4.5,

$$\frac{\text{effective design width}}{\text{actual width}} = 0.845$$

Therefore the effective design widths of compression and tension flanges between webs are (Fig. 4.48)

$$0.845[8 - 2(0.06)] = 6.6586 \text{ in.}$$

Using the full areas of webs, the moment of inertia about the x-axis is

$$I_x = 4[3.22356(0.06)(2.5 - 0.03)^2 + 0.01166(2.5 - 0.073)^2]$$

$$+ 2\tfrac{1}{12}(0.06)(4.6925)^3 = 6.046 \text{ in.}^4$$
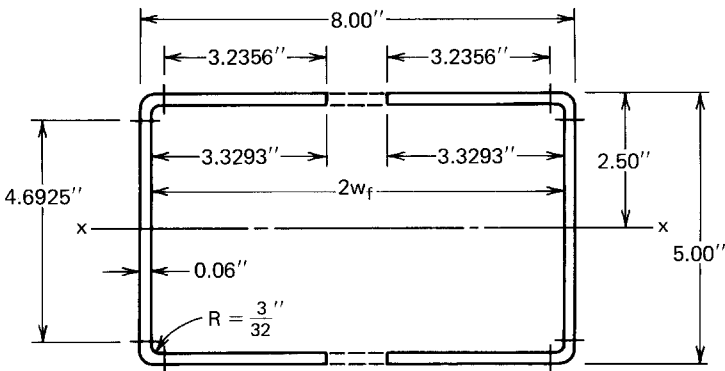
Figure 4.48   Effective design widths of compression and tension flanges for shear lag.

and the section modulus is

$$S_x = I_x/2.5 = 2.418 \text{ in.}^3$$

The nominal moment is

$$M_n = 2.418(50) = 120.9 \text{ in.-kips}$$

3. *Nominal Moment for Design.* From the above calculation, the nominal moment for design is 73.45 in.-kips. Shear lag does not govern the design.

4.2.6.2 Flange Curling When a beam with unusually wide and thin flanges is subject to bending, the portion of the flange most remote from the web tends to deflect toward the neutral axis. This is due to the effect of longitudinal curvature of the beam and bending stresses in both flanges. This subject was studied by Winter in 1940.[4.42]

Let us consider an I-beam which is subject to pure bending as shown in Fig. 4.49. The transverse component q of the flange force $f_{av}t$ per unit width can be determined by

$$q = \frac{f_{av}t\,d\phi}{dl} = \frac{f_{av}t}{r_b} = \frac{f_{av}t}{EI/M} = \frac{2f_{av}^2 t}{Ed} \qquad (4.108)$$

where f_{av} = average bending stress in flanges
t = flange thickness
$d\phi$, dl, r_b = as shown in Fig. 4.49
E = modulus of elasticity
I = moment of inertia of beam
d = depth of beam

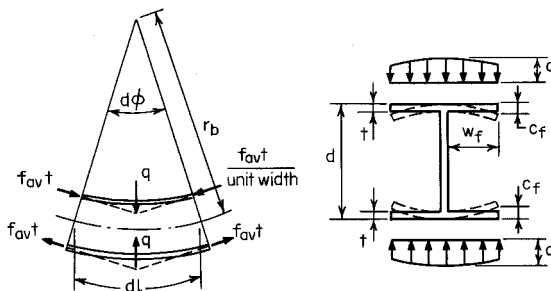If the value of q is considered to be a uniformly distributed load applied

Figure 4.49 Flange curling of I-beam subject to bending.[4.42]

on the flange, the deflection or curling at the outer edge of the flange can be computed by the conventional method for a cantilever plate, namely,

$$c_f = \frac{qw_f^4}{8D} = 3\left(\frac{f_{av}}{E}\right)^2\left(\frac{w_f^4}{t^2 d}\right)(1 - \mu^2) \tag{4.109}$$

where c_f = deflection at outer edge
w_f = projection of flange beyond web
D = flexural rigidity of plate, = $Et^3/12(1 - \mu^2)$

By substituting $E = 29.5 \times 10^3$ ksi (203 GPa) and $\mu = 0.3$ in Eq. (4.109), the following formula for the maximum width of an unusually wide stiffened or unstiffened flange in tension and compression can be obtained:

$$\begin{aligned} w_f &= \sqrt{\frac{1800td}{f_{av}}} \times \sqrt[4]{\frac{100c_f}{d}} \\ &= \sqrt{0.061tdE/f_{av}}\sqrt[4]{100c_f/d} \end{aligned} \tag{4.110}$$

where c_f = permissible amount of curling, in.
f_{av} = average stress in full unreduced flange width, ksi
w_f, t, and d were defined previously

When members are designed by the effective design width procedure, the average stress equals the maximum stress times the ratio of the effective design width to the actual width. Equation (4.110) is included in Sec. B1.1(b) of the AISI Specification to limit the width of unusually wide flanges.

The above formula for determining w_f is derived on the basis of a constant transverse component q. As soon as flange curling develops, the distance from the flange to the neutral axis becomes smaller at the outer edge of the flange. This results in the reduction of bending stresses. Therefore the values of q vary along the flange as shown in Fig. 4.49. Since the amount of c_f is usually limited to a small percentage of the depth, the error in the determination of w_f by using Eq. (4.110) is negligible and on the conservative side.

The above approximate treatment for I-beams can also be applied to the design of box and U-type beams, except that for the latter the flanges of the box beams may be regarded as simple plates freely supported at webs and that w_f is to be measured as half of the distance between webs. Using the same analogy, one can determine the flange curling c_f for box sections as follows:

$$c_f = \frac{5}{384} \times \frac{q(2w_f)^4}{D} = 5 \left(\frac{f_{av}}{E}\right)^2 \left(\frac{w_f^4}{t^2 d}\right)(1 - \mu^2) \qquad (4.111)$$

A comparison of Eqs. (4.109) and (4.111) indicates that the use of Eq. (4.110), which is derived on the basis of I-beams, to determine w_f for box beams, may result in a possible error of 13%. This is because $\sqrt[4]{5/3} = 1.13$. However, this discrepancy can be reduced if the restraint of webs and the variable values of the transverse component q are taken into consideration.

No specific values are given by the AISI Specification for the maximum permissible amount of curling. However, it is indicated in a footnote that the amount of curling that can be tolerated will vary with different kinds of sections and must be established by the designer. An amount of curling on the order of 5% of the depth of the section is usually not considered excessive.

Assuming $c_f/d = 0.05$, Eq. (4.110) can be simplified as

$$w_f = 0.37 \sqrt{\frac{t d E}{f_{av}}}$$

In general, the problem of flange curling is not a critical factor to limit the flange width. However, when the appearance of the section is important, the out-of-plane distortion should be closely controlled in practice.

Example 4.15   Determine the amount of curling for the compression flange of the hat section used in Example 4.3, when the section is subjected to the allowable moment. Use the ASD method.

Solution. The curling of the compression flange of the hat section can be computed by Eq. (4.110). In the calculation,

$$w_f = \tfrac{1}{2}(15.0 - 2 \times 0.105) = 7.395 \text{ in.}$$

$$t = 0.105 \text{ in.}$$

$$d = 10.0 \text{ in.}$$

$$f_{av} = \frac{40.69}{1.67} \times \frac{4.934}{14.415} = 8.34 \text{ ksi}$$

Using Eq. (4.110),

$$7.395 = \sqrt{\frac{0.061 \times 0.105 \times 10 \times 29,500}{8.34}} \times \sqrt[4]{\frac{100 c_f}{10}} = 26.77 \sqrt[4]{c_f}$$

$$c_f = 0.0058 \text{ in.}$$

4.3   DESIGN OF BEAM WEBS

4.3.1   Introduction

Thin-walled cold-formed steel flexural members should not only be designed for bending strength and deflection as discussed in Art. 4.2, but the webs of beams should also be designed for shear, bending, combined bending and shear, web crippling, and combined bending and web crippling. In addition, the depth of the web should not exceed the maximum value permitted by Sec. B1.2 of the AISI Specification.

The maximum allowable depth-to-thickness ratio h/t for unreinforced webs is limited to 200, in which h is the depth of the flat portion of the web measured along the plane of the web and t is the thickness of the web. When transverse stiffeners are provided only at supports and under concentrated loads, the maximum depth-to-thickness ratio may be increased to 260. When bearing stiffeners and intermediate stiffeners are used simultaneously, the maximum h/t ratio is 300. These limitations for h/t ratios are established on the basis of the studies reported in Refs. 3.60, 4.56–4.60. If a web consists of two or more sheets, the h/t ratios of the individual sheets shall not exceed the maximum allowable ratios mentioned above.

The following discussions deal with the minimum requirements for transverse stiffeners, the design strength for shear and bending in beam webs, the load or reaction to prevent web crippling, and combinations of various types of stresses.

4.3.2   Stiffener Requirements

In the 1996 edition of the AISI Specification, the following design requirements for attached transverse stiffeners and intermediate stiffeners are provided in Sec. B6. When the transverse stiffeners do not meet these requirements, the load-carrying capacity for the design of such members can be determined by tests.

a. Bearing Stiffeners. For beams having large h/t ratios, bearing stiffeners may be used at supports and/or under concentrated loads. A nominal strength, P_n, for bearing stiffeners is the smaller of the values determined by (1) and (2) as follows:

$$(1)\ P_n = F_{wy}A_c \tag{4.112}$$

(2) P_n = Nominal axial load evaluated according to Art. 5.7 with A_e replaced by A_b

$$\Omega_c = 2.00\ (\text{ASD})$$
$$\phi_c = 0.85\ (\text{LRFD})$$

where $A_c = 18t^2 + A_s$, for transverse stiffeners at interior support and under concentrated load $\tag{4.113}$

$A_c = 10t^2 + A_s$, for transverse stiffeners at end support $\tag{4.114}$

A_s = cross-sectional area of transverse stiffeners
F_{wy} = lower value of beam web, F_y, or stiffener section, F_{ys}
A_b = $b_1t + A_s$, for transverse stiffeners at interior support and under concentrated load   (4.115)
A_b = $b_2t + A_s$, for transverse stiffeners at end support   (4.116)
b_1 = $25t[0.0024(L_{st}/t) + 0.72] \le 25t$ (4.117)
b_2 = $12t[0.0044(L_{st}/t) + 0.83] \le 12t$ (4.118)
L_{st} = length of transverse stiffener
t = base thickness of beam web

In addition, the specification stipulates that w/t_s ratios for the stiffened and unstiffened elements of cold-formed steel transverse stiffeners should not exceed $1.28\sqrt{E/F_{ys}}$ and $0.42\sqrt{E/F_{ys}}$, respectively. In the above expressions, F_{ys} is the yield point in ksi and t_s the thickness in inches of the stiffener steel.

It should be noted that Eq. (4.112) is used to prevent end crushing of transverse stiffeners, while the second P_n is used to prevent column buckling of the web stiffener section. The equations for computing the effective areas A_b and A_c and the effective widths b_1 and b_2 are adopted from Nguyen and Yu.[4.59] Figures 4.50 and 4.51 show the effective areas A_c and A_b of the bearing stiffeners.

b. Intermediate Stiffeners. All intermediate stiffeners should be designed to satisfy the following requirements for spacing, moment of inertia, and gross area:

1. Spacing a between stiffeners,

$$a \le \left(\frac{260}{h/t}\right)^2 h \tag{4.119}$$
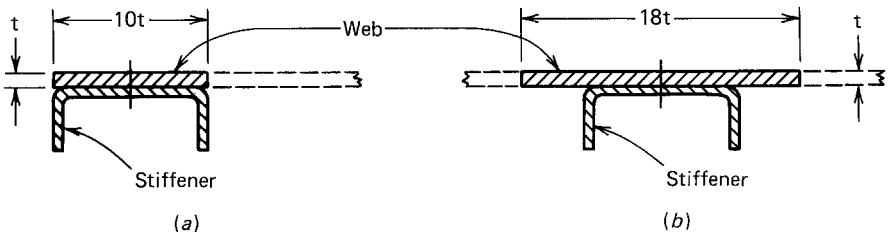
$$a \le 3h \tag{4.120}$$

Figure 4.50 Effective area A_c of bearing stiffener. (*a*) At end support. (*b*) At interior support and under concentrated load.
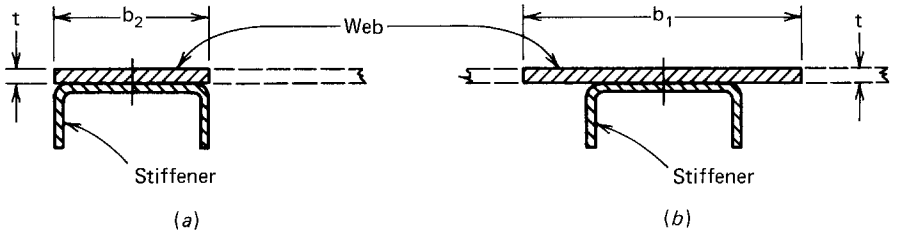
Figure 4.51   Effective area A_b of bearing stiffener. (*a*) At end support. (*b*) At interior support and under concentrated load.

2. Moment of inertia I_s of intermediate stiffeners with reference to an axis in the plane of the web,

$$I_s \geq 5ht^3 \left(\frac{h}{a} - \frac{0.7a}{h} \right) \tag{4.121}$$

$$I_s \geq \left(\frac{h}{50} \right)^4 \tag{4.122}$$

3. Gross area A_s of intermediate stiffeners,

$$A_s \geq \frac{1 - C_v}{2} \left[\frac{a}{h} - \frac{(a/h)^2}{(a/h) + \sqrt{1 + (a/h)^2}} \right] YDht \tag{4.123}$$

where

$$C_v = \begin{cases} \dfrac{1.53Ek_v}{F_y(h/t)^2}, & \text{when } C_v \leq 0.8 \tag{4.124} \\[4mm] \dfrac{1.11}{h/t} \sqrt{\dfrac{Ek_v}{F_y}}, & \text{when } C_v > 0.8 \tag{4.125} \end{cases}$$

$$k_v = \begin{cases} 4.00 + \dfrac{5.34}{(a/h)^2}, & \text{when } a/h \leq 1.0 \tag{4.126} \\[4mm] 5.34 + \dfrac{4.00}{(a/h)^2}, & \text{when } a/h > 1.0 \tag{4.127} \end{cases}$$

and a = distance between transverse stiffeners, in.
   Y = yield point of web steel/yield point of stiffener steel
   D = 1.0 for stiffeners furnished in pairs
      = 1.8 for single-angle stiffeners
      = 2.4 for single-plate stiffeners

Most of the above requirements for intermediate stiffeners are based on the AISC Specification[1.148] and the study reported in Ref. 4.59. The bearing stiffener requirement for residential construction is being studied by Fox and Schuster at the University of Waterloo.[1.299]

4.3.3 Shear

4.3.3.1 Shear Stress   In the design of beams, the actual shear stress developed in the cross section of the beam can be calculated by using the following well-known equation:[4.61]

$$f_v = \frac{VQ}{It} \tag{4.128}$$

where f_v = actual shear stress, ksi
   V = total external shear force at a section, kips
   Q = statical moment of area between the extreme fiber and the particular location at which the shear stress is desired, taken about neutral axis, in.^{3}
   I = moment of inertia of entire cross-sectional area about neutral axis, in.^{4}
   t = width of section where shear stress is desired, in.

Even though Eq. (4.128) gives the exact value at any location, it has been a general practice to use the average value in the gross area of the web as the shear stress for design purposes. This average shear stress can be computed by using the following equation:

$$f_v = \frac{V}{ht_w} \tag{4.129}$$

where h = depth of the flat portion of the web measured along the plane of the web, in.
   t_w = thickness of the web, in.

The use of Eqs. (4.128) and (4.129) is illustrated in Example 4.16.

Example 4.16   Determine the shear stress distribution at the end supports of the uniformly loaded channel shown in Fig. 4.52. Assume that the load is applied through the shear center of the cross section so that torsion is not involved.* See appendix B for a discussion of the shear center.

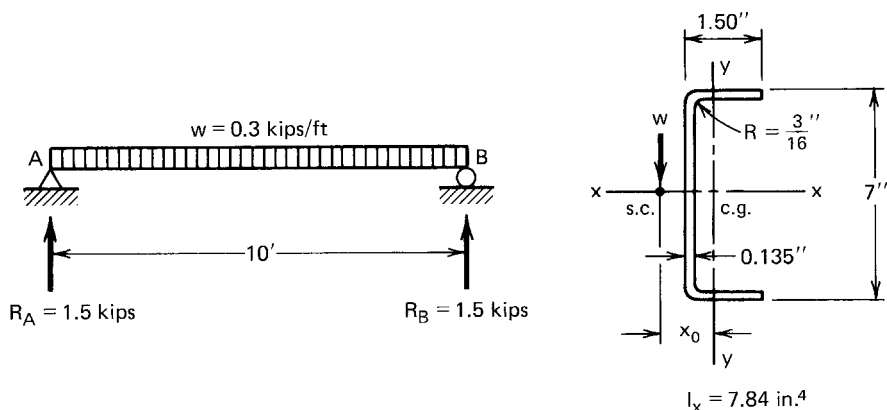*When the load does not pass through the shear center, see Appendix B.

Figure 4.52   Example 4.16.

Solution

1. *Exact Shear Stress Distribution Using Eq. (4.128).* For simplicity, use square corners and midline dimensions as shown in Fig. 4.53 for computing the exact shear stresses at various locations of the section. Shear stress at points 1 and 4:

$$V = R_A = 1.5 \text{ kips}$$

$$Q_1 = Q_4 = 0$$

$$(f_v)_{1,4} = \frac{VQ_1}{It} = 0$$

Shear stress at points 2 and 3:

$$Q_2 = Q_3 = 1.4325(0.135)(6.865/2) = 0.664 \text{ in.}^3$$

$$(f_v)_{2,3} = \frac{VQ_2}{It} = \frac{1.5(0.664)}{7.84(0.135)} = 0.941 \text{ ksi}$$

Shear stress at point 5:

$$Q_5 = Q_2 + 0.135(6.865/2)(6.865/4) = 1.46 \text{ in.}^3$$

$$(f_v)_5 = \frac{VQ_5}{It} = \frac{1.5(1.46)}{7.84(0.135)} = 2.07 \text{ ksi}$$
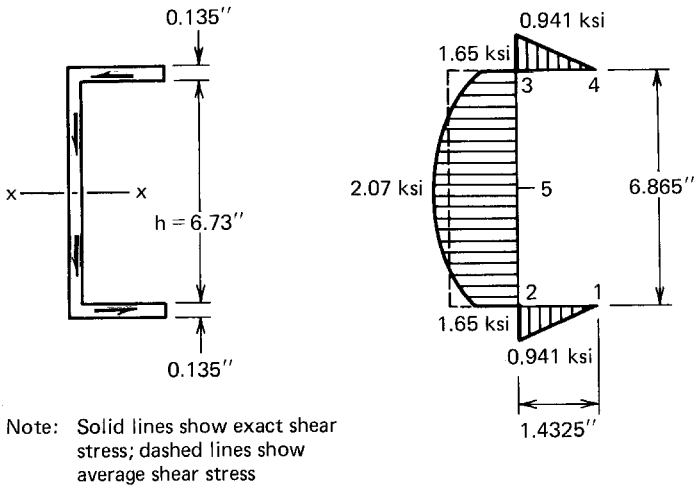
Figure 4.53   Shear stress distribution.

2. *Average Shear Stress on Beam Web by Using Eq.* (*4.129*)

$$f_v = \frac{V}{ht_w} = \frac{1.5}{6.73(0.135)} = 1.65 \text{ ksi}$$

From the above calculation it can be seen that for the channel section used in this example, the average shear stress of 1.65 ksi is 25% below the maximum value of 2.07 ksi.

4.3.3.2   Shear Strength of Beam Webs

a. Shear Yielding. When a beam web with a relatively small h/t ratio is subject to shear stress, the shear capacity of the beam is probably governed by shear yielding. The maximum shear stress at the neutral axis can be computed by Eq. (4.130):

$$\tau_y = \frac{F_y}{\sqrt{3}} \tag{4.130}$$

in which τ_y is the yield point in shear and F_y is the yield point in tension.

The nominal shear strength for yielding can be determined by the shear stress given in Eq. (4.130) and the web area, ht, as follows:

$$V_n = \left(\frac{F_y}{\sqrt{3}}\right)(ht) \cong 0.60F_y\, ht \qquad (4.131)$$

where V_n is the nominal shear strength, h is the depth of the flat portion of the web, and t is the thickness of the web.

b. Elastic Shear Buckling. For webs with large h/t ratios, the shear capacity of the web is governed by shear buckling. Figure 4.54 shows a typical pattern of shear failure.[4.56] Based on studies by Southwell and Skan on shear buckling of an infinitely long plate, the plate develops a series of inclined waves, as shown in Fig. 4.55.[4.62,4.63] The elastic critical shear buckling stress can be computed by Eq. (4.132).*

$$\tau_{cr} = \frac{k_v \pi^2 E}{12(1 - \mu^2)(h/t)^2} \qquad (4.132)$$

where k_v = shear buckling coefficient
E = modulus of elasticity of steel
μ = Poisson's ratio
h = depth of the plate
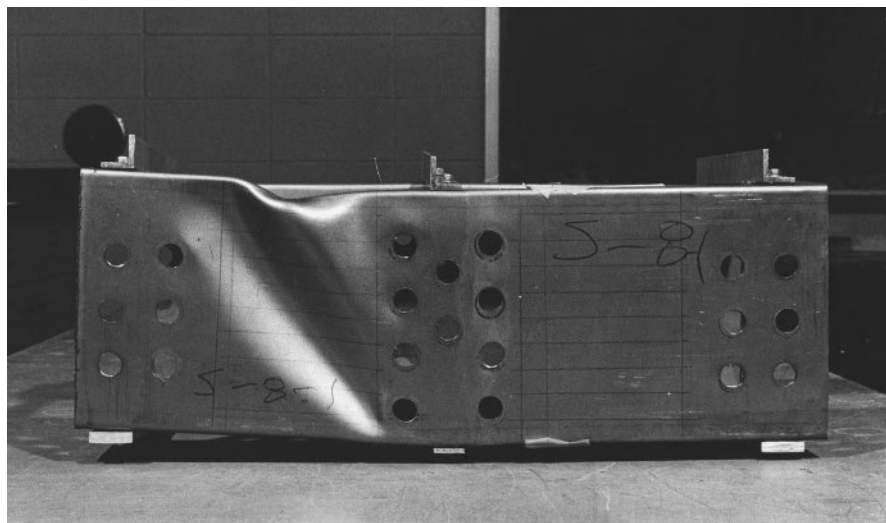
Figure 4.54   Typical shear failure pattern ($h/t = 125$).[4.56]

*The problem of shear buckling of plane plates has also been studied by Timoshenko and other investigators. For additional information see Refs. 3.1 and 4.63.
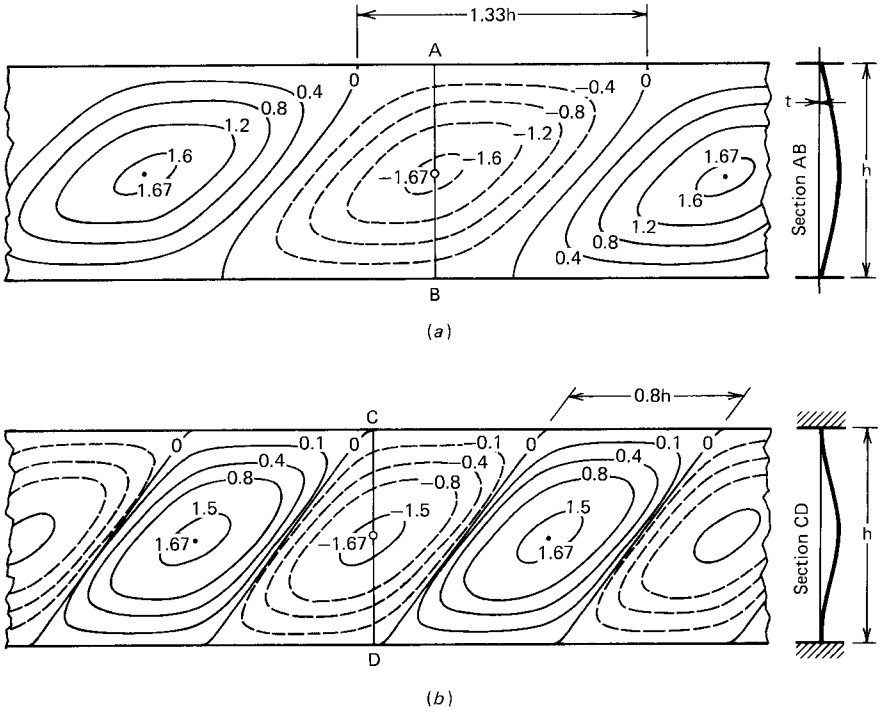
Figure 4.55   Shear buckling of infinitely long plate.[4.63] (a) Simply supported edges. (b) Fixed edges.

t = thickness of the plate

In Eq. (4.132), the value of k_v varies with the supporting conditions and the aspect ratio a/h (Fig. 4.56). For a long plate the value of k_v was found to be 5.34 for simple supports and 8.98 for fixed supports, as listed in Table 3.2.

Substituting $\mu = 0.3$ in Eq. (4.132),

$$\tau_{cr} = \frac{0.905 k_v E}{(h/t)^2}, \text{ ksi} \qquad (4.133)$$

Thus if the computed theoretical value of τ_{cr} is less than the proportional limit in shear (0.8 τ_y), the nominal shear strength for elastic buckling can be obtained from Eq. (4.134):

$$V_n = \frac{0.905 k_v E}{(h/t)^2}(ht) = \frac{0.905 k_v E t^3}{h} \qquad (4.134)$$
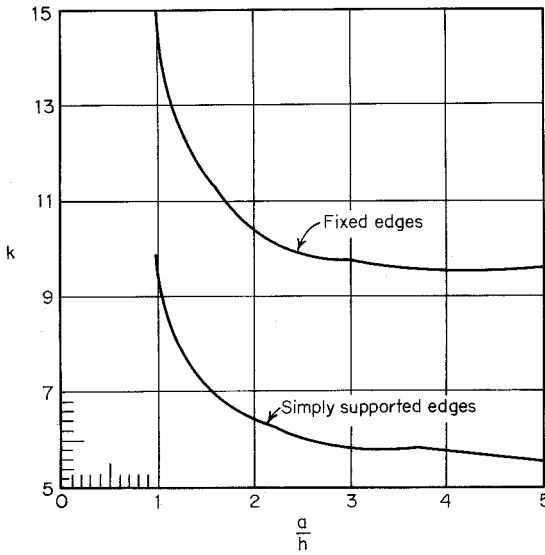
Figure 4.56   Shear buckling stress coefficient of plates versus aspect ratio a/h.[3.1]

c. Shear Buckling in the Inelastic Range. For webs having moderate h/t ratios, the computed theoretical value of τ_{cr} may exceed the proportional limit in shear. The theoretical value of the critical shear buckling stress should be reduced according to the change in the modulus of elasticity. Considering the influence of strain hardening observed in the investigation of the strength of plate girders in shear,[4.64] Basler indicated that Eq. (4.135) can be used as the reduction formula:

$$\tau_{cr} = \sqrt{\tau_{pr}\tau_{cri}} \qquad (4.135)$$

where τ_{pr} = porportional limit in shear, = $0.8\tau_y = 0.8(F_y/\sqrt{3})$
  τ_{cri} = initial critical shear buckling stress,

$$= \frac{k_v\pi^2E}{12(1 - \mu^2)(h/t)^2} \qquad (4.136)$$

By substituting the values of τ_{pr} and τ_{cri} into Eq. (4.135), one can obtain Eq. (4.137) for the shear buckling stress in the inelastic range, that is,

$$\tau_{cr} = \frac{0.64\sqrt{k_vF_yE}}{h/t} \qquad (4.137)$$

Consequently the nominal shear strength in the inelastic range can be obtained from Eq. (4.138):

$$V_n = \frac{0.64\sqrt{k_v F_y E}}{h/t}(ht) = 0.64t^2\sqrt{k_v F_y E} \qquad (4.138)$$

d. AISI Design Criteria for Shear Strength of Webs Without Holes. Based on the foregoing discussion of shear strength of beam webs, the Supplement to the 1996 edition of the AISI Specification includes the following design provisions in Sec. C3.2.1 for the ASD and LRFD methods:[1.333]

C3.2.1 Shear Strength of Webs without Holes

The nominal shear strength, V_n, at any section shall be calculated as follows:

(a) For $h/t \le 0.96\sqrt{Ek_v/F_y}$

$$V_n = 0.60F_y ht \qquad (4.139a)$$

$$\Omega_v = 1.50 \text{ (ASD)}$$

$$\phi_v = 1.0 \text{ (LRFD)}$$

(b) For $0.96\sqrt{Ek_v/F_y} < h/t \le 1.415\sqrt{Ek_v/F_y}$

$$V_n = 0.64t^2\sqrt{k_v F_y E} \qquad (4.139b)$$

$$\Omega_v = 1.67 \text{ (ASD)}$$

$$\phi_v = 0.90 \text{ (LRFD)}$$

(c) For $h/t > 1.415\sqrt{Ek_v/F_y}$

$$V_n = \frac{\pi^2 Ek_v t^3}{12(1-\mu^2)h} = 0.905Ek_v t^3/h \qquad (4.139c)$$

$$\Omega_v = 1.67 \text{ (ASD)}$$

$$\phi_v = 0.90 \text{ (LRFD)}$$

where V_n = nominal shear strength of beam
t = web thickness
h = depth of the flat portion of the web measured along the plane of the web
k_v = shear buckling coefficient determined as follows:
    1. For unreinforced webs, $k_v = 5.34$
    2. For beam webs with transverse stiffeners satisfying the requirements of Section B6

when $a/h \leq 1.0$

$$k_v = 4.00 + \frac{5.34}{(a/h)^2} \qquad (4.140a)$$

when $a/h > 1.0$

$$k_v = 5.34 + \frac{4.00}{(a/h)^2} \qquad (4.140b)$$

where a = the shear panel length for unreinforced web element
  = the clear distance between transverse stiffeners for reinforced web element.

For a web consisting of two or more sheets, each sheet shall be considered as a separate element carrying its share of the shear force.

Prior to 1996, the AISI ASD Specification employed three different factors of safety (i.e., 1.44 for yielding, 1.67 for inelastic buckling, and 1.71 for elastic buckling) for determining the allowable shear stresses in order to use the same allowable values for the AISI and AISC Specifications. To simplify the design of shear elements for using the allowable stress design method, the factor of safety for both elastic and inelastic shear buckling is taken as 1.67 in the 1996 edition of the AISI Specification. The factor of safety of 1.50 is used for shear yielding to provide the allowable shear stress of $0.40F_y$, which has been used in steel design for a long time. The use of such a smaller safety factor of 1.50 for shear yielding is justified by long-standing use and by the minor consequences of incipient yielding in shear as compared with those associated with yielding in tension and compression.

For the ASD method, the allowable shear stresses in webs are shown in Fig. 4.57 by using $E = 29,500$ ksi (203 GPa). Table 4.6 gives the allowable shear stresses for $F_y = 33$ and 50 ksi (228 and 345 MPa). Examples 4.17 through 4.19 illustrate the application of Eqs. (4.139) and (4.140).

Example 4.17   Use the ASD and LRFD methods to determine the design shear strength for the I-section used in Example 4.1. Use $F_y = 50$ ksi.

Solution

A. ASD Method

The depth-to-thickness ratio of each *individual* web element is
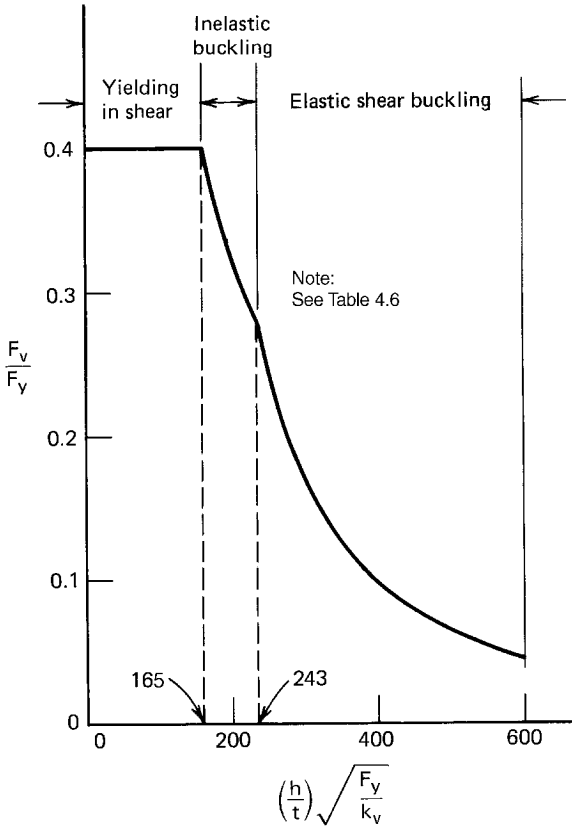
Figure 4.57   Allowable shear stress in webs for the ASD method.

$$\frac{h}{t} = \frac{8 - 2(0.135 + 0.1875)}{0.135} = \frac{7.355}{0.135} = 54.48$$

Based on the AISI design criteria, the value of k_v for unreinforced webs is 5.34. Therefore, according to Sec. C3.2.1 of the AISI Specification,

$$0.96\sqrt{Ek_v/F_y} = 0.96\sqrt{(29,500)(5.34)/50} = 53.88$$
$$1.415\sqrt{Ek_v/F_y} = 1.415\sqrt{(29,500)(5.34)/50} = 79.42$$

Since $0.96\sqrt{Ek_v/F_y} < h/t < 1.415\sqrt{Ek_v/F_y}$, use Eq. (4.139b) to compute the nominal shear strength of each web element as follows:

$$V_n = 0.64t^2 \sqrt{k_v F_y E} = 0.64(0.135)^2 \sqrt{5.34 \times 50 \times 29,500}$$
$$= 32.74 \text{ kips/web}$$

TABLE 4.6   Allowable Shear Stresses for the ASD Method, ksi

$\dfrac{h}{t}$	$F_y = 33$ ksi					$F_y = 50$ ksi				
	a/h					a/h				
	0.5	1.0	2.0	3.0	>3	0.5	1.0	2.0	3.0	>3
50	13.2	13.2	13.2	13.2	13.2	20.0	20.0	20.0	20.0	20.0
60	13.2	13.2	13.2	13.2	13.2	20.0	20.0	19.5	18.7	17.9
70	13.2	13.2	13.2	13.0	12.5	20.0	20.0	16.7	16.0	15.4
80	13.2	13.2	11.9	11.4	10.9	20.0	17.8	14.6	14.0	13.3
90	13.2	12.8	10.6	10.1	9.7	20.0	15.8	12.5	11.4	10.5
100	13.2	11.6	9.5	9.1	8.5	20.0	14.2	10.1	9.2	8.5
110	13.2	10.5	8.4	7.6	7.1	20.0	12.3	8.4	7.6	7.1
120	13.2	9.6	7.0	6.4	5.9	19.5	10.1	7.0	6.4	5.9
130	13.2	8.8	6.0	5.5	5.1	18.0	8.8	6.0	5.5	5.1
140	13.2	7.7	5.2	4.7	4.4	16.7	7.6	5.2	4.7	4.4
150	12.7	6.6	4.5	4.1	3.8	15.6	6.6	4.5	4.1	3.8
160	11.9	5.8	4.0	3.6	3.3	14.6	5.8	4.0	3.6	3.3
170	11.2	5.2	3.5	3.2	3.0	13.8	5.2	3.5	3.2	3.0
180	10.6	4.6	3.1	2.9	2.6	12.5	4.6	3.1	2.9	2.6
190	10.0	4.1	2.8	2.6	2.4	11.2	4.1	2.8	2.6	2.4
200	9.5	3.7	2.5	2.3	2.1	10.1	3.7	2.5	2.3	2.1
220	8.4	3.1	2.1	1.9	1.8	8.4	3.1	2.1	1.9	1.8
240	7.0	2.6	1.8	1.6	1.5	7.0	2.6	1.8	1.6	1.5
260	6.0	2.2	1.5	1.4	1.3	6.0	2.2	1.5	1.4	1.3
280	5.2	1.9	1.3	1.2	1.1	5.2	1.9	1.3	1.2	1.1
300	4.5	1.7	1.1	1.0	0.9	4.5	1.7	1.1	1.0	0.9

Notes:
1. Values above the single underlines are based on Eq. (4.139a); values between the single underlines and double underlines are based on Eq. (4.139b); and values below the double underlines are based on Eq. (4.139c). For the case of $a/h > 3$, $k_v = 5.34$.
2. 1 ksi = 6.9 MPa.

The allowable design shear strength for the I-section having two webs is

$$V_a = 2V_n/\Omega_v = 2(32.74)/1.67 = 39.20 \text{ kips}$$

B. LRFD Method

Using the same nominal shear strength computed in Item A, the design shear strength for the I-section having double webs is

$$2\phi_v V_n = 2(0.90)(32.74) = 58.93 \text{ kips}$$

Example 4.18   Use the ASD and LRFD methods to determine the design shear strength for the channel section used in Example 4.2. Use $F_y = 50$ ksi.

Solution

A. *ASD Method*

For the given channel section, the depth-to-thickness ratio of the web is

$$\frac{h}{t} = \frac{10 - 2(0.075 + 0.09375)}{0.075} = \frac{9.6625}{0.075} = 128.83$$

Based on $k_v = 5.34$ and $F_y = 50$ ksi

$$1.415\sqrt{Ek_v/F_y} = 1.415\sqrt{(29{,}500)(5.34)/50} = 79.42$$

Since $h/t > 1.415\sqrt{Ek_v/F_y}$, use Eq. (4.139c) to compute the nominal shear strength V_n as follows:

$$\begin{aligned}
V_n &= 0.905Ek_v t^3/h \\
&= 0.905(29{,}500)(5.34)(0.075)^3/9.6625 \\
&= 6.22 \text{ kips}
\end{aligned}$$

The allowable design shear strength using the ASD method for the design of the given channel section is

$$V_a = V_n/\Omega_v = 6.22/1.67 = 3.72 \text{ kips}$$

B. *LRFD Method*

Based on the same nominal shear strength computed in Item A, the design shear strength using the LRFD method for the design of the channel section is:

$$\phi_v V_n = (0.90)(6.22) = 5.60 \text{ kips}$$

Example 4.19   Use the ASD and LRFD methods to determine the design shear strength for the hat section used in Example 4.3. Use $F_y = 50$ ksi.

Solution

A. *ASD Method*

The depth-to-thickness ratio of the web is

$$\frac{h}{t} = \frac{10 - 2(0.105 + 0.1875)}{0.105} = \frac{9.415}{0.105} = 89.67$$

Based on $k_v = 5.34$ and $F_y = 50$ ksi,

$$1.415\sqrt{Ek_v/F_y} = 1.415\sqrt{(29,500)(5.34)/50} = 79.42$$

Since $h/t > 1.415\sqrt{Ek_v/F_y}$, use Eq. (4.139c) to compute the nominal shear strength, V_n, for the hat section having two webs as follows:

$$V_n = 2(0.905)Ek_v t^3/h$$

$$= 2(0.905)(29,500)(5.34)(0.105)^3/9.415$$

$$= 35.06 \text{ kips}$$

The allowable design shear strength using the ASD method for the design of the hat section is

$$V_a = V_n/\Omega_v = 35.06/1.67 = 20.99 \text{ kips}$$

B. LRFD Method

Based on the same nominal shear strength computed in Item A, the design shear strength using the LRFD method for the design of the hat section is

$$\phi_v V_n = (0.90)(35.06) = 31.55 \text{ kips}$$

e. AISI Design Criteria for Shear Strength of C-Section Webs with Holes. When holes are present in beam webs, the effect of web perforation on the reduction of shear strength of C-sections was investigated in the 1990s by Shan et al.,[3.184,3.197] Schuster et al.,[3.187] and Eiler.[3.192] In these studies, three hole geometries (rectangular hole with corner fillets, circular hole, and diamond-shape hole) were considered in the test programs. Based on the results of research findings, the following Sec. C3.2.2 was added in the Supplement to the 1996 edition of the AISI Specification in 1999.[1.333]

C3.2.2 Shear Strength of C-Section Webs with Holes

These provisions shall be applicable within the following limits:

1. $d_o/h < 0.7$
2. $h/t \leq 200$
3. holes centered at mid-depth of the web
4. clear distance between holes ≥ 18 in. (457 mm)

5. for non-circular holes, corner radii $\geq 2\,t$

6. for non-circular holes, $d_o \leq 2.5$ in. (64 mm) and b ≤ 4.5 in. (114 mm)

7. circular hole diameter ≤ 6 in. (152 mm)

8. $d_o > 9/16$ in. (14 mm)

The nominal shear strength, V_n, determined by Section C3.2.1 shall be multiplied by q_s:

when $c/t \geq 54$

$$q_s = 1.0 \tag{4.141a}$$

when $5 \leq c/t < 54$

$$q_s = c/(54\,t) \tag{4.141b}$$

where

$$c = h/2 - d_o/2.83 \quad \text{for circular holes} \tag{4.142a}$$

$$ = h/2 - d_o/2 \quad\;\; \text{for non-circular holes} \tag{4.142b}$$

d_o = depth of web hole

b = length of web hole

h = depth of flat portion of the web measured

along the plane of the web

Similar as Sec. B2.4 of the AISI Specification (Art. 3.6.2), the above design provisions for circular and non-circular holes apply to any hole pattern that fits within an equivalent virtual hole as shown in Figs. 3.54 and 3.55.

4.3.4   Bending

Webs of beams can buckle not only in shear but also due to the compressive stress caused by bending, for example, at the location of a maximum moment. Figure 3.27 shows a typical pattern of bending failure of beam webs.

The web buckling stress due to bending and the postbuckling strength of flat beam webs are discussed in Art. 3.5.1.2. The same article also discusses the AISI design equations for computing the effective design depth of beam webs.

For beam webs having relatively large depth-to-thickness ratios, the buckling of web elements becomes more important. The structural efficiency of such beam webs can be improved by adding longitudinal stiffeners in the

compression portion of the web, as shown in Fig. 4.58. References 4.60, 4.65, and 4.66 present the studies made by Nguyen and Yu on the structural behavior of longitudinally reinforced beam webs.

In Europe, the design methods for profiled sheeting and sections with stiffeners in the flanges and webs are provided in Refs. 1.209 and 3.56.

4.3.5 Combined Bending and Shear

When high bending and high shear act simultaneously, as in cantilever beams and at interior supports of continuous beams, the webs of beams may buckle at a lower stress than if only one stress were present without the other. Such webs must be safeguarded against buckling due to this combined bending and shear.

The critical combination of bending and shear stresses in disjointed flat rectangular plates has been studied by Timoshenko.[3.2] Figure 4.59 shows the interaction between f_b/f_{cr} and τ/τ_{cr}, in which f_b is the actual computed bending stress, f_{cr} is the theoretical buckling stress in pure bending, τ is the actual computed shear stress, and τ_{cr} is the theoretical buckling stress in pure shear. It can be seen from Fig. 4.59 that for a/h ratios ranging from 0.5 to 1.0, the relationship between f_b/f_{cr} and τ/τ_{cr} can be approximated by Eq. (4.143), which is a part of the unit circle:

$$\left(\frac{f_b}{f_{cr}}\right)^2 + \left(\frac{\tau}{\tau_{cr}}\right)^2 = 1 \qquad (4.143)$$

By using proper factors of safety, the following interaction formula has been used for the allowable stress design of beam webs subjected to the combined bending and shear stresses:

$$\left(\frac{f_{bw}}{F_{bw}}\right)^2 + \left(\frac{f_v}{F_v}\right)^2 \leq 1 \qquad (4.144)$$
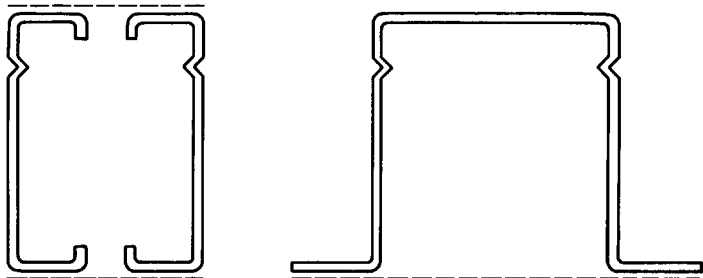
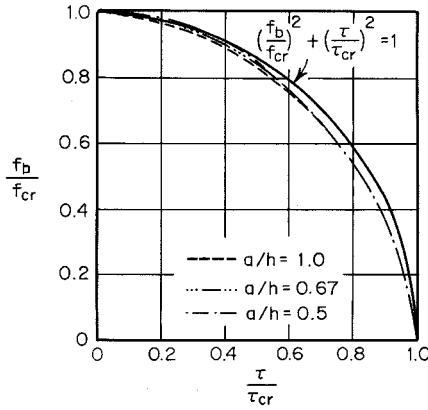**Figure 4.58** Typical sections for longitudinally reinforced beam specimens.

$$\left(\frac{f_b}{f_{cr}}\right)^2 + \left(\frac{\tau}{\tau_{cr}}\right)^2 = 1$$

a/h = 1.0
a/h = 0.67
a/h = 0.5

Figure 4.59 Interaction relationship between f_b/f_{cr} and τ/τ_{cr}.[4.63]

where f_{bw} = actual compression stress at junction of flange and web, ksi
F_{bw} = allowable compressive stress, ksi
f_v = actual average shear stress, ksi
F_v = allowable shear stress, ksi

For additional information on simply supported plates under combined shear and uniformly distributed longitudinal stresses, see Ref. 3.3.

In the past, the structural strength of beam webs subjected to a combination of bending and shear has been studied by LaBoube and Yu.[4.57,4.67] The results of 25 beam tests indicated that Eq. (4.144), originally developed for a disjointed individual sheet, would be conservative for beam webs with adequate transverse stiffeners, for which a diagonal tension field action can be developed. Based on the test results shown in Fig. 4.60, the following interaction equation was developed for beam webs with transverse stiffeners satisfying the requirements of Art. 4.3.2:

$$0.6\,\frac{f_b}{f_{b\ max}} + \frac{\tau}{\tau_{max}} = 1.3 \qquad (4.145)$$

where $f_{b\ max}$ = maximum computed stress governing bending
τ_{max} = maximum computed stress governing shear for reinforced web

Accordingly, the allowable stress design equation for webs reinforced with adequate transverse stiffeners can be expressed as follows:

$$0.6\left(\frac{f_{bw}}{F_{bw}}\right) + \frac{f_v}{F_v} \le 1.3 \qquad (4.146)$$

Equation (4.146) is applicable only when $f_{bw}/F_{bw} > 0.5$ and $f_v/F_v > 0.7$.
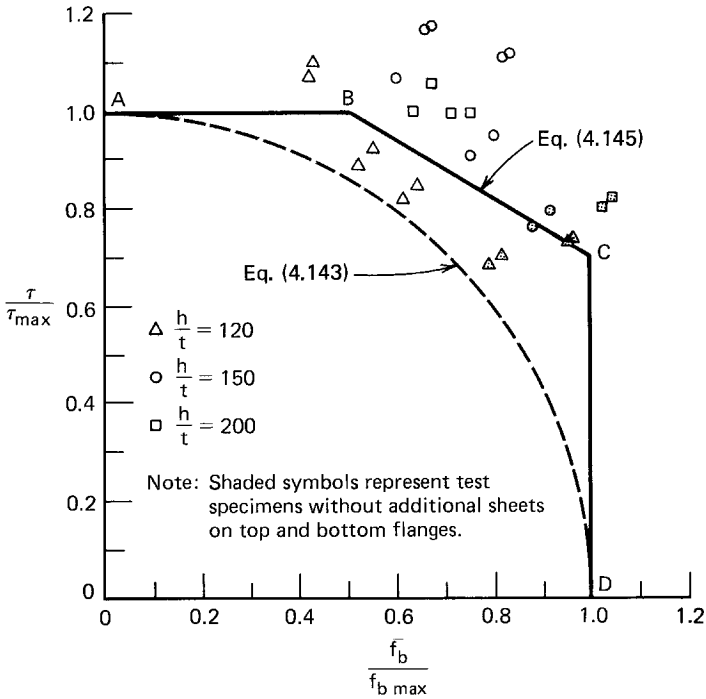
Figure 4.60   Interaction diagram for τ/τ_{max} and $f_b/f_{b\ \text{max}}$.

For other conditions, the design of beam webs is governed by either the allowable bending stress or the allowable shear stress.

Instead of using stress ratios in Eqs. (4.144) and (4.146), the 1986 and 1996 editions of the AISI Specification use strength ratios (i.e., moment ratio for bending and force ratio for shear) for the interaction equations. The following design criteria are included in Sec. C3.3 of the AISI Specification to determine the strength for combined bending and shear:

C3.3 Strength for Combined Bending and Shear

C3.3.1 ASD Method

For beams with unreinforced webs, the required flexural strength, M, and required shear strength, V, shall satisfy the following interaction equation:

$$\left(\frac{\Omega_b M}{M_{\text{nxo}}}\right)^2 + \left(\frac{\Omega_v V}{V_n}\right)^2 \leq 1.0 \qquad (4.147a)$$

For beams with transverse web stiffeners, the required flexural strength, M, and required shear strength, V, shall not exceed M_n/Ω_b and V_n/Ω_v, respectively. When $\Omega_b M/M_{\text{nxo}} > 0.5$ and $\Omega_v V/V_n > 0.7$, then M and V shall satisfy the

following interaction equation:

$$0.6 \left(\frac{\Omega_b M}{M_{nxo}} \right) + \left(\frac{\Omega_v V}{V_n} \right) \leq 1.3 \qquad (4.147b)$$

where Ω_b = factor of safety for bending (see Section C3.1.1)
$\quad\Omega_v$ = factor of safety for shear (see Section C3.2)
$\quad M_n$ = nominal flexural strength when bending alone exists
$\quad M_{nxo}$ = nominal flexural strength about the centroidal x-axis determined in accordance with Section C3.1.1
$\quad V_n$ = nominal shear force when shear alone exists

C3.3.2 LRFD Method

For beams with unreinforced webs, the required flexural strength, M_u, and the required shear strength, V_u, shall satisfy the following equation:

$$\left(\frac{M_u}{\phi_b M_{nxo}} \right)^2 + \left(\frac{V_u}{\phi_v V_n} \right)^2 \leq 1.0 \qquad (4.148a)$$

For beams with transverse web stiffeners, the required flexural strength, M_u, and the required shear strength, V_u, shall not exceed $\phi_b M_n$ and $\phi_v V_n$, respectively. When $M_u/(\phi_b M_{nxo}) > 0.5$ and $V_u/(\phi_n V_n) > 0.7$, then M_u and V_u shall satisfy the following interaction equation:

$$0.6 \left(\frac{M_u}{\phi_b M_{nxo}} \right) + \left(\frac{V_u}{\phi_v V_n} \right) \leq 1.3 \qquad (4.148b)$$

where ϕ_b = resistance factor for bending (see Section C3.1.1)
$\quad\phi_v$ = resistance factor for shear (see section C3.2)
$\quad M_n$ = nominal flexural strength when bending alone exists
$\quad M_{nxo}$ = nominal flexural strength about the centroidal x-axis determined in accordance with Section C3.1.1
$\quad V_n$ = nominal shear strength when shear alone exists

Figure 4.61 shows the AISI interaction formulas using the ASD method for the design of beam webs subjected to the combination of bending and shear. These design criteria are based on Eqs. (4.147a) and (4.147b). A recent study conducted by Almoney and Murray indicated that combined bending and shear is a possible limit state for continuous lapped Z-purlin system and that the current AISI provisions accurately predict the failure load.[4.173]

4.3.6 Web Crippling (Bearing)

When the end and load stiffeners are not used in thin-walled cold-formed steel construction, the webs of beams may cripple due to the high local intensity of the load or reaction. Figure 4.62 shows the types of failure caused
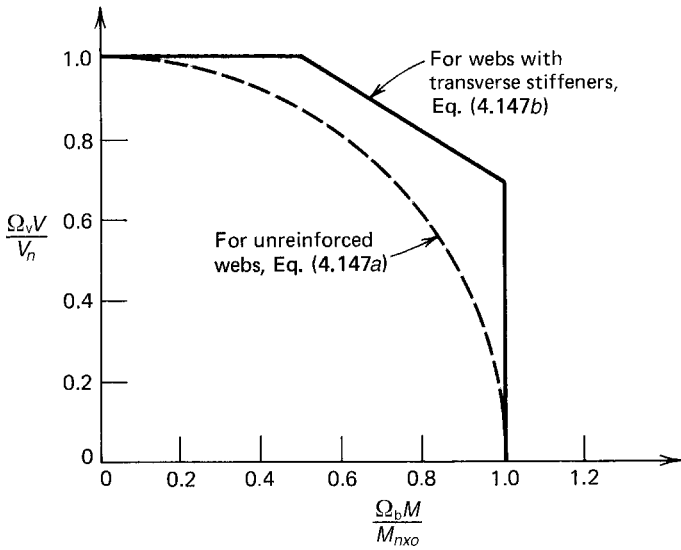
Figure 4.61   Interaction formulas for combined bending and shear.

by web crippling of unrestrained single webs and of restrained double webs. The web crippling of double restrained webs is also shown in Fig. 1.30.

The buckling problem of separate flat rectangular plates under locally distributed edge forces has been studied by numerous investigators, including Sommerfeld,[4.68] Timoshenko,[4.69] Leggett,[4.70] Hopkins,[4.71] Yamaki,[4.72] Zetlin,[4.73] White and Cottingham,[4.74] Khan and Walker,[4.75] Khan, Johns, and Hayman,[4.76] and others.[3.7] Based on Refs. 4.75 and 4.76, the buckling load for the plates subjected to locally distributed edge forces as shown in Figures 4.63 and 4.64 can be computed as

$$P_{cr} = \frac{k\pi^2 E t^3}{12(1 - \mu^2)h} \tag{4.149}$$

where k is the buckling coefficient depending on the ratios of N/h and a/h as given in these two figures.

For steel beams having webs connected to flanges, theoretical and experimental investigations on web crippling under partial edge loading have been
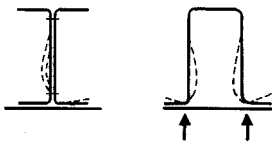
Figure 4.62   Web crippling of beams.[1.161]
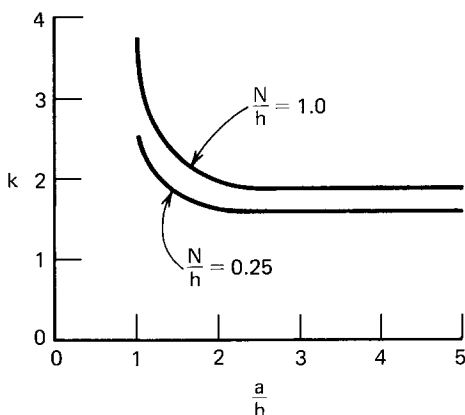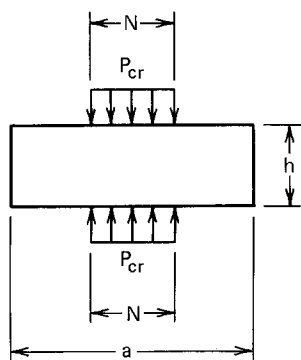
Figure 4.63 Buckling coefficient k for simply supported plates subjected to two opposite locally distributed edge forces.[1.216,4.75] (*Reproduced with permission from Walker, A. C. (ed.), Design and Analysis of Cold-Formed Sections, International Textbook Co. Ltd., Glasgow and London, 1975.*)

conducted by Lyse and Godfrey,[4.77] Rocky, Bagchi, and El-gaaly,[4.78–4.83] and Bergfelt.[4.84] However, the theoretical analysis of web crippling for cold-formed steel flexural members is rather complicated because it involves the following factors:

1. Nonuniform stress distribution under the applied load and adjacent portions of the web.
2. Elastic and inelastic stability of the web element.
3. Local yielding in the immediate region of load application.
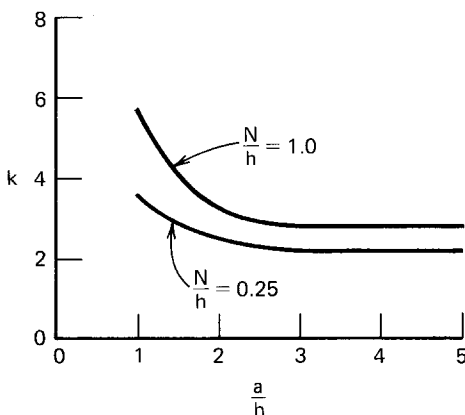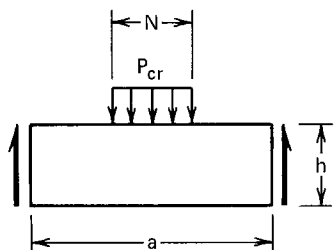
Figure 4.64 Buckling coefficient k for simply supported plates subjected to one locally distributed edge force.[4.76]

4. Bending produced by eccentric load (or reaction) when it is applied on the bearing flange at a distance beyond the curved transition of the web.
5. Initial out-of-plane imperfection of plate elements.
6. Various edge restraints provided by beam flanges and interaction between flange and web elements.
7. Inclined webs for decks and panels.

For these reasons, the present AISI design provisions for web crippling are based on the extensive experimental investigations conducted at Cornell University by Winter and Pian,[4.85] and by Zetlin[4.73] in the 1940s and 1950s, and at the University of Missouri-Rolla by Hetrakul and Yu in the 1970s.[4.58] In these experimental investigations, the web crippling tests have been carried out under the following four loading conditions for beams having single unreinforced webs and I-beams:

1. End one-flange (EOF) loading
2. Interior one-flange (IOF) loading
3. End two-flange (ETF) loading
4. Interior two-flange (ITF) loading

All loading conditions are illustrated in Fig. 4.65. In Fig. 4.65*a* and 4.65*b* the distances between bearing plates were kept to no less than 1.5 times the web depth in order to avoid the two-flange action.

4.3.6.1 Beams Having Single Unreinforced Webs   In the 1950s the web crippling strength of cold-formed steel beams having single unreinforced webs has been studied experimentally at Cornell University.[4.73] This investigation included the testing of 154 specimens, of which 128 tests were on hat sections and 26 tests on U-sections. The design formulas developed from this study for the web-crippling strength depend on N/t, h/t, R/t, and F_y, where N is the actual length of the bearing, h is the depth of the beam web, R is the inside bend radius, t is the thickness of the beam web, and F_y is the yield point of the web.

In the past, numerous types of steel sections made of high-strength materials have been developed for use in building construction and for other purposes. The design of such unusual shapes was beyond the original scope of the AISI design provisions, which were developed previously on the basis of the Cornell research. For this reason, additional web crippling tests have been conducted in the United States[4.58,4.86] and some other countries[4.87–4.89] in order to refine the design criteria.

Based on the results of 224 web crippling tests conducted at Cornell University and the University of Missouri-Rolla, the AISI design formulas were slightly modified in the 1980 edition of the specification. Similar equations with minor modifications were included in Sec. C3.4.1 of the Supplement to the 1996 edition of the AISI Specification.[1.333] All design equations for de-
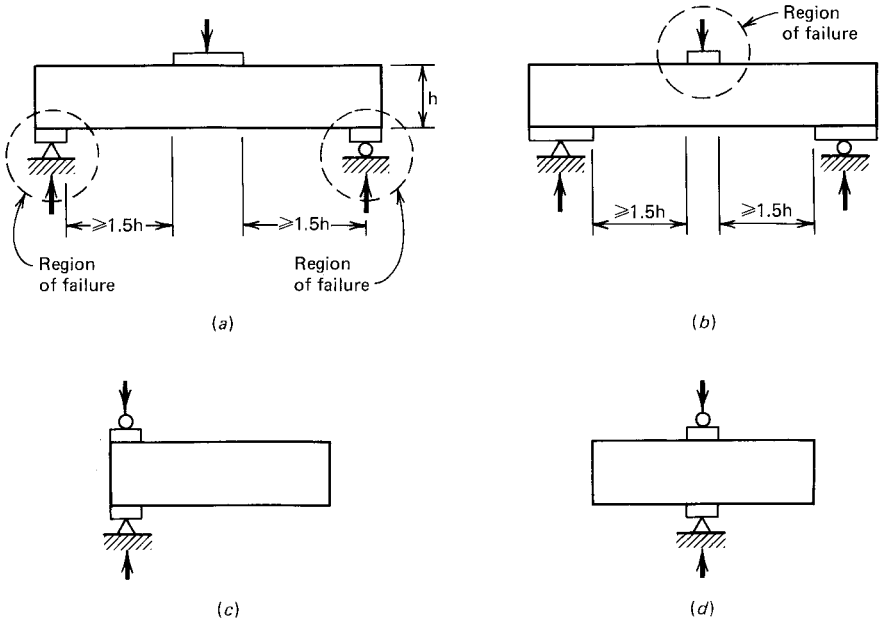
Figure 4.65 Loading conditions for web crippling tests. (*a*) EOF loading. (*b*) IOF loading. (*c*) ETF loading. (*d*) ITF loading.

termining the nominal web crippling strength for channels, Z-sections, hat sections, square or rectangular tubes, steel decks, and panels are given in Table 4.7. Figure 4.66 shows the applications of Eqs. (4.150) to (4.154) for different types of loading. It should be noted that these equations can only be used for unreinforced flat webs (i.e., webs without stiffeners) having $h/t \leq 200$. $N/t \leq 210$, $N/h \leq 3.5$, $R/t \leq 6$ for beams, $R/t \leq 7$ for decks, and $45° \leq \theta \leq 90°$. In the design equations,

$$C_1 = 1.22 - 0.22k \tag{4.155a}$$

$$C_2 = 1.06 - 0.06\left(\frac{R}{t}\right) \leq 1.0 \tag{4.155b}$$

$$C_3 = \text{not used in the Supplement}^{1.333}$$

$$C_4 = 1.15 - 0.15 \left(\frac{R}{t}\right) \leq 1.0 \text{ but no less than } 0.5 \tag{4.155c}$$

$$C_9 = 1.0 \text{ for U.S. customary units; } 6.9 \text{ for metric units} \tag{4.155d}$$

$$C_\theta = 0.7 + 0.3 \left(\frac{\theta}{90}\right)^2 \tag{4.156}$$

TABLE 4.7   Nominal Web Crippling Strength for Single Unreinforced Webs, P_n, kips(N)/web[1.314,1.333]
$\Omega_w = 1.85$ (ASD)
$\phi_w = 0.75$ (LRFD)

Shapes Having Single Unreinforced Webs Such as Channels, Z-Sections, Hat Sections, Tubular Members, Desks and Panels

At locations of one concentrated load or reaction acting on either top or bottom flange, when clear distance between the bearing edges of this and adjacent opposite concentrated loads or reacitons is greater than 1.5h	For end reactions of beams or concentrated loads on end of cantilever when distance from edge of bearing to end of beam is less than 1.5h (EOF)	Stiffened flanges $t^2 k C_1 C_4 C_9 C_\theta [331 - 0.61(h/t)]$ $\times [1 + 0.01(N/t)]$ (4.150)
		Unstiffened flanges $t^2 k C_1 C_4 C_9 C_\theta [217 - 0.28(h/t)]$ $\times [1 + 0.01(N/t)]^a$ (4.151)
	For reactions and concentrated loads when distance from edge of bearing to end of beam is equal to or larger than 1.5h (IOF)	Stiffened and unstiffened flanges $t^2 k C_1 C_2 C_9 C_\theta [538 - 0.74(h/t)]$ $\times [1 + 0.007(N/t)]^b$ (4.152)
At locations of two opposite concentrated loads or of a concentrated load and an opposite reaction acting simultaneously on top and bottom flanges, when clear distance between their adjacent bearing edges is equal to or less than 1.5h	For end reactions of beams or concentrated loads on end of cantilever when distance from edge of bearing to end of beam is less than 1.5h (ETF)	Stiffened and unstiffened flanges $t^2 k C_1 C_4 C_9 C_\theta [244 - 0.57(h/t)]$ $\times [1 + 0.01(N/t)]$ (4.153)
	For reactions and concentrated loads when distance from edge of bearing to end of beam is equal to or larger than 1.5h (ITF)	Stiffened and unstiffened flanges $t^2 k C_1 C_2 C_9 C_\theta [771 - 2.26(h/t)]$ $\times [1 + 0.0013(N/t)]$ (4.154)

[a] When $N/t > 60$, the factor $[1 + 0.01 (N/t)]$ may be increased to $[0.71 + 0.015 (N/t)]$.
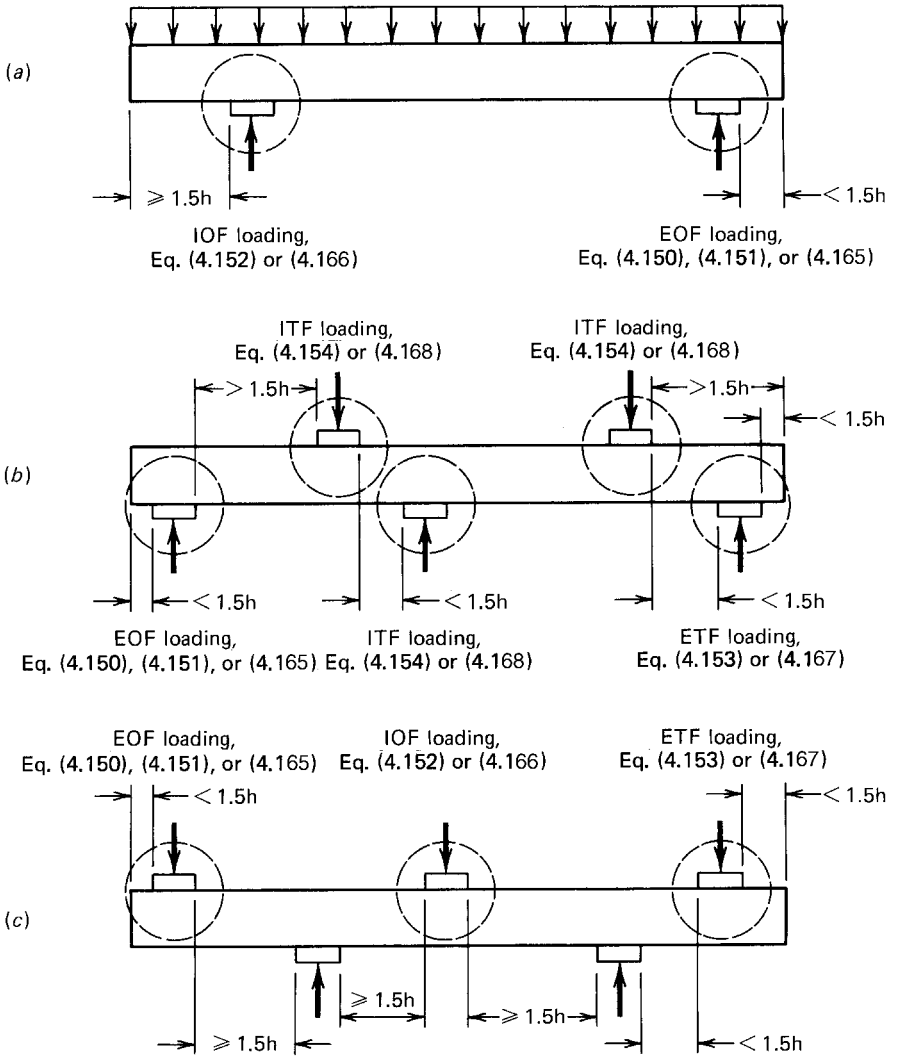[b] When $N/t > 60$, the factor $[1 + 0.007 (N/t)]$ may be increased to $[0.75 + 0.011 (N/t)]$.

Figure 4.66 Application of AISI equations listed in Tables 4.7 and 4.8.[1.159]

F_y = yield point used in design of the web, ksi (MPa)

h = depth of the flat portion of the web measured along plane of the web, in. (mm)

$$k = 894 \, F_y / E \tag{4.157}$$

t = web thickness, in. (mm)

N = actual length of bearing, in (mm). For the case of two equal and opposite concentrated loads distributed over unequal bearing lengths, the smaller value of N should be used in design

R = inside bend radius, in. (mm)

θ = angle between plane of web and plane of bearing surface, $\geq 45°$ but not more than $90°$

In the 1990s, additional research conducted by Bhaka, Cain, LaBoube, and Yu on web crippling indicated that a Z-section having its end support flange bolted to the section's supporting member through two ½-in. (12.7-mm) diameter bolts exhibits an increase in end-one-flange (EOF) web crippling strength.[4.174,4.175] For this reason, the 1996 edition of the AISI Specification permits that for a Z-section having its flange bolted to the section's end support member, Eq. (4.150) may be multiplied by 1.3. This is valid only for sections meeting the following limitations: (1)$h/t \leq 150$, (2) $R/t \leq 4$, (3) cross-section base metal thickness larger than or equal to 0.06 in. (1.52 mm), and (4) support member thickness larger than or equal to 3/16 in. (4.76 mm).

In addition, for two nested Z-sections, the 1996 edition of the AISI Specification permits the use of slightly different safety factor (Ω_w = 1.80 for ASD) and resistance factor (ϕ_w = 0.85 for LRFD) when evaluating the web crippling strength for interior-one-flange loading by using Eq. (4.152). Based on the research work conducted at the University of Wisconsin-Milwaukee and the University of Missouri-Rolla, LaBoube, Nunnery, and Hodges indicated that the web crippling behavior of unreinforced two nested Z-sections is enhanced because of the rotational restraint exhibited by the nested Z configuration and the narrow range of section parameters that represented in the industry standard sections.[4.176]

From Eqs. (4.150) to (4.154) it can be seen that the nominal web crippling strength for beams having single unreinforced webs depends on the ratios of N/t, h/t, and R/t, the web thickness t, the design yield stress of F_y, and the web inclination angle θ. The design strengths are based on the applicable safety factor and resistance factor. The use of a relatively small factor of safety against the maximum capacity obtained from tests was due to the fact that the specimens represent the lowest degree of web restraint likely to be found in practice.

In the 1996 edition of the AISI Specification, HSLAS Grades 70 and 80 of A653 and A715 steels were added in Specification Sec. A3.1. These two grades of steels have minimum yield points of 70 ksi (483 MPa) for Grade 70 and 80 ksi (522 MPa) for Grade 80. Because the AISI provisions for web crippling strengths were previously developed on the basis of the experimental investigations using steels having F_y less than 44 ksi (379 MPa), Eqs. (4.150) to (4.154) were limited only to $F_y \leq 66.5$ ksi (459 MPa). When F_y exceeds the above limit, the value of kC_3 was taken as 1.34 in a footnote of the 1996

edition of the Specification. Recent research at the University of Missouri-Rolla indicated that the web crippling strength increased for beams using the yield point of steel exceeding 66.5 ksi (459 MPa).[4.183,4.192] Based on the results of 262 web crippling tests using yield strength from 58.2 ksi (401 MPa) to 165.1 ksi (1138 MPa), the original constant C_3 used in Eqs. (4.150), (4.151), and (4.153) was replaced by C_1 with the deletion of a footnote as stated in the AISI Supplement to the 1996 Specification.[1.333]

Also included in the AISI 1999 Supplement is the addition of the following new Section C3.4.2 for web crippling strength of C-section webs with holes:[1.333]

C3.4.2 Web Crippling Strength of C-Section Webs with Holes

When a web hole is within the bearing length, a bearing stiffener shall be used. For beam webs with holes, the web crippling strength shall be computed by using Specification Section C3.4.1 multiplied by the reduction factor, R_c, given in this section.

These provisions shall be applicable within the following limits:

1. $d_o/h < 0.7$
2. $h/t \leq 200$
3. holes centered at mid-depth of the web
4. clear distance between holes $\geq$ 18 in. (457 mm)
5. distance between the end of the member and the edge of the hold $\geq d$
6. for non-circular holes, corner radii $\geq 2\ t$
7. for non-circular holes, $d_o \leq 2.5$ in. (64 mm) and $b \leq 4.5$ in. (114 mm)
8. circular hole diameter $\leq$ 6 in. (152 mm)
9. $d_o > 9/16$ in. (14 mm)

   a. For using Equations (4.150) and (4.151) when a web hole is not within the bearing length:

   $$R_c = 1.01 - 0.325 d_o/h + 0.083\ x/h \leq 1.0 \tag{4.158}$$

   $$N \geq 1 \text{ in. (25 mm)}$$

   b. For using Equation (4.152) when any portion of a web hole is not within the bearing length:

   $$R_c = 0.90 - 0.047 d_o/h + 0.053\ x/h \leq 1.0 \tag{4.159}$$

   $$N \geq 3 \text{ in. (76 mm)}$$

where b = length of web hole
d = depth of cross section
d_o = depth of web hole
h = depth of flat portion of the web measured along the plane of the web
x = nearest distance between the web hole and the edge of bearing
N = bearing length

The above provisions were based on the studies conducted by Langan et al.,[3.198] Uphoff,[3.199] and Deshmukh[3.200] for the reduction in web crippling strength when a hole is present in a C-section beam web. These studies investigated both the end-one-flange and interior-one-flange loading conditions for $h/t \leq 200$ and $d_o/h \leq 0.81$. The reduction in web crippling strength is influenced primarily by the size and location of the hole represented by the d_o/h and x/h ratios.

As in Specification Sections B2.4 and C3.2.2, the above design provisions apply to any hole pattern that fits within an equivalent virtual hole as shown in Figs. 3.54 and 3.55.

The application of Eqs. (4.150) to (4.154) is illustrated in Examples 4.20 and 4.21 for beam webs having single unreinforced webs without holes.

In other countries, the Australian/New Zealand Standard[1.175] and the British Standard[1.194] use the similar design provisions as the AISI Specification. In Canada, the Canadian Standard, CSA Standard S136-94, uses the following format for determining the web crippling strength:[1.177,4.177,4.178]

$$P_n = Ct^2 F_y(\sin\theta)(1 - C_R\sqrt{R^*})(1 + C_N\sqrt{N^*})(1 - C_H\sqrt{H^*}) \quad (4.160)$$

in which C is the web crippling coefficient, C_H is the web slenderness coefficient, C_N is the bearing length coefficient, C_R is inside bend radius coefficient, $H^* = h/t$, $N^* = N/t$, and $R^* = R/t$. All coefficients are listed in three separate tables for built-up sections (I-beams), shapes having single webs, and deck sections (multiple webs). Equation (4.160) was based on the research conducted by Wing, Prabakaran, and Schuster at the University of Waterloo.[4.89,4.177] Similar design format is being considered by the AISI Committee on Specifications for the Design of Cold-Formed Steel Structural Members at the present time (1999).

In the Swedish specification[4.87] and the European recommendations,[1.209] the web crippling load for interior-one-flange loading depends on N/t, $\sqrt{R/t}$, t, F_y, and the angle θ. The design formula can be used for $R/t \leq 10$, $50° \leq \theta \leq 90°$, and $h/t \leq 170$.

4.3.6.2 I-Beams having a High Degree of Restraint against Rotation of the Web

In the 1940s, the web crippling behavior of I-beams was investigated by Winter and Pain at Cornell University.[4.85] In this phase of study, a total of 136 tests were performed on I-sections made of channels, as shown in Fig. 4.67. The h/t ratios of the specimens ranged from 30 to 175 and the N/t ratios varied from 7 to 77. The yield stresses of steel were from 30 to 38 ksi (207 to 262 MPa). Equations (4.161) through (4.164) were developed from the Cornell tests.
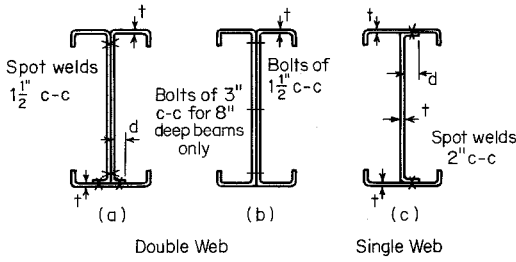
For end one-flange loading,

Figure 4.67 Typical cross sections used in investigation of web crippling.[4.85]

$$P_n = t^2 F_y (10 + 1.25\sqrt{N/t}) \qquad (4.161)$$

For interior one-flange loading,

$$P_n = t^2 F_y (15 + 3.25\sqrt{N/t}) \qquad (4.162)$$

For end two-flange loading,

$$P_n = t^2 F_y (10 + 1.25\sqrt{N/t}) \qquad (4.163)$$

For interior two-flange loading

$$P_n = t^2 F_y (15 + 3.25\sqrt{N/t}) \qquad (4.164)$$

Additional tests on the web crippling of I-beams made of high-strength materials and thinner steel sheets were conducted by Hetrakul and Yu at the University of Missouri-Rolla in the 1970s.[4.58] For these latter tests, the yield stresses of steels ranged from 33 to 54 ksi (228 to 372 MPa) and the h/t ratios were increased to 266. Based on the results of 230 tests reported in Refs. 4.85 and 4.58, the design formulas originally developed from the Cornell research have been modified as given in Table 4.8 for the I-beams having a high degree of restraint against rotation of the web.
    In Table 4.8,

P_n = nominal web crippling strength, kips/web

TABLE 4.8 Nominal Web Crippling Strength for I-Sections, P_n, kips(N)/web
$\Omega_w = 2.00$ (ASD)
$\phi_w = 0.80$ (LRFD)

I-Beams Made of Two Channels Connected Back to Back or Similar Sections, Which Provide a High Degree of Restraint against Rotation of the Web, such as I-Sections Made by Connecting Two Angles to a Channel

At locations of one concentrated load or reaction acting on either top or bottom flange, when clear distance between the bearing edges of this and adjacent opposite concentrated loads or reactions is greater than 1.5h	For end reactions of beams or concentrated loads on end of cantilever when distance from edge of bearing to end of beam is less than 1.5h (EOF)	Stiffened and unstiffend flanges $t^2F_yC_6(10.0 + 1.25\sqrt{N/t})$	(4.165)
	For reactions and concentrated loads when distance from edge of bearing to end of beam is equal to or larger than 1.5h (IOF)	Stiffened and unstiffened flanges $t^2F_yC_5(0.88 + 0.12m)(15.0 + 3.25\sqrt{N/t})$	(4.166)
At locations of two opposite concentrated loads or of a concentrated load and an opposite reaction acting simultaneously on top and bottom flanges, when clear distance between their adjacent bearing edges is equal to or less than 1.5h	For end reactions of beams or concentrated loads on end of cantilever when distance from edge of bearing to end of beam is less than 1.5h (ETF)	Stiffened and unstiffened flanges $t^2F_yC_8(0.64 + 0.31m)(10.0 + 1.25\sqrt{N/t})$	(4.167)
	For reactions and concentrated loads when distance from edge of bearing to end of beam is equal to or larger than 1.5h (ITF)	Stiffened and unstiffened flanges $t^2F_yC_7(0.82 + 0.15m)(15.0 + 3.25\sqrt{N/t})$	(4.168)

$$C_5 = 1.49 - 0.53k \geq 0.6 \tag{4.169}$$

$$C_6 = \begin{cases} 1 + \dfrac{h/t}{750}, & \text{when } h/t \leq 150 & (4.170a) \\[3mm] 1.20, & \text{when } h/t > 150 & (4.170b) \end{cases}$$

$$C_7 = \begin{cases} 1/k, & \text{when } h/t \leq 66.5 & (4.171a) \\[3mm] \left(110 - \dfrac{h/t}{665}\right)/k, & \text{when } h/t > 66.5 & (4.171b) \end{cases}$$

$$C_8 = \left(0.98 - \dfrac{h/t}{865}\right)/k \tag{4.172}$$

$$k = 894F_y/E \tag{4.173}$$

$$m = \dfrac{t}{0.075}, \qquad \text{when } t \text{ is in inches} \tag{4.174}$$

$$m = \dfrac{1}{1.91}, \qquad \text{when } t \text{ is in mm} \tag{4.175}$$

The symbols F_y, N, and t were defined previously.

Based on Eqs. (4.165) to (4.168) with the applicable safety factor and resistance factor, the design web crippling strength can be computed for I-beams made of two channels connected back to back or for similar sections which provide a high degree of restraint against rotation of the web, such as I-sections made by connecting two angles to a channel. The use of Eqs. (4.165) to (4.168) is also limited to $h/t \leq 200$, $N/t \leq 210$, $N/h \leq 3.5$, and $R/t \leq 6$. Example 4.22 illustrates the design of an I-section by using Eq. (4.165).

For the ASD method, the use of a relatively larger factor of safety of 2.0 for I-beams is based on the fact that the results of tests showed considerable scatter and that the tested specimens used in the program represent the optimum amount of web restraint likely to be met in practice.[1.161]

4.3.7   Combined Web Crippling and Bending

In Art. 4.3.6 the web crippling limit state of cold-formed steel beams was discussed in detail. The AISI design formulas were used to prevent any localized failure of webs resulting from the bearing pressure due to reactions or concentrated loads without consideration of the effect of other stresses.

In practical applications a high bending moment may occur at the location of the applied concentrated load in simple span beams. For continuous beams, the reactions at supports may be combined with high bending mo-

ments and/or high shear. Under these conditions, the web crippling strength as determined in Art. 4.3.6 may be reduced significantly due to the effect of bending moment. The interaction relationship for the combination of bearing pressure and bending stress has been studied by numerous researchers.[4.58,4.80,4.81,4.86–4.88,4.90–4.92] Based on the results of beam tests with combined web crippling and bending, interaction formulas have been developed for use in several design specifications.

4.3.7.1 Shapes Having Single Webs

Based on the results of 49 channel specimens and 17 hat sections tested for combined web crippling and bending at Cornell University, the University of Missouri-Rolla,[4.58] and United States Steel Research Laboratory,[4.92] the following conclusions have been drawn in Ref. 4.58.

1. For beam specimens having single unreinforced webs subjected to combined bending and web crippling, the presence of bending moments will noticeably reduce the web crippling capacity when the ratio of $M_{\text{test}}/M_{\text{n comp}}$ exceeds about 0.35. Equation (4.176) provides a good correlation with the test results, as shown in Fig. 4.68. Also shown in this figure are some test data for web crippling combined with small bending moments.

$$1.07 \, \frac{P_{\text{test}}}{P_{\text{n comp}}} + \frac{M_{\text{test}}}{M_{\text{n comp}}} = 1.42 \tag{4.176}$$

where P_{test} = maximum concentrated load or reaction in the presence of bending moment

$P_{\text{n comp}}$ = computed maximum concentrated load or reaction in the absence of bending moment (Table 4.7)

M_{test} = maximum bending moment at or immediately adjacent to concentrated load or reaction

$M_{\text{n comp}}$ = computed nominal flexural strength of the section if bending only exists

2. *ASD Method* When the actual shear force V in the beam is less than or equal to 40% of the nominal shear strength of the beam V_{n}, the presence of shear force does not significantly reduce the web crippling load. It is expected that even for beams having high shear stress, the web crippling strength will not be reduced significantly.

By using a safety factor of 1.85 for web crippling load and a safety factor of 1.67 for bending moment, the following allowable design equation (AISI Eq. C3.5.1-1) can be derived from Eq. (4.176) for the ASD method:

$$1.2 \left(\frac{\Omega_{\text{w}} P}{P_{\text{n}}} \right) + \left(\frac{\Omega_{\text{b}} M}{M_{\text{nxo}}} \right) \le 1.5 \tag{4.177}$$
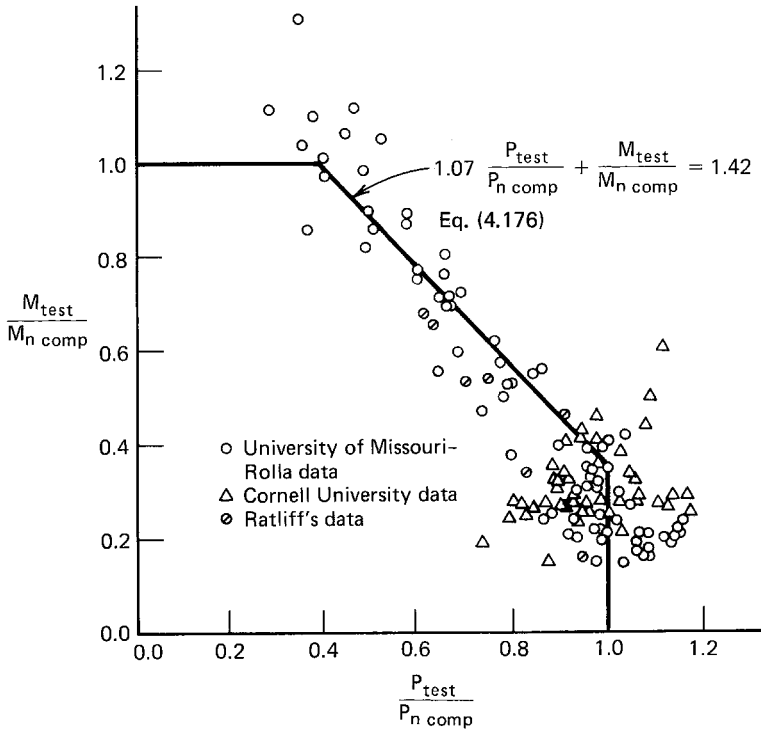
Figure 4.68 Graphic presentation for web crippling (IOF loading) and combined web crippling and bending for specimens having single unreinforced webs.[4.58]

where Ω_b = factor of safety for bending

Ω_w = factor of safety for web crippling

P = concentrated load or reaction in the presence of bending moment

P_n = nominal web crippling strength in the absence of bending moment determined in accordance with Table 4.7

M = applied bending moment at or immediately adjacent to the point of application of the concentrated load or reaction P

M_{nxo} = nominal flexural strength of the section if bending stress only exists, excluding lateral buckling

The relationship between the ratios of $\Omega_b M/M_{nxo}$ and $\Omega_w P/P_n$ is shown in Fig. 4.69. It can be seen that Eq. (4.177) is used only for $\Omega_w P/P_n > 0.417$ and $\Omega_b M/M_{nxo} > 0.3$. The effect of the bending moment on the web crippling load is considered in Example 4.20.

In the AISI Specification, an exception clause is included for the interior supports of continuous spans using the decks and beams as shown in Fig. 4.70. This is because the results of continuous beam tests of steel decks[4.86] and several independent studies of individual manufacturers indicate that for
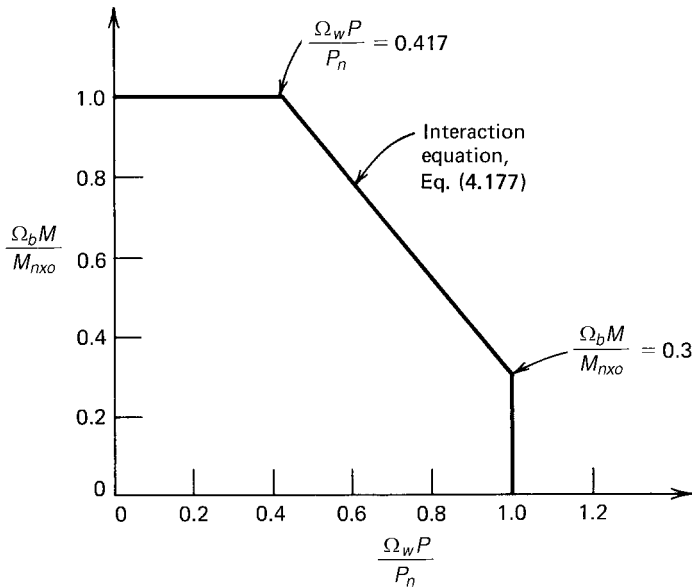
Figure 4.69 AISI ASD interaction equation for combined web crippling and bending (shapes having single unreinforced webs).

these types of members the postbuckling behavior of beam webs at interior supports differs from the type of failure mode occurring under concentrated loads on single-span beams. This postbuckling strength enables the member to redistribute the moments in continuous beams. For this reason, Eq. (4.177) may be found to be conservative for determining the load-carrying capacity of continuous spans on the basis of the conventional elastic design. If local-
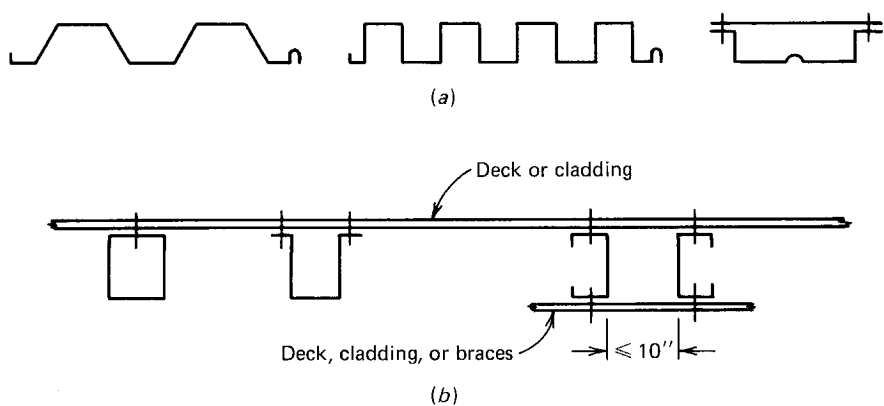
Figure 4.70 Sections used for AISI exception clauses.[1.159] (*a*) Decks. (*b*) Beams.

ized distortions of webs over interior supports as shown in Fig. 4.71 are permitted, the inelastic flexural reserve capacity due to partial plastification of beam cross section and moment redistribution may be used as discussed in Art. 4.3.8.

3. *LRFD Method* For the LRFD method, the AISI provisions specify that for shapes having single unreinforced webs subjected to a combination of bending and concentrated load or reaction shall be designed to meet the following requirements:

$$1.07 \left(\frac{P_u}{\phi_w P_n} \right) + \left(\frac{M_u}{\phi_b M_{nxo}} \right) \leq 1.42 \qquad (4.176a)$$

where ϕ_b = resistance factor for bending
 ϕ_w = resistance factor for web crippling
 P_u = required strength for the concentrated load or reaction in the presence of bending moment
 P_n = nominal strength for concentrated load or reaction in the absence of bending moment (Table 4.7)
 M_u = required flexural strength at, or immediately adjacent to, the point of application of the concentrated load or reaction P_u
 M_{nxo} = nominal flexural strength about the centroidal *x*-axis determined in accordance with Section C3.1.1 of the AISI Specification
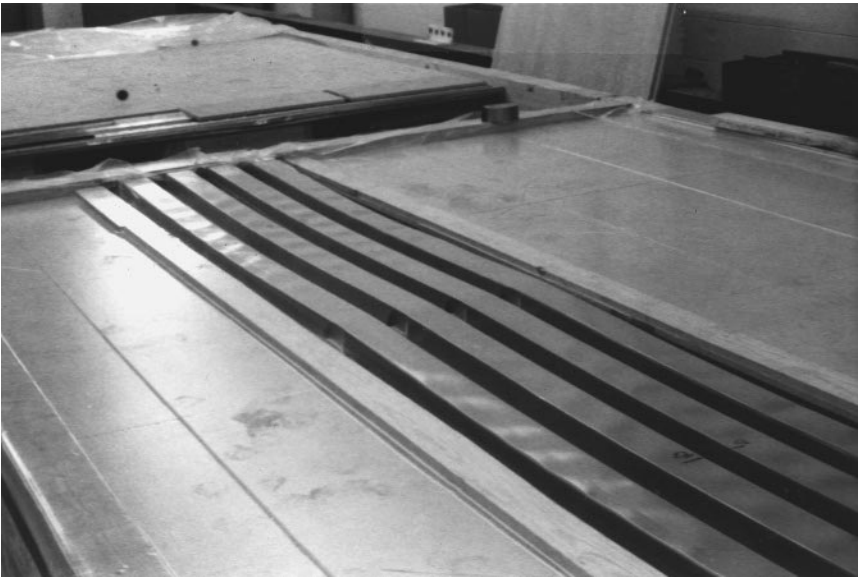
Figure 4.71 Two-span continuous beam tests using uniform loading.

It can be seen that the above equation for using the LRFD approach is based on Eq. (4.176). As with the ASD method, an exception clause is included for interior support of continuous spans.

4.3.7.2 *I-Beams Having a High Degree of Restraint against Rotation of Web*

In Ref. 4.58 the results of 106 beam tests conducted at Cornell[4.85] and the University of Missouri-Rolla[4.94] were used to evaluate the interaction between bending and web crippling for I-beams (Fig. 4.67) having a high degree of restraint against rotation of the web. It was found that when I-beams have $h/t \leq 2.33/\sqrt{F_y/E}$ and $\rho = 1$, the bending moment has little or no effect on the web crippling load, as shown in Fig. 4.72. For I-beams having web slenderness ratios h/t and flange flat-width ratios w/t other than the above combination, Eq. (4.178) can provide a good correlation with the test data as shown in Fig. 4.73:

$$0.82 \frac{P_{\text{test}}}{P_{\text{n comp}}} + \frac{M_{\text{test}}}{M_{\text{n comp}}} = 1.32 \tag{4.178}$$

where P_{test}, $P_{\text{n comp}}$, M_{test}, and $M_{\text{n comp}}$ are as defined previously.
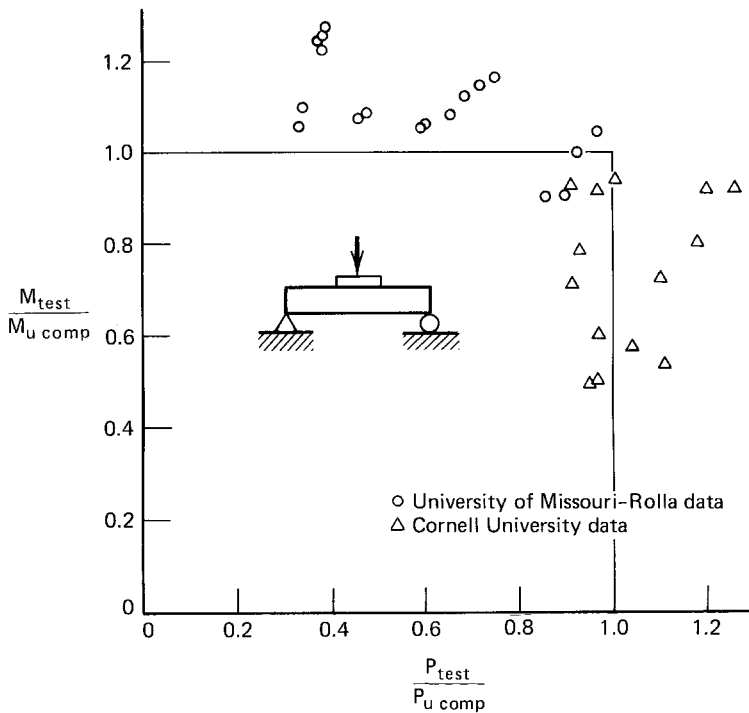
Figure 4.72 Interaction between web crippling and bending for I-beam specimens having unreinforced webs [when $h/t \leq 2.33/\sqrt{E_y/E}$ and $\rho = 1$].[4.58]
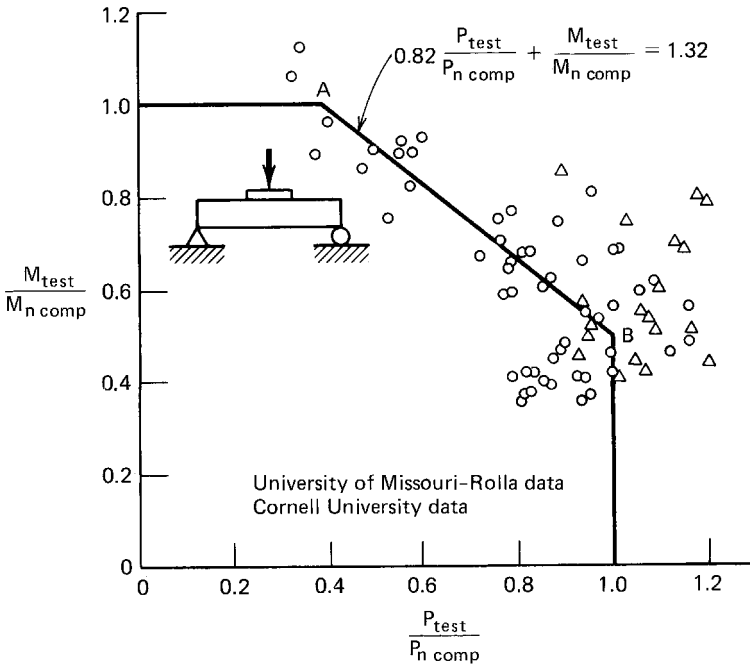
Figure 4.73 Interaction between web crippling and bending for I-beam specimens having unreinforced webs [when $h/t \leq 2.33/\sqrt{F_y/E}$ combined with $\rho < 1$, and $2.33/\sqrt{F_y/E} < h/t \leq 200$ combined with any value of w/t] (IOF loading).[4.58]

As far as the combination of shear force and web crippling is concerned, Ref. 4.58 concludes that when the shear ratio $V/V_n \leq 0.80$, the presence of shear force does not affect the web crippling load significantly.

1. *ASD Method* By applying a safety factor of 2.0 for web crippling load and a safety factor of 1.67 for bending moment, the following AISI design formula for I-beams can be derived from Eq. (4.178) for the ASD method:

$$1.1 \left(\frac{\Omega_w P}{P_n} \right) + \left(\frac{\Omega_b M}{M_{nxo}} \right) \leq 1.5 \qquad (4.179)$$

This design criterion can be used for any I-beams subjected to combined bending and web crippling, except that when $h/t \leq 2.33/\sqrt{F_y/E}$ and $\rho = 1$, the nominal web crippling strength given in Table 4.8 can be used for design without any reduction.

Figure 4.74 shows that the AISI interaction formula [Eq. (4.179)] is used only for $\Omega_w P/P_n > 0.455$ and $\Omega_b M/M_{nxo} > 0.4$.
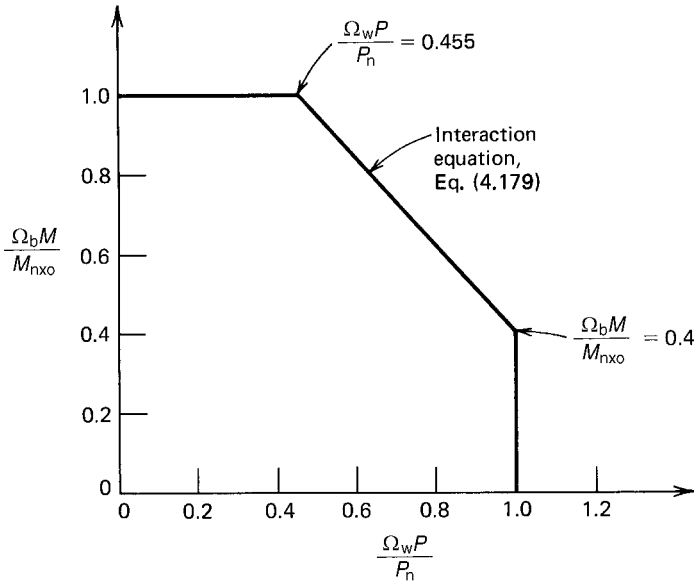
Figure 4.74 AISI ASD interaction equation for combined web crippling and bending (I-beams).

2. *LRFD Method* For the LRFD method, the AISI provisions specify that I-beams subjected to a combination of bending and concentrated load or reaction shall be designed to meet the following requirements:

$$0.82\left(\frac{P_u}{\phi_w P_n}\right) + \left(\frac{M_u}{\phi_b M_{nxo}}\right) \leq 1.32 \qquad (4.178a)$$

All symbols were defined previously. It can be seen that the above equation for using the LRFD method is based on Eq. (4.178). As with the ASD method, an exception clause is included to permit the use of the nominal web crippling strength without the use of the interaction formula.

4.3.7.3 Nested Z-Shapes In the 1996 edition of the AISI Specification, design provisions were added for nested Z-shapes. When two nested Z-shapes are subject to a combination of bending and concentrated load or reaction, these members shall be designed to meet the following requirements by using the ASD method:

$$\frac{M}{M_{no}} + \frac{P}{P_n} \leq \frac{1.67}{\Omega} \qquad (4.180)$$

where M_{no} is the nominal flexural strength for the two nested Z-sections, and $\Omega = 1.67$.

For using the LRFD method, the Z-shapes shall be designed to meet the following requirements:

$$\frac{M_u}{M_{no}} + \frac{P_u}{P_n} \leq 1.68\phi \tag{4.181}$$

in which $= \phi = 0.90$. Other symbols were defined previously.

Because the above two equations were derived from the experimental work summarized in Ref. 4.176, these equations are valid only for the shapes that meet the following limits: $h/t \leq 150$, $N/t \leq 140$, $F_y \leq 70$ ksi (483 MPa), and $R/t \leq 5.5$. In addition, the following conditions shall also be satisfied: (1) the ends of each section shall be connected to other section by a minimum of two ½-in. (12.7-mm) diameter A307 bolts through the web, (2) the combined section shall be connected to the support by a minimum of two ½-in. (12.7-mm) diameter A307 bolts through the flanges, (3) the webs of the two sections shall be in contact, and (4) the ratio of the thicker-to-thinner part shall not exceed 1.3.

Example 4.20   For the channel section shown in Fig. 4.75 to be used as a simply supported beam:

1. Determine the allowable end reaction P_{max} to prevent web crippling by considering it as a one-flange loading condition with $N = 3.5$ in.
2. Determine the allowable interior load to prevent web crippling by considering the load as a one-flange loading condition with $N = 5$ in., and assuming that the applied bending moment M at the location of the interior load is less than 30% of the allowable bending moment M_{nxo}/Ω_b permitted if bending stress only exists.
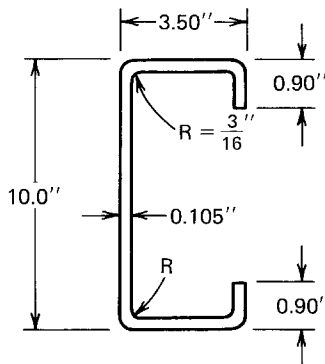

Figure 4.75   Example 4.20.

3. Same as item 2, except that the applied bending moment M at the location of the interior load is equal to the allowable bending moment M_{nxo}/Ω_b.

Use $F_y = 50$ ksi and the ASD method.

Solution

1. *Allowable End Reaction for Web Crippling (One-Flange Loading).* Since

$$h/t = [10 - 2(0.105 + 0.1875)]/0.105 = 89.67 < 200$$
$$N/t = 3.5/0.105 = 33.33 < 210$$
$$N/h = 3.5/[10 - 2(0.105 + 0.1875)] = 0.37 < 3.5$$
$$R/t = 0.1875/0.105 = 1.786 < 6$$
$$\theta = 90°$$
$$k = 894(50)/29,500 = 1.515$$

Eqs. (4.150) through (4.154) can be used for the design of the channel section. By using Eq. (4.150) for beams having stiffened flanges, the nominal strength to prevent web crippling at end support is

$$P_n = t^2 k C_1 C_4 C_9 C_\theta [331 - 0.61(h/t)][1 + 0.01(N/t)]$$
$$= (0.105)^2(1.515)[1.22 - 0.22(1.515)][1.15 - 0.15(1.786)](1)$$
$$\times [0.7 + 0.3(90/90)^2][331 - 0.61(89.67)][1 + 0.01(33.33)]$$
$$= 4.82 \text{ kips}$$

The allowable end reaction $P_a = P_n/\Omega_w = 4.82/1.85 = 2.61$ kips

2. *Allowable Interior Load for Web Crippling ($M < 0.3M_{nxo}/\Omega_b$).* According-ing to Eq. (4.152), the nominal web crippling strength for interior load without considering the effect of the bending moment is

$$P_n = t^2 k C_1 C_2 C_9 C_\theta [558 - 0.74(h/t)][1 + 0.007(N/t)]$$
$$= (0.105)^2(1.515)[1.22 - 0.22(1.515)][1.06 - 0.06(1.786)](1)$$
$$\times [0.7 + 0.3(90/90)^2][538 - 0.74(89.67)][1 + 0.007(5/0.105)]$$
$$= 8.87 \text{ kips}$$

The allowable interior load for web crippling is $P_a = P_n/\Omega_w = 8.87/$

$1.85 = 4.79$ kips. Because the applied moment M at the location of the interior load is less than 30% of the allowable bending moment M_{nxo}/Ω_b permitted if bending stress only exists, Eq. (4.177) is not applicable. For this case, the computed allowable interior load of 4.79 kips should be used without any reduction due to combined web crippling and bending (see Fig. 4.69).

3. *Allowable Interior Load for Web Crippling* ($M = M_{nxo}/\Omega_b$). From item 2 the computed allowable interior load for web crippling is 4.79 kips. Because the beam is to be designed for the maximum allowable bending moment (i.e., $\Omega_b M/M_{nxo} = 1.0$), the applied concentrated load should be reduced according to Eq. (4.177), as shown in Fig. 4.69, in order to account for the effect of the bending moment. Accordingly,

$$1.2 \left(\frac{\Omega_w P}{P_n} \right) + 1.0 = 1.5$$

or

$$\frac{\Omega_w P}{P_n} = 0.417$$

For this case, the allowable interior load for web crippling is

$$P_a = 0.417 P_n / 1.85 = 2.00 \text{ kips}$$

Example 4.21 Use the ASD method to determine the allowable end reaction for the hat section used in Example 4.3 to prevent web crippling. Assume that the length of bearing is 3.5 in. and $F_y = 50$ ksi. Also use the LRFD method to determine the design web crippling strength.

Solution

A. ASD Method

$$\text{Since } h/t = [10 - 2(0.105 + 0.1875)]/0.105 = 89.67 < 200$$
$$N/t = 3.5/0.105 = 33.33 < 210$$
$$N/h = 3.5/[10 - 2(0.105 + 0.1875)] = 0.37 < 3.5$$
$$R/t = 0.1875/0.105 = 1.786 < 6$$
$$\theta = 90°$$
$$k = 894(50)/29,500 = 1.515$$

Equations (4.150) through (4.154) can be used for the design of this hat

section having single unreinforced webs.

In view of the fact that the bottom flange of the section, which contacts the bearing plates at both end supports, is the unstiffened type, Eq. (4.151) should be used for design.

$$P_n = t^2 k C_1 C_4 C_9 C_\theta [217 - 0.28(h/t)][1 + 0.01(N/t)]$$

$$= (0.105)^2(1.515)[1.22 - 0.22(1.515)][1.15 - 0.15(1.786)](1)(1)$$

$$\times [217 - 0.28(89.67)][1 + 0.01(33.33)]$$

$$= 3.34 \text{ kips/web}$$

The allowable end reaction, per web, is

$$P_a = P_n/\Omega_w = 3.34/1.85 = 1.81 \text{ kips/web}$$

For two webs, the total allowable end reaction is

$$2P_a = 2(1.81) = 3.62 \text{ kips}$$

B. LRFD Method

The nominal web crippling strength for the LRFD method is the same as that computed for the ASD method. From Item A above, the nominal web crippling strength for end reaction is

$$P_n = 3.34 \text{ kips/web}$$

The design strength to prevent web crippling of the hat section having two webs is

$$2\phi_w P_n = 2(0.75)(3.34) = 5.01 \text{ kips}$$

Example 4.22 Use the ASD and LRFD methods to determine the allowable end reaction for the I-section used in Example 4.1 to prevent web crippling. Assume that the length of bearing is 3.5 in. and $F_y = 50$ ksi. The dead load to live load ratio is assumed to be 1/5.

Solution

A. ASD Method

As the first step, check the AISI limits on h/t, N/t, N/h, and R/t for using Eqs. (4.165) through (4.168):

$$h/t = [8 - 2(0.135 + 0.1875)]/0.135 = 54.48 < 200$$
$$N/t = 3.5/0.135 = 25.93 < 210$$
$$N/h = 3.5/7.355 = 0.48 < 3.5$$
$$R/t = 0.1875/0.135 = 1.39 < 6$$

Because the above ratios are within the AISI limits, use Eq. (4.165) to determine the allowable end reaction for web crippling:

$$P_n = t^2 F_y C_6 (10.0 + 1.25\sqrt{N/t})$$
$$= (0.135)^2 (50)(1 + 54.48/750)(10.0 + 1.25\sqrt{25.93})$$
$$= 16.00 \text{ kips/web}$$

For the I-section having double webs, the total allowable end reaction is

$$P_a = 2P_n/\Omega_w = 2(16.00)/2.00 = 16.00 \text{ kips}$$

B. LRFD Method

Use the same equation employed in Item A for the ASD method, the nominal web crippling strength for the I-section have double webs is

$$P_n = 2(16.00) = 32.00 \text{ kips}$$

The design web crippling strength is

$$\phi_w P_n = 0.80(32.00) = 25.6 \text{ kips}$$

Based on the load combination of Eq. (3.5a), the required strength is

$$P_u = 1.4P_D + P_L = 1.4P_D + 5P_D = 6.4P_D$$

where P_D = end reaction due to dead load
P_L = end reaction due to live load

Similarly, based on the load combination of Eq. (3.5b), the required strength is

$$P_u = 1.2P_D + 1.6P_L = 1.2P_D + 1.6(5P_D) = 9.2P_D \qquad \text{Controls}$$

Using $P_u = \phi_w P_n$, the end reaction due to dead load can be computed as follows:

$$9.2P_D = 25.6 \text{ kips}$$

$$P_D = 2.78 \text{ kips}$$

$$P_L = 5P_D = 13.90 \text{ kips}$$

The allowable end reaction to prevent web crippling on the basis of the LRFD method is

$$P_a = P_D + P_L = 2.78 + 13.90 = 16.68 \text{ kips}$$

It can be seem that for the given I-section, the LRFD method permits a slightly larger end reaction than the ASD method. The difference is about 4%.

4.3.8 Moment Redistribution of Continuous Beams

Article 4.2.2.3 dealt with the increase of bending moment capacity due to the plastification of the cross section. Studies of continuous beams and steel decks conducted by Yener and Pekoz,[4.2] Unger,[4.5] Ryan,[4.9] and Yu,[4.86] indicate that the inelastic flexural reserve capacity of continuous beams due to moment redistribution may be used in the design of cold-formed steel sections, provided that the following conditions are met:

1. The member is not subject to twisting, lateral, torsional, or torsional–flexural buckling.
2. The effect of cold-forming is not included in determining the yield stress F_y.
3. Localized distortions caused by web crippling over supports are permitted.
4. Reduction of the negative moment capacity over interior support due to inelastic rotation is considered.
5. Unreinforced flat webs of shapes subjected to a combination of bending and reaction are designed to meet the following requirements:
   a. For beams having single webs,

$$1.07\left(\frac{P}{P_n}\right) + \left(\frac{M}{M_n}\right) \leq 1.42$$

   b. For I-beams,

$$0.82\left(\frac{P}{P_n}\right) + \left(\frac{M}{M_n}\right) \leq 1.32$$

   where P_n = nominal web crippling load computed from Art. 4.3.6

and M_n is the ultimate bending moment defined in Art. 4.2.2.3. The values of P and M should not exceed P_n and M_n, respectively.

4.3.9 Additional Information on Web Crippling

During the past 15 years, the web crippling strength of various sections has been studied by numerous investigators. Additional information on web crippling can be found in Ref. 4.95 thorough 4.107 and 4.177 through 4.184.

4.3.10 Effect of Holes on Web Strength

In recent years, cold-formed steel members have been widely used in residential and commercial construction. Holes are usually punched in the webs of joists and wall studs for the installation of utilities. Additional research has been conducted to study the effect of holes on bending strength, shear strength, web crippling strength, and the combination thereof. A Design Guide for Cold-Forming Steel Beams with Web Penetration was published by AISI in 1997.[4.185] For further information, see Refs. 1.284, 3.179, 3.181, 3.184, 3.185, 3.187, 3.189, 3.190, 3.192, and 3.193.

In 1999, the AISI Supplement to the 1996 edition of the Specification included additional design provisions for (a) C-section webs with holes under stress gradient (Art. 3.6.2), (b) shear strength of C-section webs with holes (Art. 4.3.3.2), and (c) web crippling strength of C-section webs with holes (Art. 4.3.6.1).

4.4 BRACING REQUIREMENTS OF BEAMS

4.4.1 Single-Channel Beams

4.4.1.1 Neither Flange Connected to Sheathing When single-channel sections are used as beams, adequate bracing must be provided to prevent rotation about the shear center, as shown in Fig. 4.76, if the load is applied in the plane of the web.
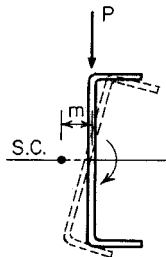

Figure 4.76 Rotation of channel section about its shear center.

The shear center is the point through which the external load must be applied in order to produce bending without twisting. It is located on the axis of symmetry at a distance m from the midplane of the web of the channel section. The value of m can be determined by Eq. (4.182) or Eq. (4.183) for different types of flanges:*

1. For channels without stiffening lips at the outer edges,

$$m = \frac{w_f^2}{2w_f + d/3} \tag{4.182}$$

2. For channels with stiffening lips at the outer edges,

$$m = \frac{w_f dt}{4I_x} \left[w_f d + 2D \left(d - \frac{4D^2}{3d} \right) \right] \tag{4.183}$$

where m = distance from shear center to midplane of web of a channel section, in.

   w_f = projection of flanges from inside face of web, in. (For channels with flanges of unequal widths, w_f shall be taken as the width of the wider flange.)

   d = depth of channel, in.

   D = overall depth of simple lip (edge stiffener), in.

   I_x = moment of inertia of one channel about its centroidal axis normal to web, in.[4]

Since the spacing between braces is usually larger than the spacing of connections required for connecting two channels to form an I-beam (Art. 8.9), each channel section may rotate slightly between braces and result in additional stress. For this reason, braces must be arranged and designed so that the rotation of the beam is small and the additional stresses will not significantly affect the load-carrying capacity of the channel section.

The spacing and strength of bracing required to counteract the twisting tendency of channel beams have been investigated theoretically and experimentally by Winter, Lansing, and McCalley.[4.108] A simplified design method has been developed on the basis of the studies of braced and unbraced channels and verified by test data.

It has been found that even for impractically small spans, the unbraced channel section [depth = 12 in. (305 mm), flange width = $3\frac{1}{2}$ in. (88.9 mm), depth of flange lip = 1 in. (25.4 mm), and t = 0.135 in. (3.4 mm)] made of steels having a yield point of 33 ksi (228 MPa) can only carry less than half of the load that each continuously braced channel would carry before yield-

---

*See Appendix B for location of shear center for other open sections.

ing.[4.108] See Fig. 4.77 for the bracing ration $a/l = 1.0$. In addition, the angle of rotation at the midspan exceeds $2°$ if the span length is larger than 40 in. (1016 mm) (Fig. 4.78).

However, as shown in Fig. 4.77, for braced channels, even for the spacing of braces equal to 0.478 times the span length, the ultimate loads for all practical purposes are the same as for continuous bracing. This fact indicates that the localized overstresses at corners do not affect the strength of the channel sections, since plastic redistribution allows the initially understressed portions of the section to carry additional load. Furthermore, analyses for a great variety of practical loading conditions show that it is unnecessary to provide more than three braces between supports in order to limit the over-stresses to 15% of the simple bending stress $f' = M_c/I$, which equals the yield point at a load equal to the design load times the safety factor, except that additional bracing should be provided at the location of a concentrated load.[4.108] This criterion has been used in the past as a basis in the development of the AISI Specification for a minimum number of braces. The same study also showed that for the 15% limitation of overstress, the rotation of the section at midspan for a deflection of $\frac{1}{360}$ of the span under design load would not exceed $1.5°$, as shown in Fig. 4.79.

The above discussion deals with the number of braces required to limit the additional stress induced by the twisting of channels between braces. The lateral force to be resisted by bracing can be determined by calculating the reaction of a continuous beam consisting of half a channel loaded by a horizontal force $F = Pm/d$ since the load P applied in the plane of the web is
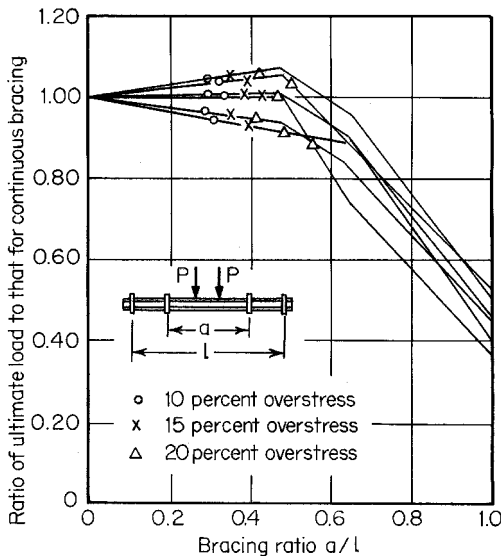

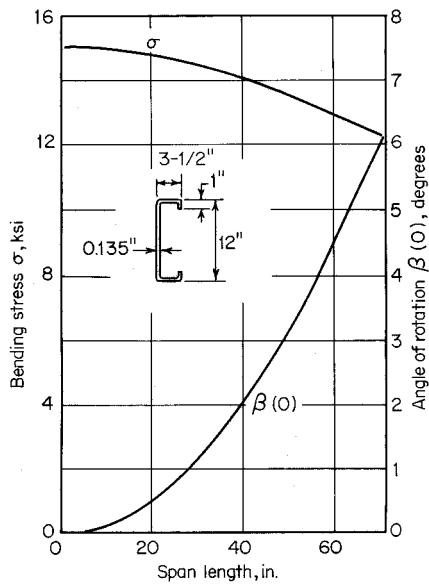**Figure 4.77**   Effect of use of bracing.[4.108]

Figure 4.78   Results of analysis for channel beam indicated.[4.108]
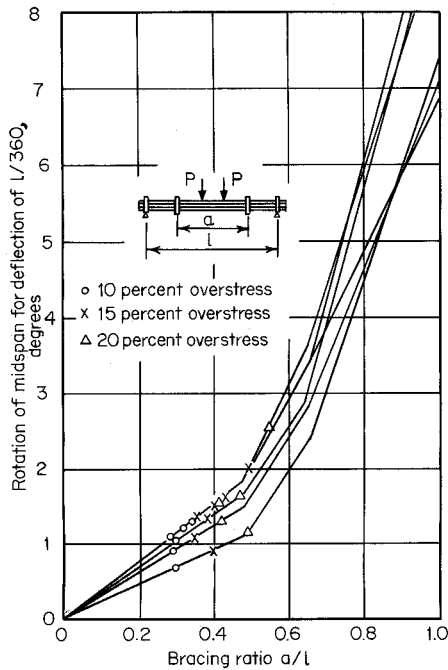

Figure 4.79   Rotations for load resulting in central vertical deflections equal to span/360.[4.108]

equivalent to the same load P applied at the shear center plus two forces applied at both flanges, as shown in Fig. 80.

Based on the research work and practical considerations, the following AISI design criteria have been developed and included in the AISI Specification during the period from 1956 through 1996 for bracing single-channel beams when they are loaded in the plane of the web and neither flange is braced by deck or other means:

> Braces are to be attached to both the top and bottom flanges of the section at the ends and at intervals not greater than one-quarter of the span length in such a manner as to prevent tipping at the ends and lateral deflection of either flange in either direction at intermediate braces. Additional bracing is to be placed at or near the center of the loaded length if one-third or more of the total load is concentrated over a length of one-twelfth or less of the span of the beam. However, when all loads and reactions on a beam are transmitted through members which frame into the section in such a manner as to effectively restrain the section against the rotation and lateral displacement, no additional braces will be required.

In the early 1990s, beam tests conducted by Ellifritt, Sputo, and Haynes[4.186] showed that for typical sections, a mid-span brace may reduce service load horizontal deflections and rotations by as much as 80% when compared to a completely unbraced beam. However, the restraining effect of braces may change the failure mode from lateral–torsional buckling to distortional buckling of the flange and lip at a brace point. The natural tendency of the member under vertical load is to twist and translate in such a manner as to relieve the compression on the lip. When such movement is restrained by intermediate braces, the compression on the stiffening lip is not relieved, and may increase. In this case, distortional buckling may occur at loads lower than that predicted by the lateral buckling equations of Sec. C3.1.2 of the AISI Specification.

The same research[4.186] has also shown that the AISI lateral buckling equations predict loads which are conservative for cases where only one mid-span
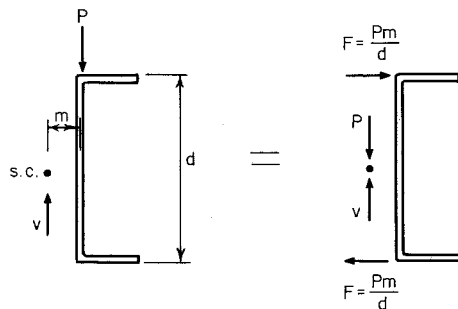

Figure 4.80   Lateral force for design of brace for channels.

brace is used but may be unconservative where more than one intermediate brace is used. Based on such research findings, Sec. D3.2.2 of the AISI Specification was revised in 1996 to eliminate the requirement of quarter-point bracing. Consequently Sec. D3.2.2 of the 1996 edition of the AISI Specification includes the following three requirements for spacing of braces:

1. Braces shall be designed to avoid local crippling at the points of attachment to the member.
2. When braces are provided, they shall be attached in such a manner to effectively restrain the section against later deflection of both flanges at the ends and at any intermediate brace points.
3. When all loads and reactions on a beam are transmitted through members which frame into the section in such a manner as to effectively restrain the section against torsional rotation and lateral displacement, no additional braces will be required except those required for strength according to Sec. C3.1.2 of the Specification.

Each intermediate brace, at the top and bottom flanges, shall be designed to resist a lateral force P_L determined as follows:

(a) For uniform load,

$$P_L = 1.5K'W \tag{4.184}$$

(b) For concentrated load,

$$P_L = K'\left[P + 1.4 \sum \left(1 - \frac{x}{a}\right) P'\right] \tag{4.185}$$

where $K' = m/d$ for channels

x = distance from concentrated load P' to brace, in.

a = length of bracing interval, in.

m = distance from shear center to midplane of web of channel section, in.

d = depth of channel, in.

W = total uniform load (nominal loads for ASD or factored loads for LRFD) within a distance of $0.5a$ from each side of brace

P' = each individual concentrated load (nominal load for ASD or factored load for LRFD) located farther than $0.3a$ but not farther than a from brace

P = concentrated load (nominal load for ASD or factored load for LRFD) within a distance of $0.3a$ from each side of brace

Example 4.23 Use the ASD method to determine the allowable uniform load and design lateral braces for the channel section used as a simple beam shown in Fig. 4.81. Use A570 Grad 50 steel ($F_y = 50$ ksi).

Solution

1. *Determination of Allowable Uniform Load Based on Section Strength* By using the design procedure illustrated in Example 4.1, the allowable moment based on section strength is

$$M_a = S_e F_y / \Omega_b = (3.123)(50)/1.67$$

$$= 93.50 \text{ in.-kips}$$

For the concentrated load of 2 kips, the moment at point C is

$$M_C = PL(12)/4 = (2)(8)(12)/4 = 48 \text{ in.-kips}$$

The moment permissible for the uniform load is

$$M = M_a - M_C = 93.50 - 48 = 45.50 \text{ in.-kips}$$

$$\frac{wL^2}{8}(12) = 45.50 \text{ in.-kips}$$

$$w = 0.474 \text{ kip/ft, including the weight of the beam}$$

2. *Determination of Allowable Uniform Load Based on Lateral Buckling Strength* Use Art. 4.4.1 or Sec. D3.2.2 of the AISI Specification, and assume that braces are attached to both top and bottom flanges of the channel section at both ends and at intervals not greater than one-quarter of the span length. Using an interval of 24 in., the allowable moment
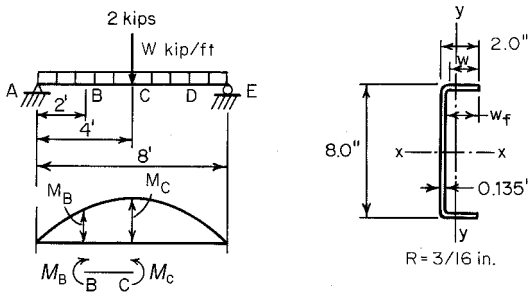
Figure 4.81 Example 4.23.

for portion *BC* (Fig. 4.81) on the basis of lateral buckling strength (Art. 4.2.3.3) can be determined as follows: From Eq. (4.65),

$$F_e = \frac{C_b r_o A}{S_f} \sqrt{\sigma_{ey} \sigma_t}$$

where

$$C_b = \frac{12.5 M_{max}}{2.5 M_{max} + 3M_1 + 4M_2 + 3M_3}$$

in which $M_{max} = 93.50$ in.-kips, maximum moment at point *C*
$M_1 = 69.11$ in.-kips, at ¼ point of unbraced length
$M_2 = 78.66$ in.-kips, at midpoint of unbraced length
$M_3 = 86.79$ in.-kips, at ¾ point of unbraced length

$$C_b = \frac{12.5(93.50)}{2.5(93.50) + 3(69.11) + 4(78.66) + 3(86.79)}$$
$$= 1.15$$

Based on Sec. C3.1.2.1 of the AISI Specification,

$$r_o = \sqrt{r_x^2 + r_y^2 + x_0^2} = 3.09 \text{ in.}$$

Using the full cross-sectional area,

$$A = 1.554 \text{ in.}^2$$

From Eq. (4.68),

$$\sigma_{ey} = \frac{\pi^2 E}{(K_y L_y / r_y)^2} = \frac{\pi^2 (29,500)}{(1 \times 2 \times 12/0.559)^2} = 158.0 \text{ ksi}$$

From Eq. (4.69),

$$\sigma_t = \frac{1}{A r_o^2} \left[GJ + \frac{\pi^2 E C_w}{(K_t L_t)^2} \right]$$

$$= \frac{1}{(1.554)(3.09)^2} \left[(11,300)(0.00944) + \frac{\pi^2 (29,500)(5.56)}{(1 \times 2 \times 12)^2} \right]$$

$$= 196.60 \text{ ksi}$$

In the above equation, the values of *J* and C_w are computed from the Design Manual or from Appendix B. Therefore, the elastic critical lateral–torsional buckling stress is

$$F_e = \frac{(1.15)(3.09)(1.554)}{3.269} \sqrt{(158.0)(196.60)} = 297.72 \text{ ksi}$$

For the yield point of steel $F_y = 50$ ksi,

$$0.56 \, F_y = 28.00 \text{ ksi}$$

$$2.78 F_y = 139.00 \text{ ksi}$$

Since $F_e > 2.78 \, F_y$, according to Eq. (4.64a), the critical buckling stress is

$$F_e = F_y = 50 \text{ ksi}$$

Based on Eq. (4.63), the nominal moment for lateral–torsional buckling is

$$M_n = S_c F_c = (3.123)(50) = 156.15 \text{ in.-kips}$$

The allowable moment for lateral–torsional buckling is

$$M_a = M_n / \Omega_b = 156.15 / 1.67 = 93.50 \text{ in.-kips}$$

Because the allowable moment for lateral–torsional buckling is the same as that allowed for section strength, therefore, the allowable uniform load is

$$w = 0.474 \text{ kip/ft including the weight of the beam.}$$

3. *Design of Braces*   Based on Eqs. (4.184) and (4.185), the braces used at midspan should be designed to resist the following force P_{L1}:

$$P_{L1} = 1.5 K' W + K' \left[P + 1.4 \sum \left(1 - \frac{x}{a} \right) P' \right]$$

where $K' = \dfrac{m}{d} = \dfrac{0.544}{8.0} = 0.068$

$\quad\quad d = 8.0$ in.

$\quad\quad m = \dfrac{w_f^2}{2w_f + d/3} = \dfrac{(1.865)^2}{2(1.865) + 8/3} = 0.544$ in.

$\quad\quad W = 2(0.474) = 0.948$ kips

$\quad\quad P = 2$ kips

$\quad\quad P' = 0$

$$P_{L1} = 1.5(0.068)(0.948) + 0.068(2) = 0.232 \text{ kips}$$

The braces used at $\frac{1}{4}$ points (points B and D) should be designed to resist the following force P_{L2}:

$$P_{L2} = 1.5K'W = 1.5(0.068)(0.948)$$

$$= 0.097 \text{ kips}$$

4.4.1.2 Top Flange Connected to Sheathing

Article 4.4.1.1 deals only with single-channel beams when neither flange is connected to deck or sheathing material. For C-sections designed according to section strength (Art. 4.2.2) and having deck or sheathing fastened directly to the top flanges in such a manner shown to effectively inhibit relative movement between the deck or sheathing and the purlin flange, provisions should be made according to Sec. D3.2.1 of the AISI Specification to restrain the flanges so that the maximum top flange lateral displacements with respect to the purlin reaction points do not exceed the span length divided by 360. Section D3.2.1(a) of the Supplement to the 1996 edition of the AISI Specification states that for roof systems using C-sections for purlins with all compression flanges facing in the same direction, a system possessing a restraint force, P_L, in addition to resisting other loading, shall be provided as follows:

$$P_L = (0.05\alpha \cos\theta - \sin\theta)W$$

where W = total vertical load (nominal load for ASD, factored load for LRFD) supported by all purlin lines being restrained. When more than one brace is used at a purlin line, the restraint force P_L shall be divided equally between all braces.

α = +1 for purlin facing upward direction, and
  = −1 for purlin facing downslope direction.
θ = angle between the vertical and the plane of the web of the C-section, degrees.

The above equation was added in the Supplement in 1999 for calculating the anchorage forces for C-sections.[1.333] A positive value for the force, P_L, means that restraint is required to prevent movement of the purlin flange in the upward roof slope direction, and a negative value means that restraint is required to prevent movement of purlin flange in the downward slope direction. If the top flanges of the adjacent lines of purlins face in opposite directions, a restraint system shall be provided to resist the down-slope component of the total gravity load.

Anchored braces may be connected to only one line of purlins in each purlin bay of each roof slope if provision is made to transmit forces from other purlin lines through roof deck and its fastening system. Anchored braces

shall be as close as possible to the flange which is connected to the deck or sheathing. Anchored braces shall be provided for each purlin bay.

For other bracing arrangements, the AISI Specification requires that special tests be performed to ensure that the type and/or spacing of braces selected are such that the tested strength of the purlin assembly is equal to or greater than its nominal flexural strength.

4.4.2   Z-Beams

4.4.2.1   Neither Flange Connected to Sheathing   For Z-beams, when a load is applied in the plane of the web, the section does not tend to rotate in the same manner as channels because the shear center coincides with its centroid. However, in view of the fact that in Z-sections the principal axes are oblique, even though such a section is loaded vertically, it will deflect vertically and horizontally. If the section deflects in the horizontal direction, the applied load will also move with the beam and is no longer in the same plane with the reactions at both ends. As a result, the section also twists in addition to vertical and horizontal deflections. The additional stress caused by the twist reduces the load-carrying capacity of the member.

The investigation carried out by Zetlin and Winter to study the bracing requirement for Z-beams consisted of testing 19 beams of three different shapes.[4.109] An approximate method of analysis indicated that the braced Z-beams can be analyzed in the same way as braced channels, except that the fictitious horizontal load P_L applied at the point of each actual vertical load should be determined by $P_L = P(I_{xy}/I_x) = PK'$.

For this reason, the AISI Specification specifies the same bracing requirements for channels and Z-sections with the exception that the term K' should be determined by I_{xy}/I_x.

For simplification of design, the vertical and horizontal deflections and the corresponding stresses can be determined by the summations of the values computed for the actual and fictitious loads by using the following modified moments of inertia (I_{mx} and I_{my}):[4.109]

$$I_{mx} = \frac{I_x I_y - I_{xy}^2}{I_y} \tag{4.186}$$

$$I_{my} = \frac{I_x I_y - I_{xy}^2}{I_x} \tag{4.187}$$

4.4.2.2   Top Flange Connected to Sheathing   When Z-sections are used in roof and wall construction to support the attached deck or sheathing directly, use the same design approach as discussed in Art. 4.4.1.2 for channels except that the following AISI requirements should be satisfied.

For roof systems having 4 to 20 Z-purlin lines with all top flanges facing in the direction of the upward roof slope, and with restraint braces at the purlin supports, midspan or one-third points, each brace shall be designed to resist a force determined as follows (Ref. 1.333):

1. Single-Span System with Restraints at the Supports:

$$P_L = 0.5 \left[\frac{0.220b^{1.50}}{n_p^{0.72}d^{0.90}t^{0.60}} \cos\theta - \sin\theta \right] W \qquad (4.188)$$

2. Single-Span System with Third-Point Restraints:

$$P_L = 0.5 \left[\frac{0.474b^{1.22}}{n_p^{0.57}d^{0.89}t^{0.33}} \cos\theta - \sin\theta \right] W \qquad (4.189)$$

3. Single-Span System with Midspan Restraint:

$$P_L = \left[\frac{0.224b^{1.32}}{n_p^{0.65}d^{0.83}t^{0.50}} \cos\theta - \sin\theta \right] W \qquad (4.190)$$

4. Multiple-Span System with Restraints at the Supports:

$$P_L = C_{tr} \left[\frac{0.053b^{1.88}L^{0.13}}{n_p^{0.95}d^{1.07}t^{0.94}} \cos\theta - \sin\theta \right] W \qquad (4.191)$$

with $C_{tr} = 0.63$ for braces at end supports of multiple-span systems

$C_{tr} = 0.87$ for braces at the first interior supports

$C_{tr} = 0.81$ for all other braces

5. Multiple-Span Systems with Third-Point Restraints:

$$P_L = C_{th} \left[\frac{0.181b^{1.15}L^{0.25}}{n_p^{0.54}d^{1.11}t^{0.29}} \cos\theta - \sin\theta \right] W \qquad (4.192)$$

with $C_{th} = 0.57$ for outer braces in exterior spans
$C_{th} = 0.48$ for all other braces

6. Multiple-Span System with Midspan Restraints:

$$P_L = C_{ms} \left[\frac{0.116b^{1.32}L^{0.18}}{n_p^{0.70}d^{1.00}t^{0.50}} \cos\theta - \sin\theta \right] W \qquad (4.193)$$

with $C_{ms} = 1.05$ for braces in exterior spans
$C_{ms} = 0.90$ for all other braces

where b = flange width, in.

d = depth of section, in.
t = thickness, in.
L = span length, in.
θ = angle between the vertical and the plane of the web of the Z-section, degrees
n_p = number of parallel purlin lines
W = total vertical load supported by the purlin lines between adjacent supports, pounds

The force, P_L, is positive when restraint is required to prevent movement of the purlin flanges in the upward roof slope direction.

For systems having less than four purlin lines, the brace force can be determined by taking 1.1 times the force found from Eqs. (4.188) through (4.193), with $n_p = 4$. For systems having more than 20 purlin lines, the brace force can be determined from Eqs. (4.188) through (4.193), with $n_p = 20$.

Equations (4.188) through (4.193) were derived from a study conducted by Murray and Elhouar in 1985.[4.110] These requirements are included in the AISI Specification since 1986 for the design of Z-purlins and girts. Because the original research was done assuming the roof was flat and the applied loading was parallel to the purlin webs, the "$\cos\theta$" term was added in 1999 to compute the component of the vertical loading parallel to the purlin webs.

4.4.3 I-Beams

For I-beams, braces should be attached to top and bottom flanges at both ends. According to Eqs. (4.63) and (4.64), if F_e is greater than or equal to $2.78F_y$ and $S_c = S_f$, no intermediate braces are required, except that additional braces should be placed at the locations of concentrated loads.

In case the value of F_e is less than $2.78F_y$ but greater than $0.56F_y$, the intervals of braces should not exceed the required unbraced length determined from Eqs. (4.63) and (4.64b). If F_e is less than or equal to $0.56F_y$ the required unbraced length should be determined from Eqs. (4.63) and (4.64c).

The design of braces is not specified in the AISI provisions. However, the bracing members may be designed for a capacity of 2% of the force resisted by the compression portion of the beam. This is a frequently used rule of thumb but is a conservative approach, as proven by a rigorous analysis.

4.4.4 Continuous Lateral Bracing for Beams

When the compression flange of the cold-formed steel beam is closely connected to decking or sheathing material as to effectively restrain lateral deflection of the flange and twisting of the member, previous studies made by Winter[1.157,4.111] indicate that the required resistance to be provided by decking may be approximated as follows:

$$F_{req} = d_i \left(\frac{\beta_{id}}{1 - \beta_{id}/\beta_{act}} \right) \tag{4.194}$$

where F_{req} = required lateral force provided by decking

d_i = initial crookedness

β_{act} = extensional stiffness of decking material, $= AE/L'$, in which A is area of decking, E is modulus of elasticity, and L' is length

β_{id} = spring constant of elastic support computed as follows:

1. When $\beta_{id}L^2 \leq 30P_e$,

$$\beta_{id} = \frac{\pi^2}{L^2} (P_{cr} - P_e) \tag{4.195}$$

2. When $\beta_{ib}L^2 > 30P_e$,

$$\beta_{id} = \frac{\pi^2 P_e}{4L^2} \left(\frac{P_{cr}}{P_e} - 0.6 \right)^2 \tag{4.196}$$

In Eqs. (4.195) and (4.196),

L = length of beam

P_e = Euler critical load, $= \pi^2 EI_{yc}/L^2$

P_{cr} = critical load for compressed half of beam buckling out of its plane as a column

I_{yc} = moment of inertia of compressed portion of beam about its weak axis

During the past three decades, the strength and behavior of diaphragm-braced beams loaded in the plane of the web have been studied by numerous investigators at Cornell University and several other institutions. The published research reports and technical papers provide a better understanding of such a complicated problem.[4.112–4.136] These documents contain valuable background information for developing new design recommendations for channels and Z-sections when one flange is connected to deck or sheathing material.

4.5   TORSIONAL ANALYSIS OF BEAMS

In the design of beams, if the transverse load does not pass through the shear center of the cross section, the beam will be subjected to a combination of plane bending and torsional moment.[2.45,4.140] The types of stress caused by plane bending and torsion are discussed in Appendix B.

4.6   ADDITIONAL INFORMATION ON PURLINS

During the past two decades, the structural strength of cold-formed steel pur-lins has been investigated by a large number of researchers and engineers. For further information on this subject, the reader is referred to Refs. 4.137 through 4.139, 4.141 through 4.155, and 4.187 through 4.191.

5 Compression Members

5.1 GENERAL REMARKS

Similar to the heavy hot-rolled steel sections, thin-walled cold-formed steel compression members can be used to carry a compressive load applied through the centroid of the cross section. The cross section of steel columns can be of any shape that may be composed entirely of stiffened elements (Fig. 5.1*a*), unstiffened elements (Fig. 5.1*b*), or a combination of stiffened and unstiffened elements (Fig. 5.1*c*). Unusual shapes and cylindrical tubular sections are also often found in use.

Cold-formed sections are made of thin material, and in many cases the shear center does not coincide with the centroid of the section. Therefore in the design of such compression members, consideration should be given to the following limit states depending on the configuration of the section, thickness of material, and column length used:

1. Yielding
2. Overall column buckling
   a. Flexural buckling: bending about a principal axis
   b. Torsional buckling: twisting about shear center
   c. Torsional–flexural buckling: bending and twisting simultaneously
3. Local buckling of individual elements

Design provisions for the overall flexural buckling and the effect of local buckling on column strength have long been included in the AISI Specification. The provisions for torsional–flexural buckling were added to the specification in 1968 following a comprehensive investigation carried out by Winter, Chajes, Fang, and Pekoz at Cornell University.[1.161,5.1,5.2]

The current AISI design provision are based on the unified approach developed in 1986 and discussed by Pekoz in Ref. 3.17. This approach consists of the following steps for the design of axially loaded compression members:

1. Calculate the elastic column buckling stress (flexural, torsional, or torsional–flexural) for the full unreduced section.
2. Determine the nominal failure stress (elastic buckling, inelastic buckling, or yielding).
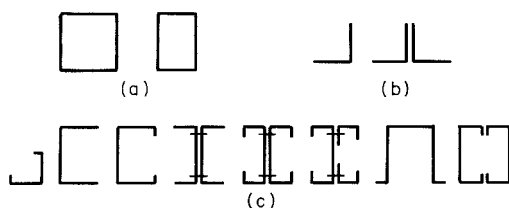
Figure 5.1 Types of compression members, (*a*) Members composed entirely of stiffened elements. (*b*) Members composed entirely of unstiffened elements. (*c*) Members composed of both stiffened and unstiffened elements.

3. Calculate the nominal column load based on the governing failure stress and the effective area.
4. Determine the design column load from the nominal column load using the specified safety factor for ASD or the resistance factor for LRFD.

For column design tables and example problems, reference should be made to Part III of the AISI Design Manual.

The column strengths for different types of failure mode are discussed in subsequent articles. References 5.3 through 5.8 deal with some relatively recent experimental work on columns.

5.2 YIELDING

It is well known that a very short, compact column under axial load may fail by yielding. For this case, the yield load is simply

$$P_y = AF_y \tag{5.1}$$

where A = full cross-sectional area of column
$\quad\ \ F_y$ = yield point of steel

5.3 FLEXURAL COLUMN BUCKLING

5.3.1 Elastic Buckling

A slender axially loaded column may fail by overall flexural buckling if the cross section of the column is a doubly symmetric shape (I-section), closed shape (square or rectangular tube), cylindrical shape, or point-symmetric shape (Z-shape or cruciform). For singly symmetric shapes, flexural buckling is one of the possible failure modes as discussed in Art. 5.4.2. If a column

has a cross section other than the above discussed shapes but is connected to other parts of the structure such as wall sheating material, the member can also fail by flexural buckling. For other possible buckling modes, see Art. 5.4.

The elastic critical buckling load for a long column can be determined by the Euler formula:

$$P_e = \frac{\pi^2 EI}{(KL)^2} \tag{5.2}$$

where P_e = Euler buckling load
  E = modulus of elasticity
  I = moment of inertia
  L = column length
  K = effective length factor

Substituting $I = Ar^2$ in Eq. (5.2), the following Euler stress for elastic column buckling can be obtained:

$$\sigma_e = \frac{\pi^2 E}{(KL/r)^2} \tag{5.3}$$

where KL/r is the effective slenderness ratio and r is the least radius of gyration.

Equation (5.3) is graphically shown as curve A in Fig. 5.2, which is applicable to the ideal columns made of sharp-yielding type steel having stress–strain characteristics as shown in Fig. 2.1a without consideration of residual stress or effects of cold working. In view of the fact that many steel sheets and strips used in cold-formed structural members are of the gradual-yielding
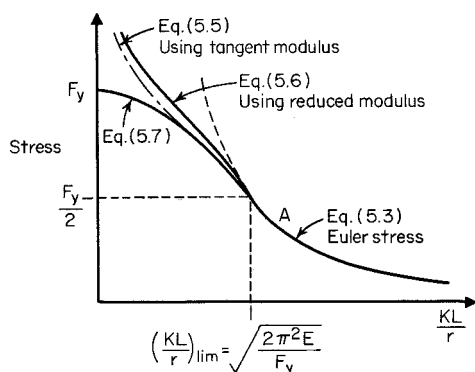
Figure 5.2   Flexural columns buckling stress.

type as shown in Fig. 2.1*b* and the cold-forming process tends to lower the proportional limit as discussed in Art. 2.7, Eq. (5.3) would not be suitable for columns made of gradual-yielding steel having small and moderate slenderness ratios. This is because when the stress is above the proportional limit, the column will buckle in the inelastic range.

5.3.2   Inelastic Buckling

For the analysis of flexural column buckling in the inelastic range, two concepts have been used in the past. They are the tangent modulus method and the reduced modulus method.[2.45,3.3]

The tangent modulus method was proposed by Engesser in 1889. Based on this method, the tangent modulus load is

$$P_{\mathrm{T}} = \frac{\pi^2 E_t I}{(KL)^2} \tag{5.4}$$

and the critical buckling stress is

$$\sigma_{\mathrm{T}} = \frac{\pi^2 E_t}{(KL/r)^2} \tag{5.5}$$

where E_t is the tangent modulus.

In 1895 Jasinky pointed out that the tangent modulus concept did not include the effect of elastic unloading. Engesser then corrected his theory and developed the reduced modulus or double modulus concept, in which

$$P_{\mathrm{r}} = \frac{\pi^2 E_r I}{(KL)^2} \qquad \text{or} \qquad \sigma_{\mathrm{R}} = \frac{\pi^2 E_r}{(KL/r)^2} \tag{5.6}$$

where E_r = reduced modulus, $E(I_1/I) + E_t(I_2/I)$
I_1 = moment of inertia about neutral axis of the area on unloading side after buckling
I_2 = moment of inertia about neutral axis of the area on loading side after buckling

Engineers were puzzled for about 50 years regarding these two concepts for the determination of column strength. After his careful experimental and analytical investigation, Shanley[5.9] concluded that

1. The tangent modulus concept gives the maximum load up to which an initially straight column remains straight.
2. The actual maximum load exceeds the tangent modulus load, but it cannot reach the reduced modulus load.

Many other investigators have proved Shanley's findings and have indicated that for the case studied, the maximum load is usually higher than the tangent modulus load by 5% or less.[2.45]

In view of the fact that the tangent modulus strength provides an excellent prediction of the actual column strength, the Column Research Council* has suggested that design formulas for steel columns should be on the basis of the tangent modulus concept.[3.84] For this reason, whenever the computed Euler stress is above the proportional limit, the tangent modulus should be used to compute the buckling stress.

The tangent modulus can be determined by the techniques described in Technical Memorandum 2 of the Structural Stability Research Council, "Notes on the Compression Testing of Metals,"[3.84,1.158] However, it is impossible to provide stress–strain curves and values of tangent moduli for all types of sheets and strip, in particular when the cold work of forming is utilized. In the design of hot-rolled shapes, the Structural Stability Research Council has indicated that Eq. (5.5) can be conservatively approximated by the following formula if the effect of residual stress is considered and the effective proportional limit is assumed to be equal to one-half the yield point.[1.161,3.84]

$$\sigma_{\mathrm{T}} = F_{\mathrm{y}} \left(1 - \frac{F_{\mathrm{y}}}{4\sigma_{\mathrm{e}}} \right)$$

$$= F_{\mathrm{y}} - \left(\frac{F_{\mathrm{y}}^2}{4\pi^2 E} \right) \left(\frac{KL}{r} \right)^2 \tag{5.7}$$

in which F_{y} is the minimum yield point. The above formula can also be used for cold-formed sections if the residual stress induced by cold forming of the section and the stress–strain characteristics of the gradual-yielding steel sheets and strip are considered.

As shown in Fig. 5.2, the value of $\sqrt{2\pi^2 E/F_{\mathrm{y}}}$ is the limiting KL/r ratio corresponding to a stress equal to $F_{\mathrm{y}}/2$. When the KL/r ratio is greater than this limiting ratio, the column is assumed to be governed by elastic buckling, and when the KL/r ratio is smaller than this limiting ratio, the column is to be governed by inelastic buckling. Equation (5.7) has been used for the design of cold-formed steel columns up to 1996.

In the 1996 edition of the AISI Specification, the design equations for calculating the nominal inelastic and elastic flexural buckling stresses were changed to those used in the AISC LRFD Specification as follows:[3.150]

$$(F_{\mathrm{n}})_{\mathrm{I}} = \left(0.658^{\lambda_{\mathrm{c}}^2} \right) F_{\mathrm{y}}, \qquad \text{when} \quad \lambda_{\mathrm{c}} \leq 1.5 \tag{5.7a}$$

$$(F_{\mathrm{n}})_{\mathrm{e}} = \left[\frac{0.877}{\lambda_{\mathrm{c}}^2} \right] F_{\mathrm{y}}, \qquad \text{when} \quad \lambda_{\mathrm{c}} > 1.5 \tag{5.3a}$$

---

*The Column Research Council has been renamed Structural Stability Research Council.

where $(F_n)_I$ is the nominal inelastic buckling stress, $(F_n)_e$ is the nominal elastic buckling stress, λ_c is the column slenderness parameter $= \sqrt{F_y/\sigma_e}$, in which σ_e is the theoretical elastic flexural buckling stress of the column determined by Eq. (5.3).

The reasons for changing the design equations from Eq. (5.7) to Eq. (5.7a) for the nominal inelastic buckling stress and from Eq. (5.3) to Eq. (5.3a) for the nominal elastic buckling stress are:[1.159]

1. The revised column design equations (Eqs. 5.7a and 5.3a) are based on a different basic strength model and were shown to be more accurate by Pekoz and Sumer.[5.103] In this study, 299 test results on columns and beam-columns were evaluated. The test specimens included members with component elements in the post-local buckling range as well as those that were locally stable. The test specimens included members subjected to flexural buckling as well as torsional–flexural buckling, to be discussed in Art. 5.4.

2. Because the revised column design equations represent the maximum strength with due consideration given to initial crookedness and can provide the better fit to test results, the required factor of safety for the ASD method can be reduced. In addition, the revised equations enable the use of a single factor of safety for all λ_c values even though the nominal axial strength of columns decreases as the slenderness increases due to initial out-of-straightness. With the use of the selected factor of safety and resistance factor given in the Specification (Art. 5.7), the results obtained from the ASD and LRFD approaches would be approximately the same for a live-to-dead load ratio of 5.0.

Figure 5.3 shows a comparison of the nominal critical flexural buckling stresses used in the 1986 edition of the ASD Specification, the 1991 edition of the LRFD Specification, and the 1996 edition of the combined ASD/LRFD Specification.

5.4 TORSIONAL BUCKLING AND TORSIONAL–FLEXURAL BUCKLING

Usually, closed sections will not buckle torsionally because of their large torsional rigidity. For open thin-walled sections, however, three modes of failure are considered in the analysis of overall instability (flexural buckling, torsional buckling, and torsional–flexural buckling) as previously mentioned. Distortional buckling has been considered in some design standards but not in the 1996 edition of the AISI Specification.

When an open section column buckles in the torsional–flexural mode, bending and twisting of the section occur simultaneously. As shown in Fig. 5.4, the section translates u and v in the x and y directions and rotates an
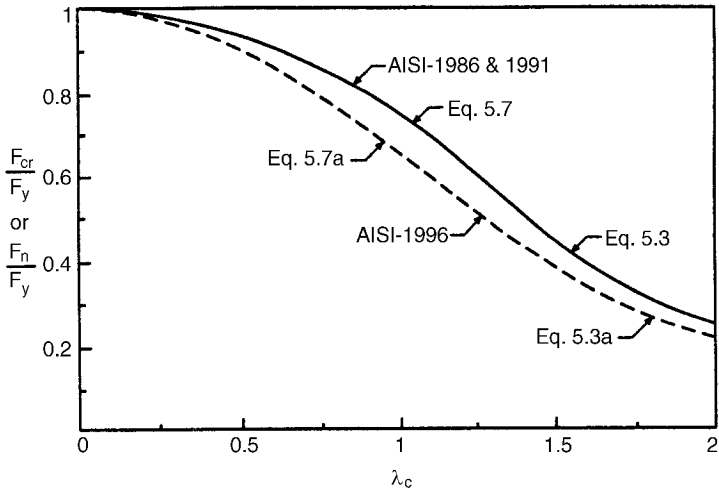
Figure 5.3   Comparison between the critical buckling stress equations.

angle ϕ about the shear center. This problem was previously investigated by Goodier, Timoshenko, and others.[5.10,5.11,3.3] It has been further studied by Winter, Chajes, and Fang for development of the AISI design criteria.[5.1,5.2]

The equilibrium of a column subjected to an axial load P leads to the following differential equations.[5.2,5.11]

$$EI_x v^{iv} + Pv'' - Px_0\phi'' = 0 \tag{5.8}$$

$$EI_y u^{iv} + Pu'' + Py_0\phi'' = 0 \tag{5.9}$$

$$EC_w \phi^{iv} - (GJ - Pr_0^2)\phi'' + Py_0 u'' - Px_0 v^+ = 0 \tag{5.10}$$
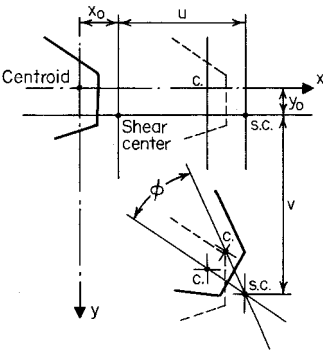
Figure 5.4   Displacement of a nonysmmetric section during torsional–flexural buckling.[5.2]

where I_x = moment of inertia about x-axis, in.[4]

$\quad\quad I_y$ = moment of inertia about y-axis, in.[4]

$\quad\quad u$ = lateral displacement in x direction, in.

$\quad\quad v$ = lateral displacement in y direction, in.

$\quad\quad \phi$ = angle of rotation, rad

$\quad\quad x_0$ = x-coordinate of shear center, in.

$\quad\quad y_0$ = y-coordinate of shear center, in.

$\quad\quad E$ = modulus of elasticity, = 29.5×10^3 ksi (203 GPa)

$\quad\quad G$ = shear modulus, = 11.3×10^3 ksi (78 GPa)

$\quad\quad J$ = St. Venant torsion constant of cross section, in.[4], = $\frac{1}{3} \Sigma\, l_i t_i^3$

$\quad\quad C_w$ = warping constant of torsion of cross section, in.[6] (Appendix B)

$\quad EC_w$ = warping rigidity

$\quad\quad GJ$ = torsional rigidity

$\quad\quad r_0$ = polar radius of gyration of cross section about shear center,
$\quad\quad\quad$ = $\sqrt{r_x^2 + r_y^2 + x_0^2 + y_0^2}$

$r_y,\, r_y$ = radius of gyration of cross section about x- and y-axis, in.

All derivatives are with respect to z, the direction along the axis of the member.

Considering the boundary conditions for a member with completely fixed ends, that is, at $z = 0, L$,

$$u = v = \phi = 0$$
$$u' = v' = \phi' = 0 \tag{5.11}$$

and for a member with hinged ends, that is, at $z = 0, L$,

$$u = v = \phi = 0$$
$$u'' = v'' = \phi'' = 0 \tag{5.12}$$

Equations (5.8) to (5.10) result in the following characteristic equation:

$$r_0^2(P_{cr} - P_y)(P_{cr} - P_y)(P_{cr} - P_z) - (P_{cr})^2(y_0)^2(P_{cr} - P_x)$$
$$- (P_{cr})^2(x_0)^2(P_{cr} - P_y) = 0 \tag{5.13}$$

where P_x = Euler flexural buckling load about x-axis,

$$= \frac{\pi^2 E I_x}{(K_x L_x)^2} \tag{5.14}$$

$\quad P_y$ = Euler flexural buckling load about y-axis,

$$= \frac{\pi^2 E I_y}{(K_y L_y)^2} \tag{5.15}$$

P_z = torsional buckling load about z-axis,

$$= \left[\frac{\pi^2 E C_w}{(K_t L_t)^2} + GJ\right]\left(\frac{1}{r_0^2}\right) \tag{5.16}$$

KL = effective length of column; theoretically, for hinged ends, $K = 1$ and for fixed ends, $K = 0.5$.

The buckling mode of the column can be determined by Eq. (5.13). The critical buckling load is the smallest value of the three roots of P_{cr}. The following discussion is intended to indicate the possible buckling mode for various types of cross section.

5.4.1 Doubly Symmetric Shapes

For a doubly symmetric shape, such as an I-section or a cruciform, the shear center coincides with the centroid of the section (Fig. 5.5), that is,

$$x_0 = y_0 = 0 \tag{5.17}$$

For this case, the characteristic equation, Eq. (5.13), becomes

$$(P_{cr} - P_x)(P_{cr} - P_y)(P_{cr} - P_z) = 0 \tag{5.18}$$

The critical buckling load is the lowest value of the following three solutions:

$$(P_{cr})_1 = P_x \tag{5.19}$$

$$(P_{cr})_2 = P_y \tag{5.20}$$

$$(P_{cr})_3 = P_z \tag{5.21}$$

An inspection of the above possible buckling loads indicates that for dou-
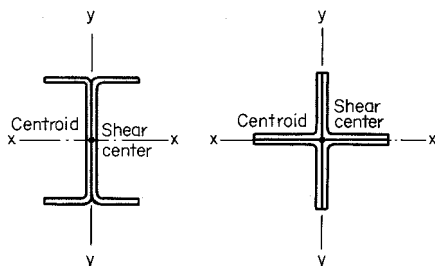
Figure 5.5 Doubly symmetric shapes.

bly symmetric sections, the column fails either in pure bending or in pure torsion, depending on the column length and the shape of the section. Usually compression members are so proportioned that they are not subject to torsional buckling. However, if the designer wishes to evaluate the torsional buckling stress σ_t, the following formula based on Eq. (5.16) can be used:

$$\sigma_t = \frac{1}{A r_0^2} \left[GJ + \frac{\pi^2 E C_w}{(K_t L_t)^2} \right] \tag{5.22}$$

The critical stress for flexural buckling was discussed in Art. 5.3.

5.4.2   Singly Symmetric Shapes

Angles, channels, hat sections, T-sections, and I-sections with unequal flanges (Fig. 5.6) are singly symmetric shapes. If the x axis is the axis of symmetry, the distance y_0 between the shear center and the centroid in the direction of the y axis is equal to zero. Equation (5.13) then reduces to

$$(P_{cr} - P_y)[r_0^2(P_{cr} - P_x)(P_{cr} - P_z) - (P_{cr}x_0)^2] = 0 \tag{5.23}$$

For this case, one of the solutions is

$$(P_{cr})_1 = P_y = \frac{\pi^2 E I_y}{(K_y L_y)^2} \tag{5.24}$$

which is the critical flexural buckling load about the y axis. The other two solutions for the torsional–flexural buckling load can be obtained by solving the following quadratic equation:

$$r_0^2(P_{cr} - P_x)(P_{cr} - P_z) - (P_{cr}x_0)^2 = 0 \tag{5.25}$$

Let $\beta = 1 - (x_0/r_0)^2$,
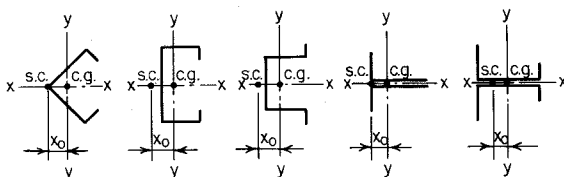
Figure 5.6   Singly symmetric shapes.

$$(P_{cr})_2 = \frac{1}{2\beta} [(P_x + P_z) + \sqrt{(P_x + P_z)^2 - 4\beta P_x P_z}] \qquad (5.26)$$

$$(P_{cr})_3 = \frac{1}{2\beta} [(P_x + P_z) - \sqrt{(P_x + P_z)^2 - 4\beta P_x P_z}] \qquad (5.27)$$

Because $(P_{cr})_3$ is smaller than $(P_{cr})_2$, Eq. (5.27) can be used as the critical torsional–flexural buckling load, which is always smaller than P_x and P_z, but it may be either smaller or larger than P_y [Eq. (5.24)] (Fig. 5.7).

Dividing Eq. (5.27) by the total cross-sectional area A, the following equation can be obtained for the elastic torsional–flexural buckling stress:

$$\sigma_{TFO} = \frac{1}{2\beta} [(\sigma_{ex} + \sigma_t) - \sqrt{(\sigma_{ex} + \sigma_t)^2 - 4\beta \sigma_{ex} \sigma_t}] \qquad (5.28)$$

where σ_{TFO} is the elastic torsional–flexural buckling stress in ksi and

$$\sigma_{ex} = \frac{P_x}{A} \qquad (5.29)$$

$$\sigma_t = \frac{P_z}{A} \qquad (5.30)$$

In summary, it can be seen that a singly symmetric section may buckle
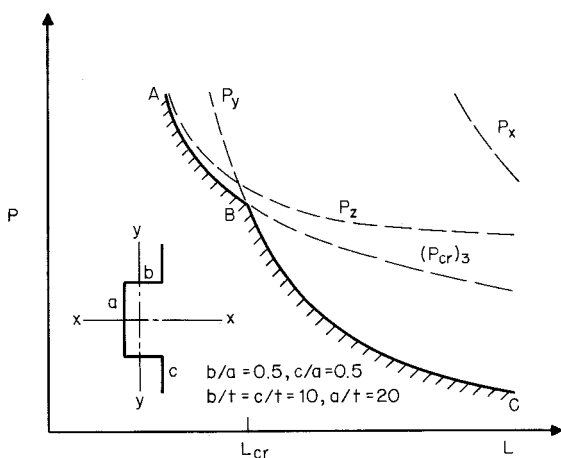
Figure 5.7 Comparison of P_{cr} with P_x, P_y, and P_z for hat section ($K_x L_x = K_y L_y = K_t L_t = L$).

either in bending about the y-axis* or in torsional–flexural buckling (i.e., bending about the x axis and twisting about the shear center), depending on the dimensions of the section and the effective column length. For the selected hat section used in Fig. 5.7, the critical length L_{cr}, which divides the flexural buckling mode and the torsional–flexural buckling mode, can be determined by solving $P_y = (P_{cr})_3$. This means that if the effective length is shorter than its critical length, the torsional–flexural buckling load $(P_{cr})_3$, represented by curve AB, will govern the design. Otherwise if the effective length is longer than the critical length, the load-carrying capacity of the given member is limited by the flexural buckling load P_y, represented by curve BC. The same is true for other types of singly symmetric shapes, such as angles, channels, T-sections, and I-sections having unequal flanges.

In view of the fact that the evaluation of the critical torsional–flexural buckling load is more complex as compared with the calculation of the Euler load, design charts, based on analytical and experimental investigations, have been developed for several commonly used sections,[5.1,1.159] from which we can determine whether a given section will buckle in the torsional–flexural mode. Such a typical curve is shown in Fig. 5.8 for a channel section. If a column section is so proportioned that torsional–flexural buckling will not occur for the given length, the design of such a compression member can then be limited to considering only flexural and local buckling. Otherwise, torsional–flexural buckling must also be considered.

As indicated in Fig. 5.8, the possibility of overall column buckling of a singly symmetric section about the x-axis may be considered for three different cases. Case 1 is for torsional–flexural buckling only. This particular case is characterized by sections for which $I_y > I_x$. When $I_y < I_x$, the section will fail either in case 2 or in case 3. In case 2, the channel will buckle in either the flexural or the torsional–flexural mode, depending on the specific

1 Torsional–flexural buckling only
2 Buckling mode depends on value of tL/a^2
3 Flexural buckling only
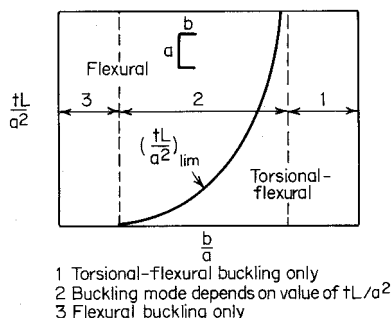
Figure 5.8   Buckling mode for channel section.[5.2]

*It is assumed that the section is symmetrical about the x-asix.

ratio of b/a and the parameter tL/a^2, where b is the flange width, a is the depth of the web element, t is the thickness, and L is the effective length. For a given channel section and column length if the value of tL/a^2 is above the $(tL/a^2)_{\lim}$ curve, the section will fail in the flexural buckling mode. Otherwise it will fail in the torsional–flexural buckling mode. In case 3, the section will always fail in the flexural mode, regardless of the value of tL/a^2. The buckling mode curves for angles, channels, and hat sections are shown in Figs. 5.9 to 5.11. These curves apply only to compatible end conditions, that is,

$$K_x L_x = K_y L_y = K_t L_t = L$$

In Part VII of the AISI design manual,[1.159] a set of design charts such as Fig. 5.12 are provided for determining the critical length for angles, channels, and hat sections. From this type of graphic design aid, the critical length can be obtained directly according to the dimensions and shapes of the member.

The preceding discussion deals with torsional–flexural buckling in the elastic range for which the compression stress is less than the proportional limit. Members of small or moderate slenderness will buckle at a stress lower than the value given by the elastic theory if the computed critical buckling stress exceeds the proportional limit.

Similar to the case of flexural buckling, the inelastic torsional–flexural buckling load may be obtained from the elastic equations by replacing E with E_t, and G with $G(E_t/E)$, where E_t is the tangent modulus, which depends on the effective stress–strain relationship of the entire cross section, that is, for inelastic torsional–flexural buckling,

$$(P_x)_T = \left(\frac{E_t}{E}\right) P_x \tag{5.31}$$

$$(P_z)_T = \left(\frac{E_t}{E}\right) P_z \tag{5.32}$$

$$(P_{cr})_T = \left(\frac{E_t}{E}\right) P_{cr} \tag{5.33}$$

With regard to the determination of E_t, Bleich[3.3] indicates that

$$E_t = CE \left[\frac{\sigma}{F_y}\left(1 - \frac{\sigma}{F_y}\right)\right] \tag{5.34}$$

where
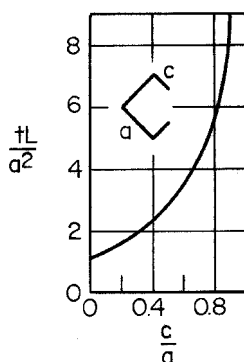
Figure 5.9   Buckling mode curve for angles.[5.2]

$$C = \frac{1}{(\sigma_{pr}/F_y)(1 - \sigma_{pr}/F_y)} \tag{5.35}$$

F_y and σ_{pr} are the yield point and the proportional limit of the steel, respectively. The values of C obtained from an experimental study[5.2] ranged from 3.7 to 5.1. Based on Eq. (5.35) and using $C = 4$ (assuming $\sigma_{pr} = \frac{1}{2}F_y$), the tangent modulus E_t for the inelastic buckling stress is given by

$$E_t = 4E \frac{\sigma_{TFT}}{F_y}\left(1 - \frac{\sigma_{TFT}}{F_y}\right) \tag{5.36}$$

where σ_{TFT} is the inelastic torsional–flexural buckling stress. Substituting the above relationship into Eq. (5.33), the following equation for inelastic torsional–flexural buckling stress can be obtained:
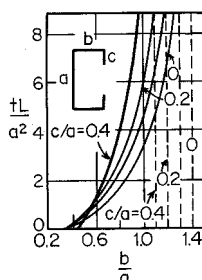
Figure 5.10   Buckling mode curves for channels.[5.2]
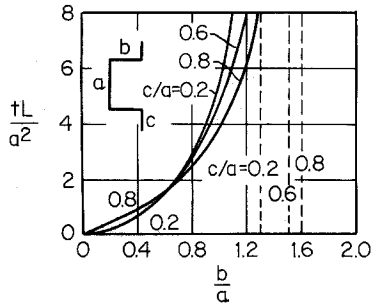
Figure 5.11   Buckling mode curves for hat sections.[5.2]

$$\sigma_{\text{TFT}} = F_y \left(1 - \frac{F_y}{4\sigma_{\text{TFO}}} \right) \tag{5.37}$$

in which σ_{TFO} is the elastic torsional–flexural buckling stress determined by Eq. (5.28). Equation (5.37) is shown graphically in Fig. 5.13.
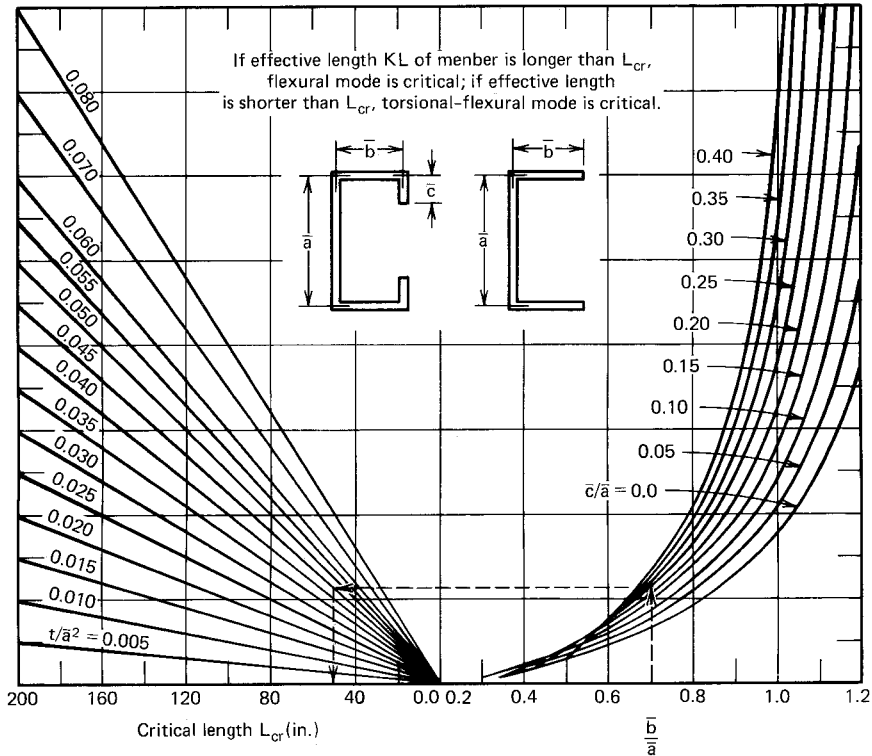
Figure 5.12   AISI chart for determining critical length of channels. [1.159]
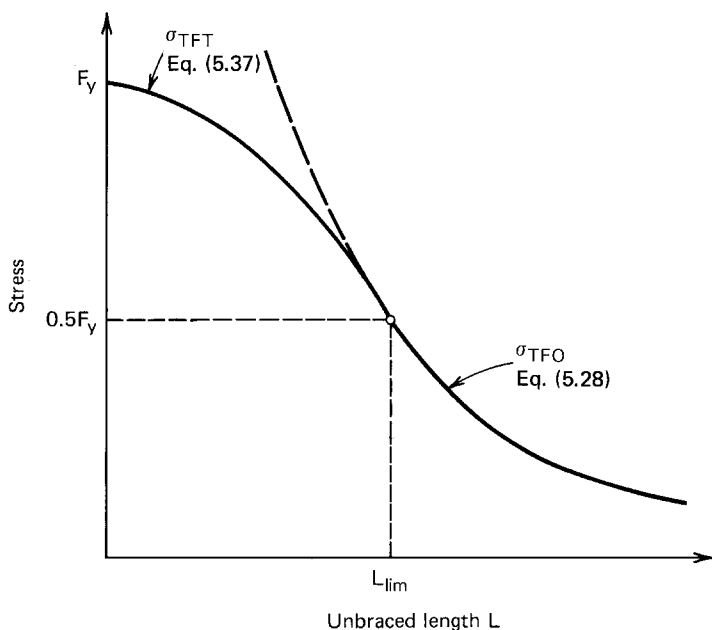
Figure 5.13   Maximum stress for torsional–flexural buckling.

To verify the design procedure described above, a total of eight columns were tested for elastic torsional–flexural buckling and 30 columns were tested for inelastic torsional–flexural buckling at Cornell University.[5.2] The results of the inelastic column tests are compared with Eq. (5.37) in Fig. 5.14.

Similar to the case for flexural column buckling, Eq. (5.37) was used in the AISI Specification up to 1996. In the 1996 edition of the Specification, the nominal inelastic torsional–flexural buckling stress is computed by Eq. (5.7a), in which $\lambda_c = \sqrt{F_y/\sigma_{\mathrm{TFO}}}$.
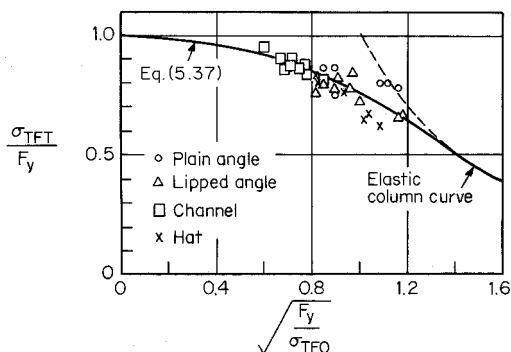
Figure 5.14   Correleation of analytical and experimental investigations.[5.2]

Following an evaluation of the test results of angles reported by Madugula, Prabhu, Temple, Wilhoit, Zandonini, and Zavellani,[5.12–5.14] Pekoz indicated in Ref. 3.17 that angle sections are more sensitive to initial sweep than lipped channels. It was also found that the magnitude of the initial sweep equal to $L/1000$ would give reasonable results for the specimens considered in his study. On the basis of the findings summarized in Ref. 3.17, an out-of-straightness of $L/1000$ is used in Sec.C5.2 of the 1996 edition of the AISI Specification for computing additional bending moments M_x, M_y (for ASD) or M_{ux}, M_{uy} (for LRFD). For the design of angles, additional information can be found in Refs. 5.15 through 5.19 and Ref. 5.100.

5.4.3 Point-Symmetric Sections

A point-symmetric section is defined as a section symmetrical about a point (centroid), such as a Z-section having equal flanges or a cruciform section.[5.17] For this case the shear center coincides with the centroid and $x_0 = y_0 = 0$.

Similar to doubly symmetric sections, Eq. (5.13) leads to

$$(P_{cr} - P_x)(P_{cr} - P_y)(P_{cr} - P_z) = 0 \tag{5.38}$$

Therefore the section may fail either in bending (P_x or P_y) or twisting (P_z), depending on the shape of the section and the column length. It should be noted that the x- and y-axes are principal axes.

Although the curve for determining the buckling mode is not available for Z-sections, a limited investigation has been carried out at Cornell.[5.2] It was found that plain and lipped Z-sections will always fail as simple Euler columns regardless of their size and shape, provided that the effective length for bending about the minor principal axis is equal to or greater than the effective length for twisting.

5.4.4 Nonsymmetric Sections

If the open section has no symmetry either about an axis or about a point, all three possible buckling loads P_{cr} are of the torsional–flexural type. The lowest value of P_{cr} is always less than the lowest of the three values P_x, P_y, and P_z.

In the design of compact nonsymmetric sections, the elastic torsional–flexural buckling stress σ_{TFO} may be computed from the following equation by trial and error:[1.159]

$$\left(\frac{\sigma^3_{TFO}}{\sigma_{ex}\sigma_{ey}\sigma_t}\right)\alpha - \left(\frac{\sigma^2_{TFO}}{\sigma_{ey}\sigma_t}\right)\gamma - \left(\frac{\sigma^2_{TFO}}{\sigma_{ex}\sigma_t}\right)\beta - \left(\frac{\sigma^2_{TFO}}{\sigma_{ex}\sigma_{ey}}\right)$$

$$+ \frac{\sigma_{TFO}}{\sigma_{ex}} + \frac{\sigma_{TFO}}{\sigma_{ey}} + \frac{\sigma_{TFO}}{\sigma_t} = 1 \tag{5.39}$$

In the calculation, the following equation may be used for the first approximation:

$$\sigma_{\text{TFO}} = [(\sigma_{\text{ex}}\sigma_{\text{ey}} + \sigma_{\text{ex}}\sigma_{\text{t}} + \sigma_{\text{ey}}\sigma_{\text{t}})$$
$$-\sqrt{(\sigma_{\text{ex}}\sigma_{\text{ey}} + \sigma_{\text{ex}}\sigma_{\text{t}} + \sigma_{\text{ey}}\sigma_{\text{t}})^2 - 4(\sigma_{\text{ex}}\sigma_{\text{ey}}\sigma_{\text{t}})(\gamma\sigma_{\text{ex}} + \beta\sigma_{\text{ey}} + \sigma_{\text{t}})]}$$
$$\times \left[\frac{1}{2(\gamma\sigma_{\text{ex}} + \beta\sigma_{\text{ey}} + \sigma_{\text{t}})} \right] \tag{5.40}$$

where

$$\sigma_{\text{ex}} = \frac{\pi^2 E}{(K_x L_x / r_x)^2} \qquad \text{ksi} \tag{5.41}$$

$$\sigma_{\text{ey}} = \frac{\pi^2 E}{(K_y L_y / r_y)^2} \qquad \text{ksi} \tag{5.42}$$

$$\sigma_{\text{t}} = \frac{1}{Ar_0^2}\left[GJ + \frac{\pi^2 E C_{\text{w}}}{(K_t L_t)^2} \right] \qquad \text{ksi} \tag{5.43}$$

and

E = modulus of elasticity, = 29.5×10^3 ksi (203 GPa)
KL = effective length of compression member, in.
r_x = radius of gyration of cross section about x-asix, in.
r_y = radius of gyration of cross section about y-axis, in.
A = cross-sectional area, in.^{2}
$r_0 = \sqrt{r_x^2 + r_y^2 + x_0^2 + y_0^2}$.
G = shear modulus, = 11.3×10^3 ksi (78 GPa)
J = St. Venant torsion constant of cross section, in^4
$\alpha = 1 - (x_0/r_0)^2 - (y_0/r_0)^2$
$\beta = 1 - (x_0/r_0)^2$
$\gamma = 1 - (y_0/r_0)^2$
x_0 = distance from shear center to centroid along principal x-axis, in.
y_0 = distance from shear center to centroid along principal y-axis, in.
C_{w} = warping constant of torsion of cross section, in.[6] (Appendix B)

5.5   EFFECT OF LOCAL BUCKLING ON COLUMN STRENGTH

Cold-formed steel compression members may be so proportioned that local buckling of individual component plates occurs before the applied load reaches the overall collapse load of the column. The interaction effect of the local and overall column buckling may result in a reduction of the overall column strength.

In general, the influence of local buckling on column strength depends on the following factors:

1. The shape of the cross section
2. The slenderness ratio of the column
3. The type of governing overall column buckling (flexural buckling, torsional buckling, or torsional–flexural buckling)
4. The type of steel used and its mechanical properties
5. Influence of cold work
6. Effect of imperfection
7. Effect of welding
8. Effect of residual stress
9. Interaction between plane components
10. Effect of perforations

During the past 50 years, investigations on the interaction of local and overall buckling in metal columns have been conducted by numerous researchers.[1.11,3.70,5.20–5.63] Different approaches have been suggested for analysis and design of columns.

5.5.1 *Q*-Factor Method

The effect of local buckling on column strength was considered in the AISI Specification during the period from 1946 through 1986 by using a form factor Q in the determination of allowable stress for the design of axially loaded compression members. Winter and Fahy were the principal contributors to the development of this Q factor. Accumulated experience has proved that the use of such a form factor as discussed below is a convenient and simple method for the design of cold-formed steel columns.[1.161]

As previously discussed, if an axially loaded short column has a compact cross section, it will fail in yielding rather than buckling, and the maximum load P can be determined as follows:

$$P = AF_y \tag{5.44}$$

where A = full cross-sectional area
   F_y = yield point of steel

However, for the same length of the column if the w/t ratios of compression elements are relatively large, the member may fail through local buckling at a stress less than F_y. Assuming the reduced stress is QF_y instead of F_y, then

$$P = A(QF_y) \tag{5.45}$$

where Q is a form factor, which is less than unity, representing the weakening influence due to local buckling.

From the above two equations it can be seen that the effect of local buck-ling on column strength can be considered for columns that will fail in local buckling by merely replacing F_y by QF_y. The same is true for columns having moderate KL/r ratios.

The value of form factor Q depends on the form or shape of the section. It can be computed as follows for various types of sections:

1. Members Composed Entirely of Stiffened Elements

When a short compression member is composed entirely of stiffened elements such as the tubular member shown in Fig. 5.1a, it will fail when the edge stress of the stiffened elements reaches the yield point. Using the effective width concept, the column will fail under a load

$$P = A_{\text{eff}} F_y \tag{5.46}$$

where A_{eff} is the sum of the effective areas of all stiffened elements.
Comparing the above equation with Eq. (5.45), it is obvious that

$$Q_{\text{a}} = \frac{A_{\text{eff}}}{A} \tag{5.47}$$

where Q_{a} is the area factor.

2. Members Composed Entirely of Unstiffened Elements

If a short compression member is composed entirely of unstiffened el-ements, it will buckle locally under a load

$$P = A\sigma_{\text{cr}} \tag{5.48}$$

where σ_{cr} is the critical local buckling stress of the unstiffened element.
Comparing the above equation again with Eq. (5.45), it is found that

$$Q_{\text{s}} = \frac{\sigma_{\text{cr}}}{F_y} = \frac{F_{\text{c}}}{F} \tag{5.49}$$

where Q_{s} = stress factor
F_{c} = allowable compressive stress
F = basic design stress ($0.60F_y$) for the ASD method

3. Members Composed of Both Stiffened and Unstiffened Elements

If a short compression member is composed of both stiffened and un-

stiffened elements as shown in Fig. 5.1c,* the useful limit of the member may be assumed to be reached when the stress in the weakest unstiffened element reaches the critical local buckling stress σ_{cr}. In this case, the effective area A'_{eff} will consist of the full area of all unstiffened elements and the sum of the reduced or effective areas of all stiffened elements. That is,

$$P = A'_{eff}\sigma_{cr} \tag{5.50}$$

Comparing the above equation with Eq. (5.45),

$$
\begin{aligned}
Q &= A'_{eff}\frac{\sigma_{cr}}{AF_y} \\
&= \left(\frac{A'_{eff}}{A}\right)\left(\frac{\sigma_{cr}}{F_y}\right) = \left(\frac{A'_{eff}}{A}\right)\left(\frac{F_c}{F}\right) \\
&= Q'_a Q_s
\end{aligned}
\tag{5.51}
$$

where Q = form factor
Q_a' = area factor
Q_s = stress factor

5.5.2 Unified Approach

Even though the Q-factor method has been used successfully in the past for the design of cold-formed steel compression members, additional investigations at Cornell University and other institutions have shown that this method is capable of improvement.[3.17,5.26–5.28,5.49] On the basis of test results and analytical studies of DeWolf, Pekoz, Winter, Kalyanaraman, and Loh, Pekoz shows in Ref. 3.17 that the Q-factor approach can be unconservative for compression members having stiffened elements with large width-to-thickness ratios, particularly for those members having slenderness ratios in the neighborhood of 100. On the other hand, the Q-factor method gives very conservative results for I-sections having unstiffened flanges, especially for columns with small slenderness rations. Consequently, the Q-factor was eliminated in the 1986 edition of the AISI Specification. In order to reflect the effect of local buckling on column strength, the nominal column load is determined by the governing critical buckling stress and the *effective area*, A_e, instead of the full sectional area. When A_e cannot be calculated, such as when the compression member has dimensions or geometry outside the range of applicability of the generalized effective width equations of the AISI Specification,

---

*The stiffeners are considered as unstiffened elements.

the effective area A_e can be determined experimentally by stub column tests as described in Ref. 3.17. For C- and Z-shapes, and single-angle sections with unstiffened flanges, the nominal column load has been limited by the column buckling load, which is calculated by the local buckling stress of the unstiffened flange and the area of the full, unreduced cross section. This requirement was included in Sec. C4(b) of the 1986 edition of the AISI Specification. It was deleted in 1996 on the basis of the study conducted by Rasmussen and Hancock (Refs. 5.101 and 5.102).

The current AISI design provisions are discussed in Art. 5.7 followed by design examples.

5.6   EFFECT OF COLD WORK ON COLUMN BUCKLING

The discussions in Arts. 5.1 to 5.5 were based on the assumption that the compression members have uniform mechanical properties over the entire cross section. However, as shown in Fig. 2.3, the yield point and tensile strength of the material vary from place to place in the cross section due to the cold work of forming. The column strength of the axially loaded compression member with nonuniform mechanical properties throughout the cross section may be predicted by Eq. (5.52) on the basis of the tangent modulus theory if we subdivide the cross section into j subareas, for which each subarea has a constant material property.[2.14,2.17,5.64,5.65]

$$\sigma_T = \frac{\pi^2}{A(KL)^2} \sum_{i=1}^{j} E_{ti}I_i \tag{5.52}$$

where E_{ti} = tangent modulus of ith subarea at a particular value of strain
I_i = moment of inertia of ith subarea about neutral axis of total cross section

In order to investigate the strength of cold-formed compression members subjected to an axial load, six specimens made of channels back to back have been tested by Karren and Winter at Cornell University.[2.14,2.17] The test data are compared graphically with Eqs. (5.5), (5.7), and (5.52) in Fig. 5.15. In addition four pairs of joist sections have also been tested at Cornell. Results of tests are compared in Fig. 5.16.[2.17]

Based on the test data shown in Figs. 5.15 and 5.16,[2.17] it may be concluded that with the exception of two channel tests, Eq. (5.52) seems to produce a somewhat better correlation because it considers the variable material properties over the cross section. Equations (5.5) and (5.7) based on the average of compressive and tensile yield points also predict satisfactory column buckling stress in the inelastic range with reasonable accuracy, particularly for
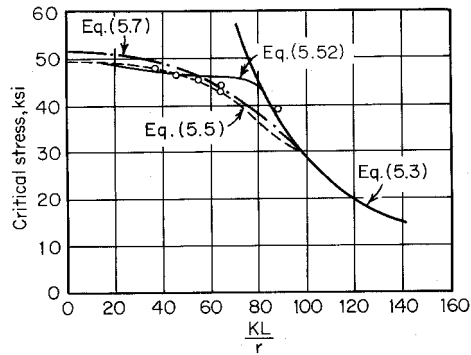
Figure 5.15   Comparison of column curves for channel sections.[2.17]

columns with a slenderness ratio around 60. Equation (5.7) could provide a lower boundary for column buckling stress if the tensile yield point is to be used.[2.14]

5.7   AISI DESIGN FORMULAS FOR CONCENTRICALLY LOADED COMPRESSION MEMBERS

Based on the discussions of Arts. 5.2 through 5.5, appropriate design provisions are included in the AISI Specification for the design of axially loaded compression members. The following excerpts are adopted from Sec. C4 of the 1996 edition of the AISI Specification for the ASD and LRFD methods:

C4   Concentrically Loaded Compression Members

This section applies to members in which the resultant of all loads acting on the member is an axial load passing through the centroid of the effective section calculated at the stress, F_n, defined in this section.
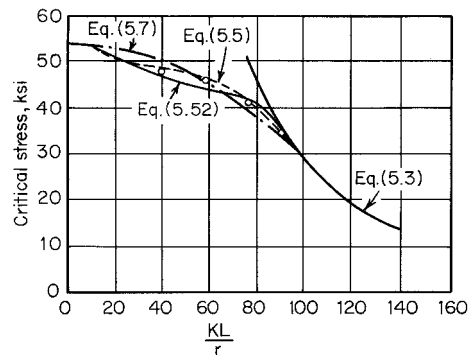
Figure 5.16   Comparison of column curves for joist chord sections.[2.17]

(a) The nominal axial strength, P_n, shall be calculated as follows:

$$P_n = A_e F_n \tag{5.53}$$

$$\Omega_c = 1.80 \text{ (ASD)}$$

$$\phi_c = 0.85 \text{ (LRFD)}$$

where $A_e =$ Effective area at the stress F_n. For sections with circular holes, A_e shall be determined according to Section B2.2a, subject to the limitations of that section. If the number of holes in the effective length region times the hole diameter divided by the effective length does not exceed 0.015, A_e can be determined ignoring the holes.

F_n is determined as follows:

$$\text{For } \lambda_c \leq 1.5 \qquad F_n = (0.658^{\lambda_c^2})F_y \tag{5.54}$$

$$\text{For } \lambda_c > 1.5 \qquad F_n = \left[\frac{0.877}{\lambda_c^2}\right] F_y \tag{5.55}$$

where

$$\lambda_c = \sqrt{\frac{F_y}{F_e}}$$

$F_e =$ the least of the elastic flexural, torsional, and torsional–flexural buckling stress determined according to Sections C4.1 through C4.3.

(b) concentrically loaded angle sections shall be designed for an additional bending moment as specified in the definitions of M_x, M_y (ASD), or M_{ux}, M_{uy}, (LRFD) in Section C5.2.

C4.1 Sections Not Subject to Torsional or Torsional–Flexural Buckling

For doubly symmetric sections, closed cross sections and any other sections which can be shown not to be subject to torsional or torsional–flexural buckling, the elastic flexural buckling stress, F_e, shall be determined as follows:

$$F_e = \frac{\pi^2 E}{(KL/r)^2} \tag{5.56}$$

where E = modulus of elasticity
    K = effective length factor*
    L = unbraced length of member
    r = radius of gyration of the full, unreduced cross section

C4.2   Doubly or Singly Symmetric Sections Subject to Torsional or Torsional–Flexural Buckling

For singly symmetric sections subject to torsional or torsional–flexural buckling, F_e shall be taken as the smaller of F_e calculated according to Sec. C4.1 and F_e calculated as follows:

$$F_e = \frac{1}{2\beta} [(\sigma_{ex} + \sigma_t) - \sqrt{(\sigma_{ex} + \sigma_t)^2 - 4\beta\sigma_{ex}\sigma_t}] \qquad (5.57)$$

Alternatively, a conservative estimate of F_e can be obtained using the following equation:

$$F_e = \frac{\sigma_t \sigma_{ex}}{\sigma_t + \sigma_{ex}} \qquad (5.58)$$

where σ_t and σ_{ex} are as defined in C3.1.2:

$$\beta = 1 - (x_0/r_0)^2 \qquad (5.59)$$

For singly symmetric sections, the x-axis is assumed to be the axis of symmetry.

For doubly symmetric sections subject to torsional buckling, F_e shall be taken as the smaller of F_e calculated according to Section C4.1 and $F_e = \sigma_t$, where σ_t is defined in Section C3.1.2.

C4.3   Nonsymmetric Sections

For shapes whose cross sections do not have any symmetry, either about an axis or about a point, F_e shall be determined by rational analysis. Alternatively, compression members composed of such shapes may be tested in accordance with Chapter F.

---

*In frames where lateral stability is provided by diagonal bracing, shear walls, attachment to an adjacent structure having adequate lateral stability, or floor slabs or roof decks secured horizontally by walls or bracing systems parallel to the plane of the frame, and in trusses, the effective length factor, K, for compression members which do not depend upon their own bending stiffness for lateral stability of the frame or truss, shall be taken as unity, unless analysis shows that a smaller value may be used. In a frame which depends upon its own bending stiffness for lateral stability, the effective length, KL, of the compression members shall be determined by a rational method and shall not be less than the actual unbraced length.

C4.4 Compression Members Having One Flange Through-Fastened to Deck or Sheathing

These provisions are applicable to C- or Z-sections concentrically loaded along their longitudinal axis, with only one flange attached to deck or sheathing with through fasteners.

The nominal axial strength of simple span or continuous C- or Z-sections shall be calculated as follows:

(a) For weak axis nominal strength

$$P_n = \frac{C_1\, C_2\, C_3 AE}{29,500} \text{ kips (Newtons)} \tag{5.60}$$

$$\Omega = 1.80 \text{ (ASD)}$$

$$\phi = 0.85 \text{ (LRFD)}$$

where

$$C_1 = (0.79x + 0.54) \tag{5.61}$$

$$C_2 = (1.17t + 0.93) \text{ when } t \text{ is in inches} \tag{5.62a}$$

$$C_2 = (0.0461t + 0.93) \text{ when } t \text{ is in millimeters} \tag{5.62b}$$

$$C_3 = (2.5b - 1.63d + 22.8) \text{ when } b \text{ and } d \text{ are in inches} \tag{5.63a}$$

$$C_3 = (0.0984b - 0.0642d + 22.8) \text{ when } b \text{ and } d \text{ are in millimeters} \tag{5.63b}$$

For Z-sections:

$x =$ the fastener distance from the outside web edge divided by the flange width, as shown in Figure C4.4

For C-sections:

$x =$ the flange width minus the fastener distance from the outside web edge divided by the flange width, as shown in Figure C4.4.

$t =$ C- or Z-section thickness
$b =$ C- or Z-section flange width
$d =$ C- or Z-section depth
$A =$ the full unreduced cross-sectional area of the C- or Z-section
$E =$ modulus of elasticity of steel
  $= 29,500$ ksi for U.S. customary units
  $= 203,000$ MPa for SI units
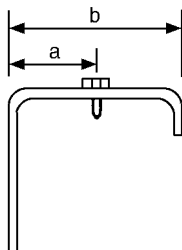
Figure C4.4   Definition of x

$$\text{For Z-sections, } x = \frac{a}{b} \tag{5.64a}$$

$$\text{For C-sections, } x = \frac{b - a}{b} \tag{5.64b}$$

Eq. (5.60) shall be limited to roof and wall systems meeting the following conditions:

(1) t not exceeding 0.125 in. (3.22 mm)
(2) 6 in. (152 mm) $\le d \le$ 12 in. (305 mm)
(3) flanges are edge stiffened compression elements
(4) 70 $\le d/t \le$ 170
(5) 2.85 $\le d/b <$ 5
(6) 16 $\le$ flange flat width/$t <$ 50
(7) both flanges are prevented from moving laterally at the supports
(8) steel roof or steel wall panels with fasteners spaced 12 in. (305 mm) on center or less and having a minimum rotational lateral stiffness of 0.0015 k/in./in. (10,300 N/m/m) (fastener at mid-flange width) as determined by the AISI test procedure*
(9) C- and Z-sections having a minimum yield point of 33 ksi (228MPa)
(10) span length not exceeding 33 ft (10 m)

(b) For strong axis nominal strength, the equations contained in Sections C4 and C4.1 of the Specification shall be used.

In addition to the discussion of Arts. 5.2 through 5.5, the following comments are related to some of the current AISI design provisions:

---

*Further information on the test procedure should be obtained from "Rotational–Lateral Stiffness Test Method for Beam-to-Panel Assemblies," *Cold-Formed Steel Design Manual*, Part VIII.

1. *Factor of Safety.* In the 1986 and earlier editions of the AISI Specification, the allowable axial load for the ASD method was determined by either a uniform safety factor of 1.92 or a variable safety factor ranging from 1.67 to 1.92 for wall thickness not less than 0.09 in. (2.3 mm) and F_e $> F_y/2$. The use of the smaller safety factors for the type of relatively stocky columns was occasioned by their lesser sensitivity to accidental eccentricities and the difference in structural behavior between the compression members having different compactness. The latter fact is illustrated by the stress–strain curves of the more compact and less compact stub-column specimens, as shown in Fig. 5.17. In the experimental and analytical investigations conducted by Karren, Uribe, and Winter,[2.14,2.17] both types of specimens shown in Fig. 5.17 were so dimensioned that local buckling would not occur at stresses below the yield point of the material. Test data did indicate that the less compact stub column (curve A for cold-reduced killed press braked hat section) reached the ultimate compressive load at strains in the range of 3 to 5×10^{-3} in./in., after which the load dropped off suddenly because yielding was followed by local crippling. However, the more compact stub column (curve B for hot-rolled semikilled roll-formed channel section) showed a long stable plateau and, after some strain hardening, reached the ultimate load at much higher values of strain in the range of 16 to 27×10^{-3} in./in. For this reason, the use of a smaller safety factor for more compact sections is justified and appropriate as far as the overall safety of the compression member is concerned.

As discussed in Art. 5.3.2, the AISI design equations were changed in 1996 on the basis of a different strength model. These equations enable the use of a single safety factor of 1.80 for all λ_c values. Figure 5.18 shows a comparison of design axial strengths permitted by the 1986 and 1996 Specifications. It can be seen that the design capacity is increased by using the 1996 Specification for thin columns with low slenderness parameters and decreased for high slenderness parameters. However the difference would be less than 10%.
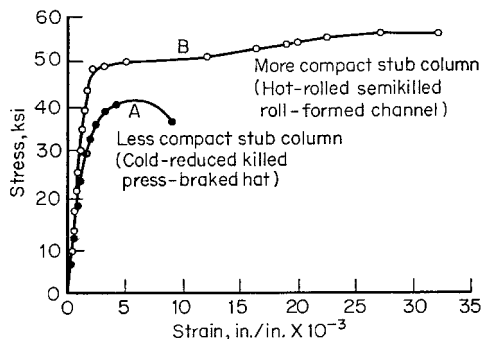
Figure 5.17 Stress-strain curves for more compact and less compact stub columns.[2.17]
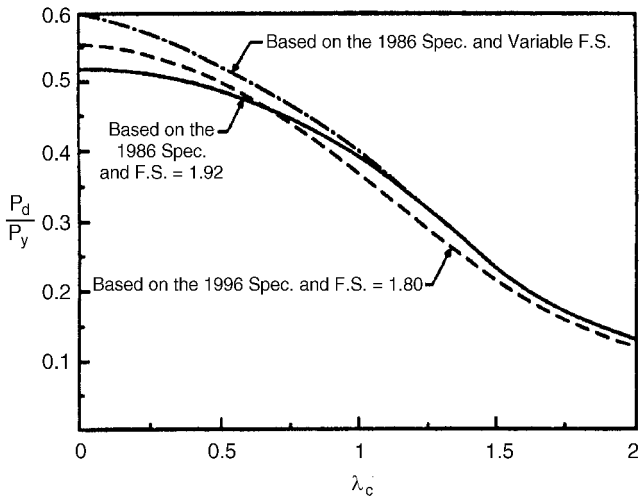
Figure 5.18   Comparison between the design axial strengths, P_d, for the ASD method.

For the LRFD method, the differences between the nominal axial strengths used for the 1991 and the 1996 LRFD design provisions are shown in Fig. 5.19. The resistance factor of $\phi_c = 0.85$ is the same as the AISC Specification[3.150] and the 1991 edition of the AISI LRFD Specification.[3.152]

2. *Maximum Slenderness Ratio*. In Sec. C4 of the 1996 AISI Specification, the maximum allowable slenderness ratio KL/r of compression members is
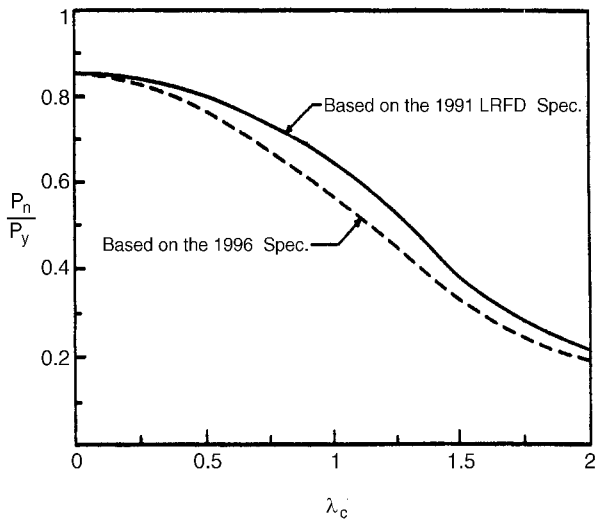
Figure 5.19   Comparison between the nominal axial strengths, P_n, for the LRFD method.

preferably limited to 200, except that during construction the maximum KL/r ratio is 300. This limitation on the slenderness ratio is the same as that used by the AISC for the design of hot-rolled heavy steel compression members. Even though the design formulas are equally applicable to columns having slenderness ratios larger than 200, any use of the unusually long columns will result in an uneconomical design due to the small capacity to resist buckling. In 1999, the AISI Committee on Specifications moved the KL/r limit from the Specification to the Commentary.[1.333]

3. *Simplified Equation for Torsional–Flexural Buckling.* The simplified equation for torsional–flexural buckling (Eq. 5.58) is based on the following formula given by Pekoz and Winter in Ref. 5.66:

$$\frac{1}{P_{\text{TFO}}} = \frac{1}{P_{\text{x}}} + \frac{1}{P_{\text{z}}}$$

(5.65)

or

$$\frac{1}{\sigma_{\text{TFO}}} = \frac{1}{\sigma_{\text{ex}}} + \frac{1}{\sigma_{\text{t}}}$$

(5.66)

4. *Compression Members Having One Flange Through-Fastened to Deck or Sheathing.* In 1996, new design provisions were added in Sec. C4.4 of the AISI Specification for calculating the weak axis capacity of axially loaded C- or Z-sections having one flange attached to deck or sheathing and the other flange unbraced. Equation (5.60) was developed by Glaser, Kaehler, and Fisher[5.104] and is also based on the work contained in the reports of Hatch, Easterling, and Murray[5.105] and Simaan.[5.106]

When a roof purlin or wall girt is subject to wind- or seismic-generated compression forces, the axial load capacity of such a compression member is less than that of a fully braced member, but greater than that of an unbraced member. The partial restraint for weak axis buckling is a function of the rotational stiffness provided by the panel-to-purlin connection. It should be noted that Eq. (5.60) is applicable only for the roof and wall systems meeting the conditions listed in Sec. C4.4 of the Specification. This equation is not valid for sections attached to standing seam roofs.

5. *Design Tables* Part III of the AISI Design Manual[1.159] contains a number of design tables for column properties and nominal axial strengths of C-sections with and without lips. The tables are prepared for $F_{\text{y}} = 33$ and 55 ksi (228 and 379 MPa).

6. *Distortional Buckling of Compression Members.* The distortional buckling mode for flexural members was discussed in Art. 4.2.3.6. For column design, flange distortional buckling is also one of the important failure modes as shown in Fig. 5.20. This type of buckling mode involves the rotation of each flange and lip about the flange–web junction.
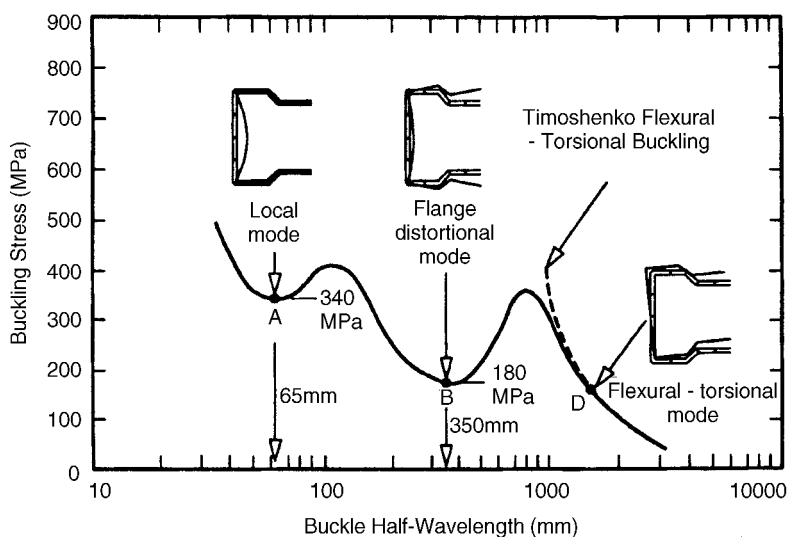
Figure 5.20 Rack section column buckling stress versus half-wavelength for concentric compression.[1.69]

During the past two decades, the distortional buckling mode of compression members was studied by Hancock,[5.108,4.164] Lau and Hancock,[5.109–5.111] Charnvarnichborikarn and Polyzois,[5.112] Kwon and Hancock,[5.113,5.114] Hancock, Kwon, and Bernard [5.115] Hancock, Rogers, and Schuster,[4.165] Schafer,[3.195] Davies, Jiang, and Ungureanu,[4.168] Bambach, Merrick, and Hancock, [3.173] and others. Research findings are well summarized by Hancock in Ref. 1.69. In the same publication, Hancock also discusses the background information on the Australian design provisions for distortional buckling of flexural members and compression members.

Even though design provisions for distortional buckling are included in some design standards, the AISI Specification does not include specific design requirements for this subject at the present time (1999).

5.8 EFFECTIVE LENGTH FACTOR *K*

In steel design, lateral bracing is generally used to resist lateral loads, such as wind or earthquake loads, or to increase the strength of members by preventing them from deforming in their weakest direction.[4.111] The use of such bracing may affect the design of compression members.

In Arts. 5.3 to 5.7, the effective length *KL* of the column was used to determine buckling stresses. The factor *K* (a ratio of the effective column length to the actual unbraced length) represents the influence of restraint against rotation and translation at both ends of the column.

The theoretical *K* values and the design values recommended by the Structural Stability Research Council are tabulated in Table 5.1. In practice, the value of *K* = 1 can be used for columns or studs with X bracing, diaphragm bracing, shear-wall construction, or any other means that will prevent relative horizontal displacements between both ends.[1.161] If translation is prevented and restraint against rotation is provided at one or both ends of the member, a value of less than 1 may be used for the effective length factor.

In the design of trusses, it is realized that considerable rotational restraint could be provided by continuity of the compression chord as long as the tension members do not yield. In view of the fact that for the ASD method tension members are designed with a factor of safety of $\frac{5}{3}$ and compression members are designed with relatively large factors of safety, it is likely that the tension members will begin to yield before the buckling of compression members. Therefore the rotational restraint provided by tension members may not be utilized in design as discussed by Bleich.[3.3] For this reason, compression members in trusses can be designed for *K* = 1.[1.161] However, when sheathing is attached directly to the top flange of a continuous chord, recent research has shown that the *K* value may be taken as 0.75.[5.107]

TABLE 5.1   Effective Length Factor *K* for Axially Loaded Columns with Various End Conditions

	(a)	(b)	(c)	(d)	(e)	(f)
Buckled shape of column is shown by dashed line						
Theoretical K value	0.5	0.7	1.0	1.0	2.0	2.0
Recommended K value when ideal conditions are approximated	0.65	0.80	1.2	1.0	2.10	2.0

End condition code		
Rotation fixed	Translation fixed
Rotation free	Translation fixed
Rotation fixed	Translation free
Rotation free	Translation free

Source: Reproduced from *Guide to Stability Design Criteria for Metal Structures*, 4th ed., 1988. (*Courtesy of* John Wiley and Sons, Inc.)

For unbraced frames, the structure depends on its own bending stiffness for lateral stability. If a portal frame is not externally braced in its own plane to prevent sidesway, the effective length KL is larger than the actual unbraced length, as shown in Fig. 5.21, that is, $K > 1$. This will result in a reduction of the load-carrying capacity of the columns when sideways is not prevented.

For unbraced portal frames, the effective column length can be determined from Fig. 5.22 for the specific ratio of $(I/L)_{beam}/(I/L)_{col}$ and the condition of the foundation. If the actual footing provides a rotational restraint between hinged and fixed bases, the K value can be obtained by interpolation.

The K values to be used for the design of unbraced multistory or multibay frames can be obtained from the alignment chart in Fig. 5.23.[1.158] In the chart, G is defined as

$$G = \frac{\Sigma(I_c/L_c)}{\Sigma(I_b/L_b)}$$

in which I_c is the moment of inertia and L_c is the unbraced length of the column, and I_b is the moment of inertia and L_b is the unbraced length of the beam.

In practical design, when a column base is supported by but not rigidly connected to a footing or foundation, G is theoretically infinity, but unless actually designed as a true friction-fee pin, it may be taken as 10. If the column end is rigidly attached to a properly designed footing, G may be taken as 1.0.[1.158,5.67]

In the use of the chart, the beam stiffness I_b/L_b should be multiplied by a factor as follows when the conditions at the far end of the beam are known:
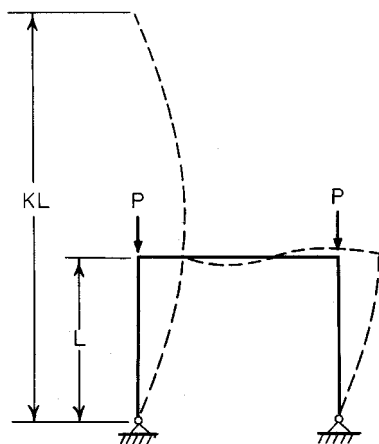
Figure 5.21   Laterally unbraced portal frame.[1.161]

$$\frac{(I/L)_{beam}}{(I/L)_{col}}$$
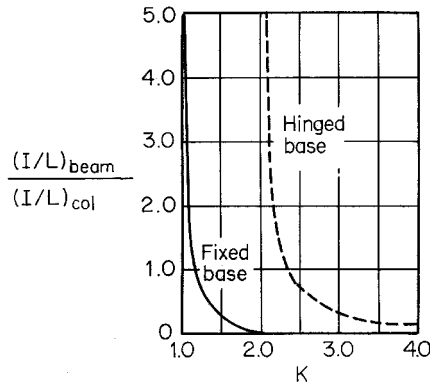
Figure 5.22   Effective length factor *K* in laterally unbraced portal frames.[1.161]

1. Sidesway is prevented,
   1.5 for far end of beam hinged
   2.0 for far end of beam fixed
2. Sidesway is not prevented
   0.5 for far end of beam hinged
   0.67 for far end of beam fixed
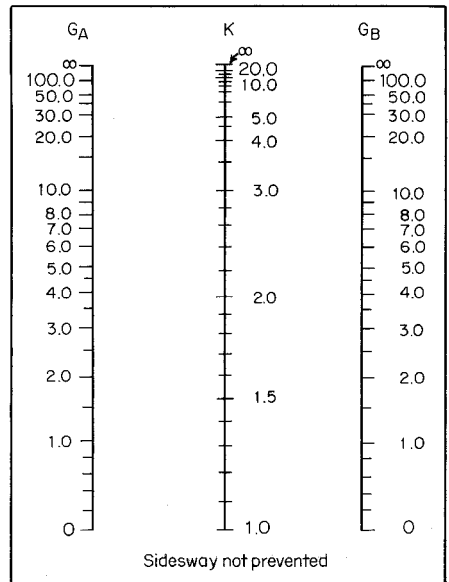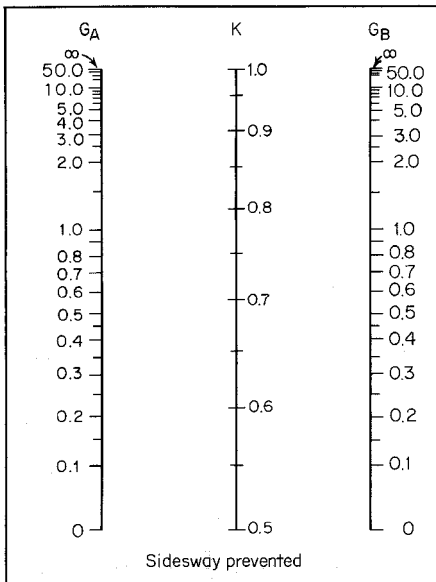
Figure 5.23   Alignment charts developed by L.S. Lawrence for effective length of column in continuous frames. (*Jackson & Moreland Division of United Engineers & Constructors, Inc.*)[1.158]

After determining G_A and G_B for joints A and B at two ends of the column section, the K value van be obtained from the alignment chart of Fig. 5.23 by constructing a straight line between the appropriate points on the scales for G_A and G_B.

5.9 DESIGN EXAMPLES

Example 5.1 Determine the allowable axial load for the square tubular column shown in Fig. 5.24. Assume that $F_y = 40$ ksi, $K_x L_x = K_y L_y = 10$ ft, and the dead-to-live load ratio is 1/5. Use the ASD and LRFD methods.

Solution

A. ASD Method

Since the square tube is a doubly symmetric closed section, it will not be subject to torsional–flexural buckling. It can be designed for flexural buckling.

1. *Sectional Properties of Full Section*

    $w = 8.00 - 2(R + t) = 7.415$ in.

    $A = 4(7.415 \times 0.105 + 0.0396) = 3.273$ in.^{2}

    $I_x = I_y = 2(0.105)[(1/12)(7.415)^3 + 7.415(4 - 0.105/2)^2]$
    $\quad + 4(0.0396)(4.0 - 0.1373)^2$

    $\quad = 33.763$ in.^{4}

    $r_x = r_y = \sqrt{I_x/A} = \sqrt{33.763/3.273} = 3.212$ in.

2. *Nominal Buckling Stress, F_n* According to Eq. (5.56), the elastic flexural buckling stress, F_e, is computed as follows:
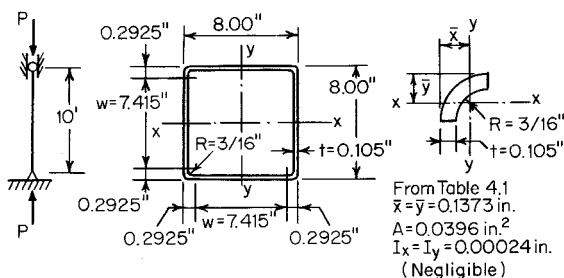
Figure 5.24 Example 5.1.

$$\frac{KL}{r} = \frac{10 \times 12}{3.212} = 37.36 < 200 \text{ O.K.}$$

$$F_e = \frac{\pi^2 E}{(KL/r)^2} = \frac{\pi^2 (29500)}{(37.36)^2} = 208.597 \text{ ksi}$$

$$\lambda_c = \sqrt{\frac{F_y}{F_e}} = \sqrt{\frac{40}{208.597}} = 0.438 < 1.5$$

$$F_n = (0.658^{\lambda_c^2})F_y = (0.658^{0.438^2})40 = 36.914 \text{ ksi}$$

3. *Effective Area, A_e*. Because the given square tube is composed of four stiffened elements, the effective width of stiffened elements subjected to uniform compression can be computed from Eqs. (3.41) through (3.44).

$$w/t = 7.415/0.105 = 70.619$$

$$\lambda = \frac{1.052}{\sqrt{k}}\left(\frac{w}{t}\right)\sqrt{\frac{F_n}{E}}$$

$$\lambda = (1.052/\sqrt{4})(70.619)\sqrt{36.914/29{,}500} = 1.314$$

Since $\lambda > 0.673$, from Eq. (3.42),

$$b = \rho w$$

where

$$\rho = (1 - 0.22/\lambda)/\lambda = (1 - 0.22/1.314)/1.314 = 0.634$$

Therefore, $b = (0.634)(7.415) = 4.701$ in.

The effective area is:

$$A_e = 3.273 - 4(7.415 - 4.701)(0.105) = 2.133 \text{ in.}^2$$

4. *Nominal and Allowable Loads*. Using Eq. (5.53), the nominal load is

$$P_n = A_e F_n = (2.133)(36.914) = 78.738 \text{ kips}$$

The allowable load is

$$P_a = P_n/\Omega_c = 78.738/1.80 = 43.74 \text{ kips}$$

B. LRFD Method

In Item (A) above, the nominal axial load, P_n, was computed to be 78.738 kips. The design axial load for the LRFD method is

$$\phi_c P_n = 0.85(78.738) = 66.93 \text{ kips}$$

Based on the load combination of dead and live loads, the required load is

$$P_u = 1.2P_D + 1.6P_L = 1.2P_D + 1.6(5P_D) = 9.2P_D$$

where

P_D = axial load due to dead load
P_L = axial load due to live load

By using $P_u = \phi_c P_n$, the values of P_D and P_L are computed as follows:

$$P_D = 66.93/9.2 = 7.28 \text{ kips}$$

$$P_L = 5P_D = 36.40 \text{ kips}$$

Therefore, the allowable axial load is

$$P_a = P_D + P_L = 43.68 \text{ kips}$$

It can be seen that the allowable axial loads determined by the ASD and LRFD methods are practically the same.

Example 5.2   Use the ASD and LRFD methods to determine the design strengths of the I-section (Fig. 5.25) to be used as a compression member. Assume that the effective length factor K is 1.0 for the x- and y-axes, and
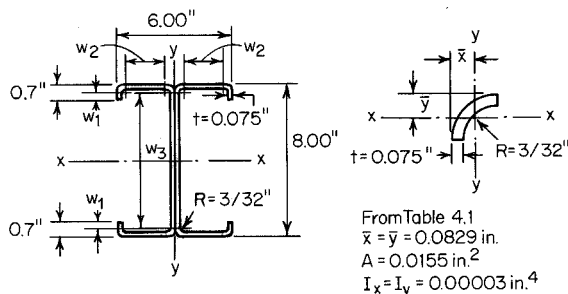
Figure 5.25   Example 5.2.

that the unbraced lengths for the x- and y-axes are 12 and 6 ft, respectively. Also assume that $K_tL_t = 6$ ft. Use $F_y = 33$ ksi.

Solution

A. ASD Method

1. *Properties of Full Section.* Based on the method used in Chap. 4, the following full section properties can be computed:

$$A = 2.24 \text{ in.}^2$$

$$I_x = 22.1 \text{ in.}^4$$

$$I_y = 4.20 \text{ in.}^4$$

$$r_x = 3.15 \text{ in.}$$

$$r_y = 1.37 \text{ in.}$$

2. *Nominal Buckling Stress, F_n.* Since the given I-section is a doubly symmetric section, the nominal buckling stress will be governed by either flexural buckling or torsional buckling as discussed in Art. 5.4.1.

   a. *Elastic Flexural Buckling.* By using Eq. (5.56), the elastic flexural buckling stress can be computed as follows:

$$K_xL_x/r_x = (1)(12 \times 12)/3.15 = 45.714$$

$$K_yL_y/r_y = (1)(6 \times 12)/1.37 = 52.555$$

use $KL/r = 52.555$ in Eq. (5.56),

$$F_e = \frac{\pi^2 E}{(KL/r)^2} = \frac{\pi^2 (29,500)}{(52.555)^2} = 105.413 \text{ ksi}$$

   b. *Elastic Torsional Buckling.* Use Eq. (5.22) of Art. 5.4.1, the torsional buckling stress is

$$F_e = \sigma_t = \frac{1}{Ar_0^2}\left[GJ + \frac{\pi^2 EC_w}{(K_tL_t)^2} \right]$$

where $A = 2.24 \text{ in.}^2$

$$r_0 = \sqrt{r_x^2 + r_y^2} = \sqrt{(3.15)^2 + (1.37)^2} = 3.435 \text{ in.}$$

$$G = 11,300 \text{ ksi}$$

$$J = 0.00418 \text{ in.}^4$$

$$C_w = 70.70 \text{ in.}^6$$

$$E = 29{,}500 \text{ ksi}$$

$$K_t L_t = 6 \text{ ft}$$

Therefore

$$F_e = \sigma_t = \frac{1}{(2.24)(3.435)^2} \left[(11300)(0.00418) + \frac{\pi^2(29{,}500)(70.70)}{(6 \times 12)^2} \right]$$

$$= 152.02 \text{ ksi}$$

The nominal buckling stress, F_n, is determined by using the smaller value of the elastic flexural buckling stress and torsional buckling stress, i.e.,

$$F_e = 105.413 \text{ ksi}$$

$$\lambda_c = \sqrt{\frac{F_y}{F_e}} = \sqrt{\frac{33}{105.413}} = 0.560 < 1.5$$

From Eq. (5.54),

$$F_n = (0.658^{\lambda_c^2})F_y = (0.658^{0.560^2})(33) = 28.941 \text{ ksi}$$

3. *Effective Area*, A_e, at stress, F_n

$$w_1 = 0.7 - (R + t) = 0.5313 \text{ in.}$$
$$w_2 = 3.0 - 2(R + t) = 2.6625 \text{ in}$$
$$w_3 = 8.0 - 2(R + t) = 7.6625 \text{ in.}$$

a. *Effective Width of the Compression Flanges* (Art. 3.5.3.2)

$$S = 1.28\sqrt{E/f} = 1.28\sqrt{29{,}500/28.941} = 40.866$$

$$S/3 = 13.622$$

$$w_2/t = 2.6625/0.075 = 35.50$$

Since $S/3 < w_2/t < S$, use Case II of Art. 3.5.3.2(a).

$$I_a = 399\{[(w_2/t)/S] - \sqrt{K_u/4}\}^3 t^4$$

$$= 399\{[35.50/40.866] - \sqrt{0.43/4}\}^3(0.075)^4$$

$$= 0.0020 \text{ in.}^4$$

$$n = 1/2$$

$$I_s = d^3 t/12 = (w_1)^3 t/12 = (0.5313)^3(0.075)/12$$

$$= 0.000937 \text{ in.}^4$$

$$C_2 = I_s/I_a = 0.000937/0.0020 = 0.469 < 1.0$$

$$C_1 = 2 - C_2 = 2 - 0.469 = 1.531$$

$$D/w_2 = 0.7/2.6625 = 0.263$$

Since $D/w_2 < 0.8$,

$$k_a = 5.25 - 5(D/w_2) = 5.25 - 5(0.263) = 3.935 < 4.0$$

$$k = C_2^n(k_a - k_u) + k_u$$

$$= (0.469)^{0.5}(3.935 - 0.43) + 0.43$$

$$= 2.830$$

Use $k = 2.830$ to compute the effective width of the compression flange.

From Eqs. (3.41) through (3.44),

$$\lambda = \frac{1.052}{\sqrt{k}}\left(\frac{w_2}{t}\right)\sqrt{\frac{f}{E}} = \frac{1.052}{\sqrt{2.830}}(35.50)\sqrt{\frac{28.941}{29500}}$$

$$= 0.695 > 0.673$$

$$\rho = \left(1 - \frac{0.22}{\lambda}\right)\Big/\lambda = \left(1 - \frac{0.22}{0.695}\right)/0.695 = 0.983$$

$$b = \rho w_2 = 0.983 \times 2.6625 = 2.617 \text{ in.}$$

b. *Effective Width of Edge Stiffeners*

$$w_1/t = 0.5313/0.075 = 7.084 < 14 \qquad \text{O.K.}$$

$$\lambda = \frac{1.052}{\sqrt{k}}\left(\frac{w_1}{t}\right)\sqrt{\frac{f}{E}} = \frac{1.052}{\sqrt{0.43}}(7.084)\sqrt{\frac{28.941}{29500}}$$

$$= 0.356 < 0.673$$

$$d'_s = w_1 = 0.5313 \text{ in.}$$

$$d_s = C_2 d'_s = (0.469)(0.5313) = 0.249 \text{ in.} < d'_s \qquad \text{O.K.}$$

c. *Effective Width of Web Elements*

$$w_3/t = 7.6625/0.075 = 102.167 < 500 \qquad \text{O.K.}$$

$$\lambda = \frac{1.052}{\sqrt{k}} \left(\frac{w_3}{t}\right) \sqrt{\frac{f}{E}} = \frac{1.052}{\sqrt{4}} (102.167) \sqrt{\frac{28.941}{29500}}$$

$$= 1.683 > 0.673$$

$$\rho = \left(1 - \frac{0.22}{\lambda}\right) / \lambda = \left(1 - \frac{0.22}{1.683}\right) / 1.683 = 0.517$$

$$b = \rho w_3 = (0.517)(7.6625) = 3.962 \text{ in.}^2$$

d. *Effective Area, A_e*

$$A_e = 2.24 - [4(0.5313 - 0.249) + 4(2.6625 - 2.617)$$
$$+ \ 2(7.6625 - 3.962)](0.075)$$
$$= 2.24 - 0.653 = 1.587 \text{ in.}^2$$

4. *Nominal and Allowable Loads.* The nominal load is

$$P_n = A_e F_n = (1.587)(28.941) = 45.93 \text{ kips}$$

The allowable load for the ASD method is

$$P_a = P_n / \Omega_c = 45.93/1.80 = 25.52 \text{ kips}$$

B. LRFD Method

From Item (A) above, $P_n = 45.93$ kips. The design strength for the LRFD method is

$$\phi_c P_n = (0.85)(45.93) = 39.04 \text{ kips}$$

Example 5.3 For the channel section shown in Fig. 5.26, determine the following items:

1. Determine the critical length, L_{cr}, below which the torsional–flexural buckling mode is critical.
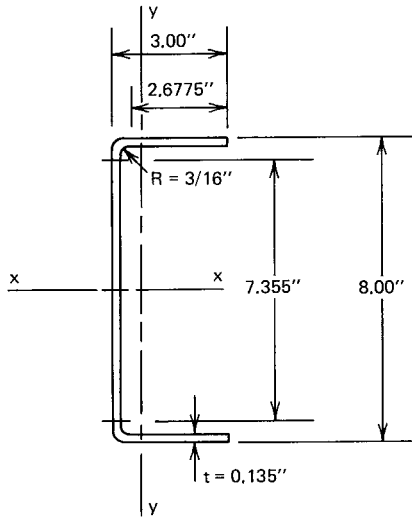
Figure 5.26 Example 5.3.

2. Use the ASD and LRFD methods to determine the design strengths if the load is applied through the centroid of the effective section.

Assume that $K_x L_x = K_y L_y = K_t L_t = 6$ ft. Use $F_y = 50$ ksi.

Solution

A. *ASD Method*

1. *Sectional Properties of Full Section.* By using the equations given in Part I of the AISI design manual or the methods discussed previously in this book, the following sectional properties can be computed:

$A = 1.824$ in.^{2} $m = 1.040$ in. $\beta = 0.7855$

$I_x = 17.26$ in.^{4} $J = 0.01108$ in.^{4}

$I_y = 1.529$ in.^{4} $C_w = 16.907$ in.^{6}

$r_x = 3.076$ in. $x_0 = 1.677$ in

$r_y = 0.916$ in. $r_0 = 3.622$ in

2. *Critical Unbraced Column Length L_{cr}.* The discussion of Art. 5.4.2 indicates that the critical unbraced column length that divides the flexural

and torsional–flexural buckling modes can be determined by either a graphic method or a theoretical solution as illustrated below.

a. *Graphic Method.* For the given channel section, the values of $\overline{b}/\overline{a}$, $\overline{c}/\overline{a}$, and $t/\overline{a}^2$ according to Fig. 5.12 are as follows:

$$\overline{a} = 8 - 0.135 = 7.865 \text{ in.}$$

$$\overline{b} = 3 - 0.135/2 = 2.9325 \text{ in.}$$

$$\overline{c} = 0$$

$$\frac{\overline{b}}{\overline{a}} = \frac{2.9325}{7.865} = 0.373$$

$$\frac{\overline{c}}{\overline{a}} = 0$$

$$\frac{t}{\overline{a}^2} = \frac{0.135}{(7.865)^2} = 0.0022$$

From Fig. 5.12, it can be seen that because the value of $t/\overline{a}^2$ is so small, it is difficult to obtain the accurate value of the critical length L_{cr} by using the graphic method.

b. *Theoretical Solution.* As shown in Fig. 5.7, and discussed in Art. 5.4.2, the critical length can be determined by solving the following equation:

$$P_y = (P_{cr})_3$$

$$= \frac{1}{2\beta} [(P_x + P_z) - \sqrt{(P_x + P_z)^2 - 4\beta P_x P_z}]$$

Since the same full area is to be used for computing P_y, P_x, and P_z, the following equation may also be used to determine L_{cr}:

$$\sigma_{ey} = \frac{1}{2\beta}[(\sigma_{ex} + \sigma_t) - \sqrt{(\sigma_{ex} + \sigma_t)^2 - 4\,\beta\sigma_{ex}\sigma_t}]$$

where

$$\sigma_{ey} = \frac{\pi^2 E}{(K_y L_y/r_y)^2} = \frac{\pi^2 (29{,}500)}{(L/0.916)^2}$$

$$\sigma_{ex} = \frac{\pi^2 E}{(K_x L_x/r_x)^2} = \frac{\pi^2 (29{,}500)}{(L/3.076)^2}$$

$$\sigma_t = \frac{1}{Ar_0^2}\left[GJ + \frac{\pi^2 EC_w}{(K_t L_t)^2}\right]$$

$$= \frac{1}{(1.824)(3.622)^2}\left[(11300)(0.01108)\right.$$

$$\left. + \frac{\pi^2(29500)(16.907)}{L^2}\right]$$

It should be noted that in the equations of σ_{ey}, σ_{ex}, and σ_t, $K_x L_x = K_y L_y = K_t L_t = L$. By solving the above equations, the critical length is 91.0 inches.

3. *Nominal and Allowable Loads*

   a. *Nominal Buckling Stress*, F_n. In view of the facts that the channel section is a singly symmetric section and that the given effective length of 72 in. is less than the computed critical length of 91 in., the nominal axial load for the given compression member should be governed by torsional–flexural buckling.

   In case that the critical length is not known, both flexural buckling and torsional–flexural buckling should be considered. The smaller value of the elastic flexural buckling stress and the elastic torsional–flexural buckling stress should be used to compute the nominal buckling stress, F_n.

   i. *Elastic Flexural Buckling Stress.* By using Eq. (5.56) of Section C4.1 of the AISI Specification, the elastic flexural buckling stress about *y*-axis can be computed as follows:

   $$K_y L_y / r_y = 6 \times 12/0.916 = 78.60 < 200 \qquad \text{O.K.}$$

   $$(F_e)_y = \frac{\pi^2 E}{(K_y L_y / r_y)^2} = \frac{\pi^2(29500)}{(78.600)^2} = 47.13 \text{ ksi}$$

   ii. *Elastic Torsional–Flexural Buckling Stress.* By using Eq. (5.57) of Sec. C4.2 of the AISI Specification, the elastic torsional–flexural buckling stress can be determined below.

   $$(F_e)_{TF} = \frac{1}{2\beta}\left[(\sigma_{ex} + \sigma_t) - \sqrt{(\sigma_{ex} + \sigma_t)^2 - 4\beta\sigma_{ex}\sigma_t}\right]$$

   where

   $$\sigma_{ex} = \frac{\pi^2 E}{(K_x L_x / r_x)^2} = \frac{\pi^2(29,500)}{(6 \times 12/3.076)^2}$$

   $$= 531.41 \text{ ksi}$$

$$\sigma_t = \frac{1}{Ar_0^2}\left[GJ + \frac{\pi^2 E C_w}{(K_t L_t)^2}\right]$$

$$= \frac{1}{(1.824)(3.622)^2}\left[(11300)(0.01108) + \frac{\pi^2(29500)(16.907)}{(6 \times 12)^2}\right]$$

$$= 44.92 \text{ ksi}$$

Substituting the values of β, σ_{ex}, and σ_t into the equation of $(F_e)_{TF}$, the elastic torsional–flexural buckling stress is

$$(F_e)_{TF} = 44.07 \text{ ksi} < (F_e)_y = 47.13 \text{ ksi}$$

$$\text{Use } F_e = 44.07 \text{ ksi}$$

$$\lambda_c = \sqrt{\frac{F_y}{F_e}} = \sqrt{\frac{50}{44.07}} = 1.065 < 1.5$$

From Eq. (5.54),

$$F_n = \left(0.658^{\lambda_c^2}\right)F_y = \left(0.658^{1.065^2}\right)(50) = 31.10 \text{ ksi}$$

b. *Effective Area, A_e*
   i. *Flange Elements*

$$w = 3 - (R + t) = 3 - (0.1875 + 0.135) = 2.6775 \text{ in}$$

$$w/t = 2.6775/0.135 = 19.83 < 60 \qquad \text{O.K.}$$

$$k = 0.43$$

$$\lambda = \frac{1.052}{\sqrt{k}}\left(\frac{w}{t}\right)\sqrt{\frac{f}{E}}$$

$$= \frac{1.052}{\sqrt{0.43}}(19.83)\sqrt{\frac{31.10}{29,500}}$$

$$= 1.033 > 0.673$$

$$\rho = \left(1 - \frac{0.22}{\lambda}\right)/\lambda = \left(1 - \frac{0.22}{1.033}\right)/1.033 = 0.762$$

$$b = \rho w = (0.762)(2.6775) = 2.040 \text{ in.}$$

ii. *Web Elements*

$$w = 8 - 2(R + t) = 8 - 2(0.1875 + 0.135) = 7.355 \text{ in.}$$

$$w/t = 7.355/0.135 = 54.48 < 500 \qquad \text{O.K.}$$

$$k = 4.0$$

$$\lambda = \frac{1.052}{\sqrt{4.0}} (54.48) \sqrt{\frac{31.10}{29,500}} = 0.930 > 6.673$$

$$\rho = \left(1 - \frac{0.22}{0.930}\right)/0.930 = 0.821$$

$$b = \rho w = (0.821)(7.355) = 6.038$$

The effective area is

$$A_e = A - [2(2.6775 - 2.040) + (7.355 - 6.038)](0.135)$$

$$= 1.824 - 0.350 = 1.474 \text{ in.}^2$$

c. *Nominal Axial Load for Column Buckling* (*Torsional–Flexural Buckling*)

$$P_n = A_e F_n = (1.474)(31.10) = 45.84 \text{ kips}$$

d. *Allowable Axial Load.* The allowable axial load for the ASD method is

$$P_a = P_n/\Omega_c = 45.84/1.80 = 25.47 \text{ kips}$$

B. LRFD Method
From Item (A) above, $P_n = 45.84$ kips. The design strength for the LRFD method is

$$\phi_c P_n = (0.85)(45.84) = 38.96 \text{ kips}$$

5.10   WALL STUDS

It is well known that column strength can be increased considerably by using adequate bracing, even though the bracing is relatively flexible. This is particularly true for those sections generally used as load-bearing wall studs which have large I_x/I_y ratios.

Cold-formed I-, Z-, channel, or box-type studs are generally used in walls with their webs placed perpendicular to the wall surface. The walls may be

made of different materials, such as fiber board, pulp board, plywood, or gypsum board. If the wall material is strong enough and there is adequate attachment provided between wall material and studs for lateral support of the studs, then the wall material can contribute to the structural economy by increasing the usable strength of the studs substantially (Fig. 5.27).

In order to determine the necessary requirements for adequate lateral support of the wall studs, theoretical and experimental investigations were conducted in the 1940s by Green, Winter, and Cuykendall.[5.68] The study included 102 tests on studs and 24 tests on a variety of wall material. It was found that in order to furnish the necessary support to the studs, the assembly must satisfy the following three requirements:

1. The spacing between attachments must be close enough to prevent the stud from buckling in the direction of the wall between attachments.
2. The wall material must be rigid enough to minimize deflection of the studs in the direction of the wall.
3. The strength of the connection between wall material and stud must be sufficient to develop a lateral force capable of resisting buckling without failure of the attachment.

Based on the findings of this earlier investigation, specific AISI provisions were developed for the design of wall studs.
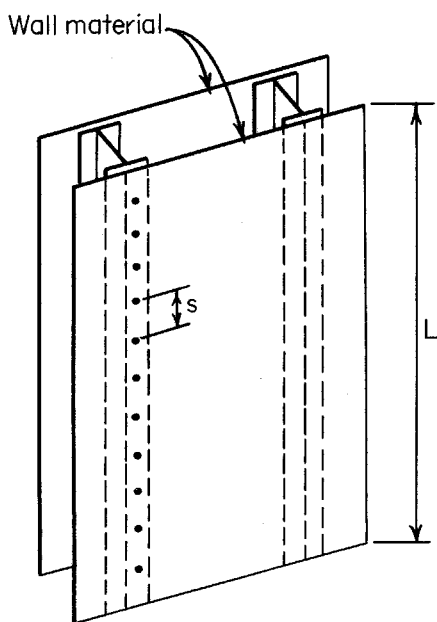
Figure 5.27   Wall studs.

In the 1970s, the structural behavior of columns braced by steel diaphragms was a special subject investigated at Cornell University and other institutions. The renewed investigation of wall-braced studs has indicated that the bracing provided for studs by steel panels is of the shear diaphragm type rather than the linear spring type, which was considered in the 1947 study. Consequently the AISI design criteria for wall studs were revised in 1980 to reflect the research findings. The same provisions were retained in the 1986 edition of the AISI Specification except that some editorial changes were made according to the unified design approach. In 1989, AISI issued an Addendum to the 1986 edition of the specification, which states that the wall stud may be designed either for a bare stud alone or for a structural assembly on the basis that sheathing (attached to one or both sides of the stud) furnishes adequate lateral support to the stud in the plane of the wall and rotational support. In addition, the 1989 Addendum moves the design limitations from the Commentary to the Specification and permits stub column tests and/or rational analysis for design of studs with perforations. In 1996, extensive revisions were made to permit the use of wall studs having either solid or perforated web. Specific limitations are included in the Specification for the size and spacing of perforations. Details of the present AISI requirements for the design of load-bearing wall studs are presented in Art. 9.3 following a general discussion of shear diaphragms.

For nonbearing wall studs, the member withstands only uniformly distributed wind loads or other lateral force. Therefore the studs used for exterior nonbearing wall construction should be designed as flexural members, for which consideration should be given to both strength and deflection requirements. This means that if the unsupported height and spacing of studs and the wind loads are given, the required sectional properties can be determined by the required bending strength of the section and the deflection limitations.

5.11   ADDITIONAL INFORMATION ON COMPRESSION MEMBERS

During past years, additional analytical and experimental studies have been conducted by many investigators. References 5.69 through 5.92 report on the research findings on doubly symmetric sections, box sections, channels, Z-sections, and multicell plate columns. The strength evaluation and design of cold-formed steel columns are discussed in Refs. 5.93 through 5.99. References 5.116 through 5.140 report on the recent studies on compression members. Additional publications can be found from other conference proceedings and engineering journals.

6 Combined Axial Load and Bending

6.1 GENERAL REMARKS

Structural members are often subject to combined bending and axial load either in tension or in compression. In the 1996 edition of the AISI Specification, the design provisions for combined axial load and bending were expanded to include specific requirements in Sec. C5.1 for the design of cold-formed steel structural members subjected to combined tensile axial load and bending.

When structural members are subject to combined compressive axial load and bending, the design provisions are given in Sec. C5.2 of the AISI Specification. This type of member is usually referred to as a *beam-column*. The bending may result from eccentric loading (Fig. 6.1*a*), transverse loads (Fig. 6.1*b*), or applied moments (Fig. 6.1*c*). Such members are often found in framed structures, trusses, and exterior wall studs. In steel structures, beams are usually supported by columns through framing angles or brackets on the sides of the columns. The reactions of beams can be considered as eccentric loading, which produces bending moments.

The structural behavior of beam-columns depends on the shape and dimensions of the cross section, the location of the applied eccentric load, the column length, the condition of bracing, and so on. For this reason, previous editions of the AISI Specification have subdivided design provisions into the following four cases according to the configuration of the cross section and the type of buckling mode:[1.4]

1. Doubly symmetric shapes and shapes not subject to torsional or torsional–flexural buckling.
2. Locally stable singly symmetric shapes or intermittently fastened components of built-up shapes, which may be subject to torsional–flexural buckling, loaded in the plan of symmetry.
3. Locally unstable symmetric shapes or intermittently fastened components of built-up shapes, which may be subject to torsional–flexural buckling, loaded in the plan of symmetry.
4. Singly symmetric shapes which are unsymmetrically loaded.
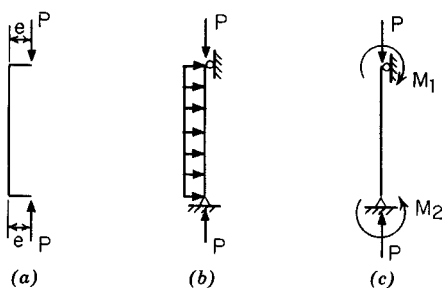
Figure 6.1   Beam-columns. (*a*) Subject to eccentric loads. (*b*) Subject to axial and transverse loads. (*c*). Subject to axial loads and end moments.

The early AISI design provisions for singly symmetric sections subjected to combined compressive load and bending were based on an extensive investigation of torsional–flexural buckling of thin-walled sections under eccentric load conducted by Winter, Pekoz, and Celibi at Cornell University.[5.66,6.1] The behavior of channel columns subjected to eccentric loading has also been studied by Rhodes, Harvey, and Loughlan.[5.34,6.2–6.5]

In 1986, as a result of the unified approach, Pekoz indicated that both locally stable and unstable beam-columns can be designed by the simple, well-known interaction equations as included in Sec. C5 of the AISI Specification. The justification of the current design criteria is given in Ref. 3.17. The 1996 design criteria were verified by Pekoz and Sumer using the available test results.[5.103]

6.2   COMBINED TENSILE AXIAL LOAD AND BENDING

6.2.1   Tension Members

For the design of tension members using hot-rolled steel shapes and built-up members, the AISC Specifications[1.148,3.150] provide design provisions for the following three limit states: (1) yielding of the full section between connections, (2) fracture of the effective net area at the connection, and (3) block shear fracture at the connection.

For cold-formed steel design, Sec. C2 of the 1996 AISI Specification gives Eq. (6.1) for calculating the nominal tensile strength of axially loaded tension members, with a safety factor for the ASD method and a resistance factor for the LRFD method as follows:

$$T_n = A_n F_y \tag{6.1}$$

$$\Omega_t = 1.67 \text{ (for ASD)}$$

$$\phi_t = 0.95 \text{ (for LRFD)}$$

where T_n = nominal tensile strength
$\quad\quad A_n$ = net area of the cross section
$\quad\quad F_y$ = design yield stress

In addition, the nominal tensile strength is also limited by Sec. E.3.2 of the Specification for tension in connected parts.

When a tension member has holes, stress concentration may result in a higher tensile stress adjacent to a hole to be about three times the average stress on the net area.[6.36] With increasing load and plastic stress redistribution, the stress in all fibers on the net area will reach to the yield stress as shown in Fig. 6.2. Consequently, the AISI Specification has used Eq. (6.1) for determining the maximum tensile capacity of axially loaded tension members since 1946. This AISI design approach differs significantly from the AISC design provisions, which consider yielding of the gross cross-sectional area, fracture of the effective net area, and block shear. The reason for not considering the fracture criterion in the 1996 AISI Specification is mainly due to the lack of research data relative to the shear lag effect on tensile strength of cold-formed steel members.

In 1995, the influence of shear lag on the tensile capacity of bolted connections in cold-formed steel angles and channels was investigated at the University of Missouri-Rolla. Design equations are recommended in Refs. 6.23 through 6.25 for computing the effective net area. This design information enables the consideration of fracture strength at connections for angles and channels. The same study also investigated the tensile strength of staggered bolt patterns in flat sheet connections.

On the basis of the results of recent research, Sec. C2 of the Specification was revised in 1999. The AISI Supplement to the Specification includes the following revised provisions for the design of axially loaded tension members:
[1.333]

C2 Tension Members

For axially loaded tension members, the nominal tensile strength, T_n, shall be the smaller value obtained according to the limit states of (a) yielding in the gross section, (b) fracture in the net section away from connections, and (c) fracture in the effective net section at the connections:
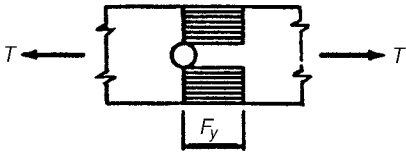
Figure 6.2   Stress distribution for nominal tensile strength.

(a) For yielding:

$$T_n = A_g F_y \tag{6.2}$$

$$\Omega_t = 1.67 \text{ (ASD)}$$

$$\phi_t = 0.90 \text{ (LRFD)}$$

(b) For fracture away from the connection:

$$T_n = A_n F_u \tag{6.3}$$

$$\Omega_t = 2.00 \text{ (ASD)}$$

$$\phi_t = 0.75 \text{ (LRFD)}$$

where T_n = nominal strength of member when loaded in tension
A_g = gross area of cross section
A_n = net area of cross section
F_y = yield stress as specified in Section A7.1
F_u = tensile strength as specified in Section A3.1 or A3.3.2

(c) For fracture at the connection:

The nominal tensile strength shall also be limited by Sections E2.7, E.3, and E4 for tension members using welded connections, bolted connections, and screw connections, respectively.

From the above requirements, it can be seen that the nominal tensile strength of axially loaded cold-formed steel members is determined either by yielding of gross sectional area or by fracture of the net area of the cross section. At connections, the nominal tensile strength is also limited by the capacities determined in accordance with Specification Sections E2.7, E3, and E4 for tension in connected parts. In addition to the strength consideration, yielding in the gross section also provides a limit on the deformation that a tension member can achieve.

6.2.2   Members Subjected to Combined Tensile Axial Load and Bending

When cold-formed steel members are subject to concurrent bending and tensile axial load, the member shall satisfy the following AISI interaction equations prescribed in Sec. C5.1 of the Specification for the ASD and LRFD methods:

C5.1 Combined Tensile Axial Load and Bending

C5.1.1 ASD Method

The required strengths T, M_x, and M_y shall satisfy the following interaction equations:

$$\frac{\Omega_b M_x}{M_{nxt}} + \frac{\Omega_b M_y}{M_{nyt}} + \frac{\Omega_t T}{T_n} \leq 1.0 \qquad (6.4a)$$

and

$$\frac{\Omega_b M_x}{M_{nx}} + \frac{\Omega_b M_y}{M_{ny}} - \frac{\Omega_t T}{T_n} \leq 1.0 \qquad (6.4b)$$

where T = required tensile axial strength
   T_n = nominal tensile axial strength determined in accordance with Sec. C2 (or Art. 6.2.1)
   M_x, M_y = required flexural strengths with respect to the centroidal axes of the section
   M_{nx}, M_{ny} = nominal flexural strengths about the centroidal axes determined in accordance with Sec. C3 (or Ch. 4)
   M_{nxt}, M_{nyt} = $S_{ft}F_y$
   S_{ft} = section modulus of the full section for the extreme tension fiber about the appropriate axis
   Ω_b = 1.67 for bending strength (Sec. C3.1.1) or for laterally unbraced beams (Sec. C3.1.2.1)
   Ω_t = 1.67

C5.1.2 LRFD Method

The required strengths T_u, M_{ux}, and M_{uy} shall satisfy the following interaction equations:

$$\frac{M_{ux}}{\phi_b M_{nxt}} + \frac{M_{uy}}{\phi_b M_{nyt}} + \frac{T_u}{\phi_t T_n} \leq 1.0 \qquad (6.5a)$$

$$\frac{M_{ux}}{\phi_b M_{nx}} + \frac{M_{uy}}{\phi_b M_{ny}} - \frac{T_u}{\phi_t T_n} \leq 1.0 \qquad (6.5b)$$

where T_u = required tensile axial strength
   M_{ux}, M_{uy} = required flexural strengths with respect to the centroidal axes
   ϕ_b = 0.90 or 0.95 for bending strength (Sec. C3.1.1), or 0.90 for laterally unbraced beams (Sec. C3.1.2.1)
   ϕ_t = 0.95
T_n, M_{nx}, M_{ny}, M_{nxt}, M_{nyt}, and S_{ft} are defined in Sec. C5.1.1.

In the AISI Specification, Eq. (6.4a) serves as an ASD design criterion to prevent yielding of the tension flange of the member subjected to combined

tensile axial load and bending. Equation (6.4*b*) provides a requirement to prevent failure of the compression flange.

For the LRFD method, Eqs. (6.5*a*) and (6.5*b*) are used to prevent the failure of the tension flange and compression flange, respectively.

6.3   COMBINED COMPRESSIVE AXIAL LOAD AND BENDING (BEAM-COLUMNS)

6.3.1   Shapes Not Subjected to Torsional or Torsional–Flexural Buckling[1.161]

When a doubly symmetric open section is subject to axial compression and bending about its minor axis, the member may fail flexurally at the location of the maximum moment by either yielding or local buckling. However, when the section is subject to an eccentric load that produces a bending moment about its major axis, the member may fail flexurally or in a torsional–flexural mode because the eccentric load does not pass through the shear center.

For torsionally stable shapes, such as closed rectangular tubes, when the bending moment is applied about the minor axis, the member may fail flexurally in the region of maximum moment, but when the member is bent about its major axis, it can fail flexurally about the major or minor axis, depending on the amount of eccentricities.

If a doubly symmetric I-section is subject to an axial load P and end moments M, as shown in Fig. 6.3*a*, the combined axial and bending stress in compression is given in Eq. (6.6) as long as the member remains straight:

$$f = \frac{P}{A} + \frac{Mc}{I} = \frac{P}{A} + \frac{M}{S}$$
$$= f_a + f_b$$

(6.6)

where f = combined stress in compression
f_a = axial compressive stress
f_b = bending stress in compression

(a)   (b)
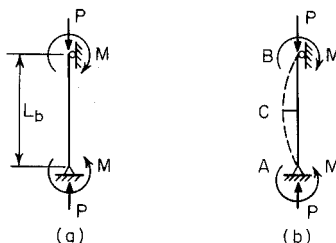
Figure 6.3   Beam-column subjected to axial loads and end moments.

P = applied axial load
A = cross-sectional area
M = bending moment
c = distance from neutral axis to extreme fiber
I = moment of inertia
S = section modulus

It should be noted that in the design of such a beam-column using the ASD method, the combined stress should be limited by certain allowable stress F, that is,

$$f_a + f_b \leq F \qquad (6.7)$$

or

$$\frac{f_a}{F} + \frac{f_b}{F} \leq 1.0$$

As discussed in Chaps. 3, 4, and 5, the safety factor for the design of compression members is different from the safety factor for beam design. Therefore Eq. (6.7) may be modified as follows:

$$\frac{f_a}{F_a} + \frac{f_b}{F_b} \leq 1.0 \qquad (6.8)$$

where F_a = allowable stress for design of compression members
F_b = allowable stress for design of beams

If the strength ratio is used instead of the stress ratio, Eq. (6.8) can be rewritten as follows:

$$\frac{P}{P_a} + \frac{M}{M_a} \leq 1.0 \qquad (6.9)$$

where P = applied axial load = Af_a
P_a = allowable axial load = AF_a
M = applied moment = Sf_b
M_a = allowable moment = SF_b

Equation (6.9) is a well-known interaction formula which has been adopted in some ASD specifications for the design of beam-columns. It can be used with reasonable accuracy for short members and members subjected to a relatively small axial load. It should be realized that in practical application, when end moments are applied to the member, it will be bent as shown in Fig. 6.3b due to the applied moment M and the secondary moment resulting

from the applied axial load P and the deflection of the member. The maximum bending moment of midlength (point C) can be represented by

$$M_{max} = \Phi M \tag{6.10}$$

where M_{max} = maximum bending moment at midlength
$\quad\quad M$ = applied end moments
$\quad\quad \Phi$ = amplification factor.

It can be shown that the amplification factor Φ may be computed by[1.161,2.45]

$$\Phi = \frac{1}{1 - P/P_e} \tag{6.11}$$

where P_e = elastic column buckling load (Euler load), = $\pi^2 EI/(KL_b)^2$.
Applying a safety factor Ω_c to P_e, Eq. (6.11) may be rewritten as

$$\Phi = \frac{1}{1 - \Omega_c P/P_e} \tag{6.12}$$

If we use the maximum bending moment M_{max} to replace M, the following interaction formula [Eq. (6.13)] can be obtained from Eqs. (6.9) and (6.12):

$$\frac{P}{P_a} + \frac{\Phi M}{M_a} \le 1.0$$

or $\tag{6.13}$

$$\frac{P}{P_a} + \frac{M}{(1 - \Omega_c P/P_e)M_a} \le 1.0$$

It has been found that Eq. (6.13), developed for a member subjected to an axial compressive load and equal end moments, can be used with reasonable accuracy for braced members with unrestrained ends subjected to an axial load and a uniformly distributed transverse load. However, it could be conservative for compression members in unbraced frames (with sidesway), and for members bent in reverse curvature. For this reason, the interaction formula given in Eq. (6.13) should be further modified by a coefficient C_m, as shown in Eq. (6.14), to account for the effect of end moments:

$$\frac{P}{P_a} + \frac{C_m M}{(1 - \Omega_c P/P_e)M_a} \le 1.0 \tag{6.14}$$

In Eq. (6.14) C_m can be computed by Eq. (6.15) for restrained compression members braced against joint translation and not subject to transverse loading:

$$C_m = 0.6 - 0.4 \frac{M_1}{M_2} \tag{6.15}$$

where M_1/M_2 is the ratio of smaller to the larger end moments.

When the maximum moment occurs at braced points, Eq. (6.16) should be used to check the member at the braced ends.

$$\frac{P}{P_{a0}} + \frac{M}{M_a} \leq 1.0 \tag{6.16}$$

where P_{a0} is the allowable axial load for $KL/r = 0$.

Furthermore, for the condition of small axial load, the influence of $C_m/ (1 - \Omega_c P/P_e)$ is usually small and may be neglected. Therefore when $P \leq 0.15 P_a$, Eq. (6.9) may be used for the design of beam-columns.

The interaction relations between Eqs. (6.9), (6.14), and (6.16) are shown in Fig. 6.4. If C_m is unity, Eq. (6.14) controls over the entire range.

Substituting $P_a = P_n/\Omega_c$, $P_{ao} = P_{no}/\Omega_c$, and $M_a = M_n/\Omega_b$ into Eqs. (6.9), (6.14), and (6.16), the AISI interaction equations for the ASD method (Sec. C5.2.1 of the Specification, can be obtained. Similarly, the interaction equa-
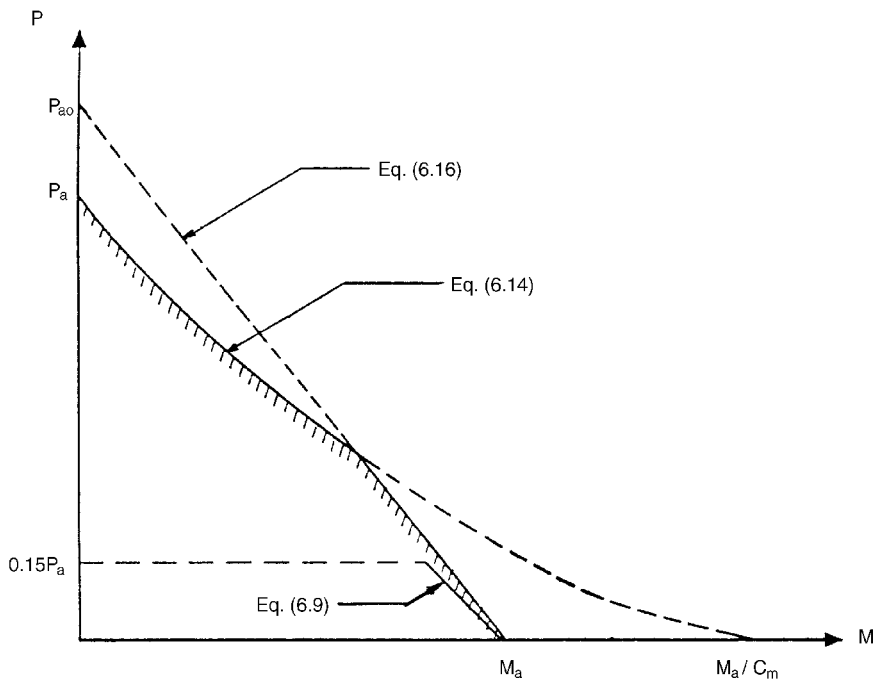
Figure 6.4 Interaction relations for the ASD method.

tions for the LRFD method (Sec. C5.2.2 of the Specification) can be obtained by using P_u, M_u, $\phi_c P_n$, and $\phi_b M_n$.

6.3.2 Open Sections That May Be Subject to Torsional–Flexural Buckling[5.66,6.1]

When singly symmetric and nonsymmetric open sections are used as beam-columns, these members may be subject to torsional–flexural buckling. The following discussion is based primarily on Ref. 6.1.

The differential equations of equilibrium governing the elastic behavior of such members are given in Eqs. (6.17) to (6.19):[3.2]

$$EI_x v^{iv} + Pv'' - Px_0 \phi'' + M_y \phi'' = 0 \tag{6.17}$$

$$EI_y u^{iv} + Pu'' + Py_0 \phi'' - M_x \phi'' = 0 \tag{6.18}$$

$$EC_w \phi^{iv} - GJ\phi'' + (Pr_0^2 + \beta_x M_x + \beta_y M_y)\phi''$$
$$+ Py_0 u'' - Px_0 v'' - M_x u'' + M_y v'' = 0 \tag{6.19}$$

where I_x = moment of inertia about x-axis, in.^{4}
I_y = moment of inertia about y-axis, in.^{4}
u = lateral displacement in x direction, in.
v = lateral displacement in y direction, in.
ϕ = angle of rotation, rad
x_0 = x-coordinate of shear center, in.
y_0 = y-coordinate of shear center, in.
E = modulus of elasticity, = 29.5×10^3 ksi (203 GPa)
G = shear modulus, = 11.3×10^3 ksi (78 GPa)
J = St. Venant torsion constant of cross section, in.^{4}, $\frac{1}{3} \Sigma l_i t_i^3$
C_w = warping constant of torsion of cross section, in.^{6} (Appendix B)
r_0 = polar radius of gyration of cross section about shear center, = $\sqrt{I_0/A} = \sqrt{r_x^2 + r_y^2 + x_0^2 + y_0^2}$
P = applied concentric load, kips
M_x, M_y = bending moments about x- and y-axes, respectively, in.-kips

and

$$\beta_x = \frac{1}{I_x} \int_A y(x^2 + y^2) \, dA - 2y_0 \tag{6.20}$$

$$\beta_y = \frac{1}{I_y} \int_A x(x^2 + y^2) \, dA - 2x_0 \qquad \text{(see Appendix C)} \tag{6.21}$$

All primes are differentiations with respect to the z-axis.

Assume that the end moments M_x and M_y are due to the eccentric loads applied at both ends of the column with equal biaxial eccentricities e_y and e_x (Fig. 6.5). Then the moments M_x and M_y can be replaced by

$$M_x = Pe_y \tag{6.22}$$

$$M_y = Pe_x \tag{6.23}$$

Consequently, Eqs. (6.17) to (6.19) can be rewritten as

$$EI_x v^{iv} + Pv'' - Pa_x \phi'' = 0 \tag{6.24}$$

$$EI_y u^{iv} + Pu'' + Pa_y \phi'' = 0 \tag{6.25}$$

$$EC_w \phi^{iv} + (P\bar{r}_0^2 - GJ)\phi'' + Pa_y u'' - Pa_x v'' = 0 \tag{6.26}$$

where

$$a_x = x_0 - e_x \tag{6.27}$$

$$a_y = y_0 - e_y \tag{6.28}$$

$$\bar{r}_0^2 = \beta_x e_y + \beta_y e_x + \frac{I_0}{A} \tag{6.29}$$

The solution of Eqs. (6.24) to (6.26) is shown in Eq. (6.30) by using Galerkin's method:
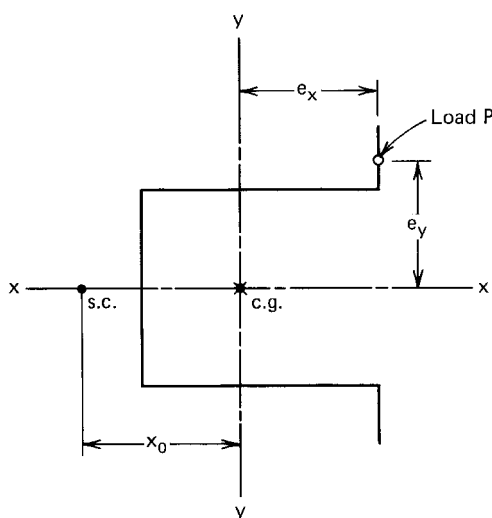
Figure 6.5 Unsymmetrically loaded hat section.

$$\begin{bmatrix} P_{ey} - P & 0 & -Pa_yK'_{13} \\ 0 & P_{ex} - P & Pa_xK'_{23} \\ -Pa_yK'_{31} & Pa_xK'_{32} & \bar{r}_0^2(P_{ex} - P) \end{bmatrix} \begin{Bmatrix} u_0 \\ v_0 \\ \phi_0 \end{Bmatrix} = \begin{Bmatrix} -\dfrac{P^2}{P_{ey}} e_xK_1 \\ -\dfrac{P^2}{P_{ex}} e_yK_2 \\ -P^2 \left(\dfrac{a_ye_x}{P_{ey}} - \dfrac{a_xe_y}{P_{ex}} \right) K_3 \end{Bmatrix}$$

$$(6.30)$$

where

$$P_{ey} = K_{11} \frac{\pi^2 EI_y}{L^2} \tag{6.31}$$

$$P_{ex} = K_{22} \frac{\pi^2 EI_x}{L^2} \tag{6.32}$$

$$P_{ez} = \frac{1}{\bar{r}_0^2} \left(K_{33}EC_w \frac{\pi^2}{L^2} + GJ \right) \tag{6.33}$$

u_0, v_0, and ϕ_0 are coefficients for deflection components. The coefficients K for various boundary conditions are listed in Table 6.1.

6.3.3 Singly Symmetric Open Shapes

Channels, angles, and hat sections are some of the singly symmetric open shapes. If these members are subject to bending moments in the plane of symmetry (x-axis as shown in Fig. 5.6), they may fail in one of the following two ways:*

1. The member deflects gradually in the plane of symmetry without twisting and finally fails by yielding or local buckling at the location of maximum moment.
2. The member starts with a gradual flexural bending in the plane of symmetry, but when the load reaches a critical value, the member will suddenly buckle by torsional–flexural buckling.

The type of failure mode, which will govern the maximum strength of the member, depends on the shape and dimensions of the cross section, the column length, and the eccentricity of the applied load.

---

*If twisting is prevented by properly designed bracing, the member will fail only flexurally by yielding or local buckling. When the bending moment is applied in any plane other than the plane of symmetry, the member will fail in the torsional-flexural buckling mode.

TABLE 6.1 Coefficients $K^{6.1}$

Boundary Conditions at $z = 0, L$	K_{11}	K_{22}	K_{33}	K_1	K_2	K_3	K'_{13}	K'_{31}	K'_{23}	K'_{32}	K_{23}
$u'' = v'' = \phi'' = 0$	1.0000	1.0000	1.0000	1.2732	1.2732	1.2732	1.0000	1.0000	1.0000	1.0000	1.0000
$u'' = v' = \phi'' = 0$	1.0000	4.1223	1.0000	1.2732	$\cdots$	1.2732	1.0000	1.0000	0.5507	1.4171	0.8834
$u' = v' = \phi'' = 0$	4.1223	4.1223	1.0000	$\cdots$	$\cdots$	1.2732	0.5507	1.4171	0.5507	1.4171	0.8834
$u'' = v' = \phi' = 0$	1.0000	4.1223	4.1223	1.2732	$\cdots$	0.6597	1.4171	0.5507	1.0000	0.8834	1.0000
$u' = v' = \phi' = 0$	4.1223	4.1223	4.1223	$\cdots$	$\cdots$	0.6597	1.0000	1.0000	1.0000	1.0000	1.0000
$u'' = v'' = \phi' = 0$	1.0000	1.0000	4.1223	1.2732	1.2732	0.6597	1.4171	0.5507	1.4171	0.5507	0.8834

The structural behavior discussed above can be explained by the solution of differential equations [Eqs. (6.24) to (6.26)]. When the eccentric load is applied in the plane of symmetry of the section, as shown in Fig. 6.5a, $e_y = y_0 = 0$. Equation (6.30) can be changed to the following two formulas:

$$(P_{ey} - P)u_0 = -\frac{P^2}{P_{ey}} e_x K_1 \tag{6.34}$$

$$\begin{bmatrix} P_{ex} - P & Pa_x K'_{23} \\ Pa_x K'_{32} & \bar{r}_0^2(P_{ex} - P) \end{bmatrix} \begin{Bmatrix} v_0 \\ \phi_0 \end{Bmatrix} = 0 \tag{6.35}$$

in which Eq. (6.34) represents the behavior of a beam-column deforming flexurally without twist, and Eq. (6.35) is related to torsional–flexural buckling.

If flexural failure governs the maximum strength of the beam-column, the design of singly symmetric shapes is to be based on the interaction formulas similar to those used in Art. 6.3.1 for doubly symmetric shapes.

However, if the singly symmetric section fails in torsional–flexural buckling, the following critical buckling load can be determined by the equation derived from Eq. (6.35) by setting the determinant of the coefficient equal to zero:

$$P_{TF} = \frac{(P_{ex} + P_{ez}) \pm \sqrt{(P_{ex} + P_{ez})^2 - 4\bar{\beta} \, P_{ex}P_{ez}}}{2\bar{\beta}} \tag{6.36}$$

where

$$\bar{\beta} = 1 - \frac{(x_0 - e_x)^2}{\bar{r}_0^2} K_{23}^2 \tag{6.37}$$

For members having simply supported ends and subjected to concentric
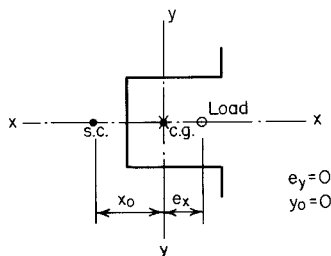
Figure 6.5a   Hat section subjected to an eccentric load in the plane of symmetry.

loading (that is, $e_x = 0$, $K_{23} = 1.0$), Eq. (6.36) can be changed to Eq. (6.38), which was used in Art. 5.4.2 for axially loaded compression members:

$$P_{TFO} = \frac{1}{2\beta} [(P_x + P_z) - \sqrt{(P_x + P_z)^2 - 4\beta P_x P_z} \qquad (6.38)$$

in which $\beta = 1 - (x_0/r_0)^2$ as previously defined in Chap. 5.

From Eq. (6.36) it can be seen that the computation of the torsional–flexural buckling load is too time-consuming for design use. A previous study made by Peköz, Celebi, and Winter indicated that the torsional–flexural buckling load may be computed by the following interaction formula if the load is applied on the side of the centroid opposite from that of the shear center.[6.1]

$$\frac{P_{TF}}{P_{TFO}} + \frac{P_{TF}e_x}{M_T} = 1.0 \qquad (6.39)$$

where P_{TF} = torsional–flexural buckling load for eccentric load having an eccentricity of e_x

P_{TFO} = torsional–flexural buckling load for concentric load [Eq. (6.38)]

M_T = critical moment causing tension on shear center side of centroid

In Eq. (6.39), if we apply the modification factor as given in Eq. (6.40)

$$\frac{C_{TF}}{1 - P_{TF}/P_e} \qquad (6.40)$$

to the moment $P_{TF}e_x$, as done previously in Art. 6.3.1, the interaction formula can be written as

$$\frac{P_{TF}}{P_{TFO}} + \frac{C_{TF}(P_{TF}e_x)}{(1 - P_{TF}/P_e)M_T} = 1.0 \qquad (6.41)$$

In the above equation, the factor C_{TF} is the same as C_m used in Art. 6.3.1.

Equation (6.41) can be used to determine the theoretical elastic torsional–flexural buckling load P_{TF} for singly symmetric sections under eccentric loads applied on the side of the centroid opposite from that of the shear center.

The critical moment M_T used in Eq. (6.41) can be obtained from the following equation:

$$M_T = -\frac{1}{2K_{23}^2} \left[\beta_y P_{ex} - \sqrt{(\beta_y P_{ex})^2 + 4K_{23}^2 \frac{P_{ex}P'_{ez}I_0}{A}} \right] \qquad (6.42)$$

where

$$P'_{ez} = P_{ez} \left(1 + \frac{e_x \beta_y A}{I_0} \right) \qquad (6.43)$$

$$K_{23} = \sqrt{K'_{23}K'_{32}} \qquad \text{(see Table 6.1)} \qquad (6.44)$$

For simply supported end conditions, Eq. (6.42) can be simplified and rearranged as

$$M_T = -P_{ex} \left[j - \sqrt{j^2 + r_0^2 \left(\frac{P_{ez}}{P_{ex}} \right)} \right] \qquad (6.45)$$

or

$$M_T = -A\sigma_{ex} \left(j - \sqrt{j^2 + r_0^2 \left(\frac{\sigma_t}{\sigma_{ex}} \right)} \right] \qquad (6.46)$$

where

$$j = \frac{\beta_y}{2} = \frac{1}{2I_y} \left(\int_A x^3 \, dA + \int_A xy^2 \, dA \right) - x_0 \qquad (6.47)$$

$$\sigma_{ex} = \frac{\pi^2 E}{(K_x L_x / r_x)^2} \qquad (6.48)$$

$$\sigma_t = \frac{1}{Ar_0^2} \left[GJ + \frac{\pi^2 E C_w}{(K_t L_t)^2} \right] \qquad (6.49)$$

If the eccentric load is applied on the side of the shear center opposite from that of the centroid, the critical moment causing compression on shear center side of centroid, M_c, can be computed as follows:

$$M_c = A\sigma_{ex} \left[j + \sqrt{j^2 + r_0^2 \left(\frac{\sigma_t}{\sigma_{ex}} \right)} \right] \qquad (6.50)$$

Both Eqs. (6.46) and (6.50) were used in Eq. (4.54) for determining the elastic critical moment for lateral buckling strength.

For the ASD method, the allowable load for torsional–flexural buckling in the elastic range can be derived from P_{TF} by using a safety factor of 1.80. The inelastic buckling stress can be computed by the equation that was used for torsional–flexural buckling of axially loaded compression members (Chap. 5).

So far we have discussed the possible failure modes for a singly symmetric section under eccentric load. However, the type of failure that will govern the maximum strength of the beam-column depends on which type of failure falls below the other for the given eccentricity. This fact can be shown in Fig. 6.6a. For the given hat section having $L/r_x = 90$, the section will fail in flexural yielding if the load is applied in region I. Previous study has indicated that for channels, angles, and hat sections, the section always fails in flexural yielding when the eccentricity is in region I (that is, $e_x < -x_0$). When the eccentricity is in region III (that is, $0 < e_x$), the section can fail either in flexural yielding or in torsional–flexural buckling. Therefore, both conditions (flexural yielding and torsional–flexural buckling) should be checked. For the given hat section shown in Fig. 6.6a, when the load is applied at the center of gravity, the section will buckle torsional-flexurally at a load P_{TFO} that is smaller than the flexural buckling load P_{ey}. At a certain eccentricity in region II (that is, $-x_0 < e_x < 0$), the failure mode changes from torsional–flexural buckling to simple flexural failure. It can also be seen that in this region, small changes in eccentricity result in large changes in failure load. Thus any small inaccuracy in eccentricity could result in nonconservative designs.

For bending about the axis of symmetry (i.e., when the eccentric load is applied along the y-axis as shown in Fig. 6.7), the following equation for determining the elastic critical moment can be derived from Eq. (6.30) on the basis of $e_x = 0$, $e_y \neq 0$, $P = 0$, and $Pe_y = M_x$:[6.1]

$$M_x = r_0\sqrt{P_{ey}P_{ez}}$$
$$= r_0 A\sqrt{\sigma_{ey}\sigma_t} \tag{6.51}$$

For the case of unequal end moments, Eq. (6.51) may be modified by multiplying by a bending coefficient C_b as follows:

$$M_x = C_b r_0 A\sqrt{\sigma_{ey}\sigma_t} \tag{6.52}$$

The above equation was used in Eq. (4.51) for lateral buckling strength consideration.

6.4   AISI DESIGN CRITERIA

The following are the AISI design provisions included in Sec. C5.2 of the 1996 edition of the AISI Specification for the design of beam-columns:
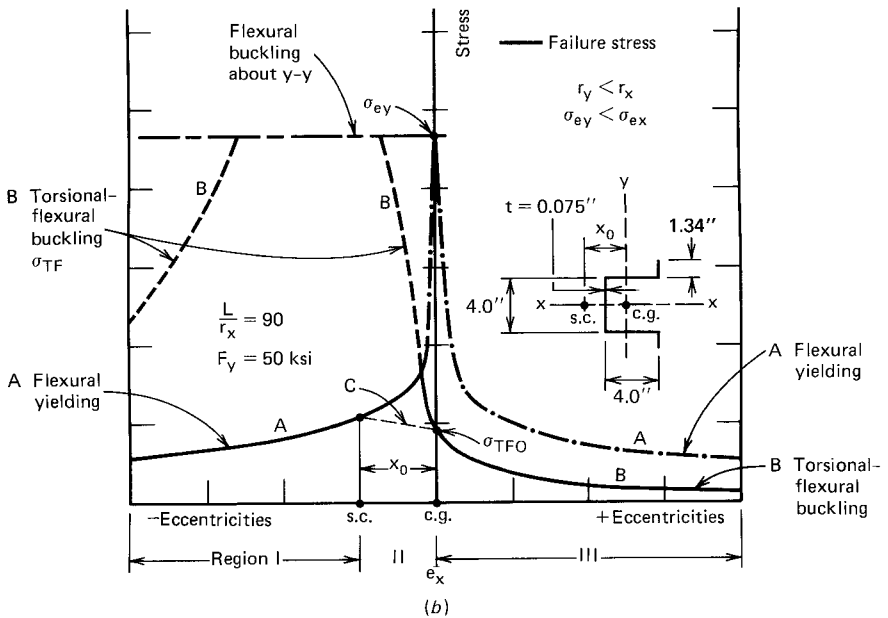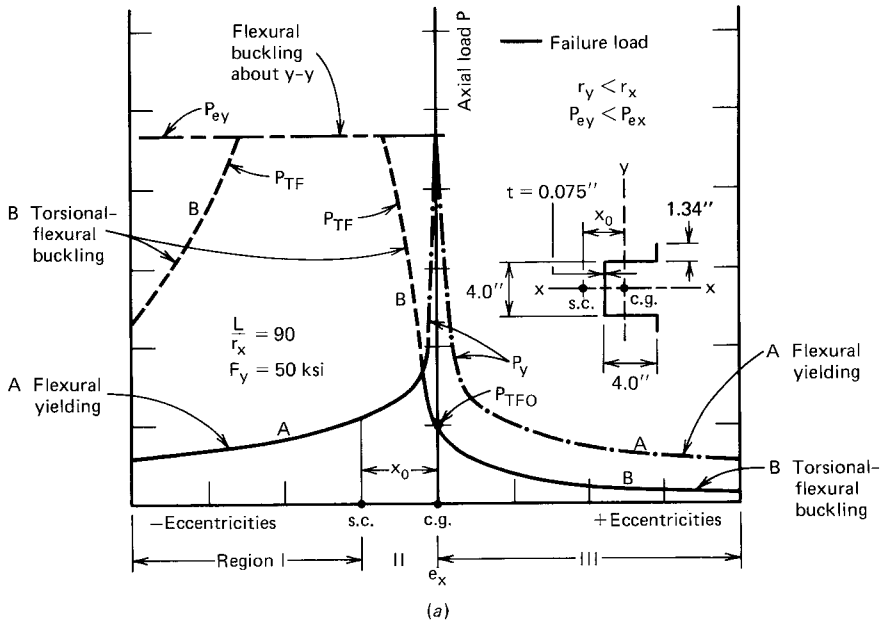
Figure 6.6 Strength of eccentrically loaded hat section.[6.1] (*a*) Load vs. e_x. (*b*) Stress vs. e_x.
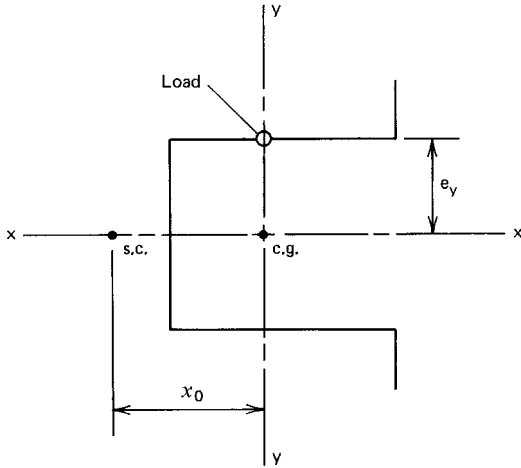
Figure 6.7   Hat section subjected to an eccentric load applied along the *y*-axis.

C5.2 Combined Compressive Axial Load and Bending

C5.2.1 ASD Method

The required strengths P, M_x, and M_y shall satisfy the following interaction equations:

$$\frac{\Omega_c P}{P_n} + \frac{\Omega_b C_{mx} M_x}{M_{nx} \alpha_x} + \frac{\Omega_b C_{my} M_y}{M_{ny} \alpha_y} \le 1.0 \tag{6.53}$$

$$\frac{\Omega_c P}{P_{no}} + \frac{\Omega_b M_x}{M_{nx}} + \frac{\Omega_b M_y}{M_{ny}} \le 1.0 \tag{6.54}$$

When $\Omega_c P / P_n \le 0.15$ the following equation may be used in lieu of the above two equations:

$$\frac{\Omega_c P}{P_n} + \frac{\Omega_b M_x}{M_{nx}} + \frac{\Omega_b M_y}{M_{ny}} \le 1.0 \tag{6.55}$$

where P = required compressive axial strength

M_x, M_y = required flexural strength with respect to the centroidal axes of the effective section determined for the required compressive axial strength alone. For angle sections, M_y shall be taken either as the required flexural strength or the required flexural strength plus $PL/1000$, whichever results in a lower permissible value of P.

P_n = nominal axial strength determined in accordance with Sec. C4

P_{no} = nominal axial strength determined in accordance with Sec. C4, with $F_n = F_y$

M_{nx}, M_{ny} = nominal flexural strength about the centroidal axes determined in accordance with Sec. C3

$$\alpha_x = 1 - \frac{\Omega_c P}{P_{Ex}} \tag{6.56}$$

$$\alpha_y = 1 - \frac{\Omega_c P}{P_{Ey}} \tag{6.57}$$

$$P_{Ex} = \frac{\pi^2 E I_x}{(K_x L_x)^2} \tag{6.58}$$

$$P_{Ey} = \frac{\pi^2 E I_y}{(K_y L_y)^2} \tag{6.59}$$

Ω_b = 1.67 for bending strength (Sec. C3.1.1) or for laterally unbraced beams (Sec. C3.1.2)

Ω_c = 1.80

I_x = moment of inertia of the full, unreduced cross section about the x-axis

I_y = moment of inertia of the full, unreduced cross section about the y-axis

L_x = actual unbraced length for bending about the x-axis

L_y = actual unbraced length for bucking about the y-axis

K_x = effective length factor for buckling about the x-axis

K_y = effective length factor for buckling about the y-axis

C_{mx}, C_{my} = coefficients whose value shall be taken as follows:

1. For compression members in frames subject to joint translation (sidesway)

$$C_m = 0.85$$

2. For restrained compression members in frames braced against joint translation and not subject to transverse loading between their supports in the plane of bending

$$C_m = 0.6 - 0.4 \, (M_1/M_2) \tag{6.60}$$

M_1/M_2 is the ratio of the smaller to the larger moment at the ends of that portion of the member under consideration which is unbraced in the plane of bending. M_1/M_2 is positive when the member is bent in reverse curvature and negative when it is bent in single curvature.

3. For compression members in frames braced against joint translation in the plane of loading and subject to transverse loading between their supports, the value of C_m may be determined by rational analysis. However, in lieu of such analysis, the following values may be used:

(a) for members whose ends are restrained, $C_m = 0.85$

(b) for members whose ends are unrestrained, $C_m = 1.0$

C5.2.2 LRFD Method

The required strengths P_u, M_{ux}, M_{uy}, shall satisfy the following interaction equations:

$$\frac{P_u}{\phi_c P_n} + \frac{C_{mx} M_{ux}}{\phi_b M_{nx} \alpha_x} + \frac{C_{my} M_{uy}}{\phi_b M_{ny} \alpha_y} \le 1.0 \tag{6.61}$$

$$\frac{P_u}{\phi_c P_{no}} + \frac{M_{ux}}{\phi_b M_{nx}} + \frac{M_{uy}}{\phi_b M_{ny}} \le 1.0 \tag{6.62}$$

When $P_u / \phi_c P_n \le 0.15$, the following equation may be used in lieu of the above two equations:

$$\frac{P_u}{\phi_c P_n} + \frac{M_{ux}}{\phi_b M_{nx}} + \frac{M_{uy}}{\phi_b M_{ny}} \le 1.0 \tag{6.63}$$

where P_u = required compressive axial strength

M_{ux}, M_{uy} = required flexural strengths with respect to the centroidal axes of the effective section determined for the required compressive axial strength alone. For angle sections, M_{uy} shall be taken either as the required flexural strength or the required flexural strength plus $P_u L / 1000$, whichever results in a lower permissible value of P_u.

$$\alpha_x = 1 - \frac{P_u}{P_{Ex}} \tag{6.64}$$

$$\alpha_y = 1 - \frac{P_u}{P_{Ey}} \tag{6.65}$$

ϕ_b = 0.90 or 0.95 for bending strength (Sec. C3.1.1), or 0.90 for laterally unbraced beams (Sec. C3.1.2)

ϕ_c = 0.85
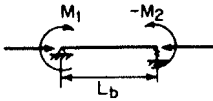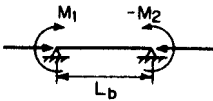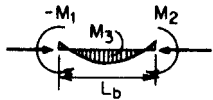
P_n, P_{no}, M_{nx}, M_{ny}, P_{Ex}, P_{Ey}, I_x, I_y, L_x, L_y, K_x, K_y, C_{mx}, and C_{my} are defined in Sec. C5.2.1.

The subscripts x and y in Eqs. (6.53) to (6.65) indicate the axis of bending about which a particular moment or design property applies.

The values of C_m are summarized in Table 6.2, which is similar to Refs. 1.148 and 6.6. The sign convention for the end moments is the same as that used for the moment distribution method (i.e., the clockwise moment is positive and counterclockwise moment negative).

In categories A and B the effective length of the member should be used in computing P_n. The effective length in the direction of bending is to be used for computing P_{Ex} or P_{Ey} whichever is applicable.

TABLE 6.2 Values of C_m[6.6.1.148]

Category	Loading Conditions $\Omega_c P/P_n > 0.15$ (ASD) $P_u/\phi_c P_n > 0.15$ (LRFD)	M	C_m	Remarks
A	Computed moments maximum at end; no transverse loading; joint translation not prevented	M_2	0.85	 $M_1 < M_2$; M_1/M_2 negative as shown. Check both Eqs. (6.53) and (6.54) for ASD; (6.61) and (6.62) for LRFD
B	Computed moments maximum at end; no transverse loading; joint translation prevented	M_2	$0.6 - 0.4\left(\pm\dfrac{M_1}{M_2}\right)$	 Check both Eqs. (6.53) and (6.54) for ASD; (6.61) and (6.62) for LRFD
C	Transverse loading; joint translation prevented	M_2 Using Eq. (6.54) or (6.62)	$1 + \psi\dfrac{\Omega_c P}{P_E}$ (ASD)*	 Check both Eqs. (6.53) and (6.54) for ASD; (6.61) and (6.62) for LRFD
		M_2 or M_3 (whichever is larger). Using Eq. (6.53) or (6.61)	$1 + \psi\dfrac{P_u}{P_E}$ (LRFD)*	

*In lieu of this formula the following values of C_m may be used:
For members whose ends are restrained, $C_m = 0.85$
For members whose ends are unrestrained, $C_m = 1.0$

In category C the actual length of the member ($K = 1.0$) is to be used for all calculations. For this case, the value of C_m can be computed by using the following equations:[5.67,6.6]

$$C_m = 1 + \psi \frac{\Omega_c P}{P_E} \text{ (ASD)} \tag{6.66a}$$
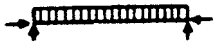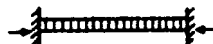
$$C_m = 1 + \psi \frac{P_u}{P_E} \text{ (LRFD)} \tag{6.66b}$$

where $\psi = (\pi^2 \delta EI / M_0 L^2) - 1$
δ = maximum deflection due to transverse loading
M_0 = maximum moment between supports due to transverse loading
P_E = P_{Ex} or P_{Ey} whichever is applicable

Values of ψ are given in Table 6.3 for various loading conditions and end restraints.[5.67,1.148,3.150]

Example 6.1   Check the adequacy of the tubular section described in Example 5.1 if it is used as a beam-column to carry an axial load of 30 kips and end moments of 60 in.-kips (Fig. 6.8). The yield point of steel is 40 ksi. The unbraced length is 10 ft and $K_x = K_y = 1.0$. The member is assumed to be bent in single curvature. Use the ASD and LRFD methods. Assume that the dead-to-live ratio is 1/5.

TABLE 6.3   Values of ψ and C_m[5.67,1.148,3.150]

Case	ψ	C_m ASD	C_m LRFD
	0	1.0	1.0
	−0.4	$1 - 0.4 \dfrac{\Omega_c P}{P_E}$	$1 - 0.4 \dfrac{P_u}{P_E}$
	−0.4	$1 - 0.4 \dfrac{\Omega_c P}{P_E}$	$1 - 0.4 \dfrac{P_u}{P_E}$
	−0.2	$1 - 0.2 \dfrac{\Omega_c P}{P_E}$	$1 - 0.2 \dfrac{P_u}{P_E}$
	−0.3	$1 - 0.3 \dfrac{\Omega_c P}{P_E}$	$1 - 0.3 \dfrac{P_u}{P_E}$
	−0.2	$1 - 0.2 \dfrac{\Omega_c P}{P_E}$	$1 - 0.2 \dfrac{P_u}{P_E}$
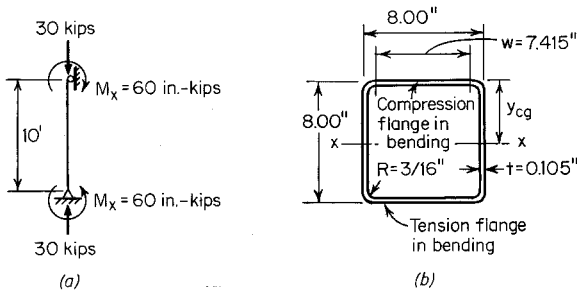
Figure 6.8   Example 6.1.

Solution

A. ASD Method

1. *Sectional Properties of Full Section.* From Example 5.1, the sectional properties of the full section are as follows:

$$A = 3.273 \text{ in.}^2$$

$$I_x = I_y = 33.763 \text{ in.}^4$$

$$r_x = r_y = 3.212 \text{ in.}$$

2. *Applied Axial Load and Moments*

$$P = 30 \text{ kips}$$

$$M_x = 60 \text{ in.-kips}$$

$$M_y = 0$$

3. *Selection of Design Equations.* Based on the design procedure discussed in Chap. 5, the nominal axial strength was computed in Example 5.1 as

$$P_n = 78.738 \text{ kips}$$

$$\Omega_c P / P_n = 1.80 \, (30) / 78.738 = 0.686 > 0.15$$

use Eqs. (6.53) and (6.54) to check the adequacy of the tubular section.

4. *Application of Eqs. (6.53) and (6.54).* Equation (6.53) is used to check the beam-column for the stability requirement between braced points.
   a. *Computation of M_{nx}.* The nominal flexural strength about x-axis should be determined according to Art. 4.2. Consideration should be given to section strength and lateral–torsional buckling strength.

i. *Section strength.* According to Art. 4.2.2, the nominal moment M_n can be computed on the basis of the initiation of yielding (Procedure I of the AISI Specification) as follows:
Corner element

$$R' = R + \frac{t}{2} = 0.240 \text{ in.}$$

Arc length

$$L = 1.57R' = 0.377 \text{ in.}$$

$$c = 0.637R' = 0.153 \text{ in.}$$

Location of neutral axis and computation of I_x and S_x. For the compression flange,

$$w = 8 - 2(R + t) = 8 - 2(0.1875 + 0.105) = 7.415 \text{ in.}$$

$$w/t = 7.415/0.105 = 70.619 < 500 \qquad \text{O.K.}$$

$$\lambda = \frac{1.052}{\sqrt{k}} \left(\frac{w}{t} \right) \sqrt{\frac{f}{E}}$$

$$= \frac{1.052}{\sqrt{4.0}} (70.619) \sqrt{\frac{40}{29,500}} = 1.368 > 0.673$$

$$\rho = \left(1 - \frac{0.22}{\lambda} \right) / \lambda = \left(1 - \frac{0.22}{1.368} \right) / 1.368 = 0.613$$

$$b = \rho w = (0.613)(7.415) = 4.545 \text{ in.}$$

By using the effective width of the compression flange and assuming the web is fully effective, the neutral axis can be located as follows:

Element	Effective Length L (in.)		Distance from Top Fiber y (in.)	Ly (in.^{2})	Ly^2 (in.^{3})
Compression flange		4.545	0.0525	0.239	0.013
Compression corners	$2 \times 0.377 =$	0.754	0.1395	0.105	0.013
Webs	$2 \times 7.415 =$	14.830	4.0000	59.320	237.280
Tension corners	$2 \times 0.377 =$	0.754	7.8605	5.927	46.588
Tension flange		7.415	7.9475	58.931	468.352
		28.298		124.522	752.248

$$y_{cg} = \frac{124.522}{28.298} = 4.400 \text{ in.} > d/2 = 8/2 = 4.000 \text{ in.}$$

The maximum stress of 40 ksi occurs in the compression flange as summed in the calculation.

Check the effectiveness of the web. Use Art. 3.5.1.2 to check the effectiveness of the web element. From Fig. 6.9,

$$f_1 = 40(4.1075/4.400) = 37.341 \text{ ksi} \qquad \text{(compression)}$$

$$f_2 = -40(3.3075/4.400) = -30.068 \text{ ksi} \qquad \text{(tension)}$$

$$\psi = f_2/f_1 = -30.068/37.341 = -0.805 < -0.236$$

$$k = 4 + 2(1 - \psi)^3 + 2(1 - \psi)$$

$$= 4 + 2[1 - (-0.805)]^3 + 2[1 - (-0.805)]$$

$$= 19.371$$

$$h/t = 7.415/0.105 = 70.619 < 200 \qquad \text{O.K.}$$

$$\lambda = \frac{1.052}{\sqrt{19.371}} (70.619) \sqrt{\frac{37.341}{29,500}} = 0.601 < 0.673$$

$$b_e = h = 7.415 \text{ in.}$$

$$b_1 = b_e/(3 - \psi) = 1.949 \text{ in.}$$

Since $\psi < -0.236$,

$$b_2 = b_e/2 = 3.708 \text{ in.}$$

$$b_1 + b_2 = 5.657 \text{ in.}$$

Because the computed value of $(b_1 + b_2)$ is greater than the compression portion of the web (4.1075 in.), the web is fully
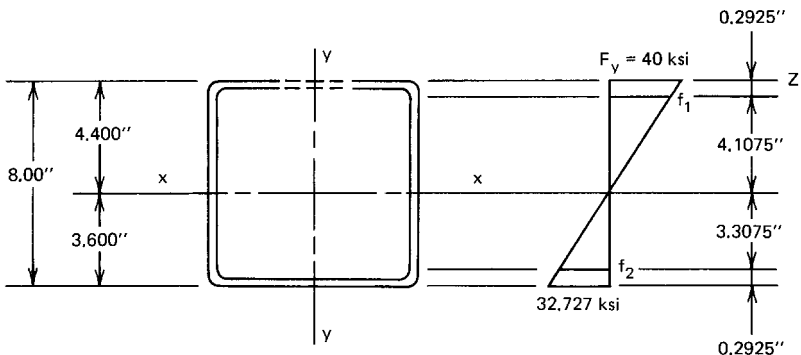
Figure 6.9   Stress distribution in webs using fully effective webs.

effective. The moment of inertia based on line element is

$$2I'_{web} = 2(\tfrac{1}{12})(7.415)^3 = \qquad 67.949$$

$$\Sigma\,(Ly^2) = \qquad \underline{752.248}$$

$$I_z = \qquad 820.197 \text{ in.}^3$$

$$-(\Sigma\,L)(y_{cg})^2 = -(28.298)(4.40)^2 = \underline{-547.849 \text{ in.}^3}$$

$$I'_x = \qquad 272.348 \text{ in.}^3$$

The actual moment of inertia is

$$I_x = I'_x(t) = (272.348)(0.105) = 28.597 \text{ in.}^4$$

The section modulus relative to the extreme compression fiber is

$$S_{ex} = 28.597/4.40 = 6.499 \text{ in.}^3$$

The nominal moment for section strength is

$$M_{nx} = S_{ex}F_y = (6.499)(40) = 259.960 \text{ in.-kips}$$

ii. *Lateral buckling strength.* Because the tubular member is a box section, the lateral buckling strength of the member can be checked by using Art. 4.2.3.4 or Sec. C3.1.2.2 of the Supplement to the 1996 edition of the AISI Specification.
According to Eq. (4.78),

$$L_u = \frac{0.36C_b\pi}{F_y S_f}\sqrt{EI_y GJ}$$

in which

$$C_b = 1.0 \text{ for combined axial load and bending}$$

$$J = \frac{2b^2 d^2 t}{(b+d)} = \frac{2(8-0.105)^4(0.105)}{2(8-0.105)} = 51.67 \text{ in.}^4$$

$$S_f = 33.763/4 = 8.44 \text{ in.}^3$$

Therefore

$$L_u = \frac{0.36(1)\pi}{40 \times 8.44} \sqrt{(29{,}500)(33.763)(11{,}300)(51.67)}$$

$$= 2{,}554.7 \text{ in.}$$

Since the unbraced length of 120 in. is less than L_u, lateral–torsional buckling will not govern the design.

iii. *Nominal moment* M_{nx}. From the above calculations, $M_{nx} = 259.960$ in.-kips

b. *Computation of* C_{mx}. Using Eq. (6.60),

$$C_{mx} = 0.6{-}0.4 \frac{M_1}{M_2}$$

$$= 0.6{-}0.4 \left(-\frac{60}{60}\right) = 1.0$$

c. *Computation of* α_x. Using Eq. (6.56),

$$\alpha_x = 1 - \frac{\Omega_c P}{P_{Ex}}$$

where

$$P_{Ex} = \frac{\pi^2 EI_x}{(K_x L_x)^2} = \frac{\pi^2 (29{,}500)(33.763)}{(1 \times 10 \times 12)^2} = 682.653 \text{ kips}$$

$$\alpha_x = 1 - \frac{1.80(30)}{682.653}$$

$$= 0.921$$

d. *Check Eq.* (*6.53*). Substituting the above computed values into Eq. (6.53),

$$\frac{\Omega_c P}{P_n} + \frac{\Omega_b C_{mx} M_x}{M_{nx} \alpha_x} = \frac{(180)(30)}{78.738} + \frac{(1.67)(1)(60)}{(259.96)(0.921)}$$

$$= 1.104 > 1.0 \text{ (no good)}$$

3. *Application of Eq.* (*6.54*). Equation (6.54) is used to check the beam-column for the yielding requirement at braced points.

a. *Computation of* P_{no}. The nominal axial strength P_{no} is computed for $KL/r = 0$ (i.e., $F_n = F_y = 40$ ksi). For stiffened compression elements,

$$\lambda = \frac{1.052}{\sqrt{4.0}} (70.619) \sqrt{\frac{40}{29,500}} = 1.368 > 0.673$$

$$\rho = \left(1 - \frac{0.22}{1.368}\right)/1.368 = 0.613$$

$$b = \rho w = (0.613)(7.415) = 4.545 \text{ in.}$$

$$A_e = 3.273 - 4(7.415 - 4.545)(0.105) = 2.068 \text{ in.}^2$$

$$P_{no} = A_e F_n = (2.068)(40) = 82.720 \text{ kips}$$

b. *Check Eq. (6.54).*

$$\frac{\Omega_c P}{P_{no}} + \frac{\Omega_b M_x}{M_{nx}} = \frac{(1.80)(30)}{82.720} + \frac{(1.67)(60)}{259.96}$$

$$= 1.038 > 1.0 \text{ (no good)}$$

Based on the above calculations for the ASD method, it can be seen that the given tubular member is inadequate for the applied load and end moments.

B. *LRFD Method*

1. *Applied Axial Load and Moments.* From the given data,

$$P_D = 5 \text{ kips}$$

$$P_L = 25 \text{ kips}$$

$$M_D = 10 \text{ in.-kips}$$

$$M_L = 50 \text{ in.-kips}$$

2. *Required Strengths.* Based on the load factors and load combinations discussed in Art. 3.3.2.2, the required strengths P_u and M_{ux} can be computed as follows:

From Eq. (3.5a),

$$(P_u) = 1.4 P_D + P_L = 1.4(5) + 25 = 32 \text{ kips}$$

$$(M_{ux})_1 = 1.4 M_D + M_L = 1.4(10) + 50 = 64 \text{ in.-kips}$$

From Eq. (3.5b),

$$(P_u)_2 = 1.2\, P_D + 1.6\, P_L = 1.2\,(5) + 1.6\,(25) = 46 \text{ kips}$$

$$(M_{ux})_2 = 1.2\, M_D + 1.6\, M_L = 1.2\,(10) + 1.6\,(50) = 92 \text{ in.-kips}$$

Use $P_u = 46$ kips and $M_{ux} = 92$ in.-kips

3. *Nominal Axial Strength and Nominal Flexural Strength.*

   From Example 5.1 and the above calculations for the ASD method,

$$P_n = 78.738 \text{ kips}$$

$$P_{no} = 82.720 \text{ kips}$$

$$P_{Ex} = 682.653 \text{ kips}$$

$$M_{nx} = 259.960 \text{ in.-kips}$$

4. *Selection of Design Equations.*

   Since $P_u/\phi_c P_n = 46/(0.85 \times 78.738) = 0.687 > 0.15$, use Eqs. (6.61) and (6.62) to check the adequacy of the tubular section.

5. *Application of Eq. (6.61).* Since the values of P_u, P_n, P_{no}, P_{Ex}, M_{ux}, M_{nx}, ϕ_c, and ϕ_b are known, calculations are needed only for C_{mx} and α_x as follows:

   From Eq. (6.60),

$$C_{mx} = 0.6 - 0.4\, \frac{M_1}{M_2} = 0.6 - 0.4\left(-\frac{92}{92}\right) = 1.0$$

   Based on (6.64),

$$\alpha_x = 1 - \frac{P_u}{P_{Ex}} = 1 - \frac{46}{682.653} = 0.933$$

   Using Eq. (6.61),

$$\frac{P_u}{\phi_c P_n} + \frac{C_{mx} M_{ux}}{\phi_b M_{nx} \alpha_x} = \frac{46}{(0.85)(78.738)} + \frac{(1)(92)}{(0.95)(259.96)(0.933)}$$

$$= 1.087 > 1.0 \text{ (no good)}$$

6. *Application of Eq. (6.62).* Based on Eq. (6.62),

$$\frac{P_u}{\phi_c P_{no}} + \frac{M_{ux}}{\phi_b M_{nx}} = \frac{46}{(0.85)(82.720)} + \frac{92}{(0.95)(259.96)}$$

$$= 1.027 > 1.0 \text{ (no good)}$$

According to the above calculations for the LRFD method, the given tubular member is also inadequate for the applied load and moments. The difference between the ASD and LRFD methods is less than 1.5%.

Example 6.2   If the I-section used in Example 5.2 is to be used as a beam-column as shown in Fig. 6.10, what is the maximum allowable transverse load P' applied at the midspan length? Assume that the axial load is 20 kips and that the beam is laterally supported at *A, B, C, D,* and *E.* Use $F_y = 33$ ksi and the ASD method.

Solution

1. *Sectional Properties of Full Section.* From Example 5.2, the sectional properties of the I-section are as follows:

$$A = 2.24 \text{ in.}^2 \qquad\qquad J = 0.00418 \text{ in.}^4$$

$$I_x = 22.1 \text{ in.}^4 \qquad\qquad C_w = 70.70 \text{ in.}^6$$

$$S_x = 5.53 \text{ in.}^3 \qquad\qquad r_0 = 3.435 \text{ in.}$$

$$I_y = 4.20 \text{ in.}^4$$

$$S_y = 1.40 \text{ in.}^3$$

$$r_x = 3.15 \text{ in.}$$

$$r_y = 1.37 \text{ in.}$$

2. *Applied Axial Load and Moments.* Since the continuous beam is subject to symmetric loads P' in two equal spans, the moment diagram can be drawn as shown in Fig. 6.11. The positive and negative moments are
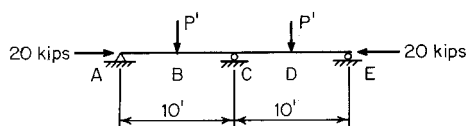
Figure 6.10   Example 6.2.
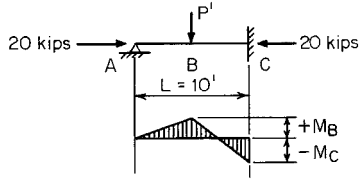
Figure 6.11 Moment diagram for the continuous beam.

$$+M_{\mathrm{B}} = \frac{5}{32} P'L = \frac{5}{32} P'(10)(12) = 18.75 \ P' \qquad \text{in.-kips}$$

$$-M_{\mathrm{C}} = \frac{3}{16} P'L = \frac{3}{16} P'(10)(12) = 22.5 \ P' \qquad \text{in.-kips}$$

As given in the problem, the applied axial load is

$$P = 20 \text{ kips}$$

3. *Computation of P_{n}*
   a. *Nominal buckling stress, F_{n}*
      i. *Elastic flexural buckling.* By using Eq. (5.56), the elastic flexural buckling stress can be computed as follows:

$$K_x L_x/r_x = (1 \times 10 \times 12)/3.15 = 38.10$$

$$K_y L_y/r_y = (1 \times 5 \times 12)/1.37 = 43.80 < 200 \qquad \text{O.K.}$$

$$F_{\mathrm{e}} = \frac{\pi^2 E}{(KL/r)^2} = \frac{\pi^2(29,500)}{(43.80)^2} = 151.77 \text{ ksi}$$

   ii. *Elastic torsional buckling.* From Eq. (5.22) of Art. 5.4.1 or Sec. C3.1.2.1(a) of the AISI Specification, the torsional buckling stress is

$$F_{\mathrm{e}} = \sigma_{\mathrm{t}} = \frac{1}{Ar_0^2} \left(GJ + \frac{\pi^2 E C_{\mathrm{w}}}{(K_t L_t)^2} \right)$$

$$= \frac{1}{(2.24)(3.435)^2}[(11,300)(0.00418) + \frac{\pi^2(29,500)(70.70)}{(5 \times 12)^2})$$

$$= 218.13 \text{ ksi}$$

The nominal buckling stress, F_{n}, is determined by using the smaller value of the elastic flexural buckling stress and torsional buckling stress, i.e.,

$$F_e = 151.77 \text{ ksi}$$

$$\lambda_c = \sqrt{\frac{F_y}{F_e}} = \sqrt{\frac{33}{151.77}} = 0.466 < 1.5$$

From Eq. (5.54),

$$F_n = (0.658^{\lambda_c^2})F_y = (0.658^{0.466^2})(33) = 30.13 \text{ ksi}$$

b. *Effective area, A_e, at the stress F_n.* From Example 5.2, the flat widths of edge stiffener, flange and web are

$$w_1 = 0.5313 \text{ in., } w_1/t = 7.084 < 14 \quad \text{O.K.}$$

$$w_2 = 2.6625 \text{ in., } w_2/t = 35.50$$

$$w_3 = 7.6625 \text{ in., } w_3/t = 102.167 < 500 \quad \text{O.K.}$$

i. *Effective width of the compression flange*

$$S = 1.28\sqrt{E/f} = 1.28\sqrt{29,500/30.13} = 40.05$$
$$S/3 = 13.35$$
$$w_2/t = 35.50$$

Since $S/3 < w_2/t < S$, use Case II of Art. 3.5.3.2(a),

$$I_a = 399\{[(w_2/t)/S] - \sqrt{k_u/4}\}^3 t^4$$
$$= 399\{[35.50/40.05] - \sqrt{0.43/4}\}^3(0.075)^4$$
$$= 0.0022 \text{ in.}^4$$
$$n = 1/2$$
$$I_s = d^3t/12 = (0.5313)^3(0.075)/12 = 0.000937 \text{ in.}^4$$
$$C_2 = I_s/I_a = 0.000937/0.0022 = 0.426$$
$$C_1 = 2 - C_2 = 2 - 0.426 = 1.574$$
$$D/w_2 = 0.7/2.6625 = 0.263$$

Since $D/w_2 < 0.8$, from Eq. (3.86),

$$k_a = 5.25 - 5(D/w_2) = 5.25 - 5(0.263) = 3.935 < 4.0$$

$$k = C_2^n(k_a - k_u) + k_u$$

$$= (0.426)^{0.5}(3.935 - 0.43) + 0.43$$

$$= 2.718$$

Use $k = 2.718$ to compute the effective width of the compression flange. From Eqs. (3.41) through (3.44),

$$\lambda = \frac{1.052}{\sqrt{2.718}} (35.50) \sqrt{\frac{30.13}{29,500}} = 0.724 > 0.673$$

$$\rho = \left(1 - \frac{0.22}{\lambda}\right)/\lambda = \left(1 - \frac{0.22}{0.724}\right)/0.724 = 0.962$$

$$b = \rho w_2 = (0.962)(2.6625) = 2.561 \text{ in.}$$

ii. *Effective width of edge stiffeners*

$$w_t/t = 7.084$$

$$\lambda = \frac{1.053}{\sqrt{0.43}} (7.084) \sqrt{\frac{30.13}{29,500}} = 0.363 < 0.673$$

$$d_s' = w_1 = 0.5313 \text{ in.}$$

$$d_s = C_2 d_s' = (0.426)(0.5313)$$

$$= 0.226 < d_s' \qquad \text{O.K.}$$

iii. *Effective width of web elements*

$$w_3/t = 102.167$$

$$\lambda = \frac{1.052}{\sqrt{4.0}} (102.167) \sqrt{\frac{30.13}{29,500}} = 1.717 > 0.673$$

$$\rho = \left(1 - \frac{0.22}{1.717}\right)/1.717 = 0.508$$

$$b = \rho w_3 = (0.508)(7.6625) = 3.893 \text{ in.}$$

iv. *Effective area, A_e*

$$A_e = 2.24 - [4(0.5313 - 0.226) + 4(2.6625 - 2.561)$$

$$+ 2(7.6625 - 3.893)](0.075) = 1.553 \text{ in.}^2$$

c. *Nominal load, P_n*

$$P_n = A_e F_n = (1.553)(30.13) = 46.79 \text{ kips}$$

4. *Selection of Design Equations*

$$\Omega_c P / P_n = (1.80)(20)/46.79 = 0.769 > 0.15$$

use Eqs. (6.53) and (6.54).

5. *Application of Eq. (6.53)*
   a. *Computation of M_{nx}*
      i. *Section strength based on initiation of yielding* (Art. 4.2.2.1).

For corner element,

$$R' = R + \frac{t}{2} = 0.09375 + \frac{0.075}{2} = 0.1313 \text{ in.}$$

The arc length is

$$L = 1.57 \, R' = 0.206 \text{ in.}$$

$$c = 0.637 \, R' = 0.0836 \text{ in.}$$

For the compression flange, the effective width for $f = F_y = 33$ ksi is $b = 2.430$ in. For the compression edge stiffener, the compression stress is conservatively assumed to be $f = F_y = 33$ ksi. Following the same procedure used in Item 3.b, the effective length of the edge stiffener at a stress of 33 ksi is 0.184 in. By using the effective widths of the compression flange and edge stiffener and assuming the web is fully effective, the neutral axis can be located as follows:

Element	Effective Length L (in.)		Distance from Top Fiber y (in.)	Ly (in.^{2})	Ly^2 (in.^{3})
Compression flange	2×2.430	$= 4.860$	0.0375	0.182	0.007
Compression corners	4×0.206	$= 0.824$	0.0852	0.070	0.006
Compression stiffeners	2×0.184	$= 0.368$	0.2608	0.096	0.025
Webs	2×7.6625	$= 15.325$	4.0000	61.300	245.200
Tension stiffeners	2×0.5313	$= 1.063$	7.5656	8.042	60.843
Tension corners	4×0.206	$= 0.824$	7.9148	6.522	51.620
Tension flange	2×2.6625	$= 5.325$	7.9625	42.400	337.610
		28.589		118.612	695.311

$$y_{cg} = \frac{118.612}{28.589} = 4.149 \text{ in.}$$

Since $y_{cg} > d/2 = 4.000$ in., the maximum stress of 33 ksi occurs in the compression flange as assumed in the above calculation.

The effectiveness of the web is checked according to Art. 3.5.1.2.

From Fig. 6.12,

$$f_1 = 33(3.9802/4.149) = 31.66 \text{ ksi} \qquad \text{(compression)}$$

$$f_2 = -33(3.6822/4.149) = -29.29 \text{ ksi} \qquad \text{(tension)}$$

$$\psi = f_2/f_1 = -29.29/31.66 = -0.925$$

$$k = 4 + 2(1 + 0.925)^3 + 2(1 + 0.925) = 22.116$$

$$h/t = w_3/t = 102.167$$

$$\lambda = \frac{1.052}{\sqrt{22.116}} (102.167) \sqrt{\frac{31.66}{29,500}} = 0.749 > 0.673$$

$$\rho = \left(1 - \frac{0.22}{0.749}\right)/0.749 = 0.943$$

$$b_e = 0.943(7.6625) = 7.229 \text{ in.}$$

$$b_1 = 7.229/(3 + 0.925) = 1.842 \text{ in.}$$

Since $\psi < -0.236$, $b_2 = 7.229/2 = 3.614$ in.

$$b_1 + b_2 = 1.842 + 3.614 = 5.456 \text{ in.}$$

Because the computed value of $(b_1 + b_2)$ is greater than the com-
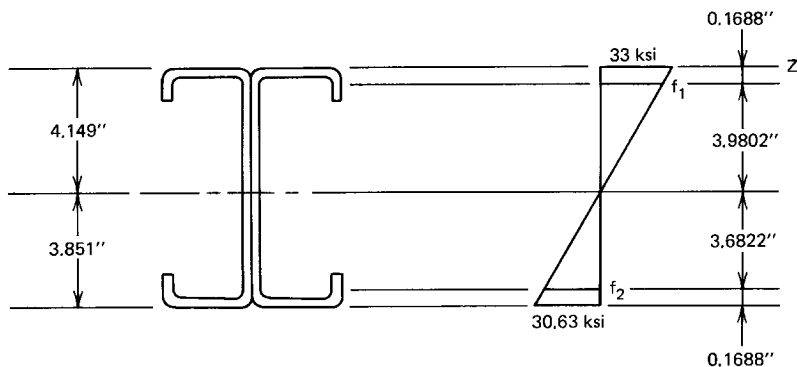
Figure 6.12 Stress distribution in webs.

pression portion of the web (3.9802 in.), the web is fully effective. The moment of inertia based on line elements is

$$2I'_{web} = 2\left(\frac{1}{12}\right)(7.6625)^3 = \quad 74.983$$

$$2I'_{comp.\ stiffener} = 2\left(\frac{1}{12}\right)(0.184)^3 = \quad 0.001$$

$$2I'_{tension\ stiffener} = 2\left(\frac{1}{12}\right)(0.531)^3 = \quad 0.025$$

$$\Sigma(Ly^2) = \underline{695.311}$$

$$I_z = \quad 770.320 \text{ in.}^3$$

$$-(\Sigma L)(y_{cg})^2 = -(28.589)(4.149)^2 = \underline{-492.137}$$

$$I'_x = \quad 278.183 \text{ in.}^3$$

The actual moment of inertia is

$$I_x = I'_x(t) = (278.183)(0.075) = 20.864 \text{ in.}^4$$

The section modulus relative to the extreme compression fiber is

$$S_{ex} = 20.864/4.149 = 5.029 \text{ in.}^3$$

The nominal moment for section strength is

$$M_{nx} = S_{ex}F_y = (5.029)(33) = 165.96 \text{ in.-kips}$$

ii. *Lateral buckling strength.* For segment AB, $L = 5$ ft. According to Eq. (4.73a),

$$F_e = \frac{\pi^2 E C_b dI_{yc}}{S_f L^2}$$

In the above equation, $C_b = 1.0$ according to the definition of C_b given on page 208 for members subject to combined compressive axial load and bending moment.

Therefore, $F_e = \dfrac{\pi^2(29{,}500)(1.00)(8)(4.20/2)}{(5.53)(5 \times 12)^2} = 245.70$ ksi

$$0.56\, F_y = 18.48 \text{ ksi}$$

$$2.78\, F_y = 91.74 \text{ ksi}$$

Since $F_e > 2.78\, F_y$, $F_c = F_y = 33$ ksi

Because the elastic section modulus of the effective section calculated at a stress of $f = 33$ ksi in the extreme compression fiber is $S_c = S_{ex} = 5.029$ in.^{3}, the nominal moment for lateral buckling is

$$M_{nx} = S_c F_c = (5.029)(33) = 165.96 \text{ in.-kips}$$

For segment BC, $L = 5$ ft, $M_B = 18.75 P'$ and $M_c = 22.5 P'$ in.-kips. The value of C_b is also 1.0 for the member subject to combined axial load and bending moment.

$$F_e = \dfrac{\pi^2(29{,}500)(1.00)(8)(4.20/2)}{(5.53)(5 \times 12)^2} = 245.70 \text{ ksi}$$

Since $F_e > 2.78\, F_y$, $F_c = F_y = 33$ ksi

$$M_{nx} = S_c F_c = 165.96 \text{ in.-kips}$$

Based on section strength and lateral–torsional buckling strength,

$$M_{nx} = 165.96 \text{ in.-kips}$$

b. *Computation of C_{mx}.* Based on Case 3 of the definition of C_{mx}, use

$$C_{mx} = 1.0$$

c. *Computation of α_x.* Using Eq. (6.56),

$$\alpha_x = 1 - \frac{\Omega_c P}{P_{Ex}}$$

where

$$P_{Ex} = \frac{\pi^2 EI_x}{(K_x L_x)} = \frac{\pi^2 (29,500)(22.1)}{(1 \times 10 \times 12)^2}$$

$$= 446.84 \text{ kips}$$

Therefore,

$$\alpha_x = 1 - \frac{1.80(20)}{446.84}$$

$$= 0.919$$

d. *Allowable load P' based on Eq. (6.53).* Using Eq. (6.53),

$$\frac{\Omega_c P}{P_n} + \frac{\Omega_b C_{mx} M_x}{M_{nx} \alpha_x} = \frac{(1.80)20}{46.79} + \frac{(1.67)(1)(22.5P')}{(165.96)(0.919)} = 1.0$$

$$P' = 0.936 \text{ kips}$$

6. *Application of Eq. (6.54)*
   a. *Computation of P_{no}.* For $KL/r = 0$, $F_n = F_y = 33$ ksi. Using the same procedure illustrated in Item 3,

$$A_e(\text{for } F_y = 33 \text{ ksi}) = 1.469 \text{ in.}^2$$

$$P_{n0} = A_e F_n = 48.48 \text{ kips}$$

   b. *Allowable load P' based on Eq. (6.54)*

$$\frac{\Omega_c P}{P_{no}} + \frac{\Omega_b M_x}{M_{nx}} = \frac{(1.80)20}{48.48} + \frac{(1.67)22.5P'}{165.96} = 1.0$$

$$P' = 1.137 \text{ kips}$$

7. *Allowable Load P'.* Based on Eqs. (6.53) and (6.54), the allowable load based on the ASD method is 0.936 kips, which is governed by the stability requirement. For the LRFD method, Eqs. (6.61) and (6.62) should be used with the load factors and combinations given in Art. 3.3.2.2.

Example 6.3   For the braced channel column shown in Fig. 6.13, determine the allowable load if the load at both ends are eccentrically applied at point *A* (that is, $e_x = +2.124$ in.) along the *x*-axis (Fig. 6.13*a*). Assume $K_xL_x = K_yL_y = K_zL_z = 14$ ft. Use $F_y = 50$ ksi and the ASD method.

Solution

1. *Properties of Full Section.* From the equation given in Part I of the AISI Design Manual,[1.159] the following full section properties can be computed:

$$A = 1.553 \text{ in.}^2 \qquad x = 0.876 \text{ in.}$$

$$I_x = 15.125 \text{ in.}^4 \qquad J = 0.0571 \text{ in.}^4$$

$$S_x = 3.781 \text{ in.}^3 \qquad C_w = 24.1 \text{ in.}^6$$

$$r_x = 3.12 \text{ in.} \qquad j = \beta_y/2 = 4.56 \text{ in.}$$

$$I_y = 1.794 \text{ in.}^4 \qquad r_0 = 3.97 \text{ in.}$$

$$S_y = 0.844 \text{ in.}^3 \qquad x_0 = 2.20 \text{ in.}$$

$$r_y = 1.075 \text{ in.}$$

2. *Applied Axial Load and End Moments*

(a)   (b)
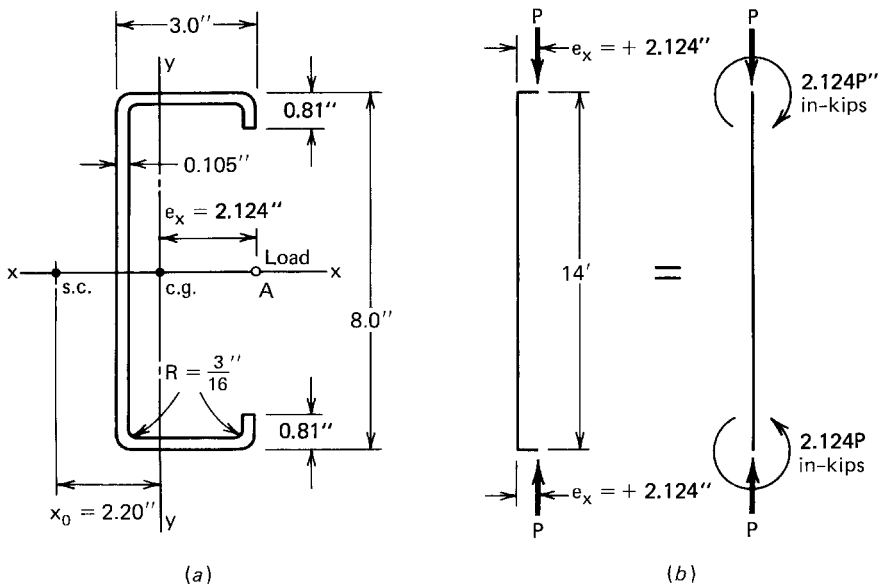
Figure 6.13   Example 6.3.

$$P = \text{axial load to be determined}$$

$$M_x = 0$$

$$M_y = 2.124P \text{ in.-kips}$$

3. *Computation of P_n*
   a. *Nominal buckling stress, F_n*
      i. *Elastic flexural buckling stress.* Since $K_x L_x = K_y L_y$ and $r_x > r_y$,

$$KL/r = K_y L_y/r_y = (1)(14 \times 12)/1.075 = 156.28 < 200 \qquad \text{O.K.}$$

$$F_e = \frac{\pi^2 E}{(KL/r)^2} = \frac{\pi^2(29,500)}{(156.28)^2} = 11.921 \text{ ksi.}$$

      ii. *Elastic torsional-flexural buckling stress.* According to Eq. (5.57),

$$F_e = \frac{1}{2\beta} [(\sigma_{ex} + \sigma_t) - \sqrt{(\sigma_{ex} + \sigma_t)^2 - 4\beta\sigma_{ex}\sigma_t}$$

where

$$\beta = 1 - \left(\frac{x_0}{r_0}\right)^2 = 1 - \left(\frac{2.20}{3.97}\right)^2 = 0.693$$

$$\sigma_{ex} = \frac{\pi^2 E}{(K_x L_x/r_x)^2} = \frac{\pi^2(29,500)}{(1 \times 14 \times 12/3.12)^2} = 100.418 \text{ ksi}$$

$$\sigma_t = \frac{1}{Ar_0^2}\left[GJ + \frac{\pi^2 EC_w}{(K_t L_t)^2}\right]$$

$$= \frac{1}{(1.553)(3.97)^2}\left[(11300)(0.00571) + \frac{\pi^2(29,500)(24.1)}{(1 \times 14 \times 12)^2}\right]$$

$$= 12.793 \text{ ksi.}$$

Therefore

$$F_e = \frac{1}{2(0.693)} [(100.418 + 12.793)$$

$$- \sqrt{(100.418 + 12.793)^2 - 4(0.693)(100.418)(12.793)]}$$

$$= 12.269 > 11.921 \text{ ksi}$$

use $F_e = 11.921$ ksi for computing F_n.

$$\lambda_c = \sqrt{\frac{F_y}{F_e}} = \sqrt{\frac{50}{11.921}} = 2.048 > 1.5$$

From Eq. (5.55),

$$F_n = \left[\frac{0.877}{\lambda_c^2}\right] F_y = \left[\frac{0.877}{(2.048)^2}\right] (50) = 10.455 \text{ ksi}$$

b. *Effective area, A_e, at the stress F_n*
   i. *Effective width of the compression flange*

$$S = 1.28\sqrt{E/f} = 1.28\sqrt{29,500/10.455} = 67.992$$
$$S/3 = 22.664$$
$$w/t = 2.415/0.105 = 23 < 60 \qquad \text{O.K.}$$

Since $S/3 < w/t < S$, use Case II of Art. 3.5.3.2(a)

$$I_a = 399\{[(w/t)/S] - \sqrt{k_u/4}\}^3 t^4$$
$$= 399\{[23/67.992] - \sqrt{0.43/4}\}^3 (0.105)^4 = 5.46 \times 10^{-8} \text{ in.}^4$$
$$n = 1/2$$
$$I_s = d^3 t/12 = (0.5175)^3 (0.105)/12 = 0.00121 \text{ in.}^4$$

From Eq. (3.83),

$$C_2 = I_s/I_a = \frac{0.00121}{5.46 \times 10^{-8}} = 2.216 \times 10^4 \geq 1.0$$

Use $C_2 = 1.0$

$$C_1 = 2 - C_2 = 1.0$$
$$D/w = 0.81/2.415 = 0.335$$

Since $D/w < 0.8$, from Eq. (3.86),

$$k_a = 5.25 - 5(D/w) = 5.25 - 5(0.335) = 3.575 < 4.0$$

$$k = C_2^n(k_a - k_u) + k_u$$

$$= (1)^{0.5}(3.575 - 0.43) + 0.43$$

$$= 3.575$$

$$\lambda = \frac{1.052}{\sqrt{3.575}} (23) \sqrt{\frac{10.455}{29,500}} = 0.241 < 0.673$$

$b = w = 2.415$ in. The flange is fully effective.

ii. *Effective width of edge stiffeners*

$$w/t = 0.5175/0.105 = 4.929 < 14 \qquad \text{O.K.}$$

$$\lambda = \frac{10.52}{\sqrt{0.43}} (4.929) \sqrt{\frac{10.455}{29,500}} = 0.149 < 0.673$$

$$d_s' = d = 0.5175 \text{ in.}$$

$$d_s = C_2 d_s' = (1)(0.5175)$$

$$= 0.5175 \text{ in.}$$

The edge stiffener is fully effective.

iii. *Effective width of web element.*

$$w/t = 7.415/0.105 = 70.619 < 500 \qquad \text{O.K.}$$

$$\lambda = \frac{1.052}{\sqrt{4.0}} (70.619) \sqrt{\frac{10.455}{29,500}} = 0.699 > 0.673$$

$$\rho = \left(1 - \frac{0.22}{0.699}\right)/0.699 = 0.980$$

$$b = \rho w = (0.980)(7.415) = 7.267 \text{ in.}$$

iv. *Effective area, A_e*

$$A_e = 1.553 - (7.415 - 7.267)(0.105) = 1.537 \text{ in.}^2$$

b. *Nominal load P_n*

$$P_n = A_e F_n = (1.537)(10.455) = 16.069 \text{ kips}$$

4. *Selection of Design Equations*

$$\Omega_c P / P_n = (1.80) P / 16.069 = P / 8.927$$

Assume that $\Omega_c P / P_n > 0.15$, use Eqs. (6.53) and (6.54) to determine the allowable load P.

5. *Application of Eq. (6.53)*

   a. *Computation of M_{ay}*

      i. *Section strength based on initiation of yielding.* Assume that the maximum compressive stress of $f = F_y = 50$ ksi occurs in the extreme fiber of edge stiffeners and that both flanges are fully effective as shown in Fig. 6.14. For edge stiffeners,

$$\lambda = \frac{1.052}{\sqrt{0.43}} (4.929) \sqrt{\frac{50}{29,500}} = 0.326 < 0.673$$

$$b = w = 0.5175 \text{ in.}$$

$$a = 2.124 \text{ in.}$$
$$b = 2.124 - 0.2925 = 1.8315 \text{ in.}$$
$$c = 3 - 2.124 = 0.876 \text{ in.}$$
$$d = c - 0.2925 = 0.5835 \text{ in.}$$
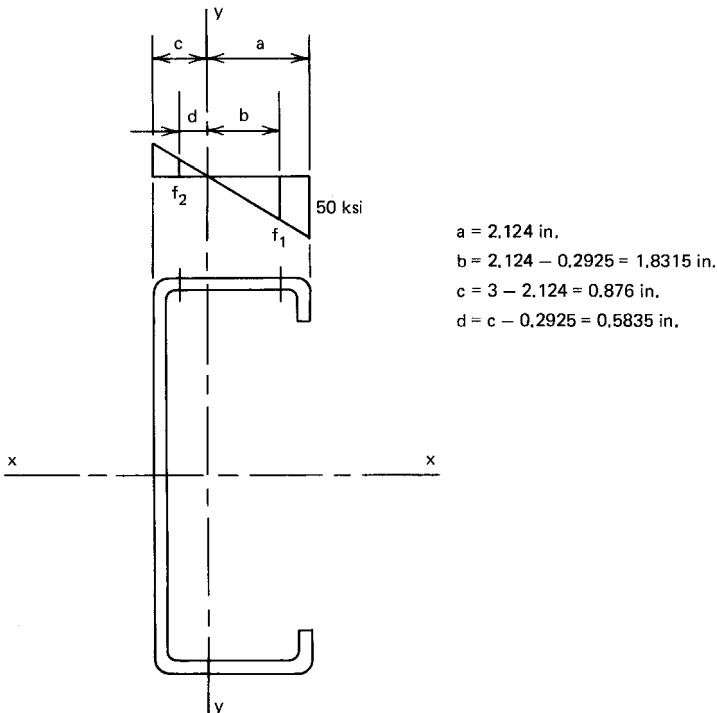
Figure 6.14   Stress distribution in flanges.

To check if flange is fully effective. From Fig. 6.14,

$$f_1 = 50(1.8315/2.124) = 43.114 \text{ ksi} \qquad \text{(compression)}$$

$$f_2 = -50(0.5835/2.124) = -13.736 \text{ ksi} \qquad \text{(tension)}$$

$$\psi = f_2/f_1 = -13.736/43.114 = -0.319 < -0.236$$

$$k = 4 + 2(1 - \psi)^3 + 2(1 - \psi) = 4 + 2(1.319)^3 + 2(1.319)$$
$$= 11.222$$

$$\lambda = \frac{1.052}{\sqrt{11.222}} \text{ (23)} \sqrt{\frac{43.114}{29,500}} = 0.276 < 0.673$$

$$b_e = w = 2.415 \text{ in.}$$

$$b_1 = b_e/(3 - \psi) = 2.415/3.319 = 0.728 \text{ in.}$$

Since $\psi < -0.236$, $b_2 = b_e/2 = 2.415/2 = 1.2075$ in.

$$b_1 + b_2 = 0.728 + 1.2075 = 1.9355 \text{ in.}$$

Because the computed value of $(b_1 + b_2)$ is greater than the compression portion of the flange (1.8315 in.), the flange is fully effective.

In view of the fact that all elements are fully effective, the section modulus relative to the extreme compression fiber is

$$S_e = S_y \text{ (for full section)} = 0.844 \text{ in.}^3$$

$$M_{ny} = S_e F_y = 0.844(50) = 42.2 \text{ in.-kips}$$

for section strength.

ii. *Lateral–torsional buckling strength.* According to Eq. (4.66), the elastic critical lateral–torsional buckling stress for bending about the centroidal axis perpendicular to the symmetry axis for singly symmetric channel section is

$$F_e = \frac{C_s A \sigma_{ex}}{C_{TF} S_f} \left[j + C_s \sqrt{j^2 + r_0^2(\sigma_t/\sigma_{ex})} \right]$$

where $C_s = -1$
$\quad A = 1.553$ in.^{2} (see Item 1)
$\quad \sigma_{ex} = 100.418$ ksi (see Item 3.a.ii)
$\quad \sigma_t = 12.793$ ksi (see Item 3.a.ii)
$\quad j = 4.56$ in. (see Item 1)

$r_0 = 3.97$ in. (see Item 1)

$C_{TF} = 1.0$ [see Eq. (4.71)]

$S_f = S_y = 0.844$ in.^{3} (see Item 1)

Substituting all values into the equation for F_e, the elastic critical buckling stress is

F_e

$$= \frac{(-1.553)(100.418)[4.56 - \sqrt{4.56^2 + 3.97^2 (12.793/100.418)}]}{(1)(0.844)}$$

$= 39.744$ ksi

$$0.56F_y = 0.56(50) = 28 \text{ ksi}$$

$$2.78F_y = 2.78(50) = 139 \text{ ksi}$$

Since $2.78F_y > F_e > 0.56F_y$, use Eq. (4.64b) to compute F_c, i.e.,

$$F_c = \frac{10}{9} F_y \left(1 - \frac{10F_y}{36F_e}\right)$$

$$= \frac{10}{9} (50) \left(1 - \frac{10 \times 50}{36 \times 39.744}\right)$$

$$= 36.141 \text{ ksi}$$

Following the same procedure used in Item 5.a.i, the elastic section modulus of the effective section calculated at a stress of $f = F_c = 36.141$ ksi in the extreme compression fiber is

$S_c = S_y = 0.844$ in.^{3}

$M_n = S_c F_c = 30.503$ in.-kips for lateral–

torsional buckling strength

iii. *Controlling Nominal Moment M_{ny}*. Use the smaller value of M_n computed for section strength and lateral–torsional buckling strength, i.e.,

$$M_{ny} = 30.503 \text{ in.-kips}$$

b. *Computation of C_{my}*. Based on Eq. (6.60),

$$C_{my} = 0.6 - 0.4(M_1/M_2) = 0.6 - 0.4(-1.0) = 1.0$$

c. *Computation of α_y.* Using Eq. (6.57)

$$\alpha_y = 1 - (\Omega_c P/P_{Ey})$$

where

$$\Omega_c = 1.80$$

$$P_{Ey} = \frac{\pi^2 EI_y}{(K_y L_y)^2} = \frac{\pi^2 (29{,}500)(1.794)}{(14 \times 12)^2} = 18.507 \text{ kips}$$

$$\alpha_y = 1 - (1.80P/18.507) = 1 - 0.0973P$$

d. *Eccentricity of the applied load based on effective area.* In the given data, the eccentricity of $e_x = 2.124$ in. is relative to the centroid of the full section. However, in the calculation of Item 3.b.iv, it was found that for the web element, the effective width b of 7.267 in. is less than the flat width of 7.415 in. The effective area was found to be 1.537 in.^{2} For this reason, the actual eccentricity is reduced slightly in Fig. 6.15. The movement of the centroid can be computed as follows:

$$\frac{[(7.415 - 7.267)(0.105)][0.876 - 0.0525]}{1.537} = 0.0083 \text{ in.}$$

The eccentricity relative to the centroid of the effective section is
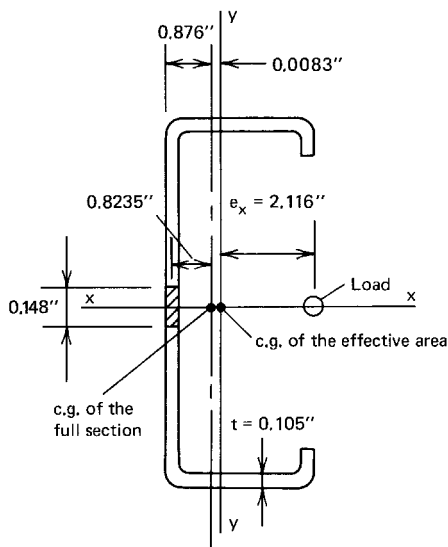
Figure 6.15 Movement of the centroid.

$$e_x = 2.124 - 0.0083 = 2.116 \text{ in.}$$

e. *Allowable load P based on Eq. (6.53).* Using Eq. (6.53),

$$\frac{\Omega_c P}{P_n} + \frac{\Omega_b C_{my} M_y}{M_{ny} \alpha_y}$$

$$= \frac{(1.80)P}{16.069} + \frac{1.67(1)(2.116)P}{(30.503)(1 - 0.0973P)} = 1.0$$

$$P = 3.48 \text{ kips}$$

6. *Application of Eq. (6.54)*
   a. *Computation of P_{no}.* For $KL/r = 0$, $F_n = F_y = 50$ ksi. Using the same procedure illustrated in Item 3,

   $$A_e = 1.176 \text{ in.}^2$$

   $$P_{n0} = A_e F_n = 1.176(50) = 58.80 \text{ kips}$$

   b. *Allowable load P based on Eq. (6.54)*

   $$\frac{\Omega_c P}{P_{n0}} + \frac{\Omega_b M_y}{M_{ny}} = \frac{(1.80)P}{58.80} + \frac{(1.67)(2.116)P}{30.503} = 1.0$$

   $$P = 6.83 \text{ kips}$$

7. *Allowable Load P.* Based on Eqs. (6.53) and (6.54), the allowable load P is 3.48 kips, which is governed by the stability requirement.

6.5   ADDITIONAL INFORMATION ON BEAM-COLUMNS

For additional information on beam-columns, the reader is referred to Refs. 6.7 through 6.35, 5.103, and 5.135.

7 Cylindrical Tubular Members

7.1 GENERAL REMARKS

The design of square and rectangular tubular sections as flexural and compression members is discussed in Chaps. 3 to 6. This chapter deals with the strength of cylindrical tubular members and the design practice for such members used as either flexural or compression members.

Thin-walled cylindrical tubular members are economical sections for compression and torsional members because of their large ratio of radius of gyration to area, the same radius of gyration in all directions, and the large torsional rigidity. In the past, the structural efficiency of such tubular members has been recognized in building construction. A comparison made by Wolford on the design loads for round and square tubing and hot-rolled steel angles used as columns indicates that for the same size and weight, round tubing will carry approximately $2\frac{1}{2}$ and $1\frac{1}{2}$ times the column load of hot-rolled angles when the column length is equal to 36 and 24 times the size of section, respectively.[7.1]

7.2 TYPES OF CYLINDRICAL TUBES

The buckling behavior of cylindrical tubes, which will be discussed later, is considerably affected by the shape of the stress–strain curve of the material, the geometric imperfections such as out of roundness, and the residual stress. It would therefore be convenient to classify tubular members on the basis of their buckling behavior.

In general, cylindrical tubes may be grouped as (1) manufactured tubes and (2) fabricated tubes.[7.2] Manufactured tubes are produced by piercing, forming and welding, cupping, extruding, or other methods in a plant. Fabricated tubes are produced from plates by riveting, bolting, or welding in an ordinary structural fabrication shop. Since fabricated tubes usually have more severe geometric imperfections, the local buckling strength of such tubes may be considerably below that of manufactured tubes.

Manufactured structural steel tubes include the following three types:

1. Seamless tubes
2. Welded tubes
3. Cold-expanded or cold-worked tubes

For the seamless tubes, the stress–strain curve is affected by the residual stress resulting from cooling of the tubes. The proportional limit of a full-sized tube is usually about 75% of the yield point. This type of tube has a uniform property across the cross section.

Welded tubes produced by cold forming and welding steel sheets or plates have gradual-yielding stress–strain curves, as shown in Fig. 2.2 due to the Bauschinger effect and the residual stresses resulting from the manufacturing process. The proportional limit of electric-resistance welded tubes may be as low as 50% of the yield point.

Cold-worked tubes also have this type of gradual yielding because of the Bauschinger effect and the cold work of forming.

7.3 FLEXURAL COLUMN BUCKLING

The basic column formulas for elastic and inelastic buckling discussed in Chap. 5 [Eqs. (5.3a) and (5.7a) are usually applicable to tubular compression members having a proportional limit of no less than 70% of the yield point. For electric-resistance welded tubes having a relatively low proportional limit, Wolford and Rebholz recommended the following formulas on the basis of their tests of carbon steel tubes with yield strengths of 45 and 55 ksi (310 and 379 MPa):[7.3]

1. For $KL/r \leq \sqrt{3\pi^2 E/F_y}$,

$$\sigma_T = F_y \left[1 - \frac{2}{3\sqrt{3}} \sqrt{\frac{F_y}{\pi^2 E}} \left(\frac{KL}{r} \right) \right] \tag{7.1}$$

2. For $KL/r > \sqrt{3\pi^2 E/F_y}$,

$$\sigma_e = \frac{\pi^2 E}{(KL/r)^2} \tag{7.2}$$

where F_y, E, K, and L are as defined in Chap. 5. The radius of gyration r of cylindrical tubes can be computed as

$$r = \frac{\sqrt{D_o^2 + D_i^2}}{4} \simeq \frac{R}{\sqrt{2}} \tag{7.3}$$

where D_o = outside diameter
$\quad\;\; D_i$ = inside diameter
$\quad\;\; R$ = mean radius of tube

The correlation between the test results and Eqs. (5.3), (5.7), (7.1), and (7.2) is shown in Fig. 7.1.[3.84,7.4,7.5] Also shown in this figure are the test data reported by Zaric.[7.6]

Because cylindrical tubes are now commonly used in offshore structures, extensive analytical and experimental studies of the strength of tubular members have recently been made by numerous investigators throughout the world.[7.7–7.15]

7.4   LOCAL BUCKLING

Local buckling of cylindrical tubular members can occur when members are subject to

1. Axial compression
2. Bending
3. Torsion
4. Transverse shear
5. Combined loading

Each item will be discussed separately as follows.
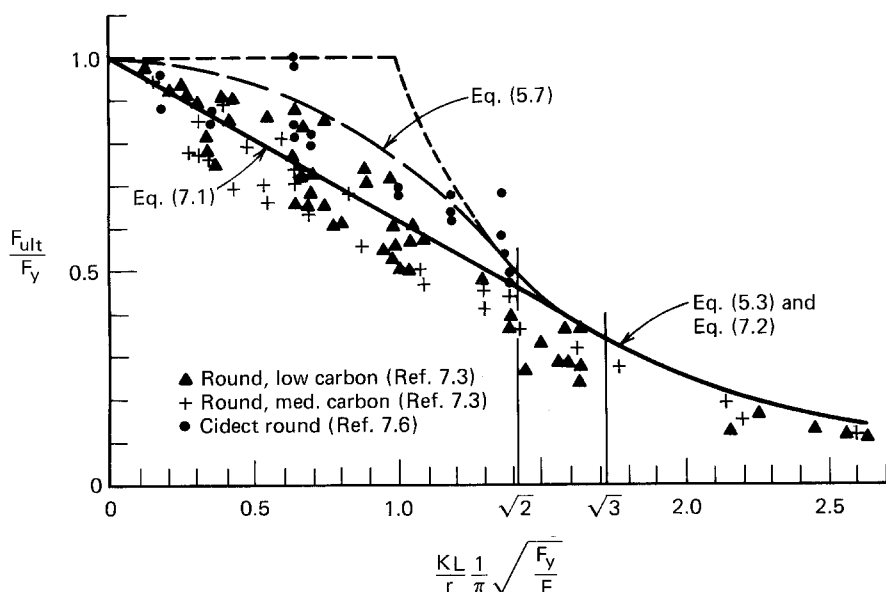
Figure 7.1   Test data for column buckling of axially loaded cylndrical tubes.[3.84]

7.4.1   Local Buckling under Axial Compression

When a cylindrical tube is subject to an axial compressive load, the elastic stability of the tube is more complicated than is the case for a flat plate. Based on the small deflection theory, the structural behavior of a cylindrical shell can be expressed by the following eighth-order partial differential equation:[7.16]

$$\nabla^8 \omega + \frac{1}{D} \nabla^4 \left(N_x \frac{\partial^2 \omega}{\partial x^2} \right) + \frac{Et}{DR^2} \frac{\partial^4 \omega}{\partial x^4} = 0 \qquad (7.4)$$

where

$$\nabla^8 \omega = \nabla^4 (\nabla^4 \omega) \qquad (7.5)$$

$$\nabla^4 \omega = \frac{\partial^4 \omega}{\partial x^4} + 2 \frac{\partial^4 \omega}{\partial x^2 \, \partial y^2} + \frac{\partial^4 \omega}{\partial y^4}$$

and

x = coordinate in x direction
y = coordinate in tangential direction
ω = displacement in radial direction
N_x = axial load applied to cylinder
t = thickness of tube
R = radius of tube
E = modulus of elasticity of steel, = 29.5×10^3 ksi (203 GPa)
$D = \dfrac{Et^3}{12(1 - \mu^2)}$
μ = Poisson's ratio, =0.3

See Fig. 7.2 for dimensions of a cylindrical tube subjected to axial compression.

For a given cylindrical tube the buckling behavior varies with the length of the member. For this reason, from the structural stability point of view, it has been divided into the following three categories by Gerard and Becker:[7.16]

1. Short tubes, $Z < 2.85$
2. Moderate-length tubes, $2.85 < Z < 50$
3. Long tubes, $Z > 50$

Here
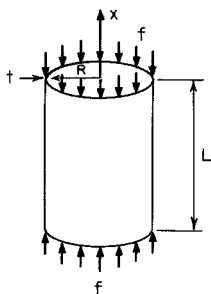
Figure 7.2   Cylindrical tube subjected to axial compression.

$$Z = \frac{L^2}{Rt} \sqrt{1 - \mu^2}$$

$$= 0.954 \, \frac{L^2}{Rt}$$

(7.6)

For very short tubes (i.e., the radius of the tube is extremely large compared with its length), the critical local buckling stress is

$$f_{cr} = \frac{\pi^2 E (t^2/12)}{(1 - \mu^2) L^2}$$

(7.7)

which is identical with the Euler stress for a plate strip of unit width.

For extremely long tubes, the tube will buckle as a column. The critical buckling load is

$$P_{cr} = \frac{\pi^2 EI}{L^2}$$

(7.8)

where I is the moment of inertia of the cross section of the tube,

$$I = \pi R^3 t$$

(7.9)

Therefore, for long tubes the critical buckling stress is

$$f_{cr} = \frac{\pi^2 E}{2} \left(\frac{R}{L} \right)^2$$

(7.10)

Moderate-length tubes may buckle locally in a diamond pattern as shown in Fig. 7.3. The critical local buckling stress is
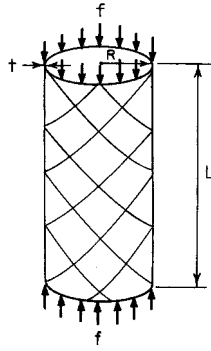
Figure 7.3   Local buckling of moderate-length tubes.

$$f_{cr} = CE\,\frac{t}{R} \tag{7.11}$$

According to the classic theory (small-deflection theory) on local buckling, the value of C can be computed as

$$C = \frac{1}{\sqrt{3(1-\mu^2)}} = 0.605 \tag{7.12}$$

Therefore

$$f_{cr} = \frac{E}{\sqrt{3(1-\mu^2)}}\left(\frac{t}{R}\right) = 0.605E\left(\frac{t}{R}\right) \tag{7.13}$$

Whenever the buckling stress exceeds the proportional limit, the theoretical local buckling stress is in the inelastic range, which can be determined by

$$f_{cr} = aCE\left(\frac{t}{R}\right) \tag{7.14}$$

Here a is the plasticity reduction factor,[7.2]

$$a = \left(\frac{1-\mu^2}{1-\mu_p^2}\right)^{1/2}\left(\frac{E_s}{E}\right)\left(\frac{E_t}{E}\right)^{1\,2} \tag{7.15}$$

where μ = Poisson's ratio in the elastic range, = 0.3
μ_p = Poisson's ratio in the plastic range, = 0.5
E_s = secant modulus
E_l = tangent modulus
E = modulus of elasticity

Results of numerous tests indicate that the actual value of C may be much lower than the theoretical value of 0.605 due to the postbuckling behavior of the cylindrical tubes, which is strongly affected by initial imperfections.

The postbuckling behavior of the three-dimensional cylindrical tubes is quite different from that of two-dimensional flat plates and one-dimensional columns. As shown in Fig. 7.4a, the flat plate develops significant transverse-tension membrane stresses after buckling because of the restraint provided by the two vertical edges. These membrane stresses act to restrain lateral motion, and therefore the plate can carry additional load after buckling.

For columns, after flexural buckling occurs, no significant transverse-tension membrane stresses can be developed to restrain the lateral motion, and therefore, the column is free to deflect laterally under critical load.

For cylindrical tubes, the inward buckling causes superimposed transverse compression membrane stresses, and the buckling form itself is unstable. As a consequence of the compression membrane stresses, buckling of an axially loaded cylinder is coincident with failure and occurs suddenly, accompanied by a considerable drop in load (snap-through buckling).

Since the postbuckling stress of a cylindrical tube decreases suddenly from the classic buckling stress, the stress in an imperfect tube reaches its maximum well below the classic buckling stress (Fig. 7.5).

On the basis of the postbuckling behavior discussed above, Donnell and Wan developed a large-deflection theory which indicates that the value of C
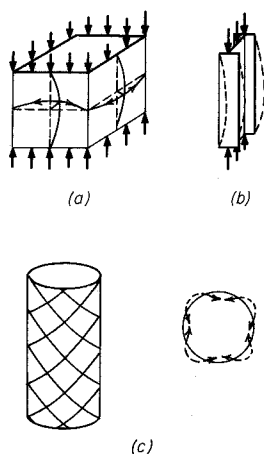
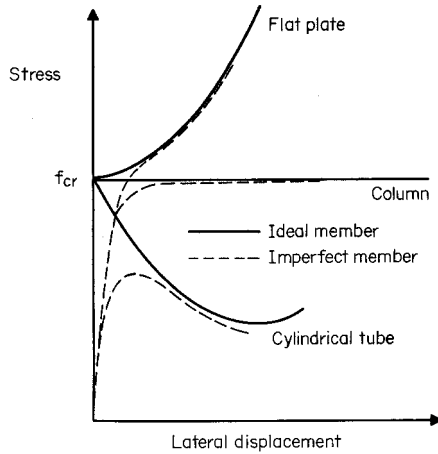Figure 7.4   Buckling patterns of various structural components.

Figure 7.5 Postbuckling behavior of flat plates, columns, and cylindrical tubes.[7.16]

varies with R/t ratio as shown in Fig. 7.6, which is based on average imperfections.[7.17]

During recent years the local buckling strength of cylindrical tubes subjected to axial compression has been studied at Lehigh University,[7.18–7.20] the University of Alberta,[7.21] the University of Tokyo,[7.22] the University of Toronto,[6.30] and others.[7.11–7.15,7.31] The test data obtained from previous and recent research projects have been used in the development and improvement of various design recommendations.[1.4,7.23–7.25]
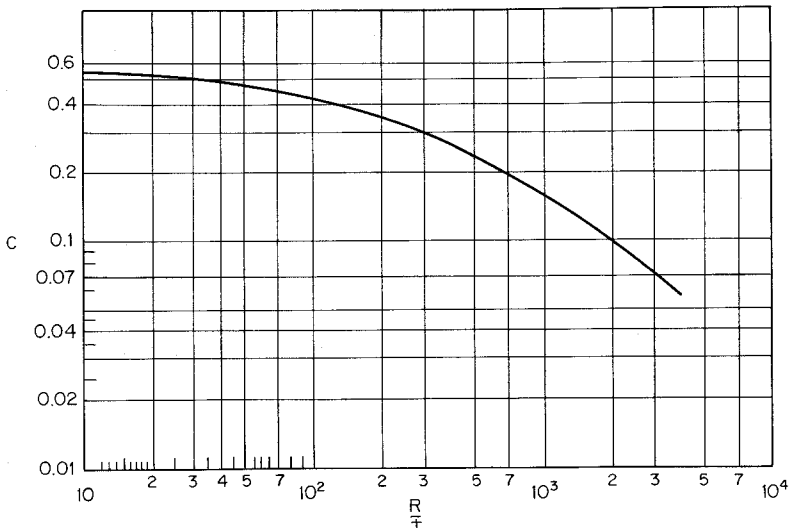
Figure 7.6 Local buckling imperfection parameter versus R/t ratio.[7.16]

7.4.2   Local Buckling under Bending

The local buckling behavior in the compression portion of a flexural tubular member is somewhat different compared with that of the axially loaded compression member. On the basis of their tests and theoretical investigation, Gerard and Becker[7.16] suggested that elastic local buckling stress for bending be taken as 1.3 times the local buckling stress for axial compression. This higher elastic buckling stress for bending results from the beneficial effect of the stress gradient that exists in bending. However, some investigators have indicated that there is not much difference between the critical stress in bending and that in axial compression.[3.84]

The bending strength of cylindrical tubes has been studied by Sherman,[7.26] and by Stephens, Kulak, and Montgomery.[7.21]

7.4.3   Local Buckling under Torsion

The theoretical local buckling stress of moderate-length tubes subjected to torsion can be computed by[7.2]

$$
\begin{aligned}
(\tau_{cr})_{\text{torsion}} &= \frac{0.596a}{(1-\mu^2)^{5/8}} E \left(\frac{t}{R}\right)^{5/4} \left(\frac{R}{L}\right)^{1/2} \\
&= 0.632aE \left(\frac{t}{R}\right)^{5/4} \left(\frac{R}{L}\right)^{1/2}
\end{aligned}
\tag{7.16}
$$

where τ_{cr} is the critical shear buckling stress due to torsion and,

$$
a = \left(\frac{1-\mu^2}{1-\mu_p^2}\right)^{3/4} \left(\frac{E_s}{E}\right) = 1.16 \frac{E_s}{E}
\tag{7.17}
$$

Previous studies indicate that the effect of imperfection on torsional postbuckling is much less than the effect on axial compression. Test data indicate that due to the effect of initial imperfection, the actual strength of the member is smaller than the analytical result.

7.4.4   Local Buckling under Transverse Shear

In Ref. 7.2, Schilling suggests that in the elastic range, the critical shear buckling stress in transverse shear be taken as 1.25 times the critical shear buckling stress due to torsion, that is,

$$
\begin{aligned}
(\tau_{cr})_{\text{transverse shear}} &= 1.25 \times 0.632aE \left(\frac{t}{R}\right)^{5/4} \left(\frac{R}{L}\right)^{1/2} \\
&= 0.79aE \left(\frac{t}{R}\right)^{5/4} \left(\frac{R}{L}\right)^{1/2}
\end{aligned}
\tag{7.18}
$$

7.4.5   Local Buckling under Combined Loading

The following interaction formula may be used for any combined loading:[7.2]

$$\left(\frac{f}{f_{\text{cr}}}\right) + \left(\frac{\tau}{\tau_{\text{cr}}}\right)^2 = 1 \tag{7.19}$$

where f = actual computed normal stress
f_{cr} = critical buckling stress for normal stress alone
τ = actual computed shear stress
τ_{cr} = critical buckling stress for shear stress alone

7.5   AISI DESIGN CRITERIA[1.314]

The AISI design criteria for cylindrical tabular members were revised in the 1986 and 1996 editions of the specification on the basis of Refs. 1.158, 7.5, and 7.30. For additional information, the reader is referred to Refs. 8.25 through 8.32.

7.5.1   Local Buckling Stress

Considering the postbuckling behavior of the axially compressed cylinder and the important effect of the initial imperfection, the design provisions included in the AISI Specification were originally based on Plantema's graphic representation[7.27] and the additional results of cylindrical shell tests made by Wilson and Newmark at the University of Illinois.[7.28,7.29]

From the tests of compressed tubes, Plantema found that the ratio $F_{\text{ult}}/F_{\text{y}}$ depends on the parameter $(E/F_{\text{y}})(t/D)$, in which t is the wall thickness, D is the mean diameter of the tubes, and F_{ult} is the ultimate stress or collapse stress. As shown in Fig. 7.7, line 1 corresponds to the collapse stress below the proportional limit, line 2 corresponds to the collapse stress between the proportional limit and the yield point (the approximate proportional limit is 83% of F_{y} at point B), and line 3 represents the collapse stress occurring at yield point. In the range of line 3, local buckling will not occur before yielding, and no stress reduction is necessary.

In ranges 1 and 2, local buckling occurs before the yield point is reached. In these cases the stress should be reduced to safeguard against local buckling.

As shown in Fig. 7.7, point A represents a specific value of $(E/F_{\text{y}})(t/D) = 8$, which divides yielding and local buckling. Using $E = 29.5 \times 10^3$ ksi (203 GPa), it can be seen that tubes with D/t ratios of no more than 0.125 E/F_{y} are safe from failure caused by local buckling. Specifically, Plantema's equations are as follows:[7.4]
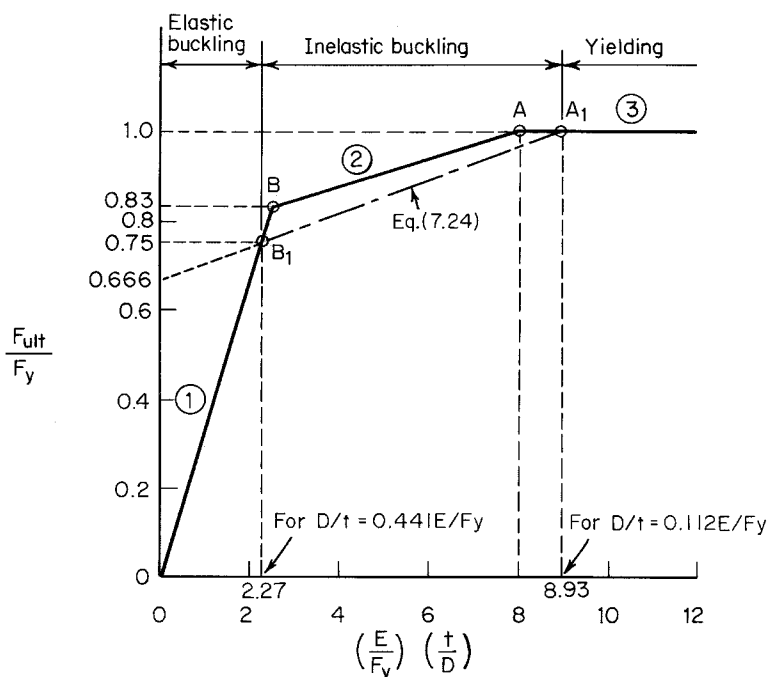
Figure 7.7   Ultimate strength of cylindrical tubes for local buckling.

1. For $D/t \leq 0.125E/F_y$ (yielding failure criterion represented by line 3),

$$\frac{F_{ult}}{F_y} = 1 \tag{7.20}$$

2. For $0.125E/F_y < D/t \leq 0.4E/F_y$ (inelastic buckling criterion represented by line 2),

$$\frac{F_{ult}}{F_y} = 0.031 \left(\frac{E}{F_y}\right)\left(\frac{t}{D}\right) + 0.75 \tag{7.21}$$

3. For $D/t > 0.4E/F_y$ (elastic buckling criterion represented by line 1),

$$\frac{F_{ult}}{F_y} = 0.33 \left(\frac{E}{F_y}\right)\left(\frac{t}{D}\right) \tag{7.22}$$

Based on a conservative approach, AISI specifies that when the D/t ratio is smaller than or equal to $0.112E/F_y$, the tubular member shall be designed for yielding. This provision is based on point A_1, for which $(E/F_y)(t/D) = 8.93$.

When $0.112E/F_y < D/t < 0.441\ E/F_y$, the design of tubular members is based on the local buckling criteria. For the purpose of developing a design formula for inelastic buckling, point B_1 was selected by AISI to represent the proportional limit. For point B_1,

$$\left(\frac{E}{F_y}\right)\left(\frac{t}{D}\right) = 2.27 \quad \text{and} \quad \frac{F_{ult}}{F_y} = 0.75 \tag{7.23}$$

Using line A_1B_1, the maximum stress of tubes can be represented by

$$\frac{F_{ult}}{F_y} = 0.037\left(\frac{E}{F_y}\right)\left(\frac{t}{D}\right) + 0.667 \tag{7.24}$$

The correlation between the available test data and Eq. (7.24) is shown in Fig. 7.8.

Let A be the area of the unreduced cross section and A_0 be the reduced area due to local buckling, then

$$AF_{ult} = A_0F_y \tag{7.25}$$

or
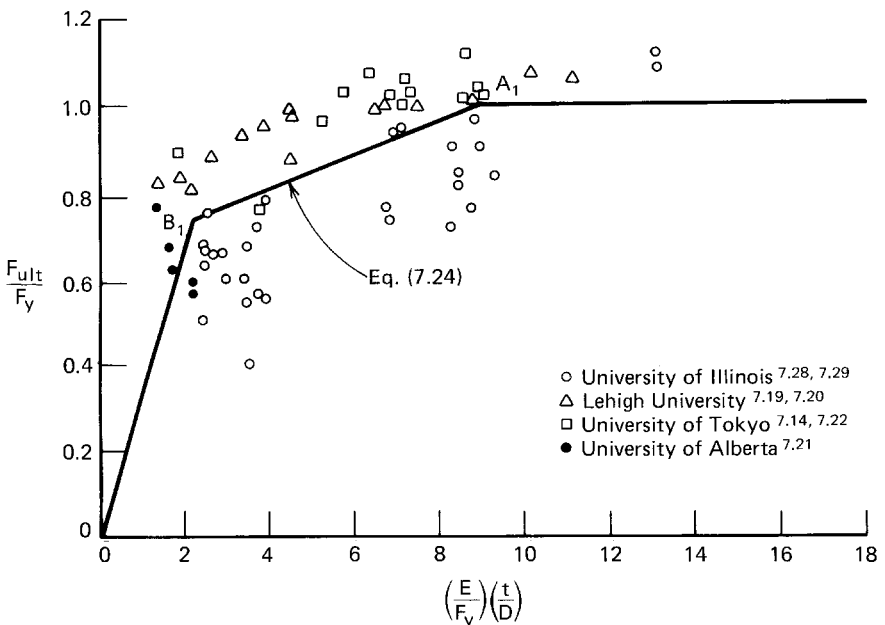
Figure 7.8   Correlation between test data and AISI criteria for local buckling of cylindrical tubes under axial compression.

$$A_0 = \left(\frac{F_{ult}}{F_y}\right) A \tag{7.26}$$

Substituting Eq. (7.24) into Eq. (7.26), the following equation can be obtained for $D/t \leq 0.441E/F_y$:

$$A_0 = \left[\frac{0.037}{(D/t)(F_y/E)} + 0.667\right] A \leq A \tag{7.27}$$

where D is the outside diameter of the cylindrical tubular member.

7.5.2 Compressive Strength

When a cylindrical tubular member is subject to a compressive load in the direction of the member axis passing through the centroid of the section, the AISI design provision was changed in the 1996 Specification to reflect the results of additional studies of cylindrical tubular members and to be consistent with Sec. C4 of the Specification. The following equations are now included in Sec. C6.2 of the AISI Specification and Supplement No. 1 for determining the nominal axial strength P_n of cylindrical tubular members having a ratio of outside diameter to wall thickness, D/t, not greater than $0.441E/F_y$.[1.314,1.333]

$$P_n = F_n A_e \tag{7.28}$$

where P_n = nominal axial strength of the member
      F_n = flexural buckling stress determined as follows:

For $\lambda_c \leq 1.5$,

$$F_n = (0.658^{\lambda_c^2})F_y \tag{7.29}$$

For $\lambda_c > 1.5$,

$$F_n = \left[\frac{0.877}{\lambda_c^2}\right] F_y \tag{7.30}$$

where

$$\lambda_c = \sqrt{\frac{F_y}{F_e}} \tag{7.31}$$

In the above equations,

F_e = the elastic flexural buckling stress determined according to Sec. C4.1 of the Specification

A_e = effective area of the cylindrical tubular member under axial compression determined as follows:[1.333]

$$A_e = A_0 + R (A - A_0) \tag{7.32}$$

$$R = F_y/2F_e \le 1.0 \tag{7.33}$$

$$A_0 = \left[\frac{0.037}{(DF_y)/(tE)} + 0.667 \right] A \le A \tag{7.34}$$

A = area of the unreduced cross section

Equations (7.28) through (7.34) can be summarized in Fig. 7.9. It can be seen that Eq. (7.32) gives $A_e = A_0$ when $\lambda_c = 0$, and $A_e = A$ when $\lambda_c = \sqrt{2}$. The latter is due to the fact that for long columns the stresses at which the column buckles are so low that they will not cause local buckling before primary buckling has taken place.

Consequently, for the design of axially loaded cylindrical tubular members, the allowable axial load P_a for the ASD method is determined by Eq. (7.35):
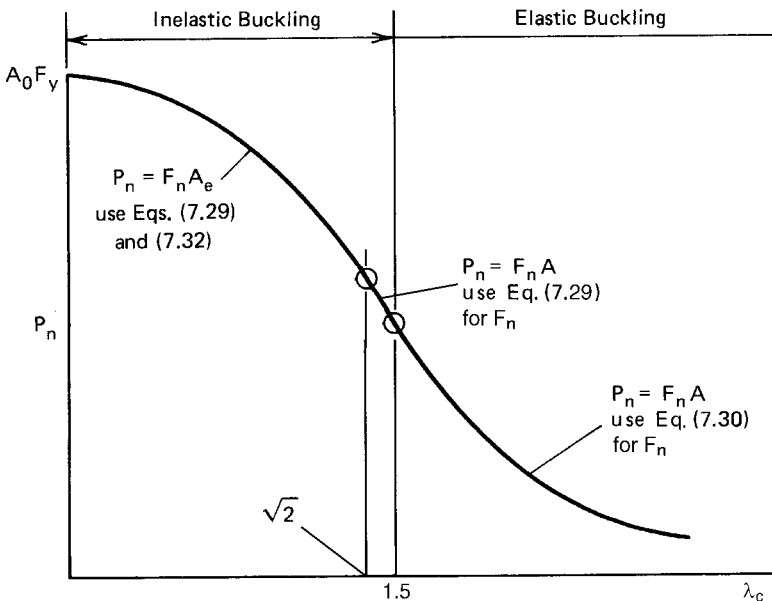
Figure 7.9 Nominal compressive load of cylindrical tubular members.

$$P_a = P_n/\Omega_c \tag{7.35}$$

where Ω_c = factor of safety for axial compression = 1.80. For the LRFD method, the design axial strength is $\phi_c P_n$, in which ϕ_c = 0.85.

7.5.3 Bending Strength

In Art. 7.4.2, it was pointed out that for cylindrical tubular members, the elastic local buckling stress for bending is higher than the elastic local buckling stress for axial compression. In addition, it has been recognized that for thick cylindrical members subjected to bending, the initiation of yielding does not represent the failure condition as is generally assumed for axial loading. For relatively compact members with $D/t \leq 0.0714\ E/F_y$, the flexural strength can reach the plastic moment capacity, which is at least 1.25 times the moment at first yielding. As far as the local buckling is concerned, the conditions for inelastic buckling are not as severe as the case of axial compression due to the effect of stress gradient. Based on the results of recent studies, the following AISI design provisions for determining the nominal flexural strength are included in Sec. C6.1 of the Supplement to the 1996 edition of the Specification for tubular members having $D/t \leq 0.441E/F_y$.[1.314,1.333]

1. For $D/t \leq 0.0714E/F_y$:

$$M_n = 1.25\ F_y S_f \tag{7.36}$$

2. For $0.0714E/F_y < D/t \leq 0.318E/F_y$:

$$M_n = \left[0.970 + 0.020\ \frac{(E/F_y)}{(D/t)} \right] F_y S_f \tag{7.37}$$

3. For $0.318E/F_y < D/t \leq 0.441E/F_y$:

$$M_n = [0.328E/(D/t)]S_f \tag{7.38}$$

where M_n = nominal flexural strength
S_f = elastic section modulus of the full, unreduced cross section

The allowable bending moment, M_a, for the ASD method is determined by using Eq. (7.39):

$$M_a = M_n/\Omega_b \tag{7.39}$$

where Ω_b = factor of safety for bending = 1.67. For the LRFD method, the design flexural strength is $\phi_b M_n$, in which ϕ_b = 0.95.

Equations (7.36) through (7.38) are shown graphically in Fig. 7.10. As compared with the 1980 edition of the AISI Specification, it can be shown that the increases of the nominal moment range from about 13 to 25% according to the value of the $(E/F_y)(t/D)$.

7.5.4 Combined Bending and Compression

The interaction formulas presented in Chap. 6 can also be used for the design of beam-columns using cylindrical tubular members. The nominal axial strength and nominal flexural strength can be obtained from Arts. 7.5.2 and 7.5.3, respectively.

7.6 DESIGN EXAMPLES

Example 7.1 Use the ASD and LRFD methods to determine the design axial strength for the cylindrical tube having a 10-in. outside diameter to be used as an axially loaded simply supported column. Assume that the effective
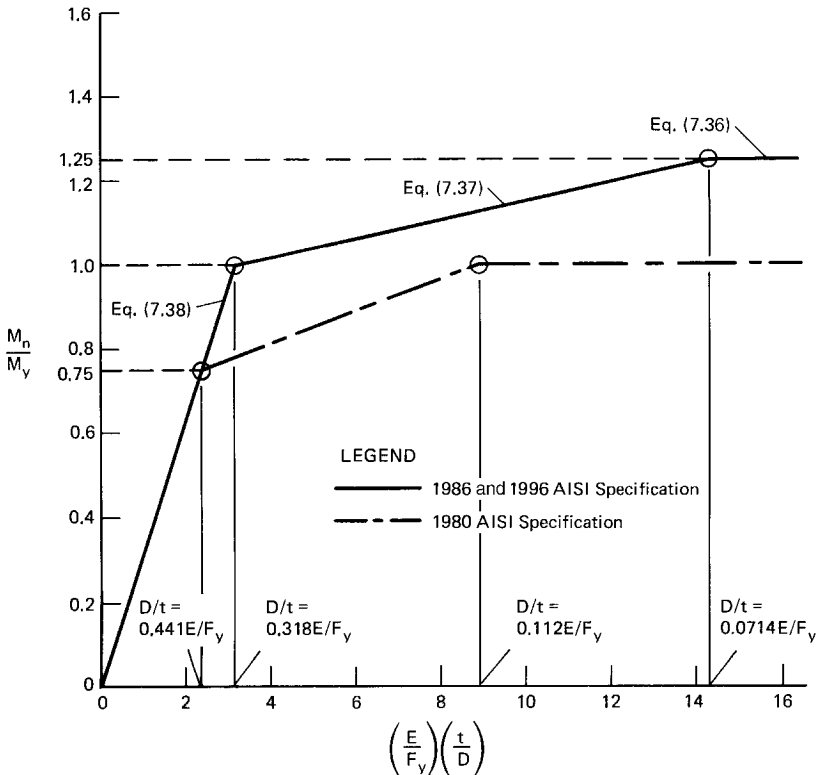
Figure 7.10 Nominal flexural strength of cylindrical tubular members.

column length is 15 ft, the yield point of steel is 33 ksi, and the thickness of the tube is 0.105 in.

Solution

A. *ASD Method.* Using the AISI design criteria, the limiting D/t ratio is

$$\left(\frac{D}{t}\right)_{\text{lim}} = 0.441 \frac{E}{F_{y}} = 0.441 \frac{29{,}500}{33} = 394.23$$

The actual D/t ratio is

$$\frac{D}{t} = \frac{10}{0.105} = 95.24 < 394.23 \qquad \text{O.K.}$$

1. *Sectional Properties of Full Section*

$$A = \frac{\pi(D_{o}^{2} - D_{i}^{2})}{4}$$

$$= \frac{\pi[(10.0)^{2} - (10.0 - 2 \times 0.105)^{2}]}{4}$$

$$= 3.264 \text{ in.}^{2}$$

$$r = \frac{\sqrt{D_{o}^{2} + D_{i}^{2}}}{4}$$

$$= \frac{\sqrt{(10.0)^{2} + (10.0 - 2 \times 0.105)^{2}}}{4} = 3.500 \text{ in.}$$

2. *Nominal Axial Strength,* P_{n}

a. $\dfrac{KL}{r} = \dfrac{15 \times 12}{3.50} = 51.43$

According to Eq. (5.56), the elastic flexural buckling stress is

$$F_{e} = \frac{\pi^{2}E}{(KL/r)^{2}} = \frac{\pi^{2}(29{,}500)}{(51.43)^{2}} = 110.08 \text{ ksi}$$

b. Based on Eq. (7.31),

$$\lambda_c = \sqrt{\frac{F_y}{F_e}} = \sqrt{\frac{33}{110.08}} = 0.548 < 1.5$$

$$F_n = (0.658^{\lambda_c^2})F_y = (0.658^{0.548^2})(33)$$

$$= 29.10 \text{ ksi}$$

c. Based on Eqs. (7.32), (7.33), and (7.34),

$$A_c = A_o + R(A - A_o)$$

where

$$R = F_y/2F_e$$

$$= 33/(2 \times 110.08) = 0.150 < 1.0 \qquad \text{O.K.}$$

$$A_0 = \left[\frac{0.037}{(D/t)(F_y/E)} + 0.667 \right] A$$

$$= \left[\frac{0.037}{(95.24)(33/29,500)} + 0.667 \right] (3.264)$$

$$= 3.311 \text{ in.}^2$$

Because $3.311 > A = 3.264 \text{ in.}^2$, use $A_0 = 3.264 \text{ in.}^2$ Therefore,

$$A_e = 3.264 + (0.150)(3.264 - 3.264)$$

$$= 3.264 \text{ in.}^2$$

From Eq. (7.28), the nominal axial load is

$$P_n = F_n A_e$$

$$= (29.10)(3.264) = 94.98 \text{ kips}$$

3. *Allowable axial load, P_a*. From Eq. (7.35), the allowable axial load is

$$P_a = P_n/\Omega_c = 94.98/1.80$$

$$= 52.77 \text{ kips}$$

B. *LRFD Method.* For the LRFD method, the design axial strength is

$$\phi_c P_n = 0.85(94.98)$$
$$= 80.73 \text{ kips}$$

Example 7.2 All data are the same as those of Example 7.1, except that the thickness of the tube is 0.06 in.

Solution

A. *ASD Method.* Use the same procedure employed in Example 7.1.

$$\left(\frac{D}{t}\right)_{\text{lim}} = 0.441 \frac{E}{F_y} = 394.23$$

The actual D/t ratio is

$$\frac{D}{t} = \frac{10}{0.06} = 166.67 < 394.23 \qquad \text{O.K.}$$

1. *Sectional Properties of Full Section*

$$A = \frac{\pi[(10.0)^2 - (10.0 - 2 \times 0.06)^2]}{4} = 1.874 \text{ in.}^2$$

$$r = \frac{\sqrt{(10.0)^2 + (10.0 - 2 \times 0.06)^2}}{4} = 3.51 \text{ in.}$$

2. *Nominal Axial Strength, P_n*

a. $\dfrac{KL}{r} = \dfrac{15 \times 12}{3.51} = 51.28$

$$F_e = \frac{\pi^2 E}{(KL/r)^2} = \frac{\pi^2(29,500)}{(51.28)^2} = 110.72 \text{ ksi}$$

b. Based on Eq. (7.31),

$$\lambda_c = \sqrt{\frac{F_y}{F_e}} = \sqrt{\frac{33}{110.72}} = 0.546 < 1.5$$

$$F_n = (0.658^{\lambda_c^2})F_y = (0.658^{0.546^2})(33)$$
$$= 29.13 \text{ ksi}$$

c. Based on Eqs. (7.32), (7.33), and (7.34),

$$A_e = A_0 + R (A - A_0)$$

where $R = F_y/2F_e = 33/(2 \times 110.72) = 0.149 < 1.0$ O.K.

$$A_0 = \left[\frac{0.037}{(166.67)(33/29,500)} + 0.667 \right](1.874) = 1.622 \text{ in.}^2$$

Since $A_0 < A = 1.874$ in.^{2}, use $A_0 = 1.622$ in.^{2}

$$A_e = 1.622 + (0.149)(1.874 - 1.622) = 1.660 \text{ in.}^2$$

The nominal axial strength is

$$P_n = F_n A_e = (29.13)(1.660) = 48.36 \text{ kips}$$

3. *Allowable Axial Load,* P_a. From Eq. (7.35), the allowable axial load is

$$P_a = P_n/\Omega_c = 48.36/1.80$$
$$= 26.87 \text{ kips}$$

B. *LRFD Method.* For the LRFD method, the design axial strength is

$$\phi_c P_n = 0.85(48.36)$$
$$= 41.11 \text{ kips}$$

Example 7.3   Use the ASD and LRFD methods to determine the design flexural strength of cylindrical tubes used in Examples 7.1 and 7.2 if these tubes are to be used as flexural members.

Solution

A. *ASD Method*
   1. Use the data given in Example 7.1,

$$F_y = 33 \text{ ksi}$$
$$D_o = 10 \text{ in.}$$
$$t = 0.105 \text{ in.}$$
$$D/t = 95.24 < 0.441E/F_y \qquad \text{O.K.}$$

a. *Section modulus of the full section.* The section modulus of the 10-in. tube having a wall thickness of 0.105 in. is

$$S_f = \frac{\pi(D_o^4 - D_i^4)}{32D_o} = 0.098175 \frac{D_o^4 - D_i^4}{D_o}$$

$$= 0.098175 \frac{(10.0)^4 - (9.79)^4}{10.0} = 7.99 \text{ in.}^3$$

b. *Nominal flexural strength, M_n*

$$0.0714E/F_y = 0.0714(29,500)/33 = 63.83$$

$$0.318E/F_y = 0.318(29,500)/33 = 284.27$$

Since $0.0714E/F_y < (D/t = 95.24) < 0.318E/F_y$, according to Eq. (7.37), the nominal flexural strength is

$$M_n = \left[0.970 + 0.020 \frac{(E/F_y)}{D/t}\right]F_y S_f$$

$$= \left[0.970 + 0.020 \frac{(29,500/33)}{95.24}\right](33)(7.99)$$

$$= 305.26 \text{ in.-kips}$$

c. *Allowable design flexural strength, M_a.* Based on Eq. (7.39), the allowable design flexural strength is

$$M_a = M_n/\Omega_b$$

$$= \frac{305.26}{1.67} = 182.79 \text{ in.-kips}$$

2. Use the data given in Example 7.2,

$$F_y = 33 \text{ ksi}$$

$$D_o = 10 \text{ in.}$$

$$t = 0.06 \text{ in.}$$

$$D/t = 166.67 < 0.441E/F_y \qquad \text{O.K.}$$

a. *Section modulus of the full section.* The section modulus of the 10-in. tube having a wall thickness of 0.06 in. is

$$S_f = 0.098175 \frac{(10.0)^4 - (9.88)^4}{10.0} = 4.628 \text{ in.}^3$$

b. *Nominal flextural strength, M_n.* Since $0.0714E/F_y < D/t < 0.318E/F_y$,

$$M_n = \left[0.970 + 0.020 \frac{(29,500/33)}{166.67} \right](33)(4.628)$$

$$= 164.53 \text{ in.-kips}$$

c. *Allowable design flexural strength, M_a.* The allowable design flexural strength is

$$M_a = M_n/\Omega_b$$

$$= \frac{164.53}{1.67} = 98.52 \text{ in.-kips.}$$

B. *LRFD Method*

Using the LRFD method, the design flexural strengths for the cylindrical tubes used in Examples 7.1 and 7.2 can be computed as follows:

1. For the cylindrical tube used in Example 7.1, the nominal flexural strength computed in Item (A) above is

$$M_n = 305.26 \text{ in.-kips}$$

The design flexural strength is

$$\phi_b M_n = 0.95(305.26) = 290.00 \text{ in.-kips}$$

2. For the cylindrical tube used in Example 7.2, the nominal flexural strength computed in Item (A) above is

$$M_n = 164.53 \text{ in.-kips}$$

The design flexural strength is

$$\phi_b M_n = 0.95(164.53) = 156.30 \text{ in.-kips}$$

8 Connections

8.1 GENERAL REMARKS

In Chaps. 4 through 7 the design of individual structural members, such as beams, columns, tension members, and cylindrical tubular members, to be used in cold-formed steel construction has been discussed. It is often found that such structural members are fabricated from steel sheets or structural components by using various types of connections. In addition, connections are required for joining individual members in overall structures.

In this chapter the types of connections generally used in cold-formed steel structures, the design criteria for various types of connections, the requirements to fabricate I- or box-shaped beams and columns by connecting two channels, and the spacing of connections in compression elements are discussed.

For connection design tables and example problems, reference should be made to Part IV of the Design Manual.

As a general rule of the AISI Specification, all connections should be designed to transmit the maximum design force in the connected member with proper regard for eccentricity.

8.2 TYPES OF CONNECTORS

Welds, bolts, cold rivets, screws, and other special devices such as metal stitching and adhesives are generally used in cold-formed steel connections.[1.159,1.161,8.1–8.10,8.63–8.65] The AISI Specification contains provisions in Sec. E for welded, bolted, and screw connections, which are most commonly used.

In the design of connections using cold rivets, the AISI provisions for bolted connections may be used as a general guide, except that the shear strength of rivets may be quite different from that of bolts, and that different failure modes such as pullout and inclination of fasteners should also be considered. Additional information on the strength of connections should be obtained from manufacturers or from tests. Article 8.6 gives a brief discussion on the application of cold rivets and press-joints.

8.3 WELDED CONNECTIONS

Welds used for building construction may be classified as arc welds and resistance welds.

430

Arc welding is a group of processes in which metals were welded together by using weld metal at the surfaces to be joined without the application of mechanical pressure or blows.

Resistance welding is a group of welding processes where coalescence is produced by the heat obtained from resistance to an electric current through the work parts held together under pressure by electrodes.

8.3.1   Arc Welds

Arc welds are often used for erection, connecting cold-formed steel members to each other, or connecting cold-formed steel members to hot-rolled framing members. Several types of arc welds generally used in cold-formed steel construction are:

1. Groove welds
2. Arc spot welds (puddle welds)
3. Arc seam welds
4. Fillet welds
5. Flare groove welds

Figure 8.1 shows different types of arc welds.

Arc spot welds used for thin sheets are similar to plug welds used for relatively thicker plates. The difference between plug welds and arc spot welds is that the former are made with prepunched holes, but for the latter no prepunched holes are required. A hole is burned in the top sheet and then filled with weld metal to fuse it to the bottom sheet or structural members. Similarly, arc seam welds are the same as slot welds, except that no prepunched holes are required for the former.

The American Welding Society (AWS) has established certain welding symbols. Figure 8.2 shows the basic symbols and the standard locations of the elements of a welding symbol used in cold-formed steel structures.[8.11]

With regard to the research work on arc welds, the earlier AISI design provisions for fillet welds and arc spot welds were based on the results of 151 tests conducted in the 1950s at Cornell University.[1.161] In the 1970s a total of 342 additional tests on fillet, flare bevel, arc spot, and arc seam welded connections were carried out at Cornell University under the sponsorship of the AISI.[8.12, 8.13] The structural behavior of the most common types of arc welds used for sheet steel has been studied in detail. Based on the research findings at Cornell University summarized by Pekoz and McGuire[8.12,8.13] and a study made by Blodgett of the Lincoln Electric Company,[8.14] the first edition of the "Specification for Welding Sheet Steel in Structures" was developed by the Subcommittee on Sheet Steel of the AWS Structural Welding Committee in 1978.[8.15] The second edition of this document, entitled "Structural Welding Code—Sheet Steel," was issued by the AWS in 1989.[8.16] Based on the same data, in 1980, the AISI design provisions for arc welds were revised
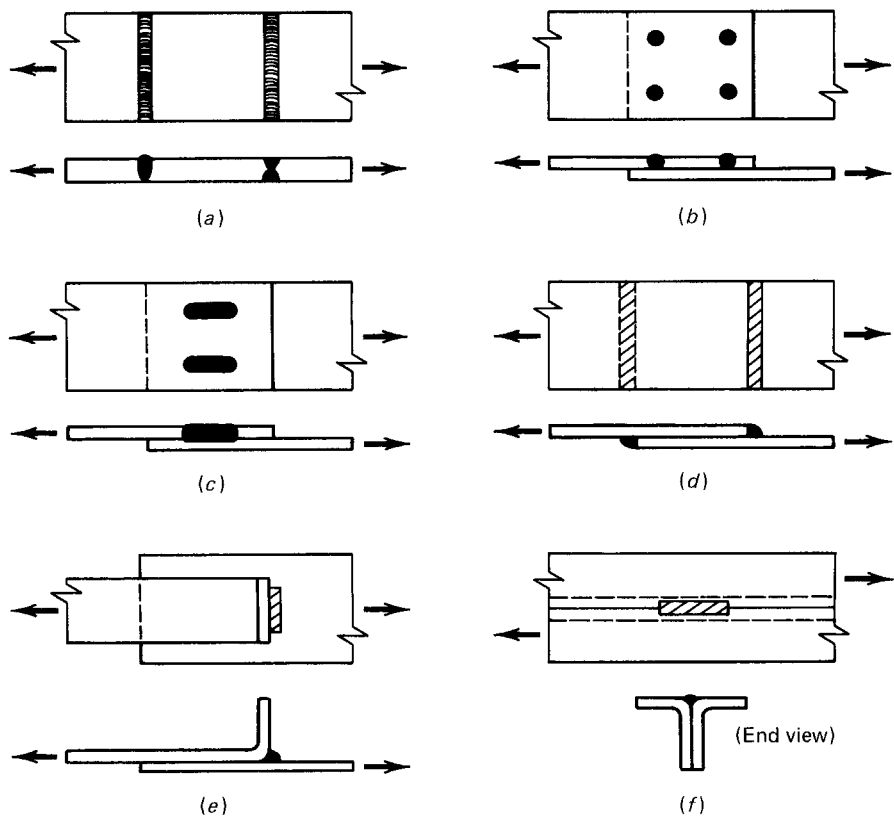
Figure 8.1   Types of arc welds. (*a*) Groove welds in butt joints. (*b*) Arc spot welds. (*c*) Arc seam welds. (*d*) Fillet welds. (*e*) Flare bevel groove weld. (*f*) Flare V-groove weld.

extensively to reflect the research results. The same design provisions were used in the 1986 AISI Specification with additional design formulas included in the 1989 Addendum for tensile load of arc spot welds. Minor revisions were made in 1996 with new figures added for the design of flare bevel groove welds. In the Supplement to the 1996 AISI Specification, design equations are used to replace tabular values for determining the nominal shear strength of resistance welds.

The following sections summarize the research findings on the structural strengths of various types of arc welds. As discussed in Refs. 8.12 and 8.13, the thickness of steel sheets used in the Cornell test program ranged from 0.019 to 0.138 in. (0.48 to 3.5 mm). The yield points of materials varied from 33 to 82 ksi (228 to 565 MPa). All specimens were welded with E6010 electrodes.
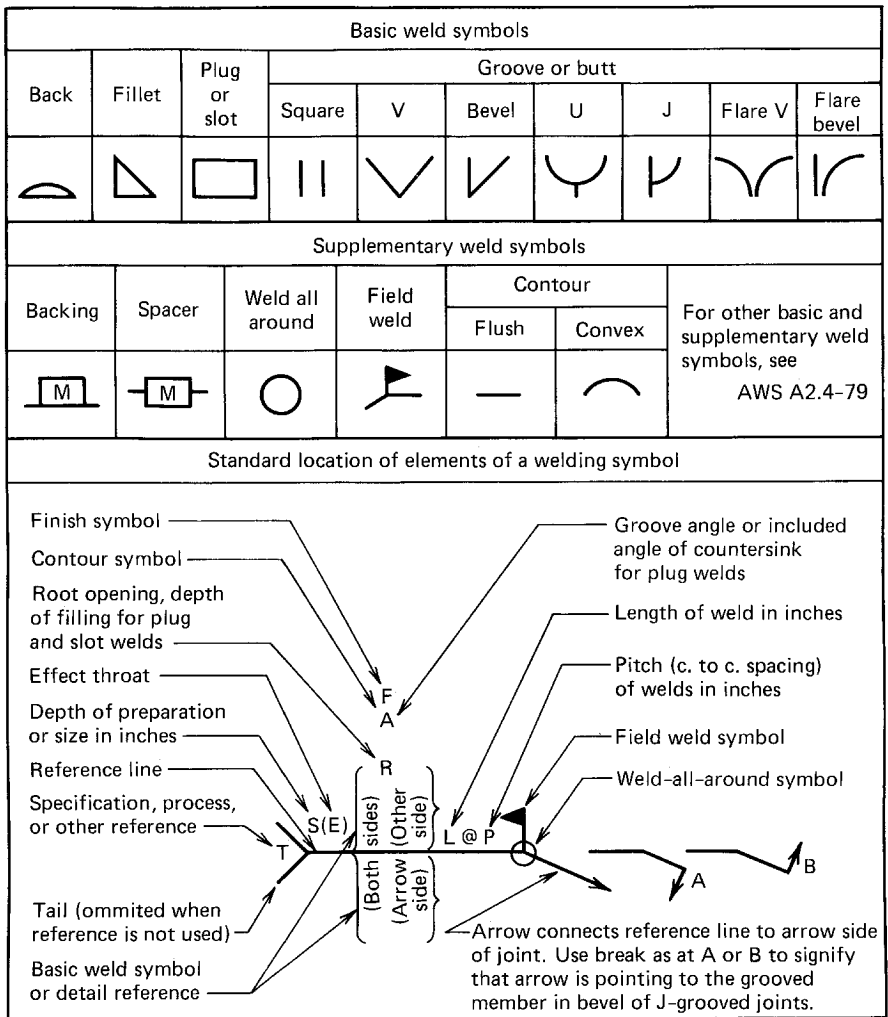
Figure 8.2   Standard symbols for welded joints.[8.11]

8.3.1.1   *Arc Spot Welds*   Based on the results of 126 tests on arc spot welds, it was found that the limit states of arc spot welds include shear failure of welds in the fused area, tearing of the sheet along the contour of the weld with the tear spreading across the sheet at the leading edge of the weld, sheet tearing combined with buckling near the trailing edge of the weld, and shearing of the sheet behind the weld.[8.12,8.13] In addition, some welds failed in part by peeling of the weld as the sheet material tore and deformed out of its own plane.

An evaluation of the test results indicates that the following equations can be used to predict the ultimate strength of connections joined by arc spot welds.

Shear Strength of Arc Spot Welds. The ultimate shear capacity per arc spot weld can be determined by[8.12]

$$P_{us} = A_s \tau_u = \left(\frac{\pi}{4} d_e^2 \right) \left(\frac{3}{4} F_{xx} \right) = \frac{3\pi}{16} d_e^2 F_{xx} \qquad (8.1)$$

where P_{us} = ultimate shear capacity per weld, kips
A_s = fused area of arc spot weld, in.^{2}
τ_u = ultimate shear strength of weld metal, which was taken as 0.75 F_{xx} in Refs. 8.12 and 8.13, ksi
F_{xx} = tensile strength of weld metal according to strength level designation in AWS electrode classification, ksi
d_e = effective diameter of fused area, in.

Based on the test data on 31 shear failures of arc spot welds, it was found that the effective diameter of the fused area can be computed as[8.12,8.13]

$$d_e = 0.7d - 1.5t \le 0.55d \qquad (8.2)$$

where d = visible diameter of outer surface of arc spot weld
t = base thickness (exclusive of coatings) of steel sheets involved in shear transfer

The correlation between the computed ratios of d_e/d and the test data is demonstrated in Fig. 8.3. Figure 8.4 shows the definitions of the visible diameter d and the effective diameter d_e.

Strength of Connected Sheets by Using Arc Spot Welds. On the basis of his analysis of stress conditions in the connected sheets around the circumference of the arc spot weld, Blodgett pointed out that the stress in the material is a tensile stress at the leading edge, becoming a shear stress along the sides, and eventually becoming a compressive stress at the trailing edge of the weld, as shown in Fig. 8.5.[8.14,8.16] If the strength of welded connections is governed by transverse tearing of the connected sheet rather than by shear failure of the weld, the ultimate load, in kips, per weld was found to be
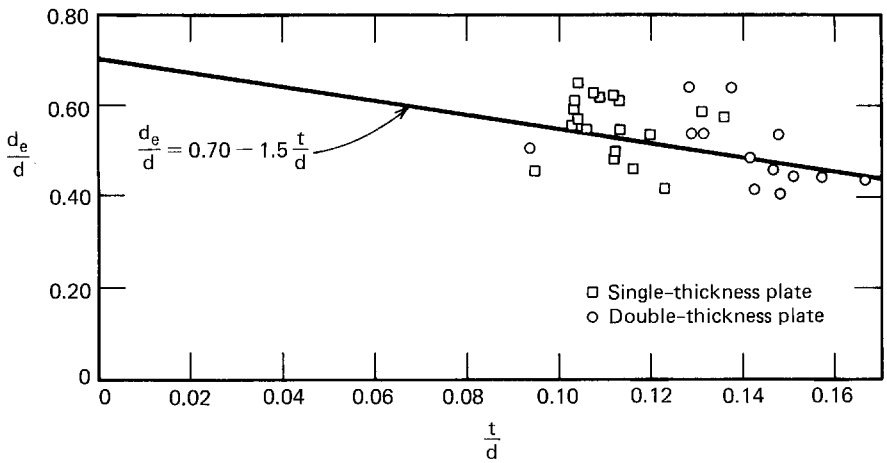
$$P_{ul} = 2.2td_a F_u \qquad (8.3)$$

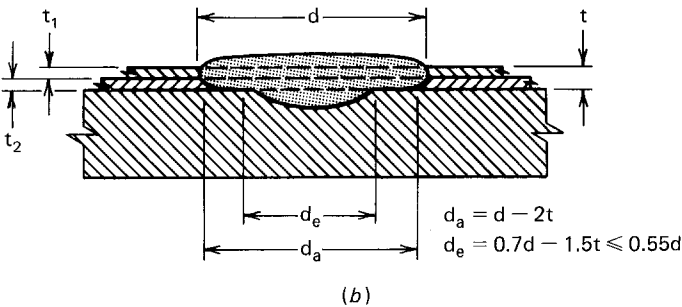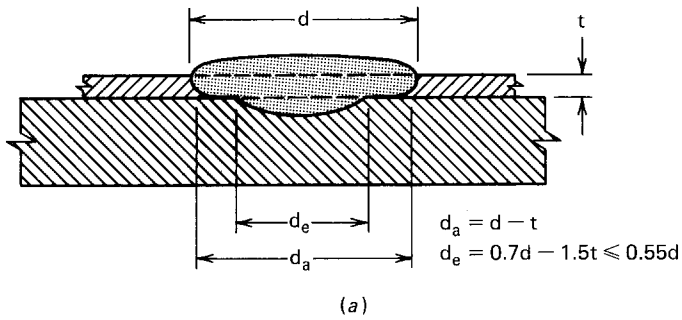**Figure 8.3** Correlation between d_e/d ratios and test data according to plate thickness.[8.13]

$$d_a = d - t$$
$$d_e = 0.7d - 1.5t \leqslant 0.55d$$

(a)

$$d_a = d - 2t$$
$$d_e = 0.7d - 1.5t \leqslant 0.55d$$

(b)

Figure 8.4 Definitions of d, d_a, and d_e in arc spot welds.[1.314] (a) Single thickness of sheet. (b) Double thickness of sheet.
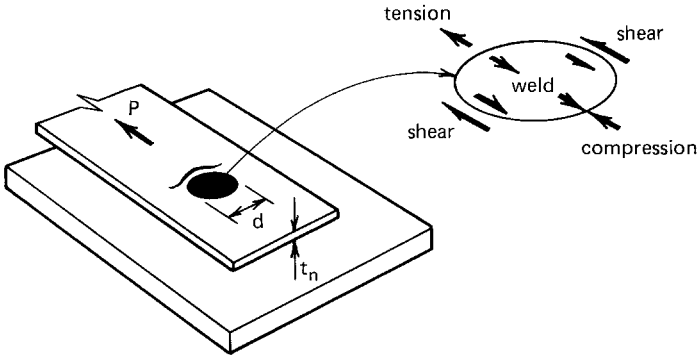
Figure 8.5   Tension, compression, and shear stresses in arc spot weld.[8.14,8.16]

where d_a = average diameter of arc spot weld at midthickness of t, in.; = $d - t$ for single sheet and = $d - 2t$ for multiple sheets (Fig. 8.4)

t = total combined base steel thickness of sheets involved in shear transfer, in.

F_u = specified minimum tensile strength of connected sheets, ksi

The same study also indicated that Eq. (8.3) is applicable only when $d_a/t \leq 140/\sqrt{F_u}$.

For thin sheets, failure will occur initially by tension at the leading edge, tearing out in shear along the sides, and then buckling near the trailing edge of the arc spot weld. By using the stress condition shown in Fig. 8.6, Blodgett developed the following equation for determining the ultimate load in kips, per weld:[8.14,8.16]

$$P_{u2} = 1.4td_aF_u \tag{8.4}$$

Equation (8.4) is applicable only when $d_a/t \geq 240/\sqrt{F_u}$.
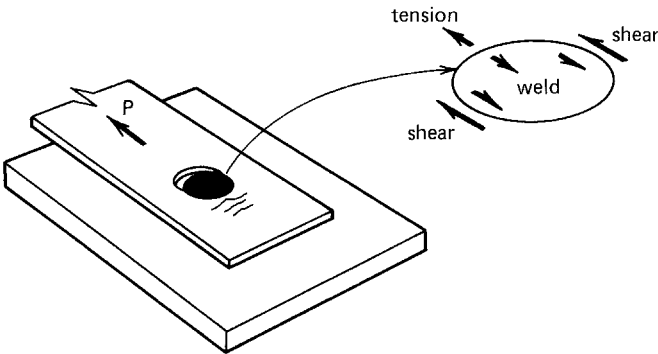
Figure 8.6   Tension and shear stresses in arc spot weld.[8.14,8.16]

For $140/\sqrt{F_\mathrm{u}} < d_\mathrm{a}/t < 240/\sqrt{F_\mathrm{u}}$, the ultimate load per weld can be determined by the following transition equation:

$$P_{\mathrm{u}3} = 0.28 \left(1 + \frac{960t}{d_\mathrm{a}\sqrt{F_\mathrm{u}}}\right) t d_\mathrm{a} F_\mathrm{u} \tag{8.5}$$

Figure 8.7 provides a graphic comparison of the observed ultimate load P_{uo} and the predicted ultimate load P_{up} according to Eq. (8.1), (8.3), (8.4), or (8.5), whichever is applicable.[8.12] Figure 8.8 summarizes Eqs. (8.3) to (8.5), which govern the failure of connected sheets.

Tensile Strength of Arc Spot Welds. In building construction, arc spot welds have been often used for connecting roof decks to support members such as hot-rolled steel beams and open web steel joists. This type of welded connection is subject to tension when a wind uplift force is applied to the roof system.

Prior to 1989, no design information was included in the AISI Specification to predict the tensile strength of arc spot welds. Based on Fung's test results[8.17] and the evaluation of test data by Albrecht[8.18] and Yu and Hsiao,[8.19] the fol-
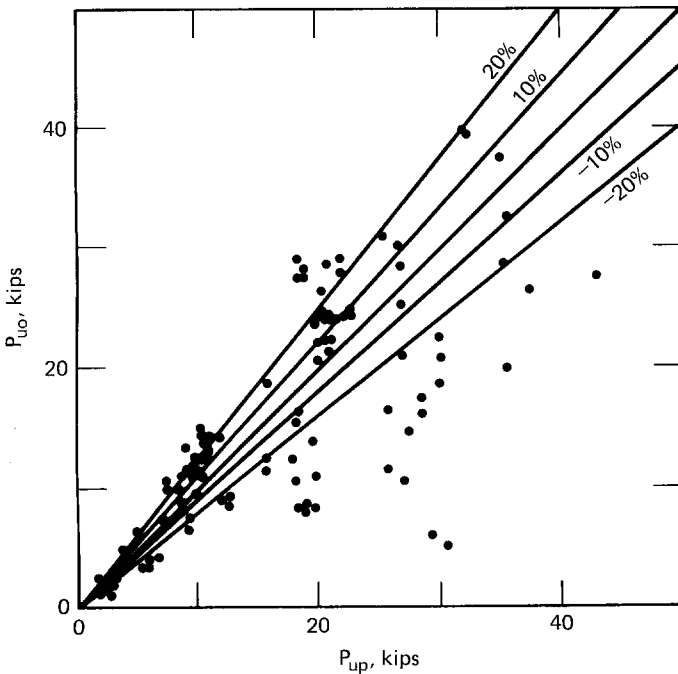
Figure 8.7   Comparison of observed and predicted ultimate loads for arc spot welds.[8.13]
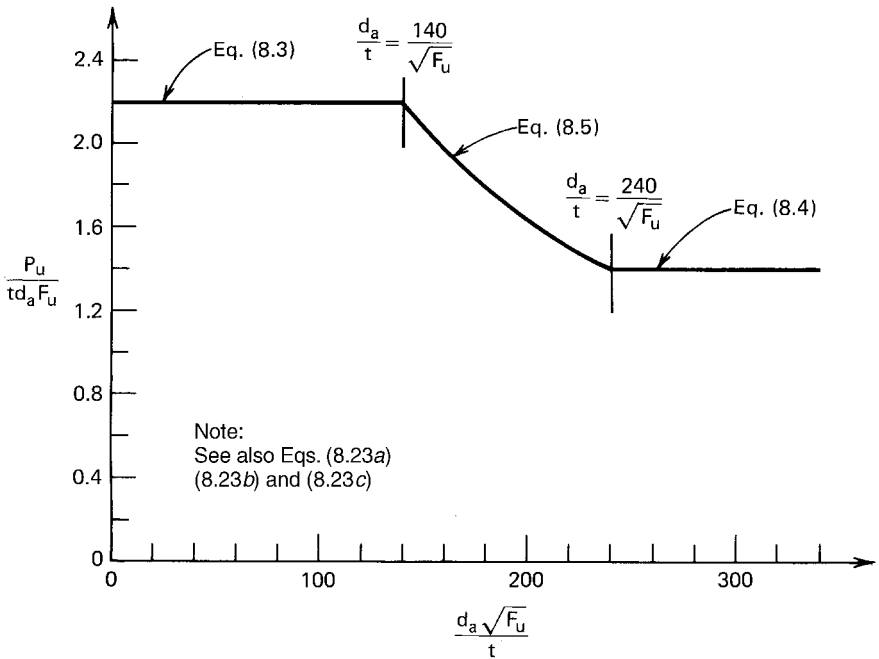
Figure 8.8 Failure load for arc spot welds.

lowing design equation was added in Section E2.2 of the 1989 Addendum to the 1986 edition of the AISI Specification:

$$P_{ut} = 0.7td_aF_u$$

in which P_{ut} is the ultimate tensile capacity per weld in kips. The symbols t, d_a, and F_u were defined previously.

The above design criterion was revised in the 1996 edition of the AISI Specification because the UMR tests[8.66,8.67] have shown that two possible limit states may occur. The most common failure mode is sheet tearing around the perimeter of the weld. This failure condition was affected by the sheet thickness, the average weld diameter, and the material tensile strength. The nominal tensile strength of concentrically loaded arc spot welds can be determined by the following equations depending on the F_u/E ratio:

1. For $F_u/E < 0.00187$:

$$P_n = [6.59 - 3150(F_u/E)]td_aF_u \leq 1.46td_aF_u \qquad (8.6a)$$

2. For $F_u/E \geq 0.00187$:

$$P_n = 0.70 \, td_a F_u \tag{8.6b}$$

In some cases, the tensile failure of the weld may occur. The tensile strength of the arc spot weld is based on the cross section of the fusion area and the tensile strength of the weld metal. Therefore, for this type of failure mode, the nominal tensile strength can be computed by Eq. (8.7):

$$P_n = \frac{\pi d_e^2}{4} F_{xx} \tag{8.7}$$

where d_e is the effective diameter of fused area and F_{xx} is the tensile strength of weld metal.

It should be noted that Eqs. (8.6) and (8.7) are subject to the following limitations:

$$e_{min} \geq d$$

$$F_{xx} \geq 60 \text{ ksi (414 MPa)}$$

$$F_u \leq 82 \text{ ksi (565 MPa)}$$

$$F_{xx} > F_u$$

where e_{min} is the minimum distance measured in the line of force from the center line of a weld to the nearest edge of an adjacent weld or to the end of the connected part toward which the force is directed. Other symbols were previously defined. When the spot weld is reinforced by a weld washer, the tensile strength given by Eqs. (8.6a) and (8.6b) can be achieved by using the thickness of the thinner sheet.

Equations (8.6) and (8.7) were derived from tests for which the applied tensile load imposed a concentric load on the spot weld, such as the interior welds on a roof system subjected to wind uplift, as shown in Fig. 8.9. For exterior welds which are subject to eccentric load due to wind uplift, tests
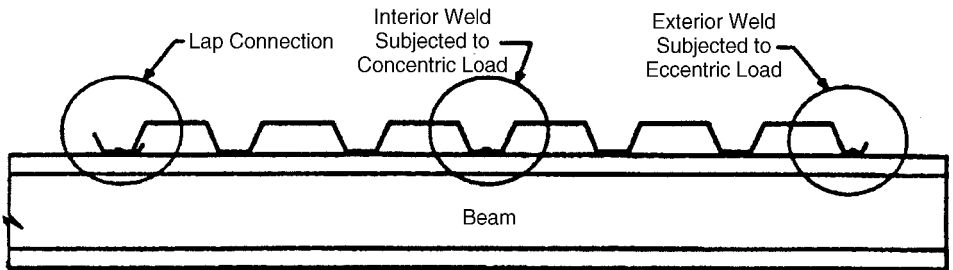

Figure 8.9   Interior weld, exterior weld, and lap connection.

have shown that only 50% of the nominal strength can be used for design. At a lap connection between two deck sections (Fig. 8.9), a 30% reduction of the nominal strength was found from the tests.[8.66,8.67]

8.3.1.2 Arc Seam Welds   As shown in Fig. 8.10, an arc seam weld consists of two half-circular ends and a longitudinal weld. The ultimate load of a welded connection is determined by the shear strength of the arc seam weld and the strength of the connected sheets.

Shear Strength of Arc Seam Welds. The ultimate shear capacity per weld is a combined shear resistance of two half-circular ends and a longitudinal weld, as given by

$$P_{us} = \left(\frac{3\pi}{16} d_e^2 + \frac{3Ld_e}{4} \right) F_{xx} \tag{8.8}$$

in which L is the length of the seam weld, not including the circular ends. For the purpose of computation, L should not exceed $3d$. Other symbols were defined in the preceding discussion.

Strength of Connected Sheets by Using Arc Seam Welds. In the Cornell research project a total of 23 welded connections were tested for arc seam welds. Based on the study made by Blodgett[8.14] and the linear regression analysis performed by Pekoz and McGuire[8.12,8.13] the following equation has been developed for determining the strength of connected sheets:

$$P_{u1} = (0.625L + 2.4d_a)tF_u \tag{8.9}$$

Equation (8.9) is applicable for all values of d_a/t. Figure 8.11 shows a comparison of the observed loads and the ultimate loads predicted by using Eq. (8.9).
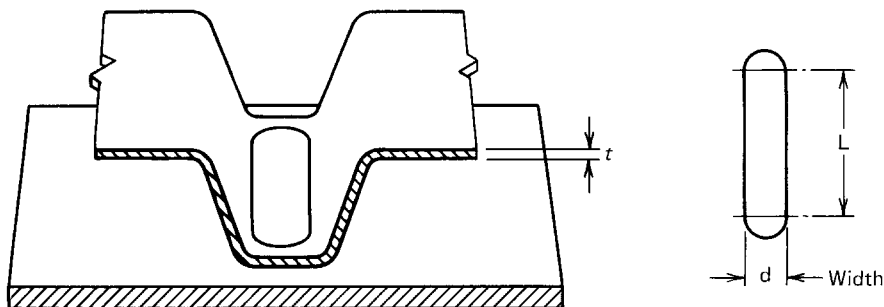

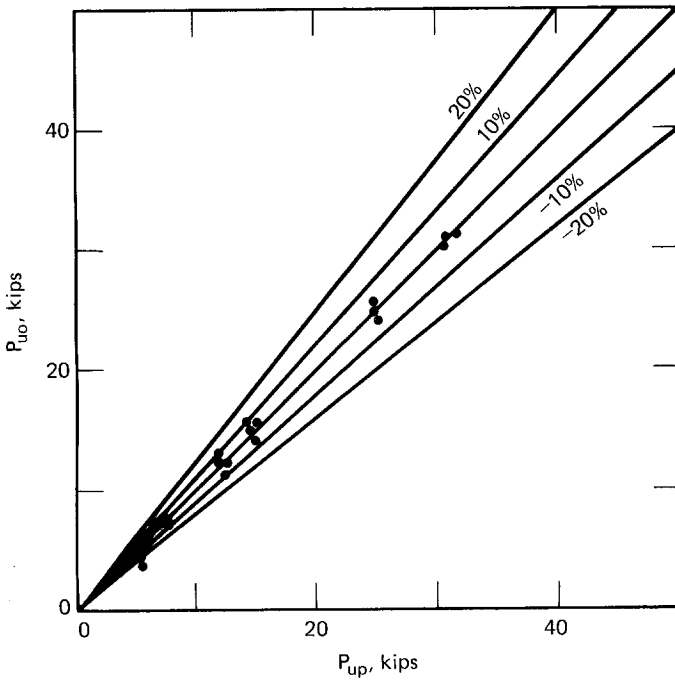**Figure 8.10**   Arc seam weld joining sheet to supporting member.[1.314]

Figure 8.11   Comparison of observed and predicted ultimate loads for arc seam welds.[8.13]

8.3.1.3   Fillet Welds   Fillet welds are often used for lap and T-joints. Depending on the arrangement of the welds, they can be classified as either longitudinal or transverse fillet welds. ("Longitudinal" means that the load is applied parallel to the length of the weld; "transverse" means that the load is applied perpendicular to the length of the weld.)

From the structural efficiency point of view, longitudinal fillet welds are stressed unevenly along the length of weld due to varying deformations. Transverse fillet welds are more uniformly stressed for the entire length. As a result, transverse welds are stronger than longitudinal welds of an equal length. The following discussion deals with the strength of welded connections using both types of fillet welds.

Shear Strength of Fillet Welds.   If the strength of welded connections is governed by the shear capacity of fillet welds, the ultimate load per weld can be determined as

$$P_{us} = \tfrac{3}{4}t_w L F_{xx} \tag{8.10}$$

where t_w = effective throat dimension
  L = length of fillet weld

F_{xx} was defined previously. As used in Eqs. (8.1) and (8.8), the shear strength of the weld metal is assumed to be 75% of its tensile strength.

Strength of Connected Sheets by Using Fillet Welds

1. *Longitudinal Welds.* A total of 64 longitudinal fillet welds were tested in the Cornell study.[8.12,8.13] An evaluation of the test data indicated that the following equations can predict the ultimate loads of the connected sheets for the failure involving tearing along the weld contour, weld shear, and combinations of the two types of failure:
   (a) For $L/t < 25$,

$$P_{u1} = \left(1 - 0.01 \frac{L}{t}\right) tLF_u \qquad (8.11a)$$

   (b) For $L/t \geq 25$,

$$P_{u2} = 0.75 tLF_u \qquad (8.11b)$$

   in which P_{u1} and P_{u2} are the predicted ultimate loads per fillet weld. Other symbols were defined previously.
2. *Transverse Welds.* Based on the results of 55 tests on transverse fillet welds, it was found that the primary failure was by tearing of connected sheets along, or close to, the contour of the welds. The secondary failure was by weld shear. The ultimate failure load per fillet weld can be computed as

$$P_{u3} = tLF_u \qquad (8.12)$$

Figures 8.12 and 8.13 show comparisons of the observed and predicted ultimate loads for longitudinal and transverse fillet welds, respectively.

8.3.1.4   Flare Groove Welds   In the Cornell research, 42 transverse flare bevel welds (Fig. 8.14) and 32 longitudinal flare bevel welds (Fig. 8.15) were tested. It was found that the following formulas can be used to determine the predicted ultimate loads.

Shear Strength of Flare Groove Welds. The ultimate shear strength of a flare groove weld is

$$P_{us} = \tfrac{3}{4} t_w LF_{xx} \qquad (8.13)$$

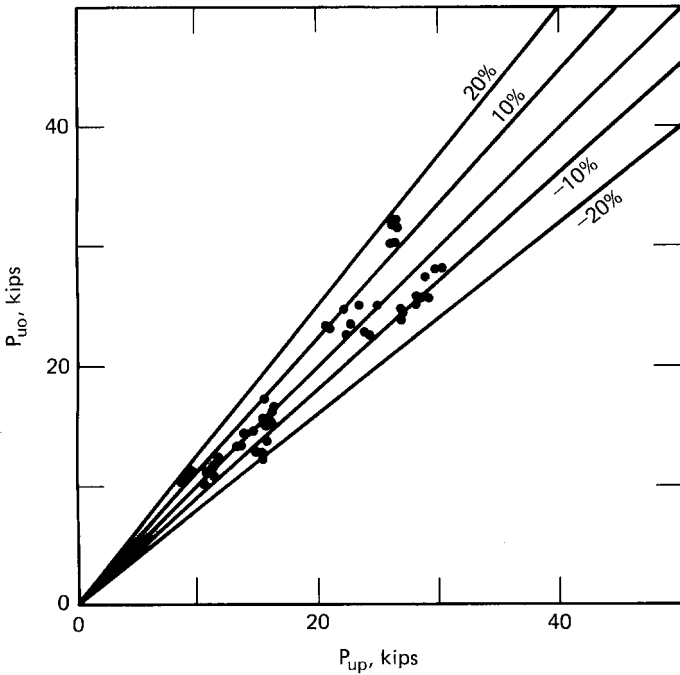The above equation is similar to Eq. (8.10) for fillet welds.

Figure 8.12 Comparison of observed and predicted ultimate loads for longitudinal fillet welds.[8.13]

Strength of Connected Sheets by Using Flare Groove Welds. If the strength of weld connections is governed by the connected sheets, the ultimate load per weld can be determined as follows:

1. *Transverse Welds*

$$P_{u1} = 0.833tLF_u \qquad (8.14)$$

2. *Longitudinal Welds.* If $t \leq t_w < 2t$ or if the lip height is less than the weld length L,

$$P_{u2} = 0.75tLF_u \qquad (8.15)$$

If $t_w \geq 2t$ and the lip height is equal to or greater than L,

$$P_{u3} = 1.5tLF_u \qquad (8.16)$$

Figures 8.16 and 8.17 show comparisons of the observed and predicted ultimate loads for transverse and longitudinal flare bevel welds, respectively.
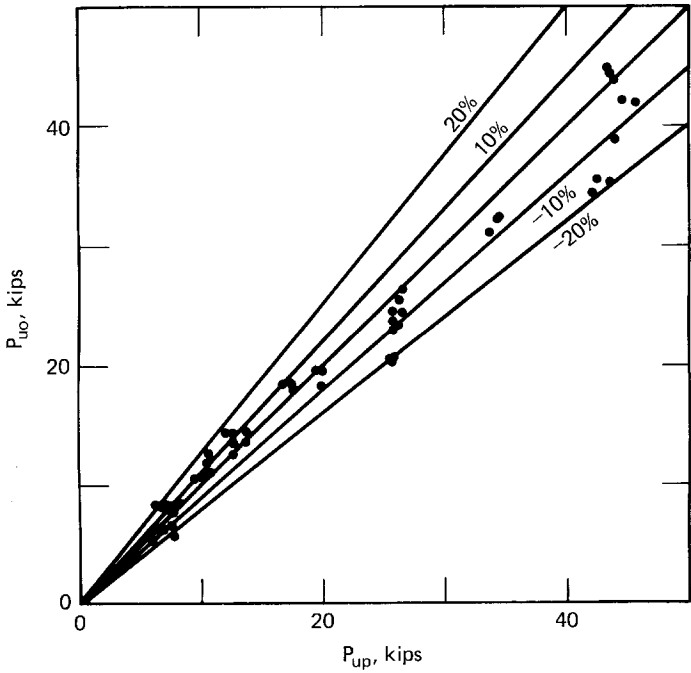
Figure 8.13   Comparison of observed and predicted ultimate loads for transverse fillet welds.[8.13]

8.3.2   AISI Design Criteria for Arc Welds

8.3.2.1   Thickness Limitations   In previous editions of the AISI Specifications, the design provisions have been used for cold-formed members and thin elements with a maximum thickness of $\frac{1}{2}$ in. (12.7 mm). Because the maximum material thickness for using the AISI Specification was increased
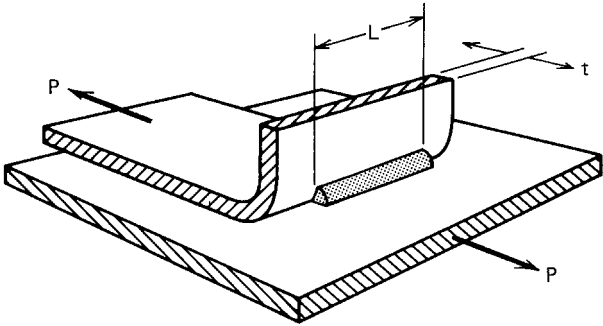

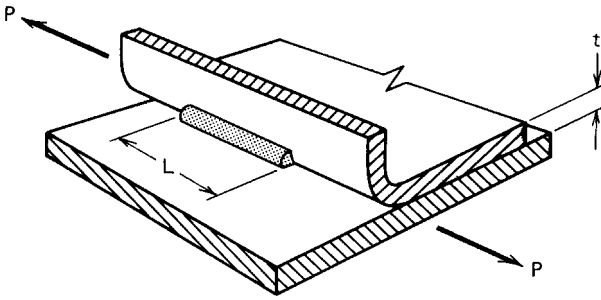**Figure 8.14**   Transverse flare bevel weld.[1.314]

Figure 8.15 Longitudinal flare bevel weld.[1.314]

to 1 in. (25.4 mm) in 1977[8.21] and the structural behavior of weld connections for joining relatively thick cold-formed members is similar to that of hot-rolled shapes, Sec. E2 of the AISI Specification is intended only for the design of arc welds for cold-formed steel members with a thickness of 0.18 in. (4.6 mm) or less.[1.134] When the connected part is over 0.18 in. (4.6 mm) in thickness, arc welds can be designed according to the AISC Specification.[1.148,3.150]
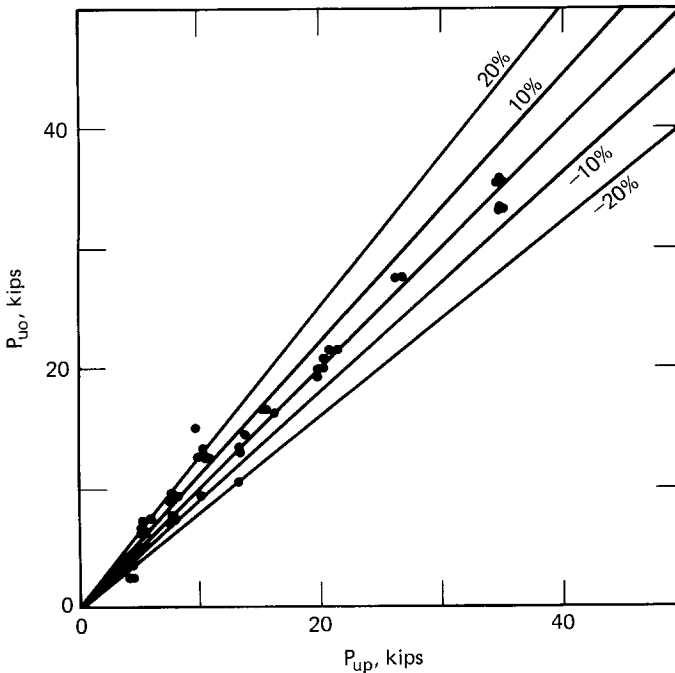

Figure 8.16 Comparison of observed and predicted ultimate loads for transverse flare bevel welds.[8.13]
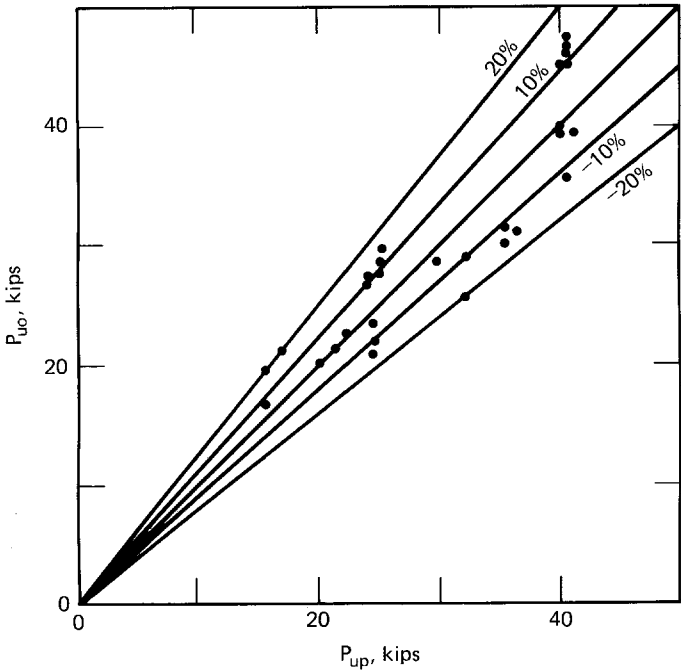
Figure 8.17 Comparison of observed and predicted ultimate loads for longitudinal flare bevel welds.[8.13]

8.3.2.2 *Criteria for Various Weld Types*   Article 8.3.1 discussed ultimate strengths of various weld types. The ultimate load, P_u, determined in Art. 8.3.1 for a given type of welds is considered to be the nominal strength of welds, P_n, used in Sec. E2 of the AISI Specification. The following are the AISI design provisions for groove welds used in butt joints, arc spot welds, arc seam welds, fillet welds, and flare groove welds:

Groove Welds in Butt Joints.   For the design of groove welds in butt joints (Fig. 8.1a), the nominal strength, P_n, with the applicable safety factor and resistance factor are given in Sec. E2.1 of the 1996 edition of the AISI Specification as follows:

a. *Tension or compression normal to the effective area or parallel to the axis of the weld*

$$P_n = Lt_eF_y \tag{8.17}$$

$$\Omega = 2.50 \text{ (ASD)}$$

$$\phi = 0.90 \text{ (LRFD)}$$

b. *Shear on the effective area.* Use the smaller value of either Eq. (8.18) or (8.19):

   i. $P_n = Lt_e(0.6F_{xx})$ (8.18)

      $\Omega = 2.50$ (ASD)

      $\phi = 0.80$ (LRFD)

  ii. $P_n = Lt_eF_y/\sqrt{3}$ (8.19)

      $\Omega = 2.50$ (ASD)

      $\phi = 0.90$ (LRFD)

where P_n = nominal strength of a groove weld
      F_{xx} = filler metal strength designation in AWS electrode classi-fication
      F_y = specified minimum yield point of the lowest strength base steel
      L = length of groove weld
      t_e = effective throat dimension for groove weld

Equations (8.17), (8.18), and (8.19) are the same as the AISC LRFD Specification.[3.150] The effective throat dimensions for groove welds are shown in Fig. 8.18.
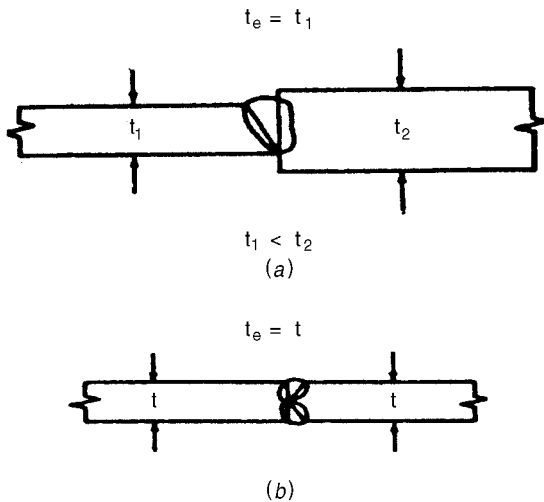

Figure 8.18 Effective dimensions for groove welds.

Arc Spot Welds (*Puddle Welds*).   Section E2.2 of the AISI Specification includes the following requirements for using arc spot welds:

1. Arc spot welds should not be made on steel where the thinnest connected part is over 0.15 in (3.8 mm) thick, nor through a combination of steel sheets having a total thickness of over 0.15 in (3.8 mm).
2. Weld washers should be used when the thickness of the sheet is less than 0.028 in. (0.7 mm). Weld washers should have a thickness of between 0.05 (1.3 mm) and 0.08 in. (2.0 mm) with a minimum prepunched hole of $\frac{3}{8}$-in. (9.5-mm) diameter.
3. The minimum allowable effective diameter d_e is $\frac{3}{8}$-in. (9.5 mm).
4. The distance measured in the line of force from the centerline of a weld to the nearest edge of an adjacent weld or to the end of the connected part toward which the force is directed should not be less than the value of e_{min} as given below:

$$e_{min} = \frac{\Omega P}{F_u t} \text{ (ASD)} \tag{8.20}$$

$$e_{min} = \frac{P_u}{\phi F_u t} \text{ (LRFD)} \tag{8.21}$$

  i. When $F_u/F_y \geq 1.08$,

$$\Omega = 2.0 \text{ (ASD)}$$
$$\phi = 0.70 \text{ (LRFD)}$$

  ii. When $F_u/F_y < 1.08$,

$$\Omega = 2.22 \text{ (ASD)}$$
$$\phi = 0.60 \text{ (LRFD)}$$

  where P = required strength (nominal force) transmitted by the weld (ASD)
  P_u = required strength (factored force) transmitted by the weld (LRFD)
  t = thickness of thinnest connected sheet
  F_u = tensile strength of steel
  F_y = yield point of steel

5. The distance from the centerline of any weld to the end or boundary of the connected member should not be less than $1.5d$. In no case should the clear distance between welds and end of member be less than $1.0d$.

6. The nominal shear strength, P_n, of each arc spot weld between sheet or sheets and supporting member should not exceed the smaller value of the loads computed by Eqs. (8.22) and (8.23):

   i. *Nominal Shear Strength Based on the Shear Capacity of Weld*

$$P_n = \frac{\pi d_e^2}{4} (0.75 F_{xx})$$ (8.22)

$$\Omega = 2.50 \text{ (ASD)}$$

$$\phi = 0.60 \text{ (LRFD)}$$

   ii. *Nominal Shear Strength Based on the Strength of Connected Sheets*
   a. For $d_a/t \leq 0.815 \sqrt{E/F_u}$:

$$P_n = 2.20 t d_a F_u$$ (8.23a)

$$\Omega = 2.50 \text{ (ASD)}$$

$$\phi = 0.60 \text{ (LRFD)}$$

   b. For $0.815 \sqrt{E/F_u} < (d_a/t) < 1.397 \sqrt{E/F_u}$:

$$P_n = 0.280 \left[1 + 5.59 \frac{\sqrt{E/F_u}}{d_a/t} \right] t d_a F_u$$ (8.23b)

$$\Omega = 2.50 \text{ (ASD)}$$

$$\phi = 0.50 \text{ (LRFD)}$$

   c. For $d_a/t \geq 1.397 \sqrt{E/F_u}$

$$P_n = 1.40 t d_a F_u$$ (8.23c)

$$\Omega = 2.50 \text{ (ASD)}$$

$$\phi = 0.50 \text{ (LRFD)}$$

   In the above requirements and design formulas for arc spot welds,

   P_n = nominal shear strength of an arc spot weld
   d = visible diameter of outer surface of arc spot weld (Fig. 8.4)
   d_a = average diameter of arc spot weld at mid-thickness of t (Fig. 8.4) = $d - t$ for a single sheet and $d - 2t$ for multiple sheets (not more than four lapped sheets over a supporting member)

d_e = effective diameter of fused area (Fig. 8.4) $= 0.7d - 1.5t$
but $\leq 0.55d$

t = total combined base steel thickness (exclusive of coating) of sheets involved in shear transfer above the plane of maximum shear transfer

F_{xx} = filler metal strength designation in AWS electrode classification

F_u = specified minimum tensile strength of steel

7. The nominal tensile strength, P_n, of each concentrically loaded arc spot weld connecting sheets and supporting members should be the smaller value of the loads computed by Eqs. (8.24) and (8.25):

   i. *Nominal Tensile Strength Based on the Capacity of Weld*

$$P_n = \frac{\pi d_e^2 F_{xx}}{4} \tag{8.24}$$

   ii. *Nominal Tensile Strength Based on the Strength of Connected Sheets*
       a. For $F_u/E < 0.00187$

$$P_n = [6.59 - 3150(F_u/E)]td_a F_u \leq 1.46 td_a F_u \tag{8.25a}$$

       b. For $F_u/E \geq 0.00187$

$$P_n = 0.70 td_a F_u \tag{8.25b}$$

For both Eqs. (8.24) and (8.25),

$$\Omega = 2.50 \text{ (ASD)}$$

$$\phi = 0.60 \text{ (LRFD)}$$

Both Eqs. (8.24) and (8.25) are limited to the following conditions: $e_{min} \geq d$, $F_{xx} \geq 60$ ksi (414 MPa), $F_u \leq 82$ ksi (565 MPa) (of connecting sheets), and $F_{xx} > F_u$. All symbols were defined previously.

It should be noted that Eq. (8.22) is derived from Eq. (8.1). Equations (8.23a), (8.23b), and (8.23c) are based on Eqs. (8.3), (8.5), and (8.4), respectively. These equations are also shown in Fig. 8.8. The background information on tensile strength was discussed previously.

Example 8.1   Use the ASD and LRFD methods to determine the allowable load for arc spot welded connection shown in Fig. 8.19. Use A607 Grade 45 steel ($F_y = 45$ ksi, $F_u = 60$ ksi). Assume that the visible diameter of the arc spot weld is $\frac{3}{4}$ in. and the dead-to-live load ratio is 1/5.
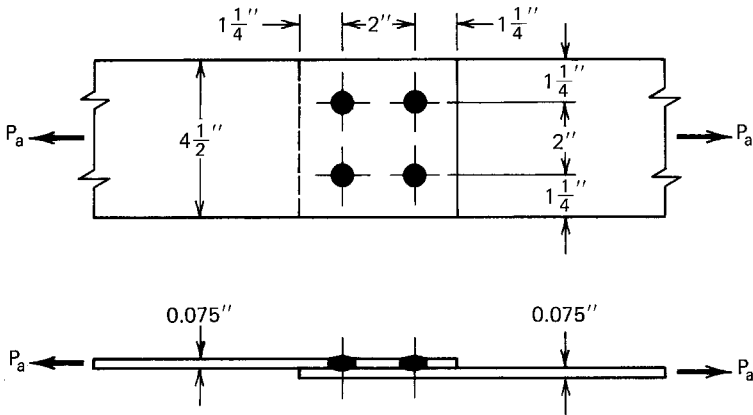
Figure 8.19 Example 8.1.

Solution

A. ASD Method. Prior to determination of the allowable load, the AISI requirements for using arc spot welds are checked as follows:

1. Since the thickness of the connected sheets is less than 0.15 in., arc spot welds can be made.
2. Because the thickness of the connected sheets is over 0.028 in., weld washers are not required.
3. The visible diameter d is $\frac{3}{4}$ in., and

$$d_a = d - t = 0.75 - 0.075 = 0.675 \text{ in.}$$

$$d_e = 0.7d - 1.5t = 0.70(0.75) - 1.5(0.075) = 0.4125 \text{ in.} = 0.55d$$

Use $d_e = 0.4125$ in. $> \frac{3}{8}$ in. (minimum size)   O.K.

4. The distance from the centerline of any weld to the end of the sheet is

$$1.25 \text{ in.} > (1.5d = 1.125 \text{ in.})   \text{O.K.}$$

5. The clear distance between welds is

$$2 - d = 1.25 \text{ in.} > d   \text{O.K.}$$

The clear distance between welds and end of member is

$$1.25 - d/2 = 0.875 \text{ in.} > d   \text{O.K.}$$

6. The allowable load for the ASD method is based on the following considerations:

   a. *Tensile Load for Steel Sheets.* Based on Sec. C2 of the Supplement to the 1996 edition of the AISI Specification,

   (i) For yielding [Eq. (6.2)],

   $$P_{al} = T_n/\Omega_t = A_g F_y/1.67$$
   $$= (4.5 \times 0.075)(45)/1.67 = 9.09 \text{ kips}$$

   (ii) For fracture away from the connection [Eq. (6.3)],

   $$P_{al} = T_n/\Omega_t = A_n F_u/2.00$$
   $$= (4.5 \times 0.075)(60)/2.00 = 10.125 \text{ kips}$$

   Use $P_{al} = 9.09$ kips

   b. *Tensile Load Based on End Distance* $(e = 1.25 \text{ in.})$

   $$\frac{F_u}{F_y} = \frac{60}{45} = 1.33 > 1.08$$

   By using Eq. (8.20),

   $$P_{a2} = 4P = 4e \, (F_u t)/2$$
   $$= 4(1.25)(60)(0.075)/2 = 11.25 \text{ kips}$$

   c. *Shear Capacity of Welds.* By using Eq. (8.22) and E60 electrodes,

   $$P_{a3} = 4 \left(\frac{\pi d_e^2}{4} \right)(0.75 F_{xx})/\Omega = \pi(0.4125)^2(0.75 \times 60)/2.50$$
   $$= 9.62 \text{ kips}$$

   d. *Strength of Connected Sheets Around Welds*

   $$\frac{d_a}{t} = \frac{0.675}{0.075} = 9 < \left(0.815 \sqrt{\frac{29,500}{60}} = 18.07 \right)$$

   By using Eq. (8.23a)

$$P_{a4} = 4(2.20 t d_a F_u)/\Omega$$

$$= 4(2.20)(0.075)(0.675)(60)/2.50 = 10.69 \text{ kips}$$

On the basis of the above considerations, the allowable load for the ASD method is the smallest value, that is, 9.09 kips, which is governed by the tensile load for yielding of steel sheets.

B. LRFD Method

As the first step of the LRFD method, the AISI requirements for using arc spot welds should be checked as the ASD method. From Items 1 through 5 for the ASD method, the layout of the spot welds are satisfied with the AISI requirements.

The design strength, ϕP_n, for the LRFD method is based on the following considerations:

a. *Tensile Load for Steel Sheets.* Based on Sec. C2 of the Supplement to the 1996 edition of the AISI Specification,
   (i) For yielding [Eq. (6.2)],

$$\phi_t P_n = \phi_t T_n = \phi_t (A_g F_y)$$

$$= (0.90)(4.5 \times 0.075)(45) = 13.67 \text{ kips}$$

   (ii) For fracture away from the connections [Eq. (6.3)],

$$\phi_t P_n = \phi_t T_n = \phi_t (A_n F_u)$$

$$= (0.75)(4.5 \times 0.075)(60) = 15.19 \text{ kips}$$

   Use $\phi_t P_n = 13.67$ kips

b. *Tensile Load Based on End Distance* ($e = 1.25$ in.)
   Using Eq. (8.21) for four spot welds ($F_u/F_y > 1.08$),

$$\phi P_n = \phi(4)(e F_u t)$$

$$= (0.70)(4)(1.25 \times 60 \times 0.075) = 15.75 \text{ kips}$$

c. *Shear Capacity of Welds.* By using Eq. (8.22) and E60 electrodes.

$$\phi P_n = \phi(4)\left(\frac{\pi d_e^2}{4}\right)(0.75 F_{xx})$$

$$= (0.60)(\pi)(0.4125)^2(0.75 \times 60) = 14.43 \text{ kips}$$

d. *Strength of Connected Sheets Around Welds*
   Since $d_a/t < 0.815\sqrt{E/F_u}$, use Eq. (8.23a)

$$\phi P_n = \phi(4)(2.20td_aF_u)$$
$$= (0.60)(4)(2.20 \times 0.075 \times 0.675 \times 60) = 16.04 \text{ kips}$$

Based on the above four considerations, the controlling design strength is 13.67 kips, which is governed by the tensile load for yielding of steel sheets.

According to the load factors and load combinations discussed in Art. 3.3.2.2, the required strength for the given dead-to-live load ratio of 1/5 is computed as follows:

$$P_{u1} = 1.4P_D + P_L = 1.4P_D + 5P_D = 6.4P_D \qquad (3.5a)$$

where

$$P_D = \text{applied load due to dead load}$$
$$P_L = \text{applied load due to live load}$$
$$P_{u2} = 1.2P_D + 1.6P_L = 1.2P_D + 1.6(5P_D) = 9.2P_D \qquad (3.5b)$$

Use

$$P_u = 9.2P_D$$

By using $9.2\,P_D = 13.67$ kips

$$P_D = 1.49 \text{ kips}$$
$$P_L = 5P_D = 7.45 \text{ kips}$$

The allowable load based on the LRFD method is

$$P_D + P_L = 1.49 + 7.45 = 8.94 \text{ kips}$$

It can be seen that the LRFD method permits a slightly smaller allowable load than the ASD method. The difference between these two design approaches for this particular case is less than 2%.

Arc Seam Welds.   For arc seam welds (Fig. 8.10), Sec. E2.3 of the AISI Specification specifies that the nominal shear strength, P_n, of an arc seam weld is the smaller of the values computed by Eqs. (8.26) and (8.27):

i. *Nominal Shear Strength Based on Shear Capacity of Weld*

$$P_n = \left(\frac{\pi d_e^2}{4} + L d_e\right) 0.75 F_{xx} \qquad (8.26)$$

ii. *Nominal Shear Strength Based on Strength of Connected Sheets*

$$P_n = 2.5 t F_u (0.25L + 0.96 d_a) \qquad (8.27)$$

For Eqs. (8.26) and (8.27),

$\Omega = 2.5$ (ASD)
$\phi = 0.60$ (LRFD)
d = width of arc seam weld
L = length of seam weld not including circular ends (for computation purposes, L should not exceed $3d$)

The definition of d_a, d_e, F_u, and F_{xx} and the requirements for minimum edge distance are the same as those for arc spot welds.

Equation (8.26) is derived from Eq. (8.8) and Eq. (8.27) is based on Eq. (8.9).

Fillet Welds. According to Sec. E2.4 of the AISI Specification, the design strength of a fillet weld in lap and T-joints should not exceed the values computed by Eq. (8.28) for the shear strength of the fillet weld and by Eq. (8.29) or Eq. (8.30) for the strength of the connected sheets as follows:

i. *Nominal Strength Based on Shear Capacity of Weld.* For $t > 0.15$ in. (3.8 mm),

$$P_n = 0.75 t_w L F_{xx}$$
$$\Omega = 2.50 \text{ (ASD)} \qquad (8.28)$$
$$\phi = 0.60 \text{ (LRFD)}$$

ii. *Nominal Strength Based on the Strength of Connected Sheets*
   a. *Longitudinal loading.* When $L/t < 25$,

$$P_n = \left(1 - 0.01 \frac{L}{t}\right) t L F_u$$
$$\Omega = 2.50 \text{ (ASD)} \qquad (8.29a)$$
$$\phi = 0.60 \text{ (LRFD)}$$

When $L/t \geq 25$,

$$P_n = 0.75tLF_u$$

$$\Omega = 2.50 \ (ASD) \qquad\qquad (8.29b)$$

$$\phi = 0.55 \ (LRFD)$$

b. *Transverse loading*

$$P_n = tLF_u$$

$$\Omega = 2.50 \ (ASD) \qquad\qquad (8.30)$$

$$\phi = 0.60 \ (LRFD)$$

In the above equations,

P_n = nominal strength of a fillet weld
L = length of fillet weld
t_w = effective throat, = 0.707 w_1 or 0.707 w_2, whichever is smaller
w_1, w_2 = leg size of fillet weld (Fig. 8.20)

The definitions of t, F_u, and F_{xx} are the same as those used for arc spot welds. It should be noted that Eqs. (8.28), (8.29), and (8.30) are based on Eqs. (8.10), (8.11), and (8.12), respectively.

Example 8.2   Use the ASD method to determine the allowable load for the welded connection using fillet welds, as shown in Fig. 8.21. Assume that A570 Grade 33 steel sheets and E60 electrodes are to be used.
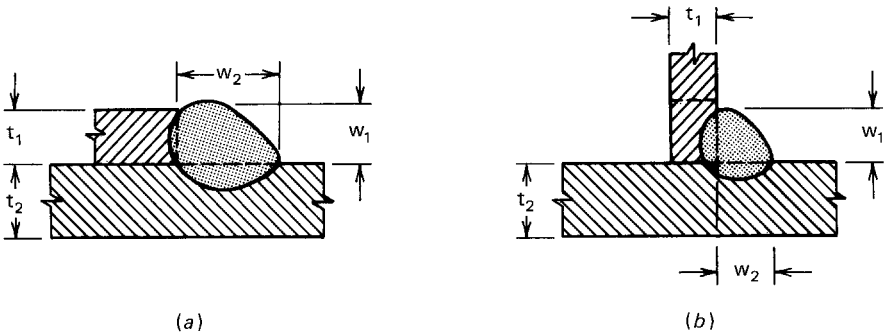

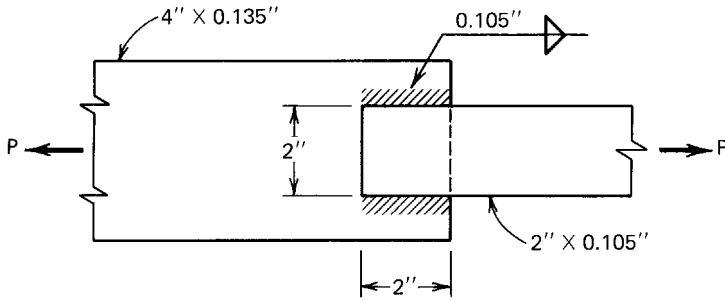**Figure 8.20**   Leg sizes of fillet welds.[1.4] (*a*) Lap joint. (*b*) T-joint.

Figure 8.21   Example 8.2.

Solution. From Table 2.1, the yield point and the tensile strength of A570 Grade 33 steel are 33 and 52 ksi, respectively. The allowable load P can be determined as follows:

1. *Allowable Tensile Load for Steel Sheet.* Based on Sec. C2 of the Supplement to the 1996 edition of the AISI Specification,
   (i) For yielding [Eq. (6.2)],

$$p_{a1} = T_n/\Omega_t = A_g F_y/1.67$$
$$= (2.0 \times 0.105)(33)/1.67 = 4.15 \text{ kips}$$

   (ii) For fracture away from the connections [Eq. (6.3)],

$$P_{a1} = T_n/\Omega_t = A_n F_n/2.00$$
$$= (2.0 \times 0.105)(52)/2.00 = 5.46 \text{ kips}$$

Use $P_{a1} = 4.15$ kips

2. *Allowable Load for Longitudinal Fillet Welds.* Since $L/t = 2/0.105 = 19.05 < 25$, use Eq. (8.29a),

$$P_L = [1 - 0.01(L/t)]tLF_u/\Omega$$
$$= [1 - 0.01(19.05)](0.105)(2)(52)/2.50 = 3.54 \text{ kips per weld}$$

Using two longitudinal welds

$$P_{a2} = 2P_L = 2 \times 3.54 = 7.08 \text{ kips}$$

Because the thickness of steel sheet is less than 0.15 in. it is not necessary to use Eq. (8.28).

Since $P_{a1} < P_{a2}$, the allowable tensile load is governed by the tensile capacity of steel sheet, that is,

$$P_a = 4.15 \text{ kips}$$

The use of the LRFD method can be handled in the same way as Example 8.1.

Flare Groove Welds.   On the basis of Sec. E2.5 of the AISI Specification, the nominal strength of each flare groove weld should be determined as follows:

  i. *Nominal Strength Based on Shear Capacity of Weld.* For $t > 0.15$ in. (3.8 mm),

$$P_n = 0.75t_wLF_{xx} \tag{8.31}$$
$$\Omega = 2.50 \text{ (ASD)}$$
$$\phi = 0.60 \text{ (LRFD)}$$

 ii. *Nominal Strength Based on Strength of Connected Sheet*
    a. *Transverse loading* (Fig. 8.14)

$$P_a = 0.833tLF_u \tag{8.32}$$

    b. *Longitudinal loading* (Figs. 8.22a thru 8.22f)

    If $t \leq t_w < 2t$ or if the lip height is less than the weld length L,

$$P_n = 0.75tLF_u \tag{8.33a}$$

    If $t_w \geq 2t$ and the lip height is equal to or greater than L,

$$P_n = 1.50tLF_u \tag{8.33b}$$

    For using Eqs. (8.32) and (8.33),
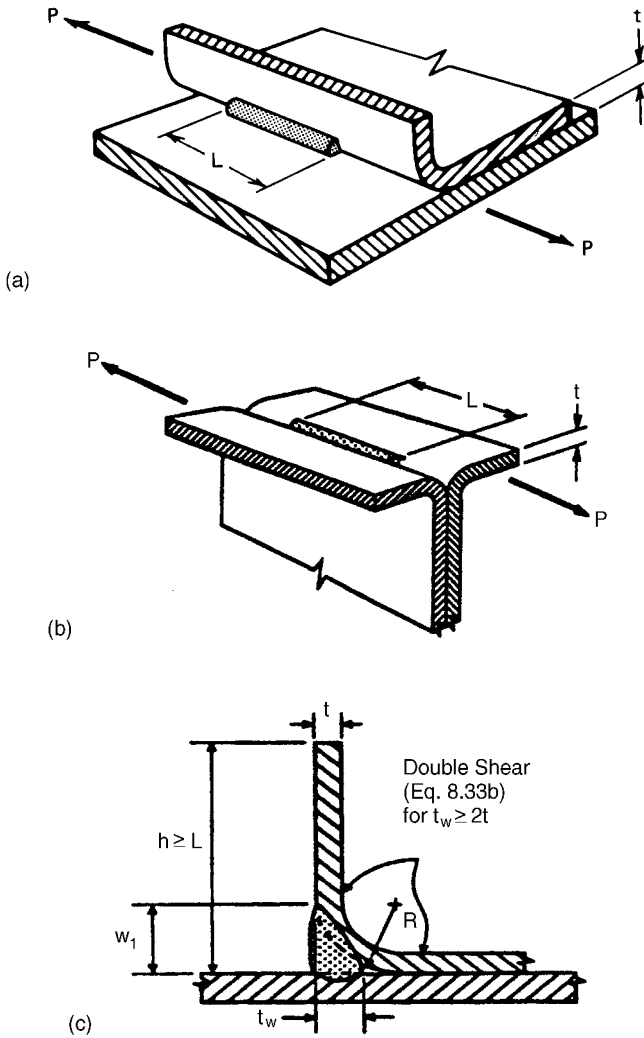
Figure 8.22   (*a*) Shear in longitudinal flare bevel groove weld.[1.314] (*b*) Shear in longitudinal flare V-groove weld.[1.314] (*c*) Flare bevel groove weld (filled flush to surface, $w_1 = R$).[1.314]

$$\Omega = 2.50 \text{ (ASD)}$$

$$\phi = 0.55 \text{ (LRFD)}$$

In Eqs. (8.31) through (8.33),

P_n = limiting nominal strength of the weld
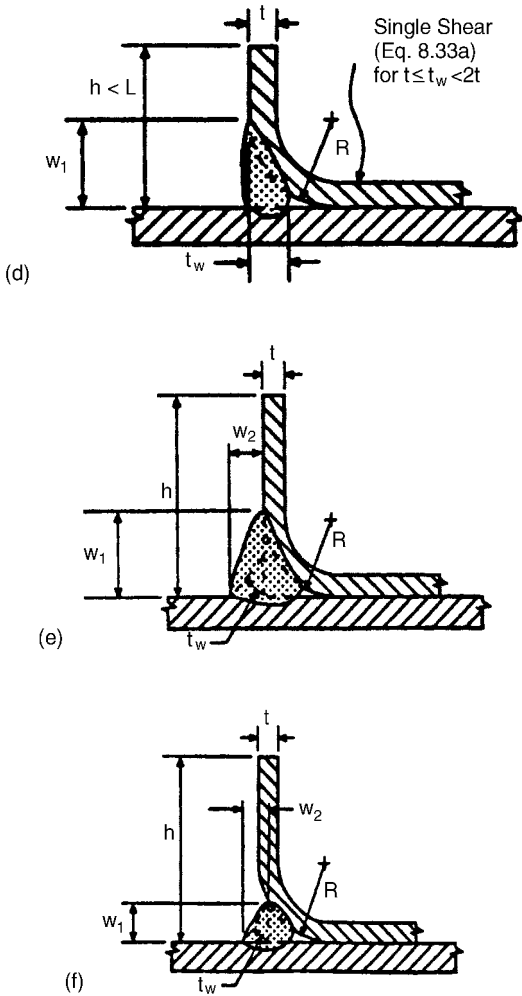h = height of lip

Figure 8.22   (*d*) Flare bevel groove weld (filled flush to surface, $w_1 = R$).[1.314] (*e*) Flare bevel groove weld (not filled flush to surface, $w_1 > R$).[1.314] (*f*) Flare bevel groove weld (not filled flush to surface, $w_1 < R$).[1.134]

L = length of the weld

t_w = effective throat of flare groove weld filled flush to surface (Figs. 8.22*c* and 8.22*d*)

　　For flare bevel groove weld = $5/16R$

　　For flare V-groove weld = $1/2R$ ($3/8R$ when $R >$ ½ in. (12.7 mm)

t_w = effective throat of flare groove weld not filled flush to surface = $0.707 w_1$ or $0.707 w_2$, whichever is smaller. (Figs. 8.22*e* and 8.22*f*)

= larger effective throat than those above shall be per-
mitted if measurement shows that the welding proce-
dure to be used consistently yields a large value of t_w.

R = radius of outside bend surface

w_1 and w_2 = Leg on weld (see Figs. 8.22e and 8.22f)

F_u and F_{xx} were defined previously.

It should be noted that Eqs. (8.31), (8.32), and (8.33) are derived from
Eqs. (8.13), (8.14), (8.15), and (8.16).

Example 8.3   Use the ASD method to design a welded connection as shown
in Fig. 8.23 for the applied load of 15 kips. Consider the eccentricity of the
applied load. Use A606 Grade 50 steel (F_y = 50 ksi and F_u = 70 ksi) and
E70 electrodes.

Solution. Considering the eccentricity of the applied load, it is desirable to
place the welds so that their centroids coincide with the centroid of the angle
section. It should be noted that weld L_1 is a flare groove weld, weld L_2 is a
transverse fillet weld, and weld L_3 is a longitudinal fillet weld.

Let P_2 be the allowable load of end weld L_2. By using Eq. (8.30) for
transverse fillet welds

$$P_2 = tLF_u/\Omega$$

$$= (0.135)(2.0)(70)/2.50 = 7.56 \text{ kips}$$

Taking moments about point A,

$$P(1.502) - P_1(2.0) - P_2(1.0) = 0$$

$$15(1.502) - P_1(2.0) - 7.56(1.0) = 0$$

$$P_1 = 7.49 \text{ kips}$$

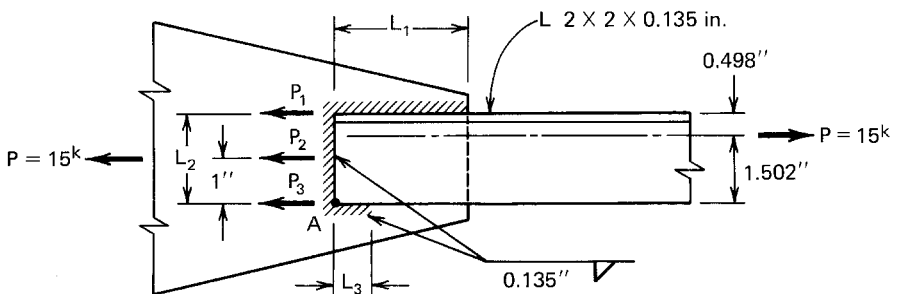$$P_3 = P - (P_1 + P_2) \simeq 0$$

Figure 8.23   Example 8.3.

For the flare groove weld subjected to longitudinal loading, with the assumption that $t \leq t_w < 2t$, the allowable load according to Eq. (8.33a) is

$$P_a = 0.75tLF_u/\Omega$$

$$= 0.75(0.135)(1)(70)/2.50 = 2.84 \text{ kips/in.}$$

The required length L_1 is

$$L_1 = \frac{P_1}{P_a} = \frac{7.49}{2.84} = 2.64 \text{ in.}; \qquad \text{use } L_1 = 3 \text{ in.}$$

For weld length L_3, use the minimum length of $\frac{3}{4}$ in. specified in Sec. 3.5 of the AWS code, even though P_3 is approximately equal to zero.

8.3.3   Additional Design Information on Welded Connections

The preceding discussion and design examples were based on the AISI Specification. For additional information concerning details of welded connections, workmanship, technique, qualification, and inspection, the reader is referred to the AWS code.[8.16]

In addition to the research work conducted at Cornell and the design criteria being used in the United States, other research projects on welded connections have been conducted by Baehre and Berggren,[8.4] Stark and Soetens,[8.22] Kato and Nishiyama,[8.23] and others. These references also discuss design considerations and testing of welded connections. An economic study of the connection safety factor has been reported by Lind, Knab, and Hall in Ref. 8.24. Design information on tubular joints can be found in Refs. 8.25 through 8.32 and 8.68 through 8.70.

8.3.4   Resistance Welds

Resistance welds (including spot welding and projection welding) are mostly used for shop welding in cold-formed steel fabrication (Fig. 8.24).
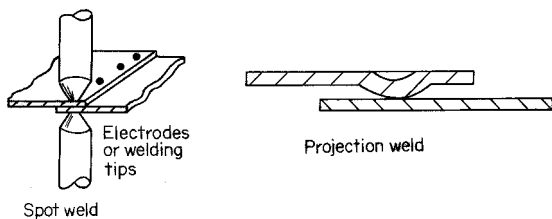

Figure 8.24   Resistance welds.

The nominal shear strengths for spot welding (Table 8.1) are based on Sec. E2.6 of the 1996 AISI Specification, which is based on Ref. 8.33 for outside sheets of 0.125 in. or less in thickness and Ref. 8.34 for outside sheets thicker than 0.125 in. The safety factor used to determine the allowable shear strength is 2.5 and the resistance factor used for the LRFD method is $\phi = 0.65$. Values for intermediate thicknesses may be obtained by straight-line interpolation.

The above tabulated values may also be applied to pulsation welding and spot welding medium-carbon and low-alloy steels with possibly higher shear strengths. It is interesting to note that if the shear strength specified in the AISI Specification is used for spot welding galvanized steel sheets, a relatively larger safety factor may be obtained for the ASD method.[8.35]

It should be noted that special welding procedures may be required for the welding of low-alloy steels. In all cases, welding should be performed in accordance with the AWS recommended practices[8.33,8.34]

In 1999, the following equations for the nominal shear strength of spot welds were developed to replace the tabulated values given in Table 8.1:[1.333]

1. For 0.01 in. (0.25 mm) $\leq t <$ 0.14 in. (3.56 mm):

$$P_n = 144t^{1.47} \text{ (for } t \text{ in inches, and } P_n \text{ in kips)} \qquad (8.34a)$$

$$= 5.51t^{1.47} \text{ (for } t \text{ in mm, and } P_n \text{ in kN)} \qquad (8.34b)$$

2. For 0.14 in. (3.56 mm) $\leq t <$ 0.18 in. (4.57 mm):

$$P_n = 43.4t + 1.93 \text{ (for } t \text{ in inches, and } P_n \text{ in kips)} \qquad (8.35a)$$

$$= 7.6t + 8.57 \text{ (for } t \text{ in mm, and } P_n \text{ in kN)} \qquad (8.35b)$$

where t = thickness of thinnest outside sheet.

The upper limit of Eq. (8.34) was selected to best fit the data provided in Table 2.1 of Ref. 8.33 and Table 1.3 of Ref. 8.34. Equation (8.35) is limited

TABLE 8.1   Nominal Shear Strength for Spot Welding[1.314]

Thickness of Thinnest Outside Sheet (in.)	Nominal Shear Strength per Spot (kips)	Thickness of Thinnest Outside Sheet (in.)	Nominal Shear Strength per Spot (kips)
0.010	0.13	0.080	3.33
0.020	0.48	0.090	4.00
0.030	1.00	0.100	4.99
0.040	1.42	0.110	6.07
0.050	1.65	0.125	7.29
0.060	2.28	0.190	10.16
0.070	2.83	0.250	15.00

to $t \le 0.18$ in. (4.57 mm) due to the thickness limit set forth in the AISI Specification.

Table 8.1 and Eqs. (8.34) and (8.35) provide only the nominal shear strength for spot welding. If tensile strength of spot welding is required, it can be obtained either from tests or from the following empirical formulas for tensile and shear strengths proposed by Henschkel:[8.36]

1. *Tensile Strength*

$$N = tF_uD \left[\frac{a}{F_u - b} + c - (fC + g\ \text{Mn}) \right]$$

2. *Shear Strength*

$$S = tF_uD \left[\alpha - \beta \left(C + \frac{\text{Mn}}{20} \right) \right]$$

where N = tensile strength of spot welding
S = shear strength of spot welding
t = sheet thickness
F_u = tensile strength of steel sheet
C = carbon content
Mn = manganese content
D = weld nugget diameter

a, b, c, f, g, α, and β are coefficients determined from test results (see Ref. 8.36 for detailed information).

It should be noted that Henschkel's study was based on the following ranges of material:

1. Thickness of steel sheet: 0.008 to 0.500 in. (0.2 to 12.7 mm)
2. Tensile strength of material: 37,500 to 163,800 psi (258 to 1129 MPa)
3. Carbon content: 0.01 to 1.09%
4. Manganese content: 0.03 to 1.37%

From the above two equations, the relationship between tensile and shear strengths of spot welding can be expressed as follows:

$$\frac{N}{S} = \frac{a}{(F_u - b)(\alpha - \beta C - 0.05\beta\text{Mn})} + \frac{c - fC - g\text{Mn}}{\alpha - \beta C - 0.05\beta\text{Mn}}$$

Using the constants given in Ref. 8.36, it can be seen that for the steels

specified in the AISI Specification, the tensile strength of spot welding is higher than 25% of the shear strength.

See Example 8.8 for the design of welded connections using resistance welds.

8.3.5 Shear Lag Effect in Welded Connections of Members

When a tension member is not connected through all elements, such as when an angle is connected through only one leg, the stress distribution in the cross section is nonuniform. This phenomenon is referred to as ''shear lag,'' which has a weakening effect on the tensile capacity of the member.

For the design of hot-rolled steel shapes, the AISC Specification uses the effective net area A_e for determining the nominal strength. The effective net area is computed as

$$A_e = UA_n$$

in which U is the reduction factor and A_n is the net area.

For cold-formed steel design, the following new Specification Section E2.7 was added in the Supplement in 1999:[1.333]

E2.7 Shear Lag Effect in Welded Connections of Members Other Than Flat Sheets

The nominal strength of a welded member shall be determined in accordance with Section C2. For fracture and/or yielding in the effective net section of the connected part, the nominal tensile strength, P_n, shall be determined as follows:

$$P_n = A_e F_u$$

$$\Omega = 2.50 \text{ (ASD)} \tag{8.36}$$

$$\phi = 0.60 \text{ (LRFD)}$$

where F_u = tensile strength of the connected part as specified in Section A3.1 or A3.3.2
A_e = AU, effective net area with U defined as follows:
  1. When the load is transmitted only by transverse welds:
    A = area of directly connected elements
    $U = 1.0$
  2. When the load is transmitted only by longitudinal welds or by longitudinal welds in combination with transverse welds:
    A = gross area of member, A_g
    $U = 1.0$ for members when the load is transmitted directly to all of the cross sectional elements, Otherwise, the reduction coefficient U is determined as follows:

(a) For angle members:

$$U = 1.0 - 1.20\, \bar{x}/L < 0.9 \qquad (8.37)$$

but U shall not be less than 0.4
(b) For channel members:

$$U = 1.0 - 0.36\, \bar{x}/L < 0.9 \qquad (8.38)$$

but U shall not be less than 0.5
$\bar{x}$ = distance from shear plane to centroid of the cross section (Fig. 8.25)
L = length of longitudinal welds (Fig. 8.25)

The above design provisions were adopted from the AISC design approach. Equations (8.37) and (8.38) are based on the research work conducted by Holcomb, LaBoube, and Yu at the University of Missouri-Rolla on bolted connections.[6.24,6.25]

8.4 BOLTED CONNECTIONS

The structural behavior of bolted connections in cold-formed steel construction is somewhat different from that in hot-rolled heavy construction, mainly because of the thinness of the connected parts. Prior to 1980, the provisions included in the AISI Specification for the design of bolted connections were developed on the basis of the Cornell tests conducted under the direction of George Winter.[8.37–8.40] These provisions were updated in 1980[1.4] to reflect the results of additional research performed in the United States[4.30,8.41–8.46] and to provide a better coordination with the specifications of the Research Council on Structural Connections[8.47] and the AISC.[1.148] In 1986, design provisions for the maximum size of bolt holes and the allowable tension stress for bolts were added in the AISI Specification. The 1996 edition of the Specification combines the ASD and LRFD design provisions with minor revisions. The
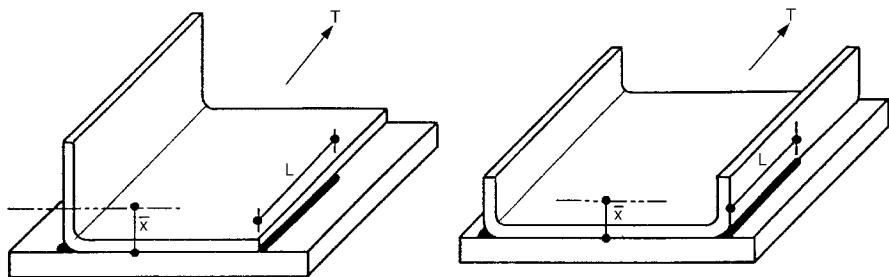

Figure 8.25 Determination of $\bar{x}$ for sections using fillet welds.[1.333]

shear lag effect on bolted connections is considered in the Supplement to the 1996 Specification.

8.4.1 Research Work and Types of Failure Mode

Since 1950, numerous bolted connections using thin sheets with A307 bolts and A325 high-strength bolts have been tested at Cornell University and other institutions. The purposes of these research projects were to study the structural performance of bolted connections and to provide necessary information for the development of reliable design methods.

In all test programs, bolts were tightened to the torque values as given in Tables 8.2 and 8.3 according to the type of bolts used in the specimens. Connections were tested with and without washers placed under bolt head and nut.

Results of tests indicate that the following four basic types of failure usually occur in the cold-formed steel bolted connections:

1. Longitudinal shearing of the sheet along two parallel lines (Fig. 8.26*a*)
2. Bearing or piling up of material in front of the bolt (Fig. 8.26*b*)
3. Tearing of the sheet in the net section (Fig. 8.26*c*)
4. Shearing of the bolt (Fig. 8.26*d*)

These four failure modes are also illustrated in Fig. 8.27. In many cases, a joint is subject to a combination of different types of failure. The tearing of the sheet is often caused by the excessive bolt rotation and dishing of the sheet material.[8.45,6.23]

8.4.1.1 *Longitudinal Shearing of Steel Sheets* (*Type I Failure*)   When the edge distance *e* as shown in Figs. 8.27*a* and 8.28 is relatively small, connections usually fail in longitudinal shearing of the sheet along two parallel lines.

TABLE 8.2   Torques Used for Installation of A307 Bolts[8.37]

Bolt Diameter (in.)	Torque (ft-lb)
$\frac{1}{4}$	5
$\frac{3}{8}$	14
$\frac{1}{2}$	40
$\frac{5}{8}$	50
$\frac{3}{4}$	110
1	250

Note: 1 in. = 25.4 mm; 1 ft-lb = 1.356 N · m.

TABLE 8.3   Torques Used for Installation of A325 High-Strength Bolts and Equivalents[8.38]

Bolt Diameter (in.)	Torque (ft-lb)
$\frac{1}{4}$	11
$\frac{3}{8}$	37.5
$\frac{1}{2}$	95
$\frac{5}{8}$	190
$\frac{3}{4}$	335
1	750

Note: 1 in. = 25.4 mm; 1 ft-lb = 1.356 N · m.

Test data shown in Figs. 8.29 through 8.34 indicate that for bolted connections having small e/d ratios, the bearing stress at failure can be predicted by

$$\frac{\sigma_b}{F_u} = \frac{e}{d} \tag{8.39}$$

where σ_b = ultimate bearing stress between bolt and connected part, ksi
  F_u = tensile strength of connected part, ksi
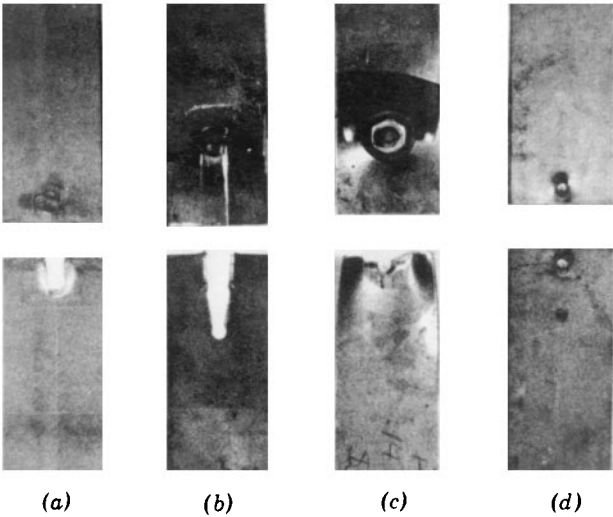 e = edge distance, in.
  d = bolt diameter, in.

(a)   *(b)*   *(c)*   *(d)*

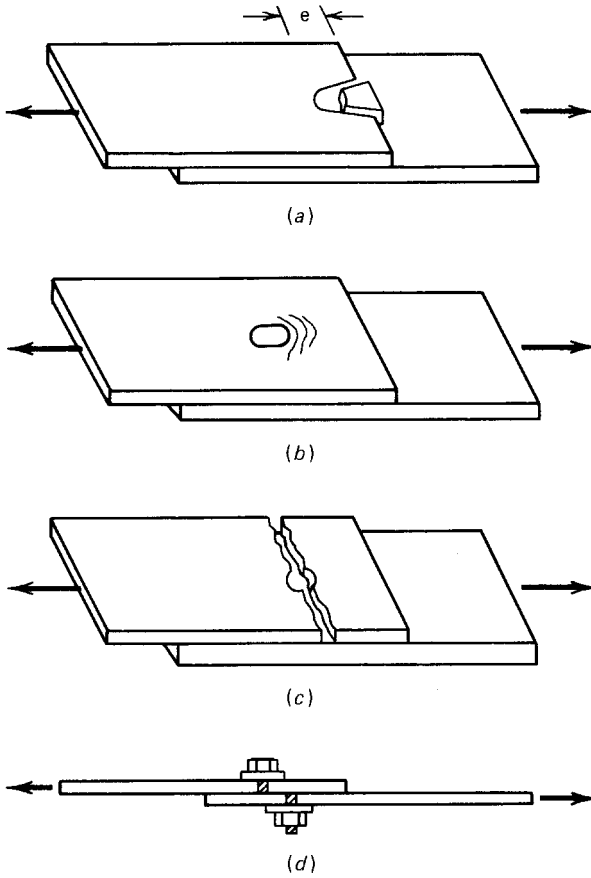**Figure 8.26**   Types of failure of bolted connections.[8.37]

Figure 8.27   Types of failure of bolted connections. (*a*) Longitudinal shear failure of sheet (type I). (*b*) Bearing failure of sheet (type II). (*c*) Tensile failure of sheet (type III). (*d*) Shear failure of bolt (type IV).
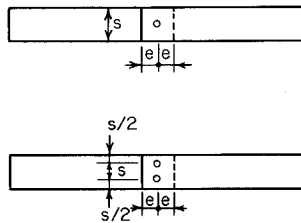

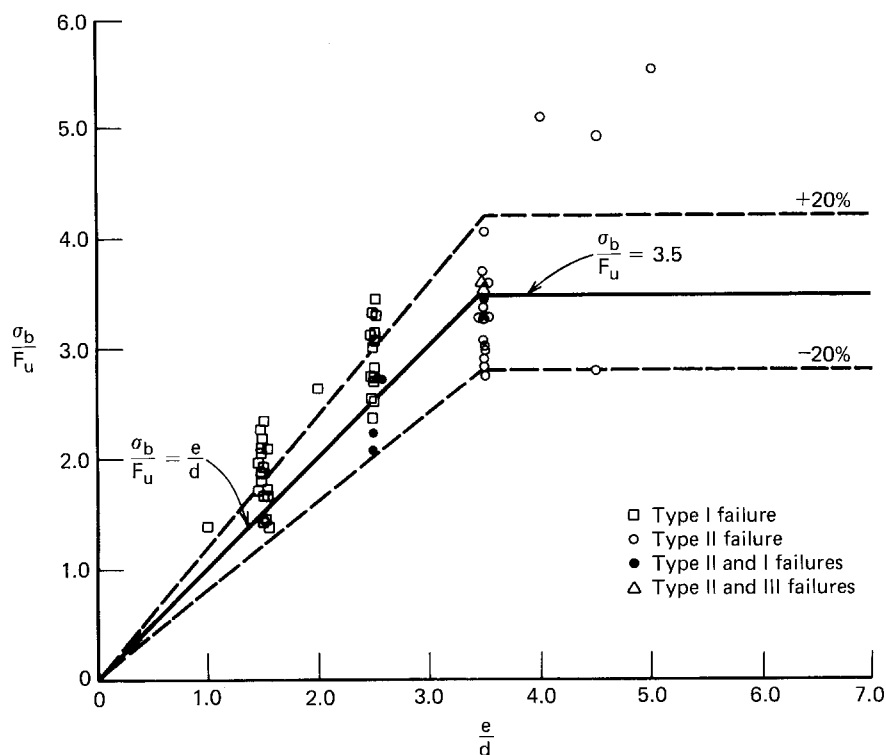**Figure 8.28**   Dimensions *s* and *e* used in bolted connections.

Figure 8.29   Single-shear connections with washers, $F_u/F_y \geq 1.15$, shear and bearing strength study.[8.46]

Equation (8.40) is based on the results of bolted connection tests with the following parameters:[8.46]

Diameter of bolt d: $\frac{3}{16}$ to 1 in. (4.8 to 25.4 mm)
Thickness of connected part t: 0.036 to 0.261 in. (0.9 to 6.6 mm)
Edge distance e: 0.375 to 2.5 in. (9.5 to 63.5 mm)
Yield point of steel F_y: 25.60 to 87.60 ksi (177 to 604 MPa)
Tensile strength of steel F_u: 41.15 to 91.30 ksi (284 to 630 MPa)
e/d ratio: 0.833 to 3.37
d/t ratio: 2.61 to 20.83
F_u/F_y ratio: 1.00 to 1.63

The dimension of the specimens and the test results are given in Ref. 8.45.
By substituting $\sigma_b = P_u/dt$ into Eq. (8.39), Eq. (8.40) can be obtained for the required edge distance e,
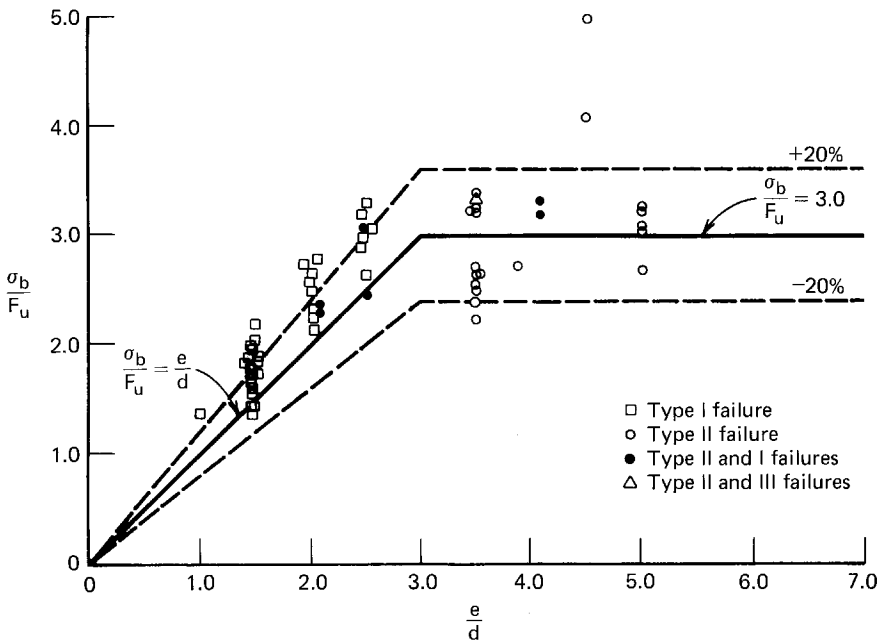
Figure 8.30   Double-shear connections with washers, $F_u/F_y \geq 1.15$, shear and bearing strength study.[8.46]
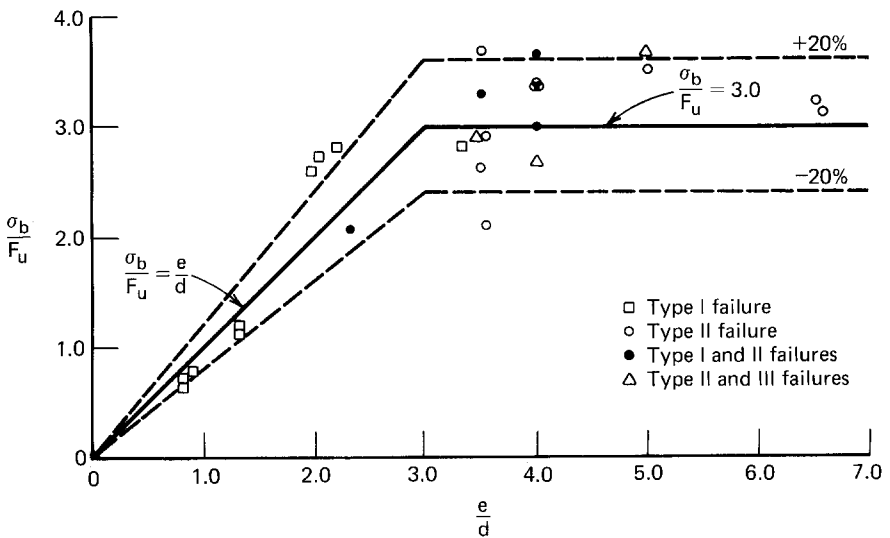

Figure 8.31   Single-shear connections with washers, $F_u/F_y < 1.15$, shear and bearing strength study.[8.46]

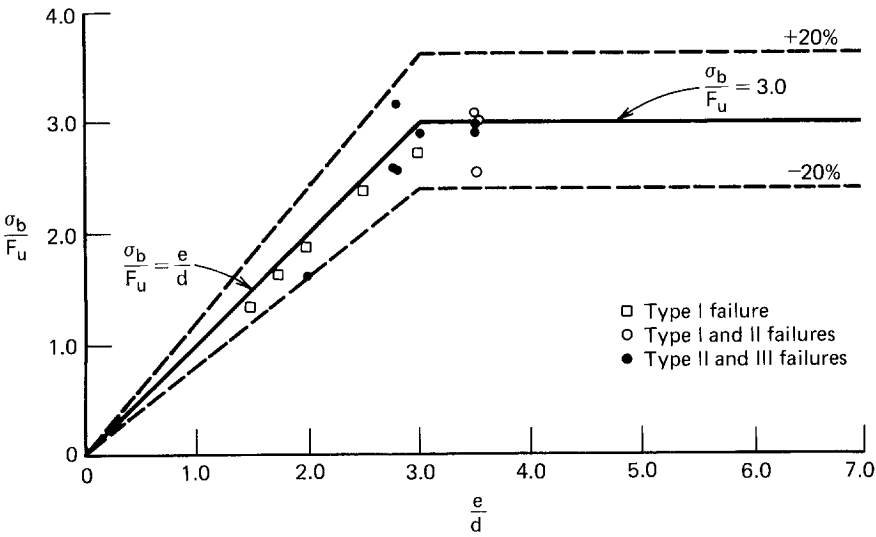**Figure 8.32**   Double-shear connections with washers, $F_u/F_y < 1.15$, shear and bearing strength study.[8.46]

$$e = \frac{P_u}{F_u t} \tag{8.40}$$

This equation is also used for the specifications of the Research Council on Structural Connections[8.47,8.48] and the AISC.[1.148]
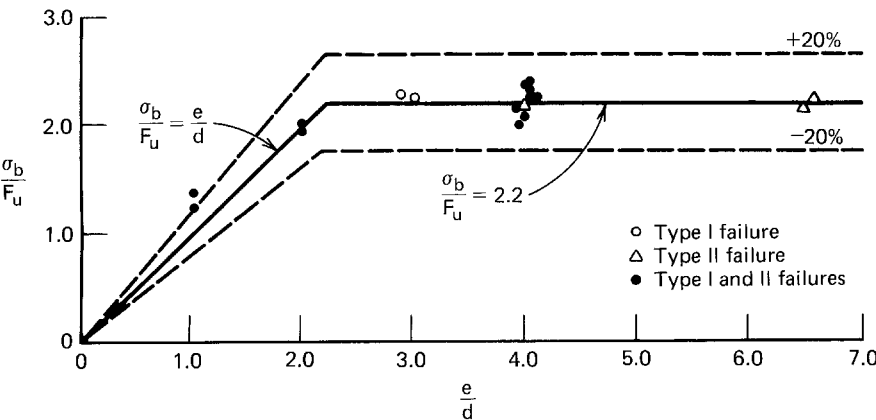

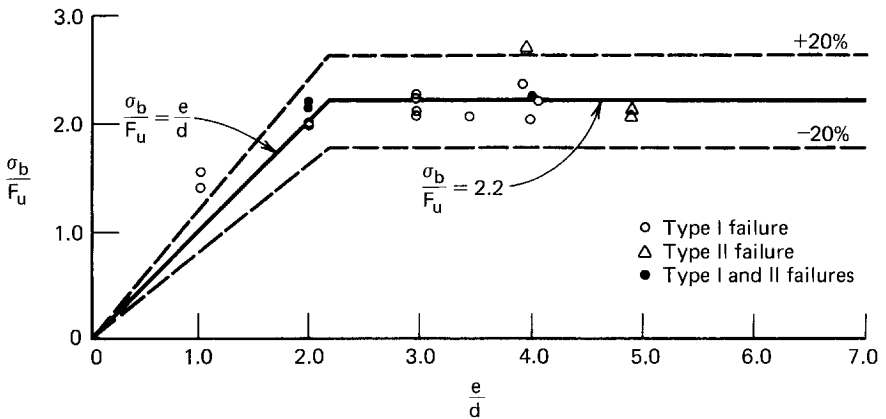**Figure 8.33**   Single-shear connections without washers, $F_u/F_y \geq 1.15$, shear and bearing strength study.[8.46]

Figure 8.34   Single-shear connections without washers, $F_u/F_y < 1.15$, shear and bearing strength study.[8.46]

8.4.1.2   *Bearing or Piling Up of Steel Sheet (Type II Failure)*   When the edge distance is sufficiently large (i.e., for large e/d ratios), the connection may fail by bearing or piling up of steel sheet in front of the bolt, as shown in Fig. 8.27b. Additional studies indicate that the bearing strength of bolted connections depends on several parameters, including the tensile strength of the connected part, the thickness of the connected part, the types of joints (lap joints or butt joint), the F_u/F_y ratio of the connected part, the use of washers, the "catenary action" of steel sheets, and the rotation of fasteners. Tables 8.4 and 8.5 list several formulas for determining the ultimate bearing stress σ_b on the basis of various conditions given in the tables. These equations were developed from the test data plotted in Figs. 8.29 through 8.35 with the following variables.[8.46]

TABLE 8.4   Bearing Strengths of Bolted Connections with Washers under Both Bolt Head and Nut

Thickness of Steel Sheet, (in.)	Type of Joint	F_u/F_y Ratio of Steel Sheet	Ultimate Bearing Stress σ_b (ksi)
< 3/16 but ≥ 0.024	Inside sheet of double-shear connections	≥1.15	$3.5F_u$
		<1.15	$3.0F_u$
	Single-shear connections and outside sheets of double-shear connections	≥1.15	$3.0F_u$
		<1.15	$3.0F_u$

Note: 1 in. = 25.4 mm; 1 ksi = 6.9 MPa.

TABLE 8.5 Bearing Strengths of Bolted Connections without Washers under Both Bolt Head and Nut

Thickness of Steel Sheet, (in.)	Type of Joint	F_u/F_y Ratio of Steel Sheet	Ultimate Bearing Stress σ_b (ksi)
< 3/16 but ≥ 0.036	Inside sheet of double-shear connections	≥1.15	$3.0F_u$
	Single-shear connections and outside sheets of double-shear connections	≥1.15	$2.2F_u$

Note: 1 in. = 25.4 mm; 1 ksi = 6.9 MPa.

Diameter of bolt d: $\frac{3}{16}$ to 1 in. (4.8 to 25.4 mm)
Thickness of connected part t: 0.024 to 0.260 in. (0.6 to 6.6 mm)
Edge distance e: 0.50 to 4.50 in. (12.7 to 114 mm)
Yield point of steel F_y: 28.1 to 82.6 ksi (194 to 570 MPa)
Tensile strength of steel F_u: 41.83 to 82.6 ksi (288 to 570 MPa)
e/d ratio: 1.02 to 6.62
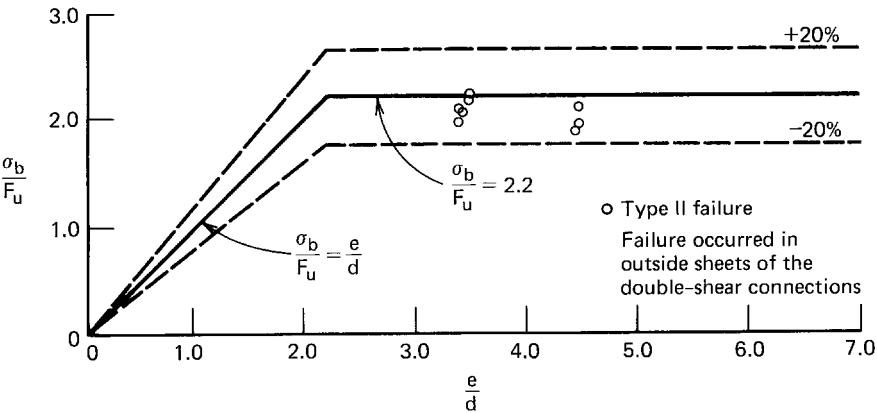d/t ratio: 3.42 to 13.50
f_u/F_y ratio: 1.00 to 1.63

Figure 8.35 Double-shear connections without washers, $F_u/F_y \geq 1.15$, bearing strength study.[8.46]

The dimensions of the specimens and detailed test data are presented in Ref. 8.45.

It should be noted that the formulas given in Tables 8.4 and 8.5 are applicable only when the deformation around the bolt holes is not a design consideration. When the deformation around the bolt holes is a design consideration, the nominal bearing strength should also be limited by the following values according to the Supplement to the 1996 edition of the Specification:[1.333]

$$P_n = (4.64t + 1.53) \, dtF_u \text{ (with } t \text{ in inches)} \qquad (8.41a)$$

For SI units:

$$P_n = (0.183t + 1.53) \, dtF_u \text{ (with } t \text{ in mm)} \qquad (8.41b)$$

All symbols were defined previously.

The above design equations were developed from the research conducted at the University of Missouri-Rolla to recognize the hole elongation prior to reaching the limited bearing strength of a bolted connection.[6.24,6.25] The movement of the connection was limited to 0.25 in. (6.4 mm), which is consistent with the permitted elongation prescribed in the AISC Specification for hot-rolled steel shapes and built-up members.

8.4.1.3   *Tearing of Sheet in Net Section* (*Type III Failure*)   In bolted connections, the type of failure by tearing of the sheet in the net section is related to the stress concentration caused by

1. The presence of holes
2. The concentrated localized force transmitted by the bolt to the sheets

Previous tests conducted at Cornell University for connections using washers under bolt head and nut have indicated that plastic redistribution is capable of eliminating the stress concentration caused by the presence of holes even for low-ductility steel.[8.39] However, if the stress concentration caused by the localized force transmitted by the bolt to the sheet is pronounced, the strength of the sheet in the net section was found to be reduced for connections having relatively wide bolt spacing in the direction perpendicular to the transmitted force. The effects of the d/s ratio on the tensile strength of bolted connections with washers are shown in Figs. 8.36 and 8.37.

An additional study conducted at Cornell on connections using multiple bolts has shown that the sharp stress concentration is much relieved when more than one bolt in line is used. As shown in Fig. 8.38, the failure in the net section in the two-bolt ($r = \frac{1}{2}$) and three-bolt ($r = \frac{1}{3}$) tests occurred at a
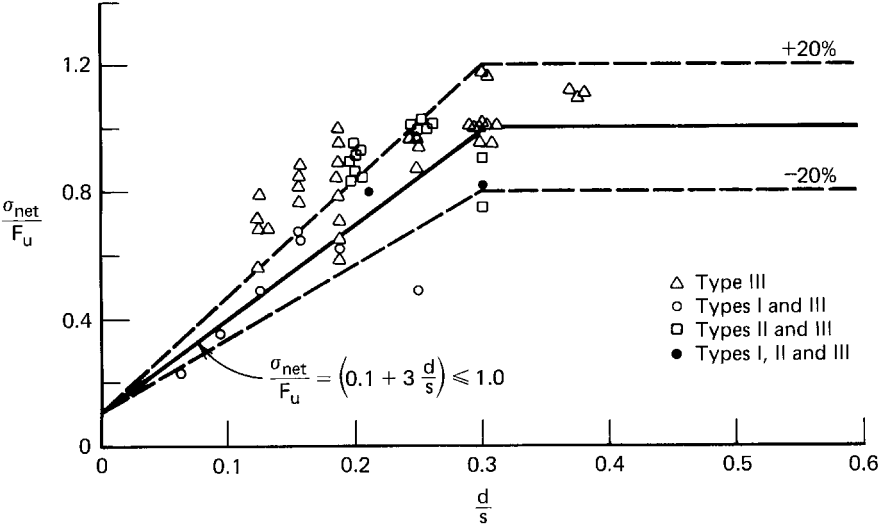
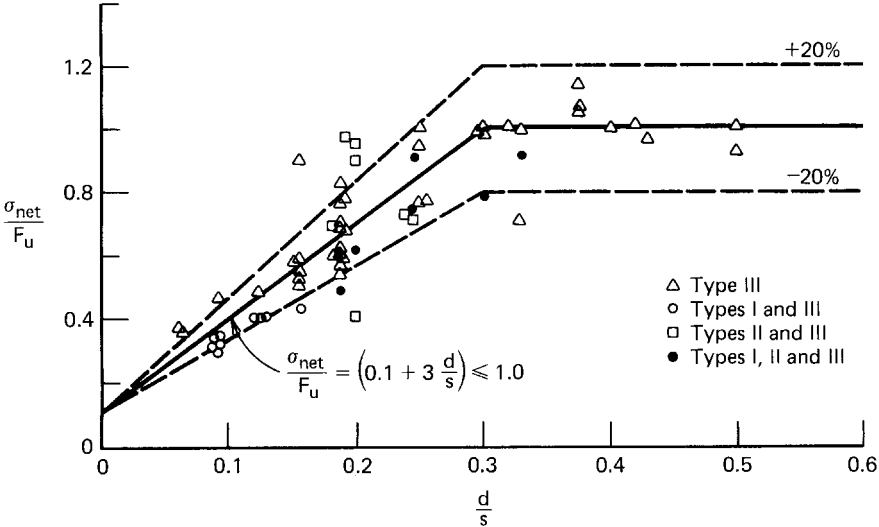**Figure 8.36** Effect of d/s on tensile strength of bolted connections with washers (double shear, one bolt).[8.46]

Figure 8.37 Effect of d/s on tensile strength of bolted connections with washers (single shear, one bolt).[8.46]
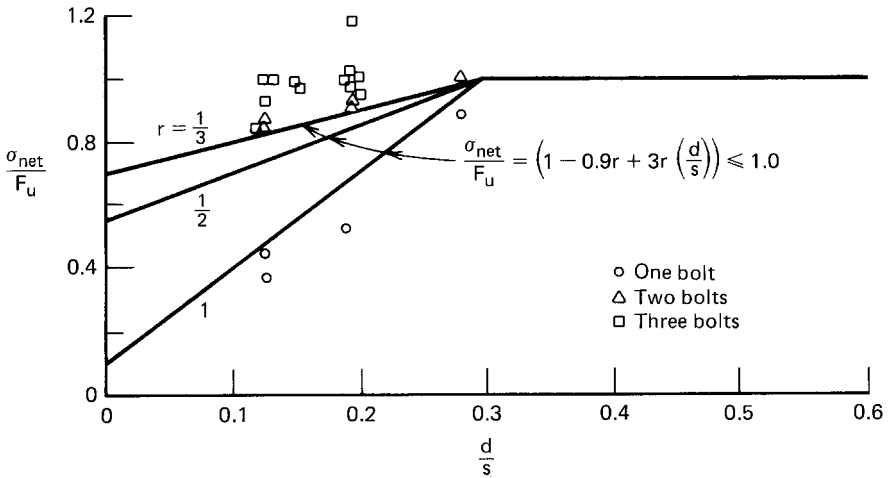
Figure 8.38   Effect of d/s on tensile strength of bolted connections with washers (single shear, multibolt).[8.46]

much higher stress than in single-bolt ($r = 1$) connections. The following formulas have been developed to predict the failure stress in the net section:

1. When $d/s \leq 0.3$,

$$\sigma_{net} = \left[1 - 0.9r + 3r \left(\frac{d}{s} \right) \right] F_u \leq F_u \qquad (8.42)$$

2. When $d/s > 0.3$,

$$\sigma_{net} = F_u \qquad (8.43)$$

where σ_{net} = failure stress in net section, ksi
r = force transmitted by bolt or bolts at the section considered, divided by the force in the member at that section
d = bolt diameter, in.
s = spacing of bolts perpendicular to line of stress, in.
F_u = ultimate tensile strength of steel sheets, ksi

The correlations between Eq. (8.42) and the test data are shown in Figs. 8.36 through 8.38. The test data were obtained with the following parameters.[8.46]

Diameter of bolt d: $\frac{1}{4}$ to $1\frac{1}{8}$ in. (6.4 to 28.6 mm)

Thickness of steel sheet t: 0.0335 to 0.191 in. (0.9 to 4.9 mm)

Width of steel sheet s: 0.872 to 4.230 in. (22 to 107 mm)

Yield point of steel F_y: 26.00 to 99.40 ksi (179 to 685 MPa)

Tensile strength of steel F_u: 41.15 to 99.80 ksi (284 to 688 MPa)

d/s ratio: 0.063 to 0.50

d/t ratio: 3.40 to 21.13

When washers are not used and when only one washer is used in bolted connections, the failure stress in the net section σ_{net} can be determined by

$$\sigma_{net} = \left[1.0 - r + 2.5r \left(\frac{d}{s} \right) \right] F_u \leq F_u \tag{8.44}$$

Figure 8.39 shows the correlation between Eq. (8.44) and the test data presented by Chong and Matlock in Ref. 8.42.

8.4.1.4   Shearing of Bolt (*Type IV Failure*)   A number of double-shear and single-shear tests have been performed at Cornell University in the 1950s to study the type of failure caused by shearing of the bolt.[8.37,8.38] It was found

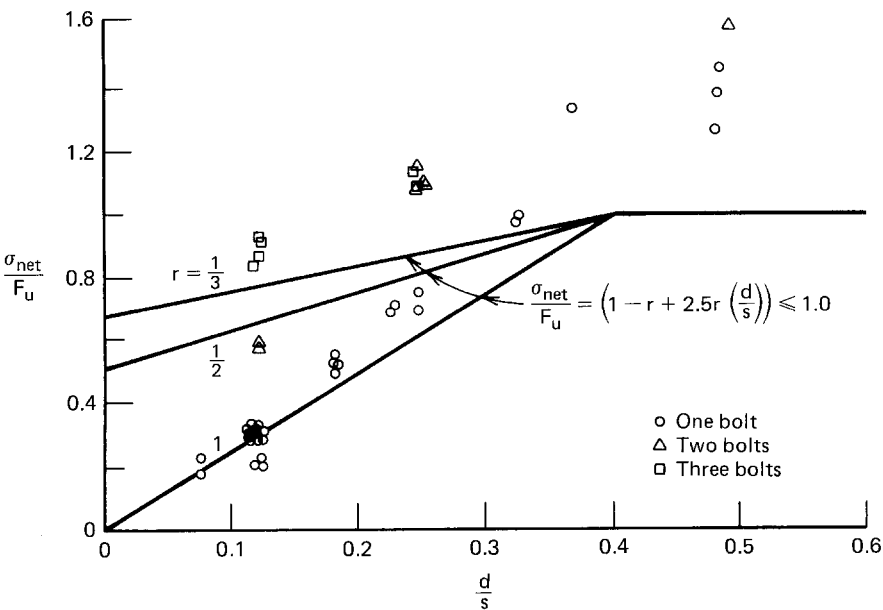**Figure 8.39**   Effect of d/s of tensile strength of bolted connections without washers (single shear, multibolt).[8.46]

that the shear-to-tension strength ratio is independent of the bolt diameter, and the ratios are equal to about 0.62 and 0.72 for double-shear and single-shear tests, respectively. In view of the fact that the failure by shearing of the bolt is more sudden than that in the sheets being connected, a conservative shear-to-tension ratio of 0.6 has been used in the past for both double- and single-shear conditions in the development of design provisions, even though the extremes of test values ranged from 0.52 to 1.0; that is, the type of failure by shearing of the bolt occurs at a strength equal to 0.6 times the tensile strength of the bolt.

8.4.2   AISI Design Criteria for Bolted Connections

Based upon the results of tests summarized in Art. 8.4.1 and past design experience, Sec. E3 of the 1996 edition of the AISI Specification and its Supplement include a number of requirements for the design of bolted connections.

8.4.2.1   Thickness Limitations   On the basis of the same reasons discussed in Art. 8.3.2.1 for the design of welded connections, Sec. E3 is applicable only to the design of bolted connections for cold-formed steel members that are less than $\frac{3}{16}$ in. (4.8 mm) in thickness. For materials not less than $\frac{3}{16}$ in. (4.8 mm), the AISC Specification[1.148,3.150] should be used for the design of bolted connections in cold-formed steel structures.

8.4.2.2   Materials   Prior to 1980, the AISI design provisions concerning the allowable shear stresses for mechanical fasteners were limited to A307 and A325 bolts. Because the maximum thickness for cold-formed steel members was increased in 1977 from $\frac{1}{2}$ in. (12.7 mm) to 1 in. (25.4 mm), other high-strength bolts, such as A354, A449, and A490 bolts were added to the 1980 Specification for bolted connections.

In view of the fact that A325 and A490 bolts are available only for a diameter of $\frac{1}{2}$ in. (12.7 mm) and larger, whenever smaller bolts [less than $\frac{1}{2}$ in. (12.7 mm) in diameter] are required in a design, A449 and A354 Grade BD bolts should be used as equivalents of A325 and A490 bolts, respectively.

For other types of fasteners, which are not listed in Sec. E3 of the AISI Specification, drawings should indicate clearly the type and size of fasteners to be employed and the design force.

8.4.2.3   Bolt Installation   The requirement for bolt installation was added to the AISI Specification since 1980 to ensure that bolts are properly tightened according to acceptable practice. Because the required pretension in bolts usually varies with the types of connected part, fasteners, applied loads, and applications, no specific provisions are provided in the AISI Specification for installation.

In Art. 8.4.1, Tables 8.2 and 8.3 give the torques used for the installation of different bolts in test specimens. The effect of torques on the strength of bolted connections has been studied in the past and was reported in Ref. 8.45.

8.4.2.4   Maximum Sizes of Bolt Holes   The 1986 and the 1996 editions of the AISI Specification include the maximum sizes of standard holes, oversized holes, short-slotted holes, and long-slotted holes as shown in Table 8.6. Standard holes should be used in bolted connections, except that oversized and slotted holes may be used as approved by the designer. Additional requirements are given in the AISI Specification for the use of oversized and slotted holes.

8.4.2.5   Shear, Spacing, and Edge Distance in Line of Stress   According to Sec. E3.1 of the AISI Specification, the nominal shear strength, P_n, of the connected part as affected by spacing and edge distance in the direction of applied force shall be calculated as follows:

$$P_n = teF_u \tag{8.45}$$

a. When $F_u/F_y \geq 1.08$:

$$\Omega = 2.0 \text{ (ASD)}$$
$$\phi = 0.70 \text{ (LRFD)}$$

b. When $F_u/F_y < 1.08$

$$\Omega = 2.22 \text{ (ASD)}$$
$$\phi = 0.60 \text{ (LRFD)}$$

TABLE 8.6   Maximum Sizes of Bolt Holes

Nominal Bolt Diameter, d (in.)	Standard Hole Diameter, d (in.)	Oversized Hole Diameter, d (in.)	Short-Slotted Hole Dimensions (in.)	Long-Slotted Hole Dimensions (in.)
$< \frac{1}{2}$	$d + \frac{1}{32}$	$d + \frac{1}{16}$	$(d + \frac{1}{32})$ by $(d + \frac{1}{4})$	$(d + \frac{1}{32})$ by $(2\frac{1}{2}d)$
$\geq \frac{1}{2}$	$d + \frac{1}{16}$	$d + \frac{1}{8}$	$(d + \frac{1}{16})$ by $(d + \frac{1}{4})$	$(d + \frac{1}{16})$ by $(2\frac{1}{2}d)$

Note: 1 in. = 25.4 mm.

where P_n = nominal resistance per bolt

e = the distance measured in the line of force from the center of a standard hole to the nearest edge of an adjacent hole or to the end of the connected part

t = thickness of thinnest connected part

F_u = tensile strength of the connected part

F_y = yield point of the connected part

Equation (8.45) was derived from Eq. (8.40) in Art. 8.4.1.1. The above design equation is the same as that used in previous editions of the AISI specification, except that the limiting F_u/F_y ratio was reduced in 1996 from 1.15 to 1.08 for the consistency with the ductility requirement prescribed in Sec. A3.3.1 of the Specification.

In addition to the above requirements, Sec. E3.1 of the AISI Specification also includes the following requirements concerning minimum spacing and edge distance in the line of stress:

1. The minimum distance between centers of bolt holes should not be less than $3d$.
2. The distance from the center of any standard hole to the end or other boundary of the connecting member should not be less than $1\frac{1}{2}d$.
3. The clear distance between edges of two adjacent holes should not be less than $2d$.
4. The distance between the edge of the hole and the end of the member should not be less than d.
5. For oversized and slotted holes, the distance between edges of two adjacent holes and the distance measured from the edge of the hole to the end or other boundary of the connecting member in the line of stress should not be less than the value of $(e - 0.5d_h)$, in which e is the required distance computed from Eq. (8.45) using the applicable safety factor for ASD and resistance factor for LRFD method, and d_h is the diameter of a standard hole defined in Table 8.6.

8.4.2.6 Tensile Strength of Connected Parts at Connection

Prior to 1999, the tensile strength on the net section of connected parts was determined in accordance with Specification Sec. E3.2 in addition to the requirements of Specification Sec. C2. In Sec. E3.2, the nominal tensile strength on the net section of the bolt connected parts was determined by the tensile strength of steel F_u and the ratios r and d/s. These design equations represent the shear lag effect on the tensile capacity of flat sheets with due consideration given to the use of washers and the type of joints, either a single shear lap joint or a double shear butt joint.

During recent years, research work has been conducted by Holcomb, LaBoube, and Yu at the University of Missouri-Rolla to study the effect of

shear lag on the tensile capacity of angles and channels as well as flat steel sheets.[6.24,6.25] The same project included a limited study of the behavior of bolted connections having staggered hole patterns. It was found that when a staggered hole pattern is involved, the net area can be determined by a design equation using the well-known parameter $s'^2/4g$.

Based on the research findings, the AISI Supplement includes the following revised Specification Sec. E3.2 to deal with the determination of the nominal tensile strength for (a) flat sheet connections not having staggered hole patterns, (b) flat sheet connections having staggered hole patterns, and (c) structural shapes including angles and channels.[1.333]

E3.2 Shear Lag Effect in Bolted Connections

The nominal tensile strength of a bolted member shall be determined in accordance with Section C2. For fracture and/or yielding in the effective net section of the connected part, the nominal tensile strength, P_n, shall be determined as follows:

(1) For flat sheet connections not having staggered hole patterns:

$$P_n = A_n F_t \tag{8.46}$$

(a) When washers are provided under both the bolt head and the nut:

$$F_t = (1.0 - 0.9r + 3rd/s) \, F_u \le F_u \tag{8.47}$$

For double shear:

$$\Omega = 2.0 \text{ (ASD)}$$
$$\phi = 0.65 \text{ (LRFD)}$$

For single shear:

$$\Omega = 2.22 \text{ (ASD)}$$
$$\phi = 0.55 \text{ (LRFD)}$$

(b) When either washers are not provided under the bolt head and the nut, or only one washer is provided under either the bolt head or the nut:

$$F_t = (1.0 - r + 2.5rd/s) \, F_u \le F_u \tag{8.48}$$
$$\Omega = 2.22 \text{ (ASD)}$$
$$\phi = 0.65 \text{ (LRFD)}$$

where A_n = net area of the connected part

r = force transmitted by the bolt or bolts at the section considered, divided by the tension force in the member at that section. If r is less than 0.2, it shall be permitted to be taken as equal to zero.

s = spacing of bolts perpendicular to line of stress; or gross width of sheet for a single line of bolts

F_u = tensile strength of the connected part as specified in Section A3.1 or A3.3.2

d is defined in Section E3.1

(2) For flat sheet connections having staggered hole patterns:

$$P_n = A_n F_t \tag{8.46}$$

$$\Omega = 2.22 \ (\text{ASD})$$

$$\phi = 0.65 \ (\text{LRFD})$$

where

F_t is determined as follows:

(a) For connections when washers are provided under both the bolt head and the nut:

$$F_t = (1.0 - 0.9r + 3rd/s) \, F_u \leq F_u \tag{8.47}$$

(b) For connections when no washers are provided under the bolt head and the nut, or only one washer is provided under either the bolt head or the nut:

$$F_t = (1.0 - r + 2.5rd/s) \, F_u \leq F_u \tag{8.48}$$

$$A_n = 0.90 \, [A_g - n_b d_h t + (\Sigma s'^2/4g)t] \tag{8.49}$$

A_g = gross area of member

s = sheet width divided by the number of bolt holes in the cross section being analyzed (when evaluating F_t)

s' = longitudinal center-to-center spacing of any two consecutive holes

g = transverse center-to-center spacing between fastener gage lines

n_b = number of bolt holes in the cross section being

analyzed

d_h = diameter of standard hole

t is defined in Section E3.1

(3) For other than flat sheet:

$$P_n = A_e F_u \tag{8.50}$$

$$\Omega = 2.22 \ (\text{ASD})$$

$$\phi = 0.65 \ (\text{LRFD})$$

where F_u = tensile strength of the connected part as specified in Section A3.1
or A3.3.2
$A_e = A_n U$, effective net area with U defined as follows:
U = 1.0 for members when the load is transmitted directly to all of the
cross-sectional elements.

Otherwise, the reduction coefficient U is determined as follows:

(a) For angle members having two or more bolts in the line of force:

$$U = 1.0 - 1.20\,\bar{x}/L < 0.9 \tag{8.51a}$$

but U shall not be less than 0.4

(b) For channel members having two or more bolts in the line of force:

$$U = 1.0 - 0.36\,\bar{x}/L < 0.9 \tag{8.51b}$$

but U shall not be less than 0.5

$\bar{x}$ = distance from shear plane to centroid of the cross section (Fig. 8.40)
L = length of the connection (Fig. 8.40)

The Specification Eqs. (8.47) and (8.48) were derived from Eqs. (8.42) and
(8.44) respectively. See Art. 8.4.1.3.

8.4.2.7 *Bearing Strength between Bolts and Connected Parts*

a. Deformation Around the Bolt Holes Is Not a Design Consideration. Based
on the ultimate bearing stress presented in Tables 8.4 and 8.5, Sec. E3.3 of
the Supplement to the 1996 edition of the Specification provides the nominal
bearing strength, P_n, as given in Tables 8.7 and 8.8, in which the values of
F_u and F_y were defined previously. For conditions not shown in these tables,
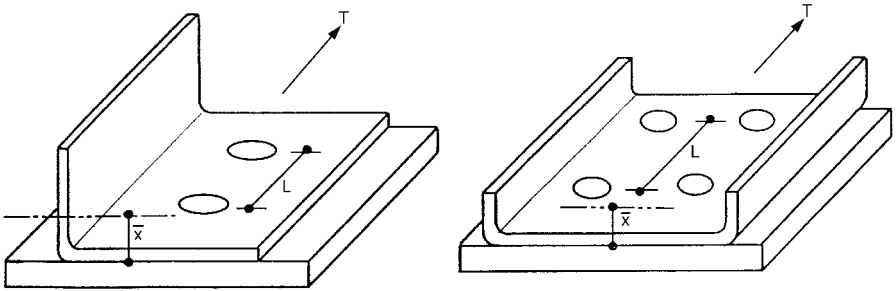
Figure 8.40   Determination of $\bar{x}$ for sections using bolted connections.[1.333]

the design bearing strength should be determined on the basis of tests. The nominal bearing strength, P_n, listed in the table is computed by Eq. (8.52), in which (dt) is the projected area and σ_b is the ultimate bearing stress.

$$P_n = \sigma_b(dt) \tag{8.52}$$

In Tables 8.7 and 8.8, the limit of F_u/F_y ratio was changed from 1.15 to 1.08 in the 1996 edition of the Specification in order to be consistent with Sec. A.3.3.1 of the Specification. In 1999, the lower thickness limit in Tables 8.7 and 8.8 was revised from 0.024 in. (0.61 mm) to 0.036 in (0.91 mm).

TABLE 8.7   Nominal Bearing Strength for Bolted Connections with Washers under Both Bolt Head and Nut[1.314,1.333]

Thickness of Connected Part, t, in. (mm)	Type of Joint	F_u/F_y ratio of Connected Part	Ω ASD	ϕ LRFD	Nominal Resistance P_n
0.036 $\leq t <$ 3/16 (0.91) $\leq t <$ (4.76)	Inside sheet of double shear connection	$\geq$1.08	2.22	0.55	3.33 $F_u dt$
		<1.08	2.22	0.65	3.00 $F_u dt$
	Single shear and outside sheets of double shear connection	No limit	2.22	0.60	3.00 $F_u dt$
$t \geq$ 3/16 (4.76)	See AISC ASD or LRFD Specification				

TABLE 8.8   Nominal Bearing Strength for Bolted Connections Without Washers under Both Bolt Head and Nut or with Only One Washer[1.314,1.333]

Thickness of Connected Part, t, in. (mm)	Type of Joint	F_u/F_y ratio of Connected Part	Ω ASD	ϕ LRFD	Nominal Resistance P_n
0.036 ≤ t < 3/16 (0.91) ≤ t < (4.76)	Inside sheet of double shear connection	≥1.08	2.22	0.60	3.00 $F_u dt$
	Single shear and outside sheets of double shear connection	≥1.08	2.22	0.70	2.22 $F_u dt$
t ≥ 3/16 (4.76)	See AISC ASD or LRFD Specification				

This revision was based on the recent research conducted by Rogers and Hancock at the University of Sydney.[2.56]

b. Deformation Around the Bolt Holes Is a Design Consideration. When the movement of the connection is critical and the deformation around bolt holes is a design consideration, nominal bearing strength should also be limited by Eq. (8.41) according to Sec. E3.3 of the Supplement to the 1996 edition of the Specification.[1.333,6.25] For using Eqs. (8.41a) and (8.41b), Ω = 2.22 (for ASD) and ϕ = 0.65 (for LRFD). See Art. 8.4.1.2 for additional discussion.

8.4.2.8   Shear and Tension in Bolts   Section E3.4 of the AISI Specification specifies that the nominal bolt strength, P_n, resulting from shear, tension, or a combination of shear and tension shall be calculated as follows:

$$P_n = A_b F \tag{8.53}$$

where A_b = gross cross-sectional area of bolt

When bolts are subject to shear or tension, the nominal stress F is given in Table 8.9 by F_{nv} for shear or F_{nt} for tension. The applicable values of Ω and ϕ are also given in the same table. When bolt tension is involved, the pull-over strength of the connected sheet at the bolt head, nut, or washer shall be considered. See Art. 8.5.1.

When bolts are subject to a combination of shear and tension:

TABLE 8.9 Nominal Tensile and Shear Strength for Bolts[1.314]

Description of Bolts	Tensile Strength			Shear Strength*		
	Factor of Safety Ω (ASD)	Resistance Factor ϕ (LRFD)	Nominal Stress F_{nt}, ksi (MPa)	Factor of Safety Ω (ASD)	Resistance Factor ϕ (LRFD)	Nominal Stress F_{nv}, ksi (MPa)
A307 Bolts, Grade A, $\frac{1}{4}$ in. (6.4 mm) $\leq d < \frac{1}{2}$ in. (12.7 mm)	2.25	0.75	40.5 (279)	2.4	0.65	24.0 (165)
A307 Bolts, Grade A, $d \geq \frac{1}{2}$ in.	2.25		45.0 (310)			27.0 (186)
A325 Bolts, when threads are not excluded from shear planes	2.0		90.0 (621)			54.0 (372)
A325 Bolts, when threads are excluded from shear planes			90.0 (621)			72.0 (496)
A354 Grade BD Bolts, $\frac{1}{4}$ in. $\leq d < \frac{1}{2}$ in. when threads are not excluded from shear planes			101.0 (696)			59.0 (407)
A354 Grade BD Bolts, $\frac{1}{4}$ in. $\leq d < \frac{1}{2}$ in. when threads are excluded from shear planes			101.0 (696)			90.0 (621)
A449 Bolts, $\frac{1}{4}$ in. $\leq d < \frac{1}{2}$ in., when threads are not excluded from shear planes			81.0 (558)			47.0 (324)
A449 Bolts, $\frac{1}{4}$ in. $\leq d < \frac{1}{2}$ in., when threads are excluded from shear planes			81.0 (558)			72.0 (496)
A490 Bolts, when threads are not excluded from shear planes			112.5 (776)			67.5 (465)
A490 Bolts, when threads are excluded from shear planes			112.5 (776)			90.0 (621)

*Applies to bolts in holes as limited by Table 8.6. Washers or back-up plates shall be installed over long-slotted holes and the capacity of connections using long-slotted holes shall be determined by load tests in accordance with Chapter F.

a. For ASD method:

  F is given by F'_{nt} in Table 8.10a (U.S. Customary Units) or 8.10b (Metric Units) with applicable safety factor.

b. For LRFD method:

  F is given by F'_{nt} in Table 8.11a (U.S. Customary Units) or 8.11b (Metric Units) with applicable resistance factor.

In Table 8.9, the allowable shear and tension stresses specified for A307, A325, and A490 bolts are approximately the same as those permitted by the AISC[1.148] and the Research Council on Structural Connections for bearing-type connections.[8.47] Slightly smaller allowable shear stresses are used for A449 and A354 Grade BD bolts with threads in the shear planes as compared with A325 and A490 bolts, respectively. Such smaller shear stresses are used because the average ratio of the root area to the gross area of the $\frac{1}{4}$-in. (6.4-mm) and $\frac{3}{8}$-in. (9.5-mm) diameter bolts is 0.585, which is smaller than the average ratio of 0.670 for the $\frac{1}{2}$-in. (12.7-mm) and 1-in. (25.4-mm) diameter bolts. According to Ref. 1.159, these design values provide safety factors ranging from 2.25 to 2.52 against the shear failure of bolts.

Example 8.4   Determine the allowable load for the bolted connection shown in Fig. 8.41. Use four $\frac{1}{2}$-in. diameter A307 bolts with washers under bolt head and nut. The steel sheets are A570 Grade 33 steel ($F_y = 33$ ksi and $F_u = 52$ ksi). Use ASD and LRFD methods. Assume that the dead-to-live load ratio is 1/5 and that the deformation around bolt holes is not a design consideration.

Solution

A.   ASD Method

In the determination of the allowable load, consideration should be given to the following items:

- Shear, spacing, and edge distance in line of stress (Art. 8.4.2.5)
- Tensile strength of connected parts at connection (Art. 8.4.2.6)
- Bearing strength between bolts and connected parts (Art. 8.4.2.7)
- Shear strength in bolts (Art. 8.4.2.8)

1. *Shear, Spacing, and Edge Distance in Line of Stress.* The distance from the center of a standard hole to the nearest edge of an adjacent hole is

$$e_1 = 2 - \frac{d + \frac{1}{16}}{2} = 2 - \frac{\frac{1}{2} + \frac{1}{16}}{2} = 1.72 \text{ in.}$$

The distance from the center of a standard hole to the end of the plate

TABLE 8.10a **(ASD) Nominal Tension Stress, F'_{nt} (ksi), for Bolts Subject to the Combination of Shear and Tension[1.314]**

Description of Bolts	Threads Not Excluded from Shear Planes	Threads Excluded from Shear Planes	Factor of Safety, Ω
A325 Bolts A354 Grade BD Bolts A449 Bolts A490 Bolts	$110–3.6f_v \leq 90$ $122–3.6f_v \leq 101$ $100–3.6f_v \leq 81$ $136–3.6f_v \leq 112.5$	$110–2.8f_v \leq 90$ $122–2.8f_v \leq 101$ $100–2.8f_v \leq 81$ $136–2.8f_v \leq 112.5$	2.0
A307 Bolts, Grade A When $\frac{1}{4}$ in. $\leq d < \frac{1}{2}$ in. When d $\geq \frac{1}{2}$ in.	$52–4f_v \leq 40.5$ $58.5–4f_v \leq 45$		2.25

The shear stress, f_v, shall also satisfy Table 8.9.

TABLE 8.10b **(ASD) Nominal Tension Stress, F'_{nt} (MPa), for Bolts Subject to the Combination of Shear and Tension**[1.314]

Description of Bolts	Threads Not Excluded from Shear Planes	Threads Excluded from Shear Planes	Factor of Safety, Ω
A325 Bolts	$758–25f_v \leq 607$	$758–19f_v \leq 607$	
A354 Grade BD Bolts	$841–25f_v \leq 676$	$841–19f_v \leq 676$	2.0
A449 Bolts	$690–25f_v \leq 552$	$690–19f_v \leq 552$	
A490 Bolts	$938–25f_v \leq 745$	$938–19f_v \leq 745$	

A307 Bolts, Grade A
   When 6.4 mm $\leq d < 12.7$ mm
   When $d \geq 12.7$ mm
	$359–28f_v \leq 276$
	$403–28f_v \leq 310$
			2.25

TABLE 8.11a (LRFD) Nominal Tension Stress, F'_{nt} (ksi), for Bolts Subject to the Combination of Shear and Tension[1.314]

Description of Bolts	Threads Not Excluded from Shear Planes	Threads Excluded from Shear Planes	Resistance Factor, ϕ
A325 Bolts A354 Grade BD Bolts A449 Bolts A490 Bolts	$113-2.4f_v \leq 90$ $127-2.4f_v \leq 101$ $101-2.4f_v \leq 81$ $141-2.4f_v \leq 112.5$	$113-1.9f_v \leq 90$ $127-1.9f_v \leq 101$ $101-1.9f_v \leq 81$ $141-1.9f_v \leq 112.5$	0.75

A307 Bolts, Grade A
    When $\frac{1}{4}$ in. $\leq d < \frac{1}{2}$ in.
    When $d \geq \frac{1}{2}$ in.
	$47-2.4f_v \leq 40.5$
	$52-2.4f_v \leq 45$
			0.75

The shear stress, f_v, shall also satisfy Table 8.9.

TABLE 8.11b (LRFD) Nominal Tension Stress, $F'ei_{nt}$ (MPa), for Bolts Subject to the Combination of Shear and Tension[1.314]

Description of Bolts	Threads Not Excluded from Shear Planes	Threads Excluded from Shear Planes	Resistance Factor, ϕ
A325 Bolts A354 Grade BD Bolts A449 Bolts A490 Bolts	$779-17f_v \leq 621$ $876-17f_v \leq 696$ $696-17f_v \leq 558$ $972-17f_v \leq 776$	$779-13f_v \leq 621$ $876-13f_v \leq 696$ $696-13f_v \leq 558$ $972-13f_v \leq 776$	0.75

A307 Bolts, Grade A
    When 6.4 mm. $\leq d < 12.7$ mm
    When $d \geq 12.7$ mm
	$324-25f_v \leq 279$
	$359-25f_v \leq 310$
			0.75
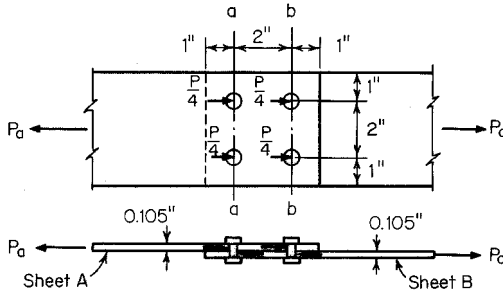
Figure 8.41 Example 8.4.

in the line of stress is

$$e_2 = 1 \text{ in.}$$

Since $e_2 < e_1$, the allowable load should be determined by e_2.

Because $F_u/F_y = 52/33 = 1.58 > 1.08$, according to Eq. (8.45), the allowable shear strength of the connected sheet using four bolts can be computed as

$$P_1 = 4P_n/\Omega = 4(te_2F_u)/2.0$$

$$= 4(0.105 \times 1 \times 52)/2.0 = 10.92 \text{ kips}$$

In addition, some other AISI requirements should be checked on the basis of Sec. E3.1 of the AISI Specification or Art. 8.4.2.5 as follows:

a. Distance between centers of bolt holes

$$2 \text{ in.} > (3d = 1.5 \text{ in.}) \qquad \text{O.K.}$$

b. Distance from center of any standard hole to end of plate

$$1 \text{ in.} > (1\tfrac{1}{2}d = 0.75 \text{ in.}) \qquad \text{O.K.}$$

c. Clear distance between edges of two adjacent holes

$$2 - (\tfrac{1}{2} + \tfrac{1}{16}) = 1.44 \text{ in.} > (2d = 1.0 \text{ in.}) \qquad \text{O.K.}$$

d. Distance between edge of hole and end of plate

$$1 - \frac{\tfrac{1}{2} + \tfrac{1}{16}}{2} = 0.72 \text{ in.} > (d = 0.5 \text{ in.}) \qquad \text{O.K.}$$

2. *Tensile Strength of Steel Sheets.* Based on the AISI design criteria, the allowable tensile strength of the steel sheet can be determined under the following considerations:

a. *Section a–a* (*Sheet A*). Based on Sec. C2 of the Supplement to the 1996 edition of the AISI Specification, the allowable tensile strength can be computed as follows:

(i) For yielding [Eq. (6.2)],

$$T_a = T_n/\Omega_t = A_g F_y/1.67$$

$$= (4.0 \times 0.105)(33)/1.67 = 8.30 \text{ kips}$$

(ii) For fracture away from the connection [Eq. (6.3)],

$$T_a = T_n/\Omega_t = A_n F_u/2.00$$

$$= (4.0 \times 0.105)(52)/2.00 = 10.92 \text{ kips}$$

Use $T_a = 8.30$ kips for the requirement of Sec. C2 of the Specification.

According to Sec. E.3.2(1) of the Supplement to the 1996 edition of the Specification for bolts with washers under bolt head and nut and for a single shear connection ($\Omega = 2.22$), the allowable tensile strength should be determined by Eq. (8.46) as follows:

$$P_a = P_n/\Omega = A_n F_t/\Omega$$

where

$$A_n = [4 - 2(1/2 + 1/16)](0.105) = 0.30 \text{ in.}^2$$

$$F_t = [1.0 - 0.9r + 3r(d/s)]F_u \le F_u$$

in which

$$r = \frac{2P_2/4}{P_2} = \frac{1}{2}$$

$$d/s = 0.5/2.0 = 0.25$$

Therefore,

$$F_t = [1.0 - 0.9(0.5) + 3(0.5)(0.25)](52)$$

$$= 48.1 \text{ ksi} < 52 \text{ ksi O.K.}$$

$$P_a = (0.30)(48.1)/2.22 = 6.50 \text{ kips}$$

Since $P_a < T_a$, use $(P_2)_a = 6.50$ kips for section a–a.
b. *Section b–b* (*Sheet A*). From the above calculation,

$$T_a = 8.30 \text{ kips}$$

$$r = \frac{2P_2/4}{P_2 - 2P_2/4} = 1$$

$$F_t = [1.0 - 0.9(1) + 3(1)(0.25)](52) = 44.2 \text{ ksi} < 52 \text{ ksi O.K.}$$

$$P_a = (0.30)(44.2)/2.22 = 5.97 \text{ kips}$$

Since $P_a < T_a$, use $P_a = 5.97$ kips.
Because at Section b–b, only 50% of the load P acts in sheet A, therefore,

$$\frac{(P_2)_b}{2} = P_a$$

$$(P_2)_b = 2P_a = 2 \times 5.97 = 11.94 \text{ kips} > (P_2)_a$$

Use $P_2 = (P_2)_a = 6.50$ kips
3. *Bearing Strength between Bolts and Steel Sheets.* Because 0.036 in. $<$ $t < \frac{3}{16}$ in. and the connection is a single shear condition, then according to Table 8.7, the allowable bearing strength per bolt is

$$P_{pa} = P_n/\Omega = 3F_u dt/2.22$$

$$= (3)(52)(\tfrac{1}{2})(0.105)/2.22 = 3.69 \text{ kips}$$

The allowable bearing strength for four bolts is

$$P_3 = 4 \times 3.69 = 14.76 \text{ kips}$$

4. *Shear Strength in Bolts.* From Table 8.9, the nominal shear stress for the $\frac{1}{2}$-in. diameter A307 bolts is 27 ksi and the gross area of the bolt is 0.196 in.[2] Therefore, the allowable shear strength for four bolts is

$$P_4 = 4(A_b F_{nv})/\Omega$$

$$= 4(0.196)(27)/2.4 = 8.82 \text{ kips}$$

Comparing P_1, P_2, P_3, and P_4, the allowable load for the given bolted connection is 6.50 kips, which is governed by the tensile strength of sheet A at section $a–a$.

B. LRFD Method

For the LRFD method, the design considerations are the same as for the ASD method. The design strength can be calculated by applying some of the values used for the ASD method.

1. *Shear, Spacing, and Edge Distance in Line of Stress.* Use Eq. (8.45) for $F_u/F_y > 1.08$, the design shear strength of connected sheet using four bolts is

$$(\phi P_n)_1 = 4(0.70)(te_2 F_u) = 4(0.70)(0.105)(1)(52)$$

$$= 15.288 \text{ kips}$$

2. *Tensile Strength of Steel Sheets*
   a. *Section a–a* (*Sheet A*). Based on Sec. C2 of the Supplement to the 1996 edition of the Specification, the design tensile strength of connected sheet is
      (i) For yielding [Eq. (6.2)],

$$\phi_t T_n = (\phi_t)(A_g F_y) = (0.90)(4 \times 0.105)(33) = 12.474 \text{ kips}$$

   (ii) For fracture away from the connection [Eq. (6.3)],

$$\phi_t T_n = \phi_t(A_n F_n) = (0.75)(4 \times 0.105)(52) = 16.38 \text{ kips}$$

   Use $\phi_t T_n = 12.474$ kips for the requirement of Sec. C2 of the Specification.
      On the basis of Sec. E3.2(1) of the Supplement to the 1996 edition of the Specification, the design tensile strength on the net section of sheet A at Section $a–a$ can be computed from Eq. (8.46) as follows:

$$\phi P_n = \phi(A_n F_t)$$

From the ASD method, $A_n = 0.30$ in.^{2} and $F_t = 48.1$ ksi. Therefore,

$$\phi P_n = (0.55)(0.30)(48.1) = 7.937 \text{ kips}$$

Since

$$\phi P_n < \phi_t T_n, \text{ use } (\phi P_n)_a = 7.937 \text{ kips}$$

b. *Section b–b (Sheet A).* From the above calculation,

$$\phi_t T_n = 12.474 \text{ kips}$$

Based on Eq. (8.46), the design tensile strength on the net section of sheet A at Section *b–b* can be computed from the values of A_n and F_t calculated for the ASD method, i.e.,

$$\phi P_n = \phi(A_n F_t) = (0.55)(0.30)(44.2) = 7.293 \text{ kips} < 12.474 \text{ kips}$$

Use $\phi P_n = 7.293$ kips
Because at Section *b–b*, only 50% of the load acts in sheet *A*, therefore, the design tensile strength based on Section *b–b* is

$$(\phi P_n)_b = 2(\phi P_n) = 2(7.293) = 14.586 \text{ kips}$$

Comparing $(\phi P_n)_a$ and $(\phi P_n)_b$, the governing design tensile strength is

$$\phi(P_n)_2 = (\phi P_n)_a = 7.937 \text{ kips}$$

3. *Bearing Strength between Bolts and Steel Sheets.* According to Table 8.7, the design bearing strength between four bolts and the steel sheet is

$$(\phi P_n)_3 = 4(0.60)(3F_u dt) = 4(0.60)(3)(52)(\tfrac{1}{2})(0.105)$$

$$= 19.656 \text{ kips}$$

4. *Shear Strength in Bolts.* Based on Table 8.9, the design shear strength of four bolts is

$$\phi(P_n)_4 = 4(0.65)(A_b F_{nv}) = 4(0.65)(0.196)(27)$$

$$= 13.759 \text{ kips}$$

Comparing the values of $(\phi P_n)_1$, $(\phi P_n)_2$, $(\phi P_n)_3$, and $(\phi P_n)_4$, the controlling design strength is 7.937 kips, which is governed by the tensile strength of sheet *A* at section *a–a*.

The required strength can be computed from Eqs. (3.5a) and (3.5b) for the dead load-to-live load ratio of 1/5.

From Eq. (3.5a),

$$(P_u)_1 = 1.4P_D + P_L = 1.4P_D + 5P_D = 6.4P_D$$

From Eq. (3.5b),

$$(P_u)_2 = 1.2P_D + 1.6P_L = 1.2P_D + 1.6(5P_D) = 9.2P_D$$

$9.2P_D$ controls.

The dead load P_D can be computed as follows:

$$9.2P_D = 7.937 \text{ kips}$$

$$P_D = 0.863 \text{ kips}$$

$$P_L = 5P_D = 4.315 \text{ kips}$$

Total allowable load based on the LRFD method is

$$P_a = P_D + P_L = 5.178 \text{ kips}$$

It can be seen that the LRFD method is more conservative than the ASD method due to the use of a relatively low resistance factor.

Example 8.5   Check the adequacy of the bearing type connection as shown in Fig. 8.42 Use four $\frac{1}{2}$-in. diameter A325 bolts and A606 Grade 50 steel sheets ($F_y = 50$ ksi and $F_u = 70$ ksi). Assume that washers are used under bolt head and nut and that threads are not excluded from shear planes. Use
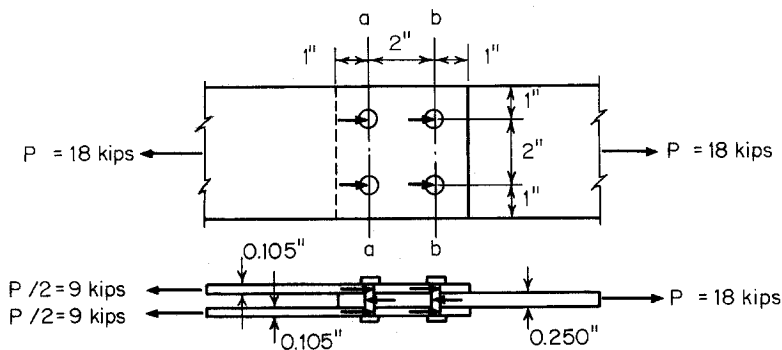

Figure 8.42   Example 8.5.

standard holes and the ASD method. The deformation around bolt holes is not a design consideration.

Solution

1. *Shear, Spacing, and Edge Distance in Line of Stress.* Since the inside sheet is thicker than the sum of the thickness of both outside sheets and the distance from the center of the hole to the end of the plate is the same for inside and outside sheets, the outside sheets will govern the design. For $F_u/F_y = 70/50 = 1.4 > 1.08$, the safety factor to be used for determining the allowable shear strength of the outside sheets is 2.0 according to Art. 8.4.2.5.

   Using Eq. (8.45), the allowable design shear strength of the outside sheet can be computed as follows:

$$P_a = \frac{P_n}{\Omega} = \frac{teF_u}{2.0} = \frac{(0.105)(1)(70)}{2.0}$$

$$= 3.675 \text{ kips/bolt} > \frac{9}{4} = 2.25 \text{ kips/bolt} \qquad \text{O.K.}$$

   In addition, the following requirements should also be checked:
   a. Distance from center of hole to edge of adjacent hole:

$$2 - \frac{\frac{1}{2} + \frac{1}{16}}{2} = 1.72 \text{ in.} > (e = 1.0 \text{ in.}) \qquad \text{O.K.}$$

   b. Distance between centers of bolt holes

$$2 \text{ in.} > (3d = 1.5 \text{ in.}) \qquad \text{O.K.}$$

   c. Distance from center of the hole to end of plate

$$1 \text{ in.} > (1\tfrac{1}{2}d = 0.75 \text{ in.}) \qquad \text{O.K.}$$

   d. Clear distance between edges of two adjacent holes

$$2 - (\tfrac{1}{2} + \tfrac{1}{16}) = 1.44 \text{ in.} > (2d = 1 \text{ in.}) \qquad \text{O.K.}$$

   e. Distance between edge of hole and end of plate

$$1 - \frac{\frac{1}{2} + \frac{1}{16}}{2} = 0.72 > (d = 0.5 \text{ in.}) \qquad \text{O.K.}$$

2. *Tensile Strength of Steel Sheets*
   a. *Section a–a* (*outside sheets*). Based on Sec. C2 of the Supplement to the 1996 edition of the Specification, the allowable tensile strength of the outside sheet can be computed as follows:
      (i) For yielding [Eq. (6.2)],

$$T_a = A_g F_y / 1.67 = (4.0 \times 0.105)(50)/1.67$$
$$= 12.57 \text{ kips} > 9 \text{ kips} \quad \text{O.K.}$$

   (ii) For fracture away from the connection [Eq. (6.3)],

$$T_a = A_n F_u / 2.00$$

   Same as Example 8.4, $A_n = 0.30 \text{ in.}^2$

$$T_a = (0.30)(70)/2.00 = 10.5 \text{ kips} > 9 \text{ kips} \quad \text{O.K.}$$

   Based on Art. 8.4.2.6, the allowable tensile strength of the outside steel sheet for double shear can be calculated from Eq. (8.46) with a safety factor of 2.0:

$$P_a = P_n / \Omega = A_n F_t / 2.0$$

   Same as Example 8.4, $r = 0.5$ and $d/s = 0.25$

$$F_t = [1.0 - 0.9(0.5) + 3(0.5)(0.25)](70)$$
$$= 64.75 \text{ ksi} < 70 \text{ ksi} \quad \text{O.K.}$$
$$P_a = (0.30)(64.75)/2.0 = 9.71 \text{ kips} > 9 \text{ kips} \quad \text{O.K.}$$

   b. *Section b–b* (*outside sheets*). Same as Example 8.4,

   $A_n = 0.30 \text{ in.}^2$

   $r = 1.0, d/s = 0.25$

   $F_t = [1.0 - 0.9(1) + 3(1)(0.25)](70) = 59.5 \text{ ksi} < 70 \text{ ksi} \quad \text{O.K.}$

   $P_a = (0.3)(59.5)/2.0 = 8.93 \text{ kips}$

   The allowable tensile strength of the outside sheet at section *b–b* (50% of the applied load) is

$$P_a = 8.93 \text{ kips} > (9/2 = 4.5 \text{ kips}) \quad \text{O.K.}$$

By inspection, it is not necessary to check the inside sheet for tensile strength because it is thicker than the sum of the thicknesses of both outside sheets,

3. *Bearing Strength between Bolts and Steel Sheets.* From Table 8.7, the allowable bearing strength can be obtained for the inside sheet and the outside sheets which are used in a double shear connection.

   a. For the inside sheet, the allowable bearing strength is

   $$P_a = 3.33F_u dt/\Omega = (3.33)(70)(0.5)(0.25)/2.22$$

   $$= 13.13 \text{ kips/bolt} > (18/4 = 4.5 \text{ kips/bolt}) \qquad \text{O.K.}$$

   b. For the outside sheets, the allowable bearing strength is

   $$P_a = 3F_u dt/\Omega = (3)(70)(0.5)(0.105)/2.22$$

   $$= 4.97 \text{ kips/bolt} > (18/4 = 4.5 \text{ kips/bolt}) \qquad \text{O.K.}$$

4. *Shear Strength in Bolts.* When threads are not excluded from shear planes, the nominal shear stress for A325 bolts can be obtained from Table 8.9, i.e.,

   $$F_{nv} = 54 \text{ ksi}$$

   The allowable shear strength for the double shear condition is

   $$P_a = (2)(A_b F_{nv})/\Omega = (2)(0.196)(54)/2.4$$

   $$= 8.82 \text{ kips/bolts} > (18/4 = 4.5 \text{ kips/bolt}) \qquad \text{O.K.}$$

   On the basis of the above calculations for the ASD method, it can be concluded that the given connection is adequate for the applied load of 18 kips. The same design considerations should be used for the LRFD method.

8.4.3   Additional Design Information on Bolted Connections

The research work reviewed at the beginning of Art. 8.4 dealt mainly with the previous studies conducted in the United States. The design criteria discussed in Art. 8.4.2 were based on the 1996 edition of the AISI Specification with its 1999 Supplement.[1.314,1.333]

In the Canadian Standard,[1.177] the coefficient used for bearing strength is a constant up to $d/t = 10$. When $d/t > 10$, the coefficient decreases depending on the ratio of d/t but not less than 2.0.

During the past few years, additional research work on bolted connections has been conducted by Baehre and Berggren,[1.25,8.4] Stark and Toma,[8.5,8.49,8.50]

Marsh,[8.51] LaBoube,[8.52] Zadanfarrokh and Bryan,[8.71] Carril, Holcomb, La-Boube, and Yu,[6.23–6.25] Seleim and LaBoube,[8.72] Kulak and Wu,[8.73] Wheeler, Clarke, Hancock, and Murray,[8.74] Rogers and Hancock[2.55–2.61] and other researchers. The criteria for the bolted connections and the additional information on mechanical fasteners have been published in Refs. 8.4, 8.7, 8.8, and 8.53. See also other design specifications mentioned in Chap. 1.

8.5   SCREW CONNECTIONS

Screws can provide a rapid and effective means to fasten sheet metal siding and roofing to framing members and to make joints in siding and roofing, as shown in Fig. 8.43. They can also be used in steel framing systems and roof trusses and to fasten drywall panels to metal channels and runners.

Dimensions for standard tapping screws are listed in Ref. 8.2. Figure 8.44 shows some types of self-tapping screws generally used in building construction.[8.2]

8.5.1   AISI Design Criteria

The AISI design provisions for screw connections were developed in 1993.[8.83] The background information on the AISI design criteria is summarized by Pekoz in Ref. 8.54. Based on the ECCS Recommendations and the British Standard with the results of over 3500 tests from the United States, Canada, Sweden, United Kingdom, and the Netherlands, the following requirements were developed as given in Sec. E4 of the 1996 edition of the AISI Specification for the design of screw connections:
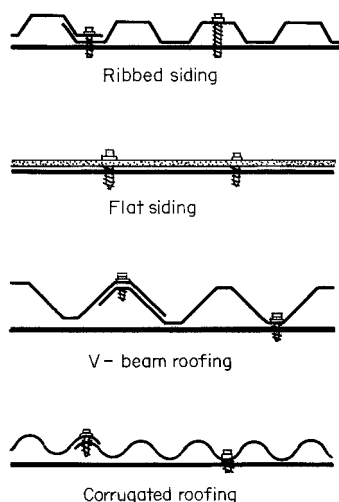

Ribbed siding

Flat siding

V – beam roofing

Corrugated roofing

Figure 8.43   Application of self-tapping screws.[8.1]

Kind of material	Thread-forming								Thread-cutting			Self-drilling	
	Type A	Type B	Type AB	Hex head B	Swage form	Swage form B	Type U	Type 21	Type F	Type L	Type B-F	Drill Kwick	Tapits
Sheet metal 0.015" to 0.050" (steel, brass, alum, monel, etc.)													
Sheet stainless steel 0.015" to 0.050"													
Sheet metal 0.050" to 0.200" (steel, brass, alum, etc.)													
Structural steel 0.200" to 1/2" thick													

Figure 8.44   Types of self-tapping screws. (*Parker-Kalon Corporation.*)[8.3]

E4 Screw Connections

The following notation applies to this section:

d = nominal screw diameter
Ω = 3.0 (ASD)
ϕ = 0.5 (LRFD)
P_{ns} = nominal shear strength per screw
P_{nt} = nominal tension strength per screw
P_{not} = nominal pull-out strength per screw
P_{nov} = nominal pull-over strength per screw
t_1 = thickness of member in contact with the screw head (Figs. 8.46 and 8.47)
t_2 = thickness of member not in contact with the screw head (Figs. 8.46 and 8.47)
F_{u1} = tensile strength of member in contact with screw head
F_{u2} = tensile strength of member not in contact with screw head
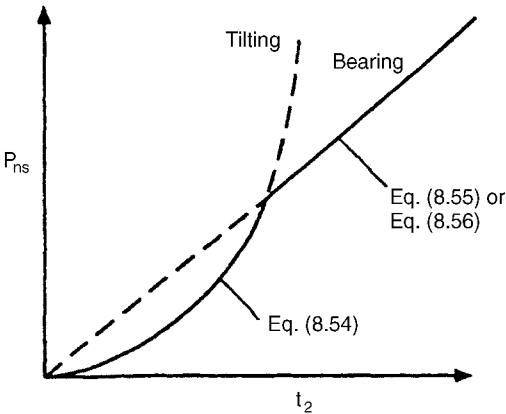
Figure 8.45   Comparison of tilting and bearing.[1.310]
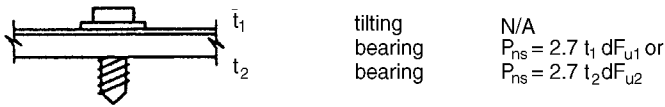
Figure 8.46 Design equations for $t_2/t_1 \geq 2.5$.

All E4 requirements shall apply to self-tapping screws with 0.08 in. (2.03 mm) $\leq d \leq 0.25$ in. (6.35 mm). The screws shall be thread-forming or thread-cutting, with or without a self-drilling point. Alternatively, design values for a particular application shall be permitted to be based on tests according to Section F. For diaphragm applications, Section D5 shall be used.

Screws shall be installed and tightened in accordance with the manufacturer's recommendations.

The nominal tensile strength on the net section of each member joined by a screw connection shall not exceed the member nominal tensile strength from Section C2 or the connection nominal tensile strength from Section E3.2.

E4.1 Minimum Spacing

The distance between the centers of fasteners shall not be less than $3d$.

E4.2 Minimum Edge and End Distance

The distance from the center of a fastener to the edge of any part shall not be less than $3d$. If the connection is subjected to shear force in one direction only, the minimum edge distance shall be $1.5d$ in the direction perpendicular to the force.

E4.3 Shear

E4.3.1 Connection Shear

The nominal shear strength per screw, P_{ns}, shall be determined as follows: For $t_2/t_1 \leq 1.0$, P_{ns} shall be taken as the smallest of

$$P_{ns} = 4.2 \, (t_2^3 d)^{1/2} F_{u2} \tag{8.54}$$

$$P_{ns} = 2.7 \, t_1 \, d \, F_{u1} \tag{8.55}$$

$$P_{ns} = 2.7 \, t_2 \, d \, F_{u2} \tag{8.56}$$

For $t_2/t_1 \geq 2.5$, P_{ns} shall be taken as the smaller of
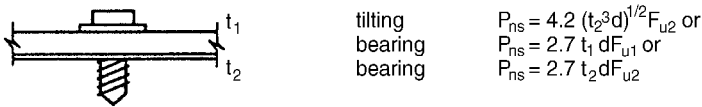
Figure 8.47 Design equations for $t_2/t_1 \leq 1.0$.

$$P_{ns} = 2.7\ t_1\ d\ F_{u1} \tag{8.55}$$

$$P_{ns} = 2.7\ t_2\ d\ F_{u2} \tag{8.56}$$

For $1.0 < t_2/t_1 < 2.5$, P_{ns} shall be determined by linear interpolation between the above two cases.

E4.3.2 Shear in Screws

The nominal strength of the screw shall be determined by test according to Section F1 (a). The nominal shear strength of the screw shall not be less than $1.25P_{ns}$. The factor of safety, Ω, for ASD design and the resistance factor, ϕ, for LRFD design shall be determined according to Section F1(a).

E4.4 Tension

For screws which carry tension, the head of the screw or washer, if a washer is provided, shall have a diameter d_w not less than 5/16 in. (7.94 mm). Washers shall be at least 0.050 in. (1.27 mm) thick.
Ω and ϕ shall be determined according to Section F1.

E4.4.1 Pull-Out

The nominal pull-out strength, p_{not}, shall be calculated as follows:

$$P_{not} = 0.85\ t_c d\ F_{u2} \tag{8.57}$$

where t_c is the lesser of the depth of the penetration and the thickness, t_2.

E4.4.2 Pull-Over

The nominal pull-over strength, P_{nov}, shall be calculated as follows:

$$P_{nov} = 1.5\ t_1 d_w\ F_{u1} \tag{8.58}$$

where d_w is the larger of the screw head diameter or the washer diameter, and shall be taken as not larger than $\frac{1}{2}$ in. (12.7 mm).

E4.4.3 Tension in Screws

The nominal tensile strength, P_{nt}, per screw shall be determined by test according to Section F1 (a). The nominal tensile strength of the screw shall not be less than 1.25 times the lesser of P_{not} and P_{nov}.
Ω and ϕ shall be determined according to Section F1.

For using the above design provisions, the AISI *Commentary* recommends that at least two screws should be used to connect individual elements.[1.310] This provides redundancy against under-torquing, over-torquing, etc., and limits lap shear connection distortion of flat unformed members such as straps. Table 8.12 lists the nominal diameter for the common number designation for

TABLE 8.12   Nominal Diameter for Screws[1.310]

Number Designation	Nominal Diameter for Screws	
	in.	mm
0	0.060	1.52
1	0.073	1.85
2	0.086	2.18
3	0.099	2.51
4	0.112	2.84
5	0.125	3.18
6	0.138	3.51
7	0.151	3.84
8	0.164	4.17
10	0.190	4.83
12	0.216	5.49
$\frac{1}{4}$	0.250	6.35

screws. Reference 8.75 contains (1) screw diameter size guidelines based on total thickness of steel, (2) common screw length, and (3) suggested capacity for screws connecting steel to steel based on Sec. E4 of the AISI Specification.

Screw connections loaded in shear can fail either in one mode or in a combination of several modes. The failure modes include shearing of the screw, edge tearing, tilting and subsequent pull-out of the screw, and bearing failure of the joined materials. Tilting of the screw followed by thread tearing out of the lower sheet reduces the connection shear capacity from that of the typical bearing strength of the connection as shown in Fig. 8.45.[1.310]

With regard to the tilting and bearing failure modes, two cases are considered in the Specification, depending on the ratio of thicknesses of the connected members. If the head of the screw is in contact with the thinner material as shown in Fig. 8.46, tilting is not a design consideration when $t_2/t_1 \geq 2.5$. However, when both members are the same thickness, or when the thicker member is in contact with the screw head as shown in Fig. 8.47, tilting must also be considered when $t_2/t_1 \leq 1.0$. Use linear interpolation for $1.0 < t_2/t_1 < 2.5$.

Screw connections subjected to tension can fail either by pulling out of the screw from the plate (pull-out), or pulling of material over the screw head and the washer (pull-over), or by tension fracture of the screw. For the failure mode of pull-out, Eq. (8.57) was derived on the basis of the modified European Recommendations and the results of a large number of tests. For the limit state of pull-over, Eq. (8.58) was derived on the basis of the modified British Standard and the results of a series of tests. The statistic data on these tests are presented by Pekoz in Ref. 8.54.

8.5.2 Additional Information on Screw Connections

During recent years, research work on screw connections has been conducted by Xu,[8.76] Daudet and LaBoube,[8.77] Serrette and Lopez,[8.78] Rogers and Hancock,[2.57,2.59] Kreiner and Ellifritt,[8.80] Anderson and Kelley,[8.81] Sokol, LaBoube, and Yu,[8.82] and other researchers.

8.6 OTHER FASTENERS

The 1996 edition of the AISI Specification provides design provisions only for welded connections (Art. 8.3), bolted connections (Art. 8.4), and screw connections (Art. 8.5). There are a number of other types of fasteners which are used in cold-formed steel construction. The following provides a brief discussion on other fasteners.

8.6.1 Rivets

Blind rivets and tubular rivets are often used in cold-formed steel construction. They are used to simplify assembly, improve appearance, and reduce the cost of connection.

***8.6.1.1 Blind Rivets*[8.3]**   Based on the method of setting, blind rivets can be classified into pull-stem rivets, explosive rivets, and drive-pin rivets.

1. *Pull-stem Rivets.* As shown in Fig. 8.48, pull-stem rivets can be subdivided into three types:
   a. Self-plugging rivets. The stem is pulled into but not through the rivet body and the projecting end is removed in a separate operation.
   b. Pull-through rivets. A mandrel or stem is pulled completely out, leaving a hollow rivet.
   c. Crimped-mandrel rivets. A part of the mandrel remains as a plug in the rivet body.
2. *Explosive Rivets.* Explosive rivets have a chemical charge in the body. The blind end is expanded by applying heat to the rivet head.
3. *Drive-Pin Rivets.* Drive-pin rivets are two-piece rivets consisting of a rivet body and a separate pin installed from the head side of the rivet. The pin, which can be driven into the rivet body by hammer, flares out the slotted ends on the blind side.

In the design of a joint using blind rivets, the following general recommendations may be used:
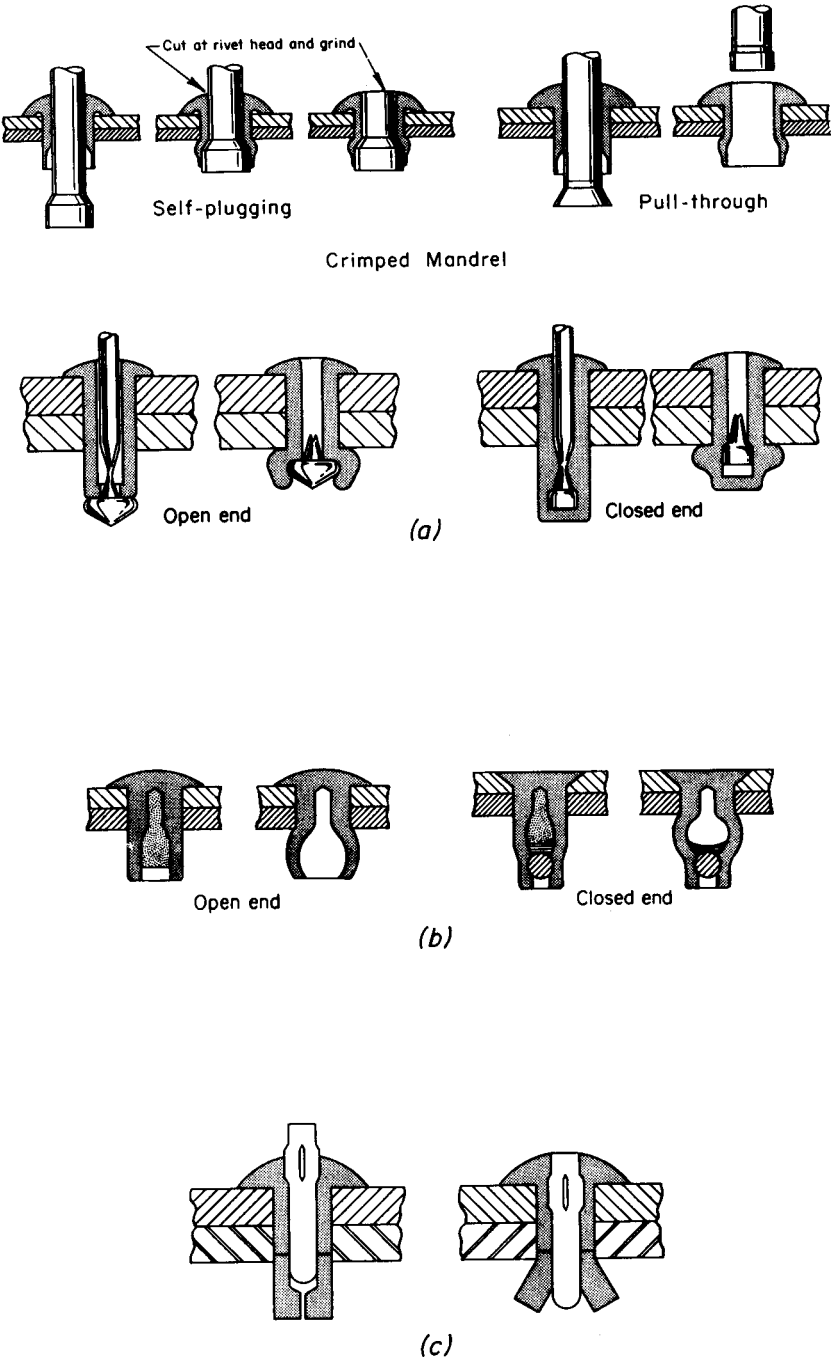
Figure 8.48   Types of blind rivets and methods of setting.[8.3] (*a*) Pull-stem rivets. (*b*) Explosive rivets. (*c*) Drive-pin rivets.

1. *Edge Distance.* The average edge distance is two times the diameter of the rivet. For lightly loaded joints, the distance can be decreased to $1\frac{1}{2}$ diameters; but for heavily loaded joints, an edge distance of 3 diameters may be needed.
2. *Spacing.* The spacing of rivets should be three times the diameter of the rivet. It may be desirable to decrease or increase the spacing depending upon the nature of the load.
3. *Tension and Bearing Stresses.* The tension stress on the net section and the bearing stress may be determined by the method used for bolted connections.
4. *Shear Stress.* The shear stress on rivets should be obtained from the manufacturer.

8.6.1.2 Tubular Rivets[8.3] Tubular rivets are also often used to fasten sheet metal. The strength in shear or compression is comparable to that of solid rivets. Nominal body diameters range from 0.032 to 0.310 in. (0.8 to 7.9 mm). The corresponding minimum lengths range from $\frac{1}{32}$ to $\frac{1}{4}$ in. (0.8 to 6.4 mm). When tubular rivets are used to join heavy- and thin-gage stock, the rivet head should be on the side of the thin sheet.

8.6.2 Press-Joints and Rosette-Joints

8.6.2.1 Press-Joints Press joining is a relatively new technique for joining cold-formed steel sections. It has many advantages over conventional connection techniques.[8.64,8.65] The joint is formed using the parent metal of the sections to be connected. The tools used to form a press-joint consist of a male and female punch and die. Figure 8.49 shows the sequence of forming a press-joint.

Press joining can be used for fabrication of beams, studs, trusses, and other structural systems. The structural strength and behavior of press-joints and fabricated components and systems have been studied recently by Pedreschi, Sinha, Davies, and Lennon at Edinburgh University.[8.64,8.65,8.84–8.86]
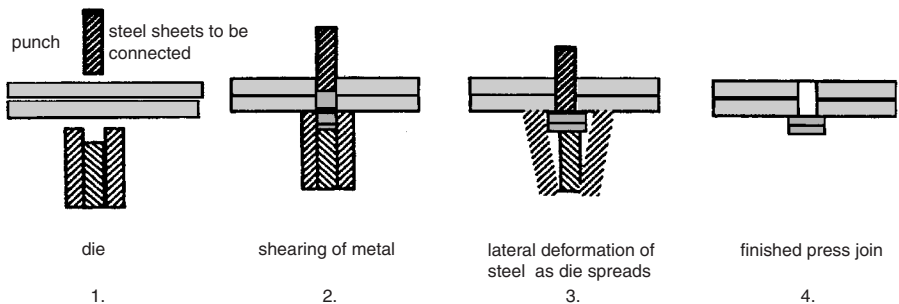
Figure 8.49 Sequence of forming press-joint.[8.65]

8.6.2.2   Rosette-Joints   Rosette-joining (Fig. 8.50) is also a new automated approach for fabricating cold-formed steel components such as stud wall panels and roof trusses.[8.87,8.88] It is formed in pairs between prefabricated holes in one jointed part and collared holes in the other part. The joining process is shown in Fig. 8.51.

During recent years, the strength and behavior of the Rosette-joints and the fabricated thin-walled sections have been investigated by Makelainen, Kesti, Kaitila, and Sahramaa at the Helsinki University of Technology.[8.87] The tests were compared with the values calculated according to the 1996 edition of the AISI Specification supported by a distortional buckling analysis on the basis of the Australian/New Zealand Standard.

8.7   RUPTURE FAILURE OF CONNECTIONS

In the design of connections, consideration should also be given to the rupture strength of the connection along a plane through the fasteners. In 1999, the AISI Specification was revised to include the following provisions in Sec. E5 of the Supplement for rupture strength.[1.333]

E5 Rupture

E5.1 Shear Rupture

At beam-end connections, where one or more flanges are coped and failure might occur along a plane through the fasteners, the nominal shear strength, V_n, shall be calculated as follows:

$$V_n = 0.6F_u A_{wn} \qquad (8.59)$$

$$\Omega = 2.0 \text{ (ASD)}$$

$$\phi = 0.75 \text{ (LRFD)}$$
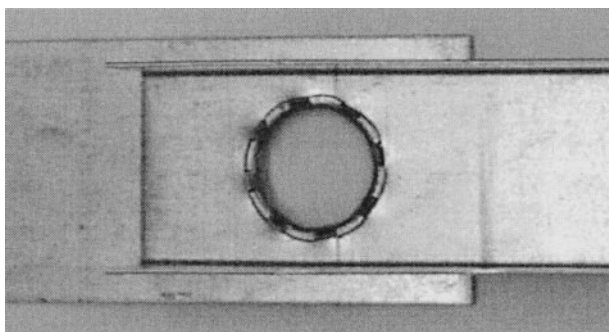
Figure 8.50   Rosette-joint.[8.87]
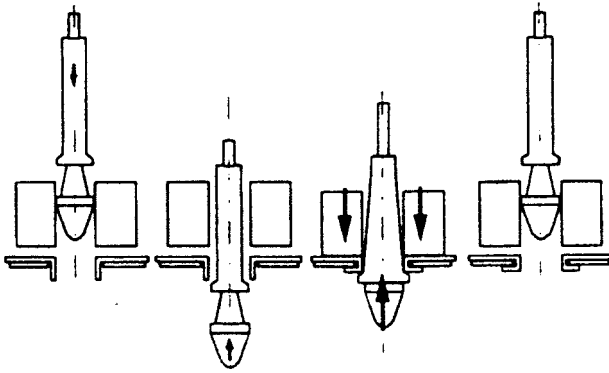
Figure 8.51   Rosette-joining process.[8.87]

where

$$A_{wn} = (h_{wc} - n_h d_h)t \qquad (8.59)$$

h_{wc} = coped flat web depth
n_h = number of holes in the critical plane
d_h = hole diameter
F_u = tensile strength of the connected part as specified in Section A3.1 or A3.3.2
t = thickness of coped web

E5.2 Tension Rupture

The nominal tensile rupture strength along a path in the affected elements of connected members shall be determined by Section E2.7 or E3.2 for welded or bolted connections, respectively.

E5.3 Block Shear Rupture

The nominal block shear rupture design strength, R_n, shall be determined as follows:
(a) When $F_u A_{nt} \geq 0.6 F_u A_{nv}$

$$R_n = 0.6 F_y A_{gv} + F_u A_{nt} \qquad (8.61)$$

(b) When $F_u A_{nt} < 0.6 F_u A_{nv}$

$$R_n = 0.6 F_u A_{nv} + F_y A_{gt} \qquad (8.62)$$

For bolted connections:

$$\Omega = 2.22 \text{ (ASD)}$$

$$\phi = 0.65 \text{ (LRFD)}$$

For welded connections:

$$\Omega = 2.50 \text{ (ASD)}$$

$$\phi = 0.60 \text{ (LRFD)}$$

where A_{gv} = gross area subject to shear
$\quad\quad A_{gt}$ = gross area subject to tension
$\quad\quad A_{nv}$ = net area subject to shear
$\quad\quad A_{nt}$ = net area subject to tension

For the AISI design provisions, Eq. (8.59) deals with the tearing failure mode along the perimeter of the holes as shown in Fig. 8.52. This design criterion was developed on the basis of the tests conducted by Birkemoe and Gilmor.[8.89] Additional information can be found in Refs. 8.90 and 8.91.

In some connections, a block of materials at the end of the member may tear out as shown in Fig. 8.53. The design equations are based on the assumption that one of the failure paths fractures and the other yields. In Eqs. (8.61) and (8.62), the gross area is used for yielding and the net area is used for fracture. The shear yield stress is taken as $0.6F_y$ and the shear strength is taken as $0.6F_u$.

8.8 I- OR BOX-SHAPED COMPRESSION MEMBERS MADE BY CONNECTING TWO C-SECTIONS

I-sections fabricated by connecting two C-sections back to back are often used as compression members in cold-formed steel construction. In order to function as a single compression member, the C-sections should be connected at a close enough spacing to prevent buckling of individual C-sections about their own axes parallel to the web at a load equal to or smaller than the buckling load of the entire section. For this reason, Sec. D1.1(a) of the AISI Specification limits the maximum longitudinal spacing of connections to

$$s_{max} = \frac{Lr_{cy}}{2r_I} \tag{8.63}$$
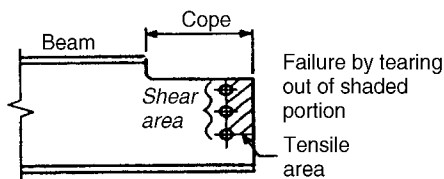
Figure 8.52   Shear rupture of beam-end connection.[1.310]
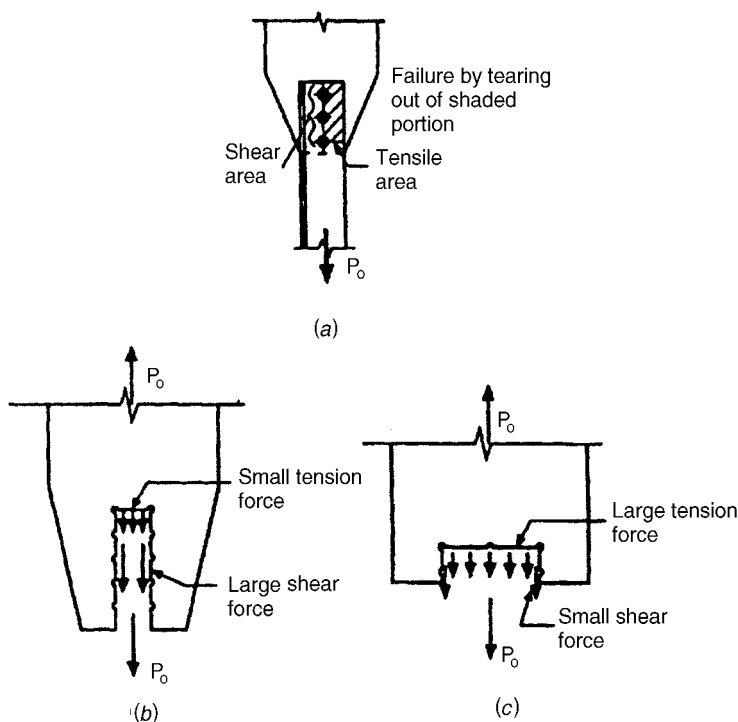
Figure 8.53   Block shear rupture in tension.[1.310]

where s_{max} = maximum permissible longitudinal spacing of connectors
L = unbraced length of compression member
r_I = radius of gyration of I-section about the axis perpendicular to the direction in which buckling would occur for the given conditions of end support and intermediate bracing
r_{cy} = radius of gyration of one C-section about its centroidal axis parallel to the web.

This requirement ensures that the slenderness ratio of the individual C-section between connectors is less than or equal to one-half of the slenderness ratio of the entire compression member in the case that any one of the connectors may be loosened or ineffective.

Box-shaped sections made by connecting two C-sections tip to tip also often found in use in cold-formed steel structures due to the relatively large torsional rigidities and their favorable radius of gyration about both principal axes. The foregoing requirement for maximum spacing of connectors for I-shaped members is also applicable to box-type compression members made by C-sections tip to tip, even though it is not specified in the AISI Specification.[1.310]

8.9 I-BEAMS MADE BY CONNECTING TWO C-SECTIONS

In cold-formed steel construction, I-beams are often fabricated from two C-sections back to back by means of two rows of connectors located close to both flanges. For this type of I-beam, Sec. D1.1(b) of the AISI Specification includes the following limitations on the maximum longitudinal spacing of connectors:

$$s_{max} = \frac{L}{6} \leq \frac{2gT_s}{mq} \tag{8.64}$$

where L = span of beam
   g = vertical distance between rows of connectors nearest to the top and bottom flanges
   T_s = design strength of connectors in tension
   q = design load on the beam for spacing of connectors (use nominal loads for ASD, factored loads for LRFD)
   m = distance from the shear center of one C-section to the midplane of its web

For simple C-sections without stiffening lips at the outer edges,*

$$m = \frac{w_f^2}{2w_f + d/3} \tag{8.65}$$

For C-sections with stiffening lips at the outer edges,*

$$m = \frac{w_f dt}{4I_x}\left[w_f d + 2D\left(d - \frac{4D^2}{3d}\right)\right] \tag{8.66}$$

where w_f = projection of flanges from inside face of web (For C-sections with flanges of unequal widths, w_f shall be taken as the width of the wider flange)
   d = depth of C-section or beam
   t = thickness of C-section
   D = overall depth of lip
   I_x = moment of inertia of one C-section about its centroid axis normal to the web

  The maximum spacing of connectors required by Eq. (8.64) is based on the fact that the shear center is neither coincident with nor located in the

---

* See Appendix B for the location of the shear center.

plane of the web; and that when a load Q is applied in the plane of the web, it produces a twisting moment Qm about its shear center, as shown in Fig. 8.54. The tensile force of the top connector T_s can then be computed from the equality of the twisting moment Qm and the resisting moment $T_s g$, that is,

$$Qm = T_s g \tag{8.67}$$

or

$$T_s = \frac{Qm}{g} \tag{8.68}$$

Considering that q is the intensity of the load and that s is the spacing of connectors, then the applied load is $Q = qs/2$. The maximum spacing s_{max} in Eq. (8.64) can easily be obtained by substituting the above value of Q into Eq. (8.68).

The determination of the load intensity q is based upon the type of loading applied to the beam.

1. For a uniformly distributed load,

$$q = 3w' \tag{8.69}$$

considering the fact of possible uneven loads.
2. For concentrated load or reaction,

$$q = \frac{P}{N} \tag{8.70}$$

where w' = uniformly distributed load based on nominal loads for ASD, factored loads for LRFD
P = concentrated load or reaction based on nominal loads for ASD, factored loads for LRFD
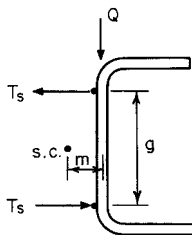
Figure 8.54   Tensile force developed in the top connector for C-section.

$$N = \text{length of bearing}$$

If the length of bearing of a concentrated load or reaction is smaller than the spacing of the connectors ($N < s$), the required design strength of the connectors closest to the load or reaction is

$$T_s = \frac{P_s m}{2g} \tag{8.71}$$

where P_s is a concentrated load or reaction based on nominal loads for ASD, factored loads for LRFD.

It should be noted that the required maximum spacing of connectors s_{max} depends upon the intensity of the load applied at the connection. If a uniform spacing of connectors is used over the entire length of the beam, it should be determined at the point of maximum load intensity. If this procedure results in uneconomically close spacing, either one of the following methods may be adopted:[1.314]

1. The connector spacing may be varied along the beam length according to the variation of the load intensity.
2. Reinforcing cover plates may be welded to the flanges at points where concentrated loads occur. The strength in shear of the connectors joining these plates to the flanges shall then be used for T_s, and the depth of the beam can be used as g.

In addition to the above considerations on the required strength of connectors, the spacing of connectors should not be so great as to cause excessive distortion between connectors by separation along the top of flange. In view of the fact that C-sections are connected back to back and are continuously in contact along the bottom flange, a maximum spacing of $L/3$ may be used. Considering the possibility that one connector may be defective, a maximum spacing of $s_{max} = L/6$ is required in the AISI Specification.

Example 8.6 Determine the maximum longitudinal spacing of welds for joining two $6 \times 2\frac{1}{2} \times 0.105$ in. channels tip to tip to make a box-shaped section (Fig. 8.55) for use as a simply supported column member. Assume that the column length is 10 ft.

Solution. Using the method described in Chaps. 3 to 5, the radius of gyration of the single-channel section ($6 \times 2\frac{1}{2} \times 0.105$ in.) about the y-axis is

$$r_{cy} = 0.900 \text{ in.}$$

The radii of gyration of the box-shaped section ($6 \times 5 \times 0.105$ in.) about the x- and y-axes are
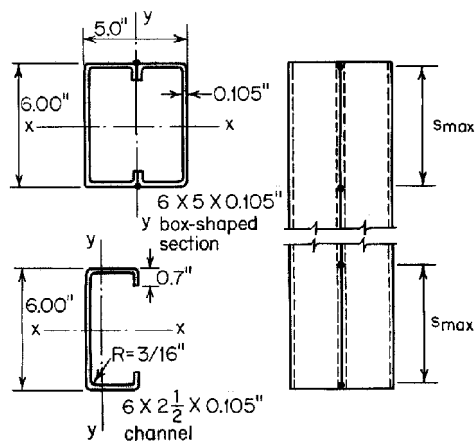
Figure 8.55 Example 8.6.

$$r_x = 2.35 \text{ in.}$$
$$r_y = 1.95 \text{ in.}$$

Since $r_y < r_x$, the governing radius of gyration for the box-shaped section is $r = 1.95$ in. Based on Eq. (8.63), the maximum longitudinal spacing of welds is

$$s_{\max} = \frac{Lr_{cy}}{2r} = \frac{(10 \times 12)(0.900)}{2 \times 1.95} = 27.7 \text{ in.}$$

Use 27 in. as the maximum spacing of welds.

Example 8.7   Use the ASD and LRFD methods to determine the maximum longitudinal spacing of $\frac{1}{4}$-in. A307 bolts joining two $6 \times 1\frac{1}{2} \times 0.105$ in. C-sections to form an I-section used as a beam. Assume that the span length of the beam is 12 ft, the applied uniform load is 0.4 kips/ft, and the length of bearing is 3.5 in. (Fig. 8.56). Assume that the dead-to-live load ratio is $\frac{1}{3}$.

Solution

A. ASD Method

1. *Spacing of Bolts between End Supports.* The maximum permissible longitudinal spacing of $\frac{1}{4}$-in. bolts can be determined by Eq. (8.64) as follows:

$$s_{\max} = \frac{L}{6} = \frac{12 \times 12}{6} = 24 \text{ in.}$$
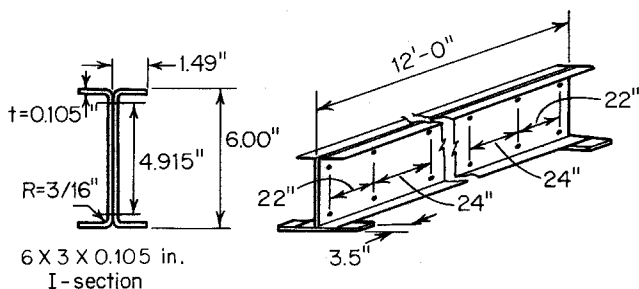
Figure 8.56   Example 8.7.

and

$$s_{\max} \leq \frac{2gT_s}{mq}$$

Using

$$g = d - 2(t + R) - 2(\tfrac{1}{4})$$

$$= 6.0 - 2(0.105 + 0.1875) - 0.5 = 4.915 \text{ in.}$$

From Table 8.9,

$$T_s = \text{(gross area)(nominal tensile stress of bolts)}/\Omega$$

$$= 0.049 \times 40.5/2.25 = 0.88 \text{ kips}$$

From Eq. (8.65),

$$m = \frac{(1.49 - 0.105)^2}{2(1.49 - 0.105) + \tfrac{6}{3}} = 0.402 \text{ in.}$$

From Eq. (8.69),

$$q = \frac{3 \times 0.40}{12} = 0.10 \text{ kips/in.}$$

Then based on Eq. (8.64),

$$s_{\max} \leq \frac{2(4.915)(0.88)}{0.402(0.1)} = 215 \text{ in.}$$

Since the maximum longitudinal spacing determined by $L/6$ will govern

the design, use 24 in. as the maximum spacing of bolts between end supports.

2. *Spacing of Bolts at End Supports.* The maximum spacing of bolts at the end supports can be computed as follows:

$$s_{max} \leq \frac{2gT_s}{mq}$$

in which

$$q = \frac{P}{N} = \frac{6 \times 0.4}{3.5} = 0.686 \text{ kips/in.}$$

and g, T_s, and m are the same as those used in item 1 above. Then

$$s_{max} \leq \frac{2(4.915)(0.88)}{0.402(0.686)} = 31.4 \text{ in.}$$

Use $s_{max} = 24$ in.

Since $N < s_{max}$, from Eq. (8.71) the required design strength of bolts closest to the reaction is

$$T_s = \frac{P_s m}{2g} = \frac{0.4(6)(0.402)}{2(4.915)}$$

$$= 0.098 \text{ kips} < 0.88 \text{ kips}$$

$$\text{(furnished design strength of bolts)} \qquad \text{O.K.}$$

B. LRFD Method

1. *Spacing of Bolts between End Supports.* From Item A.1, the maximum spacing of bolts is

$$s_{max} = \frac{L}{6} = 24 \text{ in.}$$

and

$$s_{max} \leq \frac{2gT_s}{mq}$$

where

$$g = 4.915 \text{ in.}$$

From Table 8.9,

$$T_s = \phi T_n = (0.75)(A_g F_{nt})$$
$$= (0.75)(0.049 \times 40.5) = 1.49 \text{ kips}$$

From Eq. (8.65),

$$m = 0.402 \text{ in.}$$

From Eq. (8.69),

$$q = 3(1.2\, w'_D + 1.6\, w'_L)/12$$
$$= 3(1.2 \times 0.1 + 1.6 \times 0.3)/12 = 0.15 \text{ kips/in.}$$

Based on Eq. (8.64),

$$s_{max} \leq \frac{2(4.915)(1.49)}{(0.402)(0.15)} = 242.9 \text{ in.}$$

use $s_{max} = 24$ in.

2. *Spacing of Bolts at End Supports.* The maximum spacing of bolts at end supports can be computed as follows:

$$s_{max} \leq \frac{2g T_s}{mq}$$

in which

$$q = \frac{P}{N}$$
$$P = 6(1.2 \times 0.1 + 1.6 \times 0.3) = 3.6 \text{ kips}$$
$$q = \frac{3.6}{3.5} = 1.029 \text{ kips/in.}$$
$$s_{max} \leq \frac{2(4.915)(1.49)}{(0.402)(1.029)} = 35.4 \text{ in.}$$

Use

$$s_{max} = 24 \text{ in.}$$

Since $N < s_{max}$, from Eq. (8.71), the required design strength of bolts closest to the reaction is

$$T_s = \frac{P_s m}{2g} = \frac{3.6(0.402)}{2(4.915)}$$

$$= 0.147 \text{ kips} < 1.49 \text{ kips (furnished design strength)} \qquad \text{O.K.}$$

8.10 SPACING OF CONNECTIONS IN COMPRESSION ELEMENTS

When compression elements are joined to other sections by connections such as shown in Fig. 8.57, the connectors must be spaced close enough to provide structural integrity of the composite section. If the connectors are properly spaced, the portion of the compression elements between rows of connections can be designed as stiffened compression elements.

In the design of connections in compression elements, consideration should be given to:

1. The required shear strength
2. Column buckling behavior of compression elements between connections
3. Possible buckling of unstiffened elements between the center of the connection lines and the free edge

For this reason, Sec. D1.2 of the AISI Specification contains the following design criteria:

The spacing s in the line of stress of welds, rivets, or bolts connecting a cover plate, sheet, or a nonintegral stiffener in compression to another element shall not exceed
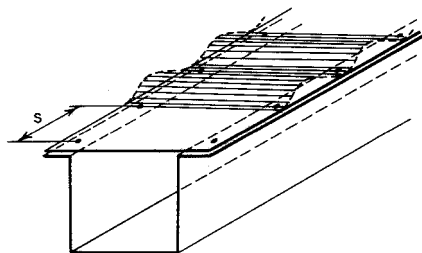
Figure 8.57 Spacing of connectors in composite section.[1.161]

1. that which is required to transmit the shear between the connected parts on the basis of the design strength per connection specified elsewhere herein; nor
2. $1.16t\sqrt{(E/f_c)}$, where t is the thickness of the cover plate or sheet, and f_c is the stress at design load in the cover plate or sheet; nor
3. three times the flat width, w, of the narrowest unstiffened compression element tributary to the connections, but need not be less than $1.11t\sqrt{(E/F_y)}$ if $w/t < 0.50\sqrt{(E/F_y)}$, or $1.33t\sqrt{(E/F_y)}$ if $w/t \geq 0.50\sqrt{(E/F_y)}$, unless closer spacing is required by 1 or 2 above.

In the case of intermittent fillet welds parallel to the direction of stress, the spacing shall be taken as the clear distance between welds, plus one-half inch (12.7 mm). In all other cases, the spacing shall be taken as the center-to-center distance between connections.

Exception: The requirements of this Section do not apply to cover sheets which act only as sheathing material and are not considered as load-carrying elements.

According to item 1, the spacing of connectors for the required shear strength is

$$s = \frac{(\text{total shear strengths of connectors})(I)}{VQ} \tag{8.72}$$

where s = spacing of connectors, in.
      I = moment of inertia of section, in.^{4}
     V = total shear force, kips
     Q = static moment of compression element being connected about neutral axis, in.^{3}

The requirement of item 2 is based on the following Euler formula for column buckling:

$$\sigma_{cr} = \frac{\pi^2 E}{(KL/r)^2} \tag{8.73}$$

by substituting $\sigma_{cr} = 1.67f_c$, $K = 0.6$, $L = s$, and $r = t/\sqrt{12}$. This provision is conservative because the length is taken as the center distance instead of the clear distance between connections, and the coefficient K is taken as 0.6 instead of 0.5, which is the theoretical value for a column with fixed end supports.

The requirement of item 3 is to ensure the spacing of connections close enough to prevent the possible buckling of unstiffened elements.

Additional information can be found in Refs. 8.60–8.62 and 8.92–8.94.

Example 8.8   Use the ASD method to determine the required spacing of spot welds for the compression member made of two channels and two sheets (0.105 in. in thickness), as shown in Fig. 8.58. Assume that the member will carry an axial load of 45 kips based on the yield point of 33 ksi and an unbraced length of 14 ft.

Solution.   Using a general rule, the following sectional properties for the combined section can be computed:

$$A = 3.686 \text{ in.}^2$$

$$I_x = 26.04 \text{ in.}^4$$

$$I_y = 32.30 \text{ in.}^4$$

$$r_x = 2.65 \text{ in.}$$

$$r_y = 2.96 \text{ in.}$$

The spacing of spot welds connecting the steel sheets to channel sections should be determined on the basis of the following considerations:

1. *Required Spacing Based on Shear Strength.* Even though the primary function of a compression member is to carry an axial load, as a general practice, built-up compression members should be capable of resisting a shear force of 2% of the applied axial load, that is,

$$V = 0.02(45) = 0.9 \text{ kips}$$

   If the shear force is applied in the y direction, then the longitudinal shear stress in line a–a is

$$vt = \frac{VQ_x}{I_x}$$
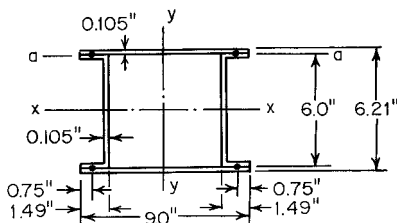
Figure 8.58   Example 8.8

Since

$$s(vt) = s\left(\frac{VQ_x}{I_x}\right) = 2 \times (\text{shear strength per spot})$$

then

$$s = \frac{2 \times (\text{shear strength per spot}) \times I_x}{VQ_x}$$

$$= \frac{2(2.10)(26.04)}{0.9(9 \times 0.105)(3.0 + 0.105/2)} = 42.1 \text{ in.}$$

In the above calculation, the shear strength of spot welds is obtained from Eq. (8.34a) using a safety factor of 2.50.

If the shear force is applied in the x direction, then the shear stress is

$$vt = \frac{VQ_y}{I_y}$$

and

$$s = \frac{2 \times (\text{shear strength per spot}) \times I_y}{VQ_y}$$

$$= \frac{2(2.10)(32.30)}{0.9[(6.0 \times 0.105 \times 3.0625) + (2 \times 1.385 \times 0.105 \times 3.808)]}$$

$$= 49.6 \text{ in.}$$

2. *Required Spacing Based on Column Buckling of Individual Steel Sheets Subjected to Compression.* Based on the AISI requirements, the maximum spacing of welds is

$$s = 1.16t\sqrt{E/f_c}$$

in which

$$f_c = \frac{P}{A} = \frac{45.0}{3.686} = 12.2 \text{ ksi}$$

Then

$$s = 1.16(0.105)\sqrt{29,500/12.2} = 6.0 \text{ in.}$$

3. *Required Spacing Based on Possible Buckling of Unstiffened Elements*

$$s = 3w = 3 \times 0.75 = 2.25 \text{ in.}$$

However, based on Item (3) of the AISI requirements,

$$w/t = 0.75/0.105 = 7.14$$
$$0.50\sqrt{E/F_y} = 0.50\sqrt{29,500/33} = 14.95$$

Since $w/t < 0.50\sqrt{E/F_y}$, the required spacing determined above need not be less than the following value:

$$1.11t\sqrt{E/F_y} = 1.11(0.105)\sqrt{29,500/33} = 3.48 \text{ in.}$$

Comparing the required spacings computed in items 1, 2, and 3, a spacing of 3.5 in. may be used for the built-up section.

If the LRFD method is used in design, the shear force applied to the member should be computed by using the factored loads and the design shear strength should be determined by ϕP_n.

9 Steel Shear Diaphragms and Shell Roof Structures

9.1 GENERAL REMARKS

During the past several decades a large number of research projects conducted throughout the world have concentrated on the investigation of the structural behavior not only of individual cold-formed steel components but also of various structural systems. Shear diaphragms and shell roof structures (including folded plate and hyperbolic parabolid roofs) are some examples of the structural systems studied in the past.

As a result of the successful studies of shear diaphragms and shell roof structures accompanied by the development of new steel products and fabrication techniques, the applications of steel structural assemblies in building construction have been increased rapidly.

In this chapter the research work and the design methods for the use of shear diaphragms and shell roof structures are briefly discussed on the basis of the available information. For details, the reader is referred to the related references.

9.2 STEEL SHEAR DIAPHRAGMS

9.2.1 Introduction

In building construction it has been a common practice to provide a separate bracing system to resist horizontal loads due to wind load, blast force, or earthquake. However, steel floor and roof panels (Fig. 1.11), with or without concrete fill, are capable of resisting horizontal loads in addition to the beam strength for gravity loads if they are adequately interconnected to each other and to the supporting frame.[1.6,9.1,9.2] The effective use of steel floor and roof panels can therefore eliminate separate bracing systems and result in a reduction of building costs (Fig. 9.1).

For the same reason, wall panels can provide not only enclosure surfaces and support normal loads, but they can also provide diaphragm action in their own planes.

In addition to the utilization of diaphragm action, steel panels used in floor, roof, and wall construction can be used to prevent the lateral buckling of
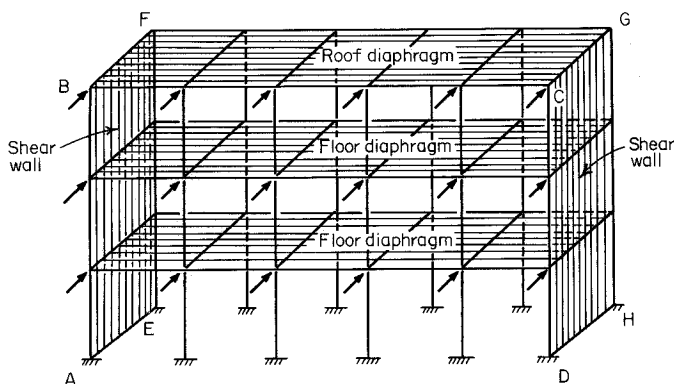
NOTE: Wall panels or other bracing system in planes ABCD and
EFGH are not shown.

Figure 9.1   Shear diaphragms.

beams and the overall buckling of columns.[4.115–4.120] Previous studies made by Winter have shown that even relatively flexible diaphragm systems can provide sufficient horizontal support to prevent the lateral buckling of beams in floor and roof construction.[4.111] The load-carrying capacities of columns can also be increased considerably if they are continuously braced with steel diaphragms.[4.116]

9.2.2   Research on Shear Diaphragms

Because the structural performance of steel diaphragms usually depends on the sectional configuration of panels, the type and arrangement of connections, the strength and thickness of the material, span length, loading function, and concrete fill, the mathematical analysis of shear diaphragms is complex. At the present time, the shear strength and the stiffness of diaphragm panels can be determined either by tests or by analytical procedures.

Since 1947 numerous diaphragm tests of cold-formed steel panels have been conducted and evaluated by a number of researchers and engineers. The diaphragm tests conducted in the United States during the period of 1947 through 1960 were summarized by Nilson in Ref. 9.2. Those tests were primarily sponsored by individual companies for the purpose of developing design data for the diaphragm action of their specific panel products. The total thickness of the panels tested generally range from 0.04 to 0.108 in. (1 to 2.8 mm). Design information based on those tests has been made available from individual companies producing such panels.

In 1962 a research project was initiated at Cornell University under the sponsorship of the AISI to study the performance of shear diaphragms constructed of corrugated and ribbed deck sections of thinner materials, from

0.017 to 0.034 in. (0.4 to 0.9 mm) in total thickness. The results of diaphragm tests conducted by Luttrell and Apparao under the direction of George Winter were summarized in Refs. 9.3, 9.4, and 9.5. Recommendations on the design and testing of shear diaphragms were presented in the AISI publication, "Design of Light Gage Steel Diaphragms," which was issued by the institute in 1967.[9.6]

Since 1967 additional experimental and analytical studies of steel shear diaphragms have been conducted throughout the world. In the United States, research projects on this subject have been performed by Nilson, Ammar, and Atrek,[9.7–9.9] Luttrell, Ellifritt, and Huang,[9.10–9.13] Easley and McFarland,[9.14–9.16] Miller,[9.17] Libove, Wu, and Hussain,[9.18–9.21] Chern and Jorgenson,[9.22] Liedtke and Sherman,[9.23] Fisher, Johnson, and LaBoube,[9.24–9.26] Jankowski and Sherman,[9.90] Heagler,[9.91] Luttrell,[9.92] and others. The research programs that have been carried out in Canada include the work of Ha, Chockalingam, Fazio, and El-Hakim,[9.27–9.30] and Abdel-Sayed.[9.31]

In Europe, the primary research projects on steel shear diaphragms have been conducted by Bryan, Davies, and Lawson.[9.32–9.38] The utilization of the shear diaphragm action of steel panels in framed buildings has been well illustrated in Davies and Bryan's book on stressed skin diaphragm design.[9.39] In addition, studies of tall buildings using diaphragms were reported by El-Dakhakhni in Refs. 9.40 and 9.41.

More recently, shear diaphragms have been studied by Caccese, Elgaaly, and Chen,[9.96] Kian and Pekoz,[9.97] Miller and Pekoz,[9.98] Easterling and Porter,[9.99] Serrette and Ogunfunmi,[9.100] Smith and Vance,[9.101] Elgaaly and Liu,[9.102] Lucas, Al-Bermani, and Kitipornchai,[9.103,9.104] Elgaaly,[9.105] and others. References 1.269 and 9.106 provide additional design information on the design and use of shear diaphragms.

In addition to the shear diaphragm tests mentioned above, lateral shear tests of steel buildings and tests of gabled frames with covering sheathing have been performed by Bryan and El-Dakhakhni.[4.113,4.114] The structural behavior of columns and beams continuously braced by diaphragms has also been studied by Pincus, Fisher, Errera, Apparao, Celebi, Pekoz, Winter, Rockey, Nethercot, Trahair, Wikstrom, and others.[4.115–4.120,4.135,4.136] This subject is discussed further in Art. 9.3.

In order to understand the structural behavior of shear diaphragms, the shear strength and the stiffness of steel diaphragms are briefly discussed in subsequent sections.

9.2.2.1 Shear Strength of Steel Diaphragms

Results of previous tests indicate that the shear strength per foot of steel diaphragm is usually affected by the panel configuration, the panel span and purlin or girt spacing, the material thickness and strength, acoustic perforations, types and arrangements of fasteners, and concrete fill, if any.

Panel Configuration. The height of panels has considerable effect on the shear strength of the diaphragm if a continuous flat plate element is not provided. The deeper profile is more flexible than are shallower sections. There-

fore the distortion of the panel, in particular near the ends, is more pronounced for deeper profiles. On the other hand, for panels with a continuous flat plate connected to the supporting frame, the panel height has little or no effect on the shear strength of the diaphragm.

With regard to the effect of the sheet width within a panel, wider sheets are generally stronger and stiffer because there are fewer side laps.

Panel Span and Purlin Spacing. Shorter span panels could provide a somewhat larger shear strength than longer span panels, but the results of tests indicate that the failure load is not particularly sensitive to changes in span.

The shear strength of panels is increased by a reduction of purlin spacing; the effect is more pronounced in the thinner panels.

Material Thickness and Strength. If a continuous flat plate is welded directly to the supporting frame, the failure load is nearly proportional to the thickness of the material. However, for systems with a formed panel, the shear is transmitted from the support beams to the plane of the shear-resisting element by the vertical ribs of the panels. The shear strength of such a diaphragm may be increased by an increase in material thickness, but not linearly.

When steels with different material properties are used, the influence of the material properties on diaphragm strength should be determined by tests or analytical procedures.

Acoustic Perforations. The presence of acoustic perforations may slightly increase the deflection of the system and decreases the shear strength.

Types and Arrangement of Fasteners. The shear strength of steel diaphragms is affected not only by the types of fasteners (welds, bolts, sheet metal screws, and others) but also by their arrangement and spacing. The shear strength of the connection depends to a considerable degree on the configuration of the surrounding metal.

Previous studies indicate that if the fasteners are small in size or few in number, failure may result from shearing or separation of the fasteners or by localized bearing or tearing of the surrounding material. If a sufficient number of fasteners are closely spaced, the panel may fail by elastic buckling, which produces diagonal waves across the entire diaphragm.

The shear strength will be increased considerably by the addition of intermediate side lap fasteners and end connections.

Concrete Fill. Steel panels with a concrete fill provide a much more rigid and effective diaphragm. The stiffening effect of the fill depends on the thickness, strength, and density of the fill and the bond between the fill and the panels.

The effect of lightweight concrete fill on shear diaphragms has been studied by Luttrell.[9.11] It was found that even though this type of concrete may have a very low compressive strength of 100 to 200 psi (0.7 to 1.4 MPa), it can

significantly improve the diaphragm performance. The most noticeable influence is the increase in shear stiffness. The shear strength can also be increased, but to a lesser extent.

9.2.2.2 Stiffness of Shear Diaphragms   In the use of shear diaphragms, deflection depending upon the stiffness of the shear diaphragms is often a major design criterion. Methods for predicting the deflection of cold-formed steel panels used as diaphragms have been developed on the basis of the specific panels tested. In general the total deflection of the diaphragm system without concrete fill is found to be a combination of the following factors:[9.2,9.39]

1. Deflection due to flexural stress
2. Deflection due to shear stress
3. Deflection due to seam slip
4. Deflection due to local distortion of panels and relative movement between perimeter beams and panels at end connections

The deflection due to flexural stress can be determined by the conventional formula using the moment of inertia due to perimeter beams and neglecting the influence of the diaphragm acting as a web of a plate girder.

For simplicity the combined deflections due to shear stress, seam slip, and local distortion can be determined from the results of diaphragm tests. If shear transfer devices are provided, the deflection due to relative movement between marginal beams and shear web will be negligible.

The above discussion is based on the test results of shear diaphragms without concrete fill. The use of concrete fill will increase the stiffness of shear diaphragms considerably, as discussed in the preceding section. When the advantage of concrete fill is utilized in design, the designer should consult individual companies or local building codes for design recommendations.

9.2.3   Tests of Steel Shear Diaphragms

In general, shear diaphragms are tested for each profile or pattern on a reasonable maximum span which is normally used to support vertical loads. The test frame and connections should be selected properly to simulate actual building construction if possible. Usually the mechanical properties of the steel used for the fabrication of the test panels should be similar to the specified values. If a substantially different steel is used, the test ultimate shear strength may be corrected on the basis of Ref. 9.42.

During the past, cantilever, two-bay, and three-bay steel test frames have been generally used. Another possible test method is to apply compression forces at corners along a diagonal. Nilson has shown that the single-panel cantilever test will yield the same shear strength per foot as the three-bay frame and that the deflection of an equivalent three-bay frame can be com-

puted accurately on the basis of the single-panel test. It is obvious that the use of a cantilever test is economical, particularly for long-span panels. References 9.42–9.44 contain the test procedure and the method of evaluation of the test results.

The test frame used for the cantilever test is shown in Fig. 9.2a, and Fig. 9.2b shows the cantilever beam diaphragm test.

The three-bay simple beam test frame is shown in Fig. 9.3a, and Fig. 9.3b shows the test setup for a simple beam diaphragm test.

The test results can be evaluated on the basis of the average values obtained from the testing of two identical specimens, if the deviation from the average value does not exceed 10%. Otherwise the testing of a third identical specimen is required by Refs. 9.42–9.44. The average of the two lower values obtained from the tests is regarded as the result of this series of tests. According to Ref. 9.43, if the frame has a stiffness equal to or less than 2% of that of the total diaphragm assembly, no adjustment of test results for frame resistance need be made. Otherwise, the test results should be adjusted to compensate for frame resistance.

The ultimate shear strength S_u in pounds per foot can be determined from

$$S_u = \frac{(P_{ult})_{avg}}{b} \tag{9.1}$$

where $(P_{ult})_{avg}$ = average value of maximum jack loads from either cantilever or simple beam tests, lb

b = depth of beam indicated in Figs. 9.2a and 9.3a, ft

The computed ultimate shear strength divided by the proper load factor gives the allowable design shear S_{des} in pounds per linear foot. (See Fig. 9.4 for the tested ultimate shear strength of standard corrugated steel diaphragms.)

According to Ref. 9.42, the shear stiffness G' is to be determined on the basis of an applied load of $0.4(P_{ult})_{avg}$ for use in deflection determination.* For the evaluation of shear stiffness, the measured deflections at the free end of the cantilever beam or at one-third the span length of the simple beam for each loading increment can be corrected by the following equations if the support movements are to be taken into account:

1. For cantilever tests,

$$\Delta = D_3 - \left[D_1 + \frac{a}{b}(D_2 + D_4) \right] \tag{9.2}$$

---

*Reference 9.44 suggests that the shear stiffness G' is to be determined on the basis of a reference level of $0.33(P_{ult})_{avg}$. If the selected load level is beyond the proportional limit, use a reduced value less than the proportional limit.

NOTES:
1. Symbol ⭘ represents dial gauge.
2. Pinned connection or double–link connection should be provided at corner G for reversed loading.

(a)

Section x–x pinned connection details at C

Section y–y details at D

(b)
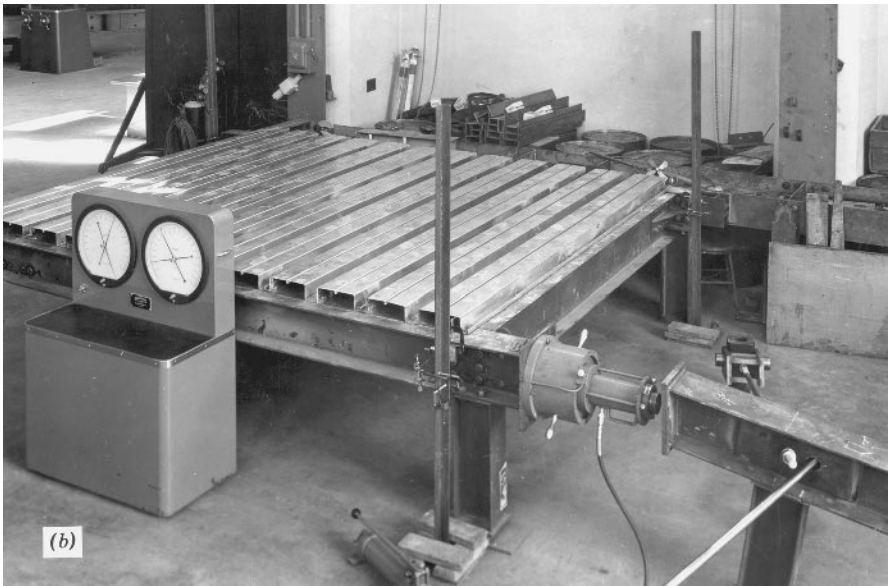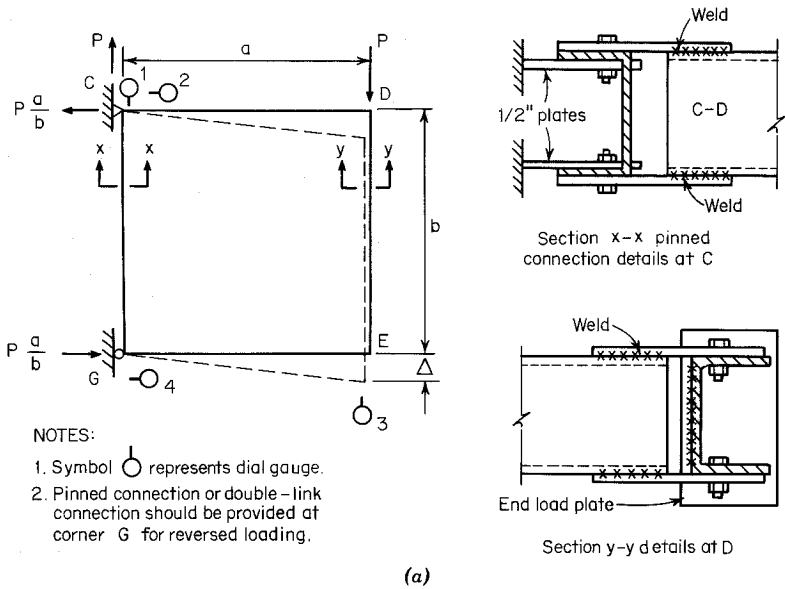
Figure 9.2 (*a*) Plan of cantilever test frame.[9.6] (*b*) Cantilever beam diaphragm test.[9.1]
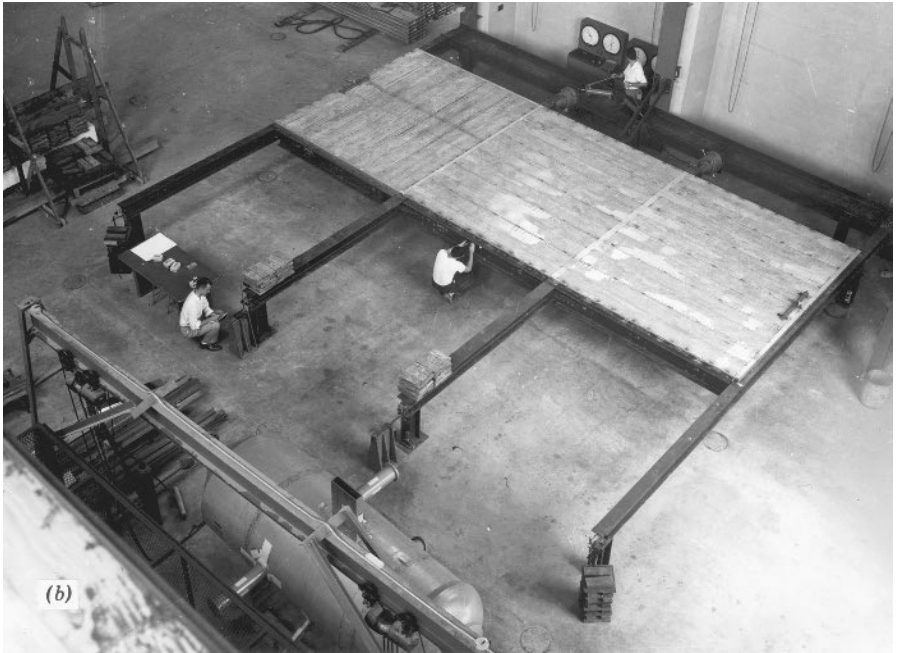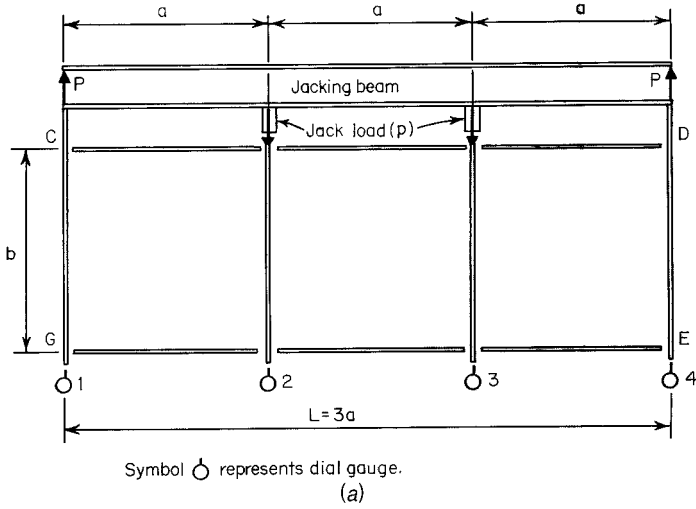
Figure 9.3   (*a*) Plan of simple beam test frame.[9.6] (*b*) Simple beam diaphragm test.[9.1]
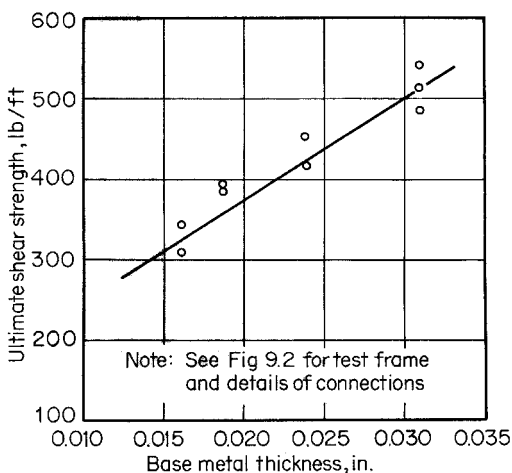
Figure 9.4 Tested ultimate shear strength of standard $2\frac{1}{2} \times \frac{1}{2}$-in. corrugated galvanized steel diaphragms.[9.42]

2. For simple beam tests,

$$\Delta = \frac{D_2 + D_3 - D_1 - D_4}{2} \tag{9.3}$$

where D_1, D_2, D_3, and D_4 are the measured deflections at locations indicated in Figs. 9.2a and 9.3a, and a/b is the ratio of the diaphragm dimensions. The load-deflection curve can then be plotted on the basis of the corrected test results.

The shear deflection for the load of $0.4(P_{ult})_{avg}$ can be computed from

$$\Delta'_s = \Delta' - \Delta'_b \tag{9.4}$$

where Δ'_s = shear deflection for load of $0.4P_{ult}$
Δ' = average value of deflections obtained from load-deflection curves for load of $0.4P_{ult}$
Δ'_b = computed bending deflection

In the computation of Δ'_b the following equations may be used for cantilever beams. The bending deflection at the free end is

$$\Delta'_b = \frac{Pa^3(12)^2}{3EI} \tag{9.5}$$

For simple beam tests, the bending deflection at one third the span length is

$$\Delta_b' = \frac{5Pa^3(12)^2}{6EI} \tag{9.6}$$

In Eqs. (9.5) and (9.6),

P = $0.4(P_{ult})_{avg}$, lb
E = modulus of elasticity of steel, 29.5×10^6 psi (203 GPa)
I = moment of inertia considering only perimeter members of test frame,
  = $Ab^2(12)^2/2$, in.^{4}
A = sectional area of perimeter members CD and GE in Figs. 9.2a and 9.3a, in.^{2}
a, b = dimensions of test frame shown in Figs. 9.2a and 9.3a, ft

Finally, the shear stiffness G' of the diaphragm can be computed as

$$G' = \frac{P/b}{\Delta_s'/a} = \frac{0.4(P_{ult})_{avg}}{\Delta_s'} \left(\frac{a}{b}\right) \tag{9.7}$$

The shear stiffness varies with the panel configuration and the length of the diaphragm. For standard corrugated sheets, the shear stiffness for any length may be computed by Eq. (9.8) as developed by Luttrell[9.5] if the constant K_2 can be established from the available test data on the same profile:

$$G' = \frac{Et}{[2(1 + \mu)g]/p + K_2/(Lt)^2} \tag{9.8}$$

where G' = shear stiffness, lb/in.
  E = modulus of elasticity of steel, =29.5×10^6 psi (203 GPa)
  t = uncoated thickness of corrugated panel, in.
  μ = Poisson's ratio, =0.3
  p = corrugation pitch, in. (Fig. 9.5)
  g = girth of one complete corrugation, in. (Fig. 9.5)
  L = length of panels from center to center of end fasteners, measured parallel to corrugations, in.
  K_2 = constant depending on diaphragm cross section and end fastener spacing, in.^{4} Knowing G' from the tested sheets, the constant K_2 can be computed as
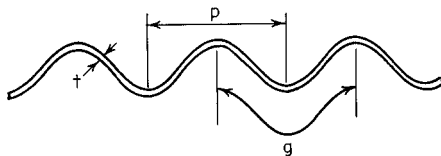
Figure 9.5 Cross section of corrugated sheets.[9.42]

$$K_2 = \left[\frac{Et}{G'} - \frac{2(1 + \mu)g}{p} \right](Lt)^2 \tag{9.9}$$

Figure 9.6 shows graphically the tested shear stiffness for 0.0198-in. (0.5-mm) thick standard corrugated diaphragms.

9.2.4   Analytical Methods for Determining Shear Strength and Stiffness of Shear Diaphragms

In Art. 9.2.3 the test method to be used for establishing the shear strength and stiffness of shear diaphragms was discussed. During the past two decades, several analytical methods have been developed for computing the shear strength and the stiffness of diaphragms. The following five methods are commonly used:

1. Steel Deck Institute (SDI) method[9.45,9.106]
2. Tri-Service method[9.46]
3. European recommendations[9.47]
4. Nonlinear finite-element analysis[9.9]
5. Simplified diaphragm analysis[9.36]

For details, the reader is referred to the referenced documents and publications.
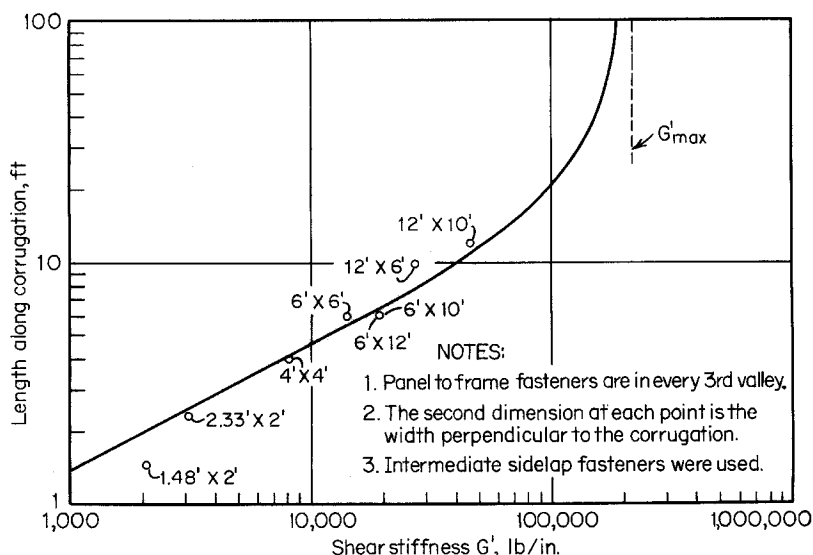
Figure 9.6   Tested shear stiffness for $2\frac{1}{2} \times \frac{1}{2}$-in. standard corrugated steel diaphragms. Thickness of panels = 0.0198 in.[9.42]

With regard to the use of the European recommendations, a design guide was prepared by Bryan and Davies in 1981.[9.48] This publication contains design tables and worked examples which are useful for calculating the strength and stiffness of steel roof decks when acting as diaphragms.

In addition to the above publications, general design rules on steel shear diaphragms can also be found in Ref. 9.49.

9.2.5 Design of Shear Diaphragms

Steel shear diaphragms can be designed as web elements of horizontal analogous plate girders with the perimeter framing members acting as the flanges. The primary stress in the web is shear stress, and in the flanges the primary stresses are axial stresses due to bending applied to the plate girder.

It has been a general design practice to determine the required sections of the panels and supporting beams based on vertical loads. The diaphragm system, including connection details, needed to resist horizontal loads, can then be designed on the basis of (1) the shear strength and the stiffness of the panels recommended by individual companies for the specific products and (2) the design provisions of local building codes.

For the design of shear diaphragms according to Sec. D5 of the AISI Specification,[1.314] the design shear strength can be determined as follows:

i. For the ASD method,

$$S_d = \frac{S_n}{\Omega_d} \tag{9.10a}$$

ii. For the LRFD method,

$$S_d = \phi_d S_n \tag{9.10b}$$

where S_d = design shear strength for diaphragm, lb/ft.
S_n = in-plane diaphragm nominal shear strength established by calculation or test, lb/ft
Ω_d = factor of safety for diaphragm shear as specified in Table 9.1
ϕ_d = resistance factor for diaphragm shear as specified in Table 9.1

In Table 9.1, the factors of safety and resistance factors are based on the statistical studies of the nominal and mean resistances from full scale tests.[4.107] This study indicated that the quality of mechanical connectors is easier to control than welded connections. As a result, the variation in the strength of mechanical connectors is smaller than that for welded connections, and their

TABLE 9.1   Factors of Safety and Resistance Factors for Diaphragms[1.314]

Ω_d	ϕ_d	Diaphragm Condition
2.65	0.60	for diaphragms for which the failure mode is that of buckling, otherwise
3.0	0.50	for diaphragms welded to the structure subjected to earthquake loads, or subjected to load combinations which include earthquake loads
2.35	0.55	for diaphragms welded to the structure subjected to wind loads, or subjected to load combinations which include wind loads
2.5	0.60	for diaphragms mechanically connected to the structure subjected to earthquake loads, or subjected to load combinations which include earthquake loads
2.0	0.65	for diaphragms mechanically connected to the structure subjected to wind loads, or subjected to load combinations which include wind loads
2.45	0.65	for diaphragms connected to the structure by either mechanical fastening or welding subjected to load combinations not involving wind or earthquake loads

performance is more predictable. Therefore, a smaller factor of safety, or larger resistance factor, is justified for mechanical connections.[1.310]

The factors of safety for earthquake loading are slightly larger than those for wind load due to the ductility demands required by seismic loading.

The stress in the perimeter framing members should be checked for the combined axial stresses due to the gravity load and the wind load or earthquake applied to the structure. According to Sec. A5.1.3 of the AISI Specification, no decrease in forces is permitted when evaluating diaphragms using the provision of Sec. D5 of the Specification.

As shown in Fig. 9.7, the axial stress in the perimeter framing members due to horizontal load (wind load or earthquake) can be determined by

$$f = \frac{F}{A} = \frac{M}{Ab} \tag{9.11}$$

where f = stress in tension or compression, psi
  F = force in tension or compression, lb, = M/b
  M = bending moment at particular point investigated, ft-lb
  A = area of perimeter framing member, in.^{2}
  b = distance between centroids of perimeter members, measured perpendicular to span length of girder, ft

Usually the shear stress in panels and the axial stress in perimeter members of such a diaphragm assembly are small, and it is often found that the framing members and panels which have been correctly designed for gravity loads
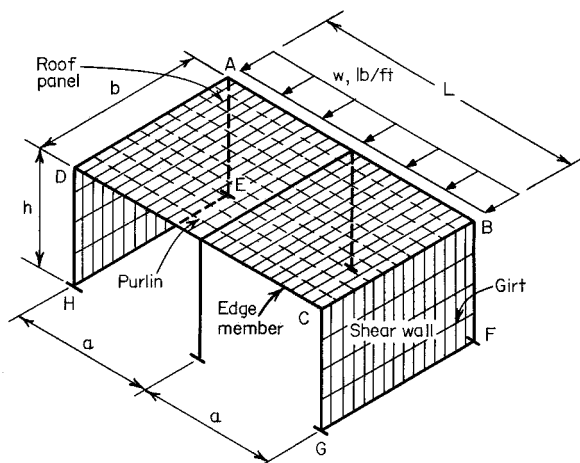
Note: Wall panels or other bracing system in planes ABFE and CDHG are not shown.

Figure 9.7   Portal frame building with wall and roof diaphragm.[9.42]

will function satisfactorily in diaphragm action with no increase in size. However, special attention may be required at connections of perimeter framing members. Ordinary connections may deform in the crimping mode if subjected to heavy axial forces along connected members.

If the panels are supported by a masonry wall rather than by a steel frame, tensile and compressive reinforcements should be provided for flange action within the walls adjacent to the diaphragm connected thereto.

In addition to designing shear diaphragm and perimeter members for their strengths, the deflection of shear diaphragms must also be considered. The total deflection of shear diaphragms may be computed as:

$$\Delta_{\text{total}} = \Delta_b + \Delta_s \tag{9.12}$$

where Δ_{total} = total deflections of shear diaphragm, in.
Δ_b = bending deflection, in.
Δ_s = shear deflection, including deflection due to seam slip and local distortion, in.

The bending deflection and shear deflection can be computed by the formulas given in Table 9.2 for various types of beams subjected to various loading conditions.

In Table 9.2 the formula for determining the shear deflection of a diaphragm is similar to the method of computing the shear deflection of a beam having relatively great depth. It can be derived from the following equation:[4.45]

TABLE 9.2   Deflection of Shear Diaphragms[9.42]

Type of Diaphragm	Loading Condition	Δ_b	$\Delta_s{}^a$
Simple beam (at center)	Uniform load	$\dfrac{5wL^4(12)^2}{384EI}$	$\dfrac{wL^2}{8G'b}$
	Load P applied at center	$\dfrac{PL^3(12)^3}{48EI}$	$\dfrac{PL}{4G'b}$
	Load P applied at each 1/3 point of span	$\dfrac{23PL^3(12)^3}{648EI}$	$\dfrac{PL}{3G'b}$
Cantilever beam (at free end)	Uniform load	$\dfrac{wa^4(12)^3}{8EI}$	$\dfrac{wa^2}{2G'b}$
	Load P applied at free end	$\dfrac{Pa^3(12)^3}{3EI}$	$\dfrac{Pa}{G'b}$

*When the diaphragm is constructed with two or more panels of different lengths, the term $G'b$ should be replaced by $\Sigma\, G_i'b_i$, where G_i' and b_i are the shear stiffness and the length of a specific panel, respectively.

$$\Delta_s = \int \frac{Vv}{G'b}\, dx \qquad (9.13)$$

where V = shear due to actual loads
$\quad\ v$ = shear due to a load of 1 lb acting at section where deflection is derived
$\quad G'$ = shear stiffness of diaphragm
$\quad\ b$ = width of shear diaphragm or depth of analogous beam.

In practical design, the total horizontal deflection of a shear diaphragm must be within the allowable limits permitted by the applicable building code or other design provisions. The following formula for masonry walls has been proposed by the Structural Engineers Association of California:

$$\text{allowable deflection} = \frac{h^2 f}{0.01Et} \qquad (9.14)$$

where h = unsupported height of wall, ft
$\quad t$ = thickness of wall, in.
$\quad E$ = modulus of elasticity of wall material, psi
$\quad f$ = allowable compressive stress of wall material, psi

9.2.6   Special Considerations

The following are several considerations which are essential in the use of steel panels as shear diaphragms.

1. If purlins and girts are framed over the top of perimeter beams, trusses, or columns, the shear plane of the panels may cause tipping of purlin and girt members by eccentric loading. For this case, rake channels or other members should be provided to transmit the shear from the plane of the panels to the flanges of the framing member or to the chords of the truss.

2. Consideration should be given to the interruption of panels by openings or nonstructural panels. It may be assumed that the effective depth of the diaphragm is equal to the total depth less the sum of the dimensions of all openings or nonstructural panels measured parallel to the depth of the diaphragm. The type of panel-to-frame fasteners used around the openings should be the same as, and their spacing equal to or less than, that used in the tests to establish the diaphragm value.

3. When panels are designed as shear diaphragms, a note shall be made on the drawings to the effect that the panels function as braces for the building and that any removal of the panels is prohibited unless other special separate bracing is provided.

4. The performance of shear diaphragms depends strongly on the type, spacing, strength, and integrity of the fasteners. The type of fasteners used in the building should be the same as, and their spacing not larger than, that used in the test to establish the diaphragm value.

5. Diaphragms are not effective until all components are in place and fully interconnected. Temporary shoring should therefore be provided to hold the diaphragms in the desired alignment until all panels are placed, or other construction techniques should be used to make the resulting diaphragm effective. Temporary bracing should be introduced when replacing panels.

6. Methods of erection and maintenance used for the construction of shear diaphragms should be evaluated carefully to ensure proper diaphragm action. Proper inspection and quality control procedures would be established to ensure the soundness and spacing of the connections.

For other guidelines on practical considerations, erection, inspection, and other design information, see Ref. 9.45.

Example 9.1   Use the ASD method to design a longitudinal bracing system by using steel shear diaphragms for a mill building as shown in Fig. 9.8*a* and *b*. Assume that a wind load of 20 psf is applied to the end wall of the building and that corrugated steel sheets having a base metal thickness of 0.0198 in. are used as roof and wall panels.

Solution

A. Alternate I   Longitudinal X-bracing is usually provided for a mill building in the planes of the roof, side walls and the lower chord of the truss,* as

---

*See Alternate II, in which the X-bracing is eliminated in the plane of the lower chord of the truss.

(a)

(b)

(c)

(d)
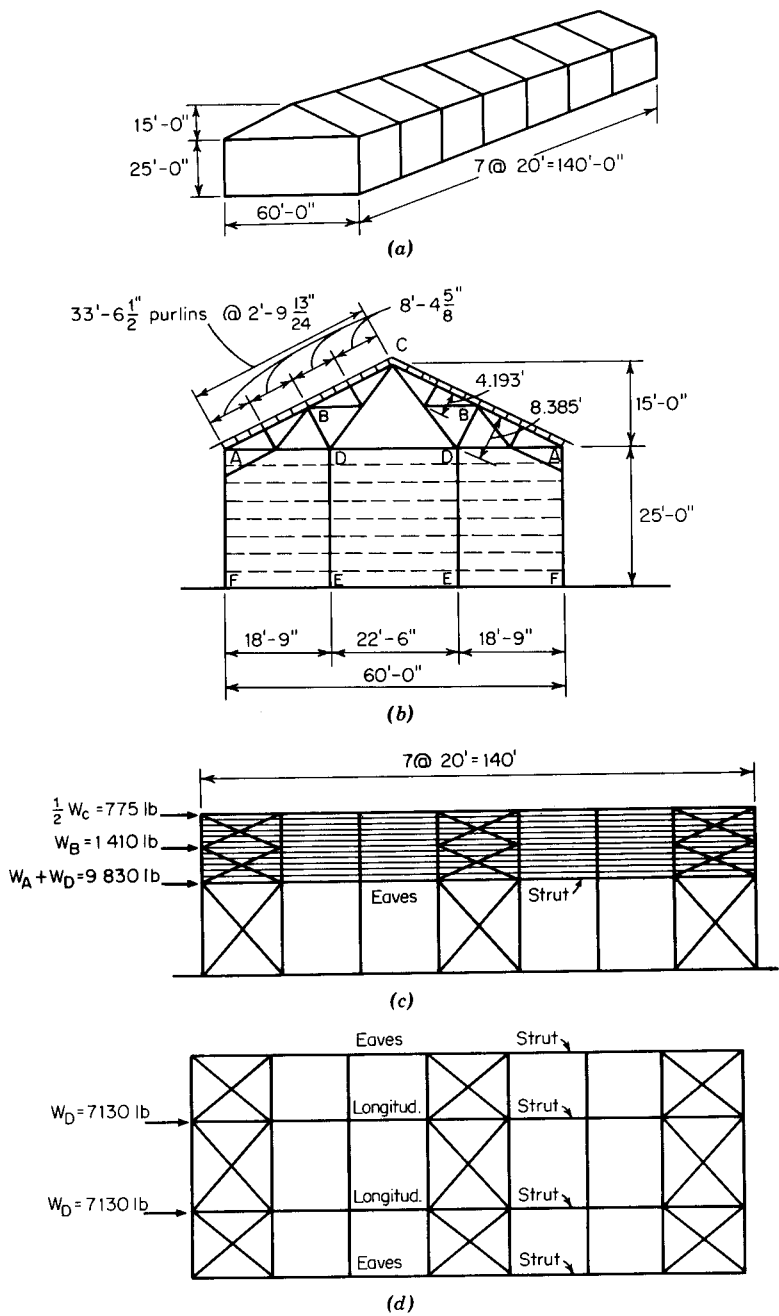
Figure 9.8 (*a*) Mill building. (*b*) End elevation. (*c*) Wind bracing in planes of roof and side walls, side elevation. (*d*) Bracing in plane of lower chord. (*e*) Assumed area of wind load to be carried at *A*, *B*, *C*, and *D*. (*f*) Shear diaphragms in planes of roof and side walls, side elevation. (*g*) Assumed area of wind load to be carried in planes of roof and bottom chord of truss. (*h*) End wall columns run all the way to roof plane.
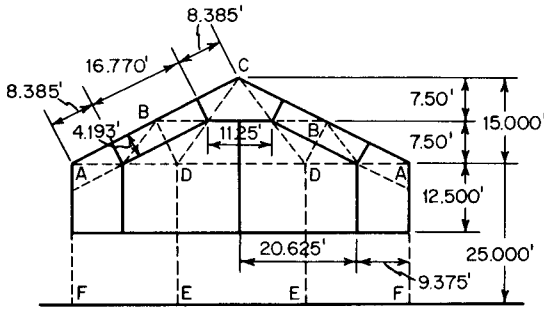
(e)
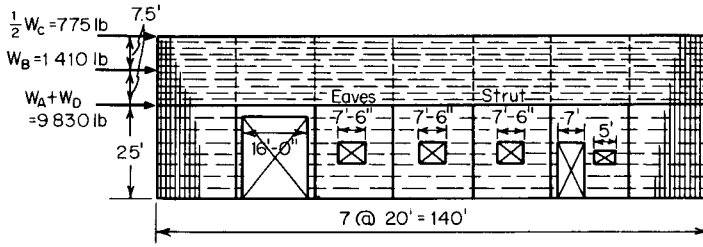
(f)
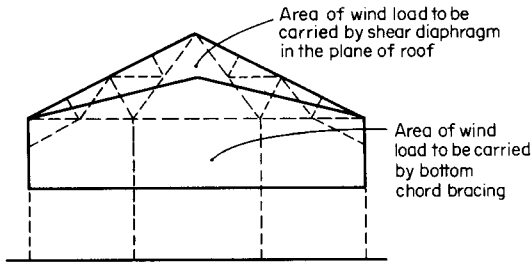
(g)
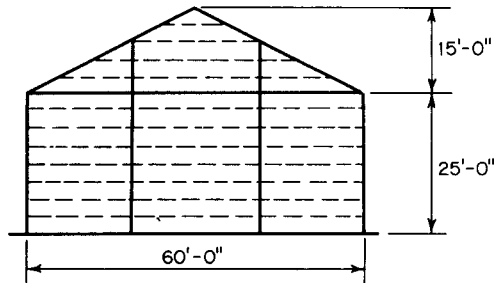
(h)

Figure 9.8   (*Continued*)

shown in Fig. 9.8c and d. The intent of this example is to illustrate the use of shear diaphragms in the planes of the roof and side walls instead of the X-bracing system. The design of the roof truss and other structural members is beyond the scope of this example.

1. *Wind Panel Loads.*   The wind panel loads at A, B, C, and D can be computed as follows based on the assumed area in Fig. 9.8e:

$$W_A = 20(9.375 \times 12.5 + \tfrac{1}{2} \times 8.385 \times 4.193) = 2700 \text{ lb}$$
$$W_B = 20(16.77 \times 4.193) = 1410 \text{ lb}$$
$$W_C = 20(8.385 \times 4.193 + \tfrac{1}{2} \times 11.25 \times 7.5) = 1550 \text{ lb}$$
$$W_D = 20(20.635 \times 12.5 + 5.625 \times 7.5 + \tfrac{1}{2} \times 7.5 \times 15.0) = 7130 \text{ lb}$$

2. *Shear Diaphragm in Plane of Roof.*   Considering that the planes of the side walls and the lower chord of the truss are adequately braced, the wind loads to be resisted by the roof panels used as a shear diaphragm are $\tfrac{1}{2}W_C$ and W_B as indicated in Fig. 9.8f. Consequently the shear developed along the eave struts is

$$v = \frac{775 + 1410}{140} = \frac{2185}{140} = 15.6 \text{ lb/ft}$$

From Table A.1 of Appendix A of Ref. 9.42, the average nominal shear strength for the corrugated sheets having a base metal thickness of 0.0198 in. is 370 lb/ft. Using a safety factor of 2.00 as recommended by AISI for screw connectors, the allowable shear strength for the design is

$$S_{\text{des}} = \frac{370}{2.00} = 185 \text{ lb/ft}$$

Since the allowable shear is much larger than the actual shear value of 15.6 lb/ft developed in the roof due to the wind load, the roof panels are adequate to resist the wind load applied to the end wall, even though no intermediate fasteners are provided. Usually intermediate fasteners are used for roof panels, and as a result, additional strength will be provided by such fasteners.

3. *Shear Diaphragm in Plane of Side Wall.*   As far as the shear diaphragms in the planes of the side walls are concerned, the total load to be resisted by one side wall as shown in Fig. 9.8f, is

$$P = W_A + W_B + \tfrac{1}{2}W_C + W_D$$
$$= 2700 + 1410 + 775 + 7130 = 12{,}015 \text{ lb}$$

The effective diaphragm width b_{eff} is the length of the building with the widths of doors and windows subtracted. This is based on the consideration that the wall panels are adequately fastened to the perimeter members around openings, that is,

$$b_{eff} = 140 - (16.0 + 3 \times 7.5 + 7.0 + 5.0) = 89.5 \text{ ft}$$

Therefore the shear to be resisted by the diaphragm is

$$v = \frac{P}{b_{eff}} = \frac{12,015}{89.5} = 134 \text{ lb/ft}$$

or the required static ultimate shear resistance should be

$$S_u = S_d \times \text{SF} = 134 \times 2.00 = 263 \text{ lb/ft}$$

Since the average nominal shear strength for the 0.0198-in. thick corrugated sheets spanning at 3 ft is 370 lb/ft, which is larger than the computed value of 268 lb/ft, the corrugated sheets are adequate for shear diaphragm action.

In determining the wind load to be resisted in the planes of roof and side walls, assumptions may be made as shown in Fig. 9.8g. Based on this figure, the wind load to be resisted by the shear diaphragm in the plane of the roof is 2250 lb, which is slightly larger than the load of 2185 lb used previously. The total load to be used for the design of the shear diaphragm in the planes of side walls is the same as the load computed from Fig. 9.8f.

4. *Purlin Members.*   It should be noted that the shear force in the plane of roof panels can cause the tipping of purlins due to eccentricity. Rake channels or other means may be required to transmit the shear force from the plane of roof panels to chord members. This can become important in short wide buildings if purlins are framed over the top of trusses.

B.   Alternate II   When end wall columns run all the way to the roof plane, as shown in Fig. 9.8h, there is no need for X-bracing in the plane of the bottom chord. For this case, the force to be resisted by one side of the roof diaphragm is

$$P = 20 \times \tfrac{1}{2}[(12.5 + 20) \times 30] = 9750 \text{ lb}$$

and

$$v = \frac{9750}{140} = 69.7 \text{ lb/ft.}$$

The above shear developed along the eave struts is smaller than the allowable shear of 180 lb/ft for 0.0198-in. thick corrugated sheets. Therefore, the roof panels are adequate to act as a diaphragm.

For side walls, the shear to be resisted by the diaphragm is

$$v = \frac{P}{b_{\text{eff}}} = \frac{9750}{89.5} = 109 \text{ lb/ft}$$

or the required static ultimate shear resistance is

$$S_{\text{u}} = 109 \times 2.00 = 218 \text{ lb/ft}$$

Since the above computed S_{u} is less than the nominal shear strength of 370 lb/ft for the 0.0198-in. thick sheets, the wall panels are also adequate to act as a shear diaphragm. The X-bracing in the plane of the side walls can therefore be eliminated.

9.3 STRUCTURAL MEMBERS BRACED BY DIAPHRAGMS

9.3.1 Beams and Columns Braced by Steel Diaphragms

In Art. 9.2 the application of steel diaphragms in building construction was discussed. It has been pointed out that in addition to utilizing their bending strength and diaphragm action, the steel panels and decking used in walls, roofs, and floors can be very effective in bracing members of steel framing against overall buckling of columns and lateral buckling of beams in the plane of panels. Both theoretical and experimental results indicate that the failure load of diaphragm-braced members can be much higher than the critical load for the same member without diaphragm bracing.

In the past, investigations of thin-walled steel open sections with and without bracing have been conducted by numerous investigators. Since 1961 the structural behavior of diaphragm-braced columns and beams has been studied at Cornell by Winter, Fisher, Pincus, Errera, Apparao, Celebi, Pekoz, Simaan, Soroushian, Zhang and others.[4.115–4.118,4.123,4.125–4.128,4.133,4.136,9.50–9.57] In these studies, the equilibrium and energy methods have been used for diaphragm-braced beams and columns. In addition to the Cornell work, numerous studies have been conducted at other institutions and several individual steel companies.[4.119–4.122,4.124,4.129–4.132,4.134,4.135,9.58–9.66]

9.3.2 Diaphragm-Braced Wall Studs

In Art. 5.10 the application of wall studs in building construction was briefly discussed. Because the shear diaphragm action of wall material can increase the load-carrying capacity of wall studs significantly, the effect of sheathing material on the design load of wall studs is considered in Sec. D4(b) and Secs. D4.1 through D4.3 of the AISI Specification. However, it should be noted that these AISI design requirements are now limited only to those studs that have identical wall material attached to both flanges. For studs with wall material on one flange only see Sec. C4.4 of the Specification. When unidentical wall materials are attached to two flanges, the reader is referred to Refs. 9.52–9.55.

In the evaluation of the load-carrying capacity of wall studs, consideration should be given to the structural strength and stiffness of the wall assembly. As far as the structural strength is concerned, the maximum load that can be carried by wall studs is governed by either (1) column buckling of studs between fasteners in the plane of the wall (Fig. 9.9) or (2) overall column buckling of studs (Fig. 9.10). The following discussion deals with the critical loads for these types of buckling.

9.3.2.1 Column Buckling of Wall Studs between Fasteners When the stud buckles between fasteners, as shown in Fig. 9.9, the failure mode may be (1) flexural buckling, (2) torsional buckling, or (3) torsional–flexural buckling, depending on the geometric configuration of the cross section and the spacing
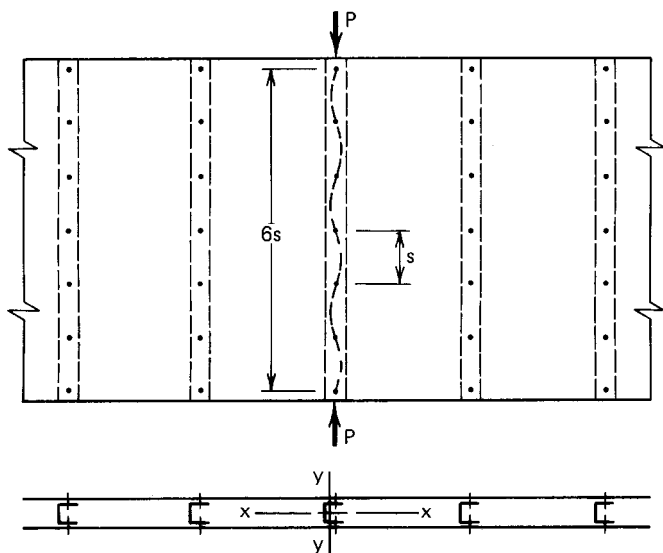
Figure 9.9 Buckling of studs between fully effective fasteners.
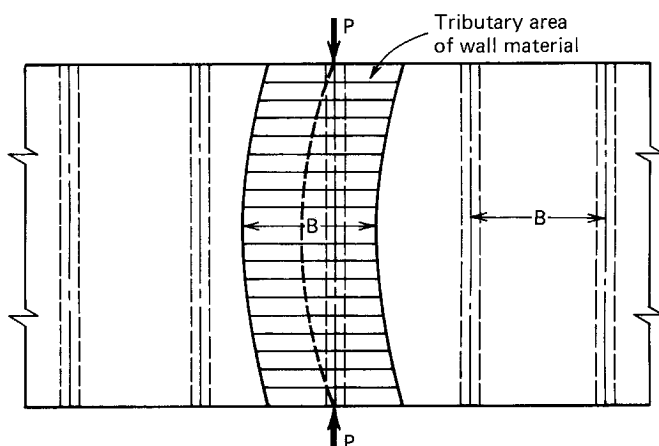
Figure 9.10   Overall column buckling of studs.

of fasteners. For these types of column buckling, the critical loads are based on the stud itself, without any interaction with the wall material. Therefore the design formulas given in Arts. 5.3 and 5.4 are equally applicable to these cases.

9.3.2.2 Overall Column Buckling of Wall Studs Braced by Shear Diaphragms on Both Flanges

The overall column buckling of wall studs braced by sheathing material has been studied extensively at Cornell University and other institutions. The earlier AISI provisions were developed primarily on the basis of the Cornell work.[9.52–9.55] Even though the original research has considered the shear rigidity and the rotational restraint of the wall material that is attached either on one flange or on both flanges of the wall studs, for the purpose of simplicity, the AISI design requirements are provided only for the studs braced by shear diaphragms on both flanges. In addition, the rotational restraint provided by the wall material is neglected in the AISI provisions.

Based on their comprehensive studies of wall assemblies, Simaan and Pekoz have shown several stability equations for determining the critical loads for different types of overall column buckling of wall studs.[9.55] The following buckling load equations are used for channels or C-sections, Z-sections, and I-sections having wall materials on both flanges:

1. *Singly Symmetric Channels or C-sections*
   a. *Flexural buckling about y-axis*

$$P_{cr} = P_y + \overline{Q} \tag{9.15}$$

b. *Torsional–flexural buckling*

$$P_{cr} = \frac{1}{2\beta} [(P_x + P_{zQ}) - \sqrt{(P_x + P_{zQ})^2 - 4\beta P_x P_{zQ}}] \quad (9.16)$$

where P_{cr} = critical buckling load, kips
P_x = Euler flexural buckling load about x-axis of wall studs, kips, i.e.

$$\frac{\pi^2 EI_x}{(K_x L_x)^2} \qquad (9.17)$$

P_y = Euler flexural buckling load about y-axis of wall studs, kips, i.e.,

$$\frac{\pi^2 EI_y}{(K_y L_y)^2} \qquad (9.18)$$

P_z = torsional buckling load about z-axis of wall studs, kips, i.e.

$$\left[\frac{\pi^2 EC_w}{(K_t L_t)^2} + GJ \right] \left(\frac{1}{r_0^2} \right) \qquad (9.19)$$

$$P_{zQ} = P_z + \frac{\overline{Q}d^2}{4r_0^2} \qquad (9.20)$$

$\overline{Q}$ = shear rigidity for two wallboards, kips
d = depth of channel or C-section, in.

Other symbols are as defined in Arts. 5.4 and 5.7.

2. *Z-Sections*

a. *Torsional buckling about z-axis*

$$P_{cr} = P_{zQ} = P_z + \frac{\overline{Q}d^2}{4r_0^2} \qquad (9.21)$$

b. *Combined flexural buckling about x- and y-axes*

$$P_{cr} = \tfrac{1}{2}[(P_x + P_y + \overline{Q}) \\ - \sqrt{(P_x + P_y + \overline{Q})^2 - 4(P_x P_y + P_x \overline{Q} - P_{xy}^2)}] \qquad (9.22)$$

where

$$P_{xy} = \frac{\pi^2 E I_{xy}}{(K_x K_y L^2)} \qquad (9.23)$$

and I_{xy} is the product of the inertia of wall studs, in.[4]

3. *Doubly Symmetric I-Sections*
   a. *Flexural buckling about y-axis*

$$P_{cr} = P_y + \overline{Q} \qquad (9.24)$$

   b. *Flexural buckling about x-axis*

$$P_{cr} = P_x \qquad (9.25)$$

   c. *Torsional buckling about z-axis*

$$P_{cr} = P_{zQ} = P_z + \frac{\overline{Q}d^2}{4r_0^2} \qquad (9.26)$$

By using the above equations for critical loads, the critical elastic buckling stress σ_{cr} can be computed as

$$\sigma_{cr} = \frac{P_{cr}}{A} \qquad (9.27)$$

9.3.2.3 AISI Design Criteria for Wall Studs   The following excerpts are adopted from Sec. D4 of the AISI Specification for the design of wall studs:[1.314]

D4 Wall Studs and Wall Stud Assemblies

Wall studs shall be designed either on the basis of an all steel system in accordance with Section C or on the basis of sheathing in accordance with Section D4.1 through D4.3. Both solid and perforated webs shall be permitted. Both ends of the stud shall be connected to restrain rotation about the longitudinal stud axis and horizontal displacement perpendicular to the stud axis.

(a) All Steel Design

Wall stud assemblies using an all steel design shall be designed neglecting the structural contribution of the attached sheathings and shall comply with the requirements of Section C. In the case of circular web perforations, see Section B2.2, and for non-circular web perforations, the effective area shall be determined as follows:

The effective area, A_e, at a stress F_n, shall be determined in accordance

with Sec. B, assuming the web to consist of two unstiffened elements, one on each side of the perforation, or the effective area, A_e, shall be determined from stub-column tests.

When A_e is determined in accordance with Section B, the following limitations related to the size and spacing of perforations and the depth of the stud shall apply:

(1) The center-to-center spacing of web perforations shall not be less than 24 inches (610 mm).

(2) The maximum width of web perforations shall be the lesser of 0.5 times the depth, d, of the section or 2-1/2 inches (63.5 mm).

(3) The length of web perforations shall not exceed 4-1/2 inches (114 mm).

(4) The section depth-to-thickness ratio, d/t, shall not be less than 20.

(5) The distance between the end of the stud and the near edge of a perforation shall not be less than 10 inches (254 mm).

(b) Sheathing Braced Design

Wall stud assemblies using a sheathing braced design shall be designed in accordance with Sections D4.1 through D4.3 and in addition shall comply with the following requirements:

In the case of perforated webs, the effective area, A_e, shall be determined as in (a) above.

Sheathing shall be attached to both sides of the stud and connected to the bottom and top horizontal members of the wall to provide lateral and torsional support to the stud in the plane of the wall.

Sheathing shall conform to the limitations specified under Table D4. Additional bracing shall be provided during construction, if required.

The equations given are applicable within the following limits:

Yield strength, $F_y \leq 50$ ksi (345 MPa)

Section depth, $d \leq 6.0$ in. (152 mm)

Section thickness, $t \leq 0.075$ in. (1.91 mm)

Overall length, $L \leq 16$ ft (4.88 mm)

Stud spacing, 12 in. (305 mm) minimum; 24 in. (610 mm) maximum

D4.1 Wall Studs in Compression

For studs having identical sheathing attached to both flanges, and neglecting any rotational restraint provided by the sheathing, the nominal axial strength, P_n, shall be calculated as follows:

$$P_n = A_e F_n \tag{9.28}$$

$$\Omega_c = 1.80 \text{ (ASD)}$$

$$\phi_c = 0.85 \text{ (LRFD)}$$

where A_e = Effective area determined at F_n

F_n = The lowest value determined by the following three conditions:

(a) To prevent column buckling between fasteners in the plane of the wall, F_n shall be calculated according to Section C4 with KL equal to two times the distance between fasteners.

(b) To prevent flexural and/or torsional overall column buckling, F_n shall be calculated in accordance with Section C4 with F_e taken as the smaller of the two σ_{CR} values specified for the following section types, where σ_{CR} is the theoretical elastic buckling stress under concentric loading.

1. Singly symmetric C-sections

$$\sigma_{CR} = \sigma_{ey} + \overline{Q}_a \tag{9.29}$$

$$\sigma_{CR} = \frac{1}{2\beta}\left[(\sigma_{ex} + \sigma_{tQ}) - \sqrt{(\sigma_{ex} + \sigma_{tQ})^2 - (4\beta\sigma_{ex}\sigma_{tQ})}\right] \tag{9.30}$$

2. Z-Sections

$$\sigma_{CR} = \sigma_t + \overline{Q}_t \tag{9.31}$$

$$\sigma_{CR} = \frac{1}{2}\{(\sigma_{ex} + \sigma_{ey} + \overline{Q}_a) \\ - \sqrt{[(\sigma_{ex} + \sigma_{ey} + \overline{Q}_a)^2 - 4(\sigma_{ex}\sigma_{ey} + \sigma_{ex}\overline{Q}_a - \sigma_{exy}^2)]}\} \tag{9.32}$$

3. I-Sections (doubly symmetric)

$$\sigma_{CR} = \sigma_{ey} + \overline{Q}_a \tag{9.33}$$

$$\sigma_{CR} = \sigma_{ex} \tag{9.34}$$

In the above formulas:

$$\sigma_{ex} = \frac{\pi^2 E}{(L/r_x)^2} \tag{9.35}$$

$$\sigma_{exy} = (\pi^2 E I_{xy})/(AL^2) \tag{9.36}$$

$$\sigma_{ey} = \frac{\pi^2 E}{(L/r_y)^2} \tag{9.37}$$

$$\sigma_t = \frac{1}{Ar_0^2}\left[GJ + \frac{\pi^2 E C_w}{(L)^2}\right] \tag{9.38}$$

$$\sigma_{tQ} = \sigma_t + \overline{Q}_t \tag{9.39}$$

$$\overline{Q} = \overline{Q}_o(2 - s/s') \tag{9.40}$$

where s = fastener spacing, in. (mm); 6 in. (152 mm) $\leq s \leq$ 12 in. (305 mm)

s' = 12 in. (305 mm)

$\underline{Q}_\text{o}$ = See Table D4

$Q_\text{a} = \overline{Q}/A$ (9.41)

A = area of full unreduced cross section

L = length of stud

$Q_\text{t} = (\overline{Q}d^2)/(4Ar_0^2)$ (9.42)

d = depth of section

I_{xy} = product of inertia

(c) To prevent shear failure of the sheathing, a value of F_n shall be used in the following equations so that the shear strain of the sheathing, γ, does not exceed the permissible shear strain, $\overline{\gamma}$. The shear strain, γ, shall be determined as follows:

$$\gamma = (\pi/L)[C_1 + (E_1 d/2)] \tag{9.43}$$

where

C_1 and E_1 are the absolute values of C_1 and E_1 specified below for each section type:

1. Singly Symmetric C-Sections

$$C_1 = (F_\text{n}C_0)/(\sigma_\text{ey} - F_\text{n} + \overline{Q}_\text{a}) \tag{9.44}$$

$$E_1 = \frac{F_\text{n}[(\sigma_\text{ex} - F_\text{n})(r_0^2 E_0 - x_\text{o}D_0) - F_\text{n}x_0(D_0 - x_0 E_0)]}{(\sigma_\text{ex} - F_\text{n})r_0^2(\sigma_\text{tQ} - F_\text{n}) - (F_\text{n}x_0)^2} \tag{9.45}$$

2. Z-Sections

$$C_1 = \frac{F_\text{n}[C_0(\sigma_\text{ex} - F_\text{n}) - D_0\sigma_\text{exy}]}{(\sigma_\text{ey} - F_\text{n} + \overline{Q}_\text{a})(\sigma_\text{ex} - F_\text{n}) - \sigma_\text{exy}^2} \tag{9.46}$$

$$E_1 = (F_\text{n}E_0)/(\sigma_\text{tQ} - F_\text{n}) \tag{9.47}$$

3. I-Sections

$$C_1 = (F_\text{n}C_0)/(\sigma_\text{ey} - F_\text{n} + \overline{Q}_\text{a}) \tag{9.48}$$

$$E_1 = 0$$

where x_0 = distance from shear center to centroid along principal x-axis, in. (absolute value)

C_0, E_0, and D_0 are initial column imperfections which shall be assumed to be at least

C_0 = L/350 in a direction parallel to the wall   (9.49)

$$D_0 = \text{L/700 in a direction perpendicular to the}$$
$$\text{wall} \tag{9.50}$$
$$E_0 = \text{L/(d} \times \text{10,000), rad, a measure of the initial twist of the stud}$$
$$\text{from the initial ideal, unbuckled shape} \tag{9.51}$$

If $F_n > 0.5 \, F_y$, then in the definitions for σ_{ey}, σ_{ex}, σ_{exy} and σ_{tQ}, the parameters E and G shall be replaced by E' and G', respectively, as defined below

$$E' = 4EF_n(F_y - F_n)/F_y^2 \tag{9.52}$$

$$G' = G(E'/E) \tag{9.53}$$

Sheathing parameters $\overline{Q}_o$ and $\overline{\gamma}$ shall be permitted to be determined from representative full-scale tests, conducted and evaluated as described by published documented methods (see Commentary), or from the small-scale-test values given in Table D4.

D4.2 Wall Studs in Bending

For studs having identical sheathing attached to both figures, and neglecting any rotational restrain provided by the sheathing, the nominal flexural strengths are M_{nxo}, and M_{nyo} where
For sections with stiffened or partially stiffened compression flanges:

$$\Omega_b = 1.67 \text{ (ASD)}$$

$$\phi_b = 0.95 \text{ (LRFD)}$$

For sections with unstiffened compression flanges:

$$\Omega_b = 1.67 \text{ (ASD)}$$

$$\phi_b = 0.90 \text{ (LRFD)}$$

M_{nxo} and M_{nyo} = Nominal flexural strengths about the centroidal axes determined in accordance with Section C3.1, excluding the provisions of Section C3.1.2 (lateral buckling)

D4.3 Wall Studs with Combined Axial Load and Bending

The required axial strength and flexural strength shall satisfy the interaction equations of Section C5 with the following redefined terms:

P_n = Nominal axial strength determined according to Section D4.1

M_{nx} and M_{ny} in Equations C5.2.1-1, C5.2.1-2 and C5.2.1-3 for ASD or C5.2.2-1, C5.2.2-2 and C5.2.2-3 shall be replaced by nominal flexural strengths, M_{nxo} and M_{nyo}, respectively.

TABLE D4   Sheathing Parameters[(1)]

Sheathing[(2)]	$\overline{Q}_o$		$\overline{\gamma}$
	k	kN	length/length
3/8 in. (9.5 mm) to 5/8 in. (15.9 mm) thick gypsum	24.0	107.0	0.008
Lignocellulosic board	12.0	53.4	0.009
Fiberboard (regular or impregnated)	7.2	32.0	0.007
Fiberboard (heavy impregnated)	14.4	64.1	0.010

(1) The values given are subject to the following limitations:
All values are for sheathing on both sides of the wall assembly.
All fasteners are No. 6, type S-12, self-drilling drywall screws with pan or bugle head, or equivalent.

(2) All sheathing is 1/2 in. (12.7 mm) thick except as noted.
For other types of sheathing, $\overline{Q}_o$ and $\overline{\gamma}$ shall be permitted to be determined conservatively from representative small-specimen tests as described by published documented methods (see Commentary)

It should be noted that in 1996, the AISI design provisions for wall studs were revised to permit (a) *all-steel design* and (b) *sheathing braced design* of wall studs with either solid or perforated webs. For sheathing braced design, in order to be effective, sheathing must retain its design strength and integrity for the expected service life of the wall.

For the case of all-steel design, the approach of determining effective areas in accordance with Specification Section D4(a) is being used in the RMI Specification[1.165] for the design of perforated rack columns. The validity of this approach for wall studs was verified in a Cornell project on wall studs reported by Miller and Pekoz.[9.98] The limitations for the size and spacing of perforations and the depth of studs are based on the parameters used in the program. For sections with perforations which do not meet these limits, the effective area can be determined by stub column tests.

In the foregoing AISI design provisions, Sec. D4.1(a) is based on the discussion given in Art. 9.3.2.1, except that the effective length KL is taken as two times the distance between fasteners. Thus even if an occasional attachment is defective to a degree that it is completely inoperative, the allowable design load will still be sufficient.

In Sec. D4.1(b) of the specification, Eqs. (9.29) through (9.34) were derived from Eqs. (9.15) through (9.25) with $K_x = K_y = K_t = 1.0$. The type of torsional buckling of doubly symmetric I-sections [Eq. (9.26)] is not considered in the AISI requirements because it is not usually a failure mode.

The design shear rigidity $\overline{Q}$ for two wallboards was determined in the 1980 and 1986 editions of the Specification as

$$\overline{Q} = \overline{q}B \qquad (9.55)$$

in which the value $\overline{q}$ was defined as the design shear rigidity for two wall-boards per inch of stud spacing. Based on the discussions presented in Ref. 9.55, $\overline{q}$ can be determined by

$$\overline{q} = \frac{2G'}{SF} \qquad (9.56)$$

where G' = diaphragm shear stiffness of a single wallboard for a load of $0.8P_{ult}$,

$$= \frac{0.8P_{ult}/b}{\Delta_d/a} = \frac{0.8P_{ult}}{\Delta_d}\left(\frac{a}{b}\right), \text{ kips/in.} \qquad (9.57)$$

P_{ult} = ultimate load reached in shear diaphragm test of a given wall-board, kips (Fig. 9.11)

Δ_d = shear deflection corresponding to a load of $0.8P_{ult}$, in. (Fig. 9.11)

a, b = geometric dimensions of shear diaphragm test frame, ft (Fig. 9.11)

SF = safety factor, = 1.5

The reason for using $0.8P_{ult}$ for G' is that the shear deflection and thus the shear rigidity at the ultimate load P_{ult} are not well defined and reproducible. A safety factor of 1.5 was used to avoid premature failure of the wallboard.
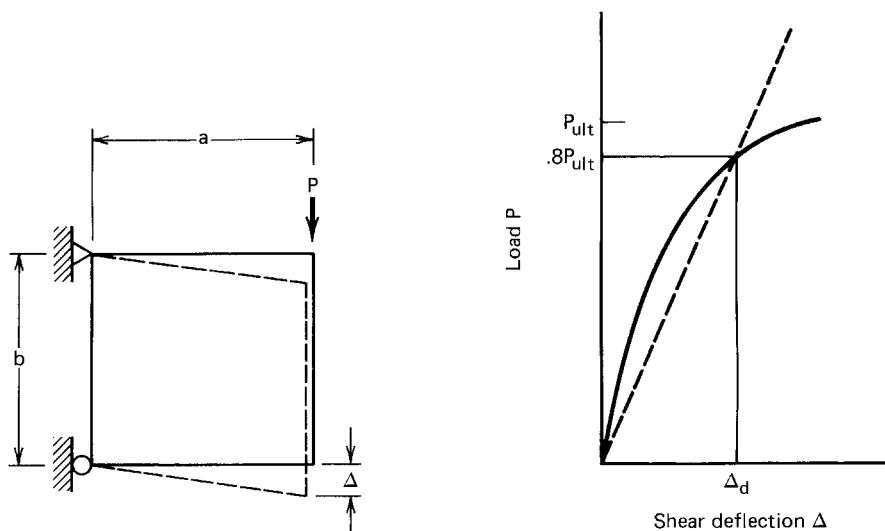
Figure 9.11   Determination of shear rigidity, $\overline{Q}$.[9.55]

By substituting the equation of G' and the safety factor into Eq. (9.56), the design shear rigidity for wallboards on both sides of the stud can be evaluated as

$$\bar{q} = \frac{0.53 \, P_{\text{ult}}}{\Delta_{\text{d}}} \left(\frac{a}{b}\right) \tag{9.58}$$

Based on the results of a series of shear diaphragm tests using different wallboards with No. 6, type S-12, self-drilling drywall screws at 6- to 12-in. (152- to 305-mm) spacing, some typical values of $\bar{q}_0$ have been developed and were given in Table D4 of the 1980 and 1986 editions of the AISI Specification. In this table, the value of $\bar{q}_0$ was computed by

$$\bar{q}_0 = \frac{\bar{q}}{2 - s/12} \tag{9.59}$$

where s is the fastener spacing, in.

In the 1996 edition of the AISI Specification, the equation for the design shear rigidity $\bar{Q}$ for sheathing on both sides of the wall was rewritten on the basis of a recent study of gypsum-sheathed cold-formed steel wall studs. In Ref. 9.108, Miller and Pekoz indicated that the strength of gypsum wall board-braced studs was observed to be rather intensive to stud spacing. Moreover, the deformations of gypsum wallboard panel (in tension) were observed to be localized at the fasteners, and not distributed throughout the panel as in a shear diaphragm. The $\bar{Q}_o$ values listed in Table D4 were determined from $\bar{Q}_o = 12\bar{q}_o$, in which the $\bar{q}_o$ values were obtained from the 1986 edition of the AISI Specification. The values given in Table D4 for gypsum are based on dry service conditions.

In addition to the requirements discussed above, the AISI Specification considers the shear strain requirements as well. In this regard, Sec. D4.1(c) specifies that the computed shear strain γ according to Eq. (9.43) and for a value of F_n, should not exceed the permissible shear strain of the wallboard $\bar{\gamma}$ given in Table D4 of the specification. From Eqs. (9.43) through (9.48) it can be seen that the shear strain in the wallboard is affected by the initial imperfections of wall studs, for which some minimum values for sweep, camber, and possible twist of studs, are recommended in Eqs. (9.49) through (9.51) to represent the general practice.

Example 9.2   Use the ASD and LRFD methods to compute the allowable axial load for the C-section shown in Fig. 9.12 if it is to be used as wall studs having a length of 12 ft. Assume that the studs are spaced at every 12 in. and that $\frac{1}{2}$-in. thick gypsum boards are attached to both flanges of the stud. All fasteners are No. 6, type S-12, self-drilling drywall screws at 12-in. spacing. Use $F_y = 33$ ksi. Assume that the dead-to-live load ratio is 1/5.
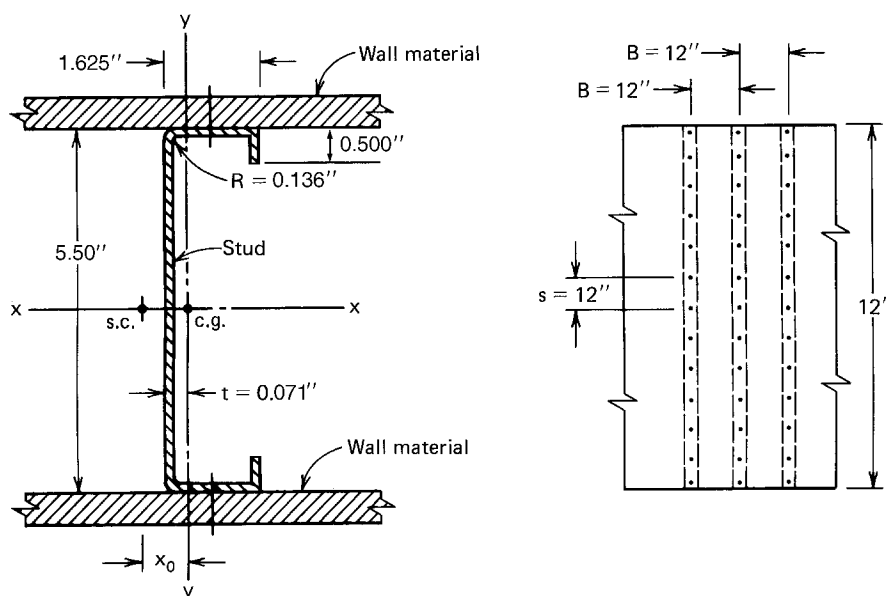
Figure 9.12   Example 9.2.

Solution

A. *ASD Method*

1. *Sectional Properties.* Using the methods discussed in Chaps. 4 and 5 and the AISI Design Manual the following sectional properties can be computed on the basis of the full area of the given C-section:

$$A = 0.651 \text{ in.}^2$$

$$I_x = 2.823 \text{ in.}^4$$

$$I_y = 0.209 \text{ in.}^4$$

$$r_x = 2.08 \text{ in.}$$

$$r_y = 0.566 \text{ in.}$$

$$J = 0.00109 \text{ in.}^4$$

$$C_w = 1.34 \text{ in.}^6$$

$$x_0 = 1.071 \text{ in.}$$

$$r_0 = 2.41 \text{ in.}$$

2. *Allowable Axial Load.* According to Sec. D4.1 of the AISI Specification, the allowable axial load for the given stud having identical sheathing attached to both flanges and neglecting any rotational restraint provided by the sheathing can be determined by Eq. (9.28) as follows:

$$P_a = A_e F_n / \Omega_c$$

In the above equation, the nominal buckling stress F_n is the lowest value determined by the following three conditions:

$(F_n)_1 =$ nominal buckling stress for column buckling of stud between fasteners in the plane of the wall
$(F_n)_2 =$ nominal buckling stress for flexural and/or torsional-flexural overall column buckling
$(F_n)_3 =$ nominal buckling stress to limit shear strain of wallboard to no more than the permissible value

      a. *Calculation of* $(F_n)_1$. In order to prevent column buckling of the study between fasteners in the plane of the wall, consideration should be given to flexural buckling and torsional–flexural buckling of the singly symmetric C-section. In the calculation of the elastic buckling stress, the effective length KL is taken to be two times the distance between fasteners.

      i. *Nominal buckling stress for flexural buckling*

$$KL = 2 \times \text{(spacing of screws)}$$
$$= 2 \times 12 = 24 \text{ in.}$$
$$\frac{KL}{r} = \frac{24}{r_y} = 42.40$$

Using Eq. (5.56)

$$F_e = \frac{\pi^2 E}{(KL/r)^2} = \frac{\pi^2(29,500)}{(42.40)^2} = 161.95 \text{ ksi}$$

$$\lambda_c = \sqrt{\frac{F_y}{F_e}} = \sqrt{\frac{33}{161.95}} = 0.451 < 1.5$$

From Eq. (5.54),

$$F_n = (0.658^{\lambda_c^2})F_y = (0.658^{0.451^2})(33)$$

$$= 30.31 \text{ ksi}$$

ii. *Nominal buckling stress for torsional–flexural buckling.* From Eq. (5.57),

$$F_e \frac{1}{2\beta} [(\sigma_{ex} + \sigma_t) - \sqrt{(\sigma_{ex} + \sigma_t)^2 - 4\,\beta\sigma_{ex}\sigma_t}]$$

where $\beta = 1 - \left(\dfrac{x_0}{r_0}\right)^2 = 0.803$

$$\sigma_{ex} = \frac{\pi^2 E}{(KL/r_x)^2} = \frac{\pi^2(29{,}500)}{(24/2.08)^2} = 2187 \text{ ksi}$$

$$\sigma_t = \frac{1}{Ar_0^2}\left[GJ + \frac{\pi^2 EC_w}{(KL)^2}\right]$$

$$= \frac{1}{0.651(2.41)^2}\left[11{,}300 \times 0.00109\right.$$
$$\left. + \frac{\pi^2(29{,}500)(1.34)}{(24)^2}\right]$$

$$= 182.4 \text{ ksi}$$

Therefore

$$F_e = 179.2 \text{ ksi}$$

$$\lambda_c = \sqrt{\frac{F_y}{F_e}} = \sqrt{\frac{33}{179.2}} = 0.429 < 1.5$$

From Eq. (5.54),

$$F_n = (0.658^{\lambda_c^2})F_y = (0.658^{0.429^2})(33)$$

$$= 30.55 \text{ ksi}$$

The governing nominal buckling stress is the smaller of the values F_n computed in items (i) and (ii) above, i.e.,

$$(F_n)_1 = 30.31 \text{ ksi}$$

b. *Calculation of* $(F_n)_2$. In order to prevent flexural and/or torsional–flexural overall column buckling, the theoretical elastic buckling stress F_e should be the smaller of the two σ_{CR} values computed for the singly symmetric C-section as follows:

For flexural overall column buckling,

$$\sigma_{CR} = \sigma_{ey} + \overline{Q}_a \tag{9.29}$$

For torsional–flexural overall column buckling,

$$\sigma_{CR} = \frac{1}{2\beta} [(\sigma_{ex} + \sigma_{tQ}) \\ - \sqrt{(\sigma_{ex} + \sigma_{tQ})^2 - 4\beta\sigma_{ex}\sigma_{tQ}}] \tag{9.30}$$

In Eq. (9.29)

$$\sigma_{ey} = \frac{\pi^2 E}{(KL/r_y)^2} = \frac{\pi^2(29,500)}{(12 \times 12/0.566)^2} = 4.50 \text{ ksi}$$

$$\overline{Q}_a = \frac{\overline{Q}}{A}$$

From Eq. (9.40) and Table D4 of the AISI Specification,

$$\overline{Q} = \overline{Q}_o (2 - s/s') = (24.0)(2 - 12/12)$$

$$= 24 \text{ kips}$$

$$\overline{Q}_a = \frac{24}{0.651} = 36.87 \text{ ksi}$$

According to Eq. (9.29), the theoretical elastic critical buckling stress is

$$\sigma_{CR} = 4.50 + 36.87 = 41.37 \text{ ksi} \tag{9.29a}$$

In Eq. (9.30),

$$\beta = 0.803$$

$$\sigma_{ex} = \frac{\pi^2 E}{(KL/r_x)^2} = \frac{\pi^2(29,500)}{(12 \times 12/2.08)^2} = 60.75 \text{ ksi}$$

$$\sigma_{tQ} = \sigma_t + \overline{Q}_t$$

where $\sigma_t = \dfrac{1}{Ar_0^2} \left(GJ + \dfrac{\pi^2 E C_w}{L^2} \right)$

$$= \frac{1}{0.651(2.41)^2} \left[11,300 \times 0.00109 + \frac{\pi^2(29,500)(1.34)}{(12 \times 12)^2} \right]$$

$$= 8.23 \text{ ksi}$$

$$\overline{Q}_t = \frac{\overline{Q}d^2}{4Ar_0^2}$$
$$= \frac{(24)(5.50)^2}{4(0.651)(2.41)^2} = 48.00 \text{ ksi}$$

and

$$\sigma_{tQ} = 8.23 + 48.00 = 56.23 \text{ ksi}$$

From Eq. (9.30),

$$\sigma_{CR} = \frac{1}{2(0.803)} [(60.75 + 56.23)$$
$$- \sqrt{(60.75 + 56.23)^2 - 4(0.803)(60.75)(56.23)}]$$
$$= 40.41 \text{ ksi} \tag{9.30a}$$

Use the smaller value given in Eqs. (9.29a) and (9.30a)

$$F_e = 40.41 \text{ ksi}$$
$$\lambda_c = \sqrt{\frac{F_y}{F_e}} = \sqrt{\frac{33}{40.41}} = 0.904 < 1.5$$

From Eq. (5.54),

$$(F_n)_2 = (0.658^{\lambda_c^2})F_y = (0.658^{0.904^2})(33)$$
$$= 23.44 \text{ ksi}$$

c. *Calculation of* $(F_n)_3$. In items (a) and (b) it was found that in order to prevent column buckling, the nominal buckling stress should not exceed 23.44 ksi. According to Sec. D4.1(c) of the AISI Specification, in order to prevent shear failure of the sheathing, a value of F_n should be used in the given equations so that the shear strain of the sheathing, γ, computed by Eq. (9.43) does not exceed the permissible value of $\overline{\gamma} = 0.008$ in./in., which is given in Table D4 of the AISI Specification for $\frac{1}{2}$-in.-thick gypsum board.

Based on Eq. (9.43), the shear strain of the sheathing can be computed as follows:

$$\gamma = \frac{\pi}{L}\left(C_1 + E_1 \frac{d}{2}\right) \tag{9.43}$$

where

$$C_1 = \frac{F_n C_0}{\sigma_{ey} - F_n + \overline{Q}_a} \tag{9.44}$$

$$E_1 = \frac{F_n[(\sigma_{ex} - F_n)(r_0^2 E_0 - x_0 D_0) - F_n x_0 (D_0 - x_0 E_0)]}{(\sigma_{ex} - F_n) r_0^2 (\sigma_{tQ} - F_n) - (F_n x_0)^2} \tag{9.45}$$

As the first approximation, let

$$F_n = (F_n)_2 \text{ of item } b = 23.44 \text{ ksi}$$

$$C_0 = \frac{L}{350} = \frac{12 \times 12}{350} = 0.411 \text{ in.}$$

$$E_0 = \frac{L}{d \times 10,000} = \frac{12 \times 12}{5.50 \times 10,000} = 0.0026 \text{ rad.}$$

$$D_0 = \frac{L}{700} = \frac{12 \times 12}{700} = 0.206 \text{ in.}$$

Therefore, from Eqs. (9.44) and (9.45),

$$C_1 = \frac{23.44 \times 0.411}{(4.50 - 23.44 + 36.87)} = 0.537$$

$$E_1 = \frac{\begin{array}{c} 23.44[(60.75 - 23.44)(2.41^2 \times 0.0026 - 1.071 \times 0.206) \\ - 23.44 \times 1.071(0.206 - 1.071 \times 0.0026)] \end{array}}{(60.75 - 23.44)(2.41)^2(56.23 - 23.44) - (23.44 \times 1.071)^2}$$

$$= -0.0462$$

Use an absolute value, $E_1 = 0.0462$
Substituting the values of C_1, E_1, L, and d into Eq. (9.43), the shear strain is

$$\gamma = \left(\frac{\pi}{12 \times 12}\right)\left[0.537 + \frac{0.0462 \times 5.5}{2}\right]$$

$$= 0.0145 \text{ in./in.} > (\overline{\gamma} = 0.008 \text{ in./in.})$$

Since the computed γ value for $F_n = 23.44$ ksi is larger than the permissible $\overline{\gamma}$ value, a smaller F_n value should be used. After several trials, it was found that a value of $F_n = 17.50$ ksi would give the permissible shear strain of 0.008 in./in. as shown below.

Try $F_n = 17.50$ ksi

Since $F_n > (F_y/2 = 16.5$ ksi), use E' and G' to compute the values of σ_{ex}, σ_{ey}, σ_t, and σ_{tQ}.

$$E' = 4EF_n(F_y - F_n)/F_y^2$$
$$= 4(E)(17.50)(33 - 17.50)/(33)^2 = 0.996E, \text{ ksi.}$$

$$G' = G(E'/E) = 0.996G \text{ ksi}$$

$$\sigma_{ex} = 60.75 \left(\frac{E'}{E}\right) = 60.51 \text{ ksi}$$

$$\sigma_{ey} = 4.50 \left(\frac{E'}{E}\right) = 4.48 \text{ ksi}$$

$$\sigma_t = 8.23 \left(\frac{E'}{E}\right) = 8.20 \text{ ksi}$$

$$\sigma_{tQ} = \sigma_t + \overline{Q}_t = 8.20 + 48.00 = 56.20$$

$$C_1 = 0.302 \text{ in.}$$

$$E_1 = 0.0238 \text{ rad.}$$

and $\gamma = 0.008$ in./in. $= (\overline{\gamma} = 0.008$ in./in.)   O.K.
Therefore $(F_n)_3 = 17.50$ ksi.

d. *Determination of F_n.* From items (a), (b), and (c), the following three values of nominal buckling stress were computed for different design considerations:

$$(F_n)_1 = 30.31 \text{ ksi}$$
$$(F_n)_2 = 23.44 \text{ ksi}$$
$$(F_n)_3 = 17.50 \text{ ksi}$$

The smallest value of the above three stresses should be used for computing the effective area and the allowable axial load for the given C-section stud. i.e.,

$$F_n = 17.50 \text{ ksi}$$

e. *Calculation of the effective area.* The effective area should be computed for the governing nominal buckling stress of 17.50 ksi.

i. *Effective width of compression flanges (Art. 3.5.3.2)*

$$S = 1.28\sqrt{E/f} = 1.28\sqrt{29,500/17.50} = 53.55$$

$$S/3 = 17.52$$

$$w_1/t = [1.625 - 2(0.136 + 0.071)]/0.071$$

$$= 1.211/0.071 = 17.06$$

Since $w_1/t < S/3$, $b_1 = w_1 = 1.211$ in.
The flanges are fully effective.

ii. *Effective width of edge stiffeners (Art. 3.5.3.2)*

$$w_2/t = [0.500 - (0.136 + 0.071)]/0.071$$

$$= 0.293/0.071 = 4.13 < 14 \qquad \text{O.K.}$$

$$\lambda = \frac{1.052}{\sqrt{k}}\left(\frac{w_2}{t}\right)\sqrt{\frac{f}{E}} = \frac{1.052}{\sqrt{0.43}}(4.13)\sqrt{\frac{17.50}{29,500}}$$

$$= 0.161 < 0.673$$

$$d_s' = w_2 = 0.293 \text{ in.}$$

$$d_s = d_s' = 0.293 \text{ in.}$$

The edge stiffeners are fully effective.

iii. *Effective width of webs (Art. 3.5.1.1)*

$$w_3/t = [5.50 - 2(0.136 + 0.071)]/0.071$$

$$= 5.086/0.071 = 71.63$$

$$\lambda = \frac{1.052}{\sqrt{4}}(71.63)\sqrt{\frac{17.50}{29,500}} = 0.918 > 0.673$$

$$\rho = (1 - 0.22/\lambda)/\lambda = (1 - 0.22/0.918)/0.918$$

$$= 0.828$$

$$b_3 = \rho w_3 = 0.828\,(5.086) = 4.211 \text{ in.}$$

iv. *Effective area, A_e*

$$A_e = A - (w_3 - b_3)(t) = 0.651 - (5.086 - 4.211)(0.071)$$

$$= 0.589 \text{ in.}^2$$

f. *Nominal axial load and allowable axial load.* Based on $F_n = 17.50$ ksi and $A_e = 0.589$ in.^{2}, the nominal axial load is

$$P_n = A_e F_n = (0.589)(17.50) = 10.31 \text{ kips}$$

The allowable axial load is

$$P_a = \frac{P_n}{\Omega_c} = \frac{10.31}{1.80} = 5.73 \text{ kips}$$

B. *LRFD Method*

For the LRFD method, the design strength is

$$\phi_c P_n = (0.85)(10.31) = 8.76 \text{ kips}$$

Based on the load combinations given in Art. 3.3.2.2, the governing required axial load is

$$P_u = 1.2 P_D + 1.6 P_L = 1.2 P_D + 1.6(5 P_D) = 9.2 P_D$$

Using $P_u = \phi_c P_n$,

$$P_D = 8.76/9.2 = 0.95 \text{ kips}$$

$$P_L = 5 P_D = 4.75 \text{ kips}$$

The allowable axial load is

$$P_a = P_D + P_L = 5.70 \text{ kips}$$

It can be seen that both ASD and LRFD methods give approximately the same result for this particular case. It should also be noted that the C-section stud used in this example is selected from page I-12 of the 1996 edition of the *AISI Cold-Formed Steel Design Manual.*[1.159] This C-section with lips is designated as 5.5CS1.625 × 071. The North American Steel Framing Alliance (NASFA) has recently announced the new universal designator systems for cold-formed steel studs, joists and track sections. For details, see Ref. 9.109 or visit the NASFA website: www.steel-framingalliance.com.

The preceding discussion and Example 9.2 dealt with the wall studs under concentric loading. For studs subjected to axial load and bending moment, the design strength of the studs should be determined according to Sec. D4.3 of the AISI Specification. A study of wall studs with combined compression and lateral loads was reported in Ref. 9.66. Additional studies on the behavior

of steel wall stud assemblies and developments of a structural system using cold-formed steel wall studs have been conducted and reported in Refs. 9.93 through 9.95.

For fire-resistance ratings of load-bearing steel stud walls with gypsum wallboard protection, the reader is referred to the AISI publication.[9.67,1.277]

9.4   SHELL ROOF STRUCTURES

9.4.1   Introduction

Steel folded-plate and hyperbolic paraboloid roof structures have been used increasingly in building construction for churches, auditoriums, gymnasiums, classrooms, restaurants, office buildings, and airplane hangars.[1.77–1.84,9.68–9.76] This is because such steel structures offer a number of advantages as compared with some other types of folded-plate and shell roof structures to be discussed. Since the effective use of steel panels in roof construction is not only to provide an economical structure but also to make the building architecturally attractive and flexible for future change, structural engineers and architects have paid more attention to steel folded-plate and hyperbolic paraboloid roof structures during recent years.

The purpose of this discussion is mainly to describe the methods of analysis and design of folded-plate and hyperbolic paraboloid roof structures which are currently used in engineering practice. In addition, it is intended to review briefly the research work relative to steel folded-plate and shell roof structures and to compare the test results with those predicted by analysis.

In this discussion, design examples will be used for illustration. The shear strength of steel panels, the empirical formulas to determine deflection, and the load factors used in various examples are for illustrative purposes only. Actual design values and details of connections should be based on individual manufacturers' recommendations on specific products.

9.4.2   Folded-Plate Roofs

9.4.2.1   General Remarks   A folded-plate structure is a three-dimensional assembly of plates. The use of steel panels in folded-plate construction started in this country about 1960. Application in building construction has increased rapidly during recent years. The design method used in engineering practice is mainly based on the successful investigation of steel shear diaphragms and cold-formed steel folded-plate roof structures.[1.77–1.81,1.84,9.1,9.2,9.70]

9.4.2.2   Advantages of Steel Folded-Plate Roofs   Steel folded-plate roofs are being used increasingly because they offer several advantages in addition to the versatility of design:

1. *Reduced Dead Load.* A typical steel folded plate generally weighs about 11 lb/ft^2 (527 N/m^2), which is substantially less than some other types of folded plates.
2. *Simplified Design.* The present design method for steel plates roofs is simpler than the design of some other types of folded plates, as discussed later.
3. *Easy Erection.* Steel folded-plate construction requires relatively little scaffolding and shoring. Shoring can be removed as soon as the roof is welded in place.

9.4.2.3   Types of Folded-Plate Roofs   Folded-plate roofs can be classified into three categories: single-bay, multiple-bay, and radial folded plate, as shown in Fig. 9.13. The folded plates can be either prismatic or nonprismatic.

The sawtooth folded-plate roof shown in Fig. 9.13*b* has been found to be the most efficient multiple-bay structure and is commonly used in building construction. Figure 9.14 shows a folded-plate structure of the sawtooth type used for schools.
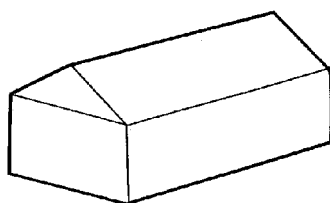
(a)
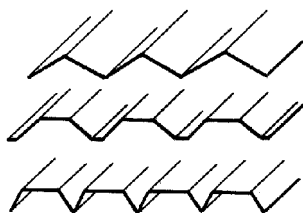
(b)
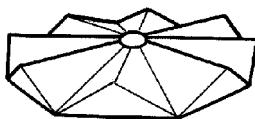
(c)

Figure 9.13   Types of folded-plate roofs. (*a*) Single-bay. (*b*) Multiple-bay. (*c*) Radial.

Figure 9.14   Cold-formed steel panels used in folded-plate roof. (*H. H. Robertson Company.*)

9.4.2.4   Analysis and Design of Folded Plates   A folded-plate roof structure consists mainly of three components, as shown in Fig. 9.15:

1. Steel roof panels.
2. Fold line members at ridges and valleys.
3. End frames or end walls.

In general, the plate width (or the span length of roof panels) ranges from about 7 to 12 ft (2.1 to 3.7 m), the slope of the plate varies from about 20° to 45°, and the span length of the folded plate may be up to 100 ft (30.5 m).
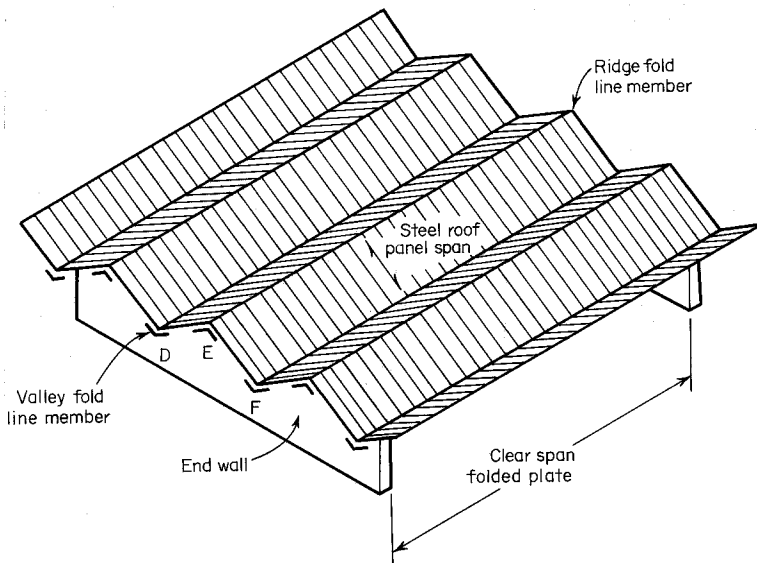
Figure 9.15   Folded-plate structure.

Since unusually low roof slopes will result in excessive vertical deflections and high diaphragm forces, it is not economical to design a roof structure with low slopes.

In the analysis and design of folded-plate roofs, two methods are available to engineers. They are the simplified method and the finite-element method. The former provides a direct technique that will suffice for use in the final design for many structures. The latter permits a more detailed analysis for various types of loading, support, and material.[1.81]

In the simplified method, steel roof panels as shown in Fig. 9.15 are designed as simply supported slabs in the transverse direction between fold lines. The reaction of the panels is then applied to fold lines as a line loading, which resolves itself into two components parallel to the two adjacent plates, as shown in Fig. 9.16. These load components are then carried by an inclined deep girder spanned between end frames or end walls (Fig. 9.15). These deep girders consist of fold line members as flanges and steel panels as a web element. The longitudinal flange force in fold line members can be obtained by dividing the bending moment of the deep girder by its depth. The shear force is resisted by the diaphragm action of the steel roof panels. Therefore the shear diaphragm discussed in Art. 9.2 is directly related to the design of the folded-plate structure discussed in this article.

In the design of fold line members, it is usually found that the longitudinal flange force is small because of the considerable width of the plate. A bent plate or an angle section is often used as the fold line member.

Referring to Fig. 9.15, an end frame or end wall must be provided at the ends of the folded plates to support the end reaction of the inclined deep girder. In the design of the end frame or end wall, the end reaction of the plate may be considered to be uniformly distributed through the entire depth of the girder. Tie rods between valleys must be provided to resist the horizontal thrust. If a rigid frame is used, consideration should be given to such a horizontal thrust.

When a masonry bearing wall is used, a steel welding plate should be provided at the top of the wall for the attachment of panels. It should be capable of resisting the force due to the folded-plate action.

Along the longitudinal exterior edge, it is a general practice to provide a vertical edge plate or longitudinal light framing with intermittent columns to
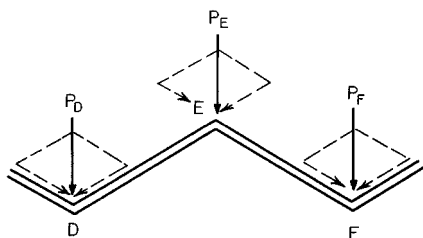
Figure 9.16   Force components along fold lines.

carry vertical loads. If an exterior inclined plate is to cantilever out from the fold line, a vertical edge plate will not be necessary.

In addition to the consideration of beam strength, the deflection character-istics of the folded-plate roof should also be investigated, particularly for long-span structures. It has been found that a method similar to the Williot diagram for determining truss deflections can also be used for the prediction of the deflection of a steel folded-plate roof. In this method the in-plane deflection of each plate should first be computed as a sum of the deflections due to flexure, shear, and seam slip, considering the plate temporarily sepa-rated from the adjacent plates. The true displacement of the fold line can then be determined analytically or graphically by a Williot diagram. When deter-mining flexural deflection, the moment of inertia of the deep girder may be based on the area of the fold line members only. The shear deflection and the deflection due to seam slip should be computed by the empirical formulas recommended by manufacturers for the specific panels and the system of connection used in the construction. In some cases it may be found that the deflection due to seam slip is negligible.

Example 9.3   Discuss the procedures to be used for the design of an interior plate of a multiple-bay folded-plate roof (Fig. 9.17) by using the simplified ASD method.
Given:

Uniform dead load w_D, psf (along roof surface).
Uniform live load w_L, psf (on horizontal projection).
Span L, ft.
Unit width B, ft.
Slope distance b between fold lines, ft (or depth of analogous plate girder).

Solution

1. *Design of Steel Panels—Slab Action in Transverse Direction*

$$M_1 = \tfrac{1}{8} \times w_L B^2 + \tfrac{1}{8} w_D bB \quad \text{ft-lb}$$

Select a panel section to meet the requirements of beam design and deflection criteria.
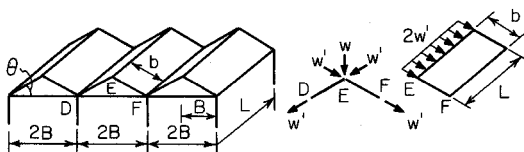
Figure 9.17   Example 9.3.

2. *Design of Fold Line Members.* The vertical line loading is

$$w = w_L B + w_D b \quad \text{lb/ft}$$

The load component in the direction of the inclined girder is w'. The total load applied to the inclined deep girder EF is $2w'$.

$$M_2 = \frac{1}{8} \times 2w'L^2 \quad \text{ft-lb}$$

Select a fold line member to satisfy the required moment.

3. *Design for Plate Shear*

$$V = 2w' \times \frac{L}{2} = w'L \quad \text{lb}$$

$$v = \frac{V}{b} \quad \text{lb/ft}$$

Select an adequate welding system on the basis of the manufacturer's recommendations.

4. *Deflection*

   a. *In-plane flexural deflection* (considering that the inclined plate is temporarily separated)

   $$\Delta_b = \frac{5}{384} \times \frac{2w'L^4}{EI} (12) \quad \text{in.}$$

   where

   $$I = 2A_f \left(\frac{b}{2} \right)^2$$

   $$E = 29.5 \times 10^6 \text{ psi}$$

   b. *In-plane shear deflection* (including the deflection due to seam slip)

   $$\Delta_s = \frac{2w'L^2}{2G'b} \quad \text{in.}$$

   where G' is the shear stiffness of steel panels obtained from diaphragm tests, lb/in. See Art. 9.2.

c. *Total in-plane deflection*

$$\Delta = \Delta_b + \Delta_s \quad \text{in.}$$

d. *Total vertical deflection.* After the in-plane deflection is computed, the maximum vertical deflection of fold line members can be determined by a Williot diaphragm, as shown in Fig. 9.18.

9.4.2.5   Research on Folded-Plate Roofs   Full-size folded-plate assemblies have been tested by Nilson at Cornell University[1.77] and by Davies, Bryan, and Lawson at the University of Salford.[9.77] The following results of tests were discussed in Ref. 1.77 for the Cornell work.

The test assembly used by Nilson was trapezoidal in cross section and was fabricated from $1\frac{1}{2}$-in. (38-mm) deep cold-formed steel panels as plates (five plates) and $3\frac{1}{2} \times \frac{1}{4} \times 3\frac{1}{2}$-in. ($89 \times 6.4 \times 89$-mm) bent plate as fold line members. The span length of the test structure was 42 ft 6 in. (13 m), and the width of the assembly was 14 ft (4.3 m), as shown in Fig. 9.19. The test setup is shown in Fig. 9.20. It should be noted that the jack loads were applied upward because of the convenience of testing.

In Ref. 1.77 Nilson indicated that the experimental structure performed in good agreement with predictions based on the simplified method of analysis, which was used in Example 9.3. It was reported that the tested ultimate load was 11% higher than that predicted by analysis and that the observed stresses in fold line members were about 20% lower than indicated by analysis due to the neglect of the flexural contribution of the steel panel flat plate elements. In view of the fact that this difference is on the safe side and the size of the fold line members is often controlled by practical considerations and clearance requirements rather than by stress, Nilson concluded that no modification of the design method would be necessary. As far as the deflection of the structure is concerned, the measured values were almost exactly as predicted.

In the 1960s, AISI sponsored a research project on cold-formed steel folded plates at Arizona State University to study further the methods of analysis and design of various types of folded-plate roofs, including rectangular and
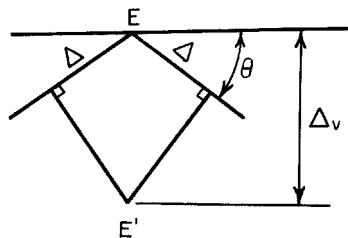
Figure 9.18   Williot diagram used for determining total vertical deflection.
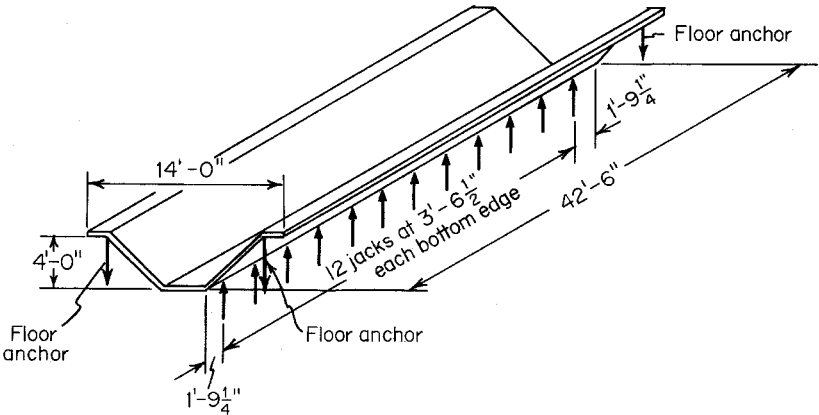
Figure 9.19 Steel folded-plate assembly.[1.77]

circular planforms. In this project, both the simplified analysis and the finite-element approach were studied in detail by Schoeller, Pian, and Lundgren.[1.81]

For a multiple sawtooth folded-plate structure with a span of 40 ft (12.2 m), the analytical results obtained from the simplified method and the finite-element method are compared as follows:[1.81]
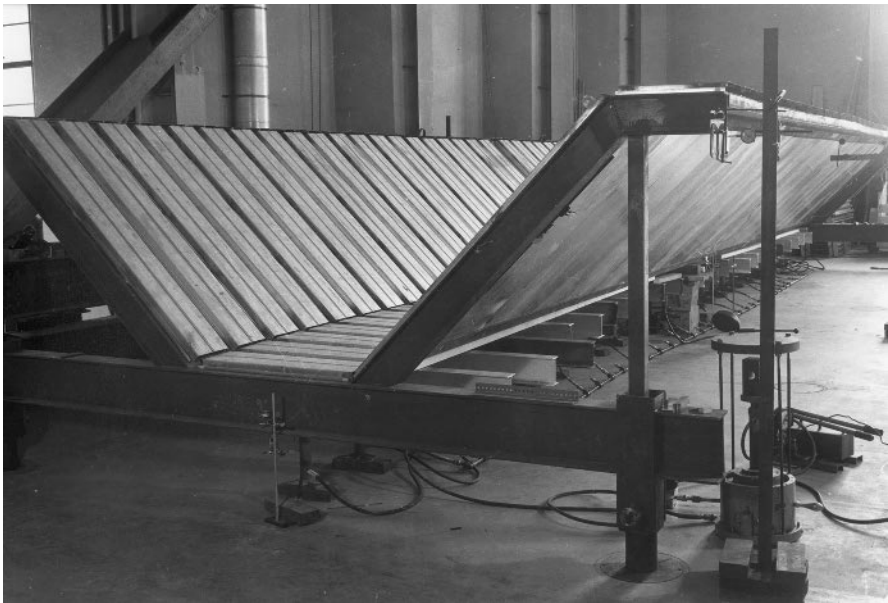
Figure 9.20 Setup for test of folded-plate assembly.[1.77]

	Simplified Method	Finite-Element Method
Maximum fold line force, lb	22,500	23,400
Maximum plate shear, lb/ft	1,024	958

9.4.2.6   Truss-Type Folded-Plate Roofs   The above discussion is related to the analysis and design of membrane-type folded-plate roofs in which the steel roof panels not only support normal loads but also resist shear forces in their own planes. This type of structure is generally used for spans of up to about 100 ft (30.5 m).

For long-span structures, a folded-plate roof may be constructed by utilizing inclined simple trusses as basic units, covering them with steel panels. In this case steel panels will resist normal loads only. The design of basic trusses is based on the conventional method. Additional information on the design and use of folded-plate roofs can be found in Refs. 1.84 and 9.78.

9.4.3   Hyperbolic Paraboloid Roofs

9.4.3.1   General Remarks   The hyperbolic paraboloid roof has also gained increasing popularity during recent years due to the economical use of materials and its attractive appearance. The hyperbolic paraboloid shell is a doubly curved surface which seems difficult to construct from steel but in fact can be built easily with either single-layer or double-layer standard steel roof deck panels. This is so because the doubly-curved surface of a hyperbolic paraboloid has the practical advantage of straight line generators as shown in Fig. 9.21.

Figure 1.14 shows the Frisch restaurant building in Cincinnati, Ohio, which consists of four paraboloids, each 33.5 ft (10.2 m) square, having a common column in the center and four exterior corner columns, giving a basic building of 67 ft (20.4 m) square. The roof of the building is constructed of laminated $1\frac{1}{2}$-in. (38-mm) steel deck of 26-in. (660-mm) wide panels. The lower layer
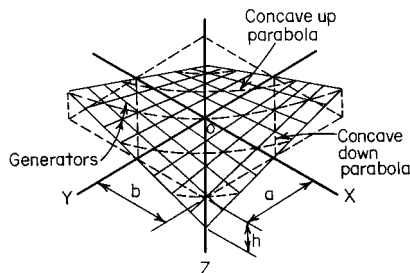
Figure 9.21   Surface of hyperbolic paraboloid.[9.79]

is 0.0516-in. (1.3-mm) thick steel panels, and the upper layer is 0.0396-in. (1-mm)-thick steel panels placed at right angles and welded together. The reason for using a two-layer laminated hyperbolic paraboloid roof was to achieve additional stiffness and resistance to point loading. The use of 0.0516-in. (1.3-mm)-thick steel panels in the lower layer was for ease of welding. The roof plan and the structure details of the Frisch restaurant building, designed by H. T. Graham, are shown in Fig. 9.22.

In 1970 Zetlin, Thornton, and Tomasetti used hyperbolic paraboloids to construct the world's largest cold-formed steel superbay hangars for the American Airlines Boeing 747s in Los Angeles and San Francisco, California (Fig. 1.15).[1.82] The overall dimensions of the building shown in Fig. 9.23 are 450 ft (137 m) along the door sides and 560 ft (171 m) at the end wall. The central core of the building is 100 ft (30.5 m) wide and 450 ft (137 m) long. The hangar area is covered by a 230-ft (70-m) cantilever on each side of the core.
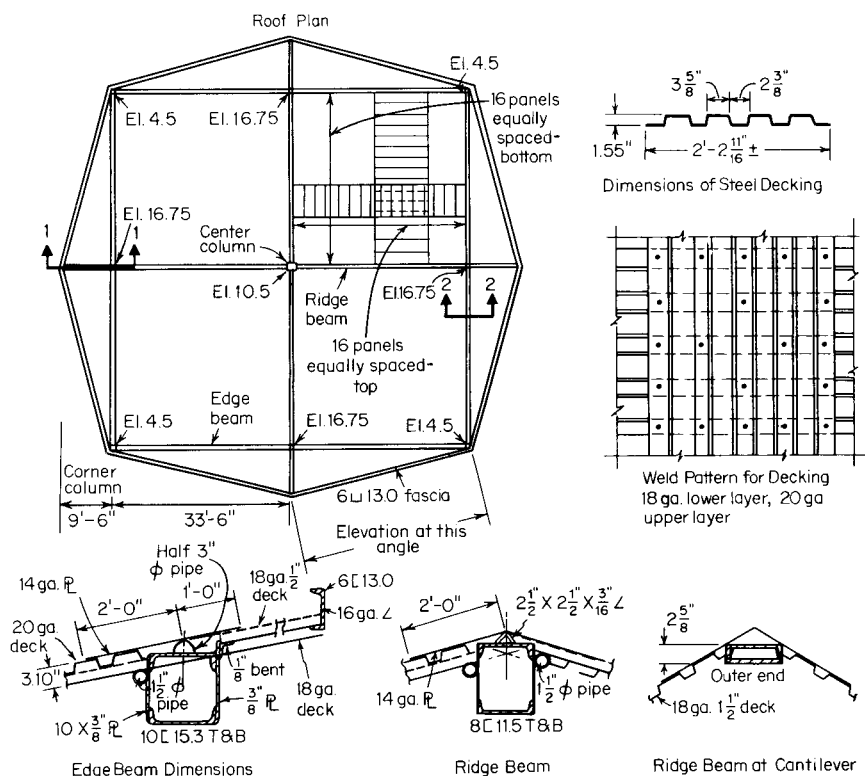
Figure 9.22   Roof plan and structural details of Frisch Restaurant, Cincinnati, Ohio, of hyperbolic paraboloid construction. (*Reprinted from Architectural Record, March 1962, copyrighted by McGraw-Hill Book Co., Inc.*)[1.79]
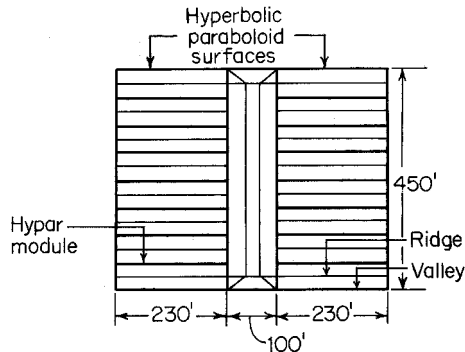
Figure 9.23   Roof plan of superbay hangar. (*Lev Zetlin Associates, Inc.*)[1.82]

As shown in Figs. 9.23 and 9.24, the roof system is composed of 16 basic structural modules. Each roof module consists of a ridge member, two valley members, edge members, and the warped hyperbolic paraboloids, as indicated in Fig. 9.24. The ridge and valley members are hot-rolled steel shapes. The hyperbolic paraboloids were made of cold-formed steel decking consisting of a flat 0.0934-in. (2.4-mm)-thick sheet, 26 in. (660 mm) wide, with two 9-in. (229-mm) wide by $7\frac{1}{2}$-in. (191-mm) deep 0.0516-in. (1.3-mm)-thick steel hat sections welded to the flat sheets. Figure 9.25 shows typical cross section of the steel deck used.

In order to be able to use this type of structural system in any area of the world, prestressed cables are incorporated into the shell structures (Fig. 9.26). Since the structural strand cables induce a prestress in the shell, the system is readily adaptable to any geographic site.
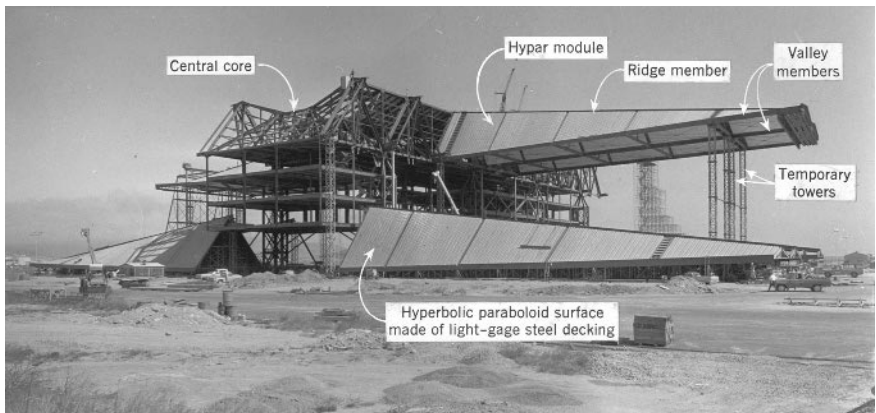
Figure 9.24   Construction of superbay hangar. (*Lev Zetlin Associates, Inc.*)[1.82]
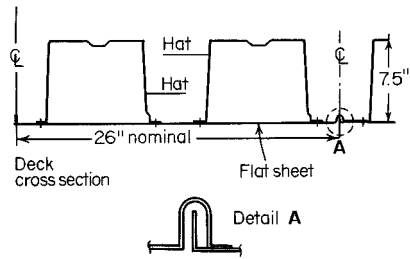
Figure 9.25 Cross section of steel deck used in superbay hangar. (*Lev. Zetlin Associates, Inc.*)[1.82]

A comparison of various types of designs indicate that this type of building with its hyperbolic paraboloids weighs approximately 40% less than a conventional steel construction.

9.4.3.2 *Types of Hyperbolic Paraboloid Roofs* The surface of a hyperbolic paraboloid may be defined by two methods.[1.80] As shown in Fig. 9.21, with the *x*-, *y*-, and *z*-axes mutually perpendicular in space, the surface is formu-
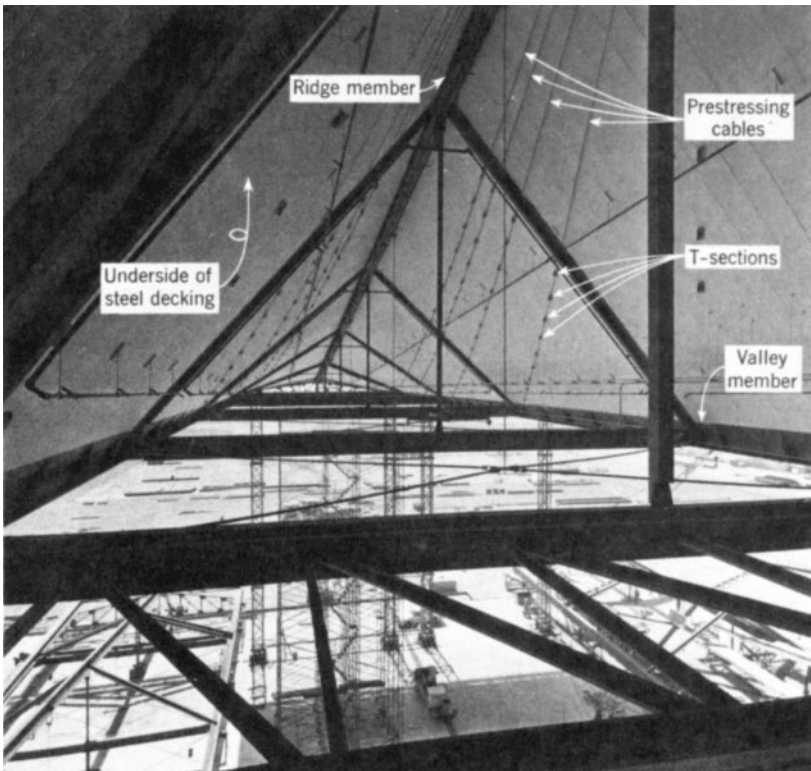
Figure 9.26 Prestressed cables used in hangar roof. (*Lev Zetlin Associates, Inc.*)[1.82]

lated by two straight lines called generators. One line, parallel to the xz plane, rotates about and moves along the *y*-axis; the other, parallel to the *yz* plane, rotates about and moves along the *x*-axis. The intersection of the generators is contained in the surface of the hyperbolic paraboloid.

Figure 9.27 shows several types of hyperbolic paraboloid roofs which may be modified or varied in other ways to achieve a striking appearance.

In general, type I is the most pleasing of the shapes available. The edge beams are in compression and are usually tubular members. For this type of roof, the most serious problem is the horizontal thrust at the supporting columns. Usually the columns are kept short in order to transfer the thrust down to the floor where tie rods can be hidden. Four units of this type with a common center column probably provide the most rigid roof structure, as shown in Fig. 1.14.

Type II is an inverted umbrella, which is the easiest and the least expensive to build. The edge members of this type are in tension, and engineers usually use angles as edge members.

Type III is the most useful type for canopy entrance structures. The edge members connected to the columns are in compression and are usually tubes, while the outside edge members are in tension and could be angles or channels. In some cases, one half of the roof may be kept horizontal and the other half tilts up.

Generally speaking, type IV is the most useful of all the available shapes. The entire building can be covered with a completely clear span. The horizontal ties between columns on four sides can be incorporated in the wall construction.

9.4.3.3 Analysis and Design of Hyperbolic Paraboloid Roofs
The selection of the method of analysis of hyperbolic paraboloid roofs depends on the curvature of the shell used. If the uniformly loaded shell is deep (i.e., when
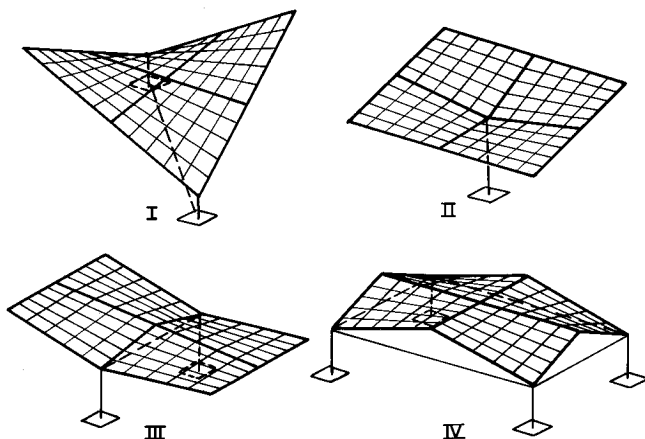
Figure 9.27 Types of hyperbolic paraboloid roofs.

the span-to-corner-depression ratio a/h shown in Fig. 9.21 is less than or equal to approximately 5.0), the membrane theory may be used. For the cases of a deep shell subjected to unsymmetrical loading and a shallow shell, the finite-element method will provide accurate results.[9.80]

In the membrane theory, the equation of the surface of a hyperbolic paraboloid can be defined from Fig. 9.28. Since

$$\frac{h}{c} = \frac{b}{x} \quad \text{and} \quad \frac{c}{z} = \frac{a}{y} \tag{9.60}$$

$$z = \frac{cy}{a} = \frac{hxy}{ab} = kxy \tag{9.61}$$

where $k = h/ab$, in which h is the amount of corner depression of the surface having the horizontal projections a and b.

If we rotate coordinate axes x and y by 45°, as shown in Fig. 9.29, the equations for two sets of parabolas can be obtained in terms of the new coordinate system using x' and y'.[9.81] Substituting

$$x = x' \cos 45° - y' \sin 45° \tag{9.62}$$

$$y = y' \cos 45° + x' \sin 45° \tag{9.63}$$

into Eq. (9.61), one can obtain a new equation for z in terms of x' and y',

$$z = \frac{1}{2} k[x'^2 - y'^2] \tag{9.64}$$

In Eq. (9.64), if the value of x' remains constant, as represented by line $a'-a'$ in Fig. 9.30, the equation for the parabolic curve can be written as

Figure 9.28   Dimensions used for defining the surface of hyperbolic paraboloid roof.

Figure 9.29 Coordinate system using x'- and y'-axes.

$$z' = -\frac{1}{2} ky'^2 \tag{9.65}$$

in which the negative sign indicates concave downward.

When the value of y' remains constant, Eq. (9.66) can be obtained for a concave upward parabola:

$$z' = \frac{1}{2} ky'^2 \tag{9.66}$$

For a constant value of z, the hyperbolic curve can be expressed by

$$\frac{2z}{k} = x'^2 - y'^2 \tag{9.67}$$

Figure 9.31 shows a concave downward parabolic arch subjected to a uni-
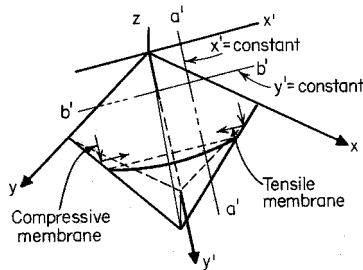
Figure 9.30 Sketch used for deriving equations for parabolic and hyperbolic curves.
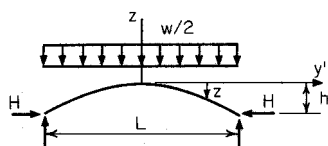
Figure 9.31   Concave downward parabolic arch.

form load of $w/2$, where w is the roof load per square foot. Since the bending moment throughout a parabolic arch supporting only a uniform load equals zero,

$$H(-h) = \frac{(w/2)L^2}{8} \tag{9.68}$$

$$H = -\frac{wL^2}{16h} \tag{9.69}$$

Use Eq. (9.65) for $y' = L/2$ and $z' = h$ then

$$h = -\frac{kL^2}{8} \tag{9.70}$$

Substituting the value of h in Eq. (9.69), one obtains Eq. (9.71) for the horizontal thrust H,

$$H = \frac{wab}{2h} \tag{9.71}$$

The above analogy can also be used for the concave upward parabolic tie.

It can be seen that if the load is applied uniformly over the horizontal projection of the surface, compressive membrane stress results in the concave downward parabolas, and tensile membrane stress results in the concave upward parabolas. These tensile and compressive membrane stresses are uniform throughout the surface and are equal to $wab/2h$, in which w is the applied load per unit surface area (Fig. 9.32). Since the compressive and tensile membrane stresses are equal in magnitude and are perpendicular to each other, a state of pure shear occurs in planes of 45° from the direction of either membrane stress. Thus only shear stress need be transmitted along the joints of the panels. The force in edge beams resulting from the shear of $q = wab/2h$ along the edge members is shown in Fig. 9.32.

Example 9.4 illustrates the design of an inverted hyperbolic umbrella by using the membrane theory.
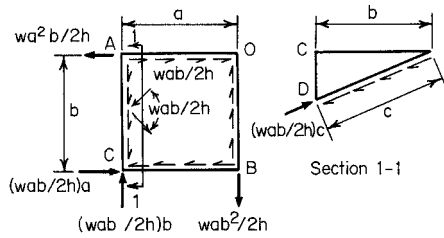
Figure 9.32 Membrane and shear stresses in panels and forces in framing members.

Example 9.4 Use the ASD method to design the inverted steel hyperbolic paraboloid umbrella roof shown in Fig. 9.33[9.76] for $w = 30$ psf on horizontal projection. Use A36 steel for framing members.

Solution

1. *Determination of Panel Shear.* The panel shear can be determined as follows:

$$v = \frac{wa^2}{2h} = \frac{30 \times (15)^2}{2 \times 4} = 845 \text{ lb/ft}$$

In accordance with Sec. D5 of the AISI Specification (Table 9.1), the factor of safety for gravity load alone is 2.45 for welded connections. The required ultimate shear strength of the roof deck system is therefore
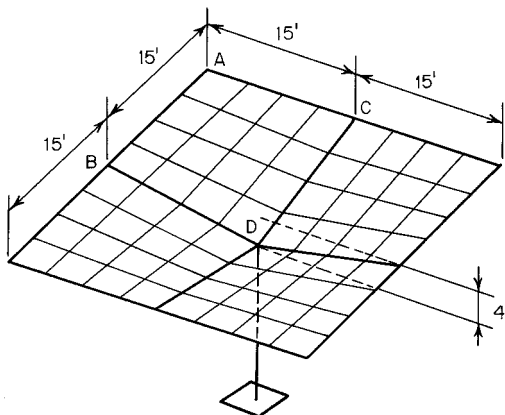
Figure 9.33 Example 9.4.

$$v_u = 845(2.45) = 2070 \text{ lb/ft}$$

2. *Selection of Steel Roof Deck.* Select a type of steel roof deck from catalogs to satisfy the following requirements:
   a. Flexural strength
   b. Shear strength
   c. Deflection
3. *Design of Framing Members*
   a. *Tension members AB and AC.* Considering the quadrant *ABCD* as shown in Fig. 9.34, the tensile force is

$$T = va = \left(\frac{wa^2}{2h}\right) a = 845(15) = 12,680 \text{ lb}$$

Using the AISC ASD Specification with an allowable stress of 22 ksi for A36 steel, the required area is

$$A = \frac{T}{F} = \frac{12.68}{22} = 0.58 \text{ in.}^2$$

Using L4 × 3 × $\frac{1}{4}$ in., the actual area is 1.69 in.^{2}

   b. *Compression members BD and CD.* Considering sec. 1-1 of Fig. 9.34, the compressive force is

$$C = vc = \left(\frac{wa^2}{2h}\right) c = 845(15.55) = 13,140 \text{ lb}$$

Since the compression member will support two quadrants, the total compressive force for design is

$$C' = 2C = 2(13,140) = 26,280 \text{ lb}$$

Using the AISC ASD Specification with an allowable stress of 22
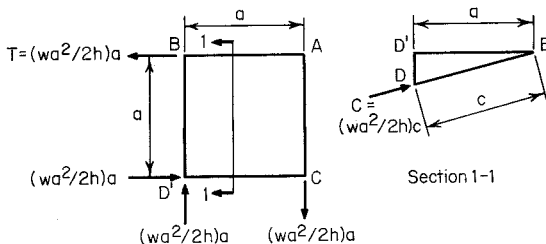
Figure 9.34   Forces in framing members.

ksi, the required area is

$$A = \frac{C'}{22} = 1.195 \text{ in.}^2$$

Selecting two L4 $\times$ 3 $\times$ $\frac{1}{4}$ in., the actual area is 3.38 in.[2] The use of an allowable stress of 22 ksi is due to the fact that the compressive force varies from zero at point B to the maximum value at point D and that the member is continuously braced by steel panels.

The above discussion is based on the requirement of strength. In some cases the deflection of hyperbolic paraboloid roofs at unsupported corners may be excessive and therefore will control the design of this type of structure. Research work[9.80] indicates that the corner deflection is affected by (1) the shear and bending stiffness of steel panels, (2) the bending and axial stiffness of edge members, (3) the type and arrangement of connections used to join steel panels and to connect steel panels to edge members, and (4) the eccentricity of the shear force transmitted from the deck to edge members. The finite-element method may be used to predict deflection.

If the corner deflection is found to be critical, the design may be improved by increasing the bending stiffness of the edge members and steel panels and the curvature of the shell.

In the design of hyperbolic paraboloid roofs, consideration should also be given to the possible buckling of steel deck and the overall buckling of edge members. The determination of the buckling load can be made either by the energy approach or by the finite-element method.[9.80]

9.4.3.4 *Research on Cold-Formed Steel Hyperbolic Paraboloid Roofs* A full-scale hyperbolic paraboloid shell constructed of one-layer standard steel roof deck sections has been tested at Cornell University by Nilson.[9.79] The test setup is shown in Fig. 9.35. Note that the jack loads are applied upward because of convenience of testing. The specimen was 15 $\times$ 15 ft (4.6 $\times$ 4.6 m) with 3-ft (0.92-m) rise, which represents one of the four quarter-surfaces of an inverted umbrella (type II), as shown in Fig. 9.27. The panels used in the specimen were standard 0.0635-in. (1.6-mm)-thick steel roof deck sections, 18 in. (457 mm) wide, with ribs 6 in. (152 mm) on centers and $1\frac{1}{2}$ in. (38 mm) high. Panels were welded to each other along the seam joints and to the perimeter frame members.

The structural feasibility of the hyperbolic paraboloid shell structure has been demonstrated by Nilson's test. The results indicate that shear values obtained from horizontal diaphragm testing can be used conservatively in the design of curved shear surfaces.

The structural behavior of hyperbolic paraboloid shell has been studied further at Cornell University by Winter, Gergely, Muskat, Parker, and Banavalkar under the sponsorship of the AISI. Findings of this study are reported
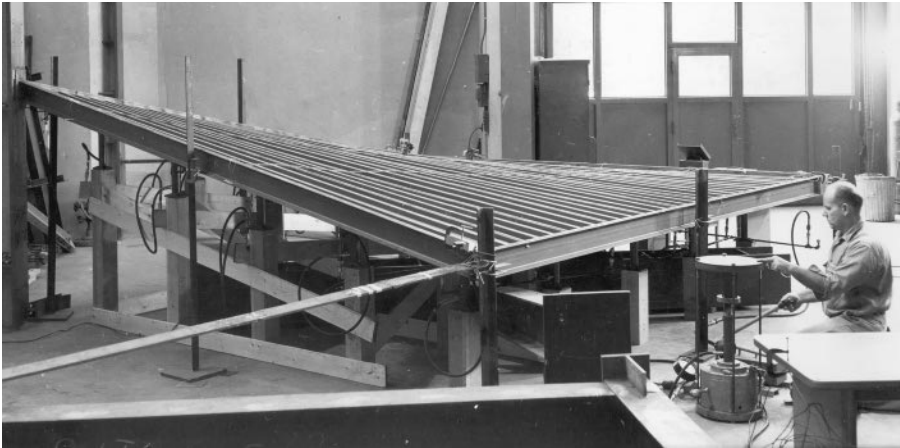
Figure 9.35 Testing of hyperbolic paraboloid shell.[9.79]

in Refs. 9.80, 9.82–9.87. In addition, investigations of hyperbolic paraboloid roofs have been conducted by individual steel companies.[9.88] It is expected that additional design information may be developed from the previous research.

9.4.3.5 Curvilinear Grid Frame Type Hyperbolic Paraboloids[9.72,9.75] The above discussion is made on the basis that the cold-formed panels are stressed as a membrane in the hyperbolic paraboloid roof. This membrane type of hyperbolic paraboloid structure is mostly used for relatively small structures. For larger structures a hyperbolic paraboloid roof may be constructed with structural members as a curvilinear grid frame. The construction shown in Fig. 9.36 was developed by Hutton of Purdue University and consists of struts
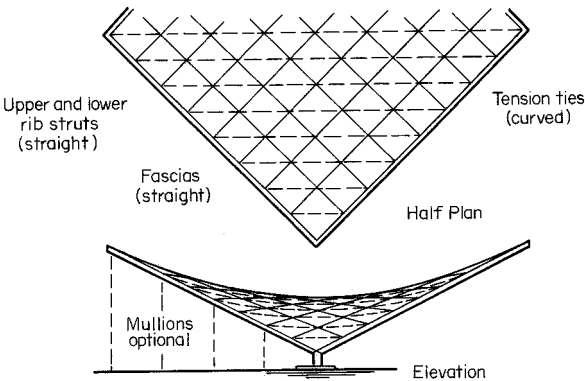
Figure 9.36 Curvilinear grid frame type hyperbolic paraboloid.[9.76]

and ties. The ties of the system can be designed as cables. Either analytical or graphic solutions are possible.

With regard to the design of ribs, the top ribs are designed for compression and bending, and the bottom ribs are designed for compression only. The fascia is designed for combined axial and bending stress. In addition, the ground tie should be provided as a tension member.

In the curvilinear grid frame type, cold-formed steel decks do not participate in shear membrane stresses; rather a grid of structural steel members supports the loads.

Two grid frame methods are possible. They are the double-arch and the orthogonal systems. For the double-arch grid system, the positive arches are compressive elements and the negative arches are curved tensile members. The analysis of this system for concentrated load and unbalanced load can be complex.

For the orthogonal grid system, as shown in Fig. 9.36, the ribs are straight members parallel to the edge members and supported by a series of ties. Two layers of corrugated steel panels may be used perpendicular to each other to replace the ribs.

In addition to the types of shell roofs discussed above, two structural systems (barrel shells and composite truss and sheet panels) generally used for lightweight utility and farm buildings have been discussed by Abdel-Sayed in Ref. 9.89.

10 Corrugated Sheets

10.1 GENERAL REMARKS

Corrugated sheets (Fig. 10.1) have been used in building construction since about 1784. This is one of the oldest types of cold-formed steel products. At present, numerous types of corrugated sheets with different coatings are being produced by many manufacturers. Several standard corrugated steel sheets are generally available for building construction and other usage.

In general, the design methods described in previous chapters are also applicable to the design and use of corrugated steel sheets. However, certain simplified formulas for computing the sectional properties of standard corrugated steel sheets can be used in design. Following an investigation conducted by the AISI during 1955–1957, a publication entitled "Sectional Properties of Corrugated Steel Sheets" was issued by the Institute in 1964 to provide the necessary design information for corrugated sheets.[1.87]

This chapter is intended to discuss the application of arc-and-tangent-type corrugated steel sheets and trapezoidal-type corrugated sheets (Fig. 10.2) and the design of such cold-formed steel products. The information included herein is based on AISI publications[1.87–1.89] and other references used in this chapter.

10.2 APPLICATIONS

Corrugated steel sheets are frequently used for roofing and siding in buildings because the sheets are strong, lightweight, and easy to erect. In many cases they are used as shear diaphragms to replace conventional bracing and to stabilize entire structures or individual members such as columns and beams. The shear diaphragms and diaphragm-braced beams and columns were discussed in Chap. 9.

Figure 1.18*a* shows the use of standard corrugated sheets for exterior curtain wall panels. The application of unusually large corrugated sections in frameless stressed-skin construction is shown in Fig. 1.18*b*. In addition, corrugated steel pipe of galvanized sheets has long been used in drainage structures for railways, highways, and airports.[1.18,1.88,1.89] Figure 10.3 shows typical corrugated metal pipe culvert used for highway systems. Other corrugated steel products have been used for retaining walls, guardrails, conveyer covers, aerial conduits, and other purposes.[1.18,1.88]
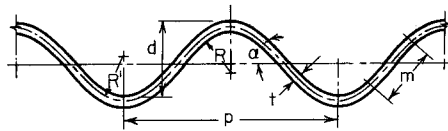
Figure 10.1 Cross section of typical arc-and-tangent-type corrugated sheets.

During recent years, corrugated sheets have been used in flooring systems for buildings and bridge construction.[1.88,10.1] These products have also been used as web elements for built-up girders in order to increase web stiffness instead of using a relatively thicker plate or a thin web with stiffeners. The Macomber Panlweb girder shown in Fig. 10.4 consists of 0.075- to 0.15-in. (1.9- to 3.8-mm) corrugated web for depths of 20 to 40 in. (0.51 to 1.02 m).[10.2] Reference 10.3 discusses the required connections for beams with corrugated webs. The fatigue strength of girders with corrugated webs was reported in Ref. 10.4.

10.3 SECTIONAL PROPERTIES AND DESIGN OF ARC-AND-TANGENT-TYPE CORRUGATED SHEETS

In 1934 Blodgett developed a method to compute the sectional properties of arc-and-tangent-type corrugated sheets.[10.5] The computation of the moment of inertia and the section modulus for standard corrugated sheets has been simplified by Wolford.[10.6] In the computation, design curves and tables can be used to determine factors C_5 and C_6 in Eqs. (10.1) and (10.2):[1.87]

$$I = C_5 bt^3 + C_6 bd^2 t \tag{10.1}$$

$$S = \frac{2I}{d + t} \tag{10.2}$$

where I = moment of inertia, in.[4]
    S = section modulus, in.[3]
    b = width of sheet, in.
    d = depth of corrugation, in.
    t = thickness of sheet, in.
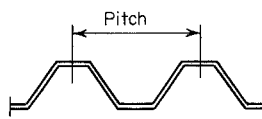
Figure 10.2 Cross section of typical trapezoidal-type corrugated sheets.
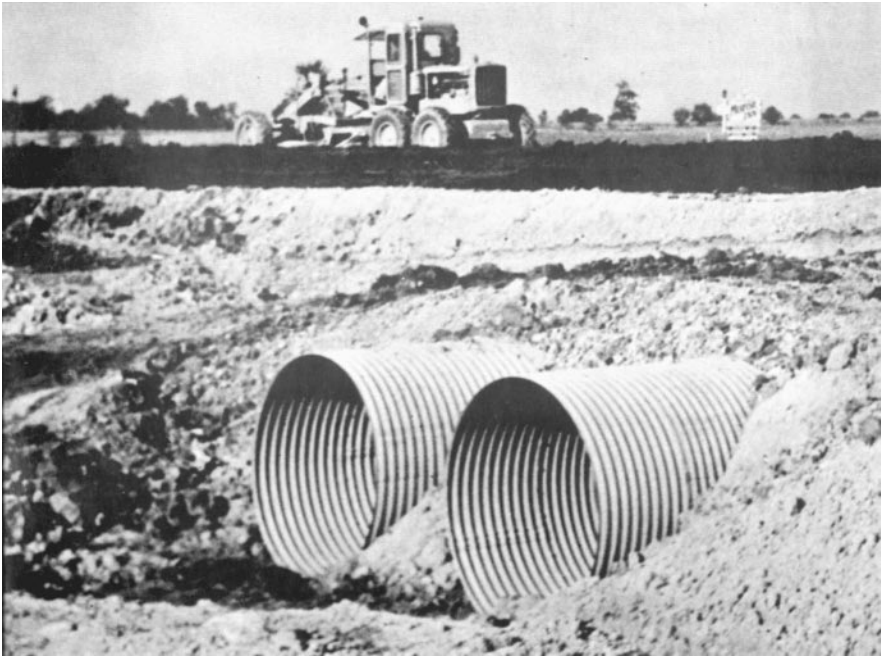
Figure 10.3   Typical corrugated metal pipe culvert installation on interstate highway system.[1.87]

The Macomber PANLWEB girder consists of Macomber V V - Section flanges and a "ribbed" light gage sheet web. Vertical posts are introduced at reactions and flange stiffeners at interior flange loading points.
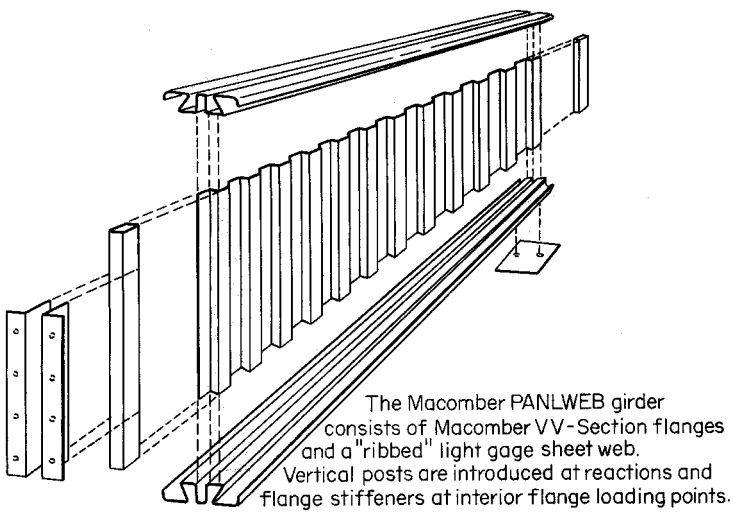
Figure 10.4   Macomber Panlweb girder.[10.2]

C_5, C_6 = factors depending on shape of arc-and-tangent-type corrugation.

Using Wolford's charts, as shown in Figs. 10.5 to 10.9, the values of the moment of inertia, section modulus, area, radius of gyration, and length of tangent can be computed by the following procedure:

1. Compute the midthickness radius R',

$$R' = R + \frac{t}{2}$$

2. Compute values of q and K,

$$q = \frac{R'}{d} \quad \text{and} \quad K = \frac{p}{d}$$

   where p is the pitch.
3. From Fig. 10.5, determine the angle α for the computed values of q and K.
4. From Figs. 10.6 and 10.7, determine C_5 and C_6 by using K and angle α.
5. From Figs. 10.8 and 10.9, determine λ and the m/d ratio.
6. Compute I and S by using Eqs. (10.1) and (10.2).
7. Compute

$$A = \lambda bt$$

8. The radius of gyration is

$$r = \sqrt{\frac{I}{A}}$$

9. The length of the tangent is $d \times \dfrac{m}{d}$
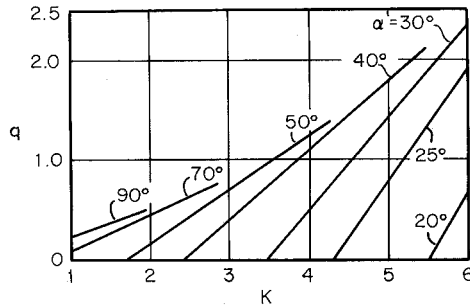
Figure 10.5 Radius-to-depth ratio versus pitch-to-depth ratio at various web angles.[10.6]
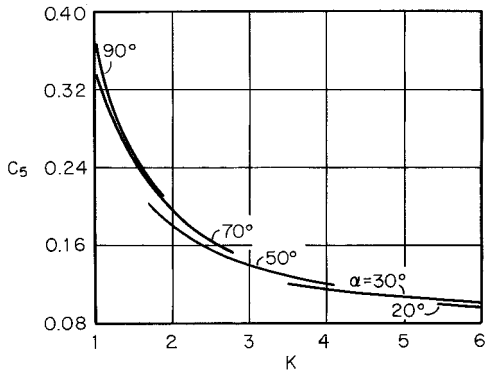
Figure 10.6   Factor C_5 versus pitch-to-depth ratio at various web angles.[10.6]

Based on the method outlined above, the sectional properties of several types of corrugated sheets have been developed and published in Refs. 1.87 and 1.88. The accuracy of Eqs. (10.1) and (10.2) has been verified by beam tests conducted under the sponsorship of the AISI. Some of the sectional properties for galvanized and uncoated corrugated sheets are reproduced in Tables 10.1 to 10.4. In these tables, the pitch of corrugation ranges from $1\frac{1}{4}$ to 6 in. (32 to 152 mm), and the depth varies from $\frac{1}{4}$ to 2 in. (6.4 to 51 mm). The thickness of steel sheets varies from 0.0135 to 0.276 in. (0.3 to 7 mm). The inelastic flexural stability of corrugations was studied by Cary in Ref. 10.11.

In determining the load-carrying capacity of corrugated sheets, the nominal flexural strength can be computed in a conventional manner as follows:
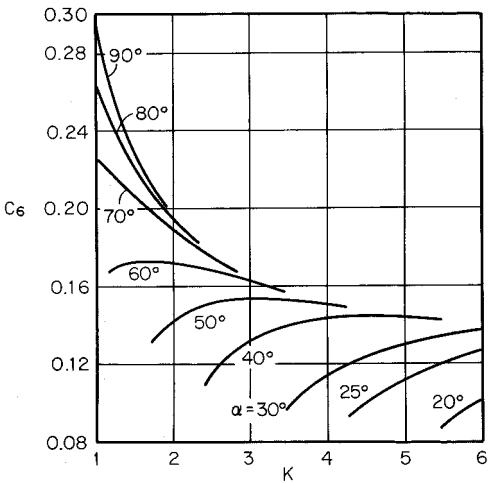
Figure 10.7   Factor C_6 versus pitch-to-depth ratio at various web angles.[10.6]
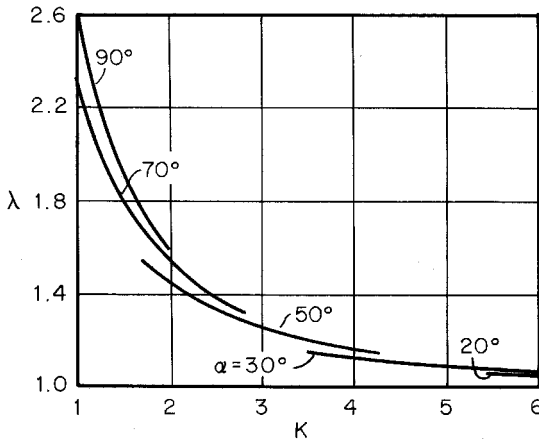
Figure 10.8 Factor λ versus pitch-to-depth ratio at various web angles.[10.6]

$$M_n = SF_y$$

where S = section modulus obtained from Tables 10.1 to 10.4
      F_y = yield point of steel

The design flexural strength can be computed by using $\Omega_b = 1.67$ for ASD and $\phi_b = 0.95$ for LRFD.

With regard to the deflection requirements, more deflection may be permitted for corrugated sheets than for other types of members. However, it should not exceed 1/90 of the span length due to the possible leakage at end laps or loss of end connections.
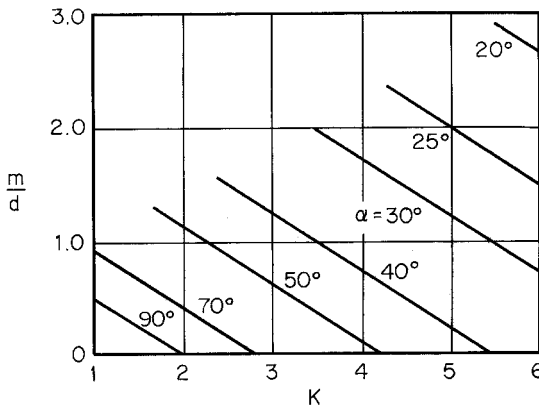
Figure 10.9 Tangent-to-depth ratio versus pitch-to-depth ratio at various web angles.[10.6]

TABLE 10.1 Sectional Properties, per Foot of Corrugated Width, of Several Types of Corrugated Galvanized Steel Sheets[1.87]

Galvanized Sheet Thickness, (in.)	$p = 1\frac{1}{4}$ in., $d = \frac{1}{4}$ in.			$p = 2\frac{2}{3}$ in., $d = \frac{1}{2}$in.			$p = 2\frac{2}{3}$ in., $d = \frac{5}{8}$ in.			$p = 2\frac{2}{3}$ in., $d = \frac{3}{4}$ in.		
	A (in.^{2})	I (in.^{4})	S (in.^{3})	A (in.^{2})	I (in.^{4})	S (in.^{3})	A (in.^{2})	I (in.^{4})	S (in.^{3})	A (in.^{2})	I (in.^{4})	S (in.^{3})
0.1084	1.396	0.0120	0.0675	1.379	0.0417	0.138	1.439	0.0683	0.187	1.503	0.1023	0.239
0.0785	1.004	0.00811	0.0497	0.991	0.0295	0.102	1.035	0.0485	0.138	1.080	0.0729	0.176
0.0635	0.807	0.00636	0.0408	0.797	0.0236	0.0839	0.832	0.0388	0.113	0.869	0.0584	0.144
0.0516	0.651	0.00504	0.0337	0.643	0.0189	0.0688	0.671	0.0312	0.0926	0.701	0.0470	0.118
0.0396	0.493	0.00377	0.0262	0.487	0.0143	0.0532	0.508	0.0236	0.0713	0.531	0.0356	0.0904
0.0336	0.415	0.00315	0.0224	0.410	0.0120	0.0451	0.427	0.0198	0.0604	0.446	0.0299	0.0765
0.0276	0.336	0.00254	0.0185	0.332	0.00971	0.0369	0.346	0.0160	0.0493	0.362	0.0242	0.0624
0.0217	0.259	0.00195	0.0145	0.225	0.00746	0.0287	0.266	0.0124	0.0383	0.278	0.0186	0.0484
0.0187	0.219	0.00165	0.0124	0.216	0.00632	0.0245	0.226	0.0105	0.0326	0.236	0.0158	0.0412
0.0172	0.199	0.00150	0.0113	0.197	0.00575	0.0223	0.206	0.00952	0.0298	0.215	0.0144	0.0375

TABLE 10.1 (***Continued***)

Galvanized Sheet Thickness, (in.)	$p = 2\frac{2}{3}$ in., $d = \frac{7}{8}$ in.			$p = 3$ in., $d = \frac{5}{8}$ in.			$p = 3$ in., $d = \frac{3}{4}$ in.		
	A (in.^{2})	I (in.^{4})	S (in.^{3})	A (in.^{2})	I (in.^{4})	S (in.^{3})	A (in.^{2})	I (in.^{4})	S (in.^{3})
0.1084	1.583	0.1471	0.300	1.411	0.0706	0.193	1.468	0.1058	0.247
0.0785	1.138	0.1050	0.221	1.014	0.0502	0.143	1.056	0.0755	0.183
0.0635	0.915	0.0843	0.180	0.816	0.0402	0.117	0.849	0.0605	0.149
0.0516	0.738	0.0679	0.147	0.658	0.0323	0.0959	0.684	0.0487	0.122
0.0396	0.560	0.0514	0.113	0.499	0.0244	0.0738	0.519	0.0369	0.0936
0.0336	0.470	0.0432	0.0952	0.419	0.0205	0.0626	0.436	0.0310	0.0792
0.0276	0.381	0.0350	0.0776	0.339	0.0166	0.0511	0.353	0.0251	0.0646
0.0217	0.293	0.0269	0.0601	0.261	0.0128	0.0397	0.272	0.0193	0.0501
0.0187	0.249	0.0228	0.0511	0.221	0.0108	0.0338	0.230	0.0163	0.0426
0.0172	0.226	0.0207	0.0466	0.202	0.00986	0.0308	0.210	0.0149	0.0389

Notes:

1. p = corrugation pitch; d = corrugation depth.

2. Steel thicknesses upon which sectional properties were based were obtained by subtracting 0.0020 in. from galvanized sheet thickness listed. This thickness allowance applies particularly to the 1.25-oz coating class (commercial).

3. Blodgett's formula was used to compute I (see Ref. 10.6).

4. 1 in = 25.4 mm.

TABLE 10.2   Sectional Properties, per Foot of Corrugated Width, of Several Types of Corrugated Uncoated Steel Sheets[1.87]

Uncoated Sheet Thickness, (in.)	$p = 1\frac{1}{4}$ in., $d = \frac{1}{4}$ in.			$p = 2\frac{2}{3}$ in., $d = \frac{1}{2}$ in.			$p = 2\frac{2}{3}$ in., $d = \frac{5}{8}$ in.			$p = 2\frac{2}{3}$ in., $d = \frac{3}{4}$ in.		
	A (in.^{2})	I (in.^{4})	S (in.^{3})	A (in.^{2})	I (in.^{4})	S (in.^{3})	A (in.^{2})	I (in.^{4})	S (in.^{3})	A (in.^{2})	I (in.^{4})	S (in.^{3})
0.1046	1.372	0.0118	0.0665	1.356	0.0410	0.136	1.412	0.0672	0.184	1.479	0.100	0.235
0.0747	0.980	0.00789	0.0486	0.968	0.0288	0.100	1.008	0.0473	0.135	1.056	0.0711	0.172
0.0598	0.784	0.00616	0.0398	0.775	0.0229	0.0818	0.807	0.0377	0.110	0.845	0.0568	0.140
0.0478	0.627	0.00485	0.0326	0.620	0.0182	0.0665	0.645	0.0301	0.0894	0.676	0.0453	0.114
0.0359	0.471	0.00360	0.0252	0.465	0.0136	0.0509	0.485	0.0226	0.0682	0.507	0.0340	0.0864
0.0299	0.392	0.00298	0.0213	0.388	0.0113	0.0428	0.404	0.0188	0.0573	0.423	0.0283	0.0725
0.0239	0.312	0.00236	0.0172	0.310	0.00906	0.0346	0.323	0.0150	0.0462	0.338	0.0226	0.0584
0.0179	0.235	0.00177	0.0132	0.232	0.00678	0.0262	0.242	0.0112	0.0349	0.253	0.0170	0.0442
0.0149	0.195	0.00147	0.0111	0.193	0.00564	0.0219	0.201	0.00933	0.0292	0.211	0.0141	0.0368
0.0135	0.177	0.00133	0.0101	0.175	0.00511	0.0199	0.182	0.00846	0.0265	0.191	0.0128	0.0334

TABLE 10.2 (*Continued*)

Uncoated Sheet Thickness, (in.)	$p = 2\frac{2}{3}$ in., $d = \frac{7}{8}$ in.			$p = 3$ in., $d = \frac{5}{8}$ in.			$p = 3$ in., $d = \frac{3}{4}$ in.		
	A (in.²)	I (in.⁴)	S (in.³)	A (in.²)	I (in.⁴)	S (in.³)	A (in.²)	I (in.⁴)	S (in.³)
0.1046	1.556	0.145	0.295	1.387	0.0694	0.190	1.444	0.104	0.243
0.0747	1.112	0.103	0.216	0.990	0.0490	0.140	1.031	0.0736	0.179
0.0598	0.890	0.0819	0.175	0.793	0.0391	0.114	0.825	0.0588	0.145
0.0478	0.711	0.0654	0.142	0.634	0.0312	0.0926	0.660	0.0469	0.118
0.0359	0.534	0.0490	0.108	0.476	0.0234	0.0707	0.495	0.0352	0.0895
0.0299	0.445	0.0408	0.0902	0.396	0.0194	0.0593	0.413	0.0293	0.0751
0.0239	0.356	0.0326	0.0726	0.317	0.0155	0.0478	0.330	0.0234	0.0605
0.0179	0.266	0.0244	0.0547	0.237	0.0116	0.0362	0.247	0.0175	0.0456
0.0149	0.222	0.0203	0.0457	0.198	0.00967	0.0302	0.206	0.0146	0.0381
0.0135	0.201	0.0184	0.0415	0.179	0.00876	0.0274	0.186	0.0132	0.0346

Notes:

1. p = corrugation pitch; d = corrugation depth.
2. Blodgett's formula was used to compute I (see Ref. 10.6).
3. 1 in. = 25.4 mm.

TABLE 10.3   Sectional Properties, per Foot of Corrugated Width, of Several Types of Corrugated Steel Sheets for Culverts[1.87]

Sheet Thickness, (in.)		$p = 2\frac{2}{3}$ in., $d = \frac{1}{2}$ in.			$p = 3$ in., $d = 1$ in.		
Galvanized	Uncoated	A (in.^{2})	I (in.^{4})	S (in.^{3})	A (in.^{2})	I (in.^{2})	S (in.^{3})
0.1681	0.1644	2.133	0.0687	0.207	2.458	0.301	0.517
0.1382	0.1345	1.744	0.0544	0.171	2.008	0.242	0.427
0.1084	0.1046	1.356	0.0411	0.136	1.560	0.186	0.336
0.0785	0.0747	0.968	0.0287	0.0998	1.113	0.131	0.243
0.0635	0.0598	0.775	0.0227	0.0812	0.890	0.104	0.196
0.0516	0.0478	0.619	0.0180	0.0659	0.711	0.0827	0.158
0.0396	0.0359	0.465	0.0135	0.0503	0.534	0.0618	0.119

Notes:
1. p = corrugation pitch; d = corrugation depth.
2. Steel thickness upon which sectional properties were based are from manufacturers standard guage for carbon steel and are close to those obtained by subtracting 0.0037 in. from galvanized sheet gauge thickness for galvanized coating of 2.00 oz/ft^2 of double-exposed surfaces by triple-spot test.
3. Blodgett's formula was used to compute I (see Ref. 10.6). Inside radii of corrugations were taken as 11/16 and 9/16 in. for $2\frac{3}{4} \times \frac{1}{2}$ and 3×1 in. corrugations, respectively.
4. 1 in. = 25.4 mm.

TABLE 10.4   Sectional Properties, per Foot of Corrugated Width, of Several Types of Corrugated Steel Plates for Culverts[1.88]

Uncoated Sheet Thickness, (in.)	$p = 5$ in., $d = 1$ in.			Uncoated Sheet Thickness, (in.)	$p = 6$ in., $d = 2$ in.		
	A (in.^{2})	I (in.^{4})	S (in.^{3})		A (in.^{2})	I (in.^{4})	S (in.^{3})
0.1644	2.186	0.3011	0.5069	0.2758	4.119	1.990	1.749
0.1345	1.788	0.2438	0.4210	0.2451	3.658	1.754	1.562
0.1046	1.390	0.1878	0.3330	0.2145	3.199	1.523	1.376
0.0747	0.992	0.1331	0.2423	0.1838	2.739	1.296	1.187
0.0598	0.794	0.1062	0.1960	0.1644	2.449	1.154	1.066
				0.1345	2.003	0.938	0.879
				0.1046	1.556	0.725	0.689

Notes:
1. p = corrugation pitch; d = corrugation depth.
2. 1 in. = 25.4 mm.

The design of corrugated steel conduits is well discussed in Chap. 3 of Ref. 1.88.

10.4   SECTIONAL PROPERTIES AND DESIGN OF TRAPEZOIDAL-TYPE CORRUGATED SHEETS

Trapezoidal corrugated sheets (or ribbed panels) have often been used as roofing, floor deck, wall panels, bridge flooring, and permanent steel bridge deck forms.

In the design of roofing, floor deck, and wall panels, the discussion on beam strength and deflection presented in Chap. 4 can be used.

Steel bridge flooring has been used to carry live loads plus 30% for impact as well as the dead load of the surfacing material and the weight of the bridge flooring. Permanent steel forms are designed for placement over or between stringers to carry the dead load of freshly poured concrete plus a 50-psf construction load. The AISI Specification[1.314] can also be used for the design of steel bridge flooring and permanent steel forms. Additional information on the design and installation of these products can be found in Refs. 1.88 and 10.7–10.10.

The most favorable cross section of steel roof panels on the basis of min-imum-weight design is discussed in Ref. 1.247. During the past decade, ad-ditional studies have been made on the use of corrugated elements as structural components. See Refs. 10.12–10.18.

11 Composite Design

11.1 GENERAL REMARKS

The use of steel-concrete composite construction began around 1926. During recent years, composite design has been widely applied in building construction. In general, composite design provides the following advantages as compared with noncomposite design:

1. Efficient use of material. As a result of composite design, the size and weight of steel beams can be reduced by as much as 15 to 30%. The cost of fireproofing can be reduced in addition to the cost reduction of steel beams.

2. Greater stiffness. The stiffness of the composite section can be increased. This reduces the deflection of the member as compared with the noncomposite beam.

3. Extra usable space. The use of shallow beams can reduce building heights. It is also possible to increase column spacings to provide larger usable space within a structure.

4. Saving in labor and other construction material. Savings in labor, facing material, piping, and wiring can be realized.

The conventional steel-concrete composite construction as now used in buildings and bridges is a series of T-beams. It is composed of three essential elements:

1. A reinforced concrete slab
2. Steel beams
3. Shear connectors

Figure 11.1 shows a composite beam section in which the reinforced concrete slab acts as the compression flange of the T-section. Shear connectors can resist the horizontal shear and provide vertical interlocking between concrete slab and steel beams to produce a composite section that acts as a single unit. Types of shear connectors include studs, channels, stiffened angles, and flat bars, as shown in Fig. 11.2. The most often-used connectors are shear studs. In building construction the studs are welded through the steel deck into the structural steel framing; in bridge construction the studs are welded directly to the framing.
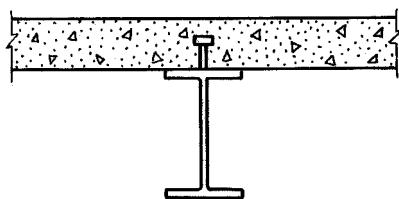
Figure 11.1   Composite construction.

In the past, the construction was usually done with wood forming and the slab was reinforced with bars. For the last 30 years, steel deck has been used as the forming material for building construction and wood is only used for bridges even though steel deck is also often used on bridges too.

11.2   STEEL-DECK-REINFORCED COMPOSITE SLABS

For steel-deck-reinforced composite slabs, the cold-formed steel deck serves in four ways. It acts as a permanent form for the concrete, provides a working platform for the various trades, provides the slab reinforcing for positive bending, and provides bracing for the steel frame by acting as a diaphragm. The placement of the steel deck is done in a fraction of the time required for wood
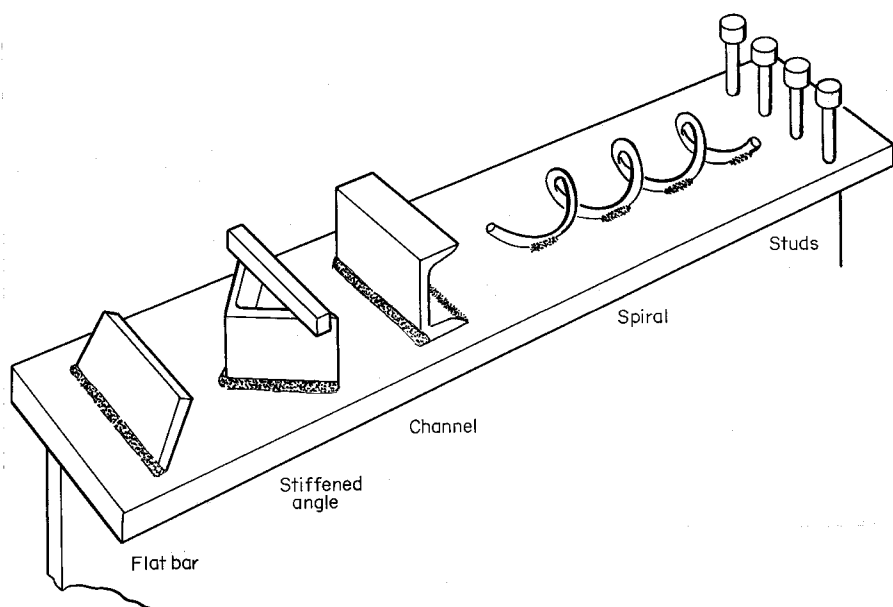
Figure 11.2   Types of shear connectors.[11.1]

forming, so it is no surprise that wood has been replaced in steel-framed building construction.

Steel deck achieves its composite bonding ability by embossments or indentations formed in the deck webs or by the deck shape (Fig. 11.3). In the past, successful composite deck was made by welding transverse wires across the deck ribs (Fig. 11.4) or by punching holes in the deck to allow concrete to fill the ribs (Fig. 11.5). Research sponsored by the Steel Deck Institute and by the American Iron and Steel Institute has shown that the shear studs used to make the beams composite also greatly enhance the composite behavior of the steel deck.[11.18,11.21]

The performance of the composite deck slab is as a one-way reinforced slab and the slab is designed with conventional reinforced concrete procedures. It is only necessary to provide reinforcement for shrinkage and sometimes, depending on the loading, for negative bending over the interior supports. The Steel Deck Institute drew on the extensive research done at Iowa State University, University of Waterloo, Lehigh University, Virginia Polytechnic Institute and State University, West Virginia University, Washington University at Seattle, and from other studies done both in the United States and overseas, to produce the uniform design method shown in the 1977 *Composite Deck Design Handbook.*[1.324] This document contains requirements and recommendations on materials, design, connections, and details of construction with some additional information on special cases. Since 1984, engineers have also used the ASCE *Standard Specification for the Design and Construction of Composite Steel Deck Slabs* prepared by the Steel Deck with Concrete Standard Committee.[1.170] In 1991, the ASCE Standard was revised and divided into two separate Standards: (1) *Standard for the Structural Design of Composite Slabs, ANSI/ASCE 3-91*[11.53] and (2) *Standard Practice for Construction and Inspection of Composite Slabs, ANSI/ASCE 9-91.*[11.54] Both Standards were approved by ANSI in December 1992. These two Standards and their Commentaries focus on the usage of composite steel-deck-reinforced slabs. Standard 3-91 addresses the design of composite slabs and Standard 9-91 focuses on construction practices and inspection. These two standards are being updated to incorporate the latest research.

11.3 COMPOSITE BEAMS OR GIRDERS WITH COLD-FORMED STEEL DECK

In building construction, one of the economical types of roof and floor construction is to combine the steel-deck-reinforced slab with the supporting steel beams or girders as a composite system.

When the composite construction is composed of a steel beam and a solid slab, as shown in Fig. 11.1, the slip between beam and slab is usually small under working load; therefore the effect of slip can be neglected. For this case, full interaction between beam and slab can be expected, and full ultimate
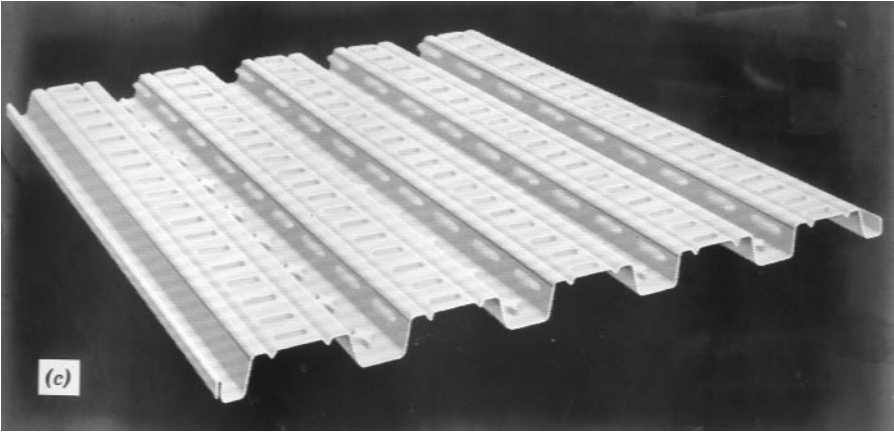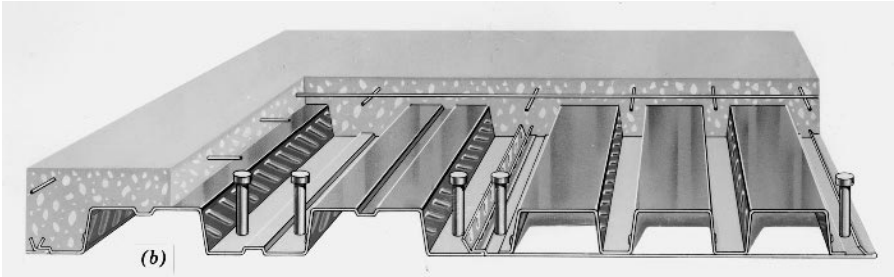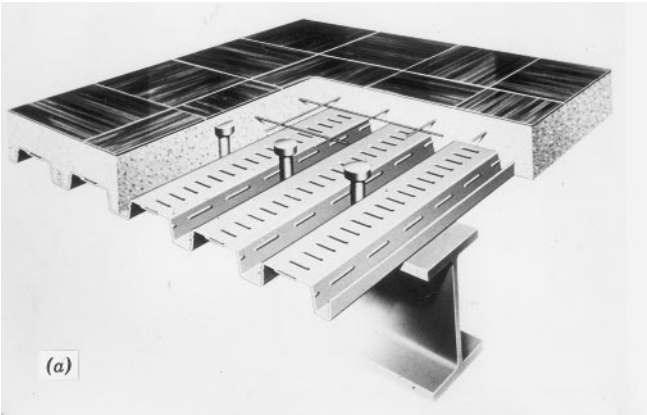
Figure 11.3 Composite systems containing embossments or indentations. (*a*) Type No. 1.[1.96,11.2] (*b*) Type No. 2.[11.3] (*c*) Type No. 3.[11.4]
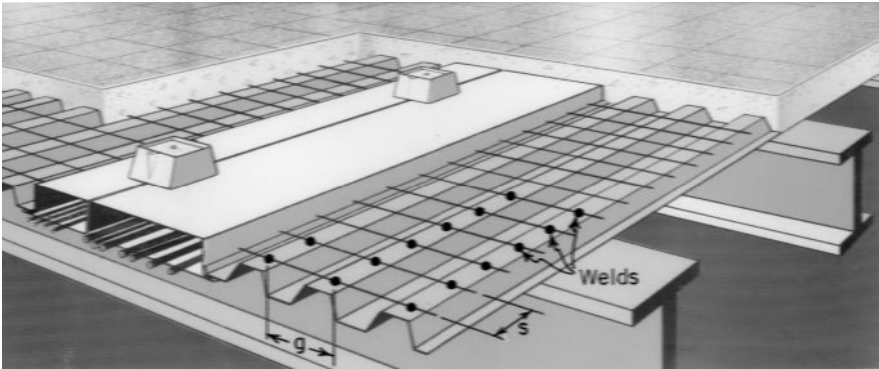
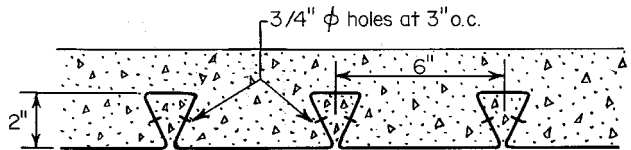**Figure 11.4**   Composite system with T-wires.[11.5]

Figure 11.5   Composite system containing punched holes.
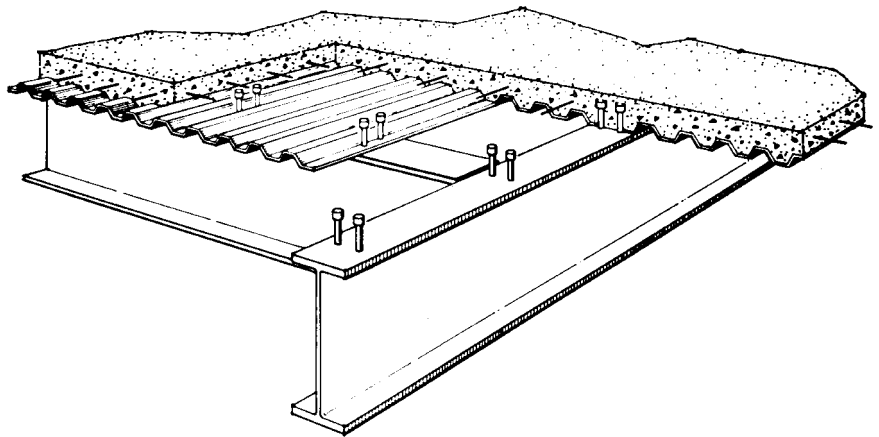
Figure 11.6   Composite beam using steel-deck-reinforced concrete slab.[1.96]
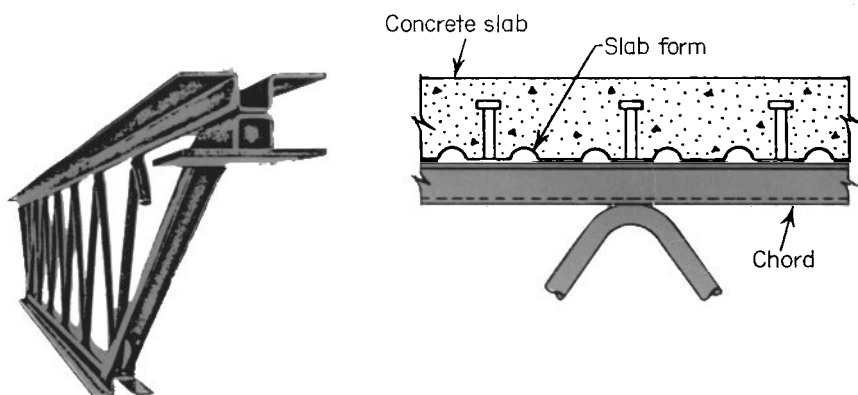
Figure 11.7   Composite joist using steel-deck-reinforced concrete slab.[1.96]

load can be achieved if adequate shear connectors are provided. This type of composite beam can be designed by the AISC Specification.[1.148]

Since 1978 the AISC Specification[1.148] has included some specific provisions for the design of composite beams or girders with cold-formed steel deck, as shown in Figs. 11.3a and 11.6. These provisions are based on the studies conducted previously by Fisher, Grant, and Slutter at Lehigh University.[1.95,11.21,11.22] This specification provides general requirements and design formulas for deck ribs oriented perpendicular or parallel to steel beams. The application of such design rules is well illustrated in Refs. 11.23–11.25. In addition to the above, the current AISC Specification also recognizes partial composite action because for some cases it is not necessary, and occasionally it may not be feasible, to provide full composite action.[1.148,11.23] In 1989, Heagler prepared the SDI LRFD Design Manual for Composite Beams and Girders with Steel Deck.[11.51] This Manual contains a large number of design tables covering a wide range of beam, deck and slab combinations that have been analyzed as composite beams using the provisions of the AISC LRFD Manual of Steel Construction.[11.52]

As far as other countries are concerned, the Canadian Sheet Steel Building Institute's Criteria for the Design of Composite Slabs[11.26] are being used in Canada. In Switzerland, design recommendations have been prepared by Badoux and Crisinel.[11.27] A book on composite design was written by Bucheli and Crisinel in 1982.[11.28] References 11.42–11.44, 11.46, and 11.48 present the additional work and developments on composite design using steel deck in Canada, United Kingdom, Switzerland, and the Netherlands. In 1999, the International Conference on Steel and Composite Structures was held in the Netherlands to discuss recent research on composite structures.

In addition to the use of conventional steel beams, composite open-web steel joists with steel deck, as shown in Fig. 11.7, have been studied by Cran and Galambos.[11.29,11.30]

With regard to shear connectors, special connectors have been developed in the past by various individual companies for use in composite construction.

Several studies have been made to investigate the composite action of cold-formed steel beams and columns with concrete.[11.17,11.49,11.50] References 11.55–11.75 report on the results of recent projects on composite slabs and construction.

12 Introduction to Stainless Steel Design

12.1 GENERAL REMARKS

Stainless steel sections are often used architecturally in building construction because of their superior corrosion resistance, ease of maintenance, and pleasing appearance. Typical applications include column covers, curtain wall panels, mullions, door and window framing, roofing and siding, fascias, railings, stairs, elevators and escalators, flagpoles, signs, and many others, such as furniture and equipment. However, their use for structural load-carrying purposes has been limited prior to 1968 because of the lack of a design specification.

In 1968 the first edition of the "Specification for the Design of Light Gage Cold-Formed Stainless Steel Structural Members"[12.1] was issued by the AISI on the basis of extensive research conducted by Johnson and Winter at Cornell University[3.5,3.16] and the experience accumulated in the design of cold-formed carbon steel structural members. This specification formulates design rules for structural members cold-formed from annealed, austenitic stainless steel types 201, 202, 301, 302, 304, and 316. The main reason for having a different specification for the design of stainless steel structural members is because the mechanical properties of stainless steel are significantly different from those of carbon steel. As a result, the design provisions of the AISI Specification prepared for carbon steel cannot be used for stainless steel without modification.

As shown in Fig. 12.1,[12.2] even annealed stainless steel has the following characteristics as compared with carbon steel:

1. Anisotropy
2. Nonlinear stress–strain relationship
3. Low proportional limits
4. Pronounced response to cold work

With regard to item 1, anisotropy, it should be recognized that stainless steel has different mechanical properties in longitudinal and transverse directions for tension and compression modes of stress. The stress–strain curves are always of the gradually yielding type accompanied by relatively low pro-
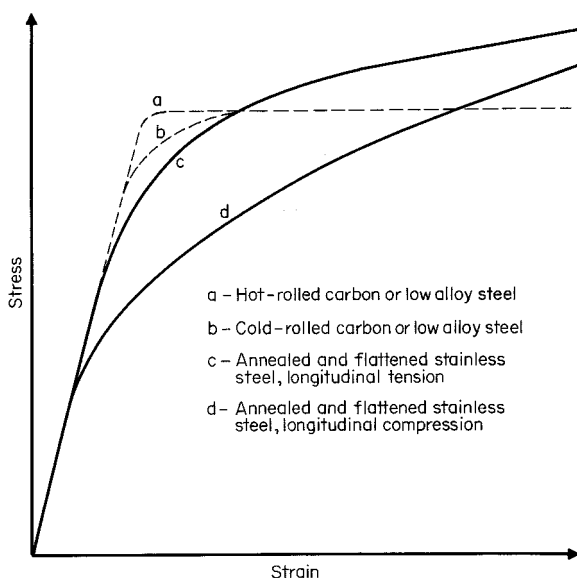
Figure 12.1   Difference between stress–strain curves of carbon and annealed stainless steels.[12.1]

portional limits. For carbon and low-alloy steels, the proportional limit is assumed to be at least 70% of the yield point, but for stainless steel the proportional limit ranges from approximately 36 to 60% of the yield strength. Lower proportional limits affect the buckling behavior and reduce the strengths of structural components and members.

Since the scope of the 1968 edition of the AISI Specification for stainless steel design was limited to the use of annealed and strain-flattened stainless steels, and $\frac{1}{4}$- and $\frac{1}{2}$-hard temper grades of stainless steel have been used increasingly in various applications as a result of their higher strengths in relation to annealed grades (Fig. 12.2), additional design provisions for the use of hard temper grades of stainless steels are needed in the engineering profession. Consequently additional research work has been conducted by Wang and Errera at Cornell University to investigate further the performance of structural members cold-formed from cold-rolled, austenitic stainless steels.[12.3,12.4] The strength of bolted and welded connections in stainless steel has also been studied by Errera, Tang, and Popowich,[12.5] Based on the research findings of these studies, the 1974 edition of the AISI "Specification for the Design of Cold-Formed Stainless Steel Structural Members"[1.160] has been issued by the Institute as Part I of the stainless steel design manual.[3.4] In this second edition of the specification, the scope was extended to include the design of structural members cold-formed from hard temper sheet, strip, plate, or flat bar stainless steels. Many design provisions and formulas were
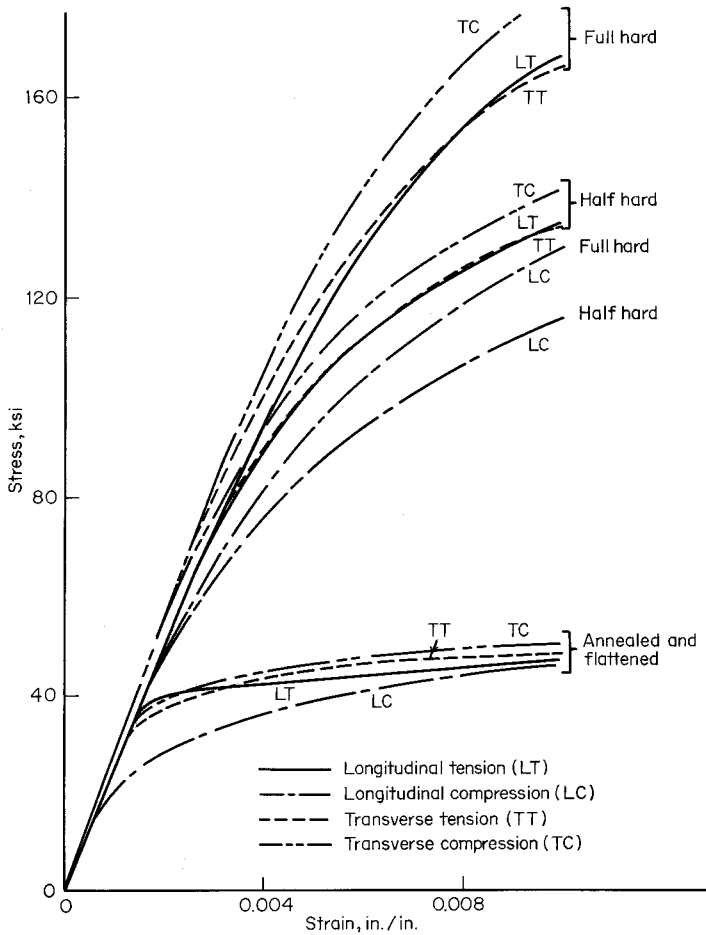
Figure 12.2 Comparison of stress–curves of annealed, half-hard, and full-hard stainless steels.[12.2]

generalized so that they can be used for different temper grades. In some cases the formulas are more complicated than heretofore because of the pronounced anisotropic material properties of the temper grades, the difference in stress–strain relationships for different grades of stainless steels, as shown in Fig. 12.2, and the nonlinear stress–strain characteristics resulting from the relatively low elastic limits for the temper grades. This revised specification covered six types of austenitic stainless steels (AISI types 201, 202, 301, 302, 304, and 316) in four different grades (Grades A, B, C, and D). Among these four grades, Grades A and B cover the annealed condition of different types of austenitic stainless steels; Grades C and D cover the $\frac{1}{4}$- and $\frac{1}{2}$-hard tempers,

respectively. The mechanical properties of the various types of stainless steels were provided in the specification[1.160] and the commentary, which is Part II of the design manual.[3.4]

In the 1980s, additional studies were conducted by Van der Merwe,[12.6] Van den Berg,[12.7] and Lin[12.8] to determine the strength of stainless steel structural members and to develop design recommendations for cold-formed austenitic and ferritic stainless steel structural members. In 1990, the ASCE Standard Specification for the Design of Cold-Formed Stainless Steel Structural Members[12.9] was developed at the University of Missouri-Rolla and approved by the ASCE Stainless Steel Cold-Formed Sections Standards Committee. This document was prepared under the financial support of the Chromium Centre in South Africa, the Nickel Development Institute in Canada, and the Specialty Steel Industry of the United States.

The ASCE Standard Specification is applicable to the use of four types of austenitic stainless steels (Types 201, 301, 304, and 316, annealed and cold-rolled in $\frac{1}{16}$-, $\frac{1}{4}$-, and $\frac{1}{2}$-hard grades) and three types of ferritic stainless steels (annealed Types 409, 430, and 439). This specification is based on the load and resistance factor design (LRFD) concept with the allowable stress design (ASD) concept as an alternative.[1.238,1.253,12.9,12.15]

In the 1990s, additional studies have been made at Rand Afrikaans University, University of Sydney, Glasgow Caledonian University, University of Strathclyde, and University of Liege. For details, see Refs. 2.63–2.65, 12.10–12.14, and 12.16–12.36.

As far as the design standards are concerned, the ASCE Standard Specification is being revised to reflect the results of additional research. Eurocode 3: Part 1.4 was published in 1994.[12.37] In 1996 the South African Bureau of Standards prepared a Draft Code of Practice for the Limit-States Design of Cold-Formed Stainless Steel Members.[12.38]

12.2   DIFFERENCES BETWEEN THE SPECIFICATIONS FOR CARBON STEELS AND STAINLESS STEELS

A comparison of the AISI Specification for carbon steels[1.314] and the specifications for stainless steels[1.160,12.9] indicates that in the latter documents modifications are necessary for the following aspects:

1. Inelastic buckling of flat elements for compression, shear, and bending modes
2. Safety factor, load factor, and resistance factor
3. Limitations of width-to-thickness ratio
4. Deflection determination
5. Anisotropy
6. Local distortion consideration

7. Lateral buckling of beams
8. Column buckling
9. Connections

12.2.1 Inelastic Buckling of Flat Elements for Compression, Shear, and Bending Modes

In order to consider inelastic buckling (i.e., when the buckling stress exceeds the proportional limit), the following plasticity reduction factors are being used in the specification for stainless steel design to modify the design formulas derived for elastic buckling:

Type of Buckling Stress for Flat Elements	Plasticity Reduction Factor
Compression	
Unstiffened	E_s/E_0
Stiffened	$\sqrt{E_t/E_0}$
Shear	G_s/G_0
Bending	E_s/E_0

E_0 = initial modulus of elasticity, E_s = secant modulus, E_t = tangent modulus, G_0 = initial shear modulus, and G_s = secant shear modulus.

The initial moduli of elasticity, initial shear moduli, secant moduli, tangent moduli, and various plasticity reduction factors are provided in the specifications for different grades of stainless steels to be used for various design considerations.

12.2.2 Safety Factor, Load Factor, and Resistance Factor

In carbon steel design specification a basic safety factor of 1.67 has been used since 1960. For stainless steel design, a relatively large safety factor of 1.85 is retained in the ASD specification because of the lack of design experience and due to the fact that in stainless steel design, it is necessary to consider the inelastic behavior at lower stresses than those used for carbon steel. For column design, the allowable stress used for stainless steel has also been derived on the basis of a relatively larger safety factor than for carbon steel.

Because the 1990 ASCE Standard Specification is based on the load and resistance factor design method with the allowable stress design method as an alternate, load factors, resistance factors, and nominal strength equations are given in the specification for the design of structural members and connections.

12.2.3   Limitations of Width-to-Thickness Ratio

Since pleasing appearance is one of the important considerations in stainless steel design, the maximum permissible width-to-thickness ratios of flat elements have been reduced in order to minimize the possible local distortion of flat elements.

12.2.4   Deflection Determination

Because the proportional limit of stainless steel is relatively low and the stress in the extreme fiber may be higher than the proportional limit under service load, special provisions are included in the stainless steel specification for computing deflections in which a reduced modulus of elasticity $E_r = (E_{ts} + E_{cs})/2$ is used, where E_r is the reduced modulus of elasticity, E_{ts} is the secant modulus corresponding to the stress in the tension flange, and E_{cs} is the secant modulus corresponding to the stress in the compression flange.

12.2.5   Anisotropy

For austenitic stainless steel, the stress-strain curves are different for longitudinal tension and compression and for transverse tension and compression, as shown in Fig. 12.2. In the ASCE stainless steel specification, the basic design stresses are based on the values obtained from a statistical analysis. This statistical analysis has been made to ensure that there is a 90% probability that the mechanical properties will be equaled or exceeded in a random selection of the material lot under consideration.

For ferritic stainless steels, a comprehensive study was made by Van der Merwe in 1987.[12.6] Figure 12.3 shows typical stress–strain curves for Types 409 and 430 stainless steels. It can be seen that these stress–strain relationships are different from those of austenitic stainless steels as shown in Fig. 12.2.

12.2.6   Local Distortion Consideration

Since for stainless steel the proportional limits are low compared with those for carbon steel and the exposed surfaces of stainless steel are important for architectural purposes, the design provisions for determining the permissible stresses for unstiffened and stiffened compression elements are included for two instances, namely, (1) no local distortion at design loads is permissible, and (2) some slight waving at design loads is permissible.

12.2.7   Lateral Buckling of Beams

In the specification for stainless steel, the theoretical equation for critical moment has been generalized by utilizing a plasticity reduction factor E_t/E_0.
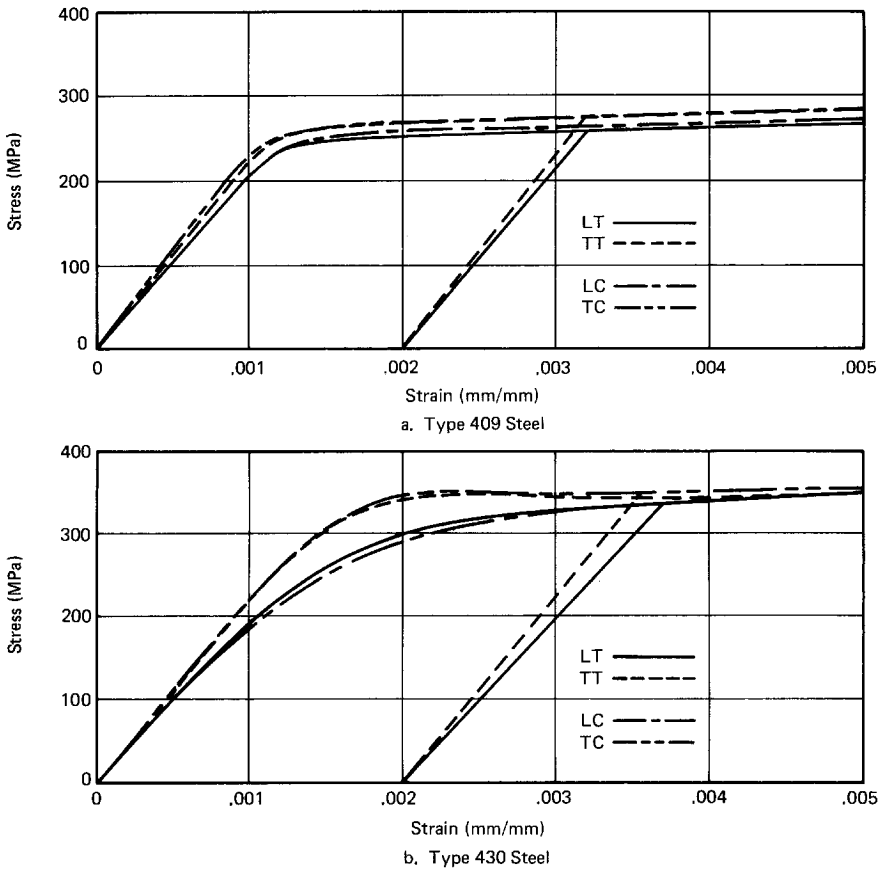
Figure 12.3 Initial portion of stress–strain curves for ferritic stainless steels.[12.6]

In addition, the allowable stress used in the stainless steel ASD specification is based on a safety factor of 1.85.

12.2.8 Column Buckling

Since the stress–strain relationships of stainless steels are different from those for carbon steel, the column buckling stress for axially loaded compression members is based on the tangent modulus theory for flexural buckling, torsional buckling, and torsional-flexural buckling. The safety factor applied in the ASD design formulas is 2.15 instead of the 1.80 used for cold-formed carbon steel design.

12.2.9 Connections

1. *Welded Connections.* The design provisions for welded connections are developed on the basis of the available research data on stainless steel connections and the AISI Specification for cold-formed carbon steel.

2. *Bolted Connections.* Based on a study of the strength of bolted and welded connections in stainless steel conducted by Errera, Tang, and Popowich,[12.5] the design provisions for bolted connections are generalized to reflect the results of research work. The design provisions are related to the determination of edge distance, tension stress, and bearing stress. Additional design information is included for the shear and tension stresses for types 201, 304, 316, and 430 stainless steel bolts.

13 Computer-Aided Design

13.1 GENERAL REMARKS

During the past 35 years, computers have been widely used in research, structural analysis, and design. There is no exception for cold-formed steel structures.

Because the research work on cold-formed steel structures usually involves studies of the structural behavior and instability of plate components, individual members, and/or the entire assembly, hand calculations are excessively lengthy and extremely difficult. Computers have been used to great advantage in obtaining solutions for complicated problems involving these structures under various boundary and loading conditions.

As discussed in the preceding chapters, the formulas used for the design of cold-formed steel structural members are quite complicated, particularly for those members having unusual cross sections. It may be found that even the determination of sectional properties requires burdensome calculations, which may involve the use of successive approximations. For this reason, various institutions and companies have used computers to develop the data necessary for the preparation of design tables and charts.

In addition, computers have also been used for the development and design of industrialized buildings, minimum-weight design of structural members, minimum-cost design of structural systems, and special structures.

Article 13.2 contains a brief review of some computer programs used for the analysis and design of cold-formed steel members and structures in the past.

13.2 COMPUTER PROGRAMS FOR THE DESIGN OF COLD-FORMED STEEL STRUCTURES

13.2.1 Sectional Properties

Computer programs have been used extensively for the preparation of the design tables included in Ref. 1.159 and in many of manufacturers' publications. The equations needed for the calculation of sectional properties of angles, channels, hat sections, I-sections, T-sections, and Z-sections are summarized in Part I of Ref. 1.159.

In some cases the calculation of the sectional properties of various types of structural members has been included as a subroutine in complete computer programs for the analysis and design of cold-formed steel structures.[13.1]

13.2.2   Optimum Design

The minimum-weight design of cold-formed steel members has been studied by Seaburg and Salmon[1.247] on the basis of the AISI Specification.[1.4] It has been found that the gradient search method requires less time than the direct search method. This optimization technique has been illustrated for the selection of the most favorable cross section of the hat-shaped roof deck.

In 1971 a computer program, DOLGAS, was developed by Klippstein for the design of steel trusses fabricated from cold-formed steel members.[13.1] It provides for the selection of minimum-weight members (channels, Z-sections, hat sections, sigma sections, or tubular sections) to meet the requirements of the AISI Specification.[1.4] This program uses STRESS to compute member forces and then check the design of members on the basis of the AISI design criteria. The output includes structural design information and the necessary data for fabrication.

In some cases, emphasis has changed to the minimum-cost design to consider the costs of material, fabrication, and erection. For example, the minimum-cost design of composite floor systems using cold-formed steel decking has been conducted by Nicholls and Merovich.[13.2] In the design, the grid search procedure has been used. This study includes the costs of cold-formed steel decking, concrete slab, rolled beams, shoring of decking as necessary, temperature mesh in slab, and the necessary fireproofing. In addition, the optimization of cold-formed steel shapes is presented by Douty in Ref. 13.3.

13.2.3   Special Structures

In Chap. 9 it was mentioned that the accurate analysis and design of special structures subjected to unsymmetrical loading and nonuniform support conditions can be achieved by using computers. For example, the analysis and the design of the world's largest cold-formed steel primary structure[1.82] have been completed by using the finite-element method.[13.4] The hypar module as shown in Fig. 9.24 has been analyzed under four different loading conditions. Reference 13.4 indicates that the computer program specially developed by Tezcan, Agrawal, and Kostro can be used to determine the deflections and stresses of any general multiwing hyperbolic paraboloid shell with any type of support and beam arrangement under any arbitrary load condition.

13.2.4   Industrialized Buildings

The conventional optimum design of industrialized buildings is usually accomplished by repeated analysis, modification, and reanalysis of redefined structural systems. The use of computers increases the design flexibility of

the building system and results in a minimum-weight or a minimum-cost design.[13.5] Computers may also be used for other operations concerning manufacturing, distribution, and administration work.

13.2.5   Decision Table and Flow Charts

A decision table is a concise tabular display of the logical conditions and the appropriate actions to be taken as the result of these conditions. It is useful in preparing computer programs which utilize the specification provisions and in identifying all combinations of factors not specifically covered by the specification.

The decision table formulation of the AISI Specification for the design of cold-formed steel structural members has been originally developed by Seaburg and modified to conform to the 1986 edition of the specification by Midgley–Clauer Associates (Ref. 13.7). The table can be converted directly into programming language.

The 1986 edition of the AISI Cold-Formed Steel Design Manual contained a series of flow charts. These charts proved to be excellent means of helping the user to understand the design provisions and to provide a clear picture of the items that need to be considered in design. They were very useful guidelines for computer programmers.

13.2.6   Computer Programs

As computer technology advances, the use of computers for the design of cold-formed steel structures is unlimited, as demonstrated by Zuehlke (Ref. 13.8) and others.

In 1991, the American Iron and Steel Institute published a document, *Cold-Formed Steel Design Computer Programs,* which contained descriptions of 12 computer programs using the AISI Specification. This document was updated by the Center for Cold-Formed Steel Structures in 1993 and 1996 to include 30 programs from the United States, Canada, Australia, and South Africa.[13.9] Most of the computer programs are now (1999) available on the Center's website.[13.10]

Recently, Helen Chen developed a set of computer programs on the basis of the 1996 edition of the AISI Specification. The example problems are dealing with (a) beam lateral buckling strength, (b) shear strength of the stiffened web, (c) web crippling strength, (d) compression members, (e) cylindrical tubes, (f) brace force for C- and Z-sections, (g) welded connections, (h) bolted connections, and (i) screw connections.[13.11] These programs can be found on the AISI website at *www.steel.org.*

13.2.7   Numerical Solutions for Cold-Formed Steel Design

In Chap. 3, the effective width design approach of *individual* elements was discussed on the basis of the current AISI Specification. It can be seen from

Eq. (3.39) that the reduction factor ρ used for calculating the effective width of a given element is a function of the critical local buckling stress f_{cr}, and the maximum compressive stress. Instead of using the AISI equation to determine the f_{cr} value for an *individual* element, Schafer and Pekoz indicate that the critical elastic buckling stress of an element or a member can be determined by numerical solutions using (a) finite element method such as ABAQUS, ANSYS, and STAGS or (b) finite strip method such as THIN-WALL[13.9] and CUFSM.[13.12–13.14] The program CUFSM was developed by Schafer and can be obtained from *http://www.cee.cornell.edu/schafer.*[13.15] The numerical solution can provide a proper handling of *element interaction for general cross sections.* It can be used to investigate various possible buckling modes for a given structural member and to determine the lowest buckling stress for design purpose. The advantages of such an approach are increased accuracy and flexibility. References 13.13 and 13.14 discuss the application of the proposed *Direct Strength Method* for the design of cold-formed steel structural members.

14 Residential Construction

14.1 GENERAL REMARKS

Cold-formed steel structural members have been used for housing for many years (Fig. 14.1). The primary advantages of cold-formed steel are price stability, light weight, high strength and stiffness, uniform quality, ease of prefabrication and mass production, economy in transportation and handling, fast and easy erection and installation, noncombustibility, and the fact that it is termite-proof and rot-proof.

During recent years, the use of cold-formed steel framing in residential construction has been on a rapidly increasing scale. In the United States, about 15,000 steel homes were built in 1993 and 75,000 in 1996.[1.282,13.14] It is expected that by the year 2002 this number may increase five-fold.

The major structural components used for housing are wall studs, floor and ceiling joists, roof rafters, roof and floor trusses, decks, and panels. Since 1960, numerous projects have concentrated on the research and development of cold-formed steel products for housing (Refs. 1.21, 1.24–1.28, 1.30, 1.39, 1.72, 1.113, 1.114, 1.282–1.285, 1.297–1.301, 5.107, 5.138, 5.139, 8.88, 14.1). However, the lack of prescriptive building code requirements has prevented cold-formed steel from gaining wider acceptance among home builders and code officials. To remedy this situation, a four-year project was conducted by the National Association of Home Builders Research Center to develop a prescriptive method for residential cold-formed steel framing.[1.280] This project was sponsored by the American Iron and Steel Institute, the U.S. Department of Housing and Urban Development (HUD), and the National Association of Home Builders (NAHB). In 1997, provisions of the prescriptive method were adopted by the International Code Council (ICC) for its One- and Two-Family Dwelling Code.

14.2 PRESCRIPTIVE METHOD

The *prescriptive method* is a guideline for the construction of one- and two-family residential dwellings using cold-formed steel framing.[1.280] It provides a prescriptive approach to build houses with cold-formed steel. This method standardizes C-Sections with lips for structural members and C-sections without lips for track sections. These requirements are supplemented by construction details and design tables.

Figure 14.1   Cold-formed steel framing used for housing. (*Elliott Steel Homes, Inc., Loveland, CO*)

In this method, the materials are limited to ASTM A653, A875, and A792 steels with specified yield points ranging from 33 to 50 ksi (227 to 348 MPa). The material thickness varies from 0.018 to 0.097 in. (0.46 to 2.46 mm). Design examples are given in the Commentary.[1.281]

14.3   AISI RESIDENTIAL MANUAL

To satisfy the needs of design and construction information, AISI published a Residential Steel Framing Manual for Architects, Engineers and Builders in the early 1990s.[1.277] This Manual presently contains (a) Residential Steel Construction Directory, (b) Introduction to Steel Framing, (c) Fasteners for Residential Steel Framing (d) Low-Rise Construction Details and Guidelines, (e) Residential Steel Beam and Column Tables, (f) Fire Resistance Rating of Load Bearing Steel Stud Walls, (g) Builders Perspectives, (h) Truss Design Guide, (i) Shear Wall Design Guide, (j) Thermal Resistance Design Guide, (k) Durability of Cold-Formed Steel Framing Members, (l) Prescriptive Method and Commentary, (m) Builders' Steel Stud Guide (n) Design Guide— CF Steel Beams with Web Penetrations, (o) Monotonic Tests of CF Steel

Shear Walls with Openings, (q) Combined Axial and Bending Load Tests/ Fully Sheathed Walls, and (r) Final Report on L-Shaped Headers.

14.4 FRAMING STANDARDS

In 1997, the AISI Construction Market Committee established a new Committee on Framing Standards to develop and maintain consensus standards for residential and light-commercial cold-formed steel framing under the Chairmanship of Jay Larson and Vice-Chairmanship of Steve Fox.[14.2] The Committee's mission is to eliminate regulatory barriers and increase the reliability and cost competitiveness of cold-formed steel framing through improved design and installation standards. The initial goals of the Committee are to develop (a) Base Standard, (b) High Wind Standard, (c) High Seismic Standard, (d) General Provisions Standard, and (e) Truss Design Standard for residential and light-commercial construction. In addition, the North American Steel Framing Alliance was formed in 1998, headed by Donald Moody.[13.10] This new organization's mission is to enable and encourage the practical and economic use of cold-formed steel framing in residential construction. Its goal is to achieve sustained annual residential construction market shipment of cold-formed steel framing products equal to 25% of the total residential market, in tons, by the year 2002.

APPENDIX A
Thickness of Base Metal

For uncoated steel sheets, the thickness of the base metal is listed in Table A.1. For galvanized steel sheets, the thickness of the base metal can be obtained by subtracting the coating thickness in Table A.2 for the specific coating designation from the equivalent thickness listed in Table A.1.

In the past, gage numbers have been used to specify sheet steel thickness, but modern practice is to use decimal values for thickness. For reference purposes, Table A.1 lists gage numbers as well as the thicknesses of uncoated and galvanized steel sheets.

In 1999, the North American Steel Framing Alliance (NASFA) announced a new universal designator system for cold-formed steel framing members. This system uses the *minimum base metal thicknesses,* which represents 95% of the design thickness according to Sec. A3.4 of the AISI Specification.[A.3,A.4]

TABLE A.1   Thicknesses of Uncoated and Galvanized Steel Sheets[a]

Gage Number[b]	Uncoated Sheet		Galvanized Sheet	
	Weight, (lb/ft²)	Thickness, (in.)	Weight, (lb/ft²)	Equivalent Thickness,[b,c] (in.)
3	10.000	0.2391		
4	9.375	0.2242		
5	8.750	0.2092		
6	8.125	0.1943		
7	7.500	0.1793		
8	6.875	0.1644	7.031	0.1681
9	6.250	0.1495	6.406	0.1532
10	5.625	0.1345	5.781	0.1382
11	5.000	0.1196	5.156	0.1233
12	4.375	0.1046	4.531	0.1084
13	3.750	0.0897	3.906	0.0934
14	3.125	0.0747	3.281	0.0785
15	2.813	0.0673	2.969	0.0710
16	2.500	0.0598	2.656	0.0635
17	2.250	0.0538	2.406	0.0575
18	2.000	0.0478	2.156	0.0516
19	1.750	0.0418	1.906	0.0456
20	1.500	0.0359	1.656	0.0396
21	1.375	0.0329	1.531	0.0366
22	1.250	0.0299	1.406	0.0336
23	1.125	0.0269	1.281	0.0306
24	1.000	0.0239	1.156	0.0276
25	0.875	0.0209	1.031	0.0247
26	0.750	0.0179	0.906	0.0217
27	0.688	0.0164	0.844	0.0202
28	0.625	0.0149	0.781	0.0187
29	0.563	0.0135	0.719	0.0172
30	0.500	0.0120	0.656	0.0157

Note: 1 lb/ft² = 47.88 N/m²; 1 in. = 25.4 mm

[a] Based on AISI and the Iron and Steel Society steel products manual.[A.1,A5]

[b] For uncoated sheets, use manufacturers' standard gage number; for galvanized sheets, use galvanized sheet gage number.

[c] The equivalent thickness for galvanized sheet includes both the base metal and the coating on both surfaces. All listed values are based on a coating thickness of 0.0037 in., which is for the coating designation of G210.

TABLE A.2 Coating Thickness to Be Deducted from the Equivalent Thickness of Galvanized Sheets

Coating Designation	Coating Weight, (oz/ft^2)	Approximate Coating Thickness (in.)
G235	2.35	0.0040
G210	2.10	0.0036
G185	1.85	0.0032
G165	1.65	0.0028
G140	1.40	0.0024
G115	1.15	0.0020
G90	0.90	0.0015
G60	0.60	0.0010

Note: 1 oz/ft^2 = 3 N/m^2; 1 in. = 25.4 mm
Based on standard specification for ASTM A653, 1997.

APPENDIX B
Torsion

B.1 INTRODUCTION

For beam design, when the transverse loads do not pass through the shear center of the cross section, the member will be subjected to a combination of plane bending and torsional moment. Consequently the following longitudinal stresses (perpendicular to the cross section) and shear stresses (in the plane of the cross section) will be developed in the member:

1. *Due to Plane Bending*

$$f = \text{longitudinal bending stress.}$$

$$v = \text{shear stress.}$$

2. *Due to Torsion*

$$\sigma_w = \text{warping longitudinal stress.}$$

$$\tau_t = \text{pure torsional shear stress (or St. Venant shear stress).}$$

$$\tau_w = \text{warping shear stress.}$$

The torsional analysis of rolled steel sections has been well presented in Refs. B.1, 2.45, and 4.140. Many textbooks on steel structures and mechanics also treat this subject in detail. In general, the longitudinal and shear stresses due to plane bending and torsional moment are computed separately and then combined for the final results. This appendix covers the location of the shear center and summarizes the methods used for determining torsional stresses. For a detailed discussion and the derivation of formulas, the reader is referred to Refs. B.1, 2.45, 4.140, and other publications.

B.2 SHEAR CENTER

For any open shapes as shown in Fig. B.1, the shear center of the cross section can be located by x_0 and y_0 as follows:[2.45,1.159]
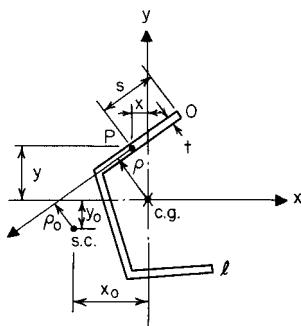
Figure B.1

$$x_0 = \frac{I_{\omega y}}{I_x} \tag{B.1}$$

$$y_0 = -\frac{I_{\omega x}}{I_y} \tag{B.2}$$

where x_0 = x coordinate of shear center
y_0 = y coordinate of shear center
I_x, I_y = moments of inertia of cross section about x- and y-axes, respectively

$$I_{\omega y} = \int_0^l \omega y t \, ds \tag{B.3}$$

$$I_{\omega x} = \int_0^l \omega x t \, ds \tag{B.4}$$

$$\omega = \int_0^s \rho \, ds \tag{B.5}$$

t = wall thickness
x, y = coordinates measured from centroid to any point P located on middle line of cross section
s = distance measured along middle line of cross section from one end to point P
l = total length of middle line of cross section
ρ = perpendicular distance to tangent line from centroid (c.g.). The magnitude of ρ is positive if the centroid is to the left of an observer standing at P and looking toward the positive direction of the tangent.

Since cold-formed sections are usually composed of flat elements, the computation of the above properties ($I_{\omega x}$, $I_{\omega y}$, and ω) can be simplified as follows by using the notations shown in Fig. B.2:[2.45]
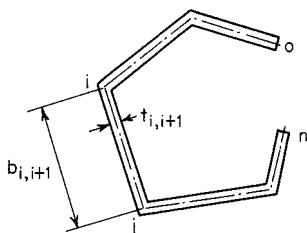
Figure B.2

$$\omega_j = \sum_{i=0}^{i=j-1} \rho_{i,i+1} b_{i,i+1} \tag{B.6}$$

$$I_{\omega x} = \frac{1}{3} \sum_{i=0}^{i=n-1} (\omega_i x_i + \omega_{i+1} x_{i+1}) t_{i,i+1} b_{i,i+1}$$

$$+ \frac{1}{6} \sum_{i=0}^{i=n-1} (\omega_i x_{i+1} + \omega_{i+1} x_i) t_{i,i+1} b_{i,i+1} \tag{B.7}$$

$$I_{\omega y} = \frac{1}{3} \sum_{i=0}^{i=n-1} (\omega_i y_i + \omega_{i+1} y_{i+1}) t_{i,i+1} b_{i,i+1}$$

$$+ \frac{1}{6} \sum_{i=0}^{i=n-1} (\omega_i y_{i+1} + \omega_{i+1} y_i) t_{i,i+1} b_{i,i+1} \tag{B.8}$$

Table B.1 includes values of x_0 and y_0 for equal-leg angles, channels, hat sections, and Z-sections (Fig. B.3). All equations are based on square corners. Reference 1.159 contains some general equations based on round corners for area and moment of inertia. If the equations in Table B.1 are to be used to compute the values of x_0, the error is usually less than 5%, except that a slightly larger error may be expected for angle sections.

B.3 TORSIONAL STRESSES

As mentioned in Art. B.1, when a torsional moment M_t is applied to the beam, as shown in Fig. B.4, the member is subjected to warping longitudinal stress, pure torsional shear stress, and warping shear stress.

B.3.1 Warping Longitudinal Stress σ_w

The warping longitudinal stress developed in the beam flange can be computed by using Eq. (B.9). It is constant across the thickness of the beam flange. The distribution of the longitudinal stresses along the flange is shown in Fig. B.5.

TABLE B.1   Values of x_0, y_0, and C_w for Angles, Channels, Hat Sections, and Z-Sections

Section	x_0	y_0	C_w
Equal-leg angle without stiffening lips (Fig. B.3a)	$\dfrac{a\sqrt{2}}{4}$	0	0
Equal-leg angle with stiffening lips (Fig. B.3b)	$\dfrac{a + c}{2\sqrt{2}}$ $+ \dfrac{tac^2}{3\sqrt{2}I_x}(3a - 2c)$	0	$\dfrac{t^2a^4c^3}{18I_x}(4a + 3c)$ where $I_x = \dfrac{t}{3}(a^3 + c^3 + 3a^2c - 3ac^2)$
Channel with unstiffened flanges (Fig. B.3c)	$\dfrac{b^2}{a + 2b} + \dfrac{3b^2}{6b + a}$	0	$\dfrac{ta^2b^3}{12}\left(\dfrac{3b + 2a}{6b + a}\right)$
Channel with stiffened flanges (Fig. B.3d)	$\dfrac{bt(b + 2c)}{A}$ $+ \dfrac{bt}{12I_x}(6ca^2$ $+ 3ba^2 - 8c^3)$	0	$\dfrac{t^2}{A}\left[\dfrac{\bar{x}Aa^2}{t}\left(\dfrac{b^2}{3} + m^2 - mb\right)\right.$ $+ \dfrac{A}{3t}[m^2a^3 + b^2c^2(2c + 3a)] - \dfrac{I_xm^2}{t}(2a + 4c)$ $+ \dfrac{mc^2}{3}\{8b^2c + 2m[2c(c - a) + b(2c - 3a)]\}$ $\left. + \dfrac{b^2a^2}{2}[(3c + b)(4c + a) - 6c^2] - \dfrac{m^2a^4}{4}\right]$

TABLE B.1 (*Continued*)

Section	x_0	y_0	C_w
			where $A = (a + 2b + 2c)t$, $m = \dfrac{bt}{12I_x}(6ca^2 + 3ba^2 - 8c^3$
			$\bar{x} = \dfrac{bt(b + 2c)}{A}$, $I_x = \dfrac{t}{12}(a^3 + 6ba^2 + 6ca^2 - 12ac^2 + 8c^3)$
Hat section (Fig. B.3*e*)	$\dfrac{bt(b + 2c)}{A}$ $+ \dfrac{bt}{12I_x}(6ca^2 + 3a^2b - 8c^3)$	0	$\dfrac{a^2}{4}\left[I_y + \bar{x}^2A\left(1 - \dfrac{a^2A}{4I_x}\right)\right] + \dfrac{2b^2tc^3}{3}$ $- ab^2c^2t + \dfrac{a^2btc^3\bar{x}A}{3I_x} - \dfrac{4b^2t^2c^6}{9I_x}$ where $A = (a + 2b + 2c)t$, $\bar{x} = \dfrac{bt(2c + b)}{A}$ $I_x = \left(\dfrac{t}{12}\right)(a^3 + 6ba^2 + 6ca^2 + 12ac^2 + 8c^3)$ $I_y = \dfrac{tb^2}{3(a + 2b + 2c)}(2ab + b^2 + 4bc + 6ca)$
Z-section (Fig. B.3*f*)	0	0	$\dfrac{(tb^3a^2/12)(b + 2a)}{2b + a}$

Notes:
1. Values of a, b, and c are middle line dimensions.
2. In this table, some formulas are obtained from Ref. B.2.
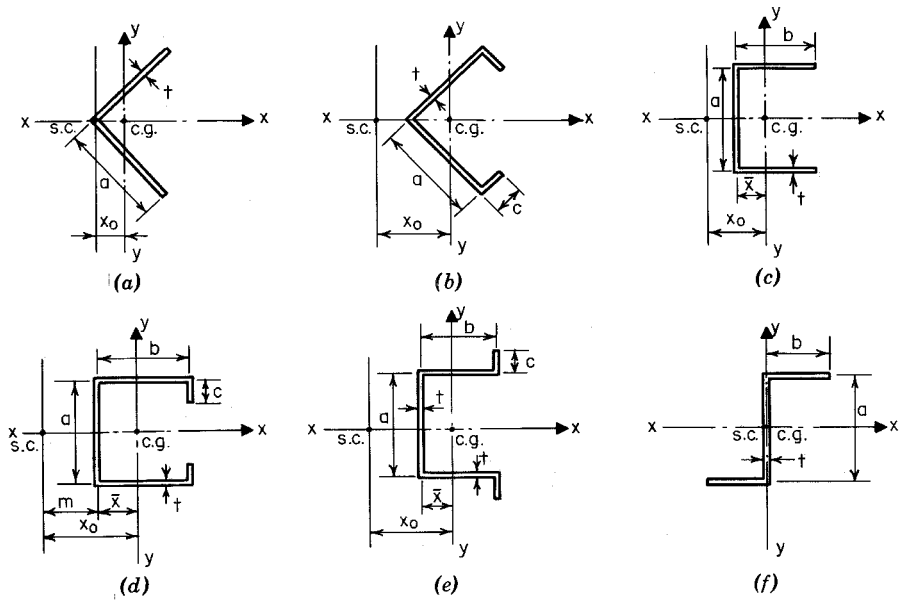
Figure B.3

$$\sigma_w = E\omega_n\phi'' \tag{B.9}$$

where E = modulus of elasticity, 29.5×10^3 ksi (203 GPa)

$$\omega_n = \text{normalized unit warping}, = \frac{1}{A}\int_0^l \omega_0 t \, ds - \omega_0 \tag{B.10}$$
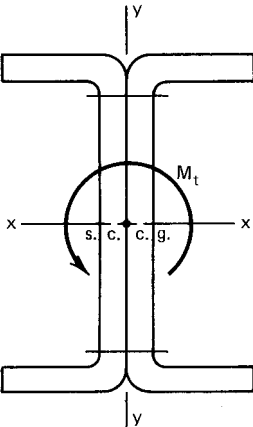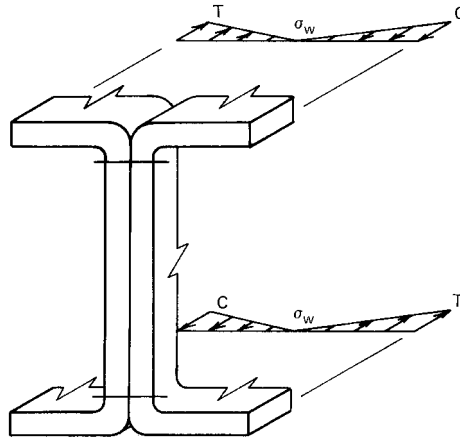
or

Figure B.4

Figure B.5

$$(\omega_{\mathrm{n}})_j = \frac{1}{A} \left\{ \frac{1}{2} \sum_{i=0}^{i=n-1} [(\omega_0)_i + (\omega_0)_{i+1}] t_{i,i+1} b_{i,i+1} \right\} - (\omega_0)_j \tag{B.11}$$

$$\omega_0 = \int_0^s \rho_0 \, ds \tag{B.12}$$

or

$$(\omega_0)_j = \sum_{i=0}^{i=j-1} (\rho_0)_{i,i+1} b_{i,i+1} \tag{B.13}$$

A = total area of cross section

ρ_0 = perpendicular distance to tangent line from shear center (s.c.) (Fig. B.1). The magnitude of ρ_0 is positive if the shear center is to the left of an observer standing at P and looking toward the positive direction of the tangent

ϕ'' = second derivative of angle of rotation ϕ with respect to z. Several typical equations for the angle of rotation ϕ are given in Table B.2
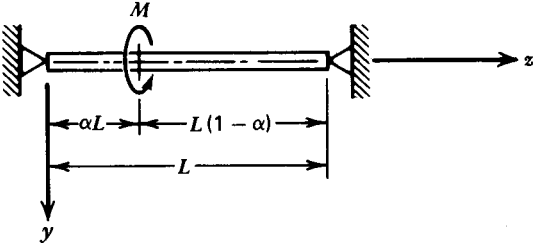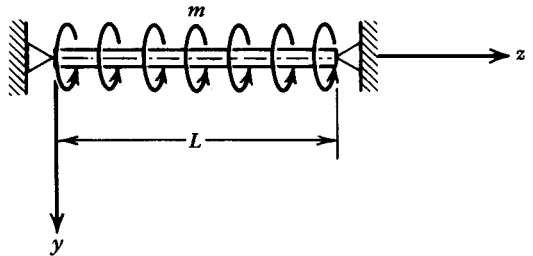
In Table B.2,

G = shear modulus, = 11.3×10^3 ksi (78 GPa)

J = St. Venant torsion constant of cross section. For thin-walled sections composed of n segments of uniform thickness,

$$J = \frac{1}{3} (l_1 t_1^3 + l_2 t_2^3 + \ldots + l_i t_i^3 + \ldots + l_n t_n^3) \tag{B.14}$$

TABLE B.2 Equations for Angle of Rotation (for Beams with Pinned Ends)[B.1]

Loading Condition	ϕ

For $0 \le z \le \alpha L$;

$$\phi = \frac{ML}{GJ}\left[(1 - \alpha)\frac{z}{L} + \left(\frac{\sinh \lambda\alpha L}{\tanh \lambda L} - \cosh \lambda\alpha L\right)\frac{1}{\lambda L}\sin \lambda z\right]$$

For $\alpha L \le zL$

$$\phi = \frac{ML}{GJ}\left[(L - z)\frac{\alpha}{L} + \frac{1}{\lambda L}\left(\frac{\sinh \lambda\alpha L \sinh \lambda z}{\tanh \lambda L} - \sinh \lambda\alpha L \cosh \lambda z\right)\right]$$

$$\phi = \frac{m}{GJ\lambda^2}\left[\frac{\lambda^2 L^2}{2}\left(\frac{z}{L} - \frac{z^2}{L^2}\right) + \cosh \lambda z - \tanh\frac{\lambda L}{2}\sinh \lambda z - 1\right]$$

Note: For other loadings and boundary conditions, see Ref. B.1.

$$\lambda = \sqrt{\frac{GJ}{EC_{\mathrm{w}}}} \tag{B.15}$$

C_{w} = warping constant of torsion of cross section,

$$= \int_0^l \omega_{\mathrm{n}}^2 t \, ds \tag{B.16}$$

or

$$C_{\mathrm{w}} = \frac{1}{3} \sum_{i=0}^{i=n-1} [(\omega_{\mathrm{n}})_i^2 + (\omega_{\mathrm{n}})_i (\omega_{\mathrm{n}})_{i+1} + (\omega_{\mathrm{n}})_{i+1}^2] t_{i,i+1} b_{i,i+1} \tag{B.17}$$

The values of C_{w} for angles, channels, hat sections, and Z-sections are also included in Table B.1. All equations are based on square corners. These C_{w} values are used for determining torsional stresses and for the design of singly symmetric and point-symmetric sections to be used as compression members.

B.3.2 Pure Torsional Shear Stress τ_{t}

The maximum pure torsional shear stress parallel to the edge of the element can be computed by using Eq. (B.18) or Eq. (B.19). These shear stresses vary linearly across the thickness of each element of the cross sections, as shown in Fig. B.6.

$$\tau_{\mathrm{t \ max}} = Gt\phi' \tag{B.18}$$

or

$$\tau_{\mathrm{t \ max}} = \frac{M_{\mathrm{t}} t}{J} \tag{B.19}$$

where M_{t} = torsional moment
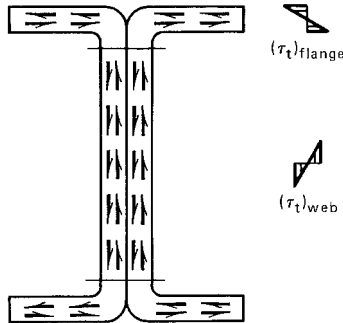ϕ' = first derivative of angle of rotation ϕ with respect to z

Figure B.6

B.3.3 Warping Shear Stress τ_w

The warping shear stress can be computed by using Eq. (B.20). These shear stresses act in the direction parallel to the edge of the element. As shown in Fig. B.7, they are constant across the thickness of an element of the cross section. The maximum stress occurs at the midwidth of the flange,

$$\tau_w = -\frac{ES_\omega \phi'''}{t} \tag{B.20}$$

where S_ω = warping statical moment at point P, shown in Fig. B.1

$$= \int_0^s \omega_n t \, ds \tag{B.21}$$

ϕ''' = third derivative of angle of rotation ϕ with respect to z

It should be noted that torsional stresses are determined by material properties (E and G), torsional properties (ω_n, S_ω, J, and C_w), cross-section dimensions, and derivatives of the angle of rotation. Torsional properties vary in the cross section, and derivatives of the angle of rotation change along the length of the member. Therefore a study should be made on the combination of plane bending stresses and torsional stresses along the length of the member with due consideration given to the direction of stress.
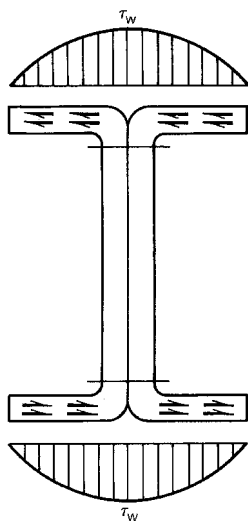
Figure B.7

Example B.1 For the beam (channel section) shown in Fig. B.8, determine the maximum longitudinal stress and shear stress under the following two conditions:

A. Uniform load applied through shear center (s.c.)
B. Uniform load applied through centroid (c.g.)

Use $E = 29{,}500$ ksi and $G = 11{,}300$ ksi. Assume that both ends of the beam are simply supported flexurally and torsionally.

Solution

A. *Uniform Load Applied through Shear Center (s.c.)* Since the uniform load is applied through the shear center of the cross section, the beam is subject only to the plane bending without torsional moment.

   1. *Sectional Properties.* Based on the methods discussed in the text, the following required sectional properties can be computed:

$$I_x = 7.84 \text{ in.}^4, \qquad S_x = 2.24 \text{ in}^3$$

   2. *Longitudinal Stress.* The maximum bending moment at midspan is

$$M = \frac{1}{8} wL^2 = \frac{1}{8}(0.3)(10^2) = 3.75 \text{ ft-kips} = 45 \text{ in.-kips}$$

Figure B.8

The maximum longitudinal stress in the flange is

$$f = \frac{M}{S_x} = \frac{45}{2.24} = 20.1 \text{ ksi}$$

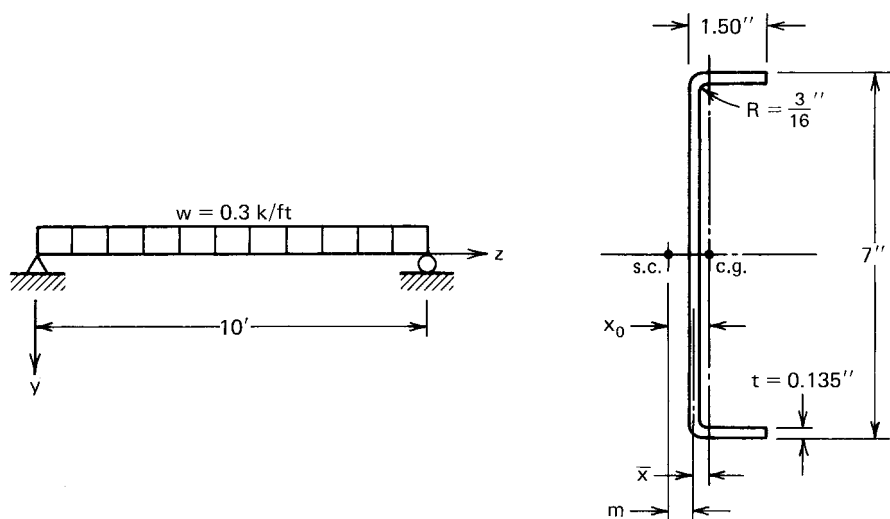3. *Shear Stress.* As discussed in Art. 4.3.3.1, the shear stress v due to plane bending can be computed by

$$v = \frac{VQ}{I_x t}$$

Therefore, as shown in Fig. B.9, the maximum shear stresses developed in the beam flange and the web are computed as follows:

$$V = \frac{1}{2} wL = \frac{1}{2} (0.3)(10) = 1.5 \text{ kips}$$

$$Q_1 = Q_4 = 0$$

$$Q_2 = Q_3 = 1.4325(0.135)\left(\frac{6.865}{2}\right) = 0.664 \text{ in.}^3$$

$$Q_5 = Q_2 + 0.135 \left(\frac{6.865}{2}\right)\left(\frac{6.865}{4}\right) = 1.459 \text{ in.}^3$$

$$v_2 = \frac{VQ_2}{I_x t} = \frac{1.5(0.664)}{7.84(0.135)} = 0.941 \text{ ksi}$$

$$v_5 = \frac{VQ_5}{I_x t} = \frac{1.5(1.459)}{7.84(0.135)} = 2.07 \text{ ksi}$$

By using the average stress method,

$$v_{av} = \frac{V}{ht} = \frac{V}{(d - 2t)t} = \frac{1.5}{[7 - 2(0.135)](0.135)} = 1.65 \text{ ksi}$$

It can be seen that for this channel section the value of v_5 is approximately 25% higher than the average value v_{av}.

B. *Uniform Load Applied through Centroid* (*c.g.*) When the uniform load is applied through the centroid, as shown in Fig. B.10a, the beam is subject to plane bending and a uniformly distributed torque because for the given channel section the shear center and the centroid do not coincide. In order to compute the longitudinal stress and the shear stresses developed from the torsional moment, the shear center should be located and torsional properties such as J, C_w, ω_n, and S_w should be computed. In addition, the equation for the angle of rotation ϕ and its derivatives must also be derived and evaluated.
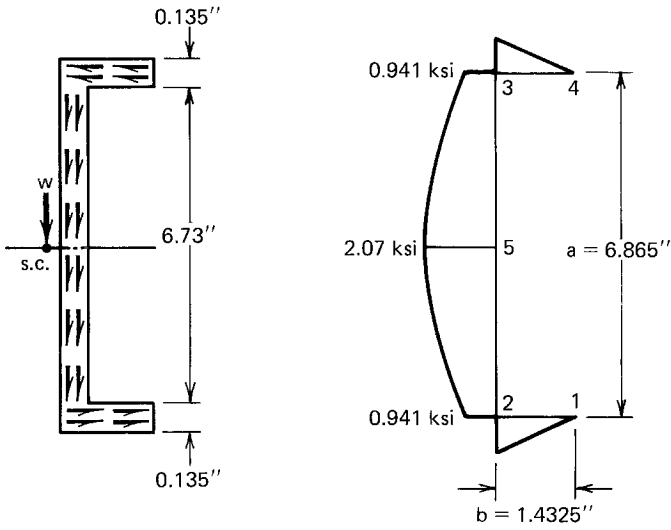
(a) Direction of shear stress   (b) Shear stress distribution

Figure B.9

Distribution of ω_n Distribution of S_ω
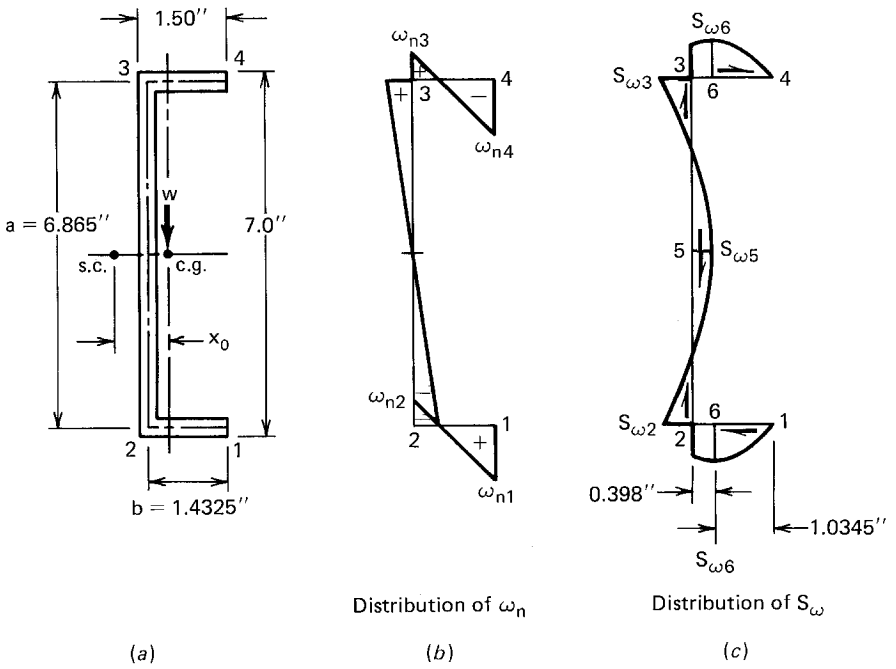
(a)   (b)   (c)

Figure B.10

The following calculations are based on the procedures given by Galambos in Ref. 2.45.

1. *Location of Shear Center.* Based on the midline dimensions shown in Fig. B.10a, the shear center of the given channel section can be located by using the value of x_0 computed from the equation given in Table B.1 for channels with unstiffened flanges:

$$x_0 = \frac{b^2}{a + 2b} + \frac{3b^2}{6b + a}$$
$$= \frac{(1.4325)^2}{6.865 + 2(1.4325)} + \frac{3(1.4325)^2}{6(1.4325) + 6.865} = 0.609 \text{ in.}$$

2. *Torsional Properties.* By using the midline dimensions, the torsional properties can be computed as follows:

   a. *St. Venant torsion constant.* From Eq. (B.14)

   $$J = \frac{1}{3} [2(1.4325) + 6.865](0.135)^3$$
   $$= 0.008 \text{ in.}^4$$

   b. *Warping constant of torsion.* From Eq. (B.17) or the equation given in Table B.1,

   $$C_w = \frac{ta^2b^3}{12} \left(\frac{3b + 2a}{6b + a} \right)$$
   $$= \frac{0.135(6.865)^2(1.4325)^3}{12} \left[\frac{3(1.4325) + 2(6.865)}{6(1.4325) + 6.865} \right]$$
   $$= 1.817 \text{ in.}^6$$

   c. *Normalized warping constant.* From Eqs. (B.10) through (B.13) or using the equations given in Ref. 2.45 for channels, the values of ω_{n1} through ω_{n4} shown in Fig. B.10b can be computed:

   $$\omega_{n1} = \omega_{n4} = \frac{ab}{2} \left(1 - \frac{3b}{6b + a} \right)$$
   $$= \frac{6.865(1.4325)}{2} \left[1 - \frac{3(1.4325)}{6(1.4325) + 6.865} \right]$$
   $$= 3.550 \text{ in.}^2$$
   $$\omega_{n2} = \omega_{n3} = \frac{ab}{2} \left(\frac{3b}{6b + a} \right)$$
   $$= \frac{6.865(1.4325)}{2} \left[\frac{3(1.4325)}{6(1.4325) + 6.865} \right]$$
   $$= 1.367 \text{ in.}^2$$

d. *Warping statical moment.* From Eq. (B.21) or using the equations given in Ref. 2.45, the values of $S_{\omega 2}$, $S_{\omega 3}$, $S_{\omega 5}$, and $S_{\omega 6}$ as shown in Fig. B.10c can be computed:

$$
\begin{aligned}
S_{\omega 2} = S_{\omega 3} &= \frac{ab^2t}{4}\left(1 - \frac{6b}{6b + a}\right) \\
&= \frac{6.865(1.4325)^2(0.135)}{4}\left[1 - \frac{6(1.4325)}{6(1.4325) + 6.865}\right] \\
&= 0.211 \text{ in.}^4 \\
S_{\omega 5} &= \frac{ab^2t}{4}\left(1 - \frac{6b + 1.5a}{6b + a}\right) \\
&= \frac{6.865(1.4325)^2(0.135)}{4}\left[1 - \frac{6(1.4325) + 1.5(6.865)}{6(1.4325) + 6.865}\right] \\
&= -0.106 \text{ in.}^4 \\
S_{\omega 6} &= \frac{ab^2t}{4}\left(1 - \frac{3b}{6b + a}\right)^2 \\
&= \frac{6.865(1.4325)^2(0.135)}{4}\left[1 - \frac{3(1.4325)}{6(1.4325) + 6.865}\right]^2 \\
&= 0.248 \text{ in.}^4
\end{aligned}
$$

3. *Equation of Angle of Rotation and its Derivatives.* From Table B.2, the following equation can be used for the angle of rotation:

$$
\phi = \frac{m}{GJ\lambda^2}\left[\frac{\lambda^2 L^2}{2}\left(\frac{z}{L} - \frac{z^2}{L^2}\right) + \cosh \lambda z - \tanh \frac{\lambda L}{2}\sinh \lambda z - 1\right]
$$

The derivatives with respect to z are as follows:

$$
\begin{aligned}
\phi' &= \frac{m}{GJ\lambda}\left[\frac{\lambda L}{2}\left(1 - \frac{2z}{L}\right) + \sinh \lambda z - \tanh \frac{\lambda L}{2}\cosh \lambda z\right] \\
\phi'' &= \frac{m}{GJ}\left(-1 + \cosh \lambda z - \tanh \frac{\lambda L}{2}\sinh \lambda z\right) \\
\phi''' &= \frac{m\lambda}{GJ}\left(\sinh \lambda z - \tanh \frac{\lambda L}{2}\cosh \lambda z\right)
\end{aligned}
$$

4. *Warping Longitudinal Stress.* The warping longitudinal stress can be computed by using Eq. (B.9):

$$
\sigma_w = E\omega_n\phi'' \tag{B.9}
$$

a. At $z = 0$,

$$
\phi'' = 0, \qquad \sigma_w = 0
$$

b. At $z = L/2$,

$$\phi'' = \frac{m}{GJ}\left(-1 + \cosh\frac{\lambda L}{2} - \tanh\frac{\lambda L}{2}\sinh\frac{\lambda L}{2}\right)$$

where

$$m = \left(\frac{0.3}{12}\right)x_0 = \left(\frac{0.3}{12}\right)(0.609) = 0.0152 \text{ in.-kips/in.}$$
$$G = 11{,}300 \text{ ksi}$$
$$J = 0.008 \text{ in.}^4$$
$$\lambda = \sqrt{\frac{GJ}{EC_w}} = \sqrt{\frac{11{,}300(0.008)}{29{,}500(1.817)}} = 0.0411 \text{ in.}^{-1}$$
$$\frac{\lambda L}{2} = \frac{0.0411(10)(12)}{2} = 2.466$$

Therefore,

$$\begin{aligned}
\phi'' &= \frac{0.0152}{11{,}300(0.008)} \\
&\quad \times [-1 + \cosh(2.466) - \tanh(2.466)\sinh(2.466)] \\
&= -0.0001398 \text{ in.}^{-2}
\end{aligned}$$

By using $E = 29{,}500$ ksi and the values of ω_{n1} through ω_{n4} given in Fig. B.10b, the warping longitudinal stresses at $z = L/2$ for points 1 through 4 shown in Fig. B.10a are computed:

$$\begin{aligned}
\sigma_{w1} &= E\omega_{n1}\phi'' \\
&= 29{,}500(3.550)(-0.0001398) = -14.64 \text{ ksi} \\
\sigma_{w2} &= 29{,}500(-1.367)(-0.0001398) = 5.64 \text{ ksi} \\
\sigma_{w3} &= 29{,}500(1.367)(-0.0001398) = -5.64 \text{ ksi} \\
\sigma_{w4} &= 29{,}500(-3.550)(-0.0001398) = 14.64 \text{ ksi}
\end{aligned}$$

The distribution of σ_w is shown in Fig. B.11a.

5. *Combined Longitudinal Stress.* From case A of this problem, the distribution of the longitudinal stress f due to plane bending is shown in Fig. B.11b. The longitudinal stresses are combined in the following table.
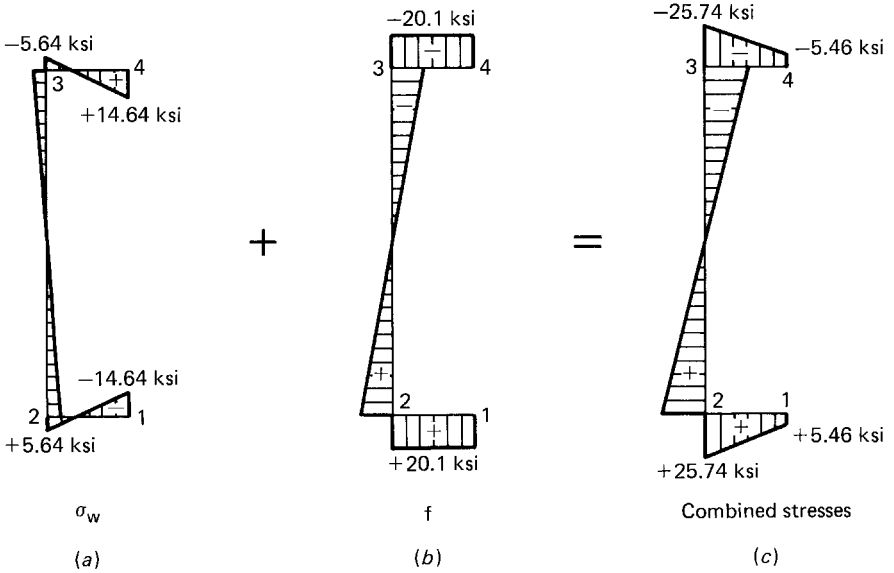
Figure B.11

Point	σ_w (ksi)	f (ksi)	$\sigma_w + f$ (ksi)
1	−14.64	+20.10	+ 5.46
2	+ 5.64	+20.10	+25.74
3	− 5.64	−20.10	−25.74
4	+14.64	−20.10	− 5.46

The combined longitudinal stresses are shown in Fig. B.11c. The maximum longitudinal stress of 25.74 ksi is 28% higher than the longitudinal stress due to plane bending.

6. *Shear Stresses Due to Torsion*

  a. *Pure torsional shear stress.* By using Eq. (B.18), the pure torsional shear stress is

$$\tau_t = Gt\phi' \tag{B.18}$$

At $z = 0$,

$$\phi' = \frac{m}{GJ\lambda} \left(\frac{\lambda L}{2} - \tanh \frac{\lambda L}{2} \right)$$

$$= \frac{0.0152}{11{,}300(0.008)(0.0411)} [2.466 - \tanh (2.466)]$$

$$= 0.00606 \text{ in.}^{-1}$$

Therefore the pure torsion shear stress in flanges and the web is

$$\tau_t = Gt\phi' = 11{,}300(0.135)(0.00606) = 9.24 \text{ ksi}$$

The distribution of τ_t is shown in Fig. B.12a and d.

b. *Warping shear stress.* By using Eq. (B.20), the warping shear stress is

Figure B.12

$$\tau_{\mathrm{w}} = \frac{ES_\omega \phi'''}{t} \qquad (B.20)$$

At $z = 0$,

$$\begin{aligned}
\phi''' &= \frac{m\lambda}{GJ}\left(-\tanh\frac{\lambda L}{2}\right) \\
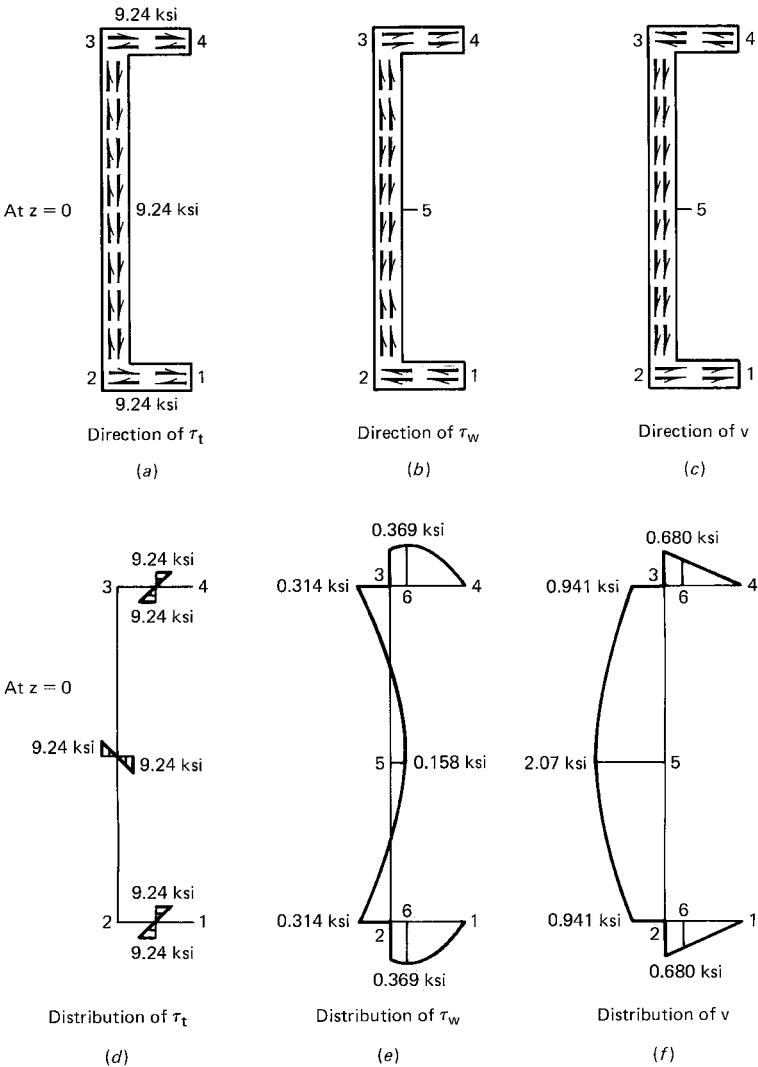&= \frac{0.0152(0.0411)}{11{,}300(0.008)}\,[-\tanh(2.466)] \\
&= -6.81 \times 10^{-6}\ \mathrm{in.}^{-3}
\end{aligned}$$

Therefore the warping shear stress is

$$\begin{aligned}
\tau_{\mathrm{w}} &= -\frac{29{,}500 S_\omega(-6.81 \times 10^{-6})}{0.135} \\
&= 1.488 S_\omega
\end{aligned}$$

Using the values of S_ω given in Fig. B. 10c,

$$\begin{aligned}
\tau_{\mathrm{w}1} &= 0 \\
\tau_{\mathrm{w}2} &= \tau_{\mathrm{w}3} = 1.488(0.211) = 0.314\ \mathrm{ksi} \\
\tau_{\mathrm{w}5} &= 1.488(-0.106) = -0.158\ \mathrm{ksi} \\
\tau_{\mathrm{w}6} &= 1.488(0.248) = 0.369\ \mathrm{ksi}
\end{aligned}$$

The distribution of τ_{w} is given in Fig. B.12b and e.

7. *Combined Shear Stresses.* The combined shear stresses at $z = 0$ can be summarized in the following table, in which the shear stress v due to plane bending is obtained from case A.

Point	τ_{t} (ksi)	τ_{w} (ksi)	v (ksi)	τ_{total} (ksi)
6	9.24 ⇄	0.369 ←	0.680 →	9.551 →
2	9.24 ⇄	0.314 ←	0.941 →	9.867 →
5	9.24 ↑↓	0.158 ↓	2.070 ↓	11.468 ↓

The maximum shear stress of 11.468 ksi occurs at point 5, which is the neutral axis of the channel section.

For additional information on torsional analysis, see Ref. B.3.

APPENDIX C
Formulas for Computing Cross-Sectional Property β_y

In Art. 6.3.2, β_x (Eq. 6.20) and β_y (Eq. 6.21) are used for the analysis of beam-columns using singly symmetric and nonsymmetric open sections.

If the x axis is the axis of symmetry of the cross section, then $\beta_y = 0$. The value of β_y for channels, hat sections, and angles can be computed by using the following equations, which are reproduced from Ref. 6.1 prepared by Pekoz and Celebi.

In the application of these equations, the axes should be oriented as shown in Fig. B.3 (x_0 and $\bar{x}$ are negative). The values of a, b, and c are midline dimensions.

1. *General*

$$\beta_y = \frac{\beta_w + \beta_f + \beta_l}{I_y} - 2x_0$$

2. *Channel* (Fig. B.3c)

$$\beta_l = 0$$

$$\beta_w = \frac{1}{12}\, t\bar{x}a^3 + t\bar{x}^3 a$$

$$\beta_f = \frac{1}{2}\, t[(b + \bar{x})^4 - \bar{x}^4] + \frac{1}{4}\, a^2 t[(b + \bar{x})^2 - (\bar{x})^2]$$

$$\bar{x} = \frac{b^2}{a + 2b}$$

3. *Hat Section* (Fig. B.3e). β_w and β_f are the same as for the channel section.

644

$$\beta_1 = 2ct(\bar{x} + b)^3 + \frac{2}{3} t(\bar{x} + b)\left[\left(\frac{a}{2} + c\right)^3 - \left(\frac{a}{2}\right)^3\right]$$

$$\bar{x} = \frac{b(b + 2c)}{a + 2b + 2c}$$

4. *Lipped Channel* (Fig. B.3d). β_w and β_f are the same as for the channel section.

$$\beta_1 = 2ct(\bar{x} + b)^3 + \frac{2}{3} t(\bar{x} + b)\left[\left(\frac{a}{2}\right)^3 - \left(\frac{a}{2} - c\right)^3\right]$$

$$\bar{x} = \frac{b(b + 2c)}{a + 2b + 2c}$$

5. *Lipped Angle* (Fig. B.3b)

$$\beta_w = 0$$

$$\beta_f = \frac{t}{\sqrt{2}} \left[(\bar{x} + b')^4 - \bar{x}^4 + \frac{4}{3} \bar{x} b'^3 + b'^4 - (\bar{x} + b')^4\right]$$

$$\beta_1 = \frac{t}{\sqrt{2}} \left\{\frac{4}{3} (\bar{x} + 2b')[b'^3 - (b' - c')^3] - b'^4 + (b' - c')^4\right\}$$

$$\bar{x} = \frac{a + c}{2\sqrt{2}}$$

where

$$b' = \frac{a}{\sqrt{2}}$$

$$c' = \frac{c}{\sqrt{2}}$$

Nomenclature

SYMBOL	DEFINITION
A	Full unreduced cross-sectional area
	Area of cross section of stud
	Constant
A_b	$b_1 t + A_s$, for transverse stiffeners at interior support and under concentrated load, and $b_2 t + A_s$, for transverse stiffeners at end support
	Gross cross-sectional area of bolt
A_c	Cross-sectional area of equivalent column
	$18t^2 + A_s$ for transverse stiffeners at interior support and under concentrated load, and $10t^2 + A_s$, for transverse stiffeners at end support
A_e	Effective area at the stress F_n
A_{ef}	Effective area of stiffener section
A_{eff}	Sum of effective areas of all stiffened elements
A'_{eff}	Effective area consisting of all unstiffened elements and sum of effective areas of all stiffened elements
A_f	Area of flange
A_{gt}	Gross area subject to tension
A_{gv}	Gross area subject to shear
A_{nt}	Net area subject to tension
A_{nv}	Net area subject to shear
A_{net}	Net area
A_o	Reduced area due to local buckling
A_s	Cross-sectional area of transverse stiffeners. Fused area of arc spot weld
A'_g	Effective area of stiffener
A_{st}	Full area of stiffener section
A_{wn}	Net web area
a	Spacing of transverse stiffeners
	Length of bracing interval
	Length of steel plate
	Depth of web element
a	Fastener distance from outside web edge
a	Shear panel length of the unreinforced web element. For a reinforced web element, the distance between transverse stiffeners

a	Lateral deflection of the compression flange at assumed load, q
a_x	$= x_o - e_x$
a_y	$= y_o - e_y$
B	Constant
	Stud spacing
B_c	Term for determining tensile yield point of corners
b	Effective design width of compression element
	Flange width
	Depth of shear diaphragm
	Overall width of compression flange, Z-section
	Midline flange width of closed box member
b_d	Effective width for deflection calculation
b_e	Effective design width of subelement or element
b_0	See Figs. 3.42 and 3.43
b_1, b_2	Width of web element for computing combined web-stiffener area; effective width defined by Fig. 3.30
C	Ratio of total corner area to total cross-sectional area of full section or full flange section
	Constant
	Carbon content
	Construction Load
C_b	Bending coefficient dependent on moment gradient
C_c	Distance from neutral axis to extreme fiber in compression flange; $= \sqrt{2\pi^2 E/F_y}$, used for column design
C_H	Web slenderness coefficient
C_{LB}	Center of rotation in lateral buckling of beams
C_m	End moment coefficient in interaction formula
C_{ms}	Coefficient for lateral bracing of Z-section
C_{mx}	End moment coefficient in interaction formula
C_{my}	End moment coefficient in interaction formula
C_N	Bearing length coefficient
C_R	Inside radius coefficient
C_s	Coefficient for lateral–torsional buckling
C_t	Distance from neutral axis to extreme fiber in tension flange
C_{TF}	End moment coefficient in interaction formula
C_{th}	Coefficient for lateral bracing of Z-section
C_{tr}	Coefficient for lateral bracing of Z-section
C_v	$1.53 E k_v/[F_y(h/t)^2]$ when $C_v \leq 0.8$; $1.1\sqrt{E k_v/F_y}/(h/t)$ when $C_v > 0.8$

C_w	Warping constant of torsion of cross section
	Nominal weight of wet concrete during construction
C_y	Factor for considering inelastic reserve strength of beams
C_0	Initial column imperfection
C_1	Term used to compute shear strain in wallboard
	Coefficient as defined in Fig. 3.46
	Term used to compute the limiting unbraced length L_u
	Axial buckling coefficient
C_2	Coefficient as defined in Fig. 3.46
	Axial buckling coefficient
	Term used to compute the limiting unbraced length L_u
$C_1, \ldots C_{11}$	Terms used to compute allowable reactions and concentrated loads for web crippling
C_θ	Factor depending on slope of beam web
c	Distance from centroidal axis to the fiber with maximum compression stress; is negative when the fiber is on shear center side of centroid
	Projection distance from center of radius to c.g. of corner
c_f	Amount of curling
D	A term determined by $Et^3/12(1-\mu^2)$
	Lateral deflection of column centroid due to a force of 1 lb applied to web at level of column centroid
	Weld nugget diameter
	Depth of corrugation
	Constant
	Number of 90° corners
	Outside diameter of cylindrical tube
	Overall depth of lip
	Shear stiffener coefficient
	Dead load
D_i	Inside diameter of cylindrical tube
D_o	Outside diameter of cylindrical tube
	Initial column imperfection
D_s	Weight of steel deck
d	Depth of section
	Diameter of bolt
	Nominal screw diameter
	Depth of corrugation
	Visible diameter of outer surface of arc spot weld
	Width of arc seam weld
	Midline web depth of closed box member

d_a	Average diameter of arc spot weld at midthickness of t
	Average width of seam weld
d_e	Effective diameter of fused area
	Effective width of arc seam weld at fused surfaces
d_h	Diameter of standard hole
d_{min}	Overall minimum depth required of simple lip
d_o	Depth of web hole
d_s	Reduced effective width of stiffener
d'_s	Actual effective width of stiffener
d_w	Larger of the screw head or washer diameter
d_{wc}	Coped web depth
d_{wx}	Screw head or washer diameter
E	Modulus of elasticity of steel, $= 29.5 \times 10^3$ ksi (203 GPa)
	Earthquake load
E_{cs}	Secant modulus in compression flange
E_r	Reduced modulus
E_s	Secant modulus
E_t	Tangent modulus
E_{ts}	Secant modulus in tension flange
E_0	Initial modulus of elasticity
	Initial column inperfection
E_1	Term used to compute shear strain in wallboard
E'	Inelastic modulus of elasticity
e	Eccentricity of axial load with respect to centroidal axis; is negative when on shear center side of centroid
	Edge distance
e_{min}	Minimum allowable distance measured in line of force from centerline of weld (or center of standard hole) to nearest edge of adjacent weld (hole) or to end of connected part toward which force is directed
F	Basic design stress
	Allowable stress on net section of tension members
	Allowable stress for tension and compression on extreme fibers of flexural members
	Fabrication factor
	Nominal load due to fluids
F_a	Maximum average compression stress
F_{at}	Allowable compression stress for torsional buckling

F_b	Maximum compression stress on extreme fibers of laterally unbraced beams
	Maximum bending stress in compression permitted where bending stress only exists
F_{bx}	Maximum bending stress in compression permitted where bending stress only exists
F_c	Critical lateral–torsional buckling stress
F_e	Elastic buckling stress
F_e'	$12\pi^2 E/[23(KL_b/r_b)^2]$
F_m	Mean value of the actual sectional properties to nominal value
F_n	Nominal buckling stress
F_{nt}	Nominal tensile strength of bolts
F_{nv}	Nominal shear strength of bolts
F_{nt}'	Nominal tensile strength for bolts subject to a combination of shear and tension
F_p	Nominal bearing stress
F_{sy}	Specified yield point
F_t	Allowable tension stress on net section
F_t'	Allowable tension stress for bolts subject to a combination of shear and tension
F_u	Tensile strength of steel
F_{uv}	Tensile strength of virgin steel
F_{u1}	Tensile strength of member in contact with screw head
F_{u2}	Tensile strength of member not in contact with screw head
F_v	Allowable average shear stress on gross area of flat web
	Allowable shear stress on the gross area of a bolt
F_{wy}	Yield point for design of transverse stiffeners
F_{xx}	Strength level designation in AWS electrode classification
F_y	Yield point
F_{ys}	Yield point of stiffener steel
F_{yv}	Tensile yield point of virgin steel
F_y'	Average tensile yield point
F_{ya}	Average yield point of section
F_{yc}	Tensile yield point of corners
F_{yf}	Weighted average tensile yield point of flat portions
f	Actual stress in compression element computed on the basis of effective design width
	Combined stress
	Longitudinal bending stress

f_a	Axial stress, $= P/A$, axial load divided by full cross-sectional area of member
f_{av}	Average stress in full unreduced flange width
f_b	Maximum bending stress, $=$ bending moment divided by section modulus of member
f_{bw}	Actual compression stress at junction of flange and web
f_c	Computed stress at design load in the cover plate or sheet
f_{cr}	Critical buckling stress for local buckling of plates and tubes
f_d	Computed compressive stress in the element being considered. Calculations are based on the effective section at the load for which deflections are determined
f_{d1}, f_{d2}	Computed stresses f_1 and f_2 as shown in Fig. 3.30. Calculations are based on the effective section at the load for which deflections are determined
f_{d3}	Computed stress f_3 in edge stiffener, as shown in Fig. 3.46. Calculations are based on the effective section at the load for which deflections are determined
f_e	Edge stress
f_{max}	Maximum actual stress
f_p	Actual bearing stress
f_t	The computed maximum compressive stress due to twisting and lateral bending
f_v	Computed shear stress on a bolt
	Actual average shear stress
f_x	Stress in x direction
f_1, f_2	Web stresses
f_3	Edge stiffener stress
G	Shear modulus of steel, 11.3×10^3 ksi (78 GPa)
G'	Shear stiffness of diaphragm; $= G(E'/E)$
G_r	Reduced shear modulus
G_s	Secant shear modulus
G_0	Initial shear modulus
g	Vertical distance between two rows of connections near or at top and bottom flanges
	Girth of one complete corrugation
	Transverse center-to-center spacing between fastener gage lines
H	Nominal load due to the weight and lateral pressure of soil and water in soil
H^*	h/t ratio

h	Depth of flat portion of web measured along plane of web
	Depth of plate
	Distance from tension flange to centroid of equivalent column
	Amount of corner depression of hyperbolic paraboloid roof
I	Moment of inertia
I'	Moment of inertia of linear elements
I_a	Adequate moment of inertia of stiffener so that each component element will behave as a stiffened element
I_b	Moment of inertia of the full unreduced section about the bending axis
	Moment of inertia of beam
I_c	Moment of inertia of column
I_f	Moment of inertia of compression flange
I_i	Moment of inertia of ith subarea about neutral axis
I_{min}	Minimum allowable moment of inertia of stiffener about its centroidal axis parallel to stiffened element
I_{mx}	Modified moment of inertia about x-axis
I_{my}	Modified moment of inertia about y-axis
I_0	Moment of inertia of effective section about its major axis
I_p	Polar moment of inertia
I_x	Actual moment of inertia of the full stiffener about its own centroidal axis parallel to the element to be stiffened
I_w	Moment of inertia about neutral axis of cover plates
I_{sf}	Moment of inertia of the full area of the multiple stiffened element, including the intermediate stiffeners, about its own centroidal axis parallel to the element to be stiffened
	Moment of inertia of side plates about neutral axis of beam
I_x	Moment of inertia about axis normal to web
I_{xc}	Moment of inertia of compression portion of section about its axis of symmetry
I_{xy}	Product of inertia
I_y	Moment of inertia about y-axis
I_{yc}	Moment of inertia of compression portion of section about gravity axis of entire section parallel to web

I_{yt}	Moment of inertia of tension portion about centerline of web
I_1	Moment of inertia about neutral axis of the area on unloading side after buckling
I_2	Moment of inertia about neutral axis of the area on loading side after buckling
I_{wx}	$\int_0^1 \omega xt\ ds$
I_{wy}	$\int_0^1 \omega yt\ ds$
J	St. Venant torsion constant of cross section
j	Section property for torsional–flexural buckling
K	Effective length factor
	Coefficient
	Constant
	Ratio of p/d
K'	Constant; $= m/d$ for channel, $= I_{xy}/I_x$ for Z-section
K_b	Effective length factor in the plane of bending
K_t	Effective length factor for torsion
K_x	Effective length factor for bending about x-axis
K_y	Effective length factor for bending about y-axis
k	Buckling coefficient; $= 894\ F_y/E$
k_a	Plate buckling coefficient
k_u	Plate buckling coefficient
k_v	Shear buckling coefficient
L	Full span for simple beams
	Distance between inflection points for continuous beams
	Twice length of cantilever beams
	Unbraced length of member
	Length of stud
	Length of element
	Length of seam weld not including circular ends
	Length of fillet weld
	Live load
L_b	Actual unbraced length in plane of bending
	Length of beam
L_c	Length of column
	Length of corner
L_f	Flat width of flange
L_r	Roof live load
L_s	Length of the portion of the span between supports where the flange that is not connected to the sheating is in compression

L_{st}	Total length of transverse stiffener
L_t	Unbraced length of compression member for torsion
L_u	Critical unbraced length for lateral buckling
L_w	Flat width of web
L_x	Unbraced length of compression number for bending about x-axis
L_y	Unbraced length of compression member for bending about y-axis
l_i	Length of middle line of segment i
M	Bending moment
	Required flexural strength, for ASD
	Applied bending moment at or immediately adjacent to point of application of concentrated load or reaction P
	Material factor
M_A	Absolute value of moment at quarter point of unbraced segment for determining C_b
M_a	Allowable bending moment permitted if bending stress only exists
	Allowable design flexural strength
M_{ax}, M_{ay}	Allowable moments about the centroidal axes
M_{allow}	Allowable bending moment permitted if bending stress only exists
M_B	Absolute value of moment at centerline of unbraced segment for determining C_b
M_C	Absolute value of moment at three-quarter point of unbraced segment for determining C_b
	Elastic critical moment causing compression on shear center side of centroid
M_c	Critical moment
M_{cr}	Critical moment
M_D	Bending moment due to dead load
M_e	Elastic critical moment
M_L	Bending moment due to live load
M_m	Mean value of the tested material properties to minimum specified values
M_{max}	Absolute value of maximum moment in the unbraced segment for determining C_b
M_n	Nominal flexural strength
	Nominal moment
	Ultimate moment causing maximum compression strain of $C_y \epsilon_y$

M_{nx}	Nominal flexural strength about x-axis
M_{ny}	Nominal flexural strength about y-axis
M_{nxo}	Nominal flexural strength about x-axis determined only for section strength
M_{nyo}	Nominal flexural strength about y-axis determined only for section strength
M_{no}	Nominal yield moment for nested Z-sections
M_{nxt}	Nominal flexural strength about x-axis determined using the gross, unreduced cross-section properties
M_{nyt}	Nominal flexural strength about y-axis determined using the gross, unreduced cross-section properties
M_p	Full plastic moment
M_T	Elastic critical moment causing tension on shear center side of centroid
M_t	Torsional moment
M_u	Required flexural strength
M_{ux}	Required flexural strength about x-axis for LRFD
M_{uy}	Required flexural strength about y-axis for LRFD
M_x	Bending moment about x-axis
M_y	Yield moment
	Bending moment about y-axis
M_0	Maximum moment between supports due to transverse loading
M_1	Smaller end moment
M_2	Larger end moment
Mn	Manganese content
m	Term for determining tensile yield point of corners
	Distance of shear center of channel from midplane of web
	Number of half sine waves
	Thickness ratio for web crippling strength
N	Actual length of bearing
	Tensile strength of spot welding
$N*$	N/t ratio
n	Number of half sine waves
	Number of holes
n_b	Number of bolt holes
n_p	Number of parallel purlin lines

P	Applied axial load
	Concentrated load or reaction
	Required strength for the concentrated load or reaction in the presence of bending moment, for ASD
	Required strength transmitted by bolt or weld, for ASD
	Required compressive axial strength for ASD
	Professional factor
P_a	Allowable load
P_{allow}	Allowable concentrated load or reaction for one transverse stiffener
	Allowable concentrated load or reaction for one solid web sheet connecting top and bottom flanges
P_{a0}	Allowable axial load determined for $L = 0$
P_{cr}	Critical load
P_D	Force due to dead load
P_{Ex}	Elastic buckling strength about x-axis
P_{Ey}	Elastic buckling strength about y-axis
P_e	Euler critical load
P_L	Force to be resisted by intermediate beam brace
	Force due to live load
P_m	Mean ratio of the experimentally determined ultimate load to the predicted ultimate load of test specimens
P_n	Nominal axial strength of member
	Nominal strength of connection component
	Nominal bearing strength
	Nominal web crippling strength
P_{no}	Nominal axial strength of member determined for $F_n = F_y$
P_{ns}	Nominal shear strength per screw
P_{nt}	Nominal tension strength per screw
P_{not}	Nominal pull-out strength per screw
P_{nov}	Nominal pull-over strength per screw
P_R	Reduced modulus load
P_s	Concentrated load or reaction
P_T	Tangent modulus load
P_u	Required strength transmitted by weld for LRFD
	Required strength for the concentrated load or reaction in the presence of bending moment for LRFD
P_{u0}	Observed ultimate load
P_{up}	Predicted ultimate load
P_{us}	Ultimate shear capacity per weld

P_x, P_y	Euler flexural buckling load about x- and y-axes, respectively
P_z	Torsional buckling load
P_{zQ}	$= P_z + \bar{Q}d^2/4r_0^2$
P_0	Initial load
p	Corrugation pitch
Q	Stress and/or area factor to modify allowable axial stress
	Shear rigidity of diaphragm
	Static moment of area between extreme fiber and the particular location at which shear stress is desired, taken about neutral axis
Q_a	Area factor to modify members composed entirely of stiffened elements
Q_a'	Area factor determined by A_{eff}'/A
Q_i	Load effect
Q_m	Mean value of load effect
Q_s	Stress factor to modify members composed entirely of unstiffened elements
$\bar{Q}$	Design shear rigidity for two wallboards
$\bar{Q}_a$	$= \bar{Q}/A$
$\bar{Q}_t$	$= \bar{Q}d^2/4Ar_0^2$
$\bar{Q}_0$	Sheathing parameter
q	Intensity of loading on beam
	Transverse component of flange force
	Ratio of R'/d
$\bar{q}$	Design shear rigidity for two wallboards per inch of studspacing
$\bar{q}_0$	Factor used to determine design shear rigidity
q_s	Factor used to reduce the shear strength due to web opening
q_w	Allowable uniform load
q_u	Maximum uniformly distributed load in the plane of the web
R	Required strength, for ASD
	Coefficient
	Inside bend radius
	Reduction factor
R_a	Allowable resistance or allowable design strength
R_c	Factor used to reduce the web crippling strength due to web opening
R_m	Mean value of resistance

R_n	Nominal resistance
R_n	Nominal strength
R_r	Roof rain load
R_u	Required strength, for LRFD
R'	Midline radius
$R*$	R/t ratio
r	Radius of gyration
	Bolt force ratio
r_b	Radius of gyration about axis of bending
r_{cy}	Radius of gyration of one C-section about its centroidal axis parallel to web
r_I	Radius of gyration of I-section about axis perpendicular to direction in which buckling would occur for given conditions of end support and intermediate bracing, if any
r_x	Radius of gyration of cross section about centroidal principal axis
r_y	Radius of gyration of cross section about centroidal principal axis
r_0	Polar radius of gyration of cross section about shear center
$\bar{r}_0$	$= \sqrt{\beta_x e_y + \beta_y e_x + I_0/A}$
S	Section modulus
	Shear strength of spot welding
	$1.28\sqrt{E/F}$
	Snow load
S_a	In-plane load carrying capacity for diaphragms
S_c	Elastic section modulus of the effective section calculated at a stress f_c relative to the extreme compression fiber
S_d	Design shear strength for diaphragm
S_e	Elastic section modulus of the effective section calculated with extreme compression or tension fiber at F_y
S_f	Elastic section modulus of full unreduced section for the extreme compression fiber
S_n	Nominal shear strength of in-plane diaphragm
S_u	Ultimate shear strength of diaphragm
S_x	Section modulus about x-axis
S'_x	Section modulus of beam computed for full web area and effective width of compression flange determined on the basis of F_y

S_{xc}	Compression section modulus of entire section about major axis
S_{yc}	Compression section modulus of entire section about axis normal to axis of symmetry
S_w	Warping statical moment
s	Fastener spacing
	Spacing in line of stress of welds, rivets, or bolts connecting a compression cover plate or sheet to a nonintegral stiffener or other element
	Weld spacing
	Spacing of bolts perpendicular to line of stress
	Distance measured along middle line of cross section from one end to point P
s'	Longitudinal center-to-center spacing of holes
s_{lim}	Limiting longitudinal spacing of connections
s_{max}	Maximum permissible longitudinal spacing of welds or other connectors joining two C-sections to form an I-section
T	Torsional reduction factor
	Self-straining forces and effects
	Required tensile axial strength, for ASD
T_a	Allowable tensile strength
T_n	Nominal tensile strength
T_s	Strength of connection in tension
T_u	Required tensile axial strength, for LRFD
t	Base steel thickness of any element or section
	Total combined base thickness (exclusive of coatings) of sheets involved in shear transfer
	Thickness of coped web
t_c	Lesser of the depth of the penetration and t_2
t_e	Effective throat dimension for groove weld
	Thickness of coped web
t_i	Steel thickness of the member for segment i
t_s	Equivalent thickness of multiple-stiffened element
t_w	Effective throat of weld
t_1	Thickness of member in contact with screw head
t_2	Thickness of member not in contact with screw head
U	Potential energy
	Reduction factor for determining effective net area
u	Deflection or displacement in x-direction
u_o	Initial deflection in x-direction

V	Required shear strength, for ASD
V_a	Allowable shear force
V_D	Shear strength due to dead load
V_F	Coefficient of variation of the fabrication factor
V_L	Shear strength due to live load
V_M	Coefficient of variation of the material ratio
V_n	Nominal shear strength
V_P	Coefficient of variation of the tested-to-predicted load ratios
V_Q	Coefficient of variation of the load effect
V_R	Coefficient of variation of the resistance
V_u	Required shear strength, for LRFD
V_1	Strain energy in twisted column
V_2	Strain energy of supporting frame
v	Deflection or displacement in y-direction
	Longitudinal shear stress
W	Total uniform load
	Wind load
$W*$	Ratio of length of centerline of full flange of flexural members, or of entire section of tension or compression members, to thickness
w	Flat width of element exclusive of fillets
	Uniformly distributed load
w_{cr}	Uniform load to cause lateral buckling of beam
w_D	Uniformly distributed dead load
w_f	Width of flange projection beyond web for I-beam and similar sections or half the distance between webs of box- or U-type sections
	Projection of flanges from inside face of web
	Flat width of flange
w_L	Uniformly distributed live load
w_s	Whole width between webs or from web to edge stiffener
w_w	Flat width of web
w_1, w_2	Leg on weld
x	Distance from concentrated load to brace
	Distance measured along x-axis
	Non-dimensional fastener location
	Nearest distance between the web hole and the edge of the bearing
x_0	Distance from shear center to centroid along principal x-axis; x coordinate of shear center, negative

$\bar{x}$	Distance from shear plane to centroid of the cross section
Y	Yield point of web steel divided by yield point of stiffener steel
y	Distance measured along y-axis
y_c	Distance from neutral axis of beam to centroid of equivalent column
y_{cg}	Distance from extreme fiber to neutral axis in y-direction
y_0	Distance from centroid of equivalent column to its shear center; y-coordinate of shear center
Z	Parameter to determine behavior of tubular members
α	Reduction factor
	$= 1 - (x_0/r_0)^2 - (y_0/r_0)^2$
	Factor for sign convention in Art. 4.4.1.2
	Parameter for determining the effective area of a stiffener
$1/\alpha_x$, $1/\alpha_y$	Magnification factors
β	$= 1 - (x_0/r_0)^2$
	Spring constant
	Coefficient
	Reliability index
β_0	Target reliability index
β_{act}	Extensional stiffness of decking material
β_{id}	Spring constant of elastic support
β_f, β_1, β_w	Terms used in Appendix C for computing β_y
β_x, β_y	Terms used in torsional and torsional–flexural buckling analysis
γ	Load factor
	$= 1 - (y_0/r_0)^2$
	Actual shear strain in the sheathing
$\bar{\gamma}$	Permissible shear strain of the sheathing
Δ	Deflection
Δ_b	In-plane flexural deflection
Δ_d	Shear deflection corresponding to a load of 0.8 P_{ult}
Δ_s	In-plane shear deflection
Δ_{ss}	In-plane deflection due to seam slip
δ_0	Maximum deflection due to transverse loading
δ_u	Horizontal displacement of shear center due to a unit load
$\delta_{u\phi}$	Horizontal displacement of shear center due to a unit moment
δ_ϕ	Rotation of column due to a unit moment
ε_{cu}	Maximum compression strain

ε_1	Local elongation
ε_u	Uniform elongation
ε_y	Yield strain
η	Plasticity reduction factor
θ	Angle between web and bearing surface, $\geq 45°$ but no more than $90°$
	Angle between the vertical and the plane of the web of the C-section or Z-section, degrees
	Angle between an element and its edge stiffener
λ	Length of half sine wave
	$= \sqrt{GJ/EC_w}$
	Slenderness factor
λ_c	Column slenderness parameter
λ_1, λ_2	Parameters used in determining compression strain factor
μ	Poisson's ratio for steel $= 0.30$
ρ	Perpendicular distance to tangent line from centroid
	Reduction factor
ρ_0	Perpendicular distance to tangent line from shear center
σ	Stress related to shear strain in sheathing
	Stress
σ_b	Bearing stress at failure of connection
σ_{bC}	Maximum compression bending stress caused by M_C
σ_{bT}	Maximum compression bending stress caused by M_T
σ_{b1}	Maximum compression bending stress in section caused by σ_{TF}, $= \sigma_{TF}ec/r_y^2$
σ_{b2}	$= \sigma_{TF}x_0c/r_y^2$
σ_{CR}	Theoretical elastic buckling stress
σ_{cr}	Critical buckling stress
σ_e	$= \pi^2 E/(KL_b/r_b)^2$
σ_{ex}	$= \pi^2 E/(K_x L_x/r_x)^2$
σ_{exy}	$= \pi^2 EI_{xy}/(AL^2)$
σ_{ey}	$= \pi^2 E/(K_y L_y/r_y)^2$
σ_{max}	Maximum local buckling stress
σ_{net}	Failure stress in net section
σ_R	Critical buckling stress based on reduced modulus method
σ_R	Standard deviation of resistance
σ_Q	Standard deviation of load effect
σ_s	Average failing stress
σ_T	Critical buckling stress based on tangent modulus method

σ_{TF}	Average elastic torsional–flexural buckling stress
σ_{TFO}	Elastic torsional–flexural buckling stress
σ_{TFT}	Inelastic torsional–flexural buckling stress
σ_t	Torsional buckling stress
σ_{tQ}	$= \sigma_t + \overline{Q}_t$
σ_w	Warping longitudinal stress
τ	E_t/E
	Shear stress
τ_{cr}	Critical shear buckling stress
τ_{cri}	Initial critical shear buckling stress
τ_{pr}	Proportional limit in shear
τ_t	Pure torsional shear stress (or St. Venant shear stress)
τ_u	Ultimate shear strength of weld metal
τ_w	Warping shear stress
τ_y	Yield point in shear
Φ	Amplification factor
ϕ	Angle of twist about z-axis.
	Resistance factor
ϕ_b	Resistance factor for bending strength
ϕ_c	Resistance factor for concentrically loaded compression member
ϕ_d	Resistance factor for diaphragm
ϕ_t	Resistance factor for tension member
ϕ_v	Resistance factor for shear strength
ϕ_w	Resistance factor for web crippling strength
ϕ_0	Initial angle of twist about z-axis
ψ	$= \pi^2 \delta_0 EI/M_0 L^2 - 1$
	f_2/f_1
ω	Deflection of plate perpendicular to surface
	$\int_0^2 \rho ds$
ω_n	Normalized unit warping
ω_0	$\int_0^s \rho_0 \, ds$
Ω	Factor of safety
Ω_b	Factor of safety for bending strength
Ω_c	Factor of safety for concentrically loaded compression member
Ω_d	Factor of safety for diaphragm
Ω_t	Factor of safety for tension member
Ω_v	Factor of safety for shear strength
Ω_w	Factor of safety for web crippling strength

Acronyms and Abbreviations

ACRONYMS

AASHTO   American Association of State Highway and Transportation Officials, 341 National Press Building, Washington, DC 20004.

AISC   American Institute of Steel Construction, One East Wacker Drive, Suite 3100, Chicago, IL 60601.

AISI   American Iron and Steel Institute, 1101 17th Street, NW, Suite 1300, Washington, DC 20036.

AREA   American Railway Engineering Association, 59 East Van Buren Street, Chicago, IL 60605.

ASCE   American Society of Civil Engineers, 1801 Alexander Bell Drive, Reston, VA 20191.

ASTM   American Society for Testing and Materials, 100 Bar Harbor Drive, West Conshohocken, PA 19428.

AWS   American Welding Society, 550 N. W. LeJeune Road, Miami, FL 33135.

CCFSS   Center for Cold-Formed Steel Structures, University of Missouri-Rolla, Rolla, MO 65409.

CRC   Column Research Council (see SSRC).

CSA   Canadian Standards Association, 178 Rexdale Boulevard, Rexdale, Ont., Canada M9W 1R3.

ECCS   European Convention for Constructional Steelwork.

IABSE   International Association for Bridge and Structural Engineering, Swiss Federal Institute of Technology, Zurich, Switzerland.

LGSEA   Light Gauge Steel Engineers Association, 2017 Galbraith, Nashville, TN 37215.

MBMA   Metal Building Manufacturers Association, 1300 Sumner Avenue, Cleveland, OH 44115.

MCA   Metal Construction Association, 104 S. Michigan Avenue, Suite 1500, Chicago, IL 60603.

NACA   National Advisory Committee for Aeronautics (see NASA).

NASA   National Aeronautics and Space Administration (formerly NACA), Washington, DC.

NASFA   North American Steel Framing Alliance, 1726 M Street, NW, Washington, DC 20036-4623.

RMI   Rack Manufacturers Institute, 8720 Red Oak Boulevard, Suite 201, Charlotte, NC 28217.

SDI   Steel Deck Institute, P.O. Box 25, Fox River Grove, IL 60021.

SJI   Steel Joist Institute, 3127 10th Ave., North Ext., Myrtle Beach, SC 29577.

SSMA	Steel Stud Manufacturers Association, 8 S. Michigan Avenue, Suite 1000, Chicago, IL 60603.
SSRC	Structural Stability Research Council (formerly CRC), University of Florida, P.O. Box 116580, Gainesville, FL 32611.

ABBREVIATIONS

ASD	Allowable stress design
c.g.	Center of gravity
EOF	End one-flange loading
ETF	End two-flange loading
ft/min	Feet per minute
GPa	Gigapascal
IOF	Interior one-flange loading
ITF	Interior two-flange loading
in.	Inch
kip	1000 pounds
kN	Kilonewton
kN/mm²	Kilonewtons per square millimeter
ksi	Kips per square inch
lb/ft	Pounds per foot
lb/ft²	Pounds per square foot
LF	Load factor
LRFD	Load and resistance factor design
MPa	Megapascal
m	Meter
m/min	Meters per minute
mm	Millimeter
N/m²	Newtons per square meter
oz/ft²	Ounces per square foot
psf	Pounds per square foot
psi	Pounds per square inch
s.c.	Shear center
s.c.e.	Stiffened compression element
SF	Safety factor
u.c.e.	Unstiffened compression element

Conversion Table

This table contains some conversion factors between U.S. Customary and S.I. Metric Units

	To Convert	To	Multiply by
Length	in.	mm	25.4
	mm	in.	0.03937
	ft	m	0.30480
	m	ft	3.28084
Area	in.^{2}	mm^2	645.160
	mm^2	in.^{2}	0.00155
	ft^2	m^2	0.09290
	m^2	ft^2	10.76391
Forces	kip force	kN	4.448
	lb	N	4.448
	kN	kip	0.2248
Stresses	ksi	MPa	6.895
	MPa	ksi	0.145
Moments	ft-kip	kN-m	1.356
	kN-m	ft-kip	0.7376
Uniform loading	kip/ft	kN/m	14.59
	kN/m	kip/ft	0.06852
	kip/ft^2	kN/m^2	47.88
	kN/m^2	kip/ft^2	0.02089
	psf	N/m^2	47.88

REFERENCES

CHAPTER 1

1.1 Kirkland, W. G.: "Cold Roll Forming Practice in the United States," presented at the Metallurgical and Engineering Aspects of Weight-Saving in Steel Structures, Conference, of The West of Scotland Iron and Steel Institute, May 1958; revised and published by American Iron and Steel Institute, Apr. 1966.

1.2 Kenedi, R. M., and W. Shearer Smith: "Applications of Cold-Formed Sections," The West of Scotland Iron and Steel Institute, May 1958.

1.3 Seaburg, P. A.: "The ABC's (and *Q*) of Cold-Formed Steel Design, *Civil Engineering,* vol. 51, pp. 52–56, Jan. 1981.

1.4 American Iron and Steel Institute: "Specification for the Design of Cold-Formed Steel Structural Members," 1986 ed. with the 1989 Addendum.

1.5 Winter, G.: "Light Gage (Thin-Walled) Steel Structures for Building in the U.S.A.," preliminary publication, 4th Congress of the International Association for Bridge and Structural Engineering, 1952.

1.6 Winter, G.: "Development of Cold-Formed Light Gage Steel Structures," AISI regional technical paper, Oct. 1, 1959.

1.7 Winter, G.: "Cold-Formed, Light Gage Steel Construction," *Journal of the Structural Division, ASCE Proceedings,* vol. 85, Nov. 1959.

1.8 American Iron and Steel Institute: "Use of Steel Cuts Costs of Home Building," *Steel Facts,* May 1970.

1.9 American Iron and Steel Institute: "The Design and Fabrication of Cold-Formed Steel Structures."

1.10 Fahy, F. E.: "Economics of Light Sections," presented at the General Meeting of the American Iron and Steel Institute, New York, May 24, 1961.

1.11 Chilver, A. H.: "Structural Problems in the Use of Cold-Formed Steel Sections," *Proceedings of the Institution of Civil Engineers,* vol. 20, Oct. 1971.

1.12 Odenhausen, H.: "Future Scope for Steel in Building, with Special Reference to Housing," *Acier-Stahl-Steel,* Oct. 1964.

1.13 Yu, W. W.: "Design of Light Gage Cold-Formed Steel Structures," West Virginia University, 1965.

1.14 Buker, P. S.: "Cold-Formed Steel Members—for Economy and Easy Assembly," *Civil Engineering,* May 1965.

1.15 Winter, G.: "Thin-Walled Steel Structures—Theoretical Solutions and Test Results," preliminary report, 8th Congress of the International Association for Bridge and Structural Engineering, Sept. 9–14, 1968, theme IIa.

1.16 Scalzi, J. B.: "Light Gage Cold-Formed Structures," preliminary report, 8th Congress of the International Association for Bridge and Structural Engineering, Sept. 9–14, 1968, theme IIb.

1.17 Kenedi, R. M., et al., "Cold-Formed Sections in Britain: Research and Its Application to Design," *Publications of the International Association for Bridge and Structural Engineering,* vol. 20, 1969.

1.18 Wolford, D. S.: "Steel Highway Accessory Structures," *Journal of the Structural Division, ASCE Proceedings,* vol. 97, July 1971.

1.19 Winter, G.: "Thin-Walled Steel for Modern Structures," *Engineering, Cornell Quarterly,* vol. 7, Spring 1972.

1.20 Pekoz, T., and G. Winter: "Cold-Formed Steel Rack Structures," *Proceedings of the 2nd Specialty Conference on Cold-Formed Steel Structures,* University of Missouri-Rolla, Oct. 1973.

1.21 Zakrzewski, A. S.: "Developments and Applications of Lightweight Steel Components in Housing," *Proceedings of the 2nd Specialty Conference on Cold-Formed Steel Structures,* University of Missouri-Rolla, Oct. 1973.

1.22 Tomasetti, R. L.: "Innovative Designs with Cold-Formed Members and Sheets," *Proceedings of the 2nd Specialty Conference on Cold-Formed Steel Structures,* University of Missouri-Rolla, Oct. 1973.

1.23 Gibson, E. B.: "Modern Use of Cold-Formed Steel Products," *Design in Cold-Formed Steel,* R. M. Schuster, Ed., University of Waterloo Press, Ont., Canada, 1974.

1.24 Bryan, E. R.: "New Developments in Light Gauge Steel Construction," Swedish Institute of Steel Construction, Stalbyggnadsdagen, 1975.

1.25 Baehre, R.: "Sheet Metal Panels for Use in Building Construction—Recent Research Projects in Sweden," *Proceedings of the 3rd International Specialty Conference on Cold-Formed Steel Structures,* University of Missouri-Rolla, Nov. 1975.

1.26 Bryan, E. R., and J. M. Davies: "Stressed Skin Construction in the U.K.," *Proceedings of the 3rd International Specialty Conference on Cold-Formed Steel Structures,* University of Missouri-Rolla, Nov. 1975.

1.27 Ife, L. W.: "The Performance of Cold-Formed Steel Products in Housing," *Proceedings of the 3rd International Specialty Conference on Cold-Formed Steel Structures,* University of Missouri-Rolla, Nov. 1975.

1.28 Zakrzewski, A. S.: "Application of Cold-Formed Steel In Foundations," *Proceedings of the 3rd International Specialty Conference on Cold-Formed Steel Structures,* University of Missouri-Rolla, Nov. 1975.

1.29 Johnson, A. L.: "AISI's Cold-Formed Steel Design Specification," *Proceedings of the 4th International Specialty Conference on Cold-Formed Steel Structures,* University of Missouri-Rolla, June 1978.

1.30 Davies, J. M.: "Developments in Inexpensive Lightweight Structures," *Proceedings of the 4th International Specialty Conference on Cold-Formed Steel Structures,* University of Missouri-Rolla, June 1978.

1.31 Pekoz, T., and G. Winter: "Cold-Formed Steel Construction," *Publications of the International Association for Bridge and Structural Engineering,* Feb. 1980.

1.32 Tarlton, D. L.: "Cold-Formed Steel in Building Application," *Conference Proceedings, Cold-Formed Steel Structures,* University of Windsor, Ont., Canada, Apr. 1980.

1.33 Johnson, A. L.: "AISI's Cold-Formed Steel Design Specification—Recent Changes," *Proceedings of the 5th International Specialty Conference on Cold-Formed Steel Structures,* University of Missouri-Rolla, Nov. 1980.

1.34   Bryan, E. R.: "European Recommendations for Cold-Formed Sheet Steel in Building," *Proceedings of the 5th International Specialty Conference on Cold-Formed Steel Structures,* University of Missouri-Rolla, Nov. 1980.

1.35   Zetlin, L.: "Light Gage Space Structures with Prestressing," *Proceedings of the 5th International Specialty Conference on Cold-Formed Steel Structures,* University of Missouri-Rolla, Nov. 1980.

1.36   Abdel-Sayed, G.: "State of the Art–Cylindrical Cold-Formed Steel Farm Structures," *Proceedings of the 5th International Specialty Conference on Cold-Formed Steel Structures,* University of Missouri-Rolla, Nov. 1980.

1.37   American Iron and Steel Institute: "Sheet Steel: A Problem-Solver for Architects."

1.38   American Iron and Steel Institute: "Lightweight Steel Framing Systems," 1975.

1.39   Baehre, R., E. R. Bryan, B. K. He, G. Moreau, T. Pekoz, and K. Sakae: "Cold-Formed Steel Applications Abroad," *Proceedings of the 6th International Specialty Conference on Cold-Formed Steel Structures,* University of Missouri-Rolla, Nov. 1982.

1.40   Rhodes, J., and A. C. Walker, Eds.: *Developments in Thin-Walled Structures—1,* Elsevier Applied Science, Publishers, London, 1982.

1.41   Rhodes, J., and A. C. Walker, Eds.: *Developments in Thin-Walled Structures—2,* Elsevier Applied Science, Publishers, London, 1984.

1.42   Rhodes, J., and A. C. Walker, Eds.: *Developments in Thin-Walled Structures—3,* Elsevier Applied Science, Publishers, London, 1987.

1.43   Rhodes, J., and J. Spence, Eds.: *Behaviour of Thin-Walled Structures,* Elsevier Applied Science Publishers, London, 1984.

1.44   Baehre, R., H. Urschel, and R. Wolfram: "Investigations Concerning the Behaviour and Load-Bearing Capacity of Built-up Light-Gauge Structures," *Thin-Walled Structures, International Journal,* vol. 2, no. 2, 1984.

1.45   Gaylord, E. H., and G. M. Wilhoite: "Transmission Towers: Design of Cold-Formed Angles," *Journal of Structural Engineering,* ASCE, vol. 111, no. 8, Aug. 1985.

1.46   Abdel-Sayed, G., F. Monasa, and W. Siddall: "Cold-Formed Steel Farm Structures, Part I: Grain Bins," *Journal of Structural Engineering,* ASCE, vol. 111, no. 10, Oct. 1985.

1.47   Abdel-Sayed, G., F. Monasa, and W. Siddall: "Cold-Formed Steel Farm Structures, Part II: Barrel Shells," *Journal of Structural Engineering,* ASCE, vol. 111, no. 10, Oct. 1985.

1.48   Zavelani, A., and P. Faggiano: "Design of Cold-Formed Latticed Transmission Towers," *Journal of Structural Engineering,* ASCE, vol. 111, no. 11, Nov. 1985.

1.49   Bryan, E. R., and J. Rhodes: "Cold-Formed Steel Structures and New British Code of Practice," *Proceedings, IABSE Colloquium,* Stockholm, 1986.

1.50   Chong, K. P.: "Sandwich Panels with Cold-Formed Thin Facings," *Proceedings, IABSE Colloquium,* Stockholm, 1986.

1.51   Zhang, Z. Q.: "Use of Cold-Formed Steel in the Building Industry of China," *Proceedings, IABSE Colloquium,* Stockholm, 1986.

1.52   Yu, W. W.: "Cold-Formed Steel for Tall Buildings," *Cold-Formed Steel, Workshop Proceedings of the 3rd International Conference on Tall Buildings,* Jan. 1986.

1.53   Wolford, D. S.: "Steel Joists," *Cold-Formed Steel, Workshop Proceedings of the 3rd International Conference on Tall Buildings,* Jan. 1986.

1.54   Schuster, R. M., S. R. Fox, and D. L. Tarlton: "An LRFD Standard for Cold-Formed Steel Design," *Cold-Formed Steel, Workshop Proceedings of the 3rd International Conference on Tall Buildings,* Jan. 1986.

1.55   Heagler, R. B.: "Composite Floor Design in Tall Buildings," *Cold-Formed Steel, Workshop Proceedings for the 3rd International Conference on Tall Buildings,* Jan. 1986.

1.56   Chong, K. P.: "Sandwich Panels," *Cold-Formed Steel, Workshop Proceedings of the 3rd International Conference on Tall Buildings,* Jan. 1986.

1.57   Fox, S. R., and D. Yates: "A Design Method for Steel Deck Shear Diaphragms," *Cold-Formed Steel, Workshop Proceedings of the 3rd International Conference on Tall Buildings,* Jan. 1986.

1.58   Van der Merwe, P.: "Stainless and Corrosion Resisting Steel Sections," *Cold-Formed Steel, Workshop Proceedings of the 3rd International Conference on Tall Buildings,* Jan. 1986.

1.59   Baehre, R.: "Functional Requirements for Tall Buildings," *Cold-Formed Steel, Workshop Proceedings of the 3rd International Conference on Tall Buildings,* Jan. 1986.

1.60   Rondal, J.: "Thin-Walled Structures," *Proceedings of 2nd Regional Colloquium on Stability of Steel Structures,* Hungary, Final Report, Sept. 25–26, 1986.

1.61   Perry, D. C., and J. N. Nunnery: "MBMA's New Low-Rise Building System Manual," *Proceedings of the 8th International Specialty Conference on Cold-Formed Steel Structures,* UMR, Nov. 1986.

1.62   Johnson, A. L.: "AISI's 1986 Cold-Formed Steel Design Specification—an Overview," *Proceedings of the 8th International Specialty Conference on Cold-Formed Steel Structures,* UMR, Nov. 1986.

1.63   Pinkham, C. W.: "Reformating the AISI Cold-Formed Steel Design Specification," *Proceedings of the 8th International Specialty Conference on Cold-Formed Steel Structures,* University of Missouri-Rolla, Nov. 1986.

1.64   Clauer, C. R.: "Features of AISI's 1986 Cold-Formed Steel Design Manual, *Proceedings of the 8th International Specialty Conference on Cold-Formed Steel Structures,* University of Missouri-Rolla, Nov. 1986.

1.65   Davies, J. M.: "Axially Loaded Sandwich Panels," *Journal of Structural Engineering,* ASCE, vol. 113, Nov. 1987.

1.66   Suunnittelu, "Kylmamuovatut Profiilit," Rautaruukki OY, Finland, 1987 (in Finnish).

1.67   Yu, W. W.: "Cold-Formed Steel Sections—The State of the Art in North America," *Steel Structures* (R. Narayanan, Ed.), Elsevier Applied Science, London, 1987.

1.68.   Rhodes, J.: "Cold-Formed Steel Section—State of the Art in Great Britain," *Steel Structures* (R. Narayanan, Ed), Elsevier Applied Science, London, 1987.

1.69   Hancock, G. J.: *Design of Cold-Formed Steel Structures* (*To Australian/New Zealand Standard AS/NZA 4600: 1996*), 3rd ed., Australian Institute of Steel Construction, 1998.

1.70   Kouhi, J.: "High Strength Steels in Building Technology," VTT Research Report 551, Technical Research Centre of Finland, Espoo, Finland, 1988.

1.71   *Der Metallbau im Konstruktiven-Ingenieurbau,* Festschrift Prof. Tekn. Dr. Rolf Baehre Zum Sechzigsten Geburtstag, Karlsruhe, Germany, February 1988.

1.72   Bryan, E. R., and J. M. Davies: "Recent Developments in Stressed Skin Design," *Der Metallbau im Konstruktiven-Ingenieurbau,* Karlsruhe, Germany, February 1988.

1.73   Johnson, A. L.: "Evolving AISI Design Provisions—an Overview," *Proceedings of the 9th International Specialty Conference on Cold-Formed Steel Structures,* University of Missouri-Rolla, Nov. 1988.

1.74   Hancock, G. J., P. Key, and C. Olsen: "Structural Behaviour of a Stressed Arch Structural System," *Proceedings of the 9th International Specialty Conference on Cold-Formed Steel Structures,* UMR, Nov. 1988.

1.75   Bats, J. O., and J. F. G. Janssen: "Industrialized Housing with Cold-Formed Sheet-Steel Elements," *Proceedings of the 9th International Specialty Conference on Cold-Formed Steel Structures,* UMR, Nov. 1988.

1.76   Hall, L.: "Computer Verifies Beam Design," *The Iron Age,* May 7, 1964.

1.77   Nilson, A. H.: "Folded-Plate Structures of Light Gage Steel," *ASCE Transactions,* pt. II, vol. 128, 1963.

1.78   Nilson, A. H.: "Steel Shell Roof Structures," *Space Forms in Steel,* American Institute of Steel Construction, 1964.

1.79   Graham, H. T.: "New Way to Build a Shell Roof is Welded Steel Deck," *Architectural Record,* Mar. 1962.

1.80   Kirkland, W. G.: "Shell Structures of Light Gage Steel Roof Panels," reprinted from *Southern Building Magazine,* Mar. 1963.

1.81   Schoeller, W. C., R. H. J. Pian, and H. R. Lundgren: "Cold-Formed Folded Plate Structures," *Proceedings of the 1st Specialty Conference on Cold-Formed Steel Structures,* University of Missouri-Rolla, Aug. 1971.

1.82   Zetlin, L., C. H. Thornton, and R. L. Tomasetti: "World's Largest Light Gage Steel Primary Structure," *Proceedings of the 1st Specialty Conference on Cold-Formed Steel Structures,* University of Missouri-Rolla, Aug. 1971.

1.83   Biswas, M., and J. S. B. Iffland: "Metal Decks Used to Form Hypar-Shell Panels," *Proceedings of the 2nd Specialty Conference on Cold-Formed Steel Structures,* University of Missouri-Rolla, Oct. 1973.

1.84   Iffland, J. S. B.: "Folded Plate Structures," *Journal of the Structural Division, ASCE Proceedings,* vol. 105, Jan. 1979.

1.85   "Prefabricated School Components, Better But Cheaper," *Engineering News-Record,* Jan. 30, 1964.

1.86   "Prefab-Steel, Techbuilt," *Progressive Architecture,* Feb. 1963.

1.87   American Iron and Steel Institute: "Sectional Properties of Corrugated Steel Sheets," 1964.

1.88   American Iron and Steel Institute: *Handbook of Steel Drainage and Highway Construction Products,* 1983.

1.89   American Iron and Steel Institute: *Modern Sewer Design,* 3rd ed., 1995.

1.90   Glasstone, S.: *The Effects of Nuclear Weapons,* United States Atomic Energy Commission, rev. ed., Feb. 1964.

1.91   Friberg, B. F.: "Combined Form and Reinforcement for Concrete Slabs," *ACI Journal,* vol. 26, May 1954.

1.92   Bryl, S.: "The Composite Effect of Profiled Steel Plate and Concrete in Deck Slabs," *Acier-Stahl-Steel,* Oct. 1967.

1.93   Ekberg, C. E., and R. M. Schuster: "Floor Systems with Composite Form-Reinforced Concrete Slabs," final report, 8th Congress, of the International Association for Bridge and Structural Engineering, Sept. 9–14, 1968.

1.94   Robinson, H.: "Composite Beam Incorporating Cellular Steel Decking," *Journal of the Structural Division, ASCE Proceedings,* vol. 95, Mar. 1969.

1.95   Fisher, J. W.: "Design of Composite Beams with Formed Metal Deck," *AISC Engineering Journal,* vol. 7, July 1970.

1.96   Oudheusden, A. J.: "Composite Construction—Applications," *Proceedings of the 1st Specialty Conference on Cold-Formed Steel Structures,* University of Missouri-Rolla, Aug. 1971.

1.97   Porter, M. L., and C. E. Ekberg: "Investigation of Cold-Formed Steel-Deck-Reinforced Concrete Floor Slabs," *Proceedings of the 1st Specialty Conference on Cold-Formed Steel Structures,* University of Missouri-Rolla, Aug. 1971.

1.98   Luttrell, L. D., and J. H. Davison: "Composite Slabs with Steel Deck Panels," *Proceedings of the 2nd Specialty Conference on Cold-Formed Steel Structures,* University of Missouri-Rolla, Oct. 1973.

1.99   Schuster, R. M.: "Composite Steel-Deck Concrete Floor Systems," *Journal of the Structural Division, ASCE Proceedings,* vol. 102, May 1976.

1.100   Porter, M. L., and C. E. Ekberg: "Design Recommendations for Steel Deck Floor Slabs," *Journal of the Structural Division, ASCE Proceedings,* vol. 102, Nov. 1976.

1.101   Stark, J. W. B.: "Design of Composite Floors with Profiled Steel Sheet," *Proceedings of the 4th International Specialty Conference on Cold-Formed Steel Structures,* University of Missouri-Rolla, June 1978.

1.102   Kubic, C. R., and J. H. Daniels: "Two-Way Flexure of Steel-Deck-Reinforced Slabs," *Journal of the Structural Division, ASCE Proceedings,* vol. 105, June 1979.

1.103   Steel Deck Institute: "Design Manual for Composite Decks, Form Decks, Roof Decks, and Cellular Metal Floor Deck with Electrical Distribution," No. 29.

1.104   Metal Building Dealers Association and Metal Building Manufacturers Association: *Metal Building Systems* (contributing authors: D. R. Buettner, J. M. Fisher, and C. B. Miller), 1980.

1.105   Canadian Sheet Steel Building Institute: "Steel Building Systems," 1982.

1.106   Metal Building Manufacturers Association: "Low Rise Building Systems Manual," 1996 ed.

1.107 Lee, G. C., R. L. Ketter, and T. L. Hsu: "*Design of Single Story Rigid Frames,* Metal Building Manufacturers Association, 1981.

1.108 Canadian Sheet Steel Building Institute: "Standard for Steel Building Systems," CSSBI 30M-95.

1.109 Ural, O., B. R. Sarchet, W. W. Yu, J. H. Emanuel, F. J. Capek, D. L. Babcock, J. H. Senne, B. H. Green, J. B. Heagler, J. E. Spooner, and L. K. Sieck: "Technique and Technology," panel 1, no. 4, submitted to Subcommittee on Housing of the Committee on Banking and Currency, House of Representatives, U.S. Government Printing Office, Washington, DC, June 1971.

1.110 Pinkham, C. W., and R. L. Klitzke: "Applications of Light-Gage Cold-Formed Members to Modular Systems of School Construction in the United States," final report, 8th Congress, International Association for Bridge and Structural Engineering, Sept. 9–14, 1968.

1.111 "Breakthrough," *Architectural Forum,* Apr. 1970.

1.112 Scalzi, J. B.: "Comments by the Author of the Introductory Report," final report, 8th Congress, International Association for Bridge and Structural Engineering, Sept. 9–14, 1968.

1.113 Eastman, R. W., and A. S. Zakrzewski: "The DOFASCO Experimental Steel House," *Proceedings of the 4th International Specialty Conference on Cold-Formed Steel Structures,* University of Missouri-Rolla, June 1978.

1.114 Machaj, E. W., and A. S. Zakrzewski: "Energy Consideration in Low-Rise Steel Buildings," *Proceedings of the 5th International Specialty Conference on Cold-Formed Steel Structures,* University of Missouri-Rolla, Nov. 1980.

1.115 Kudder, R. J., P. W. Linehan, and J. F. Wiss: "Static and Ultimate Load Behavior of Cold-Formed Steel-Joist Residential Floor Systems," *Proceedings of the 4th International Specialty Conference on Cold-Formed Steel Structures,* University of Missouri-Rolla, June 1978.

1.116 Linehan, P. W., R. J. Kudder, and J. F. Wiss: "Dynamic and Human Response Behavior of Cold-Formed Steel-Joist Residential Floor Systems," *Proceedings of the 4th International Specialty Conference on Cold-Formed Steel Structures,* University of Missouri-Rolla, June 1978.

1.117 Rockey, K. C., and H. V. Hill, Eds.: *Thin-Walled Steel Structures,* Gordon and Breach Science Publishers, New York, 1968.

1.118 Rhodes, J., and A. C. Walker, Eds.: *Thin-Walled Structures, Proceedings of the International Conference at the University of Strathclyde,* Granada Publishing, Apr. 3–6, 1979.

1.119 Halmos, G. T., Ed.: *High-Production Roll Forming,* Society of Manufacturing Engineering, Dearborn, MI, 1983.

1.120 Halmos, G. T.: "Design for Manufacturability," *Proceedings of the 5th International Specialty Conference on Cold-Formed Steel Structures,* University of Missouri-Rolla, Nov. 1980.

1.121 American Iron and Steel Institute: "Research—1966".

1.122 American Iron and Steel Institute: "Research—1969".

1.123 Wolford, D. S.: "General Review of the Related Work and Development of the AISI Design Specification," lecture note, AISI-UMR Short Course on Design of Cold-Formed Steel Structures, 1969, 1970, and 1971.

1.124 Yu, W. W., Ed.: *Proceedings of the First Specialty Conference on Cold-Formed Steel Structures,* University of Missouri-Rolla, Aug. 1971.

1.125 Yu, W. W., Ed.: "Current Research and Design Trends," *Proceedings of the 2nd Specialty Conference on Cold-Formed Steel Structures,* University of Missouri-Rolla, Oct. 1973

1.126 Yu, W. W., and J. H. Senne, Eds.: "Research and Developments in Cold-Formed Steel Design and Construction," *Proceedings of the 3rd International Specialty Conference on Cold-Formed Steel Structures,* University of Missouri-Rolla, Nov. 1975.

1.127 Yu, W. W., and J. H. Senne, Eds.: "Recent Research and Developments in Cold-Formed Steel Structures," *Proceedings of the 4th International Specialty Conference on Cold-Formed Steel Structures,* University of Missouri-Rolla, June 1978.

1.128 Yu, W. W., and J. H. Senne, Eds.: "Recent Research and Design Trends in Cold-Formed Steel Structures," *Proceedings of the 5th International Specialty Conference on Cold-Formed Steel Structures,* University of Missouri-Rolla, Nov. 1980.

1.129 Yu, W. W., and J. H. Senne, Eds.: "Recent Research and Developments in Cold-Formed Steel Design and Construction," *Proceedings of the 6th International Specialty Conference on Cold-Formed Steel Structures,* University of Missouri-Rolla, Nov. 1982.

1.130 Yu, W. W., and J. H. Senne, Eds.: "Recent Research and Developments in Cold-Formed Steel," *Proceedings of the 7th International Specialty Conference on Cold-Formed Steel Structures,* University of Missouri-Rolla, Nov. 1984.

1.131 Yu, W. W., and J. H. Senne, Eds.: "Recent Research and Developments in Cold-Formed Steel Design and Construction," *Proceedings of the 8th International Specialty Conference on Cold-Formed Steel Structures,* University of Missouri-Rolla, Nov. 1986.

1.132 Yu, W. W., and J. H. Senne, Eds.: "Recent Research and Developments in Cold-Formed Steel Structures," *Proceedings of the 9th International Specialty Conference on Cold-Formed Steel Structures,* University of Missouri-Rolla, Nov. 1988.

1.133 "Survey of Current Research on Cold-Formed Structures," ASCE Committee on Cold-Formed Members, preprint 2807, ASCE Annual Convention, Philadelphia, Sept. 1976, S. T. Wang, Subcommittee Chairman.

1.134 "Survey of Current Research on Cold-Formed Structures," ASCE Committee on Cold-Formed Members, preprint 3763, ASCE Annual Convention, Atlanta, Oct. 1979, S. T. Wang, Subcommittee Chairman.

1.135 Chowdhury, A. H.: "Current Research on Cold-Formed Steel Structures," *Proceedings of the 8th International Specialty Conference on Cold-Formed Steel Structures,* University of Missouri-Rolla, Nov. 1986.

1.136 Blandford, G. E., and A. H. Chowdhury: "Current Research on Cold-Formed Steel Structures," *Proceedings of the 9th International Specialty Conference on Cold-Formed Steel Structures,* University of Missouri-Rolla, Nov. 1988.

1.137 Pekoz, T.: "Recent Cold-Formed Steel Research and Design Specification Activities in North America," *Stability of Metal Structures, Proceedings of the Third International Colloquium,* SSRC, May 1983.

1.138   Yu, W. W.: "Research Activity of Cold-Formed Steel Structures at UMR," *Der Metallbau im Konstruktiven-Ingenieurbau,* Karlsruhe, West Germany, Feb. 1988.

1.139   "Literature Survey of Cold-Formed Structures," ASCE Committee on Cold-Formed Members, preprint 2807, ASCE Annual Convention, Philadelphia, Sept. 1976, K. P. Chong, Subcommittee Chairman.

1.140   "Literature Survey of Cold-Formed Structures," ASCE Committee on Cold-Formed Members, preprint 3762, ASCE Annual Convention, Atlanta, Oct. 1979, K. P. Chong, Subcommittee Chairman.

1.141   "Literature Survey of Cold-Formed Structures," ASCE Committee on Cold-Formed Members, *Proceedings of the 8th International Specialty Conference on Cold-Formed Steel Structures,* University of Missouri-Rolla, Nov. 1986, R. A. LaBoube, Committee Chairman.

1.142   Currie, D. M.: "Bibliography on Cold-Formed, Thin-Walled Steel Structures, 1978–86," *Building Research Establishment Report,* Building Research Station, 1987.

1.143   Polyzois, D., and F. A. Khaja: "Literature Survey on Cold-Formed Steel Structures, 1976–1986," University of Manitoba, Sept. 1987.

1.144   "Thin-Walled Metal Structures in Buildings," *Proceedings of the IABSE Colloquium,* Stockholm, 1986.

1.145   "Stability of Steel Structures," *Proceedings of the Second Regional Colloquium on Stability of Steel Structures,* Hungary, Sept. 1986.

1.146   Narayanan, R., Ed.: *Steel Structures: Advances, Design and Construction,* Proceedings of the International Conference on Steel and Aluminium Structures, Cardiff, UK, July 1987, Published by Elsevier Applied Science.

1.147   "Stability of Metal Structures—A World View," 2nd Ed., Structural Stability Research Council, 1989.

1.148   American Institute of Steel Construction: "Specification for Structural Steel Buildings—Allowable Stress Design and Plastic Design," 1989.

1.149   Williams, C. D., and E. C. Harris: *Structural Design in Metals,* The Ronald Press Company, New York, 1957, Chap. 9.

1.150   Abbett, R. W., Ed.: *American Civil Engineering Practice,* vol. III, John Wiley and Sons, New York, 1957, Sec. 31.

1.151   Ricketts, J. T., Ed.: *Building and Design Construction Handbook,* McGraw-Hill Book Company, New York, 1999, Sec. 8.

1.152   Merritt, F. S., M. K. Loftin, and J. T. Ricketts, Eds.: *Standard Handbook for Civil Engineers,* McGraw-Hill Book Company, New York, 1996, Sec. 10.

1.153   Bresler, B., T. Y. Lin, and J. B. Scalzi: *Design of Steel Structures,* John Wiley and Sons, New York, 1968, Chap. 14.

1.154   Lothers, J. E.: *Advanced Design in Structural Steel,* Prentice-Hall, Englewood Cliffs, NJ, 1960, Chap. 9.

1.155   Tall, L., Ed.-in-Chief: *Structural Steel Design,* The Ronald Press Company, New York, 1974, Chap. 12.

1.156   Gaylord, E. H., C. N. Gaylord, and J. E. Stallmeyer: *Structural Engineering Handbook,* McGraw-Hill Book Company, New York, 1997.

1.157 McGuire, W.: *Steel Structures,* Prentice-Hall, Englewood Cliffs, NJ, 1968.

1.158 Galambos, T. V., Ed.: *Guide to Stability Design Criteria for Metal Structures,* 5th ed., John Wiley and Sons, New York, 1998.

1.159 American Iron and Steel Institute: *Cold-Formed Steel Design Manual,* 1996.

1.160 American Iron and Steel Institute: ''Specification for the Design of Cold-Formed Stainless Steel Structural Members,'' 1974 ed.

1.161 Winter, G.: ''Commentary on the 1968 Edition of the Specification for the Design of Cold-Formed Steel Structural Members,'' American Iron and Steel Institute, 1970 ed.

1.162 Heagler, R. B.: *LRFD Design Manual for Composity Beams and Girders with Steel Deck,* Steel Deck Institute, No. LRFD 1.

1.163 Steel Joist Institute and American Institute of Steel Construction: ''Standard Specification for Open Web Steel Joists,'' 1994.

1.164 American Society of Civil Engineers: ''Design of Steel Transmission Pole Structures,'' prepared by the Task Committee on Updating ASCE Design Guide on Steel Transmission Poles, ASCE Manuals and Reports on Engineering Practice No. 72, 1990.

1.165 Rack Manufacturers Institute: ''Specification for the Design, Testing, and Utilization of Industrial Steel Storage Racks,'' 1990 ed.

1.166 Shelving Manufacturers Association: ''Specification for the Design, Testing, Utilization, and Application of Industrial Grade Steel Shelving,'' 1985 ed.

1.167 American Iron and Steel Institute: *Design of Light-Gage Steel Diaphragms,* 1967.

1.168 Luttrell, L. D.: *Steel Deck Institute Diaphragm Design Manual,* 2nd Ed., Steel Deck Institute, 1987.

1.169 Department of the Army—TM 5-809-10, Department of the Navy—NAVDOCKS-P-355, and Department of the Air Force—AFM 88-3; ''Seismic Design for Buildings,'' Washington, DC, Mar. 1966, Chap. 13.

1.170 American Society of Civil Engineers: ''Specification for the Design and Construction of Composite Steel Deck Slabs,'' *ASCE Standard,* Oct. 1984.

1.171 Association of the Wall and Ceiling Industries-International and Metal Lath /Steel Framing Association: ''Steel Framing Systems Manual,'' 1979.

1.172 American Iron and Steel Institute: ''Guide for Preliminary Design of Sheet Steel Automotive Structural Components,'' 1981 ed.

1.173 American Iron and Steel Institute: *Automotive Steel Design Manual,* 1998.

1.174 Johnson, A. L.: ''Cold-Formed Steel: Research to Design,'' *Proceedings of the 6th International Specialty Conference on Cold-Formed Steel Structures,* University of Missouri-Rolla, Nov. 1982.

1.175 Standards Australia and Standards New Zealand: ''Australian/New Zealand Standard on Cold-Formed Steel Structures'' AS/NZS 4600, 1996.

1.176 Lagereinrichtungen, ÖNORM B 4901, Dec. 1974.

1.177 Canadian Standards Association: ''Cold-Formed Steel Structural Members,'' CAN3-S136-M94, 1994.

1.178 Canadian Sheet Steel Building Institute: ''Standard for Steel Roof Deck'' SSBI 10M-96.

1.179 Canadian Sheet Steel Building Institute: "Standard for Composite Steel Deck" CSSBI 12M-96.

1.180 Fox, S. R., R. M. Schuster, and D. L. Tarlton: "The Canadian LRFD Standard for Cold-Formed Steel Design," *Proceedings of the 8th International Specialty Conference on Cold-Formed Steel Structures,* UMR, Nov. 1986.

1.181 Czechoslovak State Standard: "Design of Light Gauge Cold-Formed Profiles in Steel Structures," CSN 73 1402, 1987.

1.182 Finnish Ministry of Environment: "Building Code Series of Finland: Specification for Cold-Formed Steel Structures," Sept. 30, 1988 Draft.

1.183 Centre Technique Industriel de la Construction Métallique: Recommendations pour le Calcul des Constructions à Eléments Minces en Acier," Dec. 1978.

1.184 Centre Technique Industriel de la Construction Métallique: "Constructions à Eléments Minces en Acier—Calcul et Exécution," June 1968.

1.185 Indian Standards Institution: "Indian Standard Code of Practice for Use of Cold-Formed Light-Gauge Steel Structural Members in General Building Construction," IS: 801-1975.

1.186 Architectural Institute of Japan: "Recommendations for the Design and Fabrication of Light Weight Steel Structures," 1985.

1.187 Groep Stelling Fabrikanten—GSF: "Richtlijnen Voor de Berekening van Stalen Industriële Magezijnstellingen," RSM 1977.

1.188 "Technical Standard for Thin-Walled Steel Structures," GBJ 88, Beijing, People's Republic of China, 1988.

1.189 South African Institute of Steel Construction: "Code of Practice for the Design of Cold-Formed Stainless Steel Structural Members," 1995.

1.190 "Romanian Specification for Calculation of Thin-Walled Cold-Formed Steel Members," STAS 10108/2-83.

1.191 Baehre, R., and J. König: "Swedish Specification for Stressed Skin Design," BFR report BI, 1975.

1.192 National Swedish Committee on Regulations for Steel Structures: "Code for the Structural Use of Steel and Aluminium Sheeting," StBK-N5, Stockholm, 1978.

1.193 Swedish Institute of Steel Construction: "Swedish Code for Light Gauge Metal Structures," publication 76, Mar. 1982.

1.194 British Standard Institution: "British Standard: Structural Use of Steelwork in Building. Part 5. Code of Practice for Design of Cold-Formed Sections," BS 5950: Part 5: 1991.

1.195 Storage Equipment Manufacturer's Association: "Interim Code of Practice for the Design of Static Raking," Apr. 1977.

1.196 "Ergänzende Angaben zu DIN 4115," addendum to German Industry standard 4115, latest edition.

1.197 "Lager- und Betriebseinrichtungen Gütesicherung" RAL-RG 614, Oct. 1977.

1.198 Lindner, J., and T. Gregull: "Design Rules for Thin-Walled Structures Due to DIN 18800 Part 2" *Steel Structures* (R. Narayanan, Ed.), Elsevier Applied Science, London, 1987.

1.199 State Building Construction of USSR: "Building Standards and Rules: Design Standards—Steel Construction," Part II, Ch. 23, Moscow, 1988.

1.200 Gladischefski, H., H. Odenhausen, und G. Zessler: "Berechnung von Bauteilen aus kaltgeformtem dünnwandigem Stahlblech," in *Handbuch und Kommentar,* Verlag Stahleisen, Düsseldorf, 1964.

1.201 Camara Nacional de la Industria del Hierro y del Acero, Mexico: "Manual de Diseño de Secciones Estructurales de Acero Formadas en Frío de Calibre Ligero," 1965.

1.202 "Manuale per il Calcolo delle Membrature in Profilati Leggeri di Acciaio Sagomati a Freddo," ILVA Alti Forni e Acciaierie d'Italia, Genova.

1.203 Yu, W. W., and C. Y. Chuang: "Chinese Translation of the AISI Specification for the Design of Cold-Formed Steel Structural Members, 1968 ed.," SHUS Foundation, Taiwan, Republic of China, 1972.

1.204 C. V. G. Siderúrgica del Orinoco (SIDOR): "Manual de Proyectos de Estructuras de Acero," 2nd ed., Caracas, Venezuela, 1982.

1.205 European Convention for Constructional Steelwork: "European Recommendations for the Design of Composite Floors with Profiled Steel Sheet," CONSTRADO, London, May 1975.

1.206 European Convention for Constructional Steelwork: "European Recommendations for the Stressed Skin Design of Steel Structures," ECCS-XVII-77-1E, CONSTRADO, London, Mar. 1977.

1.207 European Convention for Constructional Steelwork: "European Recommendations for the Testing of Profiled Metal Sheets," ECCS-XVII-77-2E, CONSTRADO, London, Nov. 1976.

1.208 European Convention for Constructional Steelwork: "European Recommendations for the Testing of Connections in Profiled Sheeting and Other Light Gauge Steel Components," ECCS-XVII-77-3E, CONSTRADO, London, May 1978.

1.209 European Convention for Constructional Steelwork: "European Recommendations for the Design of Profiled Sheeting," 1983.

1.210 European Convention for Constructional Steelwork: "Preliminary European Recommendations for Connections in Thin-Walled Structural Steel Elements," Part 1—Design of Connections, Feb. 1981; Part 2—Mechanical Fasteners, Oct. 1981; Part 3—Testing of Fasteners, July 1982; CONSTRADO, London.

1.211 European Convention for Constructional Steelwork: "European Recommendations for Good Practice in Steel Cladding and Roofing," CONSTRADO, London, May 1983.

1.212 European Convention for Constructional Steelwork: "European Recommendations for the Design of Light Gauge Steel Members," 1st Ed., 1987.

1.213 Thomasson, P. O.: "Recent Cold-Formed Steel Research and Design Specification Activities in Europe," *Stability of Metal Structures, Proceedings of the Third International Colloquium,* Structural Stability Research Council, May 1983.

1.214 Thomasson, P. O.: "The New European Recommendations for the Design of Light Gauge Steel Members," *Proceedings of the 5th International Specialty Conference on Cold-Formed Steel Structures,* UMR, Nov. 1986.

1.215 Vlasov, V. Z.: "Thin-Walled Elastic Beams," transl. by Y. Schechtman, Israel Program for Scientific Translations, Office of Technical Services, U.S. Department of Commerce, Washington, DC, 1961.

1.216   Walker, A. C., Ed.: *Design and Analysis of Cold-Formed Sections,*: '' John Wiley and Sons, New York, 1975.

1.217   Schuster, R. M,: *Cold-Formed Steel Design Manual,* University of Waterloo, Ont., Canada, 1975.

1.218   Kenedi, R. M., and A. H. Chilver: ''The Contribution of Research in Developing the Use of Cold-Rolled Sections in Buildings,'' presented at the Symposium on Applications of Sheet and Strip Metals in Building, Institution of Structural Engineers, London, 1959.

1.219   Chilver, A. H., Ed.: *Thin-Walled Structures,* John Wiley & Sons, New York, 1966.

1.220   Rhodes, J., and K. P. Chong, Eds.: *Thin-Walled Structures,* Elsevier Applied Science, London, 1983–1999.

1.221   ''Traian Vuia'' Polytechnic Institute of Timisoara: ''Proceedings of the First Session of the 3rd International Colloquium on Stability,'' Timisoara, Oct. 16, 1982.

1.222   Karamanlidis, D., and H. Gesch-Karamanlidis: ''Geometrically and Materially Nonlinear Finite Element Analysis of Thin-Walled Frames: Numerical Studies,'' *International Journal on Thin-Walled Structures,* vol. 4, no. 4, 1986.

1.223   Wang, S. T., G. E. Blandford, and C. D. Hill: ''Nonlinear Analysis of Steel Space Trusses,'' *Proceedings of the 9th International Specialty Conference on Cold-Formed Steel Structures,* UMR, Nov. 1988.

1.224   Moore, D. B., and D. M. Currie: ''Warping Restraint Member Stability and Standards,'' *Proceedings of the 9th International Specialty Conference on Cold-Formed Steel Structures,* UMR, Nov. 1988.

1.225   Seaburg, P. A.: ''Computer Aids for the Design of Cold-Formed Steel Structural Members,'' *Proceedings of the 9th International Specialty Conference on Cold-Formed Steel Structures,* UMR, Nov. 1988.

1.226   Hassinen, P.: ''Compression Strength of the Profiled Face in Sandwich Panels,'' *Proceedings of IABSE Colloquium,* Stockholm, 1986.

1.227   Hoglund, T.: ''Load Bearing Strength of Sandwich Panel Walls with Window Openings,'' *Proceedings of IABSE Colloquium,* Stockholm, 1986.

1.228   Volkel, G., and H. G. Schiebl: ''Transmitting Wind Loads on Flats by Bending and Membrane Effects,'' *Proceedings of IABSE Colloquium,* Stockholm, 1986.

1.229   Hassinen, P., A. Helenius, J. Hieta, and A. Westerlund: ''Structural Sandwich Panels at Low Temperature,'' *Prereport of the 13th Congress, IABSE,* June 6–10, 1988.

1.230   Heinisuo, M.: ''Exact Finite Element Method for Layered Beams,'' Tempere University of Technology *Publication 56,* Tempere, Finland, 1989.

1.231   Zankert, D., and K. A. Olsson: ''DP—Sandwich—The Utilization of Thin High-Strength Steel Sheets in Compression,'' *International Journal on Thin-Walled Structures,* vol. 7, no. 2, 1989.

1.232   Benussd, F., and A. Manro: ''Half-Barrel Shells Composed of Cold-Formed Profiles,'' *Proceedings of IABSE Colloquium,* Stockholm, 1986.

1.233   Johanscon, G.: ''Built-up Roofs—Wind Uplift Resistance,'' *Proceedings of IABSE Colloquium,* Stockholm, 1986.

1.234 "Building Physics in Light-Gauge Metal Construction," Theme 4, *Proceedings of IABSE Colloquium,* Stockholm, 1986.

1.235 Sabry, A., and G. Abdel-Sayed: "Cold-Formed Steel Compression Members Embedded in Grain," *Proceedings of the 8th International Specialty Conference on Cold-Formed Steel Structures,* University of Missouri-Rolla, Nov. 1986.

1.236 Rotter, J. M.: "On the Strength and Stability of Light Gauge Silos," *Proceedings of the 8th International Specialty Conference on Cold-Formed Steel Structures,* University of Missouri-Rolla, Nov. 1986.

1.237 Rotter, J. M.: "The Structural Design of Light Gauge Silo Hoppers, *Proceedings of the 9th International Specialty Conference on Cold-Formed Steel Structures,* UMR, Nov. 1988.

1.238 Lin, S. H., W. W. Yu, and T. Y. Galambos: "ASCE Design Standard for Stainless Steel Structures," *Proceedings of the 9th International Specialty Conference on Cold-Formed Steel Structures,* UMR, Nov. 1988.

1.239 Structural Stability Research Council: "Stability of Metal Structures—A World View," 2nd Ed., vol. 2, Mar. 1989.

1.240 Zhang, Z. Q.: "The Impact of the Code Differences for Design of Cold-Formed Steel Members," *Proceedings of the SSRC 4th International Colloquium,* 1989.

1.241 Cissel, J. H., and W. E. Quinsey: "Durability of Lightweight Steel Construction, Part I—Effect of Copper and Other Alloys upon the Atmospheric Corrosion of Steel," engineering research bulletin 30, University of Michigan, June 1942.

1.242 Cissel, J. H., and W. E. Quinsey: "Durability of Lightweight Steel Construction, Part II—A Study of the Service Records of Lightweight Steel Construction," engineering research bulletin 30, University of Michigan, Nov. 1942.

1.243 American Iron and Steel Institute: "The Durability of Lightweight Types of Steel Construction," 3rd printing, Jan. 1958.

1.244 "Report of Subcommittee XIV on Inspection of Black and Galvanized Sheets," *ASTM Proceedings,* vol. 54, 1954.

1.245 American Zinc Institute: "Life Expectancy of Galvanized Steel Sheets," Aug. 1962.

1.246 "Report of Committee A-5 on Corrosion of Iron and Steel," *ASTM Proceedings,* vol. 63, 1963.

1.247 Seaburg, P. A., and C. G. Salmon: "Minimum Weight Design of Light Gage Steel Members," *Journal of the Structural Division, ASCE Proceedings,* vol. 97, Jan. 1971.

1.248 Hsiao, L. E., W. W. Yu, and T. V. Galambos: "AISI LRFD Method for Cold-Formed Steel Structural Members," *Journal of Structural Engineering, ASCE,* vol. 116, Feb. 1990.

1.249 Yu, W. W., and R. A. LaBoube, Eds.: "Recent Research and Developments in Cold-Formed Steel Design and Construction," *Proceedings of the 10th International Specialty Conference on Cold-Formed Steel Structures,* University of Missouri-Rolla, Oct. 1990.

1.250 Errera, S. J.: "The 1989 Addendum to the AISI Specification," *Proceedings of the 10th International Specialty Conference on Cold-Formed Steel Structures,* UMR, Oct. 1990.

1.251   Zhang, Z. Q.: "Main Features of the R.P.C. Specification, GBJ 18-87," *Proceedings of the 10th International Specialty Conference on Cold-Formed Steel Structures,* UMR, Oct. 1990.

1.252   Studnicka, J.: "New Czechoslovak Standard for Cold-Formed Steel Structures," *Proceedings of the 10th International Specialty Conference on Cold-Formed Steel Structures,* UMR, Oct. 1990.

1.253   Lin, S. H., W. W. Yu, and T. V. Galambos: "ASCE LRFD Method for Stainless Steel Structures," *Proceedings of the 10th International Specialty Conference on Cold-Formed Steel Structures,* UMR, Oct. 1990.

1.254   Johnson, A. L.: "Center for Cold-Formed Steel Structures," *Proceedings of the 10th International Specialty Conference on Cold-Formed Steel Structures,* UMR, Oct. 1990.

1.255   Blandford, G. E.: "Current Research on Cold-Formed Steel Structures," *Proceedings of the 5th International Specialty Conference on Cold-Formed Steel Structures,* UMR, Oct. 1990.

1.256   Maquoi, R., and J. Rondal: "From Thick to Thin or from Thin to Thick," *Proceedings, IABSE Colloquium,* Stockholm, 1986.

1.257   Cassis, J. H., and A. Sepulveda: "Optimum Design of Trusses with Buckling Constraints," *Journal of Structural Engineering,* vol. 111, no. 7, July 1985.

1.258   Packer, J. A., P. C. Birkemoe, and W. J. Tucker: "Design Aids and Design Procedures for HSS Trusses," *Journal of Structural Engineering,* vol. 112, no. 7, July 1986.

1.259   Davies, J. M.: "The Analysis of Sandwich Panels with Profiled Faces," *Proceedings of the 8th International Specialty Conference on Cold-Formed Steel Structures,* UMR, Nov. 11–12, 1986.

1.260   Makelainen, P., and J. Hyvarinen: "Stability of Arched Roof Made of Profiled Steel Sheeting," *Proceedings of the 10th International Specialty Conference on Cold-Formed Steel Structures,* UMR, Oct. 1990.

1.261   Clarke, M. J., and G. J. Hancock: "A Comparison of Finite Element Nonlinear Analysis with Tests of Stressed Arch Frames," *Proceedings of the 10th International Specialty Conference on Cold-Formed Steel Structures,* UMR, Oct. 1990.

1.262   Belyaev, V., and T. Mikhailova: "Optimal Orientation of Corrugations in Beam Webs," *Proceedings of the 10th International Specialty Conference on Cold-Formed Steel Structures,* UMR, Oct. 1990.

1.263   Martin, K. A., M. R. Ehsani, and R. Bjorhovde: "Field Testing of Highway Sign Support Structures," *Journal of Structural Engineering,* vol. 113, no. 4, Apr. 1987.

1.264   Yu, W. W.: "Applications of Cold-Formed Steel in Tall Buildings," *Tall Buildings: 2000 and Beyond,* Council on Tall Buildings and Urban Habitat, 1990.

1.265   American Iron and Steel Institute: "Cold-Formed Steel Design Computer Programs," 1991.

1.266   American Iron and Steel Institute: "Guide for Preliminary Design of Cold-Formed Steel C- and Z-Members," 1993.

1.267   Yu, W. W., D. S. Wolford, and A. L. Johnson: "Golden Anniversary of the AISI Specification," *Proceedings of the 13th International Specialty Confer-*

ence on Cold-Formed Steel Structures, University of Missouri-Rolla, Oct. 1996.

1.268   Rhodes, J., Ed.: *Design of Cold-Formed Steel Members,* Elsevier Applied Science, London, 1991.

1.269   Yu, W. W., R. Baehre, and T. Toma, Eds.: *Cold-Formed Steel in Tall Buildings,* McGraw-Hill, New York, 1993.

1.270   Rhodes, J., and W. W. Yu, Guest Eds.: *Special Issue on Cold-Formed Steel Structures, Thin-Walled Structures,* vol. 16, nos. 1–4, Elsevier Applied Science, London, 1993.

1.271   Davies, J. M., Guest Ed.: *Special Issue on Cold-Formed Steel Construction, Journal of Constructional Steel Research,* vol. 31, nos. 2–3, Elsevier Applied Science, London, 1994.

1.272   Hancock, G. J., Guest Ed.: *Special Issue on Cold-Formed Steel Structures, Engineering Structures,* vol. 16, no. 5, Butterworth-Heinemann, London, 1994.

1.273   Askar, G. A., Guest Ed.: *Special Issue on Steel and Aluminum Structures, Thin-Walled Structures,* vol. 27, no. 1, Elsevier Applied Science, London, 1997.

1.274   Rhodes, J., and K. P. Chong, Eds.: *Special Issue on Various Aspects of Thin-Walled Structural Research, Thin-Walled Structures,* vol. 28, nos. 3–4, Elsevier Applied Science, London, 1997.

1.275   Rhodes, J., and K. P. Chong, Eds.: *Special Issue on Cold-Formed Steel and Aluminum Structures, Thin-Walled Structures,* vol. 29, nos. 1–4, Elsevier Applied Science, London, 1997.

1.276   Shanmugam, N. E., and W. W. Yu, Guest Eds.: *Special Issue on Recent Developments and Future Trends in Thin-Walled Structures, Thin-Walled Structures,* vol. 32, nos. 1–3, Elsevier Applied Science, London, 1998.

1.277   American Iron and Steel Institute: *Residential Steel Framing Manual,* Washington, DC, 1997.

1.278   Scharff, R., and Eds. of Walls & Ceilings Magazine: *Residential Steel Framing Handbook,* McGraw-Hill, New York, 1996.

1.279   Newman, A.: *Metal Building Systems,* McGraw-Hill, New York, 1997.

1.280   NAHB Research Center: *Prescriptive Method for Residential Cold-Formed Steel Framing,* Upper Marlboro, MD, 1997.

1.281   NAHB Research Center: *Commentary on the Prescriptive Method for Residential Cold-Formed Steel Framing,* Upper Marlboro, MD, 1997.

1.282   Haws, R. B: "Steel—The Clear Cut Alternative," *Proceedings of the 13th International Specialty Conference on Cold-Formed Steel Structures,* University of Missouri-Rolla, Oct. 1996.

1.283   Hancock, G. J., and T. M. Murray: "Residential Applications of Cold-Formed Structural Members in Australia," *Proceedings of the 13th International Specialty Conference on Cold-Formed Steel Structures,* University of Missouri-Rolla, Oct. 1996.

1.284   LaBoube, R. A., and W. W. Yu: "Recent Research and Developments in Cold-Formed Steel Framing," *Thin-Walled Structures,* vol. 32, nos. 1–3, Elsevier Applied Science, London, 1998.

1.285   Dannemann, R. W.: "Recent Development in Cold-Formed Steel," *Proceedings of the 11th International Specialty Conference on Cold-Formed Steel Structures,* University of Missouri-Rolla, Oct. 1992.

1.286   Guo, Y. J., and S. F. Fang: "Test of a Full Scale Roof Truss," *Proceedings of the 11th International Specialty Conference on Cold-Formed Steel Structures,* University of Missouri-Rolla, Oct. 1992.

1.287   Golledge, B., T. Clayton, and G. Reardon: "Racking Performance of Plasterboard–Clad Steel Stud Walls," *Proceedings of the 11th International Specialty Conference on Cold-Formed Steel Structures,* University of Missouri-Rolla, Oct. 1992.

1.288   Tanaka, A., H. Masuda, K. Sakae, and T. Tumori: "An Experimental Study of Shear Wall Units," *Proceedings of the 11th International Specialty Conference on Cold-Formed Steel Structures,* University of Missouri-Rolla, Oct. 1992.

1.289   Glaser, N., R. Kaehler, and J. Fisher: "Axial Load Capacity of Sheeted C and Z Members," *Proceedings of the 12th International Specialty Conference on Cold-Formed Steel Structures,* University of Missouri-Rolla, Oct. 1994.

1.290   Davies, J. M., C. Jiang, and D. St. Quinton: "Design of a Purlin System," *Proceedings of the 12th International Specialty Conference on Cold-Formed Steel Structures,* University of Missouri-Rolla, Oct. 1994.

1.291   Hancock, G. J., M. Celeban, and C. Healy: "Tests of Purlins with Concealed Fixed Sheeting," *Proceedings of the 12th International Specialty Conference on Cold-Formed Steel Structures,* University of Missouri-Rolla, Oct. 1994.

1.292   Hillman, J. R., and T. M. Murray: "An Innovative Cold-Formed Floor System," *Proceedings of the 12th International Specialty Conference on Cold-Formed Steel Structures,* University of Missouri-Rolla, Oct. 1994.

1.293   Hassinen, P., and L. Martikainen: "Analysis and Design of Continuous Sandwich Beams," *Proceedings of the 12th International Specialty Conference on Cold-Formed Steel Structures,* University of Missouri-Rolla, Oct. 1994.

1.294   Fisher, J. M., and J. N. Nunnery: "Stability of Standing Seam Roof-Purlin Systems," *Proceedings of the 13th International Specialty Conference on Cold-Formed Steel Structures,* University of Missouri-Rolla, Oct. 1996.

1.295   Lucas, R. M., F. G. A. Al-Bermani, and S. Kitipornchai: "Modeling of Cold-Formed Purlin-Sheeting Systems," *Proceedings of the 13th International Specialty Conference on Cold-Formed Steel Structures,* University of Missouri-Rolla, Oct. 1996.

1.296   Serrette, R., G. Hall, and H. Nguyen: "Dynamic Performance of Light Gauge Steel Panel Shear Walls," *Proceedings of the 13th International Specialty Conference on Cold-Formed Steel Structures,* University of Missouri-Rolla, Oct. 1996.

1.297   Makelainen, P., J. Kesti, O. Kaitila, and K. J. Sahramaa: "Study on Light Gauge Steel Roof Trusses with Rosette Connections," *Proceedings of the 14th International Specialty Conference on Cold-Formed Steel Structures,* University of Missouri-Rolla, Oct. 1998

1.298   Serrette, R. L.: "Seismic Design of Light Gauge Steel Structures," *Proceedings of the 14th International Specialty Conference on Cold-Formed Steel Structures,* University of Missouri-Rolla, Oct. 1998.

1.299 Fox, S. R., and R. M. Schuster: "Testing of Cold-Formed Steel Floor Joists with Bearing Stiffeners," *Proceedings of the 14th International Specialty Conference on Cold-Formed Steel Structures,* University of Missouri-Rolla, Oct. 1998.

1.300 Kwon, I. K., K. Choi, and N. Y. Jee: "Fire Resistance on Bearing Wall Using Steel and Gypsum," *Proceedings of the 14th International Specialty Conference on Cold-Formed Steel Structures,* University of Missouri-Rolla, Oct. 1998.

1.301 Mobasher, B., S. Y. Chen, C. Young, and S. D. Rajan: "A Cost Based Approach to Design of Residential Steel Roof Systems," *Proceedings of the 14th International Specialty Conference on Cold-Formed Steel Structures,* University of Missouri-Rolla, Oct. 1998.

1.302 Yu, W. W., and R. A. LaBoube, Eds.: "Recent Research and Developments in Cold-Formed Steel Design and Construction," *Proceedings of the 11th International Specialty Conference on Cold-Formed Steel Structures,* University of Missouri-Rolla, Oct. 1992.

1.303 Yu, W. W., and R. A. LaBoube, Eds.: "Recent Research and Developments in Cold-Formed Steel Design and Construction," *Proceedings of the 12th International Specialty Conference on Cold-Formed Steel Structures,* University of Missouri-Rolla, Oct. 1994.

1.304 Yu, W. W., and R. A. LaBoube, Eds.: "Recent Research and Developments in Cold-Formed Steel Design and Construction," *Proceedings of the 13th International Specialty Conference on Cold-Formed Steel Structures,* University of Missouri-Rolla, Oct. 1996.

1.305 Yu, W. W., and R. A. LaBoube, Eds.: "Recent Research and Developments in Cold-Formed Steel Design and Construction," *Proceedings of the 14th International Specialty Conference on Cold-Formed Steel Structures,* University of Missouri-Rolla, Oct. 1998.

1.306 Centre for Advanced Structural Engineering of the University of Sydney, Australia, and Center for Cold--Formed Steel Structures of the University of Missouri-Rolla, USA: *Proceedings of the International Workshop on Cold--Formed Steel Structures,* Sydney, Australia, Feb 1993.

1.307 Academy of Sciences of the Czech Republic: *Proceedings of the International Conference on Experimental Model Research and Testing of Thin-Walled Structures,* Prague, Czech Republic, Sept. 1997.

1.308 Shanmugam, N. E., J. Y. R. Liew, and V. Thevendran, Eds.: *Thin-Walled Structures: Research and Development,* Second International Conference on Thin-Walled Structures, Elsevier Applied Science, London, 1998.

1.309 Center for Cold-Formed Steel Structures: "Research Directory and Abstracts on Cold-Formed Steel Structures," University of Missouri-Rolla, 1997.

1.310 Yu, W. W.: "Commentary on the 1996 Edition of the Specification for the Design of Cold-Formed Steel Structural Members," *Cold-Formed Steel Design Manual*—Part VI, American Iron and Steel Institute, 1997.

1.311 Yu, W. W., and R. A. LaBoube: "University of Missouri-Rolla Research on Cold-Formed Steel Structures," *Thin-Walled Structures,* vol. 28, nos. 3–4, Elsevier Applied Science, London, 1997.

1.312 Yu, W. W., and R. A. LaBoube: "Activities of the Center for Cold-Formed Steel Structures," *Proceedings of the 11th Specialty Conference on Cold-Formed Steel Structures,* University of Missouri-Rolla, 1992.

1.313 American Iron and Steel Institute: "Load and Resistance Factory Design Specification for Cold-Formed Steel Structural Members," 1991 ed.

1.314 American Iron and Steel Institute: "Specification for the Design of Cold-Formed Steel Structural Members," 1996 ed.

1.315 Brockenbrough, R. L.: "The 1996 AISI Specification," *Proceedings of the 13th International Specialty Conference on Cold-Formed Steel Structures,* University of Missouri-Rolla, Oct. 1996.

1.316 Center for Cold-Formed Steel Structures: "The AISI Combined ASD/LRFD Specification," *CCFSS Technical Bulletin,* vol. 6, no. 1, Feb. 1997.

1.317 Kaehler, R. C., and P. A. Seaburg: "A New AISI Cold-Formed Steel Design Manual," *Proceedings of the 13th International Specialty Conference on Cold-Formed Steel Structures,* University of Missouri-Rolla, Oct. 1996.

1.318 Brockenbrough, R. L. and F. S. Merritt, Eds.: *Structural Steel Designer's Handbook,* 3rd ed., McGraw-Hill, New York, 1999, Secs. 8 and 10.

1.319 Chen, W. F., Ed.: *The Civil Engineering Handbook,* CRC Press, Boca Raton, FL, 1995, Sec. VI.

1.320 Chen, W. F., Ed: *Handbook of Structural Engineering,* CRC Press, Boca Raton, FL, 1997, Sec. 7.

1.321 Wilhoite, G. M., Ed.: "Innovations in the Design of Electrical Transmission Structures," *Proceedings of a Conference Sponsored by the ASCE Structural Division,* American Society of Civil Engineers, Aug. 1985.

1.322 American Society of Civil Engineers: "Guide for Design of Steel Transmission Towers," 2nd ed., prepared by the Task Committee on Updating Manual 52 of the ASCE Structural Division, Manual 52, 1988.

1.323 American Society of Civil Engineers: "Guidelines for Electrical Transmission Line Structural Loading," prepared by the Task Committee on Structural Loadings, Manual 74, 1991.

1.324 Heagler, R. B., L. D. Luttrell, and W. S. Easterling: " Composite Deck Design Handbook," Steel Deck Institute, March 1997.

1.325 Steel Deck Institute: "SDI Manual of Construction with Steel Deck," 1992.

1.326 Standards Australia and Standards New Zealand: "Cold-Formed Steel Structures—Commentary" (Supplement 1 to AS/NZS 4600:1996), AS/NZ2 4600 Supp 1: 1998.

1.327 Canadian Standards Association: "Commentary on CSA Standard S136-94, Cold-Formed Steel Structural Members," S136.1-95, 1995.

1.328 European Committee or Standardization: "Eurocode 3: Design of Steel Structures—Part 1-3: General Rules Supplementary Rules for Cold-Formed Thin Gauge Members and Sheeting," ENV 1993-1-3: 1996/AC, Oct. 1997.

1.329 Lawson, K. M., H. H. Lawson, H. E. G. Rommal, and A. C. Tiburcio: "Accelerated Test Development for Coil-Coated Steel Building Panels," *Proceedings of the 14th International Specialty Conference on Cold-Formed Steel Structures,* University of Missouri-Rolla, Oct. 1998.

1.330   Metal Construction Association: "Selection Guidelines for Metal Composite Foam Roof Panels," Ed. 1.

1.331   Metal Construction Association: "Guide Specification for Residential Metal Roofing," Ed. 1.

1.332   Metal Construction Association: "Performed Metal Wall Guidelines," Ed. 2.

1.333   American Iron and Steel Institute: "Supplement No. 1 to the 1996 Edition of the Specification for the Design of Cold-Formed Steel Structural Member," 1999.

1.334   Center for Cold-Formed Steel Structures: "Preview of the AISI Supplement to the 1996 Edition of the Specification," *CCFSS Technical Bulletin,* vol. 8, no. 2, August 1999.

CHAPTER 2

2.1   American Society for Testing and Materials: "ASTM standards."

2.2   American Society for Testing and Materials: "Methods and Definitions for Mechanical Testing of Steel Products," ASTM designation A370, latest ed.

2.3   Wolford, D. S.: "Mechanical Properties of Steel Used in Cold-Formed Steel Construction," lecture notes, AISI-UMR Short Course on Design of Cold-Formed Steel Structures, 1969 and 1970.

2.4   American Society for Testing and Materials: "Determination of Young's Modulus at Room Temperature," ASTM designation E111-61 (reapproved 1965).

2.5   Venkataramaiah, K. R., J. Roorda, and K. R. Srinivasaiah: "Elastic Modulus of Cold-Formed Sheet Steel," *Proceedings of the 5th International Specialty Conference on Cold-Formed Steel Structures,* University of Missouri-Rolla, Nov. 1980.

2.6   Dhalla, A. K., and G. Winter: "Ductility Criteria and Performance of Low-Ductility Steels for Cold-Formed Members," *Proceedings of the 1st Specialty Conference on Cold-Formed Steel Structures,* University of Missouri-Rolla, Aug. 1971.

2.7   Dhalla, A. K., S. J. Errera, and G. Winter: "Connections in Thin Low-Ductility Steels," *Journal of the Structural Division, ASCE Proceedings,* vol. 97, Oct. 1971.

2.8   Dhalla, A. K., and G. Winter: "Steel Ductility Measurements," *Journal of the Structural Division, ASCE Proceedings,* vol. 100, Feb. 1974.

2.9   Dhalla, A. K., and G. Winter: "Suggested Steel Ductility Requirements," *Journal of the Structural Division, ASCE Proceedings,* vol. 100, Feb. 1974.

2.10   Macadam, J. N., R. L. Brockenbrough, R. A. LaBoube, T. Pekoz, and E. J. Schneider: "Low-Strain-Hardening Ductile-Steel Cold-Formed Members," *Proceedings of the 9th International Specialty Conference on Cold-Formed Steel Structures,* University of Missouri-Rolla, Nov. 1988.

2.11   Klippstein, K. H.: "Fatigue Behavior of Sheet-Steel Fabrication Details," *Proceedings of the 5th International Specialty Conference on Cold-Formed Steel Structures,* University of Missouri-Rolla, Nov. 1980.

2.12   Klippstein, K. H.: "Fatigue of Fabricated Steel-Sheet Details," paper 810436, presented at the International Congress and Exposition, Society of Automotive Engineers, Feb. 1981.

2.13   American Iron and Steel Institute: "Sheet Steel Properties and Fatigue Design for Ground Transportation Engineers," AISI SG-836.

2.14   Karren, K. W., and G. Winter: "Effects of Cold-Forming on Light-Gage Steel Members," *Journal of the Structural Division, ASCE Proceedings,* vol. 93, Feb. 1967.

2.15   Chajes, A., S. J. Britvec, and G. Winter: "Effects of Cold-Straining on Structural Sheet Steels," *Journal of the Structural Division, ASCE Proceedings,* vol. 89, Apr. 1963.

2.16   Karren, K. W.: "Corner Properties of Cold-Formed Steel Shapes," *Journal of the Structural Division, ASCE Proceedings,* vol. 93, Feb. 1967.

2.17   Winter, G., and J. Uribe: "Effects of Cold Work on Cold-Formed Steel Members," in *Thin-Walled Steel Structures* (K. C. Rockey and H. V. Hill, Eds.), Gordon and Breach Science Publishers, New York, 1968.

2.18   Karren, K. W., and M. M. Gohil: "Effects of Strain Hardening and Aging on Corner Properties of Cold-Formed Steel Shapes," *Proceedings of the 1st Specialty Conference on Cold-Formed Steel Structures,* University of Missouri-Rolla, Aug. 1971.

2.19   Lind, N. C., and D. K. Schroff: "Utilization of Cold Work in Light Gage Steel," *Proceedings of the 1st Specialty Conference on Cold-Formed Steel Structures,* University of Missouri-Rolla, Aug. 1971.

2.20   Anderson, W. C.: "Properties of Cold Compressed Steel Tubes," *Proceedings of the 2nd Specialty Conference on Cold-Formed Steel Structures,* University of Missouri-Rolla, Oct. 1973.

2.21   Gupta, S. P., A. A. Johnson, and S. P. Kodali: "Strain-Aging and the Bauschinger Effect in Steel," *Proceedings of the 2nd Specialty Conference on Cold-Formed Steel Structures,* University of Missouri-Rolla, Oct. 1973.

2.23   Yu, W. W., A. S. Liu, and W. M. McKinney: "Structural Behavior of Thick Cold-Formed Steel Members," *Journal of the Structural Division, ASCE Proceedings,* vol. 100, Nov. 1974.

2.24   Karren, K. W., and M. M. Gohil: "Strain Hardening and Aging in Cold-Formed Steel," *Journal of the Structural Division, ASCE Proceedings,* vol. 101, Jan. 1975.

2.25   Lind, N. C., and D. K. Schroff: "Utilization of Cold-Work in Cold-Formed Steel," *Journal of the Structural Division, ASCE Proceedings,* vol. 101, Jan. 1975.

2.26   Ingvarsson, L.: "Cold-Forming Residual Stress, Effect on Buckling," *Proceedings of the 3rd International Specialty Conference on Cold-Formed Steel Structures,* University of Missouri-Rolla, Nov. 1975.

2.27   Ingvarsson, L.: "Cold-Forming Residual Stresses in Thin-Walled Structures," in *Thin-Walled Structures* (J. Rhodes and A. C. Walker, Eds.), Granada Publishing, Apr. 3–6, 1979.

2.28   Jin, C. C., P. Z. Hao, and S. P. Liu: "Yield Strength of Cold-Formed Steel Shapes," *Selections from Research Papers and Reports on Steel Structures,*

vol. 2, China Technical Committee for Standards of Steel Structures, March 1983.

2.29   Weng, C. C., and R. N. White: "Cold-Bending of Thick High-Strength Steel Plates," *Journal of the Structural Engineering,* ASCE, vol. 116, no. 1, Jan. 1990.

2.30   Canadian Standards Association: "Commentary on CSA Standard S136-1974—Cold Formed Steel Structural Members," S136, 1-1995.

2.31   Culver, C. G.: "Strength of Structural Members Subjected to Fires," preprint 1542, presented at the ASCE Annual and National Environmental Engineering Meeting, St. Louis, MO, Oct 18–22, 1971.

2.32   Boring, D. F., J. C. Spence, and W. G. Wells: *Fire Protection through Modern Building Codes,* 5th ed., American Iron and Steel Institute, 1981.

2.33   Culver, C. G.: "Steel Column Buckling under Thermal Gradients," *Journal of the Structural Division, ASCE Proceedings,* vol. 98, Aug. 1972.

2.34   Uddin, T., and C. G. Culver: "Effects of Elevated Temperature on Structural Members," *Journal of the Structural Division, ASCE Proceedings,* vol. 101, July 1975.

2.35   Klippstein, K. H.: "Strength of Cold-Formed Steel Studs Exposed to Fire," *Proceedings of the 4th International Specialty Conference on Cold-Formed Steel Structures,* University of Missouri-Rolla, June 1978.

2.36   Klippstein, K. H.: "Behavior of Cold-Formed Steel Studs in Fire Tests," *Proceedings of the 5th International Specialty Conference on Cold-Formed Steel Structures,* University of Missouri-Rolla, Nov. 1980.

2.37   Makelainen, P., and K. Miller: "Mechanical Properties of Cold-Rolled Hot-Dip Zinc Coated Sheet Steel Z32 at Elevated Temperatures," Helsinki University of Technology, Finland, May 1983.

2.38   American Society for Testing and Materials: "Standard Methods of Compression Testing of Metallic Materials at Room Temperature," ASTM E9, latest ed.

2.39   Galambos, T. V., Ed.: "Notes on the Compression Testing of Metals," technical memorandum 2, *Guide to Stability Design Criteria for Metal Structures,* 5th ed., John Wiley & Sons, New York, 1998.

2.40   Galambos, T. V., Ed.: "Stub-Column Test Procedure," technical memorandum 3, *Guide to Stability Design Criteria for Metal Structures,* 5th ed., John Wiley & Sons, New York, 1998.

2.41   Sorsa, I., and P. Vierros: "The Effect of Welding on the Mechanical Properties of Cold-Formed Structural Steels," *Scandinavian Journal of Metallurgy 16,* 1987.

2.42   Huber, A. W., and L. S. Beedle: "Residual Stress and the Comparative Strength of Steel," *Welding Journal,* vol. 33, Dec. 1954.

2.43   Beedle, L. S., and L. Tall: "Basic Column Strength," *ASCE Transactions,* pt. 1, vol. 127, 1962.

2.44   Tall, L., Ed.: *Structural Steel Design,* The Ronald Press Company, New York, 1964.

2.45   Galambos, T. V.: *Structural Members and Frames,* Prentice-Hall, Englewood Cliffs, NJ, 1968.

2.46 Dat, D. T., and T. Pekoz: "The Strength of Cold-Formed Steel Columns," report No. 80-4, Department of Structural Engineering, Cornell University, Feb. 1980.

2.47 Niemi, E.: "Buckling of Cold-Formed Rectangular Hollow Sections," Seminar on Steel Tubes and Their Raw-Material Quality Requirements, Helsinki, Finland, May 1985.

2.48 Weng, C. C., and T. Pokoz: "Residual Stresses in Cold-Formed Steel Members," *Proceedings of the 9th International Specialty Conference on Cold-Formed Steel Structures,* University of Missouri-Rolla, Nov. 1988.

2.49 Weng, C. C., and R. N. White: "Residual Stresses in Cold-Bent Thick Steel Plates," *Journal of Structural Engineering,* ASCE, vol. 116, no. 1, Jan. 1990.

2.50 Kassar, M.: "Effect of Strain Rate on Material Properties of Sheet Steels and Structural Strength of Cold-Formed Steel Members," Ph.D. Thesis, University of Missouri-Rolla, 1990.

2.51 Kassar, M., and W. W. Yu: "Effect of Strain Rate on Cold-Formed Steel Stub Columns," *Proceedings of the 10th International Specialty Conference on Cold-Formed Steel Structures,* University of Missouri-Rolla, Oct. 1990.

2.52 Seely, F. B., and J. O. Smith: *Advanced Mechanics of Materials,* 2nd ed., John Wiley & Sons, New York, 1952.

2.53 Wu, S., W. W. Yu, and R. A. LaBoube: "Flexural Strength of Cold-Formed Steel Panels using Structural Grade 80 of A653 Steel," *Proceedings of the 13th International Specialty Conference on Cold-Formed Steel Structures,* University of Missouri-Rolla, Oct. 1996.

2.54 Wu, S., W. W. Yu, and R. A. LaBoube: "Flexural Strength of Cold-Formed Steel Panels Using High-Strength, Low-Ductility Steel," *Thin-Walled Structures* (N. E. Shanmugam, J. Y. R. Liew, and V. Thevendran, Eds.), Elsevier Applied Science, 1998.

2.55 Rogers, C. A., and G. J. Hancock: "Ductility of G550 Sheet Steels in Tension," *Journal of Structural Engineering, ASCE Proceedings,* vol. 123, no. 12, Dec. 1997.

2.56 Rogers, C. A., and G. J. Hancock: "Bolted Connection Tests of Thin G550 and G300 Sheet Steels," *Journal of Structural Engineering, ASCE Proceedings,* vol. 124, no. 7, 1998.

2.57 Rogers, C. A., and G. J. Hancock: "Screwed Connection Tests of Thin G550 and G300 Sheet Steels," *Journal of Structural Engineering, ASCE Proceedings,* vol. 125, no. 2, Feb. 1999.

2.58 Rogers, C. A., and G. J. Hancock: "Ductility Measurement of Thin G550 Steels," *Proceedings of the 14th International Specialty Conference on Cold-Formed Steel Structures,* University of Missouri-Rolla, Oct. 1998.

2.59 Rogers, C. A., and G. J. Hancock: "Bearing Design of Thin Sheet Steel Screwed Connections," *Proceedings of the 14th International Specialty Conference on Cold-Formed Steel Structures,* University of Missouri-Rolla, Oct. 1998.

2.60 Rogers, C. A., and G. J. Hancock: "Behaviour of Thin G550 Sheet Steel Bolted Connections," *Proceedings of the 14th International Specialty Conference on Cold-Formed Steel Structures,* University of Missouri-Rolla, Oct. 1998.

2.61   Rogers, C. A., and G. J. Hancock: "Ductile and Connection Behaviour of Thin G550 Sheet Steels," *Thin-Walled Structures,* ed. by N. E. Shanmugam, J. Y. R. Liew, and V. Thevendran, Elsevier Applied Science, 1998.

2.62   Hassan, S. K., D. Polyzois, and G. Morris: "Fatigue Behavior of Cold-Formed Steel Sections," *Proceedings of the 12th International Specialty Conference on Cold-Formed Steel Structures,* University of Missouri-Rolla, Oct. 1994.

2.63   Van den Berg, G. J., and P. van der Merwe: "Prediction of Corner Mechanical Properties for Stainless Steels Due to Cold-Forming," *Proceedings of the 11th International Specialty Conference on Cold-Formed Steel Structures,* University of Missouri-Rolla, Oct. 1992.

2.64   Macdonald, M., J. Rhodes, M. Crawford, and G. T. Taylor: "A Study of the Effect of Cold Forming on the Yield Strength of Stainless Steel Type 304—Hardness Test Approach," *Proceedings of the 13th International Specialty Conference on Cold-Formed Steel Structures,* University of Missouri-Rolla, Oct. 1996.

2.65   Laubscher, R.: "The Effect of Cold-Forming on Type 3CR12 Square Tubes," *Proceedings of the 14th International Specialty Conference on Cold-Formed Steel Structures,* University of Missouri-Rolla, Oct. 1998.

2.66   Kassar, M., and W. W. Yu: "Effect of Strain Rate on Material Properties of Sheet Steels," *Journal of Structural Engineering, ASCE Proceedings,* vol. 118, no. 11, Nov. 1992.

2.67   Kassar, M., C. L. Pan, and W. W. Yu: "Effect of Strain Rate on Cold-Formed Steel Stub Columns," *Journal of Structural Engineering, ASCE Proceedings,* vol. 118, no. 11, Nov. 1992.

2.68   Pan, C. L., and W. W. Yu: "Influence of Strain Rate on the Structural Strength of Cold-Formed Steel Automotive Components," *Proceedings of Automotive Body Materials of the International Body Engineering Conference,* Sept. 1993.

2.69   Schell, B. C., M. Y. Sheh, P. H. Tran, C. L. Pan and W. W. Yu: "Impact and Static Crush Performance of Hybrid Hat Section Stub Columns," *Proceedings of Automotive Body Design and Engineering of the International Body Engineering Conference,* Sept. 1993.

2.70   Pan, C. L., and W. W. Yu: "Structural Strength of Hybrid Cold-Formed Steel Beams under Dynamic Loading Conditions," *Proceedings of Body Design and Engineering of the International Body Design Engineering Conference,* Sept. 1996.

2.71   Pan, C. L., and W. W. Yu: "The Structural Behavior of Homogeneous and Hybrid Stub Columns under Dynamic Loading Conditions," *Thin-Walled Structures,* vol. 31, 1998.

2.72   LaBoube, R. A., and W. W. Yu: "Design of Cold-Formed Steel Structural Members and Connections for Cyclic Loading (Fatigue)," Civil Engineering Study 99-1, University of Missouri-Rolla, July 1999.

2.73   Schuster, R. M., and P. A. Sloof: "Yield Strength Increase of Cold-Formed Sections Due to Cold Work of Forming," University of Waterloo, May 1999.

CHAPTER 3

3.1   Gerard, G., and H. Becker: "Handbook of Structural Stability, Part I— Buckling of Flat Plates," NACA technical note 3781, July 1957.

3.2   Timoshenko, S. P., and J. M. Gere: *Theory of Elastic Stability,* McGraw-Hill, New York, 1961.

3.3   Bleich, F.: *Buckling Strength of Metal Structures,* McGraw-Hill, New York, 1952.

3.4   American Iron and Steel Institute: *Stainless Steel Cold-Formed Structural Design Manual,* 1974 ed.

3.5   Johnson, A. L., and G. Winter: "Behavior of Stainless Steel Columns and Beams," *Journal of the Structural Division, ASCE Proceedings,* vol. 92, Oct. 1966.

3.6   Stowell, E. Z.: "A Unifield Theory of Plastic Buckling of Columns and Plates," NACA technical note 1556, 1958.

3.7   Bulson, P. S.: *The Stability of Flat Plates,* American Elsevier, New York, 1969.

3.8   Kalyanaraman, V.: "Local Buckling of Cold-Formed Steel Members," *Journal of the Structural Division, ASCE Proceedings,* vol. 105, May 1979.

3.9   Van der Merwe, P.: "Development of Design Criteria for Ferritic Stainless Steel Cold-Formed Structural Members and Connections," Ph.D. Thesis, University of Missouri-Rolla, 1987.

3.10   Lin, S. H.: "Load and Resistance Factor Design of Cold-Formed Stainless Steel Structural Members," Ph.D. Thesis, University of Missouri-Rolla, 1989.

3.11   American Society of Civil Engineers: *Specification for the Design of Stainless Steel Structural Members,* 1990.

3.12   Von Karman, T., E. E. Sechler, and L. H. Donnell: "The Strength of Thin Plates in Compression," *Transactions ASME,* vol. 54, APM 54-5, 1932.

3.13   Winter, G.: "Strength of Thin Steel Compression Flanges" (with Appendix), bulletin 35/3, Cornell University Engineering Experiment Station, Ithaca, NY, 1947.

3.14   Winter, G: "Performance of Thin Steel Compression Flanges," preliminary publication, 3rd Congress, The International Association for Bridge and Structural Engineering, Liege, 1948.

3.15   Winter, G.: "Performance of Compression Plates as Parts of Structural Members," *Research,* Engineering Structures Supplement (Colston Papers, vol. II), London, 1949.

3.16   Johnson, A. L.: "The Structural Performance of Austenitic Stainless Steel Members," *Report 327,* Department of Structural Engineering, Cornell University, Nov. 1966.

3.17   Pekoz, T. B.: "Development of a Unified Approach to the Design of Cold-Formed Steel Members," *AISI Report SG-86-4,* Nov. 1986.

3.18   Pekoz, T.: "Development of a Unified Approach to the Design of Cold-Formed Steel Members," *Proceedings of the 8th International Specialty Con-*

ference on Cold-Formed Steel Structures, University of Missouri-Rolla, Nov. 11–12, 1986. AISI Research Report CF 87-1, Mar. 1987.

3.19   Weng, C. C., and T. Pekoz: "Subultimate Behaviour of Uniformly Compressed Stiffened Plate Elements," *Research Report,* Department of Structural Engineering, Cornell University, 1986.

3.20   Lind, N. C., M. K. Ravindra, and J. Power: "A Review of the Effective Width Formula," *Proceedings of the 1st Specialty Conference on Cold-Formed Steel Structures,* University of Missouri-Rolla, Aug. 1971.

3.21   Lind, N. C., M. K. Ravindra, and G. Schorn: "Empirical Effective Width Formula," *Journal of the Structural Division, ASCE Proceedings,* vol. 102, Sept. 1976.

3.22   Moreau, G., and N. Tebedge: "Comparison of AISI Specification for the Design of Cold-Formed Steel Structural Members and CTICM Recommendation for the Construction of Cold-Formed Steel Members," Centre Technique Industriel de la Construction Métallique, Puteaux, France, Feb. 1974.

3.23   Rhodes, J.: "Effective Widths in Plate Buckling," *Development in Thin-Walled Structures-1* (J. Rhodes and A. C. Walker, Eds.), Applied Science Publishers, London, 1982.

3.24   Rhodes, J.: "Treatment of Buckling in the New British Code," *Proceedings of the 8th International Specialty Conference on Cold-Formed Steel Structures,* University of Missouri-Rolla, Nov. 11–12, 1986.

3.25   Usami, T.: "Post-Buckling of Plates in Compression and Bending," *Journal of the Structural Division, ASCE Proceedings,* vol. 108, Mar. 1982.

3.26   Narayanan, R., and F. Y. Chow: "Effective Widths of Plates Loaded Uniaxially," *International Journal on Thin-Walled Structures,* vol. 1, no. 2, 1983.

3.27   Rondal, J., and R. Maquoi: "Stub-Column Strength of Thin-Walled Square and Rectangular Hollow Sections," *International Journal on Thin-Walled Structures,* vol. 3, no. 1, 1985.

3.28   Dawe, J. L., and G. Y. Grondin: "Inelastic Buckling of Steel Plates," *Journal of Structural Engineering,* vol. 111, no. 1, Jan. 1985.

3.29   Narayanan, R., and F. Y. Chow: "Effect of Support Conditions on Plate Strengths," *Journal of Structural Engineering,* vol. 111, no. 1, Jan. 1985.

3.30   Dubina, D., and E. Fleseriu: "Equivalent Geometric Characteristics in Stability Analysis of the Thin-Walled Cold-Formed Members," *Proceedings of the Second Regional Colloquium on Stability of Steel Structures,* Sept. 25–26, 1986, Hungary, vol. II/2.

3.31   Sun, Z. L.: "Buckling Strength of Plates," *Proceedings of the 8th International Specialty Conference on Cold-Formed Steel Structures,* University of Missouri-Rolla, Nov. 11–12, 1986.

3.32   Gradzki, R., and K. Kowal-Michalska: "Collapse Behaviour of Plates," *Thin-Walled Structures,* vol. 6, no. 1, 1988.

3.33   Dubina, D., and C. Pacoste: "Theoretical and Experimental Investigation, Concerning a New Formula for Determining the Effective Width of Thin-Walled Members," *Proceedings of the SSRC 4th International Colloquium,* 1989.

3.34   Rondal, J.: "On the Effective Width of Stiffened and Unstiffened Elements," *Proceedings of 2nd Regional Colloquium on Stability of Steel Structures,* Sept. 25–26, 1986.

3.35   Herzog, M. A. M.: "Simplified Design of Unstiffened and Stiffened Plates," *Journal of Structural Engineering,* vol. 113, no. 10, Oct. 1987.

3.36   Finnish Association for Structural Mechanics, *Journal of Structural Mechanics,* vol. 18, no. 4, 1985.

3.37   Vilnay, O., and C. Burt: "The Shear Effective Width of Aluminium Plates," *International Journal on Thin-Walled Structures,* vol. 6, no. 2, 1988.

3.38   Hu, P. C., E. E. Lundquist, and S. B. Batdorf: "Effect of Small Deviation from Flatness on the Effective Width and Buckling of Plates in Compression," NACA technical note 1124, 1946.

3.39   Abdel-Sayed, G.: "Effective Width of Thin Plates in Compression," *Journal of the Structural Division, ASCE Proceedings,* vol. 95, Oct. 1969.

3.40   Dawson, R. G., and A. C. Walker: "Postbuckling of Geometrically Imperfect Plates," *Journal of the Structural Division, ASCE Proceedings,* vol. 98, Jan. 1972.

3.41   Sherbourne, A. N., and R. M. Korol: "Postbuckling of Axially Compressed Plates," *Journal of the Structural Division, ASCE Proceedings,* vol. 98, Oct. 1972.

3.42   Hancock, G. J.: "Nonlinear Analysis of Thin Sections in Compression," *Journal of the Structural Division, ASCE Proceedings,* vol. 107, Mar. 1981.

3.43   Maquoi, R., and J. Rondal: "Parametric Study of Imperfect Compressed Plates," *Proceedings of the 2nd Regional Colloquium on Stability of Steel Structures,* Sept. 25–26, 1986, Hungary, pp. II/117–II/124.

3.44   Culver, C. G.: "Impact Loading of Cold-Formed Steel Members," preprint 1232, presented at ASCE National Meeting on Transportation Engineering, Boston, MA, July 13–17, 1970.

3.45   Culver, C. G., and R. V. Tassel: "Shock Loading of Thin Compression Elements," *Proceedings of the 1st Specialty Conference on Cold-Formed Steel Structures,* University of Missouri-Rolla, Aug. 1971.

3.46   Zanoni, E. A., and C. G. Culver: "Impact Loading of Thin-Walled Beams," *Proceedings of the 1st Specialty Conference on Cold-Formed Steel Structures,* University of Missouri-Rolla, Aug. 1971.

3.47   Culver, C. G., E. A. Zanoni, and A. H. Osgood: "Response of Thin-Walled Beams to Impact Loading," *Proceedings of the 1st Specialty Conference on Cold-Formed Steel Structures,* University of Missouri-Rolla, Aug. 1971.

3.48   Vaidya, N. R., and C. G. Culver: "Impact Loading of Thin-Walled Columns," *Proceedings of the 1st Specialty Conference on Cold-Formed Steel Structures,* University of Missouri-Rolla, Aug. 1971.

3.49   Culver, C. G.: "Cold-Formed Steel Structures Elements Subject to Time-Dependent Loading," Department of Civil Engineering, Carnegie-Mellon University, Jan. 1972.

3.50   Kassar, M., and W. W. Yu: "Effect of Strain Rate and Dynamic Loads on Structural Strength of Cold-Formed Steel Members," *Proceedings of the 10th International Specialty Conference on Cold-Formed Steel Structures,* University of Missouri-Rolla, Oct. 1990.

3.51   Bergfelt, A.: "Profiles Minces Formés a Froid (Thin-Walled Cold-Formed Trapezoidal Profiles)," *Bulletin Technique de la Suisse Romande,* vol. 99, no. 17, Aug. 1973 (in French).

3.52 Bergfelt, A., B. Edlund, and H. Larsson: "Experiments on Trapezoidal Steel Sheets in Bending," *Proceedings of the 3rd International Specialty Conference on Cold-Formed Steel Structures,* University of Missouri-Rolla, Nov. 1975.

3.53 Thomasson, P. O.: "Livbucklingens Inverkan Pa Barformagan Hos Trapetsprofilerad Stalplat (Influence of Web Buckling on the Load-Carrying Capacity of Trapezoidal Steel Sheets)," presented at the Nordiske Forskningsdager for Stalkonstruksjoner (Second Scandinavian Steel Structures Research Conference), Oslo, 1973 (in Swedish).

3.54 Kallsner, B.: "Post-Buckling Behaviour and Load-Carrying Capacity of Thin-Walled Box and Hat-Section Beams," Department of Structural Engineering, University of Lund, Sweden, 1977.

3.55 Bergfelt, A., and B. Edlund: "Effects of Web Buckling in Light Gauge Steel Beams," in *Thin-Walled Structures* (J. Rhodes and A. C. Walker, Eds.), Granada Publishing, 1980.

3.56 Hoglund, T.: "Design of Trapezoidal Sheeting Provided with Stiffeners in the Flanges and Webs," document D28, Swedish Council for Building Research, 1980.

3.57 DeWolf, J. T., and C. J. Gladding: "Post-Buckling Behavior of Beam Webs in Flexure," *Journal of the Structural Division, ASCE Proceedings,* vol. 104, July 1978.

3.58 DeWolf, J. T., and C. J. Gladding: "Web Buckling in Beams," *Proceedings of the 4th International Specialty Conference on Cold-Formed Steel Structures,* University of Missouri-Rolla, June 1978.

3.59 LaBoube, R. A., and W. W. Yu: "Effective Web Depth of Cold-Formed Steel Beams," presented at the International Colloquium on Stability of Structures under Static and Dynamic Loads, Washington, DC, May 17–19, 1977.

3.60 LaBoube, R. A., and W. W. Yu: "Structural Behavior of Beam Webs Subjected to Bending Stress," final report, civil engineering study 78-1, University of Missouri-Rolla, June 1978.

3.61 LaBoube, R. A., and W. W. Yu: "Bending Strength of Webs of Cold-Formed Steel Beams," *Journal of the Structural Division, ASCE Proceedings,* vol. 108, July 1982.

3.62 "Godkannanderegler nr 3; Tunnplatskonstrukioner (Rules for Government Approval No. 3, Thin-Walled Cold-Formed Steel Structures)," Statens Planverk, Stockholm, 1974 (in Swedish).

3.63 European Convention for Constructional Steelwork: "European Recommendations for the Design of Profiled Sheeting," *ECCS-TC7-1983,* CONSTRADO, London, Apr. 1983.

3.64 Cohen, J. M., and T. Pekoz: "Local Buckling of Plate Elements," *Research Report,* Department of Structural Engineering, Cornell University, 1987.

3.65 Johnson, D. L.: "Buckling of Beam Compression Flanges," Report submitted to American Iron and Steel Institute, Butler Manufacturing Company, Nov. 1976.

3.66 He, B. K., and T. Pekoz: "Purlin Tests," *Research Report,* Department of Structural Engineering, Cornell University, 1981.

3.67   Van Neste, A. J.: "Practical Method for the Calculation of Steel Sheeting in Bending," *Report,* Department of Architecture, Building Science and Urban Planning, Structural Engineering, Eindoven, The Netherlands, 1983.

3.68   American Iron and Steel Institute: "Specification for the Design of Cold-Formed Steel Structural Members," 1980 ed.

3.69   Kalyanaraman, V., T. Pekoz, and G. Winter: "Performance of Unstiffened Compression Elements," Department of Structural Engineering Report, Cornell University, 1972.

3.70   Kalyanaraman, V., T. Pekoz, and G. Winter: "Unstiffened Compression Elements," *Journal of the Structural Division, ASCE Proceedings,* vol. 103, Sept. 1977.

3.71   Kalyanaraman, V., and T. Pekoz: "Analytical Study of Unstiffened Elements," *Journal of the Structural Division, ASCE Proceedings,* vol. 104, Sept. 1978.

3.72   Höglund, T.: "Design of Trapezoidal Sheeting Provided with Stiffeners in the Flanges and Webs," document D28, Swedish Council for Building Research, Stockholm, 1980.

3.73   König, J.: "Transversally Loaded Thin-Walled C-Shaped Panels with Intermediate Stiffeners," document D:7, Swedish Council for Building Research, Stockholm, 1978.

3.74   König, J., and P. O. Thomasson: "Thin-Walled C-Shaped Panels Subject to Axial Compression or to Pure Bending," in *Thin-Walled Structures* (J. Rhodes and A. C. Walker, Eds.), Granada Publishing, Apr. 3–6, 1979.

3.75   Desmond, T. P., T. Pekoz, and G. Winter: "Local and Overall Buckling of Cold-Formed Compression Members," Department of Structural Engineering Report, Cornell University, 1978.

3.76   Desmond, T. P., T. Pekoz, and G. Winter: "Edge Stiffeners for Thin-Walled Members," *Journal of the Structural Division, ASCE Proceedings,* vol. 107, Feb. 1981.

3.77   Desmond, T. P., T. Pekoz, and G. Winter: "Intermediate Stiffeners for Thin-Walled Members," *Journal of the Structural Division, ASCE Proceedings,* vol. 107, Apr. 1981.

3.78   Venkataramaiah, K. R.: "Optimum Edge Stiffeners for Thin-Walled Structural Elements," technical note 7, Solid Mechanics Division, University of Waterloo, Ont., Canada, July 1971.

3.79   Skaloud, M.: "Post-critical Behavior of Compressed Plates Reinforced by Elastic Ribs," *Acta Technica CSAV,* vol. 8, no. 5, 1963.

3.80   Bulson, P. S.: "Local Stability and Strength of Structural Sections," in *Thin-Walled Structures* (A. H. Chilver, Ed.), John Wiley & Sons, New York, 1967.

3.81   Jombock, J. R., and J. W. Clark: "Postbuckling Behavior of Flat Plates," *Journal of the Structural Division, ASCE Proceedings,* vol. 87, June 1961.

3.82   Polyzois, D., and A. R. Sudharmapal: "Cold-Formed Steel Z-Sections with Sloping Edge Stiffeners under Axial Load," *Journal of Structural Engineering, ASCE,* vol. 116, no. 2, Feb. 1990.

3.83   Lind, N. C.: "Buckling of Longitudinally Stiffened Sheets," *Journal of the Structural Division, ASCE Proceedings,* vol. 99, July 1973.

3.84   Johnston, B. G., Ed.: *Guide to Stability Design Criteria for Metal Structures,* 3rd ed., John Wiley and Sons, New York, 1976.

3.85   The American Association of State Highway and Transportation Officials: "Standard Specifications for Highway Bridges," 12th ed., 1977.

3.86   American Railway Engineering Association: "Specification for Steel Railway Bridges," 1969.

3.87   Greenspan, M.: "Axial Rigidity of Perforated Structural Members," research paper RP 1568, National Bureau of Standards, Dec. 1943.

3.88   Greenspan, M.: "Theory for Axial Rigidity of Structural Members Having Ovaloid or Square Perforations," research paper RP 1737, National Bureau of Standards, Sept. 1946.

3.89   Stang, A. H., and M. Greenspan: "Perforated Cover Plates for Steel Columns: Summary of Compressive Properties," research paper RP 1880, National Bureau of Standards, May 1948.

3.90   White, M. W., and B. Thurlimann: "Study of Column with Perforated Cover Plates," AREA bulletin 531, 1956.

3.91   Levy, S., R. M. Woolley, and W. D. Kroll: "Instability of Supported Square Plates with Reinforced Circular Hole in Edge Compression," *Journal of Research of the National Bureau of Standards,* vol. 139, Dec. 1947.

3.92   Kumai, T.: "Elastic Stability of the Square Plate with a Central Circular Hole under Edge Thrust," *Reports of Research Institute for Applied Mechanics,* vol. 1, Apr. 1952.

3.93   Schlack, A. L.: "Elastic Stability of Perced Square Plates," *Experimental Mechanics,* June 1964.

3.94   Yoshiki, M., Y. Fujita, and others: "Instability of Plates with Holes (1st Report)," *Proceedings of the Society of Naval Architects of Japan,* no. 122, Dec. 1967.

3.95   Kawai, T., and H. Ohtsubo: "A Method of Solution for the Complicated Buckling Problems of Elastic Plates with Combined Use of Rayleigh-Ritz's Procedure in the Finite Element Method," *Proceedings of the 2nd Air Force Conference on Matrix Methods in Structural Mechanics,* Oct. 1968.

3.96   Hull, R. E.: "Buckling of Plates with Unknown In-Plane Stress Using the Finite Element Method," master's thesis, University of Washington, Aug. 1970.

3.97   Vann, W. P.: "Compressive Buckling of Perforated Plate Elements," *Proceedings of the 1st Specialty Conference on Cold-Formed Steel Structures,* University of Missouri-Rolla, Aug. 1971.

3.98   Yu, W. W., and C. S. Davis: "Buckling Behavior and Post-Buckling Strength of Perforated Stiffened Compression Elements," *Proceedings of the 1st Specialty Conference on Cold-Formed Steel Structures,* University of Missouri-Rolla, Aug. 1971.

3.99   Yu, W. W., and C. S. Davis: "Cold-Formed Steel Members with Perforated Elements," *Journal of the Structural Division, ASCE Proceedings,* vol. 99, Oct. 1973.

3.100   Ortiz-Colberg, R., and T. Pekoz: "Load Carrying Capacity of Perforated Cold-Formed Steel Columns," *Research Report No. 81-12,* Department of Structural Engineering, Cornell University, 1981.

3.101   Narayanan, R., and N. G. V. Der-Avanessian: "Elastic Buckling of Perforated Plates under Shear," *International Journal on Thin-Walled Structures,* vol. 2, no. 1, 1984.

3.102   Roberts, T. M., and Z. G. Azizian: "Strength of Perforated Plates Subjected to In-Plane Loading," *International Journal on Thin-Walled Structures,* vol. 2, no. 2, 1984.

3.103   Narayanan, R., and F. Y. Chow: "Ultimate Capacity of Uniaxially Compressed Perforated Plates," *International Journal on Thin-Walled Structures,* vol. 2, no. 3, 1984.

3.104   Sabir, A. B., and F. Y. Chow: "Elastic Buckling of Plates Containing Eccentrically Loaded Circular Holes," *International Journal on Thin-Walled Structures,* vol. 4, no. 2, 1986.

3.105   Brown, C. J., and A. L. Yettram: "The Elastic Stability of Square Perforated Plates under Combinations of Bending, Shear and Direct Load," *International Journal on Thin-Walled Structures,* vol. 4, no. 3, 1986.

3.106   Narayanan, R., and N. G. Verni Der-Avanessian: "Analysis of Plate Girder with Perforated Webs," *International Journal on Thin-Walled Structures,* vol. 4, no. 5, 1986.

3.107   Narayanan, R., and P. Enlotorunda: "Plate Girder Webs Containing a Central Hole, and Subjected to Bending and Shear," *Proceedings of the 2nd Regional Colloquium on Stability of Steel Structures,* Sept. 25–26, 1986, Hungary, vol. II.

3.108   Brown, C. J., A. L. Yettram, and M. Burnett: "Stability of Plates with Rectangular Holes," *Journal of Structural Engineering,* vol. 113, no. 5, May 1987.

3.109   Sivakumaran, K. S., and A. S. Banwait: "Effect of Perforation on the Strength of Axially Loaded Cold-Formed Steel Section," *Steel Structures* (R. Narayanan, Ed.), Elsevier Applied Science, London, 1987.

3.110   Narayanan, R.: "Simplified Procedures for the Strength Assessment of Axially Compressed Plates with or without Openings," *Steel Structures* (R. Narayanan, Ed.), Elsevier Applied Science, London, 1987.

3.111   Sivakumaran, K. S.: "Some Studies on Cold-Formed Steel Sections with Web Openings," *Proceedings of the 9th International Specialty Conference on Cold-Formed Steel Structures,* UMR, Nov. 8–9, 1988.

3.112   Yang, H. T. Y.: "A Finite Element Formulation for Stability Analysis of Doubly Curved Thin Shell Structures," Ph.D. dissertation, Cornell University, Jan. 1969.

3.113   Kroll, W. D.: "Instability in Shear of Simply Supported Square Plates with Reinforced Hole," *Journal of Research of the National Bureau of Standards,* vol. 43, Nov. 1949.

3.114   Rockey, K. C., R. G. Anderson, and Y. K. Cheung: "The Behavior of Square Shear Webs Having a Circular Hole," presented at the Symposium on Thin-Walled Steel Structures, University College of Swansea, 1967.

3.115   Rockey, K. C.: "The Buckling and Post-Buckling Behavior of Shear Panels which Have a Central Circular Cutout," in *Thin-Walled Structures* (J. Rhodes and A. C. Walker, Eds.), Granada Publishing, Apr. 3–6, 1979.

3.116 Kroll, W. D., G. P. Fisher, and G. J. Heimerl: "Charts for the Calculation of Critical Stress for Local Instability of Columns with I, Z, Channel, or Rectangular Tube Sections," NACA WR L-429 (ARR 3K04), 1943.

3.117 Lind, N. C.: "Numerical Buckling Analysis of Plate Assemblies," *Journal of the Structural Division, ASCE Proceedings,* vol. 104, Feb. 1978.

3.118 Fafard, M., D. Beaulieu, and G. Dhatt: "Buckling of Thin-Walled Members Forced by an Assemblage of Flat Elements by FEM," *Proceedings of the SSRC Annual Technical Session,* 1986.

3.119 Lee, S. C., and C. H. Yoo: "Interactive Buckling of Thin-Walled Members," *Proceedings of the SSRC Annual Technical Session,* 1988.

3.120 Rusmussen, K. J. R., and G. J. Hancock: "Geometric Imperfections in Plated Structures Subject to Interaction between Buckling Modes," *Thin-Walled Structures,* vol. 6, no. 6, 1988.

3.121 Dawe, J. L., A. A. Elgabry, and G. Y. Grondin: "Local Buckling of Hollow Structural Sections," *Journal of Structural Engineering,* vol. 111, no. 5, May 1985.

3.122 Rondal, J., and R. Maquoi: "Local Buckling of Hollow Structural Sections," *Journal of Structural Engineering,* vol. 113, no. 9, Sept. 1987.

3.123 Symposium on Hollow Structural Sections in Building Construction, ASCE Structural Division Structural Engineering Congress 1985, Sept. 17–18, 1985.

3.124 Pan, L. C., and W. W. Yu: "High Strength Steel Members with Unstiffened Compression Elements," *Proceedings of the 9th International Specialty Conference on Cold-Formed Steel Structures,* Nov. 8–9, 1988.

3.125 Tien, Y. L., and S. T. Wang: "Local Buckling of Beams under Stress Gradient," *Journal of the Structural Division, ASCE Proceedings,* vol. 105, Aug. 1979.

3.126 Horne, M. R., and R. Narayanan: "Design of Axially Loaded Stiffened Plates," *Journal of the Structural Division, ASCE Proceedings,* vol. 103, Nov. 1977.

3.127 Elsharkawi, K., and A. C. Walker: "Buckling of Multibay Stiffened Plate Panels," *Journal of the Structural Division, ASCE Proceedings,* vol. 106, Aug. 1980.

3.128 Sechler, E. E.: "The Ultimate Strength of Thin Flat Sheets in Compression," publication 27, Guggenhein Aeronautics Laboratory, California Institute of Technology, Pasadena, 1933.

3.129 Chilver, A. H.: "The Stability and Strength of Thin Walled Steel Struts," *The Engineer,* vol. 7, Aug. 1953.

3.130 Skaloud, M.: "Grenzzustand gedrückter Gurtplatten dünnwandiger Träger," *Acta Technica CSAV,* no. 6, 1965.

3.131 Wang, S. T.: "Cold-Rolled Austenitic Stainless Steel: Material Properties and Structural Performance," report 334, Department of Structural Engineering, Cornell University, July 1969.

3.132 Dwight, J. B., and K. E. Moxham: "Welded Steel Plates in Compression," *The Structural Engineer,* vol. 47, Feb. 1969.

3.133 Dwight, J. B., and A. T. Ractliffe: "The Strength of Thin Plates in Compression, in *Thin-Walled Steel Structures* (K. C. Rockey and H. V. Hill, eds.), Gordon and Breach Science Publishers, New York, 1968.

3.134   Vilnay, O., and K. C. Rockey: "A Generalised Effective Width Method for Plates Loaded in Compression," *Journal of Constructional Steel Research,* vol. 1, May 1981.

3.135   Parks, M. B., C. Santaputra, and W. W. Yu: "Local Buckling of Curved Elements," *Proceedings of the 8th International Specialty Conference on Cold-Formed Steel Structures,* Nov. 11–12, 1986.

3.136   Parks, M. B., and W. W. Yu: "Local Buckling Behaviour of Stiffened Curved Elements," *Thin-Walled Structures,* vol. 7, no. 1, 1989.

3.137   Fukumoto, Y., and H. Kusama: "Local Instability Tests of Plate Elements under Cyclic Uniaxial Loading," *Journal of Structural Engineering,* vol. 111, no. 5, May 1985.

3.138   Souza, M. A.: "Vibrational Characteristics of Buckled Plates," *Proceedings of the SSRC Annual Technical Session,* 1986.

3.139   Gierlinski, J. T., and T. R. Graves Smith: "The Geometric Non-Linear Analysis of Thin-Walled Structures by Finite Strips," *International Journal on Thin-Walled Structures,* vol. 2, no. 1, 1984.

3.140   Lau, S. C. W., and G. J. Hancock: "Buckling of Thin Flat-Walled Structures by a Spline Finite Strip Method," *International Journal on Thin-Walled Structures,* vol. 4, no. 4, 1988.

3.141   Mahendran, M., and N. W. Murray: "Elastic Buckling Analysis of Ideal Thin-Walled Structures under Combined Loading Using a Finite Strip Method," *International Journal on Thin-Walled Structures,* vol. 4, no. 5, 1986.

3.142   Gradzki, R., and K. Kowal-Michalska: "Stability in the Elasto-plastic Range of Rectangular Plates Subjected to Uniaxial Compression, With Unloaded Edges Clamped," *International Journal on Thin-Walled Structures,* vol. 5, no. 2, 1987.

3.143   Puckett, J. A., D. L. Wiseman, and K. P. Chong: "Compound Strip Method for the Buckling Analysis of Continuous Plates," *Thin-Walled Structures,* vol. 5, no. 5, 1987.

3.144   Lau, S. C. W., and G. J. Hancock: "Inelastic Buckling Analysis of Beams, Columns, and Plates Using the Spline Finite Strip Method," *Thin-Walled Structures,* vol. 8, nos. 3, 4, 1989.

3.145   Jakubowski, S.: "Local Buckling of Thin-Walled Girders of Triangular Cross-Section," *Thin-Walled Structures, International Journal,* vol. 8, no. 4, 1989.

3.146   Polyzois, D.: "Effect of Sloping Edge Stiffeners on the Capacity of Cold-Formed Sections," *Proceedings of the SSRC Annual Technical Session,* 1985.

3.147   Elgaaly, M., and W. L. Nunan: "Behavior of Rolled Section Web under Eccentric Edge Compressive Loads," *Journal of Structural Engineering,* vol. 115, no. 7, 1989.

3.148   Narayanan, R., and N. G. Der-Avanessian: "Design of Slender Webs Having Rectangular Holes," *Journal of Structural Engineering,* vol. 111, no. 4, Apr. 1985.

3.149   American Society of Civil Engineers: *Minimum Design Loads for Buildings and Other Structures,* ASCE Standard 7-95, 1995.

3.150   American Institute of Steel Construction: "Load and Resistance Factor Design Specification for Structural Steel Buildings" 3rd ed., 1999.

3.151 Steel Deck Institute: "LRFD Design Manual for Composite Beams and Girders with Steel Deck," 1st Ed.

3.152 American Iron and Steel Institute: "Commentary on the Load and Resistance Factor Design Specification for Cold-Formed Steel Structural Members," Aug. 1991.

3.153 Rang, T. N., T. V. Galambos, W. W. Yu, and M. K. Ravindra: "Load and Resistance Factor Design of Cold-Formed Steel Structural Members," *Proceedings of the 4th International Specialty Conference on Cold-Formed Steel Structures,* University of Missouri-Rolla, June 1978.

3.154 Galambos, T. V., T. N. Rang, W. W. Yu, and M. K. Ravindra: "Structural Reliability Analysis of Cold-Formed Steel Members," *Proceedings of the ASCE Specialty Conference on Probabilistic Mechanics and Structural Reliability,* Jan. 1979.

3.155 Rang, T. N., W. W. Yu, T. V. Galambos, and M. K. Ravindra: "Load and Resistance Factor Design of Bolted Connections," *Proceedings of the International Conference on Thin-Walled Structures,* University of Strathclyde, Glasgow, Scotland, Apr. 1979.

3.156 Galambos, T. V., and W. W. Yu: "Load and Resistance Factor Design of Cold-Formed Steel Structural Members," *Proceedings of the 7th International Specialty Conference on Cold-Formed Steel Structures,* University of Missouri-Rolla, Nov. 1984.

3.157 Snyder, B. K., L. C. Pan, and W. W. Yu: "Comparative Study of Load and Resistance Factor Design versus Allowable Stress Design," *Proceedings of the 7th International Specialty Conference on Cold-Formed Steel Structures,* University of Missouri-Rolla, Nov. 1984.

3.158 Hsiao, L. E., S. H. Lin, W. W. Yu, and T. V. Galambos: "American LRFD Design Criteria for Cold-Formed Steel Structural Members," *Proceedings of the 2nd International Conference on Steel and Aluminum Structures,* National University of Singapore, May 1991.

3.159 Hsiao, L. E., W. W. Yu, and T. V. Galambos: "Load and Resistance Factor Design of Cold-Formed Steel: Load and Resistance Factor Design Specification for the Design of Cold-Formed Steel Structural Members with Commentary," 14th Progress Report, University of Missouri-Rolla, Aug. 1990.

3.160 Ravindra, M. K., and T. V. Galambos: "Load and Resistance Factor Design of Steel," *Journal of the Structural Division, ASCE Proceedings,* vol. 104, Sept. 1978.

3.161 Ellingwood, B., T. V. Galambos, J. G. MacGregor, and C. A. Cornell: "Development of a Probability Based Load Criterion for American National Standard A58: Building Code Requirements for Minimum Design Loads in Buildings and Other Structures," NBS Special Publication 577, June 1980.

3.162 Hsiao, L. E., W. W. Yu, and T. V. Galambos: "Load and Resistance Factor Design of Cold-Formed Steel: Calibration of the AISI Design Provisions," 9th Progress Report, University of Missouri-Rolla, Feb. 1988.

3.163 Hsiao, L. E., W. W. Yu, and T. V. Galambos: "Load and Resistance Factor Design of Cold-Formed Steel: Comparative Study of Design Methods for Cold-Formed Steel," 11th Progress Report, University of Missouri-Rolla, Feb. 1988.

3.164   Ellingwood, B.: "Serviceability Guidelines for Steel Structures," *Engineering Journal,* AISC, First Quarter, 1989.

3.165   Fisher, J. M., and M. A. West: *Serviceability Design Considerations for Low-Rise Buildings,* Steel Design Guide Series, AISC, 1990.

3.166   Murray, T. M.: "Building Floor Vibrations," *Engineering Journal,* AISC, Third Quarter, 1991.

3.167   Allen, D. E., and T. M. Murray: "Designing Criterion for Vibrations Due to Walking," *Engineering Journal,* AISC, Fourth Quarter, 1993.

3.168   Schafer, B. W., and T. Pekoz: "Laterally Braced Cold-Formed Steel Flexural Members with Edge Stiffened Flanges," *Proceedings of the 14th International Specialty Conference on Cold-Formed Steel Structures,* University of Missouri-Rolla, Oct. 1998. Also *Journal of Structural Engineering,* ASCE, vol. 125, no. 2, Feb. 1999.

3.169   Kalyanaraman, V., and P. Jayabalan: "Local Buckling of Stiffened and Unstiffened Elements under Nonuniform Compression," *Proceedings of the 12th International Specialty Conference on Cold-Formed Steel Structures,* University of Missouri-Rolla, Oct. 1994.

3.170   Rogers, C. A., and R. M. Schuster: "Effective Width of a Single Edge-Stiffener Subjected to a Stress Gradient," *Proceedings of the 13th International Specialty Conference on Cold-Formed Steel Structures,* University of Missouri-Rolla, Oct. 1996.

3.171   Bernard, E. S., R. Q. Bridge, and G. J. Hancock: "Tests of Profiled Steel Decks with V-Stiffeners," *Proceedings of the 11th International Specialty Conference on Cold-Formed Steel Structures,* University of Missouri-Rolla, Oct. 1992. Also *Journal of Structural Engineering,* ASCE, vol. 119, no. 8, Aug. 1993.

3.172   Bernard, E. S., R. Q. Bridge, and G. J. Hancock: "Tests of Profiled Steel Decks with Flat-Hat Stiffeners," *Journal of Structural Engineering,* ASCE, vol. 121, no. 8, Aug. 1995.

3.173   Bambach, M. R., J. T. Merrick, and G. J. Hancock: "Distortional Buckling Formulae for Thin-Walled Channel and Z-Sections with Return Lips," *Proceedings of the 14th International Specialty Conference on Cold-formed Steel Structures,* University of Missouri-Rolla, Oct. 1998.

3.174   Papazian, R. P., R. M. Schuster, and M. Sommerstein: "Multiple Stiffened Deck Profiles," *Proceedings of the 12th International Specialty Conference on Cold-Formed Steel Structures,* University of Missouri-Rolla, Oct. 1994

3.175   Schafer, B. W., and T. Pekoz: "Design of Cold-Formed Steel Stiffened Elements with Multiple Longitudinal Intermediate Stiffeners," *Proceedings of the 13th International Specialty Conference on Cold-Formed Steel Structures,* University of Missouri-Rolla, Oct. 1996.

3.176   Schafer, B. W., and T. Pekoz: "Cold-Formed Steel Members with Multiple Longitudinal Intermediate Stiffeners," *Journal of Structural Engineering,* ASCE, vol. 124, no. 10, Oct. 1998.

3.177   Acharya, V. V., and R. M. Schuster: "Bending Tests of Hat Sections with Multiple Longitudinal Stiffeners," *Proceedings of the 14th International Specialty Conference on Cold-Formed Steel Structures,* University of Missouri-Rolla, Oct. 1998.

3.178   Acharya, V. V., and R. M. Schuster: "Analysis of Hat Sections with Multiple Intermediate Longitudinal Stiffeners," *Proceedings of the 14th International Specialty Conference on Cold-Formed Steel Structures,* University of Missouri-Rolla, Oct. 1998.

3.179   Sivakumaran, K. S., and K. M. Zielonka: "Web Crippling Strength of Thin-Walled Steel Members with Openings," *Thin-Walled Structures,* vol. 8, no. 4, 1989.

3.180   Shimizu, S., S. Yoshida, and N. Enomoto: "Buckling of Plates with a Hole under Tension," *Thin-Walled Structures,* vol. 12, 1991.

3.181   Shanmugam, N. E., and V. Thevendran: "Critical Loads of Thin-Walled Beams Containing Web Openings," *Thin-Walled Structures,* vol. 14, 1992.

3.182   Rhodes, J., and F. D. Schneider: "The Compressional Behavior of Perforated Elements," *Proceedings of the 12th International Specialty Conference on Cold-Formed Steel Structures,* University of Missouri-Rolla, Oct. 1994.

3.183   Mahendran, M., N. E. Shanmugam, and J. Y. R. Liew: "Strength of Stiffened Plates with Openings," *Proceedings of the 12th International Specialty Conference on Cold-Formed Steel Structures,* UMR, Oct. 1994.

3.184   Shan, M. Y., R. A. LaBoube, and W. W. Yu: "Bending and Shear Behavior of Web Elements with Openings," *Proceedings of the 12th International Specialty Conference on Cold-Formed Steel Structures,* University of Missouri-Rolla, Oct. 1994. Also *Journal of Structural Engineering,* vol. 122, no. 8, Aug. 1996.

3.185   Langan, J. E., R. A. LaBoube, and W. W. Yu: "Perforated Webs Subjected to End-One-Flange Loading," *Proceedings of the 12th International Specialty Conference on Cold-Formed Steel Structures,* University of Missouri-Rolla, Oct. 1994.

3.186   Miller, T. H., and T. Pekoz: "Unstiffened Strip Approach for Perforated Wall Studs," *Journal of Structural Engineering,* ASCE, vol. 120, no. 2, Feb. 1994.

3.187   Schuster, R. M., C. A. Rogers, and A. Celli: "Research into Cold-Formed Steel Perforated C-Sections in Shear," *Progress Report No. 1,* CSSBI/IRAP Project, University of Waterloo, 1995.

3.188   Rhodes, J., and M. Macdonald: "The Effects of Perforation Length on the Behavior of Perforated Elements in Compression," *Proceedings of the 13th International Specialty Conference on Cold-Formed Steel Structures,* University of Missouri-Rolla, Oct. 1996

3.189   LaBoube, R. A., W. W. Yu, J. E. Langan, and M. Y. Shan: "Cold-Formed Steel Webs with Openings: Summary Report," *Thin-Walled Structures,* vol. 27, no. 1, 1997.

3.190   Shanmugam, N. E.: "Openings in Thin-Walled Structures," *Thin-Walled Structures,* vol. 28, nos. 3–4, 1997.

3.191   Davies, J. M., P. Leach, and A. Taylor: "The Design of Perforated Cold-Formed Steel Sections Subject to Axial Load and Bending," *Thin-Walled Structures,* vol. 29, nos. 1–4, 1997.

3.192   Eiler, M. R.: "Behavior of Web Elements with Openings Subjected to Linearly Varying Shear," M.S. Thesis, University of Missouri-Rolla, 1997.

3.193   LaBoube, R. A., W. W. Yu, S. U. Deshmukh, and C. A. Uphoff: "Crippling Capacity of Web Elements with Openings," *Journal of Structural Engineering,* ASCE, vol. 125, no. 2, Feb. 1999.

3.194 Pu, Y., M. H. R. Godley, R. G. Beale, and H. H. Lau: "Prediction of Ultimate Capacity of Perforated Lipped Channels," *Journal of Structural Engineering,* ASCE, vol.125, no. 5, May 1999.

3.195 Schafer, B. W.: "Elastic Buckling Stress and Cold-Formed Steel Design," *CCFSS Technical Bulletin,* vol. 7, no. 1, University of Missouri-Rolla, Feb. 1998.

3.196 Schafer, B. W., and T. Pekoz: "Direct Strength Prediction of Cold-Formed Steel Members using Numerical Elastic Buckling Solution," *Proceedings of the 14th International Specialty Conference on Cold-Formed Steel Structures,* University of Missouri-Rolla, Oct. 1998. Also *Thin-Walled Structures: Research and Development,* ed. N. E. Shanmugam, J. Y. R. Liew, and V. Thevendran, Elsevier, 1998.

3.197 Shan, M. Y., R. A. LaBoube and W. W. Yu: "Behavior of Web Elements with Openings Subjected to Bending, Shear and the Combination of Bending and Shear," Final Report, Civil Engineering Study 94-2, University of Missouri-Rolla, 1994.

3.198 Langan, J. E., R. A. LaBoube, and W. W. Yu: "Structural Behavior of Perforated Web Elements of Cold-Formed Steel Flexural Members Subjected to Web Crippling and a Combination of Web Crippling and Bending," Final Report, Civil Engineering Study 94-3, University of Missouri-Rolla, 1994.

3.199 Uphoff, C. A.: "Structural Behavior of Circular Holes in Web Elements of Cold-Formed Steel Flexural Members Subjected to Web Crippling for End-One-Flange Loading," M.S. Thesis, University of Missouri-Rolla, 1996.

3.200 Deshmukh, S. U.: "Behavior of Cold-Formed Steel Web Elements with Web Openings Subjected to Web Crippling and a Combination of Bending and Web Crippling for Interior-One-Flange Loading," M.S. Thesis, University of Missouri-Rolla, 1996.

CHAPTER 4

4.1 Reck, H. P., T. Pekoz, and G. Winter: "Inelastic Strength of Cold-Formed Steel Beams," *Journal of the Structural Division, ASCE Proceedings,* vol. 101, Nov. 1975.

4.2 Yener, M., and T. Pekoz: "Inelastic Load Carrying Capacity of Cold-Formed Steel Beams," *Proceedings of the 5th International Specialty Conference on Cold-Formed Steel Structures,* University of Missouri-Rolla, Nov. 1980.

4.3 Yener, M., and T. Pekoz: "Partial Stress Redistribution in Cold-Formed Steel," *Journal of Structural Engineering,* vol. 111, no. 6, June 1985.

4.4 Yener, M., and T. Pekoz: "Partial Moment Redistribution in Cold-Formed Steel," *Journal of Structural Engineering,* vol. 111, no. 6, June 1985.

4.5 von Unger, B.: "Ein Beitrag zur Ermittlung der Traglast von querbelasteten Durchlaufträgern mit dünnwandigem Querschnitt, insbesondere von durchlaufenden Trapezblechen für Dach und Geschossdecken," *Der Stahlbau,* vol. 42, Jan. 1973.

4.6 Wang, S. T.: "Nonlinear Analysis of Thin-Walled Continuous Beams," *Proceedings of the 2nd Specialty Conference on Cold-Formed Steel Structures,* University of Missouri-Rolla, Oct. 1973.

4.7   Wang, S. T., and S. S. Yeh: "Post-Local-Buckling Behavior of Continuous Beams," *Journal of the Structural Division, ASCE Proceedings,* vol. 100, June 1974.

4.8   Chong, K. P., and D. M. Mosier: "Nonlinear Behavior of Continuous Cold-Formed Beams," *Proceedings of the 3rd International Specialty Conference on Cold-Formed Steel Structures,* University of Missouri-Rolla, Nov. 1975.

4.9   Ryan, T. G.: "Designing for Moment Redistribution and Ultimate Load for Continuous Beams," committee correspondence, Sept. 9, 1981.

4.10 LaBoube, R. A., M. Golovin, D. J. Montague, D. C. Perry, and L. L. Wilson: "Behavior of Continuous Span Purlin Systems," *Proceedings of the 9th International Specialty Conference on Cold-Formed Steel Structures,* UMR, Nov. 8–9, 1988.

4.11 Chong, K. P., and D. M. Harris: "Automated Design of Continuous Cold-Formed Beams," *Proceedings of the 2nd Specialty Conference on Cold-Formed Steel Structures,* University of Missouri-Rolla, Oct. 1973.

4.12 Douty, R. T., and J. O. Crooker: "Optimization of Long Span Truss Purlins," *Proceedings of the 2nd Specialty Conference on Cold-Formed Steel Structures,* University of Missouri-Rolla, Oct. 1973.

4.13 Bleustein, J. L., and A. Gjelsvik: "Rational Design of Light Gage Beams," *Journal of the Structural Division, ASCE Proceedings,* vol. 96, July 1970.

4.14 Yu, W. W.: "Discussion of Rational Design of Light Gage Beams, by J. L. Bleustein and A. Gjelsvik," *Journal of the Structural Division, ASCE Proceedings,* vol. 96, Dec. 1970.

4.15 Winter, G.: "Lateral Stability of Unsymmetrical I-Beams and Trusses," *ASCE Transactions,* vol. 198, 1943.

4.16 Galambos, T. V.: "Inelastic Lateral Buckling of Beams," *Journal of the Structural Division, ASCE Proceedings,* vol. 89, Oct. 1963.

4.17 Hill, H. N.: "Lateral Buckling of Channels and Z-Beams," *ASCE Transactions,* vol. 119, 1954.

4.18 Winter, G.: "Strength of Slender Beams," *ASCE Transactions,* vol. 109, p. 1312, 1944.

4.19 Douty, R. T.: "A Design Approach to the Strength of Laterally Unbraced Compression Flange," bulletin 37, Engineering Experiment Station, Cornell University, 1962.

4.20 Haussler, R. W.: "Strength of Elastically Stabilized Beams," *Journal of the Structural Division, ASCE Proceedings,* vol. 90, June 1964.

4.21 Fukumoto, Y., and M. Kubo: "Buckling in Steel U-Shaped Beams," *Journal of Structural Engineering,* vol. 108, May 1982, Discussion by S. Rajasekaran, *Journal of Structural Engineering,* vol. 110, no. 1, Jan. 1984.

4.22 Bradford, M. A., and G. J. Hancock: "Elastic Interaction of Local and Lateral Buckling in Beams," *International Journal on Thin-Walled Structures,* vol. 2, no. 1, 1984.

4.23 Ings, N. L., and N. S. Trahair: "Lateral Buckling of Restrained Roof Purlins," *International Journal on Thin-Walled Structures,* vol. 2, no. 4, 1984.

4.24 Kemp, A. R.: "Interaction of Plastic Local and Lateral Bucklings," *Journal of Structural Engineering,* vol. 111, no. 10, October 1985.

4.25   Roberts, T. M., and M. Benchina: "Lateral Instability of Monosysmetric Beams with Initial Curvature," *International Journal on Thin-Walled Structures,* vol. 5, no. 2, 1987.

4.26   Toneff, J. D., S. F. Stiemer, and P. Osterrieder: "Local and Overall Buckling in Thin-Walled Beams and Columns," *Journal of Structural Engineering,* vol. 113, no. 4, Apr. 1987.

4.27   Kubo, M., and Y. Fukumoto: "Lateral-Torsional Buckling of Thin-Walled I-Beams," *Journal of Structural Engineering,* vol. 114, no. 4, Apr. 1988.

4.28   Djugash, A. C. R., and V. Kalyanaraman: "Experimental Study on the Lateral Buckling Behaviour of Cold-Formed Beams," *Proceedings of the 10th International Specialty Conference on Cold-Formed Steel Structures,* University of Missouri-Rolla, Oct. 1990.

4.29   Seah, L. K., and J. Rhodes: "Behaviour of Channel Beams with Unbraced Compressions Flanges," *Proceedings of the 10th International Specialty Conference on Cold-Formed Steel Structures,* University of Missouri-Rolla, Oct. 1990.

4.30   Haussler, R. W., and R. F. Pahers: "Connection Strength in Thin Metal Roof Structures," *Proceedings of the 2nd Specialty Conference on Cold-Formed Steel Structures,* University of Missouri-Rolla, Oct. 1973.

4.31   Pekoz, T. B., and P. Soroushian: "Behavior of C- and Z-Purlins Under Uplift," *Report no. 81-2,* Department of Structural Engineering, Cornell University, Ithaca, NY.

4.32   LaBoube, R. A., and M. B. Thompson: "Static Load Tests of Braced Purlins Subjected to Uplift Load," *Final Report, Project No. 7485-G,* Midwest Research Institute, Kansas City, MO, 1982.

4.33   Pekoz, T., and P. Soroushian: "Behavior of C- and Z-Purlins under Wind Uplift," *Proceedings of the Sixth International Specialty Conference on Cold-Formed Steel Structures,* University of Missouri-Rolla, Nov. 16–17, 1982.

4.34   LaBoube, R. A.: "Laterally Unsupported Purlins Subjected to Uplift," *Final Report, Metal Building Manufacturers Association,* Dec. 1983.

4.35   Polyzois, D., and P. C. Birkemoe: "Z-Section Girts under Negative Loading," *Journal of Structural Engineering,* vol. 111, no. 3, Mar. 1985.

4.36   LaBoube, R. A.: "Roof Panel to Purlin Connection: Rotational Restraint Factor," *Proceedings of the IABSE Colloquium on Thin-Walled Metal Structures in Buildings,* Stockholm, Sweden, June, 1986.

4.37   LaBoube, R. A., et al.: "Behavior of Continuous Span Purlin System," *Proceedings of the 9th International Specialty Conference on Cold-Formed Steel Structures,* University of Missouri-Rolla, Nov. 8–9, 1988.

4.38   Haussler, R. W.: "Theory of Cold-Formed Steel Purlin/Girt Flexure," *Proceedings of the 5th International Specialty Conference on Cold-Formed Steel Structures,* University of Missouri-Rolla, Nov. 8–9, 1988.

4.39   LaBoube, R. A., and M. Golovin: "Uplift Behavior of Purlin Systems Having Discrete Braces," *Proceedings of the 10th International Specialty Conference on Cold-Formed Steel Structures,* University of Missouri-Rolla, Oct. 1990.

4.40   Hancock, G. J., M. Celeban, C. Healy, P. N. Georgiou, and N. L. Ings: "Tests of Purlins with Screw Fastened Sheeting under Wind Uplift," *Proceedings of*

the 10th International Specialty Conference on Cold-Formed Steel Structures, Oct. 1990.

4.41   Hildebrand, F. B., and E. Reissner: "Least Work Analysis of the Problem of Shear Lag in Box Beams," NACA technical note 893, 1943.

4.42   Winter, G.: "Stress Distribution in and Equivalent Width of Flanges of Wide, Thin-Wall Steel Beams," NACA technical note 784, 1940.

4.43   Miller, A. B.: "Die mittragende Breite, and über die mittragende Breite," *Luftfahrtforschung,* vol. 4, no. 1, 1929.

4.44   Tate, M. B.: "Shear Lag in Tension Panels and Box Beams," engineering report 3, Iowa Engineering Station, Iowa State College, 1950.

4.45   Roark, R. J.: *Formulas for Stress and Strain,* 4th ed., McGraw-Hill Book Company, New York, 1965.

4.46   Malcolm, D. J., and R. G. Redwood: "Shear Lag in Stiffened Box Girders," *Journal of the Structural Division, ASCE Proceedings,* vol. 96, July 1970.

4.47   Parr, D. H., and S. P. Maggard: "Ultimate Design of Hollow Thin-Walled Box Girders," *Journal of the Structural Division, ASCE Proceedings,* vol. 98, July 1972.

4.48   Van Dalen, K., and S. V. Narasimham: "Shear Lag in Shallow Wide-Flange Box Girders," *Journal of the Structural Division, ASCE Proceedings,* vol. 102, Oct. 1976.

4.49   Lamas, A. R. G., and P. J. Dowling: "Effect of Shear Lag on the Inelastic Buckling Behavior of Thin-Walled Structures," *Thin-Walled Structures* (J. Rhodes and A. C. Walker, Eds.), Granada Publishing, New York, Apr. 3–6, 1979.

4.50   Jetteur, P., R. Maquoi, and C. Massonnet: "Simulation of the Behaviour of Stiffened Box Girders with and without Shear Lag," *International Journal on Thin-Walled Structures,* vol. 1, no. 3, 1983.

4.51   Skaloud, M.: "The Effect of Shear Lag in the Light of Various Definitions of the Ultimate Limit State of Stiffened Compression Flanges," *International Journal on Thin-Walled Structures,* vol. 3, no. 4, 1985.

4.52   Chang, S. T., and F. Z. Zheng: "Negative Shear Lag in Cantilever Box Girder with Constant Depth," *Journal of Structural Engineering,* vol. 133, no. 1, Jan. 1987.

4.53   Chang, S. T., and D. Yun: "Shear Lag Effect in Box Girder with Varying Depth," *Journal of Structural Engineering,* vol. 114, no. 10, Oct. 1988.

4.54   Song, Q. G., and A. C. Scordelis: "Shear-Lag Analysis of T-, I-, and Box Beams," *Journal of Structural Engineering,* ASCE, vol. 116, May 1990.

4.55   Song, Q. G., and A. C. Scordelis: "Formulas for Shear-Lag Effect of T-, I-, and Box Beams," *Journal of Structural Engineering,* ASCE, vol. 116, May 1990.

4.56   LaBoube, R. A., and W. W. Yu: "Structural Behavior of Beam Webs Subjected Primarily to Shear," final report, civil engineering study 78-2, University of Missouri-Rolla, June 1978.

4.57   LaBoube, R. A., and W. W. Yu: "Structural Behavior of Beam Webs Subjected to a Combination of Bending and Shear," final report, civil engineering study 78-3, University of Missouri-Rolla, June 1978.

4.58   Hetrakul, N., and W. W. Yu: "Structural Behavior of Beam Webs Subjected to Web Crippling and a Combination of Web Crippling and Bending," final report, civil engineering study 78-4, University of Missouri-Rolla, June 1978.

4.59   Nguyen, P., and W. W. Yu: "Structural Behavior of Transversely Reinforced Beam Webs," final report, civil engineering study 78-5, University of Missouri-Rolla, June 1978.

4.60   Nguyen, P., and W. W. Yu: "Structural Behavioral of Longitudinally Reinforced Beam Webs," final report, civil engineering study 78-6, University of Missouri-Rolla, June 1978.

4.61   Popov, E. P.: *Mechanics of Materials,* Prentice-Hall, Englewood Cliffs, NJ, 1976.

4.62   Southwell, R. V., and S. W. Skan: "On the Stability under Shearing Forces of a Flat Elastic Strip," *Proceedings, Royal Society A,* vol. 105, no. 733, May 1924.

4.63   Rockey, K. C.: "Shear Buckling of Thin-Walled Sections," *Thin-Walled Structures* (A. H. Chilver, Ed.), John Wiley and Sons, New York, copyrighted by Chatto & Windus, 1967.

4.64   Basler, K.: "Strength of Plate Girders in Shear," *Journal of the Structural Division, ASCE Proceedings,* vol. 87, pp. 151–180, Oct. 1961.

4.65   Nguyen, P., and W. W. Yu: "Bending Strength of Cold-Formed Steel Longitudinally Reinforced Beam Webs," *Proceedings of the 5th International Specialty Conference on Cold-Formed Steel Structures,* University of Missouri-Rolla, Nov. 1980.

4.66   Nguyen, R. P., and W. W. Yu: "Longitudinally Reinforced Cold-Formed Steel Beam Webs," *Journal of the Structural Division, ASCE Proceedings,* vol. 108, Nov. 1982.

4.67   LaBoube, R. A., and W. W. Yu: "Cold-Formed Steel Web Elements under Combined Bending and Shear," *Proceedings of the 4th International Specialty Conference on Cold-Formed Steel Structures,* University of Missouri-Rolla, June 1978.

4.68   Sommerfeld, A.: *Zeitschrift für Mathematik und Physik,* vol. 54, 1906.

4.69   Timoshenko, S. P.: *Zeitschrift für Mathematik und Physik,* vol. 58, 1910.

4.70   Leggett, D. M. A.: "The Effect of Two Isolated Forces on Elastic Stability of Flat Rectangular Plate," *Proceedings, Cambridge Philosophical Society,* vol. 33, 1937.

4.71   Hopkins, H. G.: "Elastic Stability of Infinite Strips," *Proceedings, Cambridge Philosophical Society,* vol. 45, 1969.

4.72   Yamaki, N.: "Buckling of a Rectangular Plate under Locally Distributed Forces Applied on the Two Opposite Edges," 1st, 2nd, and 4th reports, The Institute of High-Speed Mechanics, Tohuku University, Japan, 1953 and 1954.

4.73   Zetlin, L.: "Elastic Instability of Flat Plates Subjected to Partial Edge Loads," *Journal of the Structural Division, ASCE Proceedings,* vol. 81, Sept. 1955.

4.74   White, R. N., and W. S. Cottingham: "Stability of Plates under Partial Edge Loadings," *Journal of the Engineering Mechanics Division, ASCE Proceedings,* vol. 88, Oct. 1962.

4.75   Khan, M. Z., and A. C. Walker: "Buckling of Plates Subjected to Localised Edge Loading," *The Structural Engineer,* vol. 50, June 1972.

4.76   Khan, M. Z., K. C. Johns, and B. Hayman: "Buckling of Plates with Partially Loaded Edges," *Journal of the Structural Division, ASCE Proceedings,* vol. 103, Mar. 1977.

4.77   Lyse, I., and H. J. Godfrey: "Investigation of Web Buckling in Steel Beams," *ASCE Transactions,* vol. 100, 1935.

4.78   Bagchi, D. K., and K. C. Rockey: "A Note on the Buckling of a Plate Girder Web Due to Partial Edge Loadings," final reports, International Association for Bridge and Structural Engineering, Sept. 1968.

4.79   Rockey, K. C., and D. K. Bagchi: "Buckling of Plate Girder Webs under Partial Edge Loading," *International Journal of Mechanical Science,* Pergamon Press, vol. 12, 1970.

4.80   Rockey, K. C., and M. A. El-gaaly: "Ultimate Strength of Plates when Subjected to In-Plane Patch Loading," *Proceedings of the Seminar on Design of Plate and Box Girders for Ultimate Strength,* International Association for Bridge and Structural Engineering, 1971.

4.81   Rockey, K. C., M. A. El-gaaly, and D. K. Bagchi: "Failure of Thin-Walled Members and Patch Loading," *Journal of the Structural Division, ASCE Proceedings,* vol. 98, Dec. 1972.

4.82   Rockey, K. C., and M. A. El-gaaly: "Stability of Load Bearing Trapezoidal Diaphragms," publications, International Association for Bridge and Structural Engineering, vol. 32-11, 1972.

4.83   Rockey, K. C., and M. A. El-gaaly: "Ultimate Strength of Plates when Subjected to In-Plane Patch Loading," presented at the Colloquium on Design Plate and Box Girders for Ultimate Strength, London, England, International Association for Bridge and Structural Engineering, July 1972.

4.84   Bergfelt, A.: "Patch Loading on a Slender Web—Influence of Horizontal and Vertical Web Stiffeners on the Load Carrying Capacity," Chalmers University of Technology, Goteborg, Sweden, 1979.

4.85   Winter, G., and R. H. J. Pian: "Crushing Strength of Thin Steel Webs," Cornell bulletin 35, pt. 1, Apr. 1946.

4.86   Yu. W. W.: "Web Crippling and Combined Web Crippling and Bending of Steel Decks," civil engineering study 81-2, University of Missouri-Rolla, Apr. 1981.

4.87   Baehre, R.: "Sheet Metal Panels for Use in Building Construction—Recent Research Projects in Sweden," *Proceedings of the 3rd International Specialty Conference on Cold-Formed Steel Structures,* University of Missouri-Rolla, Nov. 1975.

4.88   Wing, B. A., and R. M. Schuster: "Web Crippling and the Interaction of Bending and Web Crippling of Unreinforced Multi-Web Cold-Formed Steel Sections," University of Waterloo, Ont., Canada, 1981.

4.89   Wing, B. A., and R. M. Schuster: "Web Crippling of Decks Subjected to Two Flange Loading," *Proceedings of the 6th International Specialty Conference on Cold-Formed Steel Structures,* University of Missouri-Rolla, Nov. 1982.

4.90   NAHB Research Foundation, Inc.: "Tests of United States Steel Super-C Steel Joists for Interaction of Bending and Web Crippling," CR-785B, 1972.

4.91   El-gaaly, M. A., and K. C. Rockey: "Ultimate Strength of Thin-Walled Members and Patch Loading and Bending," *Proceedings of the 2nd Specialty Conference on Cold-Formed Steel Structures,* University of Missouri-Rolla, Oct. 1973.

4.92   Ratliff, G. D.: "Interaction of Concentrated Loads and Bending in C-Shaped Beams," *Proceedings of the 3rd International Specialty Conference on Cold-Formed Steel Structures,* University of Missouri-Rolla, Nov. 1975.

4.93   National Swedish Board of Urban Planning: "Swedish Specification for Design of Thin-Walled Cold-Formed Structural Members."

4.94   Hetrakul, N., and W. W. Yu: "Cold-Formed Steel I-Beams Subjected to Combined Bending and Web Crippling," *Thin-Walled Structures* (J. Rhodes and A. C. Walker, Eds.), Granada Publishing, Apr. 3–6, 1979.

4.95   Graves Smith, T. R., and J. T. Gierlinski: "Buckling of Stiffened Webs by Local Edge Loads," *Journal of Structural Engineering,* vol. 108, June 1982. Discussion by A. Bergfelt, *Journal of Structural Engineering,* vol. 110, no. 1, Jan. 1984.

4.96   Packer, J. A.: "Web Crippling of Rectangular Hollow Sections," *Journal of Structural Engineering,* vol. 110, no. 10, Oct. 1984.

4.97   Santaputra, C., M. B. Parks, and W. W. Yu: "Web Crippling Strength of High Strength Steel Beams," *Proceedings of the 8th Specialty Conference on Cold-Formed Steel Structures,* UMR, Nov. 11–12, 1986.

4.98   Wing, B. A., and R. M. Schuster: "Web Crippling of Multi-Web Deck Sections Subjected to Interior One Flange Loading," *Proceedings of the 5th International Specialty Conference on Cold-Formed Steel Structures,* UMR, Nov. 11–12, 1986.

4.99   Tsai, Y. M., and M. Crisinel: "Moment Redistribution in Profiled Sheeting," *Proceedings of the 8th International Specialty Conference on Cold-Formed Steel Structures,* UMR, Nov. 11–12, 1986.

4.100   Tsai, Y. M., and M. Crisinel: "Moment Redistribution in Continuous Profiled Steel Sheeting," *Proceedings of the IABSE Colloquium,* Stockholm, 1986.

4.101   Packer, J. A.: "Review of American RHS Web Crippling Provisions," *Journal of Structural Engineering,* vol. 113, no. 12, Dec. 1987.

4.102   Edlund, B. L. O.: "Buckling and Failure Modes in Slender Plate Girders under Patch Loading," *Der Metallbau in Konstruktiven-Ingenieurbau,* Karlsruhe, West Germany, Feb. 1988.

4.103   Jakubowski, S.: "Buckling of Thin-Walled Girders under Compound Load," *Thin-Walled Structures,* vol. 6, no. 2, 1988.

4.104   Santaputra, C., M. B. Parks, and W. W. Yu: "Web-Crippling Strength of Cold-Formed Steel Beams," *Journal of Structural Engineering,* ASCE, vol. 115, Oct. 1989.

4.105   Sivakumaran, K. S., and K. M. Zielonka: "Web Crippling Strength of Thin-Walled Steel Members with Web Opening," *Thin-Walled Structures, International Journal,* vol. 8, no. 4, 1989.

4.106   Studnicka, J.: "Web Crippling of Wide Deck Sections," *Proceedings of the 10th International Specialty Conference on Cold-Formed Steel Structures,* University of Missouri-Rolla, Oct. 1990.

4.107   Bakker, M., T. Pekoz, and J. Stark: "A Model for the Behavior of Thin Walled Flexural Members under Concentrated Loads," *Proceedings of the*

10th International Specialty Conference on Cold-Formed Steel Structures, University of Missouri-Rolla, Oct. 1990.

4.108 Winter, G., W. Lansing, and R. B. McCalley: "Performance of Laterally Loaded Channel Beams," Research, Engineering, Structures Supplement (Colston papers, vol. II). p. 49, London, 1949 (reprinted in *Four Papers on the Performance of Thin Walled Steel Structures,*" reprint 33, Cornell University Engineering Experimental Station.

4.109 Zetlin, L., and G. Winter: "Unsymmetrical Bending of Beams with and without Lateral Bracing," *ASCE Proceedings,* vol. 81, paper 774, 1955.

4.110 Murray, T. M., and S. Elhouar: "Stability Requirements of Z-Purlin Supported Conventional Metal Building Roof Systems," *Annual Technical Session Proceedings, Structural Stability Research Council,* 1985.

4.111 Winter, G.: "Lateral Bracing of Columns and Beams," *ASCE Transactions,* vol. 125, 1960.

4.112 Lautensleger, R. W.: "The Opposed Z Purlin System for Low-Sloped Metal Building Roofs," *Proceedings, Behavior of Building Systems and Building Components,* Vanderbilt University, Nashville, TN, Mar. 1979.

4.113 Bryan, E. R.: "The Effect of Sheeting on Structural Design," *Building with Steel, Journal of the British Constructional Steel Work Association,* vol. 3, Aug. 1964.

4.114 Bryan, E. R., and W. M. El-Dakhakhni: "Behavior of Sheeted Portal Frame Sheds: Theory and Experiments," *Proceedings of the Institution of Civil Engineers,* vol. 29, Dec. 1964.

4.115 Pincus, G., and G. P. Fisher: "Behavior of Diaphragm-Braced Columns and Beams," *Journal of the Structural Division, ASCE Proceedings,* vol. 92, paper 4792, Apr. 1966.

4.116 Errera, S. J., G. Pincus, and G. P. Fisher: "Columns and Beams Braced by Diaphragms," *Journal of the Structural Division, ASCE Proceedings,* vol. 93, paper 5103, Feb. 1967.

4.117 Errera, S. J., and T. V. S. R. Apparao: "Beams and Columns Braced by Thin-Walled Steel Diaphragms," final report, International Association for Bridge and Structural Engineering, Sept. 9–14, 1968.

4.118 Celebi, N., T. Pekoz, and G. Winter: "Behavior of Channel and Z-Section Beams Braced by Diaphragms," *Proceedings of the 1st Specialty Conference on Cold-Formed Steel Structures,* University of Missouri-Rolla, Aug. 1971.

4.119 Rockey, K. C., and D. A. Nethercot: "Stabilization of Beams against Lateral Buckling," *Proceedings of the 1st Specialty Conference on Cold-Formed Steel Structures,* University of Missouri-Rolla, Aug. 1971.

4.120 Wikstrom, P.: "Z and Channel-Purlins Connected with Corrugated Steel Sheeting," *Proceedings of the 1st Specialty Conference on Cold-Formed Steel Structures,* University of Missouri-Rolla, Aug. 1971.

4.121 Harvey, J. M.: "The Integral Behavior of Roof Sheets and Purlins," *Thin-Walled Structures* (K. C. Rockey and H. V. Hill, Eds.), Gordon and Breach Science Publishers, New York, 1969.

4.122 Harvey, J. M.: "Flexure of a Cold-Formed Z-Section Purlin," *Structural Engineer,* Sept. 1970.

4.123   Celebi, N., G. Winter, and T. Pekoz: "Diaphragm Braced Channel and Z-Section Beams," report 344, Cornell University, Oct. 1971.

4.124   Fisher, J. M., and D. L. Johnson: "Behavior of Light Gage Diaphragms Coupled with X-Bracing," *Proceedings of the 2nd Conference on Cold-Formed Steel Structures,* University of Missouri-Rolla, Oct. 1973.

4.125   Pekoz, T.: "Continuous Purlin Tests," final report, Cornell University, Jan. 1975.

4.126   Pekoz, T.: "Evaluation of the Results of Continuous Purlin Tests," final report, Cornell University, Jan. 1975.

4.127   Pekoz, T.: "Progress Report on Cold-Formed Steel Purlin Design," *Proceedings of the 3rd International Specialty Conference on Cold-Formed Steel Structures,* University of Missouri-Rolla, Nov. 1975.

4.128   Pekoz, T.: "Evaluation of the Results of Gravity Load Tests of C and Z Purlin Roof Systems," Cornell University, Jan. 1976.

4.129   Birkemoe, P. C.: "Behavior and Design of Girts and Purlins for Negative Pressure," *Proceedings, Canadian Structural Engineering Conference,* 1976.

4.130   Hancock, G. J., and N. S. Trahair: "Lateral Buckling of Roof Purlins with Diaphragm Restraints," research report R319, University of Sydney, Sydney, Australia, Apr. 1978.

4.131   Rhodes, J., et al.: "Tests on a Continuous Purlin Roofing System," *Proceedings of the 4th International Specialty Conference on Cold-Formed Steel Structures,* University of Missouri-Rolla, June 1978.

4.132   Birkemoe, P. C., and D. Polyzois: "The Behavior of Cold-Formed Channels Braced Continuously along Their Tensions Side and Restrained by Sag Rods," *Thin-Walled Structures* (J. Rhodes and A. C. Walker, Eds.), Granada Publishing, New York, Apr. 1979.

4.133   Razak, M. A. A., and T. Pekoz: "Ultimate Strength of Cold-Formed Steel Z-Purlins," report 80-3, Cornell University, Feb. 1980.

4.134   Polyzois, D., and P.C. Birkemoe: "Behavior and Design of Continuous Girts and Purlins," *Proceedings of the 5th International Specialty Conference on Cold-Formed Steel Structures,* University of Missouri-Rolla, Nov. 1980.

4.135   Nethercot, D. A., and N. S. Trahair: "Design of Diaphragm-Braced I-Beams," *Journal of the Structural Division, ASCE Proceedings,* vol. 101, Oct. 1975.

4.136   Errera, S. J., and T. V. S. R. Apparao: "Design of I-Shaped Beams with Diaphragm Bracing," *Journal of the Structural Division, ASCE Proceedings,* vol. 102, Apr. 1976.

4.137   LaBoube, R. A.: "Purlin Braces: Measured Forces," *Stability of Metal Structures, Proceedings of the 3rd International Colloquium,* SSRC, May 1983.

4.138   Galambos, T. V.: "Bracing of Light Roof Trusses," *Proceedings of the 2nd Regional Colloquium on Stability of Steel Structures,* Sept. 25–26, 1986, Hungary.

4.139   Polyzois, D.: "Sag Rods as Lateral Supports for Girts and Purlins," *Journal of Structural Engineering,* vol. 113, no. 7, July 1987.

4.140   Heins, C. P.: *Bending and Torsional Design in Structural Members,* Lexington Books, D. C. Heath and Company, Lexington, MA, 1975.

4.141   Davies, J. M., and G. Raven: "Design of Cold-Formed Steel Purlins," *Proceedings of the IABSE Colloquium,* Stockholm, 1986.

4.142   Murray, T. M., and V. Seshappa: "Study of Thin-Walled Metal Building Roof Systems Using Scale Models," *Proceedings of the IABSE Colloquium,* Stockholm, 1986.

4.143   Tomka, P.: "Load Bearing Capacity of Cold-Formed Z-Sections," *Proceedings of the 2nd Regional Colloquium on Stability of Steel Structures,* Sept. 25–26, 1986, Hungary.

4.144   Robertson, G. W., and C. E. Kurt: "Behavior of Nested Z-Shaped Purlins," *Proceedings of the 8th International Specialty Conference on Cold-Formed Steel Structures,* University of Missouri-Rolla, Nov. 11–12, 1986.

4.145   Elhouar, S., and T. M. Murray: "Verification of 1986 AISI Provisions for Purlin Design," *Proceedings of the 8th International Specialty Conference on Cold-Formed Steel Structures,* University of Missouri-Rolla, Nov. 11–12, 1986.

4.146   Stark, J. W. B., and A. W. Toma: "New Design Method for Cold-Formed Purlins," *Der Metallbau in Konstruktiven-Ingenieurbau,* Karlsruhe, West Germany, Feb. 1988.

4.147   Thomasson, P. O.: "On the Behavior of Cold-Formed Steel Purlins—Particularly with Respect to Cross Sectional Distortion," *Der Metallbau in Konstruktiven-Ingenieurbau,* Karlsruhe, West Germany, Feb. 1988.

4.148   Sokol, L.: "Specific Aspects of the Design of Purlins in Z-Sections," *Der Metallbau in Konstruktiven-Ingenieurbau,* Karlsruhe, West Germany, Feb. 1988.

4.149   Lindner, J.: "To the Load Carrying Capacity of Cold-Formed Purlins," *Proceedings of the 9th International Specialty Conference on Cold-Formed Steel Structures,* University of Missouri-Rolla, Nov. 8–9, 1988.

4.150   Rhodes, J., and J. Zaras: "Development and Design Analysis of a New Purlin System," *Proceedings of the 9th International Specialty Conference on Cold-Formed Steel Structures,* University of Missouri-Rolla, Nov. 8–9, 1988.

4.151   Soetens, F., and A. W. Toma: "New Design Method for Cold-Formed Purlins," *Proceedings of the 9th International Specialty Conference on Cold-Formed Steel Structures,* University of Missouri-Rolla, Nov. 8–9, 1988.

4.152   Chang, N. S., and D. S. Ellifritt: "Selecting the Optimum Lipped Channel Beam," *Proceedings of the 9th International Specialty Conference on Cold-Formed Steel Structures,* University of Missouri-Rolla, Nov. 8–9, 1988.

4.153   Lau, S. C. W., and G. J. Hancock: "Distortional Buckling Tests of Cold-Formed Channel Sections," *Proceedings of the 9th International Specialty Conference on Cold-Formed Steel Structures,* University of Missouri-Rolla, Nov. 8–9, 1988.

4.154   DeMartino, A., A. Ghersi, and F. M. Mazzolani: "Bending Behaviour of Double-C Thin Walled Beams," *Proceedings of the 10th International Specialty Conference on Cold-Formed Steel Structures,* University of Missouri-Rolla, Oct. 1990.

4.155   Brooks, S. D., and T. M. Murray: "A Method for Determining the Strength of Z- and C-Purlin Supported Standing Seam Roof Systems," *Proceedings of*

the 10th International Specialty Conference on Cold-Formed Steel Structures, University of Missouri-Rolla, Oct. 1990.

4.156   Kirby, P. A., and D. A. Nethercot: *Design for Structural Stability,* John Wiley & Sons, New York, N.Y. 1979.

4.157   Bredt, R.: "Kritische Bemerkungen zur Drehungselastizität," *Z. Ver. Deut. Ing.*, vol. 40, 1896.

4.158   Serrette, R. L., and T. Pekoz: "Local and Distortional Buckling of Thin-Walled Beams," *Proceedings of the 11th International Specialty Conference on Cold-Formed Steel Structures,* University of Missouri-Rolla, Oct. 1992.

4.159   Serrette, R. L., and T. Pekoz: "Flexural Capacity of Continuous Span Standing Seam Panels: Gravity Load," *Proceedings of the 12th International Specialty Conference on Cold-Formed Steel Structures,* University of Missouri-Rolla, Oct, 1994.

4.160   Serrette, R. L., and T. Pekoz: "Distortional Buckling of Thin-Walled Beams/Panels. I: Theory," *Journal of Structural Engineering,* ASCE, vol. 121, no. 4, Apr. 1995.

4.161   Serrete, R. L., and T. Pekoz: "Distortional Buckling of Thin-Walled Beams/Panels. II: Design Methods," *Journal of Structural Engineering,* ASCE, vol. 121, no. 4, Apr. 1995.

4.162   Serette, R. L., and T. Pekoz: "Behavior of Standing Seam Panels," *Proceedings of the 3rd International Conference on Steel and Aluminum Structures,* Bagazici University, Istanbul, Turkey, May 1995.

4.163   Hancock, G. J.: "Local, Distortional and Lateral Buckling of I-Beams," *Journal of the Structural Division, ASCE Proceedings,* vol. 104, no. 11, Nov. 1978.

4.164   Hancock, G. J.: "Design for Distortional Buckling of Flexural Members," *Thin-Walled Structures,* vol. 20, 1997.

4.165   Hancock, G. J., C. A. Rogers, and R. M. Schuster: "Comparison of the Distortional Buckling Method for Flexural Members with Tests," *Proceedings of the 13th International Specialty Conference on Cold-Formed Steel Structures,* University of Missouri-Rolla, Oct. 1996.

4.166   Buhagiar, D., J. C. Chapman, and P. J. Dowling: "Design of C-Sections Against Deformational Lip Buckling," *Proceedings of the 11th International Specialty Conference on Cold-Formed Steel Structures,* University of Missouri-Rolla, Oct. 1992.

4.167   Davies, J. M., and C. Jiang: "Design of Thin-Walled Beams for Distortional Buckling," *Proceedings of the 13th International Specialty Conference on Cold-Formed Steel Structures,* University of Missouri-Rolla, Oct. 1996.

4.168   Davies, J. M., C. Jiang, and V. Ungureanu: "Buckling Mode Interaction in Cold-Formed Steel Columns and Beams," *Proceedings of the 14th International Specialty Conference on Cold-Formed Steel Structures,* University of Missouri-Rolla, Oct. 1998.

4.169   Ellifritt, D. S., R. L. Glover, and J. D. Hern: "A Simplified Model for Distortional Buckling of Channels and Zees in Flexure," *Proceedings of the 14th International Specialty Conference on Cold-formed Steel Structures,* University of Missouri-Rolla, Oct. 1998.

4.170   Fisher, J. M.: "Uplift Capacity of Simple Span Cee and Zee Members with Through-Fastened Roof Panels," Final Report MBMA 95-01, Metal Building Manufacturers Association, 1996.

4.171   Shoemaker, W. L.: "Standing Seam Metal Roofs, The State of the Art in Engineering Roofs," *CCFSS Technical Bulletin,* vol. 14, no. 1, Feb. 1995.

4.172   American Iron and Steel Institute: "A Guide for Designing with Standing Seam Roof Panels," Design Guide CF97-1, Aug. 1997.

4.173   Almoney, K., and T. M. Murray: "Shear Plus Bending in Lapped Z-Purlins," *Proceedings of the 14th International Specialty Conference on Cold-Formed steel Structures,* University of Missouri-Rolla, Oct. 1998.

4.174   Bhaka, B. H., R. A. LaBoube, and W. W. Yu: "The Effect of Flange Restraint on Web Crippling Strength," Final Report, Civil Engineering 92-1, University of Missouri-Rolla, March 1992.

4.175   Cain, D. E., R. A. LaBoube, and W. W. Yu: "The Effect of Flange Restraint on Web Crippling Strength of Cold-Formed Z- and I-Sections," Final Report, Civil Engineering Study 95-2, University of Missouri-Rolla, May 1995.

4.176   LaBoube, R. A, J. N. Nunnery, and R. E. Hodges: "Web Crippling Behavior of Nested Z-Purlins," *Engineering Structures,* (G. J. Hancock, Guest Ed.), vol. 16, no. 5, Butterworth-Heinemann Ltd., London, July 1994.

4.177   Prabakaran, K., and R. M. Schuster: "Web Crippling Behavior of Cold-Formed Steel Members," *Proceedings of the 14th International Specialty Conference on Cold-Formed Steel Structures,* University of Missouri-Rolla, Oct. 1998.

4.178   Gerges, R. R., and R. M. Schuster: "Web Crippling of Single Web Cold-Formed Steel Members Subjected to End-One-Flange Loading," *Proceedings of the 14th International Specialty Conference on Cold-Formed Steel Structures,* University of Missouri-Rolla, Oct. 1998.

4.179   Zhao, X. L., and G. J. Hancock: "Square and Rectangular Hollow Sections under Transverse End-Bearing Force," *Journal of Structural Engineering,* ASCE, vol. 121, no. 9, Sept. 1995.

4.180   Hofmeyer, H., J. G. M. Kerstens, H. H. Snijder, and M. C. M. Bakker: "Experimental Research on the Behavior of Combined Web Crippling and Bending of Steel Deck Sections," *Proceedings of the 13th International Specialty Conference on Cold-Formed Steel Structures,* Oct. 1996.

4.181   Roberts, T. M., and A. C. B. Neware: "Strength of Webs Subjected to Compressive Edge Loading," *Journal of Structural Engineering,* ASCE, vol. 123, no. 2, Feb 1997.

4.182   Young, B., and G. J. Hancock: "Web Crippling Behavior of Cold-Formed Unlipped Channels," *Proceedings of the 14th International Specialty Conference on Cold-Formed Steel Structures,* University of Missouri-Rolla, Oct. 1998.

4.183   Wu, S., W. W. Yu, and R. A. LaBoube: "Web Crippling of Members Using High Strength Steels," *Proceedings of the 14th International Specialty Conference on Cold-Formed Steel Structures,* University of Missouri-Rolla, Oct. 1998.

4.184   Rhodes, J., and D. Nash: "An Investigation of Web Crushing Behavior in Thin-Walled Beams," *Thin-Walled Structures,* vol. 32, 1998.

4.185   American Iron and Steel Institute: "Design Guide for Cold-Formed Steel Beams with Web Penetration," Publication RG-9712, Aug. 1997.

4.186   Ellifritt, D. S., T. Sputo, and J. Haynes: "Flexural Capacity of Discretely Braced C's and Z's," *Proceedings of the 11th International Specialty Conference on Cold-Formed Steel Structures,* University of Missouri-Rolla, Oct. 1992.

4.187   Kavanagh, K. T., and D. S. Ellifritt: "Bracing of Cold-Formed Channels Not Attached to Deck or Sheating," *Is Your Structure Suitably Braced?* Structural Stability Research Council, April 1993.

4.188   Kavanagh, K. T., and D. S. Ellifritt: "Design Strength of Cold-Formed Channels in Bending and Torsion," *Journal of Structural Engineering,* ASCE, vol. 120, no. 5, May 1994.

4.189   Put, B. M, Y. L. Pi, and N. S. Trahair: "Bending and Torsion of Cold-Formed Channel Beams," *Journal of Structural Engineering,* ASCE, vol. 125, no. 5, May 1999.

4.190   Put, B. M, Y. L. Pi, and N. S. Trahair: "Lateral Buckling Tests on Cold-Formed Channel Beams," *Journal of Structural Engineering,* ASCE, vol. 125, no. 5, May 1999.

4.191   Yura, J. A.: "Fundamentals of Beam Bracing," *Is Your Structure Suitably Braced?* Structural Stability Research Council, April 1993.

4.192   Wu, S., W. W. Yu, and R. A. LaBoube: "Strength of Flexural Members Using Structural Grade 80 of A653 Steel (Web Crippling Tests)," Third Progress Report, Civil Engineering Study 97-3, University of Missouri-Rolla, February 1997.

4.193   American Society for Testing and Materials: "Standard Test Method for Structural Performance of Sheet Metal Roof and Siding Systems by Uniform Static Air Pressure Difference," ASTM designation E1592-95.

CHAPTER 5

5.1   Chajes, A., and G. Winter: "Torsional-Flexural Buckling of Thin-Walled Members," *Journal of the Structural Division, ASCE Proceedings,* vol. 91, Aug. 1965.

5.2   Chajes, A., P. J. Fang, and G. Winter: "Torsional-Flexural Buckling, Elastic and Inelastic, of Cold-Formed Thin-Walled Columns," engineering research bulletin 66-1, Cornell University, Aug. 1966.

5.3   Hegedus, L.: "Experiments on Cold-Formed Rack Columns," *Proceedings of the 2nd Regional Colloquium on Stability of Steel Structures,* Sept. 25–26, 1986, Hungary, Final reprint.

5.4   Fleseriu, E., and D. Dubina: "Experimental Investigations Concerning the Thin-Walled Cold-Formed Bars, Subjected to Centric and Eccentric Compression," *Proceedings of the 2nd Regional Colloquium on Stability of Steel Structures,* Sept. 25–26, 1986, Hungary, vol. II/2.

5.5   Szabo, G.: "Tests For Column Buckling of High Strength Steel Members," *Proceedings of the 2nd Regional Colloquium on Stability of Steel Structures,* Sept. 25–26, 1986, Hungary.

5.6   Chiew, S. P., S. L. Lee, and N. E. Shanmugam: "Experimental Study of Thin-Walled Steel Box Columns," *Journal of Structural Engineering,* vol. 113, no. 10, Oct. 1987.

5.7   Weng, C. C., and T. Pekoz: "Compression Tests of Cold-Formed Steel Columns," *Proceedings of the 9th International Specialty Conference on Cold-Formed Steel Structures,* University of Missouri-Rolla, Nov. 8–9, 1988.

5.8   Weng, C. C., and T. Pekoz: "Compression Tests of Cold-Formed Steel Columns," *Journal of Structural Engineering,* ASCE, vol. 116, May 1990.

5.9   Shanley, F. R.: "Inelastic Column Theory," *Journal of Aeronautical Science,* vol. 14, May 1947.

5.10 Goodier, J. N.: "The Buckling of Compressed Bars by Torsion and Flexure," Cornell University Experiment Station, Dec. 1941.

5.11 Timoshenko, S. P.: "Theory of Bending, Torsion and Buckling of Thin-Walled Members of Open Cross Section," *Journal of the Franklin Institute,* Apr. and May 1945.

5.12 Madugula, M. K. S., T. S. Prabhu, and M. C. Temple: "Ultimate Strength of Concentrically Loaded Cold-Formed Angles," *Proceedings of the Annual Technical Session of the Structural Stability Research Council,* 1982.

5.13 Madugula, M. K., T. S. Prabhu, and M. C. Temple: "Ultimate Strength of Concentrically Loaded Cold-Formed Angles," *Canadian Journal of Civil Engineering 10.606,* 1983.

5.14 Wilhoit, G., R. Zandonini, and A. Zavellani: "Behavior and Strength of Angles in Compression: An Experimental Investigation," ASCE Annual Convention and Structural Congress, 1984.

5.15 Kennedy, J. B., and Madugula K. S. Murty: "Buckling of Steel Angle and Tee Struts," *Journal of the Structural Division, ASCE Proceedings,* vol. 98, Nov. 1972.

5.16 Kennedy, J. B., and Madugula K. S. Murty: "Buckling of Angles: State of the Art," *Journal of the Structural Division, ASCE Proceedings,* vol. 108, Sept. 1982.

5.17 Smith, E. A.: "Buckling of Four Equal-Leg Angle Cruciform Columns," *Journal of the Structural Division, ASCE Proceedings,* vol. 109, Feb. 1983.

5.18 Chuenmei, G.: "Elastoplastic Buckling of Single Angle Columns," *Journal of Structural Engineering,* vol. 110, no. 6, June 1984.

5.19 Shan, L., and A. H. Peyrot: "Plate Element Modeling of Steel Angle Members," *Journal of Structural Engineering,* vol. 114, no. 4, Apr. 1988.

5.20 Bijlaard, P. P., and G. P. Fisher: "Interaction of Column and Local Buckling in Compression Members," NACA technical note, 2640, Mar. 1952.

5.21 Pflüger, A. von: "Thin-Walled Compression Members, Parts I, II, III," publications of Technische Hochschule, Hanover, Jan. 1959 and Mar. 1961.

5.22 Bulson, P. S.: "Local Stability and Strength of Structural Sections," *Thin-Walled Structures* (A. H. Chilver, Ed.), John Wiley and Sons, New York, 1967.

5.23   Graves Smith, T. R.: "The Ultimate Strength of Locally Buckled Columns of Arbitrary Length," paper at SSIDA Symposium on Thin-Walled Steel Structures, University College of Swansea, Sept. 1967.

5.24   Graves Smith, T. R.: "The Ultimate Strength of Locally Buckled Columns of Various Slenderness Ratios," research report 12 (Pt. 2), May 1968.

5.25   Ghobarah, A. A., and W. K. Tso: "Overall and Local Buckling of Channel Columns," *Journal of Engineering Mechanics Division, ACSE Proceedings,* vol. 95, Apr. 1969.

5.26   DeWolf, J. T., T. Pekoz, and G. Winter: "Local and Overall Buckling of Cold-Formed Members," *Journal of the Structural Division, ASCE Proceedings,* vol. 100, Oct. 1974.

5.27   DeWolf, J. T.: "Local Buckling in Channel Columns," *Proceedings of the 3rd International Specialty Conference on Cold-Formed Steel Structures,* University of Missouri-Rolla, Nov. 1975.

5.28   Pekoz, T.: "Design Procedure for Unstiffened Compression Elements and the Interaction of Local and Overall Buckling," lecture notes, AISI-UMR Short Course on Cold-Formed Steel Structures, July 1979.

5.29   Wang, S. T., and Y. L. Tien: "Post-Local-Buckling Behavior of Thin-Walled Columns," *Proceedings of the 2nd Conference on Cold-Formed Steel Structures,* University of Missouri-Rolla, Oct. 1973.

5.30   Wang, S. T., and G. E. Blandford: "Stability Analysis of Locally Buckled Frames," *Proceedings of the 4th International Specialty Conference on Cold-Formed Steel Structures,* University of Missouri-Rolla, June 1978.

5.31   Wang, S. T., and H. Y. Pao: "Stability Analysis of Locally Buckled Singly Symmetric Columns," *Thin-Walled Structures* (J. Rhodes and A. C. Walker, Eds.), Granada Publishing, Apr. 3–6, 1979.

5.32   Wang, S. T., H. Y. Pao, and R. Ekambaram: "Lateral Bracing of Locally Buckled Columns," *Proceedings of the 5th International Specialty Conference on Cold-Formed Steel Structures,* University of Missouri-Rolla, Nov. 1980.

5.33   Blandford, G. E., S. T. Wang, and N. T. Wang: "Dynamic Behavior of Locally Buckled Frames," *Proceedings of the 6th International Specialty Conference on Cold-Formed Steel Structures,* University of Missouri-Rolla, Nov. 1982.

5.34   Rhodes, J., and J. M. Harvey: "Interaction Behavior of Plain Channel Columns under Concentric or Eccentric Loading," preliminary report, *Stability of Steel Structures,* Liege, Apr. 1977.

5.35   Loughlan, J., and J. Rhodes: "Interaction Buckling of Lipped Channel Columns," *Conference on Stability of Steel Structures and Components,* Cardiff, UK, Sept. 1978.

5.36   Rhodes, J., and J. Loughlan: "Simple Design Analysis of Lipped Channel Columns," *Proceedings of the 5th International Specialty Conference on Cold-Formed Steel Structures,* University of Missouri-Rolla, Nov. 1980.

5.37   Rhodes, J.: "Some Thoughts on Future Cold-Formed Steel Design Rules," *Behaviour of Thin Walled Structures,* University of Strathclyde, Mar. 1983.

5.38   Loughlan, J., and A. R. Upadhya: "Locally Imperfect Plain Channel Columns," *Behaviour of Thin Walled Structures,* University of Strathclyde, Mar. 1983.

5.39 Maquoi, R., and C. Massonnet: "Interaction between Local Plate Buckling and Overall Buckling in Thin-Walled Compression Members-Theories and Experiments," *Buckling of Structures* (B. Budiansky, Ed.), Springer-Verlag, Berlin, 1976.

5.40 Hancock, G. J.: "Interaction Buckling in I-Section Columns," *Journal of the Structural Division, ASCE Proceedings,* vol. 107, Jan. 1981.

5.41 Baigent, A. H., and G. J. Hancock: "Structural Analysis of Assemblages of Thin-Walled Members," research report R-389, University of Sydney, Australia, June 1981.

5.42 Baigent, A. H., and G. J. Hancock: "The Strength of Cold-Formed Portal Frames," *Proceedings of the 6th International Specialty Conference on Cold-Formed Steel Structures,* University of Missouri-Rolla, Nov. 1982.

5.43 Sridharan, S., and T. V. Galambos: "Finite Strip Analysis of Postbuckling Behavior of Plate Structures—Some Recent Results," *Proceedings of the Annual Technical Session of the Structural Stability Research Council,* 1981.

5.44 Sridharan, S., and T. R. Graves-Smith: "Postbuckling Analysis with Finite Strips," *Journal of the Engineering Mechanics Division, ASCE Proceedings,* vol. 107, Oct. 1981.

5.45 Sridharan, S.: "A Finite Strip Analysis of Locally Buckled Plate Structures Subject to Nonuniform Compression," *Engineering Structures,* vol. 4, Oct. 1982.

5.46 Sridharan, S.: "A Semi-Analytical Method for the Post-Local-Torsional Buckling Analysis of Prismatic Plate Structures," *International Journal for Numerical Methods in Engineering,* vol. 18, 1982.

5.47 Sridharan, S., and R. Benito: "Interactive Buckling in Thin-Walled Columns," *Proceedings of the 6th International Specialty Conference on Cold-Formed Steel Structures,* University of Missouri-Rolla, Nov. 1982.

5.48 Usami, T., and Y. Fukumoto: "Local and Overall Buckling of Welded Box Columns," *Journal of the Structural Division, ASCE Proceedings,* vol. 108, Mar. 1982.

5.49 Mulligan, G. P., and T. Peköz: "The Influence of Local Buckling on the Structural Behavior of Singly-Symmetric Cold-Formed Steel Columns," report 83-1, Department of Structural Engineering, Cornell University, Mar. 1983.

5.50 Dawe, J. L., and G. L. Kulak: "Local Buckling of W Shape Columns and Beams," *Journal of Structural Engineering,* vol. 110, no. 6, June 1984.

5.51 Mulligan, G. P., and T. Pekoz: "Locally Buckled Thin-Walled Columns," *Journal of Structural Engineering,* vol. 110, no. 11, Nov. 1984.

5.52 Queen, D. J., and N. C. Lind: "Interactive Buckling of Thin-Walled Compression Members," *Proceedings of the SSRC Annual Technical Session,* 1985.

5.53 Gradzki, R., and K. Kowal-Michalska: "Elastic and Elasto-Plastic Buckling of Thin-Walled Columns Subjected to Uniform Compression," *International Journal on Thin-Walled Structures,* vol. 3, no. 2, 1985.

5.54 Pignataro, M., A. Luongo, and N. Rizz: "On the Effect of the Local Overall Interaction on the Postbuckling of Uniformly Compressed Channels," *International Journal on Thin-Walled Structures,* vol. 3, no. 4, 1985.

5.55   Blandford, G. E., and G. C. Glass: "Earthquake Response of Locally Buckled Frames," *Proceedings of the 8th International Specialty Conference on Cold-Formed Steel Structures,* University of Missouri-Rolla, Nov. 11–12, 1986.

5.56   Loughlan, J., and M. Nabavian: "The Behaviour of Thin-Walled I-Section Columns after Local Buckling," *Proceedings of the 8th International Specialty Conference on Cold-Formed Steel Structures,* University of Missouri-Rolla, Nov. 11–12, 1986.

5.57   Mulligan, G. P., and T. Pekoz: "Local Buckling Interaction in Cold-Formed Columns," *Journal of Structural Engineering,* vol. 113, no. 3, Mar. 1987.

5.58   Pignataro, M., and A. Luongo: "Asymmetric Interactive Buckling of Thin-Walled Columns with Initial Imperfections," *Thin-Walled Structures,* vol. 5, no. 5, 1987.

5.59   Kolakowski, Z.: "Mode Interaction in Thin-Walled Trapezoidal Column under Uniform Compression," *International Journal of Thin-Walled Structures,* vol. 5, no. 5, 1987.

5.60   Yamao, T., and T. Sakimoto: "Local and Overall Buckling of Thin-Walled H-Section Columns," *Proceedings of the SSRC Annual Technical Session,* 1988.

5.61   Kolakowski, Z.: "Some Thoughts on Mode Interactions in Thin-Walled Columns under Uniform Compression," *Thin-Walled Structures,* vol. 7, no. 1, 1989.

5.62   Liew, J. Y. R., N. E. Shanmugam, and S. L. Lee: "Local Buckling of Thin-Walled Steel Box Columns," *Thin-Walled Structures,* vol. 8, no. 2, 1989.

5.63   Gioncu, V.: "Coupled Instabilities in Bar Structures-Phenomenon, Theory, Practice," *Proceedings of the SSRC 4th International Colloquium,* 1989.

5.64   Osgood, W. R.: "The Effect of Residual Stresses on Column Strength," *Proceedings, 1st U.S. National Congress of Applied Mechanics,* New York, June 1951.

5.65   Peterson, R. E., and A. O. Bergholm: "Effect of Forming and Welding on Stainless Steel Columns," *Aerospace Engineering,* Institute of Aerospace Sciences, New York, vol. 20, Apr. 1961.

5.66   Pekoz, T. B., and G. Winter: "Torsional-Flexural Buckling of Thin-Walled Sections under Eccentric Load," *Journal of the Structural Division, ASCE Proceedings,* vol. 95, May 1969.

5.67   American Institute of Steel Construction: *Allowable Stress Design Manual of Steel Construction,* 9th ed., 1989.

5.68   Green, G. G., G. Winter, and T. R. Cuykendall: "Light Gage Steel Columns in Wall-Braced Panels," bulletin 35/2, *Engineering Experiment Station,* Cornell University, 1947.

5.69   Dabrowski, R.: "On Stability of Thin-Walled Columns with Cruciform Cross Section," *Proceedings of the 2nd Regional Colloquium on Stability of Steel Structures,* Sept. 25–26, 1986, Hungary, vol. II/2.

5.70   Szymczak, C.: "On the Buckling and Post-Buckling Behaviour of Thin-Walled Columns with Bisymmetric Open Cross-Section," *Proceedings of the 2nd Regional Colloquium on Stability of Steel Structures,* Sept. 25–26, 1986, Hungary, vol. II/2.

5.71   Sridharan, S.: "On The Behaviour and Design of Thin-Walled Columns Having Doubly Symmetric Sections," *Proceedings of the 8th International Specialty Conference on Cold-Formed Steel Structures,* University of Missouri-Rolla, Nov. 11–12, 1986.

5.72   Murtha-Smith, E., and H. R. Adibjabromi: "Restrained Warping in Cruciform Compression Members," *Journal of Structural Engineering,* vol. 114, no. 1, Jan. 1988.

5.73   Usami, T., and Y. Fukumoto: "Welded Box Compression Members," *Journal of Structural Engineering,* vol. 110, no. Oct. 1984.

5.74   Key, P. W., S. W. Hasan, and G. J. Hancock: "Column Behaviour of Cold-Formed Hollow Sections," *Proceedings of the 8th International Specialty Conference on Cold-Formed Steel Structures,* University of Missouri-Rolla, Nov. 11–12, 1986.

5.75   Key, P. W., S. W. Hansan, G. J. Hancock: "Column Behaviour of Cold-Formed Hollow Section," *Journal of Structural Engineering,* vol. 114, no. 2, Feb. 1988.

5.76   Lee, S. L., N. E. Shanmugam, and S. P. Chiew: "Thin-Walled Box Columns under Arbitrary End Loads," *Journal of Structural Engineering,* vol. 114, no. 6, June 1988.

5.77   Shanmugam, N. E., J. Y. R. Liew, and S. L. Lee: "Design Formulas for Biaxially Loaded Thin-Walled Steel Box Columns," *Proceedings of the 10th International Specialty Conference on Cold-Formed Steel Structures,* University of Missouri-Rolla, Oct. 1990.

5.78   Loughlan, J.: "The Ultimate Load Sensitivity of Lipped Channel Columns to Column Axis Imperfection," *International Journal on Thin-Walled Structures,* vol. 1, no. 1, 1983.

5.79   Batista, E., J. Rondal, and R. Maquoi: "Column Stability of Cold-Formed U and C Sections," *Steel Structures* (R. Narayanan, Ed.), Elsevier Applied Science, London, 1987.

5.80   Polyzois, D., and A. Sudharmapal: "Cold-Formed Steel Z-Sections under Axial Load," *Proceedings of the 9th International Specialty Conference on Cold-Formed Steel Structures,* University of Missouri-Rolla, Nov. 8–9, 1988.

5.81   Purnadi, R. W., J. L. Tassoulas, and D. Polyzois: "A Study of Cold-Formed Z-Section Steel Members under Axial Loading," *Proceedings of the 10th International Specialty Conference on Cold-Formed Steel Structures,* University of Missouri-Rolla, Oct. 1990.

5.82   Tillman, S. C., and A. F. Williams: "Buckling under Compression of Simple and Multicell Plate Columns," *Thin-Walled Structures,* vol. 8, no. 2, 1989.

5.83   Midgley, W. R.: "Torsional Effective Length Factors, Perforated Posts," *Proceedings of the SSRC Annual Technical Session,* 1985.

5.84   Wang, S. J.: "Torsional-Flexural Buckling of Open Thin-Walled Columns with Battens," *International Journal on Thin-Walled Structures,* vol. 3, no. 4, 1985.

5.85   Hancock, G. J.: "Distortional Buckling of Steel Storage Rack Columns," *Journal of Structural Engineering,* vol. 111, no. 12, Dec. 1985.

5.86   Wang, S. J.: "Torsional-Flexural Buckling of Partially Closed Thin-Walled Columns," *Proceedings of IABSE Colloquium,* Stockholm, 1986.

5.87   Takahashi, K., and M. Mizuno: "Distortion of Thin-Walled Open Cross Section Members," *Proceedings of IABSE Colloquium,* Stockholm, 1986.

5.88   Rutenberg, A., M. Shtarkman, and M. Eisenberger: "Torsional Analysis Methods for Perforated Cores," *Journal of Structural Engineering,* vol. 112, no. 6, June 1986.

5.89   Hancock, G. J., and O. Roos: "Flexural-Torsional Buckling of Storage Rack Columns," *Proceedings of the 8th International Specialty Conference on Cold-Formed Steel Structures,* University of Missouri-Rolla, Nov. 11–12, 1986.

5.90   Toader, I. H. I.: "A More Accurate Evaluation of Buckling Loads of Thin-Walled Members in Torsion and Torsion-Bending," *International Journal on Thin-Walled Structures,* vol. 5, no. 3, 1987.

5.91   Lau, S. C. W., and G. J. Hancock: "Distortional Buckling Formulas for Channel Columns," *Journal of Structural Engineering,* vol. 113, no. 5, May 1987.

5.92   Kanok-Nukulchai, W., and M. Sivakumar: "Degenerate Elements for Combined Flexural and Torsional Analysis of Thin-Walled Structures," *Journal of Structural Engineering,* vol. 114, no. 3, Mar. 1988.

5.93   Sridharan, S., and M. Ashraf Ali: "On the Design of Thin-Walled Columns with Doubly Symmetric Sections," *Proceedings of the SSRC Annual Technical Session,* 1986.

5.94   Kirk, P.: "Design of Cold-Formed Section Portal Frame Building System," *Proceedings of the 8th International Specialty Conference on Cold-Formed Steel Structures,* University of Missouri-Rolla, Nov. 11–12, 1986.

5.95   Chen, W. F., and S. Zhou: "C_m Factor in Load and Resistance Factor Design," *Journal of Structural Engineering,* vol. 113, no. 8, Aug. 1987.

5.96   Pekoz, T.: "Design of Cold-Formed Steel Columns," *Der Metallbau im Konstruktiven-Ingenieurbau,* Karlsruhe, West Germany, Feb. 1988.

5.97   Pekoz, T.: "Design of Cold-Formed Steel Columns," *Proceedings of the 9th International Specialty Conference on Cold-Formed Steel Structures,* University of Missouri-Rolla, Nov. 8–9, 1988.

5.98   Rhodes, J., and P. W. Khong: "A Simple Semi-Analytical, Semi-Numerical Approach to Thin-Walled Structures Stability Problems," *Proceedings of the 10th International Specialty Conference on Cold-Formed Steel Structures,* University of Missouri-Rolla, Oct. 1990.

5.99   Hatch, G. L., W. S. Easterling, and T. M. Murray: "Strength Evaluation of Strut-Purlins," *Proceedings of the 10th International Specialty Conference on Cold-Formed Steel Structures,* University of Missouri-Rolla, Oct. 1990.

5.100   Popvic, D., G. J. Hancock, and K. J. R. Rasmussen: "Axial Compression Tests of Cold-Formed Angles," *Journal of Structural Engineering,* ASCE, vol. 125, No. 5, May 1999.

5.101   Rasmussen, K. J. R., and G. J. Hancock: "Nonlinear Analyses of Thin-Walled Channel Section Columns," *Thin-Walled Structures,* vol. 13, nos. 1–2, Elsevier Applied Science, Tarrytown, N.Y., 1992.

5.102   Rasmussen, K. J. R., "Design of Thin-Walled Column with Unstiffened Flanges," *Engineering Structures,* vol. 16, no. 5, Butterworth-Heinemann, London, July 1994.

5.103 Pekoz, T. B., and O. Sumer: "Design Provisions for Cold-Formed Steel Columns and Beam-Columns," Final Report, submitted to American Iron and Steel Institute, Sept. 1992.

5.104 Glaser, N. J., R. C. Kaehler, and J. M. Fisher: "Axial Load Capacity of Sheeted C and Z Members," *Proceedings of the 12th International Specialty Conference on Cold-Formed Steel Structures,* University of Missouri-Rolla, Oct. 1994.

5.105 Hatch, J., W. S. Easterling, and J. M. Murray: "Strength Evaluation of Strut-Purlins," *Proceedings of the 10th International Specialty Conference on Cold-Formed Steel Structures,* University of Missouri-Rolla, Oct. 1990.

5.106 Simaan, A.: "Buckling of Diaphragm-Braced Columns of Unsymmetrical Sections and Applications to Wall Studs Design," Report No. 353, Cornell University, Ithaca, N.Y. 1973.

5.107 Harper, M. M., R. A. LaBoube, and W. W. Yu: "Behavior of Cold-Formed Steel Roof Trusses," Summary Report, Civil Engineering Study 95-1, University of Missouri-Rolla, May 1995.

5.108 Hancock, G. J.,: "Distortional Buckling of Steel Storage Rack Columns," *Journal of Structural Engineering,* ASCE, vol. 111, no. 12, Dec. 1985.

5.109 Lau, S. C. W., and G. J. Hancock: "Distortional Buckling Formulas for Channel Columns," *Journal of Structural Engineering,* ASCE, vol. 113, no. 5, May 1987.

5.110 Lau, S. C. W., and G. J. Hancock, "Tests of Cold-Formed Channel Sections," *Proceedings of the 9th International Specialty Conference on Cold-Formed Steel Structures,* University of Missouri-Rolla, Nov. 1988.

5.111 Lau, S. C. W., and G. J. Hancock: "Inelastic Buckling of Channel Columns in the Distortional Mode," *Thin-Walled Structures,* vol. 10, no. 1, 1990.

5.112 Charnvarnichborikarn, P., and D. Polyzois: "Distortional Buckling of Cold-Formed Steel Z-Section Columns," *Proceedings of the 11th International Specialty Conference on Cold-Formed Steel Structures,* University of Missouri-Rolla, Oct. 1992

5.113 Kwon, Y. B., and G. J. Hancock: "Design of Channels Against Distortional Buckling," *Proceedings of the 11th International Specialty Conference on Cold-Formed Steel Structures,* University of Missouri-Rolla, Oct. 1992.

5.114 Kwon, Y. B., and G. J. Hancock: "Tests of Cold-Formed Channels with Local and Distortional Buckling," *Journal of Structural Engineering,* ASCE, vol. 118, no. 7, July 1992.

5.115 Hancock, G. J., Y. B. Kwon, and E. S. Bernard: "Strength Design Curves for Thin-Walled Sections Undergoing Distortional Buckling," *Journal of Construction Steel Research,* vol. 31, nos. 2/3, 1994.

5.116 Weng, C. C.: "Effect of Residual Stress on Cold-Formed Steel Column Strength," *Journal of Structural Engineering, ASCE,* vol. 117, no. 6, June 1991.

5.117 Guo, Y. L. and S. F. Chen, "Elasto-Plastic Interaction Buckling of Cold-Formed Channel Columns," *Journal of Structural Engineering,* ASCE, vol. 117, no. 8, Aug. 1991.

5.118 Shen, Z., and Q. Zhang: "Interaction of Local and Overall Instability of Compressed Box Columns," *Journal of Structural Engineering,* ASCE, vol. 117, no. 11, Nov. 1991.

5.119   Rasmussen, K. J. R., and G. J. Hancock: "Nonlinear Analysis of Thin-Walled Channel Section Columns," *Thin-Walled Structures,* vol. 13, 1991.

5.120   Weng, C. C., and C. P. Lin: "Study on Maximum Strength of Cold-Formed Steel Columns, *Journal of Structural Engineering,* ASCE, vol. 118, No. 1, Jan. 1992.

5.121   Migita, Y., T. Aoki, and Y. Fukumoto: "Load and Interaction Buckling of Polygonal Section Steel Columns," *Journal of Structural Engineering,* ASCE, vol. 118, no. 10, Oct. 1992.

5.122   Polyzois, D., and P. Charnvarnichborikarn: "Web-Flange Interaction in Cold-Formed Steel Z-Section Columns," *Journal of Structural Engineering,* ASCE, vol. 119, no. 9, Sept. 1993.

5.123   Rasmussen, K. J. R., and G. J. Hancock: "The Flexural Behaviour of Fixed-Ended Channel Section Columns," *Thin-Walled Structures,* vol. 17, 1993.

5.124   Balut, N.: "A Practical Approach to the Spatial Buckling of Monosymmetrical Compression Members," *Thin-Walled Structures,* vol. 20, 1994.

5.125   Rasmussen, K. J. R., and G. J. Hancock: "Design of Thin-Walled Plain Channel Section Columns Against Flexural Bucking," *Thin-Walled Structures,* vol. 20, 1994.

5.126   Moldovan, A.: "Compression Tests on Cold-Formed Steel Columns with Monosymmetrical Section," *Thin-Walled Structures,* vol. 20, 1994.

5.127   Lindner, J., and Y. L. Guo: "Buckling Behavior of Cold-Formed Thin-Walled Member by Spline Finite Strip Analysis," *Proceedings of the 12th International Specialty Conference on Cold-Formed Steel Structures,* University of Missouri-Rolla, Oct. 1994.

5.128   Odaisky, D., D. Polyzois, and G. Morris: "Cold-Formed Steel Sections for Transmission Towers," *Proceedings of the 12th International Specialty Conference on Cold-formed Steel Structures,* University of Missouri-Rolla, Oct. 1994.

5.130   Davies, J. M., and C. Jaing: "Non-Linear Buckling Analysis of Thin-Walled Metal Columns," *Proceedings of the 13th International Specialty Conference on Cold-formed Steel Structures,* University of Missouri-Rolla, Oct. 1996.

5.131   Marsh, C.: "Design of Single and Multiple Angle Columns and Beams," *Journal of Structural Engineering,* ASCE, vol. 123, no. 7, July 1997.

5.132   Young, B., and K. J. R. Rasmussen: "Bifurcation of Single Symmetric Columns," *Thin-Walled Structures,* vol. 28, no. 2, 1997.

5.133   Young, B., and K. J. R. Rasmussen: "Tests of Fixed-Ended Plain Channel Columns," *Journal of Structural Engineering,* ASCE, vol. 124, no. 2, Feb. 1998.

5.134   Young, B., and K. J. R. Rasmussen: "Design of Lipped Channel Columns," *Journal of Structural Engineering,* ASCE, vol. 124, no. 2, Feb. 1998.

5.135   Rhodes, J.: "Columns Under Loads of Varying Eccentricity," *Proceedings of the 14th International Conference on Cold-Formed Steel Structures,* University of Missouri-Rolla, Oct. 1998.

5.136   Young, B., and K. J. R. Rasmussen: "Behaviour of Locally Buckling Singly Symmetric Columns," *Proceedings of the 14th International Specialty Conference on Cold-Formed Steel Structures,* University of Missouri-Rolla, Oct. 1998.

5.137 Young, B, and K. J. R. Rasmussen: "Shift of the Effective Centroid of Channel Columns," *Proceedings of the 14th International Specialty Conference on Cold-Formed Steel Structures,* University of Missouri-Rolla, Oct. 1998.

5.138 Riemann, J. A.: "The Behavior of Compression Web Members in Cold-Formed Steel Truss Assemblies," M.S. Thesis, University of Missouri-Rolla, 1996.

5.139 Ibrahim, T. M., R. A. LaBoube, and W. W. Yu: "Behavior of Compression Web Members of Cold-Formed Steel Roof Trusses," *Proceedings of the International Conference on Experimental Model Research and Testing of Thin-Walled Structures,* Academy of Science of the Czech Republic, Prague, Sept. 1997.

5.140 Ibrahim, T. M., R. A. LaBoube, and W. W. Yu: "Behavior of Cold-Formed Steel Roof Trusses Subjected to Concentrated Loads," *Journal of Constructional Steel Research,* Elsevier Science Ltd., vol. 46, nos. 1–3.

CHAPTER 6

6.1 Pekoz, T. B., and N. Celebi: "Torsional-Flexural Buckling of Thin-Walled Sections under Eccentric Load," engineering research bulletin 69-1, Cornell University, 1969.

6.2 Rhodes, J., and J. M. Harvey: "The Local Instability of Thin-Walled Sections under Combined Compression and Bending," *Proceedings of the 3rd International Specialty Conference on Cold-Formed Steel Structures,* University of Missouri-Rolla, Nov. 1975.

6.3 Rhodes, J., and J. M. Harvey: "Plain Channel Section Struts in Compression and Bending beyond the Local Buckling Load," *International Journal, Mechanics Science,* Pergamon Press, vol. 8, 1976.

6.4 Loughlan, J., and J. Rhodes: "The Interactive Buckling of Lipped Channel Columns under Concentric or Eccentric Loading," *Thin-Walled Structures* (J. Rhodes and A. C. Walker, Eds.), Granada Publishing, New York, Apr. 3–6, 1979.

6.5 Loughlan, J.: "The Ultimate Load Sensitivity of Lipped Channel Columns to Column Axis Imperfection: *Thin-Walled Structures, An International Journal,* Applied Science Publishers, England, vol. 1, no. 1, Mar. 1983.

6.6 American Institute of Steel Construction: "Commentary on the Specification for the Design, Fabrication and Erection of Structural Steel for Buildings," adopted Feb. 12, 1969.

6.7 Rack Manufacturers Institute: "Commentary and Supplementary Information-Specification for the Design, Testing and Utilization of Industrial Steel Storage Racks," 1979 ed.

6.8 Haaijer, G., P. S. Carskaddan, and M. A. Grubb: "Eccentric Load Test of Angle Column Simulated with MSC/NASTRAN Finite-Element Program," *Proceedings of the Structural Stability Research Council,* 1981.

6.9 Sridharan, S., and M. Ashraf Ali: "Interactive Buckling in Thin-Walled Beam-Columns," *Proceedings of the SSRC Annual Technical Session,* 1985.

6.10   Wang, S. J.: "Lateral Torsional Buckling of Thin-Walled Beam-Columns Having Unequal End Moments," *Proceedings of the SSRC Annual Technical Session,* 1986.

6.11   Pekoz, T.: "Combined Axial Load and Bending in Cold-Formed Steel Members," *Proceedings of the IABSE Colloquium,* Stockholm, 1986.

6.12   Goczek, J., and M. Lukowiak: "Limit State of a Thin-Walled Rectangular Hollow Beam-Column," *Proceedings of the IABSE Colloquium,* Stockholm, 1986.

6.13   Dubina, D.: "On the Stability of Thin-Walled Members Subjected to Centric Compression and Bending Compression—'Stabas' Computer Program," *Proceedings of the 2nd Regional Colloquium on Stability of Steel Structures,* Sept. 25–26, 1986, Hungary, vol. II/2.

6.14   Rondal, J., and R. Maquoi: "Optimal Ranges of Beam-Columns with Square or Rectangular Hollow Sections" *Proceedings of the 2nd Regional Colloquium on Stability of Steel Structures,* Sept. 25–26, 1986, Hungary, vol. II/2.

6.15   Weiss, S., and J. Sliwinska: "Evaluation of Post-Buckling Capacity of Box Columns Compressed on a Biaxial Eccentricity," *Proceedings of the 2nd Regional Colloquium on Stability of Steel Structures,* Sept. 25–26, 1986, Hungary, vol. II/2.

6.16   Dawe, J. L., and G. L. Kulak: "Local Buckling Behavior of Beam-Columns," *Journal of Structural Engineering,* vol. 112, no. 11, Nov. 1986.

6.17   Mahmood, H. F., and S. H. Abed: "Computer Aided Analysis of Thin-Walled Structural Components Subjected to Axial and Bending's Crush Loads," *Proceedings of the 8th International Specialty Conference on Cold-Formed Steel Structures,* UMR, 1986.

6.18   Davids, A. J., and G. J. Hancock: "Nonlinear Elastic Response of Locally Buckled Thin-Walled Beam-Columns," *International Journal on Thin-Walled Structures,* vol. 5, no. 3, 1987.

6.19   Farkas, J.: "Local Buckling Behavior of Beam-Columns," *Journal of Structural Engineering,* vol. 114, no. 4, April 1988.

6.20   Sohal, E. S., and W. F. Chen: "Local and Post-Buckling Behavior of Tubular Beam-Columns," *Journal of Structural Engineering,* vol. 114, no. 5, May 1988.

6.21   Shanmugam, N. E., J. Y. R. Liew, and S. L. Lee: "Thin-Walled Steel Box Columns under Biaxial Loading," *Journal of Structural Engineering,* vol. 115, no. 11, 1989.

6.22   Liew, J. Y. R., N. E. Shanmugam, and S. L. Lee: "Behavior of Thin-Walled Steel Box Columns Under Biaxial Loading," *Journal of Structural Engineering,* vol. 115, no. 12, 1989.

6.23   Carril, D. E., R. A. LaBoube, and W. W. Yu: "Tensile and Bearing Capacities of Bolted Connections," *First Summary Report,* Civil Engineering Study 94-1, University of Missouri-Rolla, 1994.

6.24   Holcomb, R. D., R. A. LaBoube, and W. W. Yu: "Tensile and Bearing Capacities of Bolted Connections," *Second Summary Report,* Civil Engineering Study 95-1, University of Missouri-Rolla, 1995.

6.25   LaBoube, R. A., and W. W. Yu: "Additional Design Considerations for Bolted Connections," *Proceedings of the 13th International Specialty Conference on Cold-Formed Steel Structures,* University of Missouri-Rolla, Oct. 1996.

6.26   Guo, Y., and S. Chen: "Postbuckling Interaction Analysis of Cold-Formed Thin-Walled Channel Sections by Finite Strip Method," *Thin-Walled Structures,* vol. 11, 1991.

6.27   Murtha-Smith, E., and P. Magyar: "Cold-Formed Steel Channel Struts," *Journal of Structural Engineering,* ASCE, vol. 117, no. 4, April 1991.

6.28   Chan, S. L., S. Kitipornchai, and G. A. Al-Bermani "Elastro-Plastic Analysis of Box Beam-Column Including Local Buckling Effects," *Journal of Structural Engineering,* ASCE, vol. 117, no. 7, July 1991.

6.29   Zhao, X. L., and G. J. Hancock: "Square and Rectangular Hollow Sections Subject to Combined Actions," *Journal of Structural Engineering,* ASCE, vol. 118, no. 3, March 1992.

6.30   Prion, H. G. L., and P. C. Birkemoe: "Beam-Column Behavior of Fabricated Steel Tubular Members," *Journal of Structural Engineering,* ASCE, vol. 118, no. 5, May 1992.

6.31   Miller, T. H., and T. Pekoz: "Load-Eccentricity Effects of Cold-Formed Steel Lipped-Channel Columns," *Journal of Structural Engineering,* ASCE, vol.120, no. 3, May 1994.

6.32   Sully, R. M, and G. J. Hancock: "Behavior of Cold-Formed SHS Beam-Columns," *Proceedings of the 12th International Specialty Conference on Cold-Formed Steel Structures,* University of Missouri-Rolla, Oct. 1994. Also *Journal of Structural Engineering,* ASCE, vol. 122, no. 3, March 1996.

6.33   Makelainen, P., and J. Kankaanpaa: "Structural Design Study on a Light-Gauge Steel Portal Frame with Cold-Formed Sigma Sections," *Proceedings of the 13th International Specialty Conference on Cold-Formed Steel Structures,* University of Missouri-Rolla, Oct. 1996.

6.34   Rasmussen, K. J. R., and A. S. Hasham: "Flexural and Flexural–Torsional Bifureation of Locally Buckled Beam-Columns," *Thin-Walled Structures,* vol. 29, nos. 1–4, 1997.

6.35   Hancock, G. J., and K. J. R. Rasmussen: "Recent Research on Thin-Walled Beam-Columns," *Thin-Walled Structures,* vol. 32, 1998.

6.36   Salmon, C. G., and J. E. Johnson: *Steel Structures—Design and Behavior,* 4th ed., Harper Collins, New York, 1996.

CHAPTER 7

7.1   Wolford, D. S.: "Welded Steel Tubing Solves Structural Design Problems," *Tubular Steel Progress,* vol. 4, no. 2, 1965.

7.2   Schilling, C. G.: "Buckling Strength of Circular Tubes," *Journal of the Structural Division, ASCE Proceedings,* vol. 91, Oct. 1965.

7.3   Wolford, D. S., and M. J. Rebholz: "Beam and Column Tests of Welded Steel Tubing with Design Recommendations," ASTM bulletin 233, Oct. 1958.

7.4   Sherman, D. R.: "Structural Behavior of Tubular Sections," *Proceedings of the Third International Specialty Conference on Cold-Formed Steel Structures,* University of Missouri-Rolla, Nov. 1975.

7.5   Sherman, D. R.: "Tentative Criteria for Structural Applications of Steel Tubing and Pipe," American Iron and Steel Institute, Aug. 1976.

7.6   Zaric, B.: "CIDECT Research Report," Convention Européenne de la Construction Métallique, Subcommission 8.1, Mar. 1968.

7.7   Miller, C. D.: "Buckling of Axially Compressed Cylinders," *Journal of the Structural Division, ASCE Proceedings,* vol. 103, Mar. 1977.

7.8   Chen, W. F., S. Toma, and R. L. Yuan: "Strength of Fabricated Tubular Columns in Offshore Structures," *Thin-Walled Structures* (J. Rhodes and A. C. Walker, Eds.), Granada Publishing, New York, Apr. 3–6, 1979.

7.9   Toma, S., and W. F. Chen: "Analysis of Fabricated Tubular Columns," *Journal of the Structural Division, ASCE Proceedings,* vol. 105, Nov. 1979.

7.10   Ross, D. A., W. F. Chen, and L. Tall: "Fabricated Tubular Steel Columns," *Journal of the Structural Division, ASCE Proceedings,* vol. 106, Jan. 1980.

7.11   Dowling, P. J.: "Research in Great Britain on the Stability of Circular Tubes," *Proceedings of the Structural Stability Research Council,* Lehigh University, 1982.

7.12   Foss, G.: "Research in Norway in the Stability of Circular Tubes," *Proceedings of the Structural Stability Research Council, Lehigh University, 1982.*

7.13   Sherman, D. R.: "Research in North America on the Stability of Circular Tubes," *Proceedings of the Structural Stability Research Council,* Lehigh University, 1982.

7.14   Kurobane, Y., T. Atsuta, and S. Toma: "Research in Japan in the Stability of Circular Tubes," *Proceedings of the Structural Stability Research Council,* Lehigh University, 1982.

7.15   Singer, J.: "Shell Buckling Research in Israel and Its Application to Offshore Structures," *Proceedings of the Structural Stability Research Council,* Lehigh University, 1982.

7.16   Gerard, G., and H. Becker: "Handbook of Structural Stability, Part IV— Buckling of Curved Plates and Shells," NACA technical note 3783, Aug. 1975.

7.17   Donnell, L. H., and C. C. Wan: "Effect of Imperfections on Buckling of Thin Cylinders and Columns under Axial Compression," *Journal of Applied Mathematics,* vol. 17, Mar. 1950.

7.18   Ostapenko, A.: "Local Buckling of Welded Tubular Columns," presented at the International Colloquium on Stability of Structures under Static and Dynamic Loads, Washington, DC, May 17–19, 1977.

7.19   Ostapenko, A., and S. X. Gunzelman: "Local Buckling Tests on Three Steel Large-Diameter Tubular Columns," *Proceedings of the 4th International Specialty Conference on Cold-Formed Steel Structures,* University of Missouri-Rolla, June 1978.

7.20   Grimm, D. F., and A. Ostapenko: "Local Buckling of Steel Tubular Columns," *Proceedings of the Structural Stability Research Council,* Lehigh University, 1982.

7.21 Stephens, M. J., G. L. Kulak, and C. J. Montgomery: "Local Buckling of Thin-Walled Tubular Steel Members," structural engineering report 103, University of Alberta, Canada, Feb. 1982.

7.22 Kato, B.: "Local Buckling of Steel Circular Tubes in Plastic Region," presented at the International Colloquium on Stability of Structures under Static and Dynamic Loads, Washington, DC, May 17–19, 1977.

7.23 American Water Works Association: "AWWA Standard for Steel Tanks—Standpipes, Reservoirs, and Elevated Tanks—for Water Storage," AWWA D100-79, 1979.

7.24 American Society of Mechanical Engineers: "Metals Containment Shell Buckling Design Methods," Case N-284 of the ASME Boiler and Pressure Vessel Code, 1980.

7.25 American Petroleum Institute: "Recommended Practice for Planning, Designing, and Construction of Fixed Offshore Platforms," API RP 2A, 12th ed., Jan. 1981.

7.26 Sherman, D. R.: "Tests of Circular Steel Tubes in Bending," *Journal of the Structural Division, ASCE Proceedings,* vol. 102, Nov. 1976.

7.27 Plantema, F. J.: "Collapsing Stresses of Circular Cylinders and Round Tubes," report S. 280, Nat. Luchtvaartlaboratorium, Amsterdam, Netherlands, 1946.

7.28 Wilson, W. M., and N. M. Newmark: "The Strength of Thin Cylindrical Shells as Columns," bulletin 255, University of Illinois Engineering Experiment Station, 1933.

7.29 Wilson, W. M.: "Tests of Steel Columns," bulletin 292, University of Illinois Engineering Experiment Station, 1937.

7.30 Sherman, D. R.: "Bending Equations for Circular Tubes," *Annual Technical Session Proceedings,* Structural Stability Research Council, 1984.

7.31 Gupta, N. K.: "Some Aspects of Axial Collapse of Cylindrical Thin-Walled Tubes," *Thin-Walled Structures,* vol. 32, 1998.

CHAPTER 8

8.1 Toepel, W. A.: "Selection and Application of Construction Fasteners," *Metal Building Review,* Oct. 1966.

8.2 "USA Standard Slotted and Recessed Head Tapping Screws and Metallic Drive Screws," USAS B18.6.4, 1967.

8.3 "Fastening and Joining," reference issue, *Machine Design,* 4th ed., June 15, 1967.

8.4 Baehre, R., and L. Berggren: "Jointing of Thin-Walled Steel and Aluminium Structures," National Swedish Institute for Building Research, 1971.

8.5 Stark, J. W. B., and A. W. Toma: "Connections in Cold-Formed Sections and Steel Sheets," *Proceedings of the 4th International Specialty Conference on Cold-Formed Steel Structures,* University of Missouri-Rolla, June 1978.

8.6   Johnson, D. L.: "Connections in Cold-Formed Construction," *Proceedings of the Cold-Formed Steel Structures Conference,* University of Windsor, Ont., Canada, Apr. 1980.

8.7   European Convention for Constructional Steelwork: "Design of Connections," Preliminary European Recommendations for Connections in Thin Walled Structural Steel Elements, pt. 1, prepared by Working Group TWG 7.2 of ECCS Committee TC7, Feb. 1981.

8.8   European Convention for Constructional Steelwork: "Mechanical Fasteners for Use in Thin-Walled Structural Steel Elements," Preliminary European Recommendations for Connections in Thin Walled Structural Steel Elements, pt. 2, prepared by Working Group TWG 7.2 of ECCS Committee TC7, Feb. 1981.

8.9   Heagler, R. B.: "How to Fasten Steel Deck," *Modern Steel Construction,* American Institute of Steel Construction, vol. 22, First Quarter 1982.

8.10   American Iron and Steel Institute: "Production Design Guide for Adhesive Bonding of Sheet Steel," AISI 1201-413-476.

8.11   American Welding Society: "Symbols for Welding and Nondestructive Testing," AWS A2.4, 1979.

8.12   Pekoz, T. B., and W. McGuire: "Welding of Sheet Steel," report SG 79-2, American Iron and Steel Institute, Jan. 1979.

8.13   Pekoz, T. B., and W. McGuire: "Welding of Sheet Steel," *Proceedings of the 5th International Specialty Conference on Cold-Formed Steel Structures,* University of Missouri-Rolla, Nov. 1980.

8.14   Blodgett, O. W.: "Report on Proposed Standards for Sheet Steel Structural Welding," *Proceedings of the 4th International Specialty Conference on Cold-Formed Steel Structures,* University of Missouri-Rolla, June 1978.

8.15   American Welding Society: "Specification for Welding Sheet Steel in Structures," AWS D1.3-78, 1978.

8.16   American Welding Society: "Structural Welding Code—Sheet Steel," 2nd ed., ANS1/AWS D1.3-89, 1989.

8.17   Fung, C.: "Strength of Arc-Spot Weld in Sheet Steel Construction," Final Report on CSICC Industry Research Project 175, Westeel-Rosco, Ltd., Canada, 1978.

8.18   Albrecht, R. E.: "Developments and Future Needs in Welding Cold-Formed Steel," *Proceedings of the 9th International Specialty Conference on Cold-Formed Steel Structures,* University of Missouri-Rolla, Nov. 1988.

8.19   Hsiao, L. E., and W. W. Yu: "Required Factor of Safety for Tensile Strength of Arc Spot Welds Using Allowable Stress Design Methods," committee correspondence, March 1989.

8.20   LaBoube, R. A., and W. W. Yu: "Tensile Strength of Cold-Formed Steel Welded Connections," *Proceedings of the International Conference on Steel & Aluminium Structures,* Singapore, May 1991.

8.21   American Iron and Steel Institute: "Specifications for the Design of Cold-Formed Steel Structural Members," 1968 ed., addendum 2, Feb. 4, 1977.

8.22   Stark, J. W. B., and F. Soetens: "Welded Connections in Cold-Formed Sections," *Proceedings of the 5th International Specialty Conference on Cold-Formed Steel Structures,* University of Missouri-Rolla, Nov. 1980.

8.23   Kato, B., and I. Nishiyama: "T-Joints Made of Rectangular Tubes," *Proceedings of the 5th International Specialty Conference on Cold-Formed Steel Structures,* University of Missouri-Rolla, Nov. 1980.

8.24   Lind, N. C., L. I. Knab, and W. B. Hall: "Economic Study of the Connection Safety Factor," *Proceedings of the 3rd International Specialty Conference on Cold-Formed Steel Structures,* University of Missouri-Rolla, Nov. 1975.

8.25   Wardenier, J.: *Hollow Section Joints,* Delft University Press, Delft, 1982.

8.26   Kurobane, Y., Y. Makino, and K. Ochi: "Ultimate Resistance of Unstiffened Tubular Joints," *Journal of the Structural Engineering, ASCE Proceedings,* vol. 110, no. 2, Feb. 1984.

8.27   Kurobane, Y., K. Ogawa, K. Ochi, and Y. Makino: "Local Buckling of Braces in Tubular K-Joints," *International Journal on Thin-Walled Structures,* vol. 4, no. 1, 1986.

8.28   Mäkeläinen, P., R. Puthil, and F. Bijlaard: "Strength, Stiffness and Nonlinear Behaviour of Simple Tubular Joints," *Preprint of 13th Congress, IABSE,* June 6–10, 1988.

8.29   Mäkeläinen, P. K.: "Semi-Analytical Models for the Static Behaviour of T and DT Tubular Joints," *Proceedings of the 3rd Finnish Mechanics Days* (M. A. Ranta, Ed.), Helsinki University of Technology, Finland, 1988.

8.30   Niemi, E., J. Lehtinen, and I. Sorsa: "Behaviour of Rectangular Hollow Section K-Joints at Low Temperatures," *Report 54,* Department of Mechanical Engineering, Lappeenranta University of Technology, Lappeenranta, Finland, 1988.

8.31   Niemi, E., and P. Makelainen, Eds.: *Tubular Structures,* Elsevier Applied Science, New York, 1990.

8.32   Zhao, X. L., and G. J. Hancock: "Tubular T-Joints Subject to Combined Actions," *Proceedings of the 10th International Specialty Conference on Cold-Formed Steel Structures,* University of Missouri-Rolla, Oct. 1990.

8.33   American Welding Society: "Recommended Practice for Resistance Welding Coated Low-Carbon Steels," AWS C1.3-70, 1970 (Reaffirmed 1987).

8.34   American Welding Society: "Recommended Practice for Resistance Welding," AWS C1.1-66, 1966.

8.35   Green, E. A., and J. J. Riley: "Resistance Spot Welding Galvanized Steel of Thicknesses 0.022 to 0.138 in.," *Welding Research Supplement,* Oct. 1963.

8.36   Henschkel, J.: "The Expression of Spot-Weld Properties," *Welding Journal,* Oct. 1952.

8.37   Winter, G.: "Tests on Bolted Connections in Light Gage Steel," *Journal of the Structural Division, ASCE Proceedings,* vol. 82, Mar. 1956.

8.38   Winter, G.: "Light Gage Steel Connections with High-Strength, High Torqued Bolts," publication, International Association for Bridge and Structural Engineering, vol. 16, p. 513, 1956.

8.39   Dhalla, A. K., S. J. Errera, and G. Winter: "Connections in Thin Low-Ductility Steels," *Journal of the Structural Division, ASCE Proceedings,* vol. 97, Oct. 1971.

8.40   Popowich, D. W.: "Tension Capacity of Bolted Connections in Light Gage Cold-Formed Steel," M.S. thesis, Cornell University, 1969.

8.41   McKinney, W. M., A. S. Liu, and W. W. Yu: "Study of Cold-Formed Steel Structural Members Made of Thick Sheets and Plates," final report, University of Missouri-Rolla, Apr. 1975.

8.42   Chong, K. P., and R. B. Matlock: "Light Gage Steel Bolted Connections without Washers," *Journal of the Structural Division, ASCE Proceedings,* vol. 101, July 1975.

8.43   Gilchrist, R. T., and K. P. Chong: "Thin Light-Gage Bolted Connections without Washers," *Journal of the Structural Division, ASCE Proceedings,* vol. 105, Jan. 1979.

8.44   Rang, T. N., W. W. Yu, T. V. Galambos, and M. K. Ravindra: "Load and Resistance Factor Design of Bolted Connections," *Thin-Walled Structures* (J. Rhodes and A. C. Walker, Eds.), Granada Publishing, New York, Apr. 3–6, 1979.

8.45   Yu, W. W., and R. L. Mosby: "Bolted Connections in Cold-Formed Steel Structures," final report, University of Missouri-Rolla, Jan. 1981.

8.46   Yu, W. W.: "AISI Design Criteria for Bolted Connections," *Proceedings of the 6th International Specialty Conference on Cold-Formed Steel Structures,* University of Missouri-Rolla, Nov. 1982.

8.47   Research Council on Structural Connections: "Allowable Stress Design Specification for Structural Joints Using ASTM A325 or A490 Bolts," Nov. 13, 1985.

8.48   Kulak, G. L., J. W. Fisher, and J. H. A. Struik: *Guide to Design Criteria for Bolted and Riveted Joints,* John Wiley and Sons, New York, 2nd Ed., 1987.

8.49   Stark, J. W. B., and A. W. Toma: "Fastening of Steel Sheets for Walls and Roofs on Steel Structures," *Thin-Walled Structures* (J. Rhodes and A. C. Walker, Eds.), Granada Publishing, New York, Apr. 3–6, 1979.

8.50   Stark, J. W. B., and A. W. Toma: "Connections in Thin-Walled Structures," *Developments in Thin-Walled Structures—1* (J. Rhodes and A. C. Walker, eds.), Applied Science Publishers, London, 1982.

8.51   Marsh, C.: "Tear-Out Failure of Bolt Groups," *Journal of the Structural Division, ASCE Proceedings,* vol. 105, Oct. 1979.

8.52   LaBoube, R. A.: "Strength of Bolted Connections: Is It Bearing or Net Section?" *Proceedings of the 9th International Specialty Conference on Cold-Formed Steel Structures,* University of Missouri-Rolla, Nov. 1988.

8.53   Baehre, R., and L. Berggren: "Joints in Sheet Metal Panels," document D8, National Swedish Building Research, 1973.

8.54   Pekoz, T.: "Design of Cold-Formed Steel Screw Connections," *Proceedings of the 10th International Specialty Conference on Cold-Formed Steel Structures,* University of Missouri-Rolla, Oct. 1990.

8.55   Eastman, R. W.: "Report on Screw Fastened Sheet Steel Connections," vols. I and II, DOFASCO, Hamilton, Ont., Canada, Jan. 1976.

8.56   McCavour Engineering Ltd.: "Screw Fastener Connections," research 578, Etobicoke, Ont., Canada, June 1980.

8.57   Strnad, M.: "Flexibility of Mechanical Fastenings of Very Thin-Walled Steel Structures," *International Journal of Thin-Walled Structures,* vol. 2, no. 3, 1984.

8.58 Strnad, M.: "Design of Screwed Fastenings with Regard to Their Elasto-Plastic Behaviour," *Der Metallbau im Konstruktiven-Ingenieurbau,* Karlsruhe, West Germany, February 1988.

8.59 Ellifritt, D. S., and R. Burnett: "Pull-over Strength of Screws in Simulated Building Tests," *Proceedings of the 10th International Specialty Conference on Cold-Formed Steel Structures,* University of Missouri-Rolla, Oct. 1990.

8.60 Yener, M.: "Criteria for Connection Spacing in Cold-Formed Steel," *Journal of the Structural Division, ASCE Proceedings,* vol. 110, no. 9, Sept. 1984.

8.61 Klippstein, K. H.: "Discussion of Criteria for Connection Spacing in Cold-Formed Steel by M. Yener," *Journal of Structural Engineering, ASCE Proceedings,* vol. 112, no. 12, Dec. 1986.

8.62 Yener, M.: "Spacing of Connections in Thin-Walled Compression Elements," *Proceedings, IABSE Colloquium,* Stockholm, 1986.

8.63 Brockenbrough, R. L.: "Fastening of Cold-Formed Steel Framing," American Iron and Steel Institute, Washington, DC, Sept. 1995.

8.64 Pedreschi, R. F., B. P. Sinha, and R. Davies: "Advanced Connection Techniques for Cold-Formed Steel Structures," *Journal of Structural Engineering,* ASCE, vol. 123, no. 2, Feb. 1997.

8.65 Pedreschi, R., B. Sinha, R. Davies, and R. Lennon: "Factors Influencing the Strength of Mechanical Clinching," *Proceedings of the 14th International Specialty Conference on Cold-Formed Steel Structures,* University of Missouri-Rolla, Oct. 1998.

8.66 LaBoube, R. A., and W. W. Yu: "Tensile Strength of Welded Connections," Final Report, University of Missouri-Rolla, June 1991.

8.67 LaBoube, R. A., and W. W. Yu: "Behavior of Arc Spot Weld Connections in Tension," *Journal of Structural Engineering,* ASCE, vol. 119, no. 7, July 1993. Also *Proceedings of the 11th International Specialty Conference on Cold-Formed Steel Structures,* University of Missouri-Rolla, Oct. 1992.

8.68 Zhao, X. L., and G. J. Hancock: "T-Joints in Rectangular Hollow Sections Subject to Combined Actions," *Journal of Structural Engineering,* ASCE, vol. 117, no. 8, Aug. 1991.

8.69 Zhao, X. L., and G. J. Hancock: "Butt Welds and Transverse Fillet Welds in Thin Cold-Formed RHS Members," *Journal of Structural Engineering,* ASCE, vol. 121, no. 11, Nov. 1995.

8.70 Zhao, X. L., and G. J. Hancock: "Longitudinal Fillet Weld in Thin Cold-Formed RHS Members," *Journal of Structural Engineering,* ASCE, vol. 121, no. 11, Nov. 1995.

8.71 Zadanforrokh, F., and E. R. Bryan: "Testing and Design of Bolted Connections in Cold-Formed Steel Sections," *Proceedings of the 11th International Specialty Conference on Cold-Formed Steel Structures,* University of Missouri-Rolla, Oct. 1992.

8.72 Seleim, S., and R. A. LaBoube: "Behavior of Low Ductility Steel in Cold-Formed Steel Connections," *Thin-Walled Structures,* vol. 25, no. 2, 1996.

8.73 Kulak, G. L., and E. Y. Wu: "Shear Lag in Bolted Angle Tension Members," *Journal of Structural Engineering,* vol. 123, no. 9, Sept. 1997.

8.74 Wheeler, A. T., M. J. Clarke, G. J. Hancock, and T. M. Murray: "Design Model for Bolted Moment End Plate Connections Joining Rectangular Hollow Sections," *Journal of Structural Engineering,* vol. 124, no. 2, Feb. 1998.

8.75 American Iron and Steel Institute: "Fasteners for Residential Steel Framing," *Publication* RG-933, June 1993.

8.76 Xu, Y. L.: "Fatigue Performance of Screw-Fastened Light-Gauge-Steel Roofing Sheets," *Journal of Structural Engineering,* ASCE, vol. 121, no. 3, March 1995.

8.77 Daudet, L. R., and R. A. LaBoube: "Shear Behavior of Self-Drilling Screws Used in Low Ductility Steel," *Proceedings of the 13th International Specialty Conference on Cold-Formed Steel Structures,* University of Missouri-Rolla, Oct. 1996.

8.78 Serrette, R., and V. Lopez: "Performance of Self-Tapping Screws in Lap-Shear Metal-to-Metal Connections," *Proceedings of the 13th International Specialty Conference on Cold-Formed Steel Structures,* University of Missouri-Rolla, Oct. 1996.

8.79 Fan, L. X., J. Rondal, and S. Cescotto: "Numerical Simulation of Lap Screw Connections," *Thin-Walled Structures,* vol. 29, nos. 1–4, 1997.

8.80. Kreiner, J. S., and D. S. Ellifritt: "Understanding Pullover," *Proceedings of the 14th International Specialty Conference on Cold-Formed Steel Structures,* University of Missouri-Rolla, Oct. 1998.

8.81 Anderson, G. A., and V. C. Kelley: "Lateral Load Strength of Screw Connections in 29 Ga Metal," *Proceedings of the 14th International Specialty Conference on Cold-Formed Steel Structures,* University of Missouri-Rolla, Oct. 1998.

8.82 Sokol, M. A., R. A. LaBoube, and W. W. Yu: "Determination of the Tensile and Shear Strength of Screws and the Effect of Screw Patterns on Cold-Formed Steel Connections," Civil Engineering Study 98-3, University of Missouri-Rolla, Dec. 1998.

8.83 Center for Cold-Formed Steel Structures: "AISI Specification Provisions for Screw Connections," *CCFSS Technical Bulletin,* vol. 2., no. 1, University of Missouri-Rolla, Feb. 1993.

8.84 Davies, R., R. Pedreschi, and B. P. Sinha: "The Shear Behaviour of Press-Joining in Cold-Formed Steel Structures," *Thin-Walled Structures,* vol. 25, no. 3, 1996.

8.85 Davies, R. R. Pedreschi, and B. P. Sinha: "Moment-Rotation Behaviour of Groups of Press-Joints in Cold-Formed Steel Structures," *Thin-Walled Structures,* vol. 27, no. 3, 1997.

8.86 Padreschi, R. F., B. P. Sinha, and R. J. Davies: "End Fixity in Cold-Formed Steel Sections Using Press Joining," *Thin-Walled Structures,* vol. 29, nos. 1–4, 1997.

8.87 Makelainen, P., J. Kosti, O. Kaitila, and K. J. Sahramaa: "Study on Light-Gauge Steel Roof Trusses with Rosette Connections," *Proceedings of the 14th International Specialty Conference on Cold-Formed Steel Structures,* University of Missouri-Rolla, Oct. 1998.

8.88   Metal Home Digest: "New Approach to Fabricating Light-Gauge Products Designed for Economy," Nov.–Dec. 1998.

8.89   Birkemoe, P. C., and M. I. Gilmor: "Behavior of Bearing-Critical Double-Angle Beam Connections," *AISC Engineering Journal,* 4th Quarter, 1978

8.90   Richles, J. M., and J. A. Yura: "Strength of Double-Row Bolted Web Connections," *Journal of the Structural Division,* ASCE, vol. 109, no. ST1, Jan. 1983.

8.91   Hardash, S. G., and R. Bjorhovde: "New Design Criteria for Gusset Plates in Tension," *AISC Engineering Journal,* 2nd Quarter, 1985.

8.92   Luttrell, L. D., and K. Balaji: "Properties for Cellular Deck in Negative Bending," *Proceedings of the 11th International Specialty Conference on Cold-Formed Steel Structures,* University of Missouri-Rolla, Oct. 1992.

8.93   LaBoube, R. A., W. W. Yu, and M. L. Jones: "Spacing of Connections in Compression Flanges of Built-Up Cold-Formed Steel Beams," *Proceedings of the 14th International Specialty Conference on Cold-Formed Steel Structures,* University of Missouri-Rolla, Oct. 1998.

8.94   Tillman, S. C.: "The Effects of Connector Spacing and Distribution on the Buckling Behaviour of Some Single-Cell and Twin-Cell Box Columns," *Thin-Walled Structures,* vol. 14, 1992.

CHAPTER 9

9.1   Nilson, A. H.: "Diaphragm Action in Light Gage Steel Construction," AISI regional technical paper, 1960.

9.2   Nilson, A. H.: "Shear Diaphragms of Light Gage Steel," *Journal of the Structural Division, ASCE Proceedings,* vol. 86, Nov. 1960.

9.3   Luttrell, L. D.: "Structural Performance of Light Gage Steel Diaphragms," report 319, Department of Structural Engineering, Cornell University, Aug. 1965.

9.4   Apparao, T. V. S. R.: "Tests on Light Gage Steel Diaphragms," report 328, Department of Structural Engineering, Cornell University, Dec. 1966.

9.5   Luttrell, L. D.: "Strength and Behavior of Light Gage Steel Shear Diaphragms," Department of Structural Engineering, Cornell University, 1967.

9.6   American Iron and Steel Institute: "Design of Light Gage Steel Diaphragms," 1st ed., 1967.

9.7   Nilson, A. H.: "Analysis of Light Gage Steel Shear Diaphragms," *Proceedings of the 2nd Specialty Conference on Cold-Formed Steel Structures,* University of Missouri-Rolla, Oct. 1973.

9.8   Nilson, A. H., and A. R. Ammar: "Finite Element Analysis of Metal Deck Shear Diaphragms," *Journal of the Structural Division, ASCE Proceedings,* vol. 100, Apr. 1974.

9.9   Atrek, E., and A. H. Nilson: "Nonlinear Analysis of Cold-Formed Steel Shear Diaphragms," *Journal of the Structural Division, ASCE Proceedings,* vol. 106, Mar. 1980.

9.10   Ellifritt, D. S., and L. D. Luttrell: "Strength and Stiffness of Steel Deck Shear Diaphragms," *Proceedings of the 1st Specialty Conference on Cold-Formed Steel Structures,* University of Missouri-Rolla, Aug. 1971.

9.11   Luttrell, L. D.: "Shear Diaphragms with Lightweight Concrete Fill," *Proceedings of the 1st Specialty Conference on Cold-Formed Steel Structures,* University of Missouri-Rolla, Aug. 1971.

9.12   Luttrell, L. D.: "Screw Connected Shear Diaphragms," *Proceedings of the 2nd Specialty Conference on Cold-Formed Steel Structures,* University of Missouri-Rolla, Oct. 1973.

9.13   Huang, H. T., and L. D. Luttrell: "Theoretical and Physical Evaluation of Steel Shear Diaphragms," *Proceedings of the 5th International Specialty Conference on Cold-Formed Steel Structures,* University of Missouri-Rolla, Nov. 1980.

9.14   Easley, J. T., and D. E. McFarland: "Buckling of Light-Gage Corrugated Metal Shear Diaphragms," *Journal of the Structural Division, ASCE Proceedings,* vol. 95, July 1969.

9.15   Easley, J. T.: "Buckling Formulas for Corrugated Metal Shear Diaphragms," *Journal of the Structural Division, ASCE Proceedings,* vol. 101, July 1975.

9.16   Easley, J. T.: "Strength and Stiffness of Corrugated Metal Shear Diaphragms," *Journal of the Structural Division, ASCE Proceedings,* vol. 103, Jan. 1977.

9.17   Miller, C. J.: "Drift Control with Light Gage Steel Infill Panels," *Proceedings of the 2nd Specialty Conference on Cold-Formed Steel Structures,* University of Missouri-Rolla, Oct. 1973.

9.18   Libove, C.: "On the Stiffness, Stresses and Buckling Analysis of Corrugated Shear Webs," *Proceedings of the 2nd Specialty Conference on Cold-Formed Steel Structures,* University of Missouri-Rolla, Oct. 1973.

9.19   Wu, L. H., and C. Libove: "Curvilinearly Corrugated Plates in Shear," *Journal of the Structural Division, ASCE Proceedings,* vol. 101, Nov. 1975.

9.20   Hussain, M. I., and C. Libove: "Trapezoidally Corrugated Plates in Shear," *Journal of the Structural Division, ASCE Proceedings,* vol. 102, May 1976.

9.21   Libove, C.: "Buckling of Corrugated Plates in Shear," presented at the International Colloquium on Stability of Structures under Static and Dynamic Loads, Washington, DC, May 1977.

9.22   Chern, C., and J. L. Jorgenson: "Shear Strength of Deep Corrugated Steel Panels," *Proceedings of the 2nd Specialty Conference on Cold-Formed Steel Structures,* University of Missouri-Rolla, Oct. 1973.

9.23   Liedtke, P. E., and D. R. Sherman: "Comparison of Methods Predicting Diaphragm Behavior," *Proceedings of the 5th International Specialty Conference on Cold-Formed Steel Structures,* University of Missouri-Rolla, Nov. 1982.

9.24   Fisher, J. M., and D. L. Johnson: "Behavior of Light Gage Diaphragms Coupled with X-Bracing," *Proceedings of the 2nd Specialty Conference on Cold-Formed Steel Structures,* University of Missouri-Rolla, Oct. 1973.

9.25   Fisher, J. M.: "Strength and Stiffness of Light Gauge Steel Diaphragms," *Proceedings of the Cold-Formed Steel Structures Conference,* University of Windsor, Ont., Canada, Apr. 1980.

9.26 LaBoube, R. A., and J. M. Fisher: " Diaphragm Strength of Composite Roof System," *Proceedings of the 6th International Specialty Conference on Cold-Formed Steel Structures,* University of Missouri-Rolla, Nov. 1982.

9.27 Chockalingam, S., P. Fazio, and K. Ha: "Strengths of Cold Formed Steel Shear Diaphragms," *Proceedings of the 4th International Specialty Conference on Cold-Formed Steel Structures,* University of Missouri-Rolla, June 1978.

9.28 Ha, H. K., S. Chockalingam, and P. Fazio: "Further Study on the Strength of Cold-Formed Shear Diaphragms," *Thin-Walled Structures* (J. Rhodes and A. C. Walker, Eds.), Granada Publishing, New York, Apr. 1979.

9.29 Ha, H. K.: "Corrugated Shear Diaphragms," *Journal of the Structural Division, ASCE Proceedings,* vol. 105, Mar. 1979.

9.30 Ha, H. K., N. El-Hakim, and P. P. Fazio: "Simplified Design of Corrugated Shear Diaphragms," *Journal of the Structural Division, ASCE Proceedings,* vol. 105, July 1979.

9.31 Abdel-Sayed, G.: "Critical Shear Loading of Curved Panels of Corrugated Sheets with Restrained Edges," *Proceedings of the 1st Specialty Conference on Cold-Formed Steel Structures,* University of Missouri-Rolla, Aug. 1971.

9.32 Bryan, E. R.: "Calculation of Sheet Steel Diaphragms in the U.K.," *Proceedings of the 3rd International Specialty Conference on Cold-Formed Steel Structures,* University of Missouri-Rolla, Nov. 1975.

9.33 Bryan, E. R., and J. M. Davies: "Stressed Skin Construction in the U.K.," *Proceedings of the 3rd International Specialty Conference on Cold-Formed Steel Structures,* University of Missouri-Rolla, Nov. 1975.

9.34 Davies, J. M., and R. M. Lawson: "The Shear Flexibility of Corrugated Steel Sheeting," *Proceedings of the 3rd International Specialty Conference on Cold-Formed Steel Structures,* University of Missouri-Rolla, Nov. 1975.

9.35 Davies, J. M.: "Calculation of Steel Diaphragm Behavior," *Journal of the Structural Division, ASCE Proceedings,* vol. 102, July 1976.

9.36 Davies, J. M.: "Simplified Diaphragm Analysis," *Journal of the Structural Division, ASCE Proceedings,* vol. 103, Nov. 1977.

9.37 Davies, J. M.: "Developments in Inexpensive Lightweight Structures," *Proceedings of the 4th International Specialty Conference on Cold-Formed Steel Structures,* University of Missouri-Rolla, June 1978.

9.38 Davies, J. M., and E. R. Bryan: "Design Tables for Light Gauge Steel Diaphragms," *Thin-Walled Structures* (J. Rhodes and A. C. Walker, Eds.), Granada Publishing, New York, Apr. 1979.

9.39 Davies, J. M., and E. R. Bryan: *Manual of Stressed Skin Diaphragm Design,* Granada Publishing, New York, 1982.

9.40 El-Dakhakhni, W. M.: "Shear of Light-Gage Partitions in Tall Buildings," *Journal of the Structural Division, ASCE Proceedings,* vol. 102, July 1976.

9.41 El-Dakhakhni, W. M.: "Effect of Light-Gage Partitions on Multistory Buildings," *Journal of the Structural Division, ASCE Proceedings,* vol. 103, Jan. 1977.

9.42 American Iron and Steel Institute: *Design of Cold-Formed Steel Diaphragms,* 1967.

9.43   American Society for Testing and Materials: "Standard Method for Static Load Testing of Framed Floor or Roof Diaphragm Constructions for Buildings," ANSI/ASTM E 455-76.

9.44   American Society for Testing and Materials: "Standard Method of Static Load Test for Shear Resistance of Framed Walls for Buildings," ANSI/ASTM E 564-76.

9.45   Steel Deck Institute: *Steel Deck Institute Design Manual,* Canton, Ohio, 1987.

9.46   Department of the Army—TM 5-809-10, Department of the Navy—NAVDOCKS-P-355, and Department of the Air Force—AFM 88-3, "Seismic Design for Buildings," Washington, DC, Feb. 1982, Chap. 13.

9.47   European Convention for Constructional Steelwork: "European Recommendations for the Stressed Skin Design of Steel Structures," ECCS-XVII-77-IE, Constrado, England, Mar. 1977.

9.48   Bryan, E. R., and J. M. Davies: "Steel Diaphragm Roof Decks—A Design Guide with Tables for Engineers and Architects, Granada Publishing, New York, 1981.

9.49   Canadian Sheet Steel Building Institute: "Diaphragm Action of Cellular Steel Floor and Roof Deck Construction, information bulletin 3, Dec. 1972.

9.50   Apparao, T. V. S. R., and S. J. Errera: "Design Recommendations for Diaphragm-Braced Beams, Columns and Wall Studs," report 332, Department of Structural Engineering, Cornell University, Oct. 1968.

9.51   Apparao, T. V. S. R., and S. J. Errera, and G. P. Fisher: "Columns Braced by Girts and a Diaphragm," *Journal of the Structural Division, ASCE Proceedings,* vol. 95, May 1969.

9.52   Errera, S. J., and T. V. S. R. Apparao: "Design of I-Shaped Columns with Diaphragm Bracing," *Journal of the Structural Division, ASCE Proceedings,* vol. 102, Sept. 1976.

9.53   Simaan, A.: "Buckling of Diaphragm-Braced Columns of Unsymmetrical Sections and Applications to Wall Studs Design," report 353, Department of Structural Engineering, Cornell University, Aug. 1973.

9.54   Simaan, A., and T. Pekoz: "Cold-Formed Steel Wall Stud Design," *Proceedings of the 2nd Specialty Conference on cold-Formed Steel Structures,* University of Missouri-Rolla, Oct. 1973.

9.55   Simaan, A., and T. Pekoz: "Diaphragm Braced Members and Design of Wall Studs," *Journal of the Structural Division, ASCE Proceedings,* vol. 102, Jan. 1976.

9.56   Simaan, A., and T. Pekoz: "An Exploratory Study on the Behavior of Cold-Formed Steel Wall Studs," report 82-14, Department of Structural Engineering, Cornell University, Sept. 1982.

9.57   Pekoz, T., and P. Soroushian: "Behavior of C- and Z-Purlins under Wind Uplift," *Proceedings of the 6th International Specialty Conference on Cold-Formed Steel Structures,* University of Missouri-Rolla, Nov. 1982.

9.58   Heins, C. P., and D. Blank: "Box Beam Stiffening Using Cold-Formed Decks," *Proceedings of the 2nd Specialty Conference on Cold-Formed Steel Structures,* University of Missouri-Rolla, Oct. 1973.

9.59 Thulin, F. A., and J. L. Lutfallah: "Cold-Formed Steel Framing with Gypsum Facing," *Proceedings of the 2nd Specialty Conference on Cold-Formed Steel Structures,* University of Missouri-Rolla, Oct. 1973.

9.60 McDermott, J. F.: "Load Tests on Steel-Stud Walls," *Proceedings of the 3rd International Specialty Conference on Cold-Formed Steel Structures,* University of Missouri-Rolla, Nov. 1975.

9.61 Ife, L. W.: "The Performance of Cold-Formed Steel Products in Housing," *Proceedings of the 3rd International Specialty Conference on Cold-Formed Steel Structures,* University of Missouri-Rolla, Nov. 1975.

9.62 McCreless, C. S., and T. S. Tarpy: "Experimental Investigation of Steel Stud Shear Wall Diaphragms," *Proceedings of the 4th International Specialty Conference on Cold-Formed Steel Structures,* University of Missouri-Rolla, June 1978.

9.63 Tarpy, T. S., and S. F. Havenstein: "Application of Light Gauge Steel-Stud Research in Building Design," *Thin-Walled Structures* (J. Rhodes and A. C. Walker, Eds.), Granada Publishing, New York, Apr. 1979.

9.64 Tarpy, T. S.: "Shear Resistance of Steel-Stud Wall Panels," *Proceedings of the 5th International Specialty Conference on Cold-Formed Steel Structures,* University of Missouri-Rolla, Nov. 1980.

9.65 Tarpy, T. S., and J. D. Girard: "Shear Resistance of Steel Stud Wall Panels," *Proceedings of the 6th International Specialty Conference on Cold-Formed Steel Structures,* University of Missouri-Rolla, Nov. 1982.

9.66 Schurter, P. G., R. M. Schuster, and A. S. Zakrzewski: "Combined Compression and Lateral Loads on Load-Bearing Steel Stud Walls," *Proceedings of the 6th International Specialty Conference on Cold-Formed Steel Structures,* University of Missouri-Rolla, Nov. 1982.

9.67 American Iron and Steel Institute: "Fire Resistance Ratings of Load-Bearing Steel Stud Walls with Gypsum Wallboard Protection With or Without Cavity Insulation," FT-901, 1981.

9.68 Baer, O.: "Steel Frame Folded Plate Roof," *Journal of the Structural Division, ASCE Proceedings,* vol. 87, June 1961.

9.69 Shapiro, D.: "Load Test Steel Folded-Plate Roof," *Engineer News-Record,* July 27, 1961.

9.70 Nilson, A. H.: "Light Gage Steel Shell Roofs," *Proceedings of the World Conference on Steel Structures,* Oct. 1962.

9.71 H. H. Robertson Company: "Folded Plate Design," Pittsburgh, PA, 1967.

9.72 "Ideas on Arc-Welded Steel Roofs," *Civil Engineering,* Aug. 1962.

9.73 Kirkgaard, W. H.: "Four Welded Steel Deck Sections in H-P Roof," *Modern Welded Structures,* vol. 1, The James F. Lincoln Arc Welding Foundation, 1963.

9.74 Hutton, C. R.: "Curvilinear Grid Frames," *Engineering Journal,* AISC, vol. 1, July 1964.

9.75 Hutton, C. R.: "Development of the Concepts of Curvilinear Grid Frames," Inland Steel Company, Apr. 1965.

9.76 American Institute of Steel Construction: "Design Examples—Space Forms in Steel," 1966.

9.77   Davies, J. M., E. R. Bryan, and R. M. Lawson: "Design and Testing of a Light Gauge Steel Folded Plate Roof," *Proceedings, Institution of Civil Engineers,* pt. II, June 1977.

9.78   Lawson, R. M.: "Design Formulas for Steel Folded Plate Roofs," *Journal of the Structural Division, ASCE Proceedings,* vol. 104, Oct. 1978.

9.79   Nilson, A. H.: "Testing of Light Gage Steel Hyperbolic Paraboloid Shell," *Journal of the Structural Division, ASCE Proceedings,* vol. 88, Oct. 1962.

9.80   Gergely, P.: "Design of Cold-Formed Hyperbolic Paraboloid Shells," *Proceedings of the 1st Specialty Conference on Cold-Formed Steel Structures,* University of Missouri-Rolla, Aug. 1971.

9.81   Portland Cement Association: "Elementary Analysis of Hyperbolic Paraboloid Shells," 1960.

9.82   Muskat, R.: "Buckling of Orthotropic Hyperbolic Paraboloids," doctoral dissertation, Cornell University, 1969.

9.83   Parker, J. E.: "Behavior of Light Gage Steel Hyperbolic Paraboloid Shells," doctoral dissertation, Cornell University, June 1969.

9.84   Gergely, P., and J. E. Parker: "Thin-Walled Hyperbolic Paraboloid Structures," final report, International Association for Bridge and Structural Engineering, Sept. 9–14, 1968.

9.85   Banavalkar, P. V., and P. Gergely: "Analysis of Thin Steel Hyperbolic Paraboloid Shells," preprint 1320, ASCE National Water Resources Engineering Meeting, Jan. 1971.

9.86   Gergely, P., and G. Winter: "Experimental Investigation of Thin-Steel Hyperbolic Paraboloid Structures," *Journal of the Structural Division, ASCE Proceedings,* vol. 98, Oct. 1972.

9.87   Banavalkar, P. V., and P. Gergely: "Analysis of Thin-Steel Hyperbolic Paraboloid Shells," *Journal of the Structural Division, ASCE Proceedings,* vol. 98, Nov. 1972.

9.88   McDermott, J. F.: "Single-Layer Corrugated Steel Sheet Hypars," *Journal of the Structural Division, ASCE Proceedings,* vol. 94, paper 5977, June 1968.

9.89   Abdel-Sayed, G.: "Clear Span Utility Buildings," *Proceedings of the Cold-Formed Steel Structures Conference,* University of Windsor, Ont., Canada, Apr. 1980.

9.90   Jankowski, W. A., and D. R. Sherman: "The Interaction of Shear Diaphragms and Diagonal Bracing," *Proceedings of the 9th International Specialty Conference on Cold-Formed Steel Structures,* University of Missouri-Rolla, Nov. 1988.

9.91   Heagler, R. B.: "Basic Diaphragm Design," *Proceedings of the 1988 National Steel Construction Conference,* American Institute of Steel Construction, June 1988.

9.92   Luttrell, L. D.: "Shear Diaphragm Strength," *Proceedings of the 1988 National Steel Construction Conference,* American Institute of Steel Construction, June 1988.

9.93   Tarpy, T. S.: "Shear Resistance of Steel Stud Wall Panels: A Summary Report," *Proceedings of the 7th International Specialty Conference on Cold-Formed Steel Structures,* University of Missouri-Rolla, Nov. 1984.

9.94   Miller, T. H., and T. Pekoz: "Studies on the Behavior of Cold-Formed Steel Wall Stud Assemblies," *Proceedings of the 10th International Specialty Conference on Cold-Formed Steel Structures,* University of Missouri-Rolla, Oct. 1990.

9.95   diGirolamo, E. R., T. Pekoz, and T. Bond: "Development and Verification of a Structural System Using Cold-Formed Steel Wall Studs," *Proceedings of the 10th International Specialty Conference on Cold-Formed Steel Structures,* University of Missouri-Rolla, Oct. 1990.

9.96   Caccese, V., M. Elgaaly, and R. Chen: "Experimental Study of Thin Steel-Plate Shear Walls under Cyclic Load," *Journal of Structural Engineering,* ASCE, vol. 119, no. 2, Feb. 1993.

9.97   Kian, T., and T. B. Pekoz: "Evaluation of Industry-Type Bracing Details for Wall Stud Assemblies," Final Report, Cornell University, Jan. 1994.

9.98   Miller, T. H., and T. Pekoz: "Unstiffened Strip Approach for Perforated Wall Studs," *Journal of Structural Engineering,* ASCE, vol. 120, No. 2, Feb. 1994.

9.99   Easterling, W. S., and M. L. Porter: "Steel-Deck-Reinforced Concrete Diaphragms, I and II," *Journal of Structural Engineering,* ASCE, vol. 120, no. 2, Feb. 1994.

9.100   Serrette, R., and K. Ogunfunmi: "Shear Resistance of Gypsum-Sheathed Light-Gauge Steel Stud Walls," *Journal of Structural Engineering,* vol. 122, no. 4, April 1996.

9.101   Smith, H. A., and V. L. Vance: "Model to Incorporate Architectural Walls in Structural Analysis," *Journal of Structural Engineering,* vol. 122, No. 4, April 1996.

9.102   Elgaaly, M., and Y. Liu: "Analysis of Thin-Steel-Plate Shear Walls," *Journal of Structural Engineering,* vol. 123, no. 11, Nov. 1997.

9.103   Lucas, R. M, F. G. A. Al-Bermani, and S. Kitipornchai: "Modelling of Cold-Formed Purlin-Sheeting Systems—Part I: Full Model," *Thin Walled Structures,* vol. 27, no. 3, 1997.

9.104   Lucas, R. M, F. G. A, Al-Bermani, and S. Kitipornchai: "Modelling of Cold-Formed Purlin-Sheating Systems—Part 2: Simplified Model," *Thin-Walled Structures,* vol. 27, no. 3, 1997.

9.105   Elgaaly, M.: "Thin Steel Plate Shear Walls Behavior and Analysis," *Thin-Walled Structures,* vol. 32, 1998.

9.106   Steel Deck Institute: *Diaphragm Design Manual,* 2nd ed., 1998.

9.107   Steel Deck Institute: *Diaphragm Design Manual,* 1st ed., 1981.

9.108   Miller, T. H., and T. Pekoz: "Behavior of Gypsum-Sheathed Cold-Formed Steel Walls Studs," *Journal of Structural Engineering,* vol. 120, no. 5, May 1994.

9.109   Center for Cold-Formed Steel Structures, *CCFSS Technical Bulletin,* vol. 8., no. 2, University of Missouri-Rolla, August 1999.

CHAPTER 10

10.1   Rockey, K. C., and H. R. Evans: "The Behaviour of Corrugated Flooring Systems," *Thin-Walled Structures,* Gordon and Breach Science Publishers, New York, 1968.

10.2   Macomber Inc.: "The Panlweb Girder," Canton, Ohio.

10.3   Sherman, D., and J. Fisher: "Beams with Corrugated Webs," *Proceedings of the 1st Specialty Conference on Cold-Formed Steel Structures,* University of Missouri-Rolla, Aug. 1971.

10.4   Harrison, J. D.: "Exploratory Fatigue Tests of Two Girders with Corrugated Webs," *British Welding Journal,* Mar. 1965.

10.5   Blodgett, H. B.: "Moment of Inertia of Corrugated Sheets," *Civil Engineering,* vol. 4, pp. 492–493, Sept. 1934.

10.6   Wolford, D. S.: "Sectional Properties of Corrugated Sheets Determined by Formula," *Civil Engineering,* vol. 24, pp. 103–104, Feb. 1954.

10.7   Bethlehem Steel Corporation: "Bethlehem Bridge Flooring," booklet 3324A, Bethlehem, PA, 1979.

10.8   Armco Inc.: "Armco Bridge Plank," catalog BP-8479, Middletown, OH, 1979.

10.9   United Steel Fabricators: "USF Structural Plate Bridge Flooring," folder BF1, Sidney, OH, 1981.

10.10   Wheeling Corrugating Company: "Wheeling Bridge Forms," WC-357, Wheeling, WV.

10.11   Cary, R. L.: "Inelastic Flexural Stability of Corrugations," *Proceedings of the 8th International Specialty Conference on Cold-Formed Steel Structures,* University of Missouri-Rolla, Nov. 1986.

10.12   Rauch, A. F., S. M. Sargand, and G. A. Hazan: "Behavior of Deeply Corrugated Steel Plate in Culvert," *Journal of Structural Engineering,* ASCE, vol. 120, no. 5, May 1994.

10.13   Luo, R., and B. Edlund: "Buckling Analysis of Trapezoidally Corrugated Panels Using Spline Strip Method," *Thin-Walled Structures,* vol. 18, 1994.

10.14   Lee, C. L., A. Mioduchowski, and M. G. Faulkner: "Optimization of Corrugated Claddings," *Journal of Structural Engineering,* ASCE, vol. 121, no. 8, Aug. 1995.

10.15   Elgaaly, M., R. W. Hamilton, and A. Seshadri: "Shear Strength of Beams with Corrugated Web," *Journal of Structural Engineering,* ASCE, vol. 122, no. 4, April 1996.

10.16   Elgaaly, M., A. Seshadri, and R. W. Hamilton: "Bending Strength of Steel Beams with Corrugated Webs," *Journal of Structural Engineering,* vol. 123, no. 6, June 1997.

10.17   Elgaaly, M., and A. Seshadri: "Girders with Corrugated Webs under Partial Compressive Edge Loading," *Journal of Structural Engineering,* vol. 123, no. 6, June 1997.

10.18   Luo, R., and B. Edlund: "Ultimate Strength of Girders with Trapezoidally Corrugated Webs under Patch Loading," *Thin-Walled Structures,* vol. 24, 1996.

CHAPTER 11

11.1   Blodgett, O. W.: "Design of Welded Structures," The James F. Lincoln Arc Wielding Foundation, Cleveland, OH, 1966, Sec. 4.8.

11.2   Robertson, H. H.: "Robertson Q-Lock Floor," 1966.

11.3   Inland-Ryerson: "Hi-Bond Composite Beam Design for Buildings," catalog 2715M, Nov. 1968.

11.4   Wheeling Corrugating Company: "Composite Floor Deck," 1970.

11.5   Granco Steel Products Company: "Floor, Roof Construction," catalog 99–10, Jan. 1972.

11.6   Porter, M. L., and C. E. Ekberg: "Design Recommendations for Steel Deck Floor Slabs," *Proceedings of the 3rd International Specialty Conference on Cold-Formed Steel Structures,* University of Missouri-Rolla, Nov. 1975.

11.7   Porter, M. L., and C. E. Ekberg: "Design vs Test Results for Steel Deck Floor Slabs," *Proceedings of the 3rd International Specialty Conference on Cold-Formed Steel Structures,* University of Missouri-Rolla, Nov. 1975.

11.8   Porter, M. L., C. E. Ekberg, L. F. Greimann, and H. A. Elleby: "Shear-Bond Analysis of Steel-Deck-Reinforced Slabs," *Journal of the Structural Division, ASCE Proceedings,* vol. 102, Dec. 1976.

11.9   Porter, M. L., and C. E. Ekberg: "Behavior of Steel-Deck-Reinforced Slabs," *Journal of the Structural Division, ASCE Proceedings,* vol. 103, Mar. 1977.

11.10   Porter, M. L.: "Effects of Added Reinforcement in Steel-Deck Slabs," *Proceedings of the 4th International Specialty Conference on Cold-Formed Steel Structures,* University of Missouri-Rolla, June 1978.

11.11   Porter, M. L., and C. E. Ekberg: "Coating Effects of Cold-Formed Steel Deck Slabs," *Proceedings of the 5th International Specialty Conference on Cold-Formed Steel Structures,* University of Missouri-Rolla, Nov. 1980.

11.12   Porter, M. L., and L. F. Greimann: "Composite Steel Deck Diaphragm Slabs-Design Modes," *Proceedings of the 6th International Specialty Conference on Cold-Formed Steel Structures,* University of Missouri-Rolla, Nov. 1982.

11.13   Temple, M. C., and G. Abdel-Sayed: "Fatigue Experiments on Composite Slab Floors," *Proceedings of the 4th International Specialty Conference on Cold-Formed Steel Structures,* University of Missouri-Rolla, June 1978.

11.14   Schuster, R. M.: "Composite Steel Deck Concrete Floor Slabs," *Proceedings of the Cold-Formed Steel Structures Conference,* University of Windsor, Ont., Canada, Apr. 1980.

11.15   Schuster, R. M., and W. C. Ling: "Mechanical Interlocking Capacity of Composite Slabs," *Proceedings of the 5th International Specialty Conference on Cold-Formed Steel Structures,* University of Missouri-Rolla, Nov. 1980.

11.16   Seleim, S. S., and R. M. Schuster: "Shear-Bond Capacity of Composite Slabs," *Proceedings of the 6th International Specialty Conference on Cold-Formed Steel Structures,* University of Missouri-Rolla, Nov. 1982.

11.17   Abdel-Sayed, G.: "Composite Cold-Formed Steel-Concrete Structural System," *Proceedings of the 6th International Specialty Conference on Cold-Formed Steel Structures,* University of Missouri-Rolla, Nov. 1982.

11.18   Steel Deck Institute: "Design Manual for Composite Decks, Form Decks and Roof Decks," 1981–1982.

11.19   McCabe, T. J.: "Design Example on Composite Steel Deck Floor Slabs," *Proceedings of the 3rd International Specialty Conference on Cold-Formed Steel Structures,* University of Missouri-Rolla, Nov. 1975.

11.20   Fisher, J. M., and D. R. Buettner: "Applications of Light-Gauge Steel in Composite Construction," *Handbook of Composite Construction Engineering* (G. M. Sabnis, Ed.), Van Nostrand Reinhold, New York, 1979, Chap. 3.

11.21   Grant, J. A., J. W. Fisher, and R. G. Slutter: "Composite Beams with Formed Steel Deck," *Engineering Journal,* American Institute of Steel Construction, First Quarter 1977.

11.22   Winter, G.: "Discussion of Design of Composite Beams With Formed Metal Deck, by J. W. Fisher," *AISC Engineering Journal,* vol. 8, Jan. 1971.

11.23   Nicholas J. Bouras, Inc.: "Engineers Notebook for the Design of Composite Beams and Girders with Steel Deck," Aug. 1985.

11.24   Inryco: "Inryco Composite Beam Design," manual 21-12, July 1977.

11.25   Mac-Fab Products Inc.: "Floor & Roof Systems," Jan. 1978.

11.26   Canadian Sheet Steel Building Institute: "Criteria for the Design of Composite Slabs," CSSBI S3-88, Nov. 1988.

11.27   Badoux, J. C., and M. Crisinel: "Recommendations for the Application of Cold-Formed Steel Decking for Composite Slabs in Buildings," Swiss Institute of Steel Construction, 1973.

11.28   Bucheli, P., and M. Crisinel: "Poutres Mixtes dans le Bâtiment," Swiss Institute of Steel Construction, 1982.

11.29   Cran, J. A.: "Design and Testing—Composite Open Web Steel Joists," *Proceedings of the 1st Specialty Conference on Cold-Formed Steel Structures,* University of Missouri-Rolla, Aug. 1971.

11.30   Tide, R. H. R., and T. V. Galambos: "Composite Open Web Steel Joists," *AISC Engineering Journal,* Jan. 1970.

11.31   Porter, M. L., and L. F. Greimann: "Shear-Bond Strength of Studded Steel Deck Slabs," *Proceedings of the 7th International Specialty Conference on Cold-Formed Steel Structures,* University of Missouri-Rolla, Nov. 1984.

11.32   Luttrell, L. D., and S. Prasannan: "Strength Formulations for Composite Slabs," *Proceedings of the 5th International Specialty Conference on Cold-Formed Steel Structures,* University of Missouri-Rolla, Nov. 1984.

11.33   Luttrell, L. D.: "Methods for Predicting Strength in Composite Slabs," *Proceedings of the 8th International Specialty Conference on Cold-Formed Steel Structures,* University of Missouri-Rolla, Nov. 1986.

11.34   Porter, M. L.: "Highlights of New ASCE Standard on Composite Slabs," *Proceedings of the 8th International Specialty Conference on Cold-Formed Steel Structures,* University of Missouri-Rolla, Nov. 1986.

11.35   Schuster, R. M., and R. E. Suleiman: "Composite Slabs Subjected to Repeated Point Loading," *Proceedings of the 8th International Specialty Conference on Cold-Formed Steel Structures,* University of Missouri-Rolla, Nov. 1986.

11.36   Schurter, P. G., and R. M. Schuster: "Aluminum-Zinc Alloy Coated Steel For Composite Slabs," *Proceedings of the 8th International Specialty Conference on Cold-Formed Steel Structures,* University of Missouri-Rolla, Nov. 1986.

11.37   Porter, M. L.: "Two-Way Analysis of Steel-Deck Floor Slabs," *Proceedings of the 9th International Specialty Conference on Cold-Formed Steel Structures,* University of Missouri-Rolla, Nov. 1988.

11.38 Bode, H., R. Kunzel, and J. Schanzenbach: "Profiled Steel Sheeting and Composite Action," *Proceedings of the 9th International Specialty Conference on Cold-Formed Steel Structures,* University of Missouri-Rolla, Nov. 1988.

11.39 McCuaig, L. A., and R. M. Schuster: "Repeated Point Loading on Composite Slabs," *Proceedings of the 9th International Specialty Conference on Cold-Formed Steel Structures,* University of Missouri-Rolla, Nov. 1988.

11.40 Easterling, W. S., and M. L. Porter: "Composite Diaphragm Behavior and Strength," *Proceedings of the 9th International Specialty Conference on Cold-Formed Steel Structures,* University of Missouri-Rolla, Nov. 1988.

11.41 Porter, M. L.: "New Standards for Cold-Formed Steel Deck with Concrete," *Proceedings of the 10th International Specialty Conference on Cold-Formed Steel Structures,* University of Missouri-Rolla, Oct. 1990.

11.42 McCuaig, L. A., and R. M. Schuster: "Safety Indexes for Shear-Bond Failure of Composite Slabs," *Proceedings of the 10th International Specialty Conference on Cold-Formed Steel Structures,* University of Missouri-Rolla, Oct. 1990.

11.43 Wright, H. D., and Evans: "A Review of Composite Slab Design," *Proceedings of the 10th International Specialty Conference on Cold-Formed Steel Structures,* University of Missouri-Rolla, Oct. 1990.

11.44 Daniels, B. J., D. O'Leary, and M. Crisinel: "The Analysis of Composite Slabs with Profiled Sheeting Using a Computer Based Semi-Empirical Partial Interaction Approach," *Proceedings of the 10th International Specialty Conference on Cold-Formed Steel Structures,* University of Missouri-Rolla, Oct. 1990.

11.45 Young, C. S., and W. S. Easterling: "Strength of Composite Slabs," *Proceedings of the 10th International Specialty Conference on Cold-Formed Steel Structures,* University of Missouri-Rolla, Oct. 1990.

11.46 Patrick, M.: "Long-Spanning Composite Members with Steel Decking," *Proceedings of the 10th International Specialty Conference on Cold-Formed Steel Structures,* University of Missouri-Rolla, Oct. 1990.

11.47 Lamport, W. B., and M. L. Porter: "Deflections for Composite Steel Deck Floors," *Proceedings of the 10th International Specialty Conference on Cold-Formed Steel Structures,* University of Missouri-Rolla, Oct. 1990.

11.48 Hamerlinck, R., L. Twilt, and J. Stark: "A Numerical Model for Fire-Exposed Composite Steel/Concrete Slabs," *Proceedings of the 10th International Specialty Conference on Cold-Formed Steel Structures,* University of Missouri-Rolla, Oct. 1990.

11.49 Nguyen, R. P.: "Strength of Composite Cold-Formed Steel-Concrete Beams," *Proceedings of the 9th International Specialty Conference on Cold-Formed Steel Structures,* University of Missouri-Rolla, Nov. 1988.

11.50 Lin, C. Y.: "Axial Capacity of Concrete Infilled Cold-Formed Steel Columns," *Proceedings of the 9th International Specialty Conference on Cold-Formed Steel Structures,* University of Missouri-Rolla, Nov. 1988.

11.51 Heagler, R. B.: *LRFD Design Manual for Composite Beams and Girders with Steel Deck,: " 1st Ed., Steel Deck Institute, 1989.*

11.52   American Institute of Steel Construction: *Manual of Steel Construction—Load & Resistance Factor Design,* 1st Ed., 1986.

11.53   American Society of Civil Engineers: "Standard for the Structural Design of Composite Slabs," ANSI/ASCE 3-91, 1994.

11.54   American Society of Civil Engineers: "Standard Practice for Construction and Inspection of Composite Slabs," ANSI/ASCE 9-91, 1994.

11.55   Nguyen, R. P.: "Thin-Walled, Cold-Formed Steel Composite Beams," *Journal of Structural Engineering,* ASCE, vol. 117, no. 10, Oct. 1991.

11.56   Porter, M. L.: "New ASCE Standards for Cold-Formed Steel Deck Slabs," *Proceedings of the 11th International Specialty Conference on Cold-Formed Steel Structures,* University of Missouri-Rolla, Oct. 1992.

11.57   An, L., and K. Cederwall: "Composite Slabs Analyzed by Block Bending Test," *Proceedings of the 11th International Specialty Conference on Cold-Formed Steel Structures,* University of Missouri-Rolla, Oct. 1992.

11.58   Itoh, Y., K. Komori, and H. Fujioka: "Repeated Point Loading Tests on Composite Slabs," *Proceedings of the 11th International Specialty Conference on Cold-Formed Steel Structures,* University of Missouri-Rolla, Oct. 1992.

11.59   Both, K., J. W. B. Stark, and L. Twilt: "Thermal Shielding Near Intermediate Supports of Continuous Span Composite Slab," *Proceedings of the 11th International Specialty Conference on Cold-Formed Steel Structures,* University of Missouri-Rolla, Oct. 1992.

11.60   Oehlers, D. J., H. D. Wright, and M. J. Burnet: "Flexural Strength of Profiled Beams," *Journal of Structural Engineering,* ASCE, vol. 120, no. 2, Feb. 1994.

11.61   Terry, A. S., and W. S. Easterling: "Further Studies of Composite Slab Strength," *Proceedings of the 12th International Specialty Conference on Cold-Formed Steel Structures,* University of Missouri-Rolla, Oct. 1994.

11.62   Patrick, M., and R. Q. Bridge: "Review of Concepts Concerning Bond of Steel Decking," *Proceedings of the 12th International Specialty Conference on Cold-Formed Steel Structures,* University of Missouri-Rolla, Oct. 1994.

11.63   Cheng, J. J. R., M. C. H. Yam, and E. B. Davison: "Behavior and Failure Mechanism of Composite Slabs," *Proceedings of the 12th International Specialty Conference on Cold-Formed Steel Structures,* University of Missouri-Rolla, Oct. 1994.

11.64   An, L., and K. Cederwall: "Slip and Separation of Interface of Composite Slabs," *Proceedings of the 12th International Specialty Conference on Cold-Formed Steel Structures,* University of Missouri-Rolla, Oct. 1994.

11.65   O'Shea, M. D., and R. Q. Bridge: "Tests of Thin-Walled Concrete-Filled Steel Tubes," *Proceedings of the 12th International Specialty Conference on Cold-Formed Steel Structures,* University of Missouri-Rolla, Oct. 1994.

11.66   Wright, H. D.: "Local Buckling of Filled Sections," *Proceedings of the 12th International Specialty Conference on Cold-Formed Steel Structures,* University of Missouri-Rolla, Oct. 1994.

11.67   Hariharan, S., K. Mahadevan, and V. Kalyanaraman: "Core Loaded Thin-Walled Sleeved Column System," *Proceedings of the 12th International Specialty Conference on Cold-Formed Steel Structures,* University of Missouri-Rolla, Oct. 1994.

11.68   Wright, H. D.: "Load Stability of Filled and Encased Steel Sections," *Journal of Structural Engineering,* ASCE, vol. 121, no. 10, Oct. 1995

11.69   ASCE Task Committee on Design Criteria for Composite Structures in Steel and Concrete: "Proposed Specification and Commentary for Composite Joists and Composite Trusses," *Journal of Structural Engineering,* ASCE, vol. 122, no. 4, April 1996.

11.70   Widjaja, B. R., and W. S. Easterling: "Strength and Stiffness Calculation Procedures for Composite Slabs," *Proceedings of the 13th International Specialty Conference on Cold-Formed Steel Structures,* University of Missouri-Rolla, Oct. 1996.

11.71   Lyons, J. C., W. S. Easterling, and T. M. Murray: "Strength of Headed Shear Studs in Cold-Formed Steel Deck," *Proceedings of the 13th International Specialty Conference on Cold-Formed Steel Structures,* University of Missouri-Rolla, Oct. 1996.

11.72   Wright, H. D., and M. Veljkovic: "Towards a Numerical Procedure for Composite Slab Assessment," *Proceedings of the 13th International Specialty Conference on Cold-Formed Steel Structures,* University of Missouri-Rolla, Oct. 1996.

11.73   Lee, J. S., Y. B. Kwon, and K. S. Woo: "Moment Rotation Behavior for Concrete Filled SHS Column to Composite Beam Connection," *Proceedings of the 13th International Specialty Conference on Cold-Formed Steel Structures,* University of Missouri-Rolla, Oct. 1996.

11.74   Yang, G. R., Y. S. Hwang, and Y. B. Kwon: "A Study on the Flexural Behavior of Profiled Composite Beams," *Proceedings of the 14th International Specialty Conference on Cold-Formed Steel Structures,* University of Missouri-Rolla, Oct. 1998.

11.75   Malite, M., W. A. Nimir, J. J. de Sales, and R. M. Goncalves: "Cold-Formed Shear Connectors for Composite Construction," *Proceedings of the 14th International Specialty Conference on Cold-Formed Steel Structures,* University of Missouri-Rolla, Oct. 1998.

CHAPTER 12

12.1   American Iron and Steel Institute: "Specification for the Design of Light Gage Cold Formed Stainless Steel Structural Members," 1968 ed.

12.2   Johnson, A. L., and G. A. Kelsen: "Stainless Steel in Structural Applications," *Stainless Steel for Architecture,* American Society for Testing and Materials, STP 454, Aug. 1969.

12.3   Wang, S. T.: "Cold-Rolled Austenitic Stainless Steel: Material Properties and Structural Performance," report 334, Department of Structural Engineering, Cornell University, July 1969.

12.4   Wang, S. T., and S. J. Errera: "Behavior of Cold Rolled Stainless Steel Members, *Proceedings of the 1st Specialty Conference on Cold-Formed Steel Structures,* University of Missouri-Rolla, Aug. 1971.

12.5   Errera, S. J., B. M. Tang, and D. W. Popowich: "Strength of Bolted and Welded Connections in Stainless Steel," report 335, Department of Structural Engineering, Cornell University, Aug. 1970.

12.6   Van der Merwe, P.: "Development of Design Criteria for Ferritic Stainless Steel Cold-Formed Structural Members and Connections," Ph.D. Thesis, University of Missouri-Rolla, 1987.

12.7   Van den Berg, G. J.: "The Torsional Flexural Buckling Strength of Cold-Formed Stainless Steel Columns," D.Eng. Thesis, Rand Afrikaans University, Johannesburg, South Africa, 1988.

12.8   Lin, S. H.: "Load and Resistance Factor Design of Cold-Formed Stainless Steel Structural Members," Ph.D. Thesis, University of Missouri-Rolla, 1989.

12.9   American Society of Civil Engineers: "Standard Specification for the Design of Cold-Formed Stainless Steel Structural Members," 1990.

12.10   Coetsee, J. S., G. J. Van den Berg, and P. Van der Merwe: "The Behaviour of Stainless Steel Lipped Channel Axially Loaded Compression Members," *Proceedings of the Annual Technical Session,* Structural Stability Research Council, 1990.

12.11   Carvalho, E. C. G., G. J. Van den Berg, and P. Van der Merwe: "Local Shear Buckling in Cold-Formed Stainless Steel Beam Webs," *Proceedings of the Annual Technical Session,* Structural Stability Research Council, 1990.

12.12   Rasmussen, K. J. R., and G. J. Hancock: "Stainless Steel Tubular Columns—Tests and Design," *Proceedings of the 10th International Specialty Conference on Cold-Formed Steel Structures,* University of Missouri-Rolla, Oct. 1990.

12.13   Van Wyk, M. L., G. J. Van den Berg, and P. Van der Merwe: "Lateral Torsional Buckling Strength of Doubly Symmetric Stainless Steel Beams," *Proceedings of the 10th International Specialty Conference on Cold-Formed Steel Structures,* University of Missouri-Rolla, Oct. 1990.

12.14   Coetsee, J. S., G. J. Van den Berg, and P. Van der Merwe: "The Effects of Workhardening and Residual Stresses Due to Cold Work of Forming on the Strength of Cold-Formed Stainless Steel Lipped Channel Sections," *Proceedings of the 10th International Specialty Conference on Cold-Formed Steel Structures,* University of Missouri-Rolla, Oct. 1990.

12.15   Lin, S. H., W. W. Yu, and T. V. Galambos "ASCE LRFD Method for Stainless Steel Structures," *Journal of Structural Engineering,* vol. 118, no. 4, April 1990.

12.16   Rasmussen, K. J. R., and G. J. Hancock: "Stainless Steel Tubular Beams—Tests and Design," *Proceedings of the 11th International Specialty Conference on Cold-Formed Steel Structures,* University of Missouri-Rolla, Oct. 1992.

12.17   Bredenkamp, P. J., G. J. Van den Berg, and P. Van der Merwe: "The Lateral Torsional Buckling Strength of Cold-Formed Stainless Steel Lipped Channel Beams," *Proceedings of the 11th International Specialty Conference on Cold-Formed Steel Structures,* University of Missouri-Rolla, Oct. 1992.

12.18   Rasmussen, K. J. R., and G. J. Hancock: "Design of Cold-Formed Stainless Steel Tubular Members. I: Columns," *Journal of Structural Engineering,* vol. 119, no. 8, Aug. 1993.

12.19   Rasmussen, K. J. R., and G. J. Hancock: "Design of Cold-Formed Stainless Steel Tubular Members. II: Columns," *Journal of Structural Engineering,* vol. 119, no. 8, Aug. 1993.

12.20   Bredenkamp, P. J., and G. J. Van den Berg: "The Lateral Torsional Buckling Strength of Cold-Formed Stainless Steel Beams," *Proceedings of the 12th International Specialty Conference on Cold-Formed Steel Structures,* University of Missouri-Rolla, Oct. 1994.

12.21   Korvink, S. A., and G. J. Van den Berg: "Web Crippling of Stainless Steel Cold-Formed Beams," *Proceedings of the 12th International Specialty Conference on Cold-Formed Steel Structures,* University of Missouri-Rolla, Oct. 1994.

12.22   Bruitendag, Y., and G. J Van den Berg: "The Strength of Partially Stiffened Stainless Steel Compression Members," *Proceedings of the 12th International Specialty Conference on Cold-Formed Steel Structures,* University of Missouri-Rolla, Oct. 1994.

12.23   Rasmussen, K. J. R., and B. Young: "Stainless Steel Tubular Joints—Test and Design of X- and K-Joints in Square Hollow Sections," *Proceedings of the 12th International Specialty Conference on Cold-Formed Steel Structures,* University of Missouri-Rolla, Oct. 1994.

12.24   Rasmussen, K. J. R., and A. S. Hasham: "Stainless Steel Tubular Joints Tests and Design of X- and K-Joints in Circular Hollow Sections," *Proceedings of the 12th International Specialty Conference on Cold-Formed Steel Structures,* University of Missouri-Rolla, Oct. 1994.

12.25   Rasmussen, K. J. R., and J. Rondal: "An Explicit Approach to Design of Stainless Steel Columns," *Proceedings of the 13th International Specialty Conference on Cold-Formed Steel Structures,* University of Missouri-Rolla, Oct. 1996.

12.26   Reyneke, W., and G. J. Van den Berg: "The Strength of Partially Stiffened Stainless Steel Compression Members," *Proceedings of the 13th International Specialty Conference on Cold-Formed Steel Structures,* University of Missouri-Rolla, Oct. 1996.

12.27   Prestorius, J., P. Van der Merwe, and G. J. Van den Berg: "Burst Strength of 304L Stainless Steel Tubes Subjected to Internal Pressure and Internal Forces," *Proceedings of the 12th International Specialty Conference on Cold-Formed Steel Structures,* University of Missouri-Rolla, Oct. 1996.

12.28   Rasmussen, K. J. R., and J. Rondal: "Explicit Approach to Design of Stainless Steel Columns," *Journal of Structural Engineering,* vol. 123, no. 7, July 1997.

12.29   Macdonald, M., J. Rhodes, and G. T. Taylor: "Compressional Behaviour of Stainless Steel Short Struts," *Proceedings of the 14th International Specialty Conference on Cold-Formed Steel Structures,* University of Missouri-Rolla, Oct. 1998.

12.30   Van den Berg, G. J.: "The Local Buckling Strength of Partially Stiffened Type 3CR12 Stainless Steel Compression Elements in Beam Flanges," *Proceedings of the 14th International Specialty Conference on Cold-Formed Steel Structures,* University of Missouri-Rolla, Oct. 1998.

12.31   Van den Berg, G. J., and P. Van der Merwe: *Collected Papers of the Chromium Steels Research Group,* Rand Afrikaans University, vol. 1, 1992.

12.32   Van den Berg, G. J., and P. Van der Merwe: *Collected Papers of the Chromium Steels Research Group,* Rand Afrikaans University, vol. 2, 1993.

12.33   Van den Berg, G. J., and P. Van der Merwe: *Collected Papers of the Chromium Steels Research Group,* Rand Afrikaans University, vol. 3, 1994.

12.34   Van den Berg, G. J., and P. van der Merwe: *Collected Papers of the Chromium Steels Research Group,* Rand Afrikaans University, vol. 4, 1995.

12.35   Van den Berg, G. J.: *Collected Papers of the Chromium Steels Research Group,* Rand Afrikaans University, vol. 5, 1998.

12.36   Van der Merwe, P., and G. J. Van den Berg: "Design of Stainless Steel Structural Members and Connections," *Proceedings of 4th International Conference on Steel and Aluminum Structures,* Helsinki University of Technology, June 1999.

12.37   Euro 3: Part 1.4, "Design of Steel Structures: Supplementary Rule for Stainless Steels," March 1994.

12.38   South African Bureau of Standards: "Draft Code of Practice—Limit State Design of Cold-Formed Stainless Steel Members," SABS 0162-4: 1996.

CHAPTER 13

13.1   Klippstein, K. H.: "Computer Program for the Design of Light-Gage Steel Structures," presented at the 1st Specialty Conference on Cold-Formed Steel Structures, University of Missouri-Rolla, Aug. 1971.

13.2   Nicholls, J. I., and A. T. Merovich: "Minimum Cost Design of Composite Floor Systems Using Cold-Formed Steel Decking," *Proceedings of the 1st Specialty Conference on Cold-Formed Steel Structures,* University of Missouri-Rolla, Aug. 1971.

13.3   Douty, D. T.: "Optimization of Light Gage Cold-Formed Shapes by Parametric Bandwidth Constriction," presented at the National Symposium on Computerized Structural Analysis and Design, George Washington University, Mar. 28, 1972.

13.4   Tezcan, S. S., K. M. Agrawal, and G. Kostro: "Finite Element Analysis of Hyperbolic Paraboloid Shells," *Journal of the Structural Division, ASCE Proceedings,* vol. 97, Jan. 1971.

13.5   Buker, P. S.: "Flexibility in Standardization," *Progressive Architecture,* Sept. 1961.

13.6   Seaburg, P. A.: "A Decision Table Formulation of the AISI Specification for the Design of Cold-Formed Steel Structural Members," Ph.D., Thesis, University of Wisconsin, Milwaukee, July 1971.

13.7   American Iron and Steel Institute: "Decision Tables for Use with the August 19, 1986 Edition of the Specification for the Design of Cold-Formed Steel Structural Members," Report CF 88-1, October 1988.

13.8   Zuehlke, M. T.: "Computer-Aided Design of Cold-Formed Steel Structural Members," M.S. Thesis, University of Missouri-Rolla, 1989.

13.9   Center for Cold-Formed Steel Structures: "Cold-Formed Steel Design Computer Programs," University of Missouri-Rolla, 1996.

13.10   Center for Cold-Formed Steel Structures: *CCFSS NEWS,* vol. 9, no. 2, University of Missouri-Rolla, Feb. 1999.

13.11   Chen, H.: "Example Problems Based on the 1996 AISI Specification for the Design of Cold-Formed Steel Structural Members," American Iron and Steel Institute, 1999.

13.12   Schafer, B. W.: "Elastic Buckling Stress and Cold-Formed Steel Design," *CCFSS Technical Bulletin,* vol. 7, no. 1, University of Missouri-Rolla, Feb. 1998.

13.13   Schafer, B. W., and T. Pekoz: "Direct Strength Prediction of Cold-Formed Steel Members Using Numerical Elastic Buckling Solutions," *Thin-Walled Structures: Research and Development* (N. E. Shanmugam, J. Y. R. Liew, and V. Thevendran, Eds.), Elsevier, 1998.

13.14   Pekoz, T.: "Possible Future Developments in the Design and Application of Cold-Formed Steel," *Proceedings of the Fourth International Conference on Steel and Aluminum Structures,* Helsinki University of Technology, Finland, June 1999.

13.15   Schafer, B. W.: "CUFSM User's Manual," Cornell University, 1998.

CHAPTER 14

14.1   Bats, J. O., and J. F. G. Janssen: "Industrialized Housing with Cold-Formed Sheet-Steel Elements," *Proceedings of the 9th International Specialty Conference on Cold-Formed Steel Structures,* University of Missouri-Rolla, Nov. 1988.

14.2   Center for Cold-Formed Steel Structures: *CCFSS NEWS,* vol. 8, no.2, University of Missouri-Rolla, Feb. 1998.

14.3   Center for Cold-Formed Steel Structures: *CCFSS NEWS,* vol. 9, no.2, University of Missouri-Rolla, Feb. 1999.

APPENDIX A

A.1   American Iron and Steel Institute: "Sheet Steel—Carbon, High Strength Low Alloy, and Alloy Coils and Cut Lengths," *Steel Products Manual,* Oct. 1979.

A.2   American Society for Testing and Materials: "Standard Specification for Steel Sheet, Zinc-Coated (Galvanized) or Zinc—Iron Alloy-Coated (Galvannealed) by the Hot-Dip Process," ASTM designation A653-97.

A.3   Center for Cold-Formed Steel Structures: *CCFSS Technical Bulletin,* vol. 8, no. 2, University of Missouri-Rolla, Aug. 1999.

A.4   Steel Stud Manufacturers Association: *Product Technical Information.*

A.5   Iron and Steel Society: "Sheet Steel—Carbon, High-Strength Low-Alloy, Alloy, Uncoated, Metallic Coated, Coil Coated, Coils, Cut Lengths, Corrugated Products," *Steel Products Manual,* Sept. 1999.

APPENDIX B

B.1   American Institute of Steel Construction: "Torsional Analysis of Steel Members," 1983.

B.2   Fang, P. J.: "Torsional-Flexural Buckling of Thin-Walled Open Sections," Report No. 320, Cornell University, 1965.

B.3   Gotluru, B. P., and T. Pekoz: "Torsion in Cold-Formed Steel Beams," Final Report, Cornell University, Feb. 1999.

Index